PROCESS INTENSIFICATION: SPINNING DISC REACTOR FOR THE POLYMERISATION OF STYRENE

by

K.V.K.Boodhoo MEng.

Thesis submitted for the degree of Doctor of Philosophy in the Faculty of Engineering of the University of Newcastle Upon Tyne

Process Intensification and Innovation Centre (PIIC)
Department of Chemical Engineering
University of Newcastle Upon Tyne
Newcastle Upon Tyne
U.K.

April 1999

Acknowledgements

I wish to express my gratitude to Dr R.J.Jachuck for his supervision, guidance and helpful suggestions and comments throughout this research. I am also indebted to both Dr R.J.Jachuck and Professor C. Ramshaw for the award of a university studentship for the duration of my Ph.D.

The assistance provided by Mr E.T. Horsley with photographing the apparatus and his enthusiastic team of technical staff with modification, repairs and general maintenance of the experimental rig is greatly appreciated.

The contribution of fellow students and members of staff in the Process Intensification and Innovation Centre during the preparation of this work is gratefully acknowledged. In particular, I would like to thank Miss Marija Vicevic for her time and effort in the tedious task involved in producing exceptionally good quality scans of diagrams included in this work.

A special thought goes to my parents, brother and sister whose love, consistent encouragement, moral support and understanding have kept me going throughout the years especially during the most trying times.

And finally, to Mohammed whose standards of excellence and unrelenting patience, understanding and confidence in me have been an uplifting source of inspiration in my life, I say "keep inspiring me- always".

Abstract

This investigation is concerned with the assessment of the performance of a novel spinning disc reactor (SDR) for the polymerisation of chemically initiated free-radical polymerisation of styrene. The application of high acceleration fields such as those created on the surface of the grooved rotating disc to the polymerising system is aimed at intensifying the polymerisation rate and producing a better quality polymer product.

As part of the experimental programme, four separate sets of experimental runs were conducted on a 360 mm diameter grooved rotating disc at a fixed temperature of 88-90°C to explore the effects of disc rotational speed and prepolymer feed conversion/viscosity on the extent of monomer conversion and molecular weight properties ($\overline{M}_n$, $\overline{M}_w$ and MWD) of the product from the SDR. The performance data of the SDR was compared with conventional batch polymerisation data.

Both the disc rotational speed and prepolymer feed conversion/viscosity variables were found to have a profound influence on the performance of the SDR. A steady increase in conversion, rate of polymerisation and hence time saving in one pass in the SDR were observed with a rise in the prepolymer feed conversion and rotational speed until, for the latter, an optimal speed of rotation which gave the highest rate of polymerisation was reached. The results have been explained in relation to the effect of disc speed and prepolymer feed viscosity on mean film thickness, mean residence time and film surface instabilities. Furthermore, the SDR product is seen to have generally improved characteristics in terms of narrower molecular weight distribution when compared to polymer prepared in the batch at the same conversion.

The large enhancement of the rate of styrene polymerisation in the SDR was discussed in terms of a possible improvement in the BPO initiator efficiency f and non-stationary state polymerisation conditions likely to be prevalent on the rotating disc. The general improvement in SDR product quality was ascribed to the combined effects of a reduced diffusion path length and an intense mixing mechanism within the thin film.

A separate experimental study exploring the effects of micromixing efficiency on the conversion and molecular weight properties of styrene polymerisation in the batch was also undertaken. The opposing effects of enhanced micromixing in batch and continuous polymerisation systems were contrasted in a theoretical manner.

A theoretical case study highlighting the energy efficiency of the SDR was also carried out. Savings in energy of more than 70% was calculated for a semi-batch process using an industrially adapted spinning disc reactor in comparison to a purely batch process.

Finally, a two-stage continuous industrial process for free-radical polymerisations has been proposed consisting of an enhanced tubular reactor in the first stage followed by a parallel arrangement of several rotating disc surfaces. Improvements in intrinsic safety and minimised risks of polymer degradation and thermal runaways are the expected potential benefits.

Keywords: Process Intensification, Thin Film, Spinning Disc Reactor, Free Radical Polymerisation, Polystyrene

Table of Contents

List of Figures

List of Plates

List of Tables

Chapter 1

Introduction

1. PROCESS INTENSIFICATION

The concept of Process Intensification (PI) is based on a drastic reduction of the size of process equipment in a chemical plant designed to meet a given production target. Several potential benefits can be identified by applying this technology.

Cutting down the size of Main Plant Items in a process which include reactors, heat exchangers and separators not only entails a reduction in individual equipment cost but also, and to a more appreciable extent, huge cost savings are to be expected in installation costs as a result of reduced pipeworks, civil engineering and support structure to name but a few. Furthermore, it is envisaged that smaller sized plants could become 'mobile' and hence be transported to the customer or to resources such as an oil field, for instance, for processing flare gas into methanol. The logistics associated with such small, portable plants will be greatly simplified.

The issue of safety in the chemical industry is nowadays being addressed constantly by the Health & Safety regulatory bodies after a number of fatal incidents have occurred involving large inventories of hazardous materials and exothermic runaways in batch reactors [1]. Adopting the PI approach can substantially improve the intrinsic safety of a process by having a significantly reduced volume of potentially hazardous chemical at any time in a smaller intensified unit. In addition, one of the objectives of PI is to move away from batch processing to small continuous reactors, the latter giving more efficient overall operation especially in the case of hugely exothermic reactions whereby the heat can be removed continuously as it is being released.

With regard to our environment, the application of PI technology will have tremendously appealing implications whereby a small, compact, highly intensified plant is more likely to be below the tree line, making it far less of an eyesore for the general public than the unsightly and massive steel works characterising our present chemical plants. Furthermore novel reactor designs based on the PI concept will enable 'clean technology' to be practised. In other words, high selectivity operation in intensified reactors will reduce or eliminate altogether the formation of unwanted by-products which, if not removed from the effluent before discharge, can cause irreversible damage to the environment. High purity product and hence of improved quality will consequently be obtained without incurring enormous downstream purification costs.

The improved energy efficiency foreseeable in intensified unit operations constitutes yet another highly attractive benefit of PI in a world where there is overwhelming concern over the ever growing demand on non-renewable energy resources. In this respect, there is a great and urgent need for the development of new process technologies which will utilise energy in an efficient manner. PI is a positive

step in the right direction for the chemical industry. Large enhancements in heat and mass transfer, two of the most fundamental and frequently encountered operations in chemical engineering processes, can be achieved in intensified units. Such improvements give ample reason to believe that process times and therefore the associated energy consumption can be dramatically reduced for a given operation.

Process intensification is seen as the way forward for the chemical and pharmaceutical industries alike. The idea of plant miniaturisation for the future is endorsed by IChemE in its Future Life Report [2]. Interest from the industry is potentially immense as many routine operations such as mixing and heat and mass transfer could be substantially improved by applying intensification methods [3-6]. As summed up by Semel [7], "*process intensification is the key to survival of the fittest in international competition*".

The Process Intensification and Innovation Centre (PIIC) at this university has acquired a leading edge in research in the field of PI. The idea of PI has long been actively pursued by Ramshaw [8] who has presented numerous examples suited for intensification. His vision that "small is beautiful" [9] has led the way to a wide spectrum of research activities at the centre. Recent studies into a wide range of operations which could potentially benefit from various intensification methods have thus been undertaken. These include the development of intensified catalytic plate reactors [10], rotating packed beds [11,12], spinning disc equipment [13] and polymer film compact heat exchangers [14].

1.1. INTENSIFICATION STRATEGIES

The basic principle underlying the concept of PI concerns the enhancement of equipment performance by a number of ways which can be classified as either "active" or "passive".

Passive methods involving, for example, surface roughening and surface extensions in the forms of fins, have long been implemented on a commercial basis in the field of heat transfer [15]. Such surface modifications have been shown to give improved film heat transfer coefficients in evaporators.

A number of techniques can be employed to provide "actively" intensified systems. These can broadly be categorised as:

1. Stirring
2. Scraping
3. Surface vibration
4. Surface rotation

Stirring or agitation is the simplest and most frequently encountered of all. Its use has found wide applications in mixers and reactors in general where adequate heat and mass transfer rates are required. Complex agitator designs have emerged over the years to meet more stringent functional requirements especially in high conversion polymerisation reactors. Scraping and surface vibration have more specific applications but their implementation demands more complex installation arrangements.

Surface rotation as a technique for intensification has stimulated keen interest from academic workers for many years. As early as the 1950s, Hickman's research efforts into two phase heat transfer on spinning disc surfaces culminated in the development of the first successful centrifugal evaporator used in sea-water desalination [47].

The benefits that can be extracted from the exploitation of high centrifugal fields created by rotation are numerous and are as outlined below:

1. The rotational speed of the spinning surface provides an additional degree of freedom that can be readily manipulated for optimum equipment performance.
2. The extremely high gravity fields thus generated are capable of producing very thin films in which heat transfer, mass transfer and mixing rates are likely to be greatly intensified.
3. Applications in which the solid content of a process fluid often poses a number of problems with regard to fouling in conventional devices can be handled by the rotating equipment. The rotating action in itself provides a scraping or 'self-cleaning' mechanism strong enough to shift any solid deposit away from the surface of revolution, thereby ensuring maximum exposed area at all times during operation.
4. The effect of very short and controllable residence times achieved under the centrifugal action will enable heat sensitive materials to be processed without any risk of degradation.

Several unit operations have been identified where centrifugal acceleration generated on surfaces of revolution presents remarkable potentials for success as a means for intensifying processes. The performance of multiple phase processes in particular stands more chance of being enhanced under the influence of high gravitational forces as a result of increased interphase buoyancy and slip velocity [16]. Typical operations include distillation, extraction, boiling, condensation, crystallisation, precipitation and gas-liquid reactions among others. The practical approach will involve the use of totally innovative designs which unfortunately industrialists are reluctant to embrace precisely because of the novel and therefore unestablished nature of the technology.

1.2. SPINNING DISC TECHNOLOGY

As mentioned before, high acceleration environments can be produced by rotation of various surface configurations and arrangements suitable for the particular operation to which each is to be applied. The spinning disc technology is based on a specific type of rotating equipment, namely a flat horizontal disc surface which on rotation causes the reacting fluid to flow in the form of thin films. The potential applications of such high acceleration environments in processes involving separation, heat transfer, gas liquid reactions, crystallisation etc. have been extensively reviewed by Ramshaw [16].

Previous work on rotating discs has concentrated mostly on understanding the hydrodynamics of thin film flow [13, 17-19] and measuring heat and mass transfer rates from solid to liquid and liquid to vapour [19-22]. More recently, the investigation into spinning disc surfaces was extended to look into the mixing characteristics, in particular micromixing, in the thin liquid film flowing across the

disc [23] and initial results have shown that there is reason to believe that micromixing is promoted by the formation of ripples on the free surface.

1.2.1. Areas of possible application

Reaction engineering is one area where aspects of fluid dynamics, mixing and heat and mass transfer are all intricately linked to the progress of reaction. Therefore the spinning disc surface can be invaluable as a reactor for some systems in which a combined enhancement in the mixing and heat and mass transfer rates would give much improved reaction rates and better overall process management. This may, in principle, apply to both liquid and gas-liquid reactions. The sectors of the chemical industry being targeted with the spinning disc technology are the pharmaceutical and fine chemicals industries which traditionally carry out reactions in batch processes which are associated with inherent processing difficulties especially where exothermic reactions are concerned [24]. There is therefore a clear incentive to replace batch reactors with intensified, continuous units [25].

The rotating disc surface would appear to be an attractive choice for systems which, conventionally, are or become heat and mass transfer limited during the course of the reaction. Two main categories of reactions exhibit such characteristics:

1. Inherently fast exothermic reactions
2. Polymerisation reactions

Industrially relevant examples of highly exothermic reactions governed by fast kinetics include acid-base neutralisation reactions and sulphonation of dye-stuff intermediates. The use of conventional stirred tank reactors imposes major limitations on the reaction rate so as to control the rate of heat generation in the system. This is done because the heat removal rate is strongly dependent on the mixing efficiency throughout the contents of the reactor and mixing at a molecular level (micromixing) is relatively slow in comparison to the reaction step. Hence, the fast kinetics of the reaction cannot be fully exploited to increase productivity due to poor reactor engineering in conventional stirred tanks. On the other hand, an internally cooled spinning disc reactor would be expected to give significantly enhanced heat removal from such systems and hence handle a much higher reaction rate.

Similar considerations can be applied to both addition and step growth polymerisation processes. The rather unique characteristic encountered during polymerisation reactions is the rapid viscosity build up with increasing monomer conversion. At such high viscosities, complete and efficient agitation throughout the bulk of the monomer-polymer mixture becomes increasingly difficult in stirred tank reactors giving reduced heat transfer capabilities. Non-uniformity in temperature causes broadening of the molecular weight distribution and consequently poor product quality. In extreme cases of total loss in temperature control, runaway reactions can occur and these have been responsible for a number of accidents on polymer plants. The case of equilibrium controlled reactions, such as polyester production, is special in that progress in polymerisation is heavily dependent on glycol removal from the reaction site. This removal of small glycol molecules involves diffusion through liquid polymer and mass transfer at the liquid vapour interface. Both processes become hindered at high viscosities so that the rate of polymerisation eventually drops significantly. The problem is further aggravated by insufficient surface area available

in the usually large polymer reactors. Drastic operating conditions are then applied to achieve the desired degree of polymerisation. The use of the spinning disc for polymerisation reactions could overcome the problems outlined above for a more efficient process.

Chapter 2

Literature Review

2. INTRODUCTION

This chapter aims to review the published literature considered relevant and useful to the present study of styrene polymerisation on a rotating disc. With a view to cover all the major areas of interest to this investigation, this chapter will be divided into three parts. The first part will consist of a summary of the areas of applications of spinning disc technology which have been studied so far. This will be followed by a review of reactor technologies for industrial production of polystyrene which have been developed to the present day with special emphasis placed on the limitations of such reactors. Finally, since reactor performance is closely related to reaction kinetics, a review of the kinetics of free-radical polymerisation with particular reference to styrene polymerisation will be presented in the third part of this chapter.

2.1. SPINNING DISC TECHNOLOGY

The interest in spinning disc technology gradually evolved from the realisation during the early 1900s that the flow of thin liquid films on plane surfaces due to gravity was of great practical importance in chemical engineering operations. Much of the experimental work done in the first half of this century has been devoted to the study of gravitational film flow [26-34]. The intense mixing action of the surface waves and the increased heat and mass transfer rates associated with such films subjected to the gravitational field were also extensively investigated both theoretically and experimentally [27,35-40]. Fulford [41] has presented a very comprehensive review of all the studies involving different aspects of gravitational thin film flow.

More recently, research into thin films generated by rotating surfaces have dominated the scene. The centrifugal force driving the flow is much greater than the force acting on films flowing under gravity and films produced in this way have been shown to have improved characteristics. The numerous investigations into thin films generated on a rotating surface can broadly be classified into three groups: hydrodynamic studies, heat and mass transfer studies and chemical reaction studies. Each of these categories will be reviewed in turn below.

2.1.1. Hydrodynamics

2.1.1.1. Flow models

The flow of thin liquid films on a smooth horizontal rotating disc is fully described by the modified Navier-Stokes equations for the conservation of momentum and the equation of continuity for the conservation of mass, both of which are given in Appendix A. Simplified versions of the Navier-Stokes equation are treated in several models from which expressions for velocity distribution, film thickness and residence

times on the surface of rotation can be derived. The various models are also discussed in depth in Appendix A. The equations derived from these models are applicable to smooth, fully developed laminar flow which as will be seen below is only obtained for a very restricted range of conditions.

2.1.1.2. Flow regimes

An assessment of the type of flow prevailing on a rotating disc surface under given conditions of flowrate and rotational speed is one other important aspect involved in the hydrodynamic study of thin liquid films as it directly affects the rate of mixing, heat and mass transfer in the fluid. The flow regime can be predicted on the basis of the Reynolds number defined for thin film flow. The direct visual observation of the flow pattern generated can also help to determine the operating flow regime on the rotating surface. In fact the latter method has been the subject of a number of studies undertaken by many researchers. Although most of the flow visualisation experiments were performed using smooth surfaces [13,17-19,42-45], a separate study involving tailored rotating surfaces [22] showed a marked difference in the flow regimes obtained on such mechanically treated surfaces.

2.1.1.2.1. Reynolds number criteria

The various flow regimes discussed above can be predicted on the basis of the Reynolds number for thin film flow which, in the case of smooth rotating disc, can be defined as:

$$\mathrm{Re} = \frac{4\rho Q_v}{\pi \mu D} \qquad (2.1)$$

where ρ: liquid density (kg/m^3)
Q_v: volumetric flowrate (m^3/s)
μ: liquid viscosity (Ns/m^2)
D: diameter at point of measurement on disc (m)

The criteria governing the type of flow (smooth laminar, wavy laminar and turbulent) obtained on a plane vertical surface have been measured experimentally by several researchers [27,28,32,41,46] in terms of the Reynolds number defined above. These criteria are as follows:

Re < 16: smooth laminar flow (no surface waves)
16≤ Re < 40: Undulations across the film (small amplitude waves)
40 ≤ Re < 80: Sinusoidal waves gradually replaced by regular waves
80 ≤ Re < 1000-2000: Random surface waves (wavy laminar flow)
Re ≥ 1000-2000: Turbulent regime

It is to be noted that the definition of Re as given in equation (2.1) above is based on the hydraulic diameter of an infinitely wide film. It is 4 times as large as another definition sometimes preferred by the research community in the study of thin films [31,32,46]. Hence the Re values computed in those investigations have been multiplied by the factor 4 to match the definition of Re used in this research.

Although the above criteria have been defined on the basis of film flow under gravity, they are also applicable to films formed by the action of high centrifugal fields.

2.1.1.2.2. Flow visualisation

The most recent attempt at studying wave-associated flow regimes on rotating discs was by Woods [13]. He carried out a comprehensive theoretical and experimental study on the formation and propagation of waves at the free surface of films of water mixed with a coloured dye (nigrosine) flowing on a rotating disc. The range of operating conditions employed was:

Flowrate : 7 cc/s < Q < 19 cc/s
Rotational speed: 100 rpm < N < 600 rpm

Three distinct flow regions were observed at different radial locations on the disc:

1. An inner region starting from the distributor with apparent smooth flow
2. A middle section covered with what appeared initially to be a series of concentric waves but subsequently found to be a single tightly wound spiral having a noticeably longer wavelength as the rate of rotation was stepped up.
3. An outer region right up to the periphery of the disc where a multitude of spirals with irregularities along the wavefronts eventually disintegrated into random three-dimensional wavelets on propagation across the disc. These wavelets first appeared at a radius which became smaller with increases in the speed of rotation of the disc. The effect of increased flowrate was to cause the wavelets to form more rapidly and hence occupy a greater proportion on the disc surface.

In similar flow visualisation experiments, Lim [19] investigated an extended range of flowrates from 14.5 cc/s to 60.5 cc/s and rotational speeds between 230 and 1120 rpm. His observations regarding the flow regimes are in good agreement with those of Woods [13] for the ranges of flowrates and rotational speeds considered by the latter. Also, at the highest flows and rotational speeds, Lim showed that the whole surface of the disc was covered with 'three-dimensional wavelets' or ripples. In addition, useful correlations were presented for the 'wave inception' wave amplitude and wavelength in terms of the non- dimensional Reynolds number Re and Taylor number Ta.

Previously, Charwat et al [42] had identified "stability boundaries" for different types of flow pattern generated on their 38cm diameter rotating disc. These were clearly illustrated on a plot of flowrate Q against rotational speed ω. Smooth film flow was typically characterised by low flowrates and low rotational speeds. At various other conditions of disc rotational speeds, flowrates, surface tension and viscosity of the fluid studied, different types of waves classified as concentric, spiral and irregular waves were observed. Concentric waves appeared when the flowrate increased at relatively low speeds of rotation and they were seen to remain close to the centre of the disc. Their tendency was to move radially outwards and eventually decay at a certain radial distance from the centre of the disc leaving a smooth film surface on the outer part. According to the authors, the presence of these waves was due to the outflow from the nozzle distributor and not because of surface instabilities in the film. An increase in the rotational speed of the disc at relatively low flowrates caused spiral waves to appear, originating from some radius away from the centre. They then decayed close to the edge of the disc. A combination of very high flows and rotational speeds led to the film becoming highly unstable and the spiral wave fronts were seen

to break up into numerous individual three-dimensional wavelets decaying at large radii. These observations are, for most part, consistent with Woods results [13] except for the concentric waves which, according to Woods, were in fact closely wound spirals.

Thomas et al. [45] used much higher flowrates between 7 and 15 lpm in their experiments whence the inertial effects played an important part on the flow characteristics. Two types of wave-associated flow regimes were observed on the rotating disc: the wavy-laminar flow and the radial-wave flow. Each type of waves bore close resemblance to those already described above. Wavy-laminar flow was characteristic of low rotational speeds while radial-wave flow conditions appeared at high spin rates. In the wavy-laminar flow, random patterns of low amplitude waves were observed. The transition from wavy-laminar flow to radial-wave flow was marked by the appearance of distinct V-shapes waves on the surface of thin films. With an increase in flowrate, such a transition occurred at a higher rotational speed.

The effect of built-in surface roughness on surface wave formation has also been the subject of a recent experimental study done by Jachuck and Ramshaw [22]. Three different surface configurations were tested and compared to the flow on a smooth disc: metal sprayed, re-entry grooved and normal grooved discs. It was found that for a given flowrate and rotational speed, the tailored surfaces, especially the grooved types, produced more numerous waves of small amplitude and short wavelength at the film surface than the smooth disc. When the flow characteristics on the re-entry grooved disc were compared to those on the normal grooved disc, more waves were observed for the re-entry grooves at low rotational speeds rather than at the higher rates of rotation. The normal grooved disc was more efficient at high speeds of rotation by generating more waves and hence more instabilities at the free surface of the film.

2.1.1.2.3. Heat and mass transfer

The heat transfer enhancement in thin films falling under gravity has long been recognised and exploited in condensers or evaporators such the commonly encountered falling film equipment. Under the action of much higher acceleration fields as those created on a rotating disc surface, the heat transfer coefficient during boiling/evaporation or condensation has been shown to be dramatically increased by 1000% [15]. The development by Hickman [47] of the first centrifugal evaporator used in sea-water desalination demonstrated the successful application of the spinning surface technology in the field of heat transfer. Since then, much research effort has been invested into the intensification of heat and mass transfer by the use of high acceleration fields generated by rotating surfaces. The patented development of a number of equipment such as the 'Rotex' absorption cycle heat pump [48-50] designed for combined heat and mass transfer enhancement and the Higee contactor [51,52] for intensified mass transfer operations bears evidence to the remarkable progress made in this field over the years.

Academic interest in intensified heat and mass transfer processes using the spinning disc technology has not been lacking either. The idea of spinning discs as heat exchangers has been explored by many. Thus, Woods and Watts [44] tested the heat transfer properties of a small disc rotating about a horizontal axis for water/water and water/oil systems. Their results indicated that high heat transfer rates could be

achieved by increasing the liquid flowrate and rotational speed. However, simple laminar flow theory failed to predict the increases in heat coefficients which the authors attributed instead to intense ripple formation on the film surface. Bell [17] carried out an extensive study into evaporation on the surface of a horizontal rotating disc heated by condensing steam on the underside and attempted to correlate the measured evaporation film coefficient with Reynolds number and Taylor number. As a follow up to Bell's work on heat transfer, Khan [20] investigated heat transfer on a rotating disc with and without phase change. The use of modified surface configurations of rotating discs to further improve heat transfer rates was explored by Bromley and co-workers [53] in simultaneous evaporation and condensation processes. Increases in overall heat transfer coefficients of up to 13% were reported. More recently, Jachuck and Ramshaw [22] investigated the effect of different types of grooves machined in the disc surface on the convective heat transfer characteristics of the disc using water as the test fluid. They found that, in the presence of grooves, surface instabilities and heat transfer coefficients were significantly increased to an average value of 18 kW $m^{-2}K^{-1}$ in comparison to the smooth surface which again suggests the positive influence of surface waves on the heat transfer properties. The effect of rotational speed on heat transfer coefficients for the various surface configurations is shown in Figure 2.1 below.

The heat transfer characteristics of boiling liquid films and condensing vapours on both smooth and grooved spinning disc surfaces have also been studied by Yanniotis and Kolokotsa [54,55] and their results also indicated large enhancements in heat transfer with heat coefficients of up to 16 kW/(m^2K) for boiling and 30 kW/(m^2K) for condensation with a rotational speed of 1000 rpm. More recently, a novel double disc rotating heat exchanger was developed for boiling of liquid films by the same research team [56]. The preliminary results suggested that high heat transfer rates could easily be achieved.

Many workers have also performed numerical simulations of heat transfer for thin film flow on rotating discs. For example, Rahman et al. [57-59] presented a computational analysis of the heat transfer characteristics using an iterative procedure applied to a three-dimensional boundary-fitted co-ordinate system. Numerical solutions for the case of simple heating with no evaporation and evaporation at the free surface were obtained and these showed that heat transfer coefficients became much larger with increases in radial distance, rotational speed and liquid flowrate. The effects of inertia were also taken into account. Previously, Butuzov and Rifert [60] and Sparrow and Gregg [61] had respectively analysed the evaporation from and condensation onto a spinning surface.

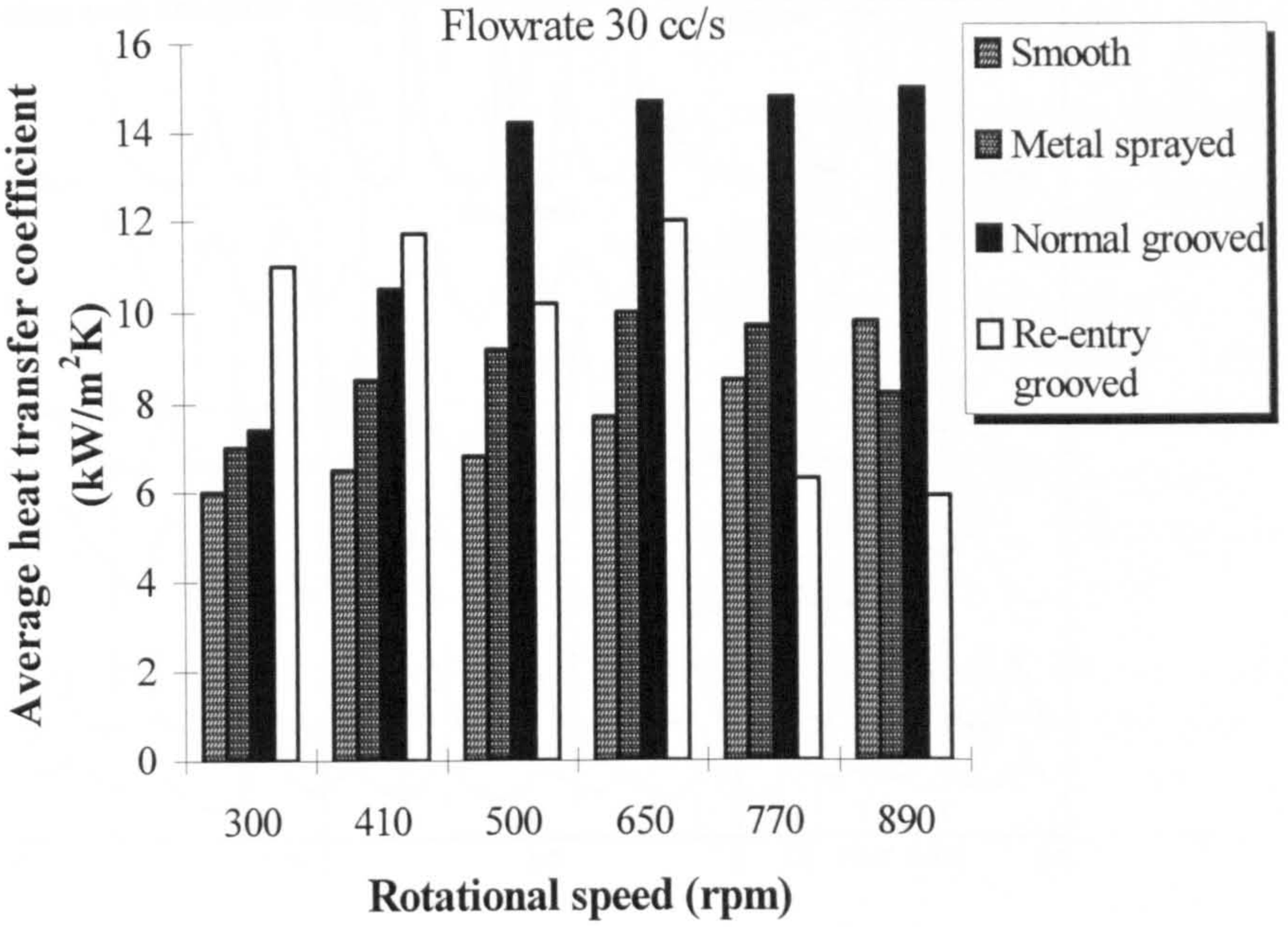

Figure 2.1. Heat transfer characteristics for different rotating surface configurations [22]

The enhancements in heat transfer on a rotating disc have naturally prompted researchers to investigate the effects of centrifugal fields on mass transfer processes. In some cases, heat and mass transfer studies have been carried out in parallel. In fact the multifunctionality of the spinning disc equipment makes it very versatile for applications where a combination of heat and mass transfer processes simultaneously take place. Lim [19] investigated the mass transfer rates during the absorption of oxygen in thin liquid films on a rotating disc and reported mass transfer coefficients much larger than can be predicted on the sole basis of molecular diffusion in a smooth laminar liquid film were. The observation was attributed to vigorous bulk mixing action of the numerous ripples formed on the film surface. Moore [21] also compared the effect of rotation on mass transfer processes using various perforated and smooth plates as the active mass transfer surfaces. Mass transfer coefficients for the perforated surfaces were much higher than those associated with the smooth disc due to excessive random turbulent waves in the former case. Interestingly, the interactions between waves and local instantaneous mass transfer coefficients for films flowing down an inclined surface under gravity have been measured directly by Brauner and Maron [62] and the time traces as shown in Figure 2.2 below represent strong evidence of the influence of waves on the associated transport mechanisms.

Several attempts at modelling mass transfer processes into thin wavy liquid films flowing on rotating surfaces have been made [63-69]. However, as with heat transfer models, there is not, so far, a universally accepted model to predict the mass transport phenomenon in the presence of surface waves on thin liquid films.

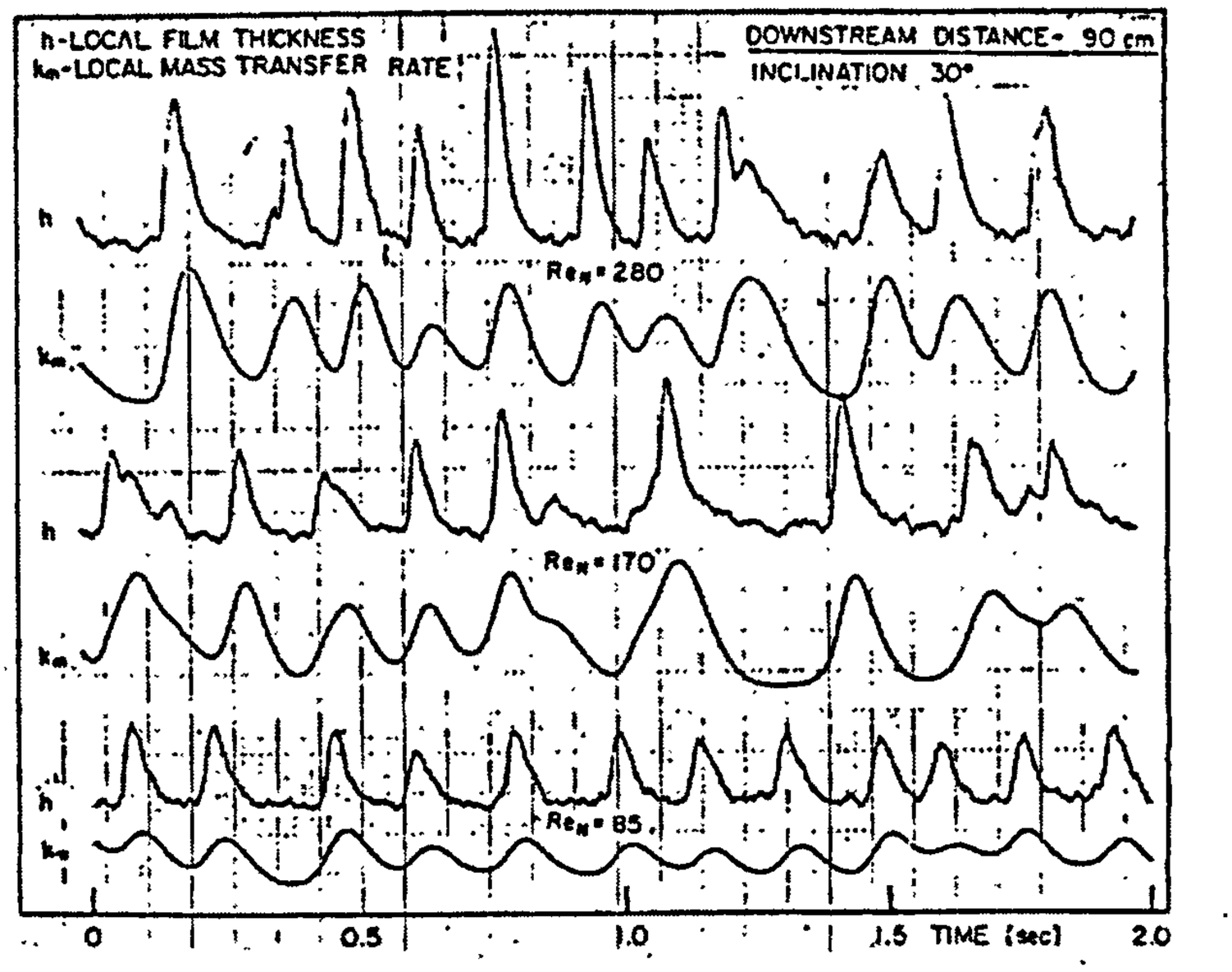

Figure 2.2. Time traces of simultaneous local instantaneous solid-liquid mass transfer rates and local film thickness for thin film flow on an inclined plane [62]

2.1.1.2.4. Chemical reaction

As has been shown in the previous section, the intense mixing activity arising from random turbulent waves on the surface of thin films flowing on a rotating disc is of paramount importance for optimal transfer of heat and mass across either the gas-liquid or liquid solid interface. It is therefore obvious that chemical reactions which rely on heat and mass interchange will also be affected by mixing efficiency.

Diffusion-controlled reactions are one type of such reactions and one very common example of diffusion-controlled reactions is polymerisation. The problems encountered in polymerisation are related to the rapid build-up of viscosity with increase in polymer concentration. Diffusion limitations arise in both condensation and free-radical polymerisations. Polycondensation reactions are controlled by the rate of removal of small molecules such as ethylene glycol or water from the bulk of the polymer melt. The benefits of carrying out the polymerisation in thin films, especially at high viscosity, are very apparent since the diffusion of the small molecules across the short path length of the film to the surface will be much easier than through a massive bulk of polymer in large tanks. In fact this principle of removal of volatiles from polymer layers has been studied in relation to the finishing reactors in continuous polycondensation processes [70-72]. However, in these studies, the primary aim of using a vertically mounted disc rotating at extremely low speeds and partially immersed in the bulk polymer melt phase is to provide a large surface area to volume ratio for the removal of volatile, the whole operation being carried out under vacuum. The idea of enhancing mass transfer by rapid diffusion through intense mixing in the thin film is evidently not considered in these reactors.

The only study known to the author, dealing with the application of a horizontal disc system rotating at speeds in excess of 500 rpm to polymerisation, is that of Jachuck and Ramshaw [73] who have tested the technology for the

condensation polymerisation of unsaturated polyester. The performance of the spinning disc surface was compared to polymerisation in a conventional batch reactor and the main conclusion from this study was that reaction on the rotating surface proceeded more rapidly than in the batch when the melt became excessively viscous.

One other study which has been reported recently involving the use of spinning disc technology in chemical reaction concerns immobilised enzyme reactors [74]. In comparison to packed columns, the rotating disc surface coated with the same weight of immobilised glucose oxidase preparation was shown to increase the initial rate of substrate conversion by removing mass transfer constraints associated with the diffusion of substrate from the bulk of the solution to the immobilised active sites. Under conditions of higher rates of substrate conversion in the rotating disc bioreactor, the utilisation of the immobilised sites was considered more efficient.

The spinning disc technology would appear to be most suitable for highly exothermic chemical reaction involving gas absorption which cannot otherwise be performed in conventional reactors because of heat removal limitations. One such reaction is the sulphonation of dyestuff intermediates with the use of gaseous SO_3 which unfortunately has not been tested on the rotating disc to the present day. It is quite obvious from the apparent lack of investigations into spinning disc surfaces for chemical reaction applications that the technology in this area is under exploited. Future research into the applications of centrifugal fields should therefore aim to fill this void.

2.2. INDUSTRIAL POLYSTYRENE REACTORS AND PROCESSES

This section gives a critical review of the different commercial processes developed to this day for the production of polystyrene with emphasis on the reactor technology. Although a large part of this section will deal with styrene polymerisation, other systems, where relevant, will be considered for comparison. It is considered worthwhile to also include a separate section dealing with the issues of stability of polystyrene reactors and more particularly with the ways in which loss of temperature control can be avoided.

All polystyrene commercial processes follow a free-radical polymerisation mechanism generally aided by the use of initiators. These different processes address the main polymerisation problem of high polymer melt viscosity that results in large difficulties in providing an adequate control of temperature and in handling the melt.

The choice of a reactor for polymerisation is strongly dependent on the type of process for which it is being used as well as the reaction kinetics, mass and energy transport capabilities and the desired polymer properties. The general types of reactors suitable for the various methods of polymerisation have been conveniently categorised by Menikheim [75]. With regard to the production of polystyrene, the processes commonly used in industry are mass or bulk polymerisation, solution polymerisation and suspension polymerisation [75]. The advantages and disadvantages attributable to each technique are discussed by Meister and Malanga [76]. It is worthwhile noting that the definition of bulk polymerisation traditionally implied the use of pure monomer while in solution polymerisation, solvents such as toluene or ethylbenzene were added as chain-transfer agents and processing aids. More recently, industrial

practice has seen the terminology "modified-bulk" adopted to describe processes involving addition of substantial amounts of solvent [77].

Styrene bulk polymerisation processes can be operated in batch or continuous mode while suspension polymerisation is only carried out batchwise. The importance of bulk batch processing for large volume productions has declined over the years mainly because of the difficulty involved in controlling the polymerisation and handling the extremely high viscosity, which will be discussed in more detail below. The bulk or modified-bulk reaction in continuous mode has become the preferred method of production for general purpose polystyrene as pointed out in the review by Ku [78,79].

Since this present work focuses on the bulk/modified-bulk method of polymerisation, batch suspension reactors will only be considered in limited detail here. As will become apparent in the following sections, different reactor types are frequently used in varying series combinations in both batch and continuous styrene polymerisation processes with each type designed mainly to operate within a selected range of conversion or viscosity.

2.2.1. Batch Processes

Batch reactors are mostly employed in mass, solution (modified-bulk process) and suspension polymerisation of styrene.

2.2.1.1. Batch-mass reactors

On a commercial level, two types of batch-mass reactors are usually used. These can be classified as low conversion kettles with mechanical agitation and high conversion unagitated reactors with provision for largely expanded cooling surfaces. Low conversion reactors where the polymer concentration is less than 20% are generally provided with large turbine agitators and jacket cooling [80]. Anchor or helical agitator designs as well as proprietary designs can be substituted for the relatively simple turbine impellers to cope with higher viscosities in the conversion range of 20-80% [80].

On the other hand, the design of high conversion batch reactors in which the viscosity can be as high as 10^5 cP, is radically different. It is extremely impractical and uneconomical to agitate such viscous mixture. Instead high conversion batch-mass reactors are unagitated, a typical example being the polymerisation press which has been described in great detail by Bishop [81]. It consists of a modified plate and frame filter press where styrene is polymerised in frames alternating between cooling platens through which water circulates and provides sufficiently good heat removal.

Other versions of the high conversion reactors include the early "Dow Tube-Tank Process" developed by the Dow Chemical Company [82]. Styrene monomer was placed in a horizontal tank equipped with internal tubes through which heat transfer fluid was circulated. Temperature was raised as polymerisation progressed to a maximum conversion of 95%. Devolatilisation was then carried out in a holding tank under vacuum.

A typical batch-mass PS process therefore involves transfer of prepolymer from the low conversion reactor to the filter press as shown in the process flow diagram presented by Bishop [81] (Figure 2.3).

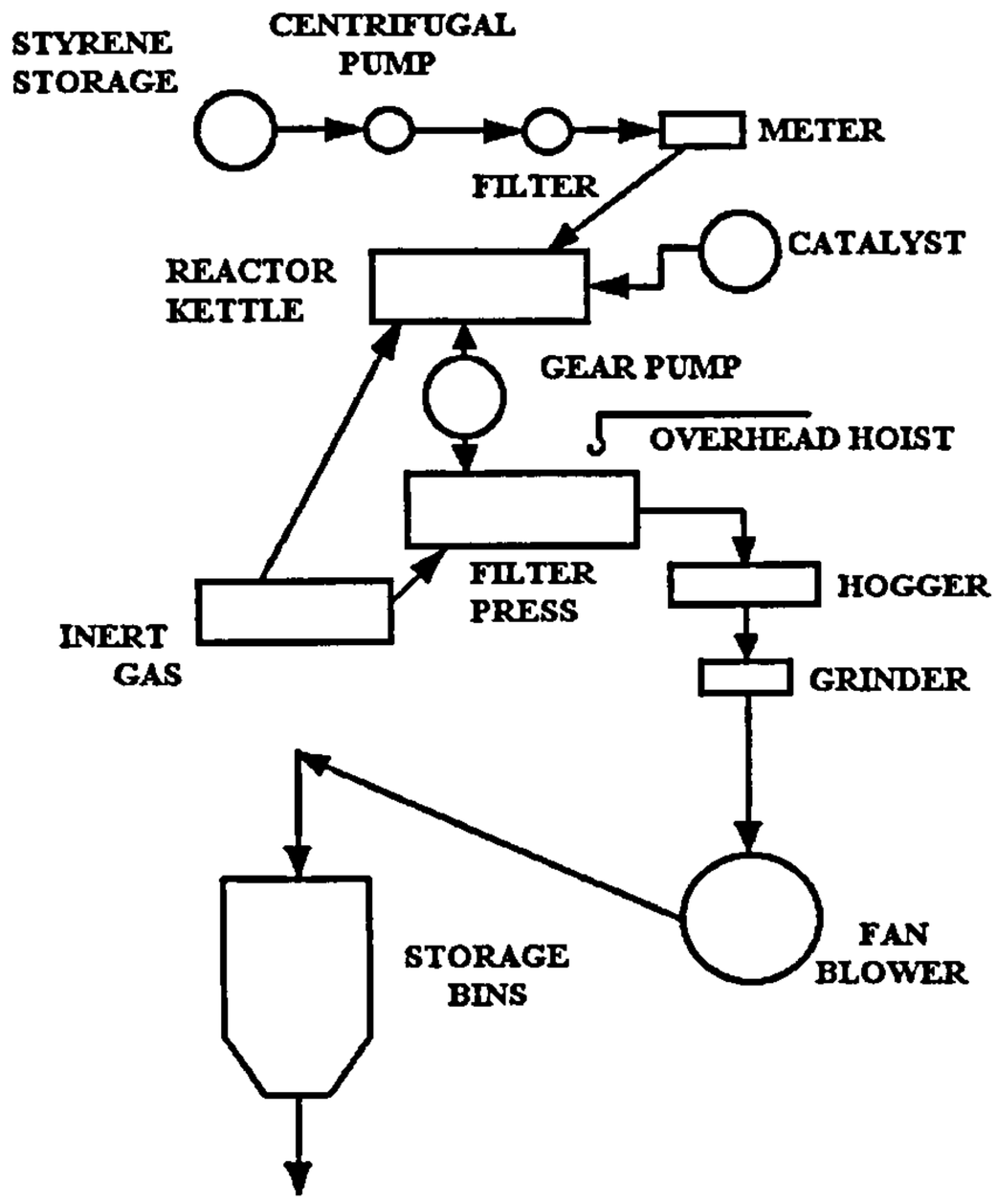

Figure 2.3. Batch-mass polymerisation of styrene [81]

Styrene monomer is charged to the low conversion prepolymerisation reactor with catalyst and other additives. When the desired conversion is attained with a gradual increase in the operating temperature, the prepolymer is discharged to the filter press. It is reported that typical cycle times in the low conversion vessel are between 6 and 14 hours while the residence time in the press can vary between 16 to 24 hours [80].

The chamber-type reactor, developed by T.Shriver and Co., is another unit which has been used by some of the major polystyrene producers in America in the batchwise production of polystyrene [83]. No mechanical agitation is employed in these reactors which contain numerous cavities where polymerisation occurs. The principles underlying the operation of the chamber-type reactors are similar to plate-and-frame filter presses. Each unit consists of several combinations of plates and frames made of cast aluminium and each frame is provided with two cavities. Styrene or partially polymerised styrene is placed in the cavities. Steam or hot water flows through the platens, heating up the styrene until the onset of polymerisation. Albright has reported that patents indicate that polymerisation is driven to completion when a 28% prepolymerised mixture is heated steadily from 90°C to 200°C over a period of 5 hours, and then held at 200°C for another hour [83]. The reactor is then cooled with water before opening it up to remove the polystyrene blocks from the cavities. Sticking of the blocks to the frames and the platens sometimes poses a problem.

Polymerisation rates are kept relatively low to minimise temperature gradients in the reaction mixture and achieve adequate temperature control which is a critical factor in the operation of the Shriver reactor. The temperature of the platens, the amount and type of initiator used, if any, and the degree of prepolymerisation of the feed material are operating variables that can be manipulated to control the reaction

and obtain high quality polymer product. The production capacity of a 56-frame reactor ranges from 7.5 to 15 million lb/year of polystyrene depending on the conversion of the prepolymer [83]. In addition, the chamber-type reactor requires a modest capital investment which makes it quite attractive for use in the bulk polymerisation of styrene.

Platzer [84] has described an unagitated batch reactor having numerous bundles of cooling coils for increased heat transfer used in the production of large amounts of crystal polystyrene. The primary advantage of this type of reactor is that any portion of the reaction mixture is within 2 inches or less of a heat transfer surface. Consequently, improved temperature control can be achieved in this reactor compared to plate-and-frame reactors. Albright [83] has suggested that the use of mechanical agitators in such reactors can provide even more rigorous temperature control, resulting in polystyrenes with better-controlled molecular-weight distributions than in continuous processes. However, Beckmann [85] argued that the presence of a bundle of coils in the middle of the reactor would most certainly interfere with the mixing of high viscosity mixtures and hence he recommended using internal cooling coils combined with agitation only in low viscosity mixtures in special cases such as the polymerisation of vinyl chloride where the exotherm is exceedingly high.

The major problems encountered in the batch-mass reactor designs discussed above are heat removal, temperature control and materials handling due to high viscosities. Such reactors are designed to provide a maximum level of heat removal capacity at the highest rate of polymerisation. It is therefore important to impose a limit on the rate of polymerisation which in turn affects the maximum conversion that can be obtained in the low conversion batch reactor. Two phenomena related to temperature variations are often encountered in a typical reactor: **hot spots** which involve temperature variation with position in the reactor and **temperature peaking** where temperature varies with time. Both occurrences lead to a broadening of the molecular weight distribution (MWD) which translates in poor polymer quality. If heat removal becomes excessively poor due to loss of cooling capability, thermal runaways are likely to occur.

The high conversion reactors face an additional problem of high viscosities which makes heat removal and temperature control more difficult. Because of the extremely high viscosities at high conversions, these reactors are unagitated. In order to promote heat dissipation, they are designed to provide extended heat transfer surfaces such as the cooled platens of the plate and frame unit. In some cases tube bundles, cans, etc. have also been used [80]. Heat is removed by conduction through the polymer to the extended heat transfer surfaces. The high heat of polymerisation of styrene (73 kJ/mole of monomer) [86] combined with the low thermal conductivity of polystyrene (between 0.154 W/m K (at 300 K)and 0.160 W/m K (400 K)) [87] leads to non-uniform temperatures in high conversion commercial reactors. It is important to keep the distance between heat transfer surfaces small to minimise this problem and hence to prevent runaway reactions and excessive hot spots in the inner part of the melt. In his account of styrene polymerisation in the press, Bishop [81] has reported that temperature peaking is almost impossible to avoid. The effect of such temperature gradients is an increase in the breadth of the MWD.

2.2.2. Batch-suspension reactors

Suspension polymerisation is probably the most widely practised and most economical method of producing expandable polystyrene and it is commercially carried out in batch mode. It differs from the mass or solution polymerisation in that both the monomer and the polymer are insoluble in the diluent, which is generally water. The initiator is first dissolved in the monomer and the solution is then dispersed in the continuous solution containing a suspending agent, usually an inorganic salt such as calcium, barium or magnesium phosphate, and a small amount of an inorganic surfactant such as dodecyl benzene sulfonate.

In a typical polystyrene plant, several suspension reactors are operated batchwise. The working volumes of some of the largest commercial reactors installed over the last few years are in the range 60-120 m^3 [78,88]. Stainless steel clad reactors have become increasingly popular on a commercial level. The polished surfaces are not only effective in minimising fouling and incredibly easy to clean but they also provide significantly higher heat-transfer coefficients (284-625 W/m^2K) than glass-lined reactors (227-340 W/m^2K) [88]. It has been highlighted that the optimum heat transfer rate can be achieved by using a thin stainless steel layer over a carbon steel reactor wall [89]. Mechanical agitators, frequently of the turbine type, and baffles provide the desired agitation. Cooling jackets around the reactor walls and water-cooled internal baffles are usually adequate for the removal of the heat of polymerisation of styrene. In contrast, provision for substantially more cooling is made in PVC suspension reactors by means of reflux condensers and jackets on the reactor head in addition to the jacketed reactor walls and baffles [88,89].

In comparison to mass processes, suspension processes offer the unrivalled advantage of rapid heat removal achieved through the suspending medium (water) to provide excellent temperature control throughout the reactor contents. The effects of hot spots and temperature peaking associated with mass processes as discussed earlier are drastically reduced or even completely eliminated giving a product with improved physical properties. Higher polymerisation rates are therefore permissible enabling cycle times to be lower. In addition, the final devolatilisation step characteristic of mass processes can be avoided altogether as the polymerisation can be driven very close to completion. Furthermore, owing to its relatively simple design, the suspension reactor is considerably less expensive to build than the specially designed reactors employed in continuous mass processes as highlighted in the section below.

Nevertheless, suspension polymerisation also presents a number of disadvantages. The water must be pure and the suspending agents are costly. To reduce the environmental impact, the effluent must be treated before discharge to remove the suspending agents and a small amount of polymer emulsion which adds to the operating costs. With regard to the properties of the finished product, the clarity is also affected by the use of the suspending agents.

2.2.3. Continuous Processes

Since as far back as the 1930's, continuous reactors have been a popular choice for the industrial production of polystyrene using mass or solution polymerisation methods. There has been significant improvement in continuous reactor designs over the years. Most of the development has focused on obtaining

better temperature control and hence better polystyrene product quality to satisfy growing demands for high quality of this commodity in today's market place.

The extensive research and development which has gone into continuous reactor technology has inevitably resulted in a wide variety of designs currently used by the major polystyrene producers world-wide. However, all continuous reactors can be conveniently classified in two general categories: the continuous stirred tank reactor (CSTR) also often referred to as a stirred autoclave and the linear flow reactor (LFR) or the tower reactor.

A CSTR is a backmixed reactor and, in the ideal case, its effluent temperature and composition are the same as the reactor contents. In actual practice, varying degrees of segregation, short-circuiting and stagnation exist in the reactor contents. CSTRs are generally more suitable for processing low viscosity mixtures in the first stages of polymerisation where conventional mixing equipment is normally adequate for the reaction mixtures. Heat transfer to the internal coils or tubes is generally good. At high viscosities, the degree of mixing is considerably reduced and some temperature and composition variations will occur unless low speed heavy duty agitators requiring high power inputs are used. Since a CSTR operates at or close to uniform conditions of temperature and composition, its kinetic and product parameters are easily predicted and controlled.

The intention with the design of an LFR is to provide for a net, progressive change in composition and perhaps temperature as the reactants move through the reactor. LFRs cannot work at low viscosities since excessive backmixing is difficult to prevent. As viscosity increases, backmixing in an LFR can be more easily reduced since flow conditions become more laminar and stratification can be more closely approached. LFRs generally run under varying temperature, viscosities and other parameters and this makes the process and product control more complicated than with a CSTR.

Flow processes using bulk polymerisation techniques employ two or more reactors in series. The initial reactor which is designed as a CSTR is referred to as the prepolymeriser where as much as 50% of styrene can be converted, depending on the design of the vessel. The polymerisation reaction is driven almost to completion in the remaining reactors down the line which are usually tower reactors or LFRs.

Now that the general characteristics of CSTRs and LFRs have been established, the different commercial processes developed to this day for the continuous production of polystyrene will be discussed. It has to be mentioned that of all the literature consulted, Albright [83] gave the first extensive review of continuous processes for polystyrene which was later updated by Simon and Chappelear [80]. The purpose of the ensuing section of this thesis attempts to combine the work of the above mentioned authors as well as describe the most recent developments in continuous reactor technology for polystyrene.

2.2.3.1. I.G. Farben Process

One of the first continuous processes for mass polymerisation of styrene was developed by I.G. Farbenindustrie at Ludwigshafen, Germany, in the early 1930s (Figure 2.4).

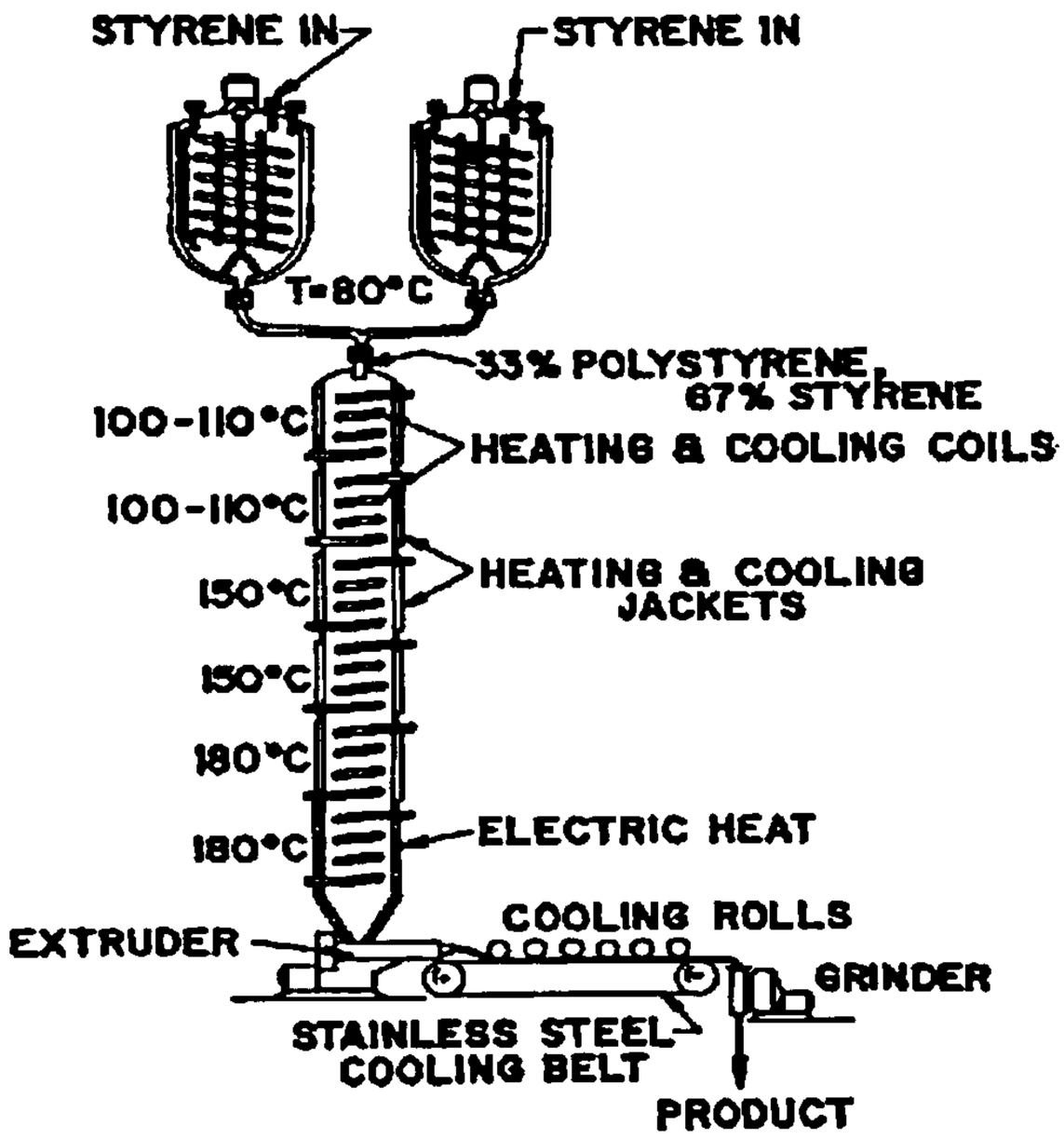

Figure 2.4. I.G. Farben continuous tower process [80]

Two stirred autoclaves or CSTRs were operated in parallel as prepolymerisers, each having a hold up capacity of 1400 kg. Aluminium was used as the base material of construction for the CSTRs which were provided with internal cooling coils and standard jackets for heat removal. Mixing was carried out by flat paddles or gate-type agitators rotating at low speeds of 50-60 rpm [83]. An inert gas such as nitrogen was used to fulfil two main purposes: (1) to act as an inert blanket over the reaction mixture preventing contact with oxygen which causes deterioration in the colour and stability of the polymer [90] and (2) to flush styrene from the region of entry of the agitator thus preventing polymer accumulation.

Approximately 30% of the styrene was converted in the prepolymerisers operating at about 80°C with an average residence time of 60-70 hours [83]. Each polymerisation line had two such reactors in parallel to compensate for the slow rates of polymerisation. As a direct consequence of the low operating temperature, the molecular weight of the polymer from the prepolymerisers was reported to be 370,000 by ultracentrifuge methods [91] or as high as 100,000 by the Staudinger method [80].

As shown in Figure 2.4 above, the second stage of the process was carried out in a vertical tower also called a linear flow reactor (LFR) which gave a final product with typical polymer concentration of 95%. No mechanical agitation was provided in this relatively small unit having reported dimensions of 0.8m in diameter and 6m in height [91,92]. The tower, made of stainless-clad steel, was divided into six sections of equal length. Each section was heated by an external electrical source to temperatures within a desired operating range: 100-110°C at the top, 150°C in the mid section and a finishing stage of 180°C at the bottom [80,83,84]. A cooling jacket around the walls together with internal helical cooling coils helped to control the temperature in each section. The absence of mechanical agitation meant that rather large temperature variations existed in each section. The early equipment had no provision for removing volatile components from the polymer so that the level of

monomer and other low molecular weight compounds in the polystyrene exiting the tower typically ran in the range of 3-5%. In the final processing step, the melt was fed to an extruder and the extruded sheet was then cooled before being granulated. Simon & Chappelear [80] reported the use of 0.02% glacial acetic acid in the extrusion step possibly to reduce the volatile components in the final polystyrene product down to 0.5%.

The I.G. Farben process as described above produced polymer containing 95% polystyrene of average molecular weight of about 170,000 -180,000 (as determined by the osmotic method) at the rate of 44 kg/hr giving an annual production output of about 800,000 lb/year [83].

Two major variations were implemented in the subsequent years following the commercialisation of the original I.G Farben process. The first involved condensing and recycling styrene vapour removed from the top of the tower [84]. This procedure helped to remove some of the heat of polymerisation. In the second variation, the polymeric syrup from the prepolymerisation step was isolated directly by feeding it into a vacuum two-roll drum dryer instead of a continuous tower [83,84,91]. In this set-up, the unreacted styrene was evaporated, recovered and then recycled while the devolatilised polymer was scraped from the drums and ground into granules. Polystyrene of very high uniform molecular weight as produced in the prepolymerisers at low temperatures could thus be obtained. However, as the economics of this process were not particularly favourable due to low production capacity, it was soon abandoned.

2.2.3.2. BASF Process

The reactor system employed by BASF is based on the early German plant at Ludwigshafen with a CSTR as prepolymeriser and a tower reactor for the final stages of polymerisation as shown in Figure 2.5 below.

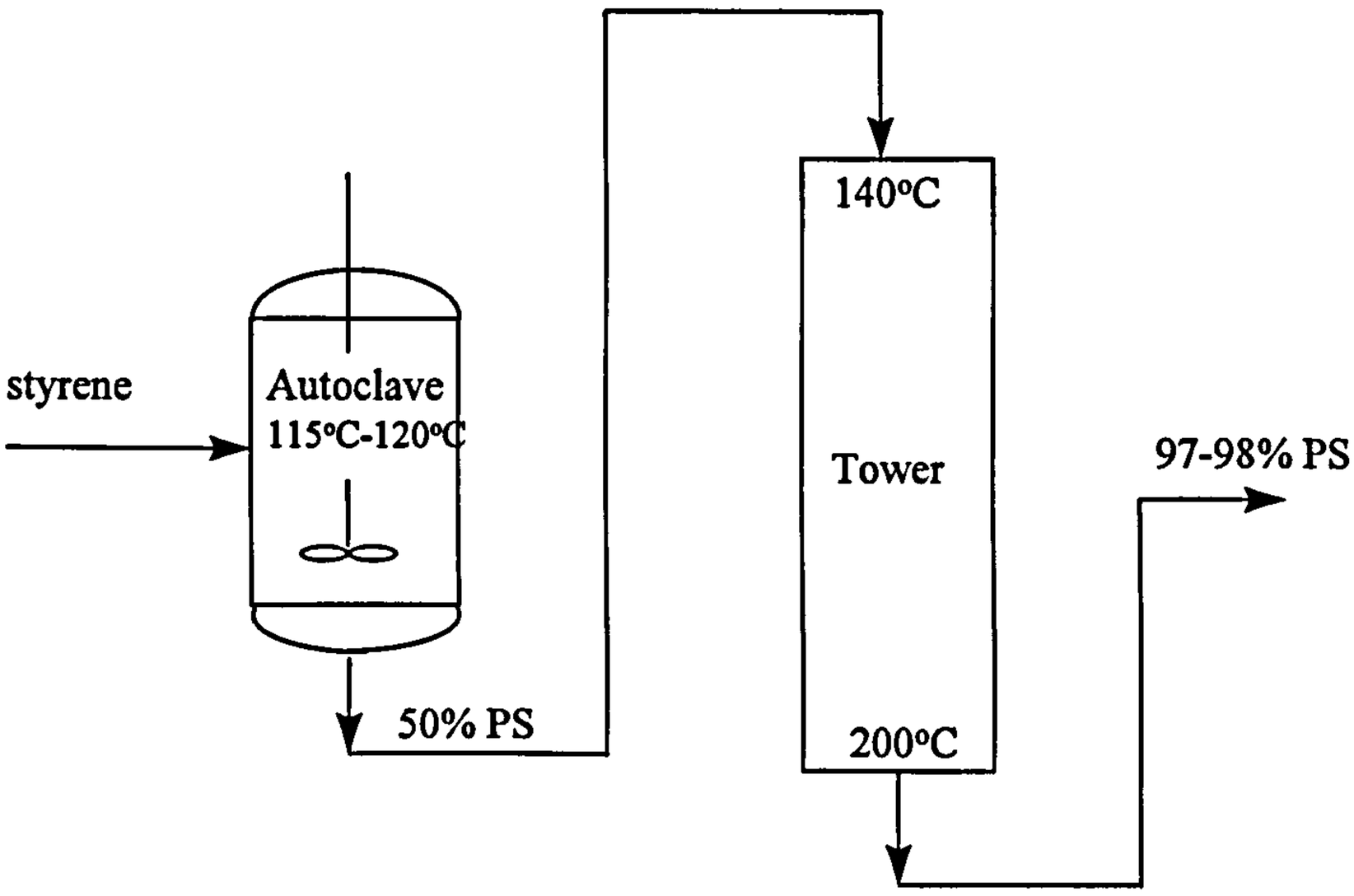

Figure 2.5. BASF continuous process [83]

The major modification implemented was a higher operating temperature of 100-130°C in the CSTR. Such an increase in temperature could be accommodated as a result of an improved reactor design providing more efficient heat removal. With a much lower residence time of about 4-5 hours, a conversion of 45-60% by weight could be obtained in the prepolymer [83].

The prepolymer is then fed to a patented tower reactor which is reportedly larger than the earlier version employed at Ludwigshafen. A temperature gradient is maintained down the tower with the top zone at 140°C and the bottom section at 200°C. The product stream out of the tower has a polystyrene content of 97-98% after the reaction mixture has been in the tower for 3-4 hours. During its passage through the tower, the stream loses some of the unreacted styrene by devolatilisation which is removed from the top of the tower, condensed and recycled to the prepolymeriser. The removal of styrene in this way helps to cool the reaction and achieve improved temperature control.

Heat removal in the BASF tower reactor is critical especially at higher temperatures and increased rates of polymerisation. It is believed that heat transfer is effected primarily by a large number of coils and tubes, the latter being reportedly arranged in horizontal banks inside the tower [83]. With an improved reactor design system for its polystyrene process, BASF could achieve higher polystyrene outputs on a given volume basis which, back in 1974, was approximated at 7-8 lb/hr of polystyrene per cubic foot of reactor volume which is a dramatic increase compared to the production capacity of 0.7 lb/(hr. ft^3) of the early I.G. Farben process [83].

2.2.3.3. Dow Chemical Process

Several polystyrene process technologies have been studied and developed by The Dow Chemical Company as early as 1944, whose progress has been documented by Amos [82]. The efforts of the researchers at Dow culminated in the commercial implementation of a continuous process for high impact polystyrene (HIPS) in 1952 in which three vertical towers or linear flow reactors are usually operated in series (Figure 2.6). This process is also applicable to the production of general purpose polystyrene.

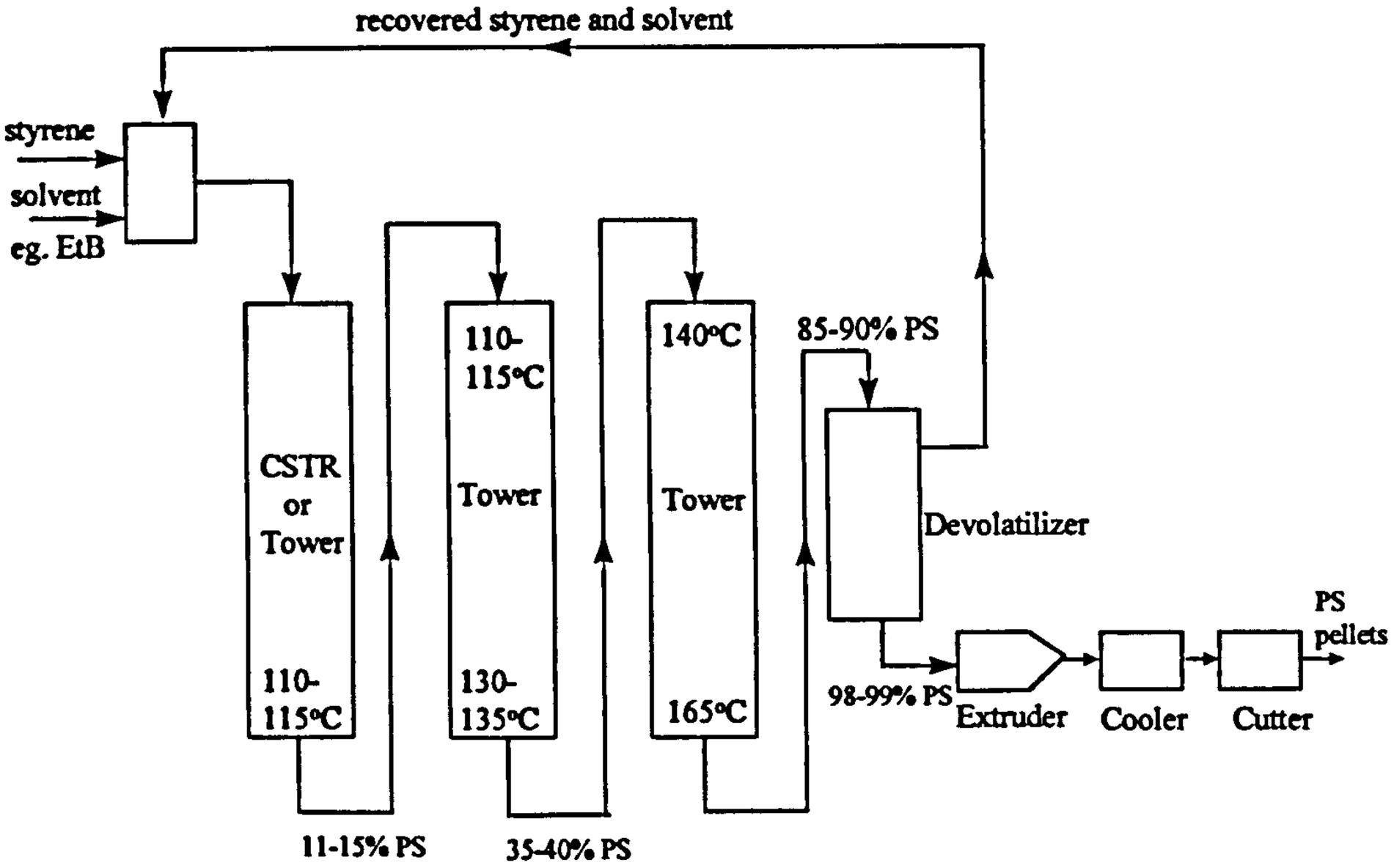

Figure 2.6. Dow Chemical Process [84]

There are two types of tower design employed in the process. One of the reactors called a "stratifier-polymeriser" [82,93] has rods mounted on a vertical shaft running along the centre of the tower. The rods revolve slowly to provide gentle agitation in the reaction mixture and they also helped in eliminating channelling of the polymerising mixture thereby promoting plug flow behaviour. The installation of several banks of horizontal tubes between adjacent agitator rods (Figure 2.7) gives efficient temperature control through the heat transfer fluid circulating in the tubes.

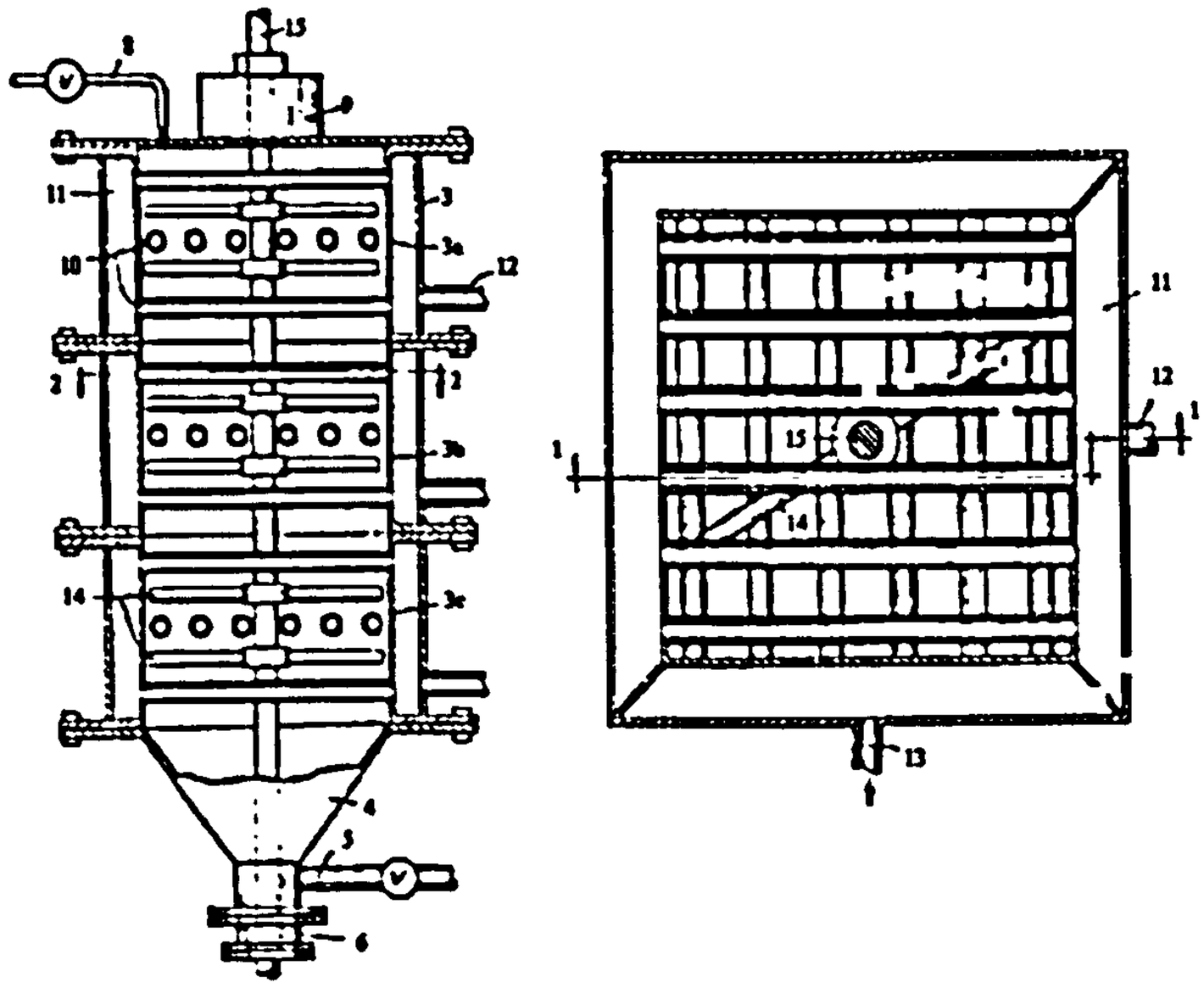

Figure 2.7. Stratifying polymerisation reactor [82,93]

The second reactor configuration has been described as an 'egg-beater' type of reactor [80,82]. It is characterised by specially designed agitators in the form of two vertical impeller shafts each being located at the axis of each of the two cylindrical cross-sections of the column. Albright has compared the cross-sectional area to a 'figure eight' shape [83]. The important features of this reactor are illustrated in Figure 2.8 below.

Rapid heat removal is possible through the jacketed walls of the reactor and the hollow shaft and attached cross arms which have provision for coolant flow. When the two impeller shafts rotate in opposite directions, the overlapping action results in effective agitation of the viscous polymerising mass in which channelling and rotation effects are minimal.

The process as illustrated in Figure 2.6 above proceeds by adding ethylbenzene, generally of concentration 5-25% [84], as solvent to the styrene monomer in the feed to reduce viscosity of the mixture during polymerisation and hence ease its flow down the tower while promoting heat transfer. It also acts as a chain transfer agent and when used in the right proportion it controls the molecular weight of the polymer product to a within a desired range. In the production of impact polystyrene, a mechanically agitated glass-lined CSTR has been used as the first reactor in the series [83]. However various other literature sources [80,84,94] indicate the use of an apparently simple, agitated tower reactor operating at temperatures between 85°C and 130°C for the general purpose polystyrene process.

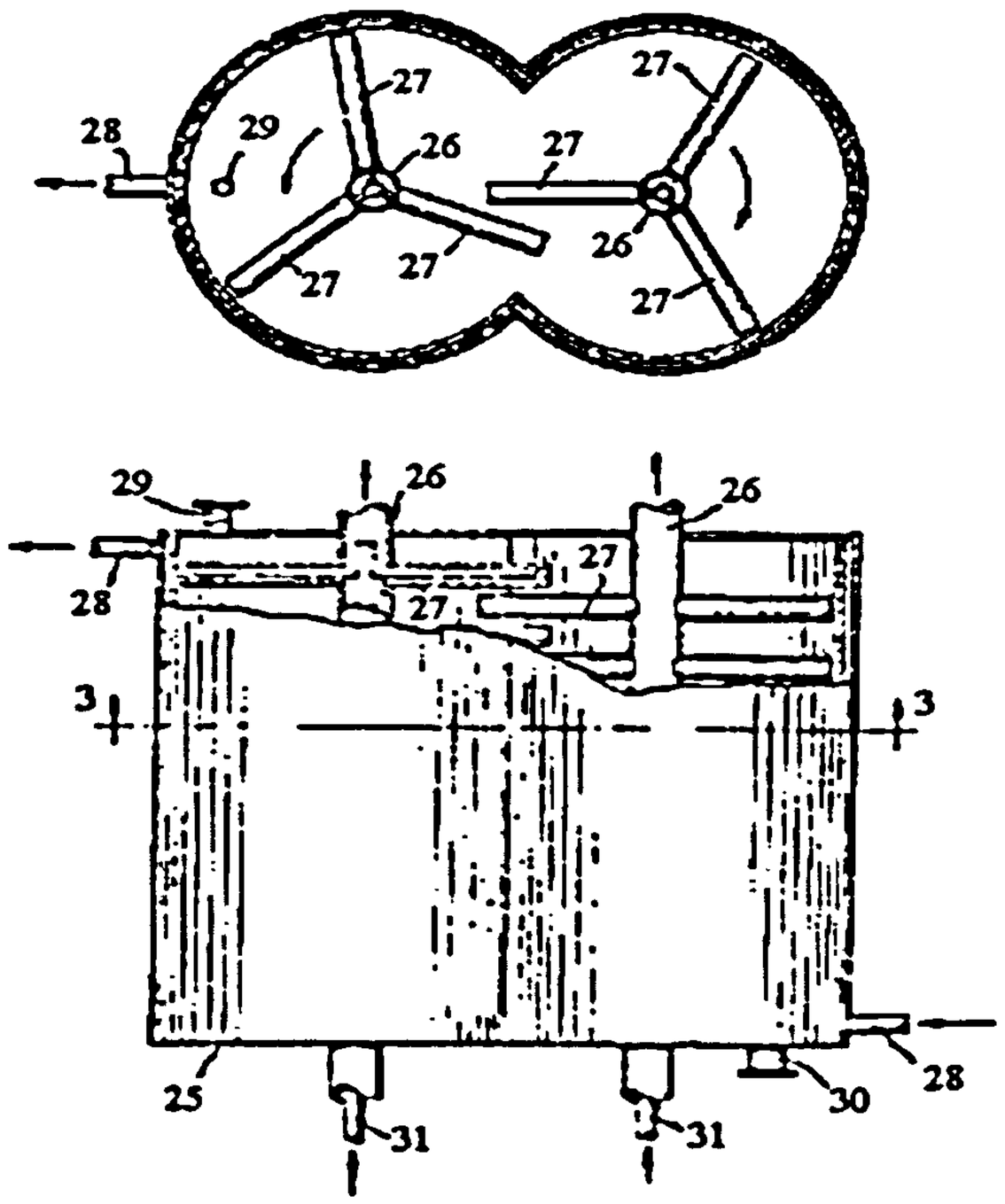

Figure 2.8. 'Egg-beater' agitated tower reactor [82]

The product exiting the bottom of the first tower has a polystyrene concentration of 25-50 %. This product is fed to the top of the second reactor which is

normally of the "egg-beater" design described earlier. According to Albright [83], a temperature rise from 112°C at the top to 133°C at the bottom with a residence time of 7 hours causes polymer conversion to increase from 11 to 37% in the case of high impact polystyrene. For crystal PS, however, higher temperatures of about 150°C at the exit of the second reactor are permissible without any major control problem giving a product containing as much as 70% of polymer [80]. The third reactor down the line is the "stratifier polymeriser" where most of the remaining monomer is converted at temperatures ranging from 165°C to 185°C for the case of general purpose PS. The exiting melt containing about 80% of polymer is heated to 220-240°C before being stripped of the solvent and the unreacted monomer while under vacuum in the devolatilisation step. The purified polystyrene is then extruded, cooled and cut into pellets.

2.2.3.4. Union Carbide Process

The continuous mass process for polystyrene patented by Union Carbide and Carbon Corporation [95] utilises a CSTR in the first stage of the polymerisation followed by a tower reactor as depicted in Figure 2.9 below.

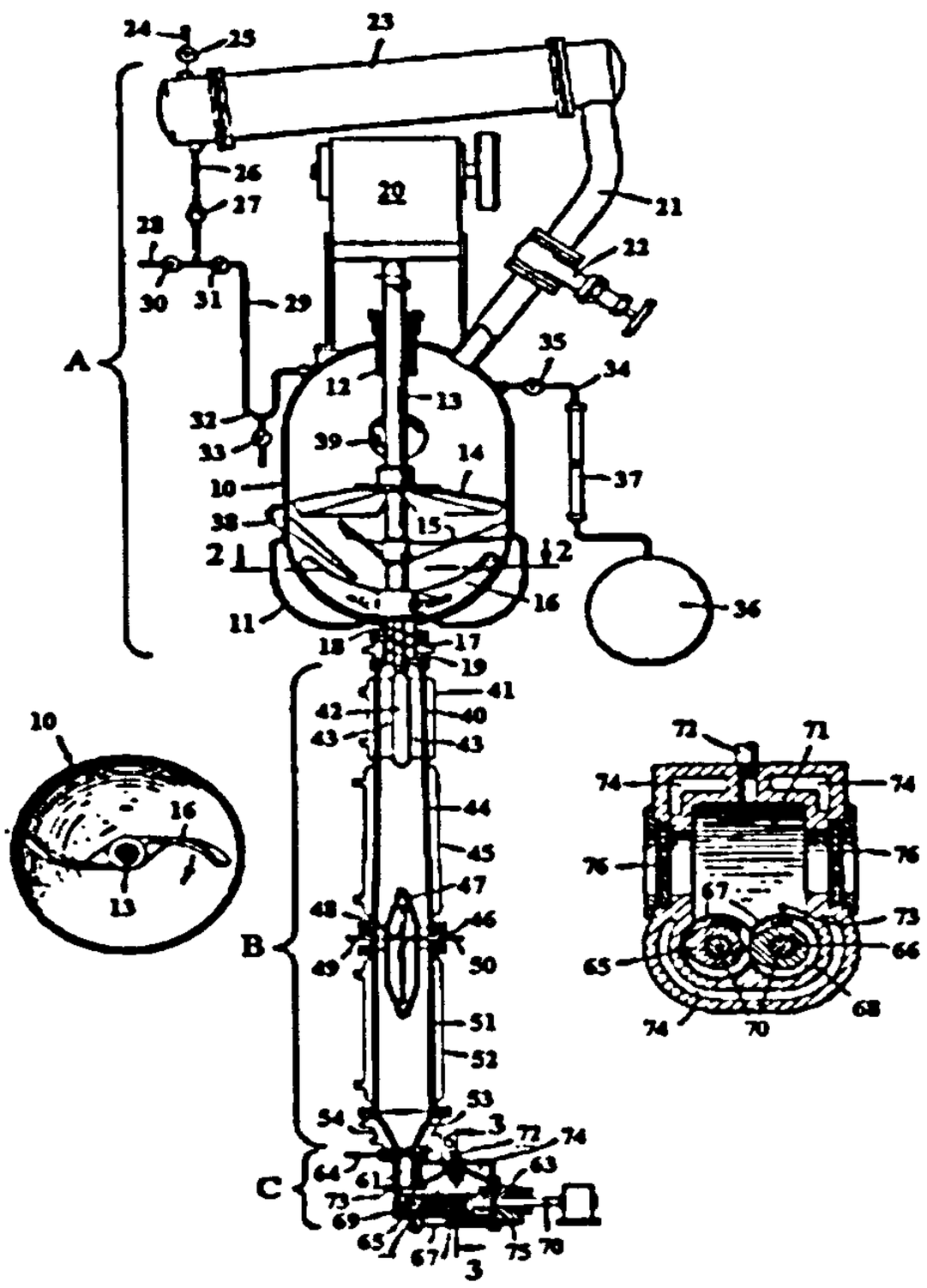

Figure 2.9. Union Carbide patented continuous process [95]

The single CSTR operates under vacuum conditions at about 125°C and the product from this reactor is 70-80% converted after a residence time of 32 hours. The agitator used in the reactor has been described as being "complex and ruggedly built" [80] and it is so designed to achieve good mixing of the highly viscous polymer mass generated with the progress of polymerisation. Heat removal by reflux cooling of the

monomer plays a vital part in temperature control aided by a conventional jacket around the lower walls of the stirred tank.

The polymerisation is driven almost to completion in the tower reactor design details of which have not been publicised. However with the high viscosity material flowing down the tower, it would be unlikely that agitation would be provided. Before its entry in the tower, the polymer mixture is heated to 175°C by means of a heat exchange unit. A residence time of about 8 hours ensures that the polystyrene content in the final product is raised from 85 to 95-97% at a discharge temperature of 215°C. The polymer produced by this process is characterised by a flow-time of 300-500 seconds, average molecular weights of 70000-110000 and a softening point of 85-90°C [95].

It has been suggested that the space-time yield of the single CSTR can be greatly improved by replacing the first reaction zone with three CSTRs in series. A schematic of the process is given in Figure 2.10.

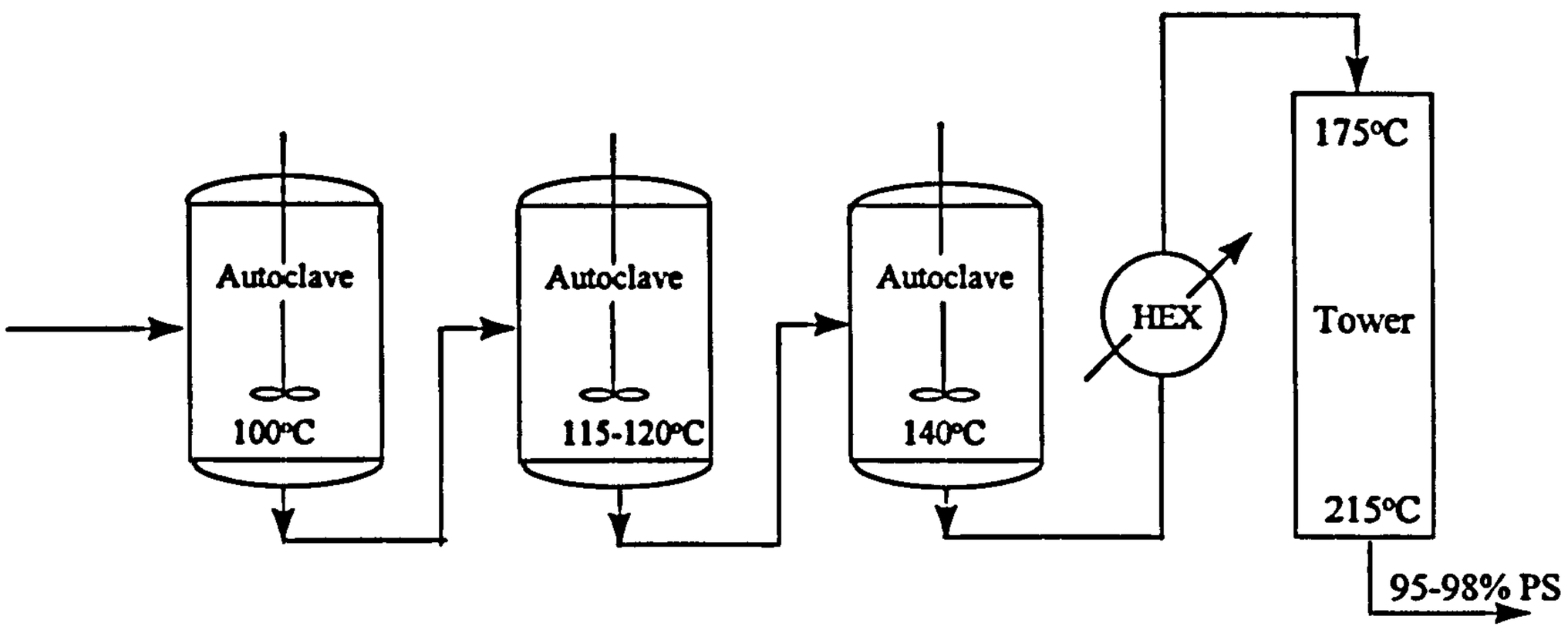

Figure 2.10. Union Carbide process with 3 CSTRs in series [83]

An increasing temperature sequence is applied down the line of reactors as shown in Figure 2.10 with exit PS concentrations rising from 35% to 85% from the third CSTR. Each of the stirred tanks is jacketed and as before the agitator design is rather complex with each built differently to cope with the increasingly viscous material down the line [83]. This reactor system offers greater flexibility than that discussed previously in that the size of each of the reactors can be optimised together with the operating temperature to obtain the maximum polymer output. Ideally, the temperature in the third reactor where polymer concentration is at the highest level is largely elevated to reduce the viscosity. However this also results in faster rates of polymerisation which in turn translates into increased rates of heat release. It then becomes important to provide smaller reactors which have higher surface-to-volume ratio to speed up heat transfer. The Union Carbide Process clearly illustrates the application of this principle whereby higher temperature zones prevail in the CSTRs downstream. Based on the rates of polymerisation estimated to be around 2%, 4% and 7.5% per hour in the first, second and third reactors respectively, the reactor volumes are expected to be in the ratio of about 6.7:2.9:1 with the amounts of polystyrene produced corresponding to 1.1, 2.2 and 4.2 lb/hr per cubic foot of reaction mixture [80,83].

2.2.3.5. Mitsui Toatsu Process

Mitsui Toatsu Chemicals, Inc. patented a polystyrene process employing three to five CSTRs operating in series [96]. The process which has been reported in the literature is illustrated in the schematic drawing below (Figure 2.11).

The first reactor is significantly different in design compared to the others and each has specific features for agitation which make it appropriate for the viscosity range being handled. For example, the first CSTR is fitted with a vertical agitator shaft having two turbine type impellers, one positioned close to the bottom and the other half-way up the shaft. The shaft rotates at moderate to high speeds to generate large recirculated volumes of "opposing axial flows" between the two turbines in the polymerising mixture thus ensuring good mixing action before discharge. This reactor has the ability to handle a maximum viscosity of 40 poise [96]. A continuous feed of cold styrene entering from the bottom of the reactor is the primary method of heat removal which is supplemented by the cooling jacket around the walls of the reactor.

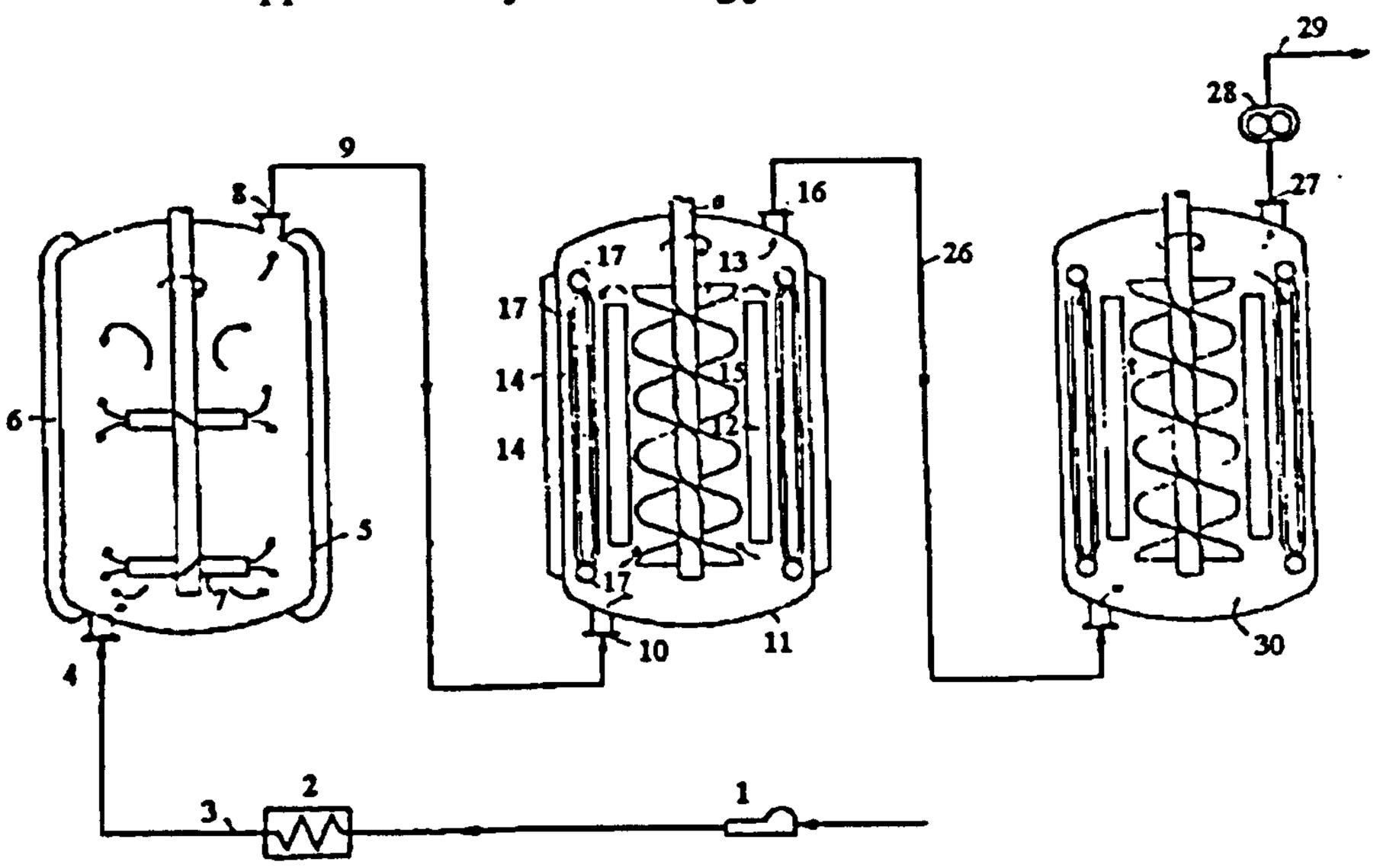

Figure 2.11. Mitsui Toatsu continuous process [96]

The operation of the remaining reactors in the sequence is based on similar principles. All of the vessels are fed through a bottom inlet and while in operation, they all hold a volume of material equal to their maximum capacity. A pumping screw mounted along the central shaft conveys the mixture upwards in the space between the screw and a draft tube around it. Coolant flows through the draft tube providing additional heat transfer surfaces to conduct the heat of polymerisation away. Once the melt reaches the top part of the screw, it falls back down along the annulus between the draft tube and cooling jacket. The presence of a number of cooled vertical tubes arranged circumferentially in the annulus removes yet more heat from the mixture in its downward path. Such a reactor design is claimed to result in exceptionally good mixing performances as well as drastically reduced temperature gradients of less than 1°C between top and bottom portions of the reaction mixture [80].

2.2.3.6. High viscosity staged CSTR

A two-stage mechanically agitated reactor was developed about 2 decades ago and it was said to be particularly appropriate for handling viscosities in the region of 100,000 cp [97]. A detailed diagram of the unit showing the direction of fluid motion within each stage is displayed in Figure 2.12 below.

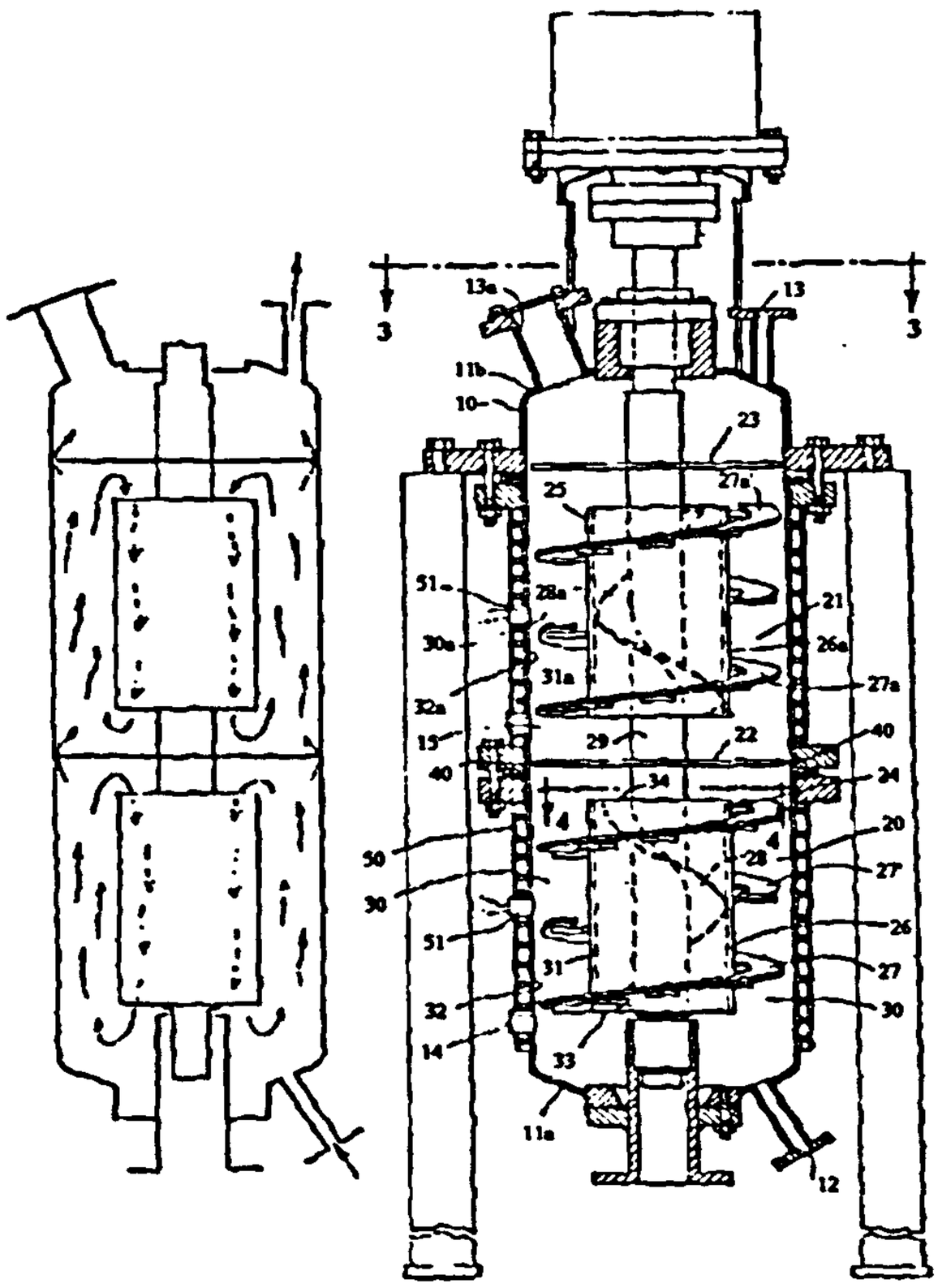

Figure 2.12. Staged CSTR reactor design [97]

There are two main design features in this reactor which are apparently responsible for promoting the blending of very viscous material. Each stage utilises a helical screw wrapped around the central agitator shaft. This screw is separated from an "interrupted ribbon agitator" by a draft tube which supports the ribbon agitator on its outer wall. An interstage rotating disc baffle is placed horizontally primarily to eliminate any potential backmixing between stages. When the two different types of agitators rotate with opposite pitches, they continuously recirculate and thoroughly mix the viscous fluid contained within each stage before passing it on to the following stage.

2.2.4. Tubular Reactors

Tubular reactors are usually designed to be non-agitated and are based on an idealised plug flow model where the fluid properties at any axial distance from the inlet is constant across the whole cross sectional area at that distance as illustrated below in Figure 2.13.

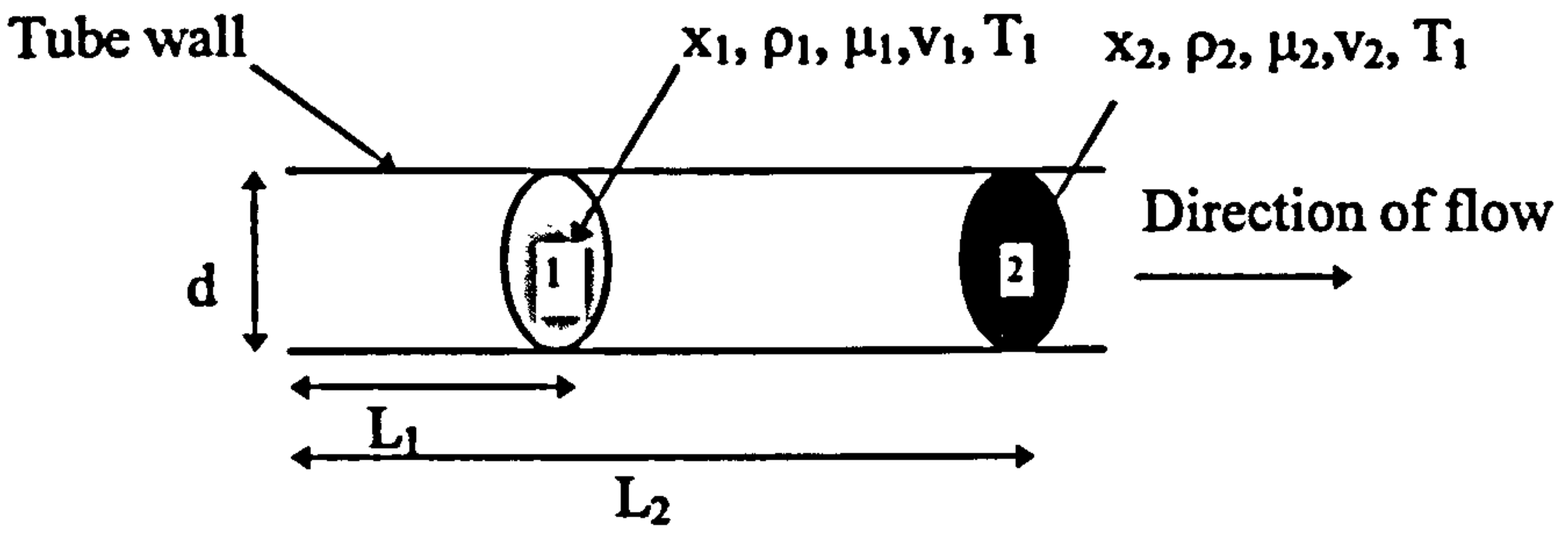

X, ρ, μ, v and T represent the fluid properties where
x : conversion
ρ: density
μ : viscosity
v: velocity
T: temperature
Subscripts 1, 2 refer to sections 1 and 2 respectively

Figure 2.13. Plug flow behaviour in a tubular reactor

Various forms of tubular reactors have been suggested and used industrially. They include the simple pipe surrounded by a conventional cooling jacket, the "shell-and-tube" reactor in which reactants pass through many tubes in parallel immersed in coolant and the batch or semi-batch vessel with very low agitation levels [98]. The simplicity and potentially low cost of tubular reactors have been their primary attractive features for investigators who have conducted styrene polymerisation experiments and performed numerical simulations in tubular reactors [99,100].

Under the ideal plug flow model, molecular diffusion only occurs within a section and not from one section to another down the tube. The definition of plug flow relies on essentially flat velocity, temperature and concentration profiles over the reactor cross section, all of which are normally obtained under turbulent flow conditions. However, in the case of polymerisation reactions, turbulent flow is impossible to achieve in viscous material at high concentrations of polymer. The numerical study on anionic polymerisation in tubular reactors by Lynn and Huff [101] reveals that laminar flow conditions in fact prevails in the reactor from the onset of polymerisation. However, due to the formation of a seriously "distorted velocity profile" with the progress of polymerisation, Lynn [102] argues that the use of the tubular reactor for styrene prepolymerisation is severely compromised. More recent experimental and mathematical modelling work into empty tubular reactors applied to polymerisation reactions [103] are indicative of the limitations inherent in such reactor designs.

Polymerisation in an empty tube suffers from heat removal limitations especially from the viscous polymerising mixture. Coolant flow around the walls of the tubular reactor would cool an already viscous polymer melt in contact with the wall making it even more viscous so that a gradually thickening layer of polymer would deposit. In order to promote heat transfer from the bulk of the melt in the middle of the tube, internal cooling coils have been used in the industrial production of polystyrene such as in the tower reactors of the I.G. Farben and the Union Carbide

Processes discussed above. Such designs are mostly applicable for the finishing polymerisation stages with small or no cooling requirements.

The recent development of static mixers has given a new dimension to polymer reactor technology in general and more specifically to tubular reactor systems. Static mixing involves the installation of "in-line motionless mixer inserts" inside the tubes, examples of such inserts being the Kenics static mixer, the Ross "low pressure drop" insert [104] and the newly commercialised Sulzer SMX static mixer elements [105,106]. Many experimental and modelling work into tubular reactors filled with static mixers of various designs have been undertaken [104,107]. It has thus been shown that the presence of static mixing elements all over the length of the pipe induces radial "turbulent" mixing of the high viscosity material thereby eliminating temperature, concentration and velocity gradients across the pipe cross section which Lynn and Huff [101] had regarded to be serious issues for polymerisation systems. As a result of the advancement in static mixing technology over the past decade, several researchers have investigated the possibility of implementing large scale tubular reactors for the production of polystyrene.

2.2.4.1. Static Mixer Reactors- SDS Process

The first completely tubular reactor system to be operated at a commercial level for the production of general purpose PS is the SDS process which started in August 1988 in Japan. A schematic of the process is given in Figure 2.14 [105]. All the major steps in this polymerisation process namely mixing, reaction, devolatilisation and final melt upgrading are performed in equipment using the static mixing principle.

During the first stage of the SDS polymerisation process, the monomer and solvent (if necessary) feed are circulated in SMR mixer-reactors in a loop connection. As highlighted by Streiff and Rogers [108], the merits of having reactors in loops reside primarily in preventing the polymerisation from spiralling out of control which is a potential risk caused by high initial monomer concentration. The loop arrangement thus allows the great heat load at the start of the polymerisation to be conducted away rapidly and efficiently. Another series of SMR plug flow reactors downstream converts more of the monomer in the mixture under an increasing temperature sequence. Specially designed for exothermic reactions, each SMR unit is made up of a large number of tubes which serve two main purposes. Firstly, they provide a passage for the flow of heat transfer fluid. Secondly they act as "flow-guiding elements" [108] in the place of the solid plates employed in conventional static mixing units so that the flow field of any portion of the polymerising mixture in the SMR mixer-reactor is constantly disrupted. Exceptionally good radial mixing thus results in uniformity in the fluid properties of the mixture. Thus the much desired plug flow pattern with a narrow residence time distribution is obtained.

Devolatilisation of the product from the SMRs is then carried out in SMXL mixer-heat exchangers followed by an upgrading step using SMX mixers to blend additives and colorant as required.

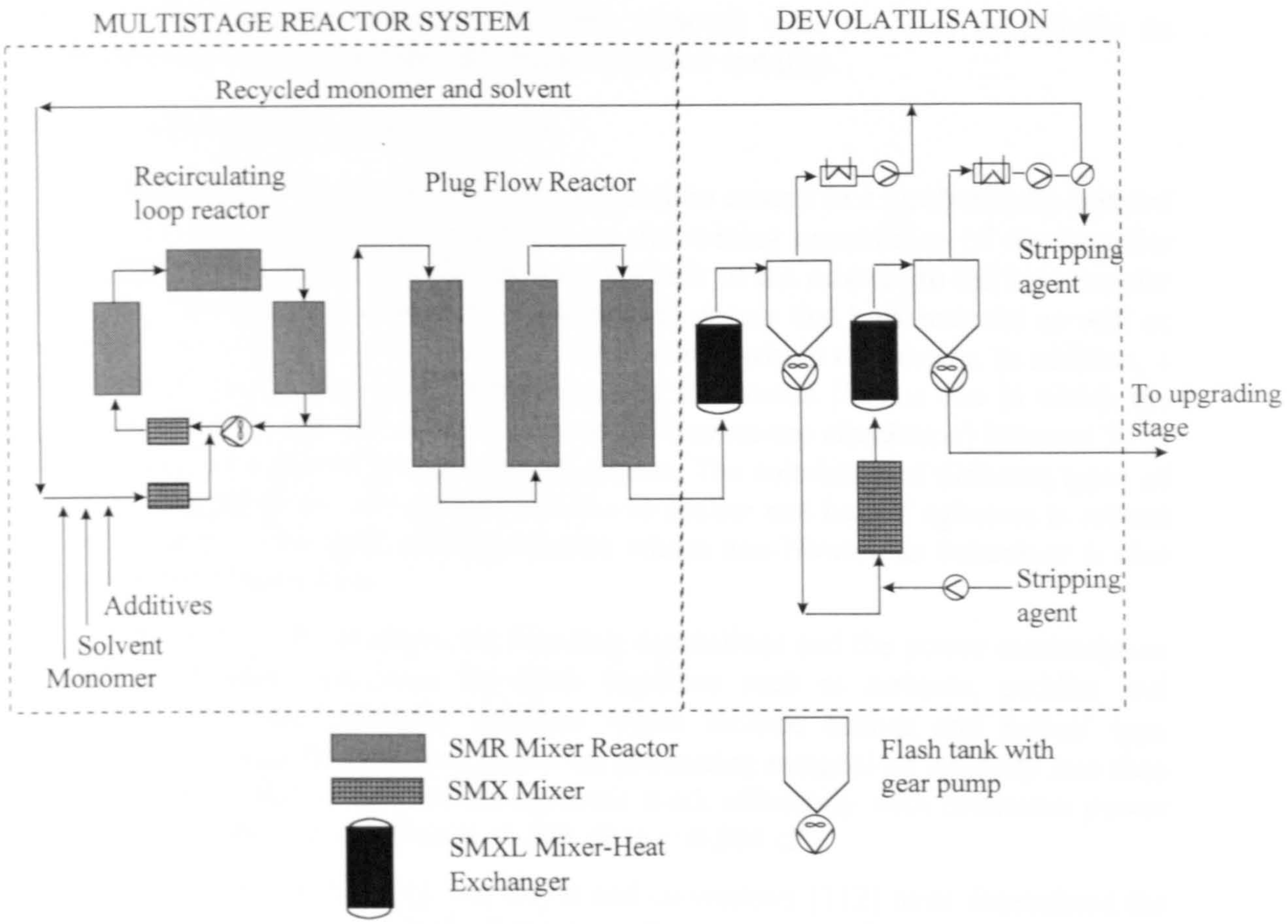

Figure 2.14. SDS Process [105]

One seemingly enormous advantage of the SMR reactor is its relatively high surface area-to-volume ratio even at reactor volumes in excess of 10^3 m^3 which means that heat transfer performance is little affected as reactor size increases [105]. On that basis alone, the SMR mixer-reactor compares most favourably with the empty tubular reactor or the stirred tank reactor. In addition, low capital investment, compactness and low maintenance costs have been identified as some of the other attractive benefits presented by the static mixer reactor.

2.2.5. Stability of polymer reactors

Reactor stability is of paramount importance in any polymerisation process and the many analytical and experimental studies carried out to this day attest to this. Polymer reactor stability is controlled by two primary factors namely agitation and heat removal. Loss of either will most definitely lead to the reaction spiralling out of control and either affect the polymer properties so seriously that the product becomes useless or in the worst case scenario can cause a thermal runaway and possible explosion. The critical nature of these two parameters is further intensified by the rapidly increasing viscosity of the reaction mixture. Henderson [109] has presented a theoretical stability analysis in a continuous stirred tank polymer reactor in relation to the effects of viscosity increases on mixing and heat transfer characteristics in the vessel and hence the steady state operating temperature. In the ensuing section the important issues of reactor stability will be reviewed with particular emphasis on the

effect of viscosity on agitation and heat removal with the aim to provide an understanding of the criteria for the limits of reactor stability.

2.2.5.1. Agitation in polymer reactors

Heat transfer rates and therefore temperature control in a mechanically agitated polymer reactor are strongly dependent on the mixing capabilities of the impeller which aids in the distribution of heat from the bulk of the mixture to the heat transfer surfaces by convection methods. It is essential to ensure that bulk material as well as material close to the walls are constantly recirculated within the reactor. In addition, a "well-mixed" reactor has been characterised by Beckmann [85] as one in which the agitator gives an "overturn" time (time for a top-bottom-top circulation) between 30 to 100 seconds for a typical polymerisation system. The suitability of different types of impellers ranging from turbines and paddles to anchor and helical agitators is related to the viscosity of the polymerising mixture whose non-Newtonian behaviour is also an important consideration.

Oldshue [110] compares the blending capabilities and the power consumption at widely different viscosities for open impellers such as turbines, paddles and propellers and close clearance agitators which include anchor and helical type agitators. Open impellers are best suited for processing material of viscosity less than 15,000 cP while anchor and helical agitators work efficiently with minimum power requirement at viscosities between 15,000 cP to 500,000 cP.

Uhl and Voznick [111] and Coyle and co-workers [112] have determined the range of viscosities over which different agitator types perform best and this is illustrated in graphical form in Figure 2.15 below.

By inducing different types of flow patterns, different agitator designs directly influence heat transfer, power requirements, rate of polymerisation and polymer product properties. The effect of the rate of agitation of several types of impellers on shear rate, power consumption and heat transfer in non-Newtonian processing media have been extensively studied and documented in the literature [113-115].

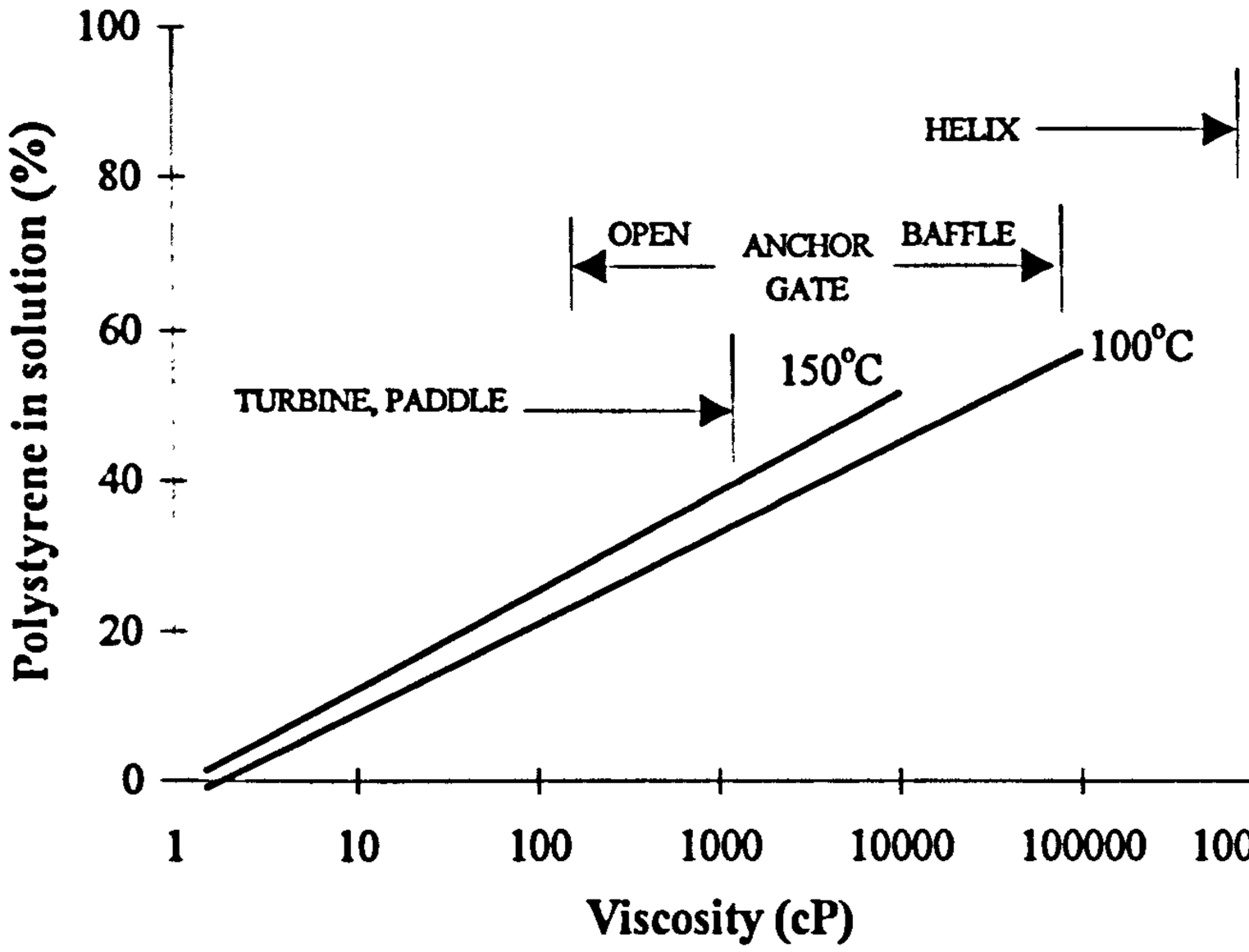

Figure 2.15. Recommended viscosity range of different agitators for polystyrene solutions [80]

2.2.5.2. Heat removal

The thermal stability of polymerisation reactors constitutes a major concern during the operation of such reactors. Polymerisation reactions are highly exothermic in nature; the polymerisation of styrene generates about 73 kJ of heat energy at 25°C per mole of reacted monomer [86]. There is an obvious need to remove the heat released in order to prevent loss of temperature control and in the worst case scenario, reactor runaway. Adequate heat transfer surfaces in polystyrene reactor designs have been provided in many forms, shapes and designs in the development of reactor technology over the years, as will be detailed in this section.

Cooled water circulation in a jacket surrounding the walls of the reactor has long been and still remains the simplest and most economical method of extracting the heat liberated in polystyrene and many other polymer reactors. Correlations for the heat transfer coefficient on the inner wall of the jacket have been developed for different Reynolds numbers [109,116]. In order to maximise productivity, it is often desirable to carry out the polymerisation in large reactor vessels. However, an increase in reactor size is accompanied by a considerable decrease in surface area to volume ratio. It therefore becomes necessary to incorporate additional heat transfer surfaces, besides the conventional cooling jacket, in large polymer reactors to aid in heat removal. Several state-of -the art designs have been developed and adopted in both batch and continuous polystyrene processes over the years.

As reported by Platzer [84] the use of water-cooled baffles positioned along the inside walls of the reactor promotes rapid heat removal from the reactor polymerising mass, although the primary purpose of the baffles is to improve the mixing characteristics of the increasingly viscous reacting mass. This method of supplementing the heat removal capacity of the reactor has been successfully

implemented in large polystyrene suspension reactors currently in use at a commercial level [88].

The cooled plates of the plate and frame filter press used for high conversion polymerisation of styrene represent another example of extended heat transfer surfaces whose proper performance is highly critical to the control of temperature and consequently to the molecular weight distribution of the polystyrene product [80,81].

The prepolymerisers and the unagitated tower down the line in the early I.G. Farben Process were fitted with internal helical cooling coils and conventional water jackets [84]. Correlations predicting heat transfer coefficients on the outside surface of internal helical cooling coils have been presented in the literature [109,116]. The extensive analytical study carried out by Henderson et *al.* [117] on the coil/jacket cooled reactor indicates that such a configuration can have serious limitations in controlling the reaction temperature at high conversions.

Temperature control in an "autorefrigerated" polystyrene reactor is also discussed in detail in Henderson's work [117]. The removal of heat by evaporation of styrene monomer and a solvent such as ethylbenzene and refluxing a fraction of the condensate material into the reactor is shown to be a more reliable means of achieving temperature stability in the polymerisation reactor. This method has been adopted commercially in the prepolymeriser of the Union Carbide two-stage continuous process for polystyrene [80,95].

The externally cooled reactor having part of its reacting mass pumped through an external heat exchanger loop is designed to achieve significantly better temperature control by separating the otherwise interacting effects of insufficient mixing of the reactor contents at the wall and heat removal [117]. However, this configuration has the disadvantages of requiring a substantial capital investment in addition to a control strategy of high complexity as opposed to the jacket/coil cooling system.

In the Dow Process, horizontal banks of cooling tubes have been installed between adjacent agitator rods in the "stratifier" reactor while heat transfer fluid flowing through the hollow shaft and arms of the "egg-beater" type of reactor helped to remove excess heat load [80,93].

The process in use at Mitsui Toatsu Chemicals, Inc. involves continuous flow of coolant in a draft tube surrounding a pumping screw at the centre of the reactor vessel [80,96]. Further provision for heat removal is made by having a number of vertical cooling tubes in the annulus between the draft tube and the reactor wall. Such an arrangement is believed to be extremely effective in achieving uniform temperature throughout the reactor contents.

More recently, the newly developed static mixer reactors as discussed above have been shown to have an inherent advantage of high surface area to volume ratio which ensures excellent heat transfer capability [105].

2.3. KINETICS OF FREE-RADICAL POLYMERISATION

Several decades of study dedicated to the subject of polymerisation have resulted in a clear understanding of the basic elements of the chemistry for the two main categories of polymerisation mechanisms: step and chain polymerisations. Flory [118] identified the rate of increase in polymer size as being the major characteristic distinguishing the two types of polymerisation. Hence, it was observed that whilst step polymers were produced by relatively slow, sequential addition of monomer, dimer, trimer and so on to one another, chain polymers of high molecular weight were being formed in an almost instantaneous manner. These distinctive features which result from different polymerisation mechanisms are illustrated in Figure 2.16 below.

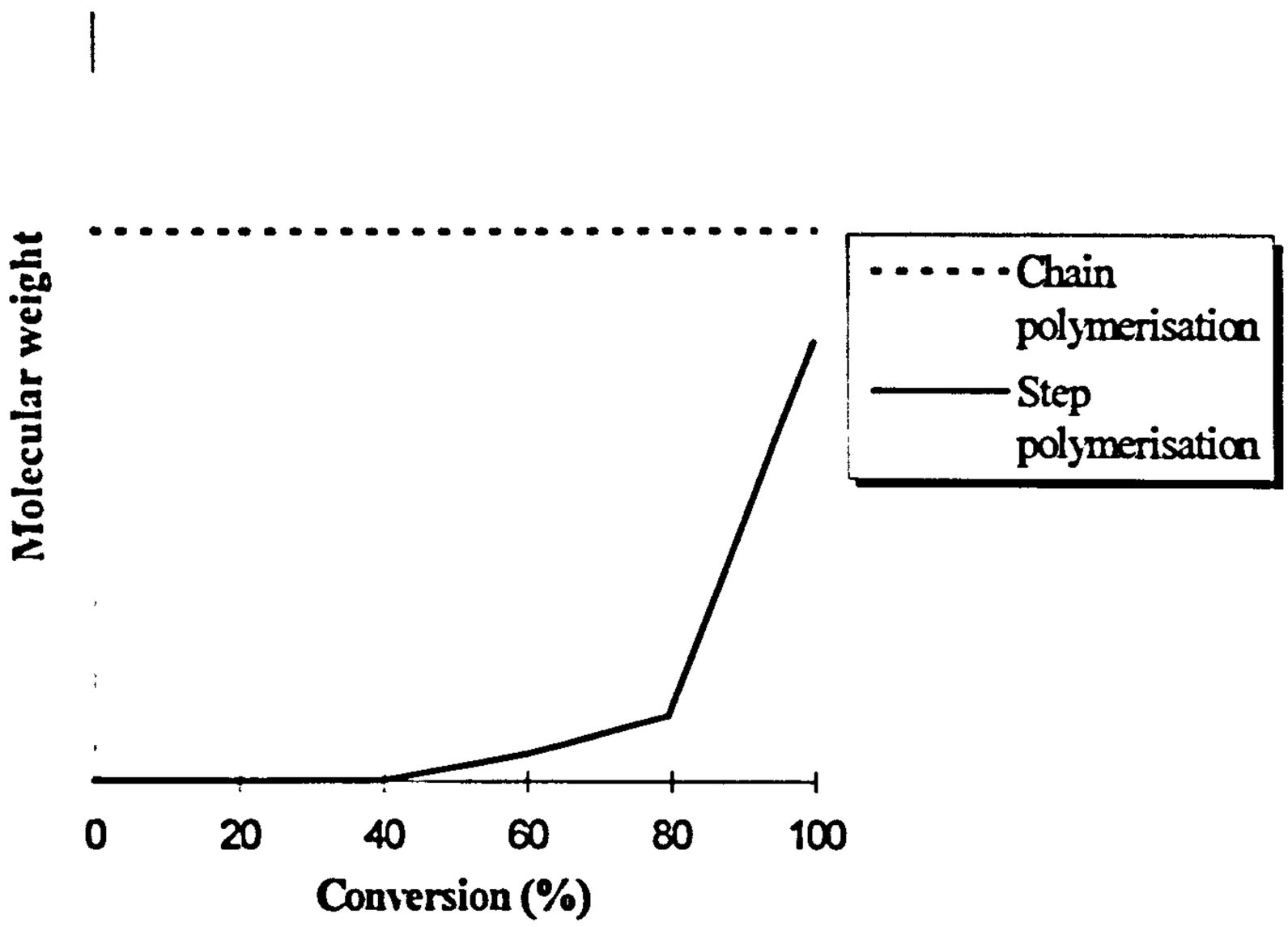

Figure 2.16. Variation of molecular weight with conversion for chain and step polymerisations [119]

Since the current research focuses entirely on chain polymerisation, more specifically of the free-radical type, the theoretical development relating to the mechanism and rate expressions pertaining to free-radical processes will be presented in this section of the literature review with particular emphasis on free-radical styrene polymerisation. Such a background is essential to the full understanding of the effect of the various process conditions not only on the rate of polymerisation but also on the structural features of the polymer product which include the average molecular weight, molecular weight distribution, branching in the polymeric chain and stereospecificity of the repeating units in the chain.

2.3.1. POLYMERISATION OF STYRENE

Chain polymerisation is further subdivided into radical, cationic or anionic polymerisations according to the type of initiators used in the reaction. Styrene and most of its substituted derivatives are among the few monomers that can be

polymerised by all three types of initiators. The ability of styrene to undergo ionic polymerisation is attributed to the presence of the phenyl group in its structure. The phenyl group exhibits a unique readiness to act as an electron-donating or electron-withdrawing centre. This electronic effect allows the growing end of the polymer chain to be either a carbocation or a carbanion with an associated counterion. A detailed and comprehensive review of the steps involved in the ionic polymerisation mechanisms of styrene can be found in various literature sources [86].

Although production of polystyrene is possible by all the above routes, only the free-radical process is of major commercial interest. The weight-average molecular weight of all commercial molding and extrusion resins lies between 100,000 and 400,000 with a distribution index (M_w/M_n) between 2 and 4 [76]. Such range of molecular weight can only be achieved at economic production rates by the free-radical polymerisation method. Anionic polymerisation of styrene is limited to the production of narrow molecular weight distribution polystyrenes in laboratory quantities which are mostly used in instrument calibration and theoretical studies of properties as functions of molecular weight. On a commercial level, anionic polymerization is the established method by which block copolymers of styrene with butadiene are produced [94]. The cationic process has been commercially adopted for the synthesis of low molecular weight polymers for use mainly in coatings and glues [94].

2.3.2. FREE-RADICAL CHAIN POLYMERISATION OF STYRENE

2.3.2.1. Mechanism

In the simplest terms, free-radical polymerisation is a chain reaction consisting of a sequence of three primary steps: initiation, propagation and termination. Normally chain transfer reactions often occur whereby the transfer of the active centre from a growing chain end to another molecule such as monomer, solvent, initiator or dead polymer takes place. The importance of the chain transfer step in controlling the molecular weight of the final polymer product is widely recognised.

2.3.2.1.1. Initiation

The initiation phase of any free-radical polymerisation is considered to involve two distinct reactions, the first being the production of free-radicals which then react with the monomer molecule resulting in an active centre. Radical generation can occur in a number of ways. The most commonly used are thermal or photo-dissociation of a suitable chemical initiator, high energy radiation initiation of monomer and free-radical initiation using suitable one electron transfer redox reactions. Since thermal initiation of monomer and chemical initiator bear most relevance to the present study, these will be discussed at length in the ensuing sections. For more detail about the other modes of initiation mentioned above, the interested reader is invited to consult the extensive literature on the particular subject [86,120-122].

2.3.2.1.1.1. Thermal Initiation

The styrene family of monomers possess the almost unique ability to undergo rapid thermal or self-initiated polymerisation by heating to temperatures in the range between 100-200°C [123,124]. Styrene acts as its own initiator in this reaction.

Experimental evidence obtained from studies into the mechanism of the initiation step strongly favours an overall termolecular reaction such as the one suggested by Mayo [125] as opposed to the bimolecular initiation mechanism initially proposed by Flory [126]. Pryor and Lasswell [127] have presented an in-depth and well researched discussion of the evidence in support of either mechanism. The most up-to-date critical review about the subject has been given by Priddy [128]. The conclusions from a recent study cited in Priddy's work looking into the spontaneous polymerisation of styrene in the presence of acid catalysts [129] lends further support to the Mayo mechanism. It is therefore widely accepted that a Diels-Alder dimer intermediate is first formed by combination of two styrene molecules as shown below [86,94,124,127]:

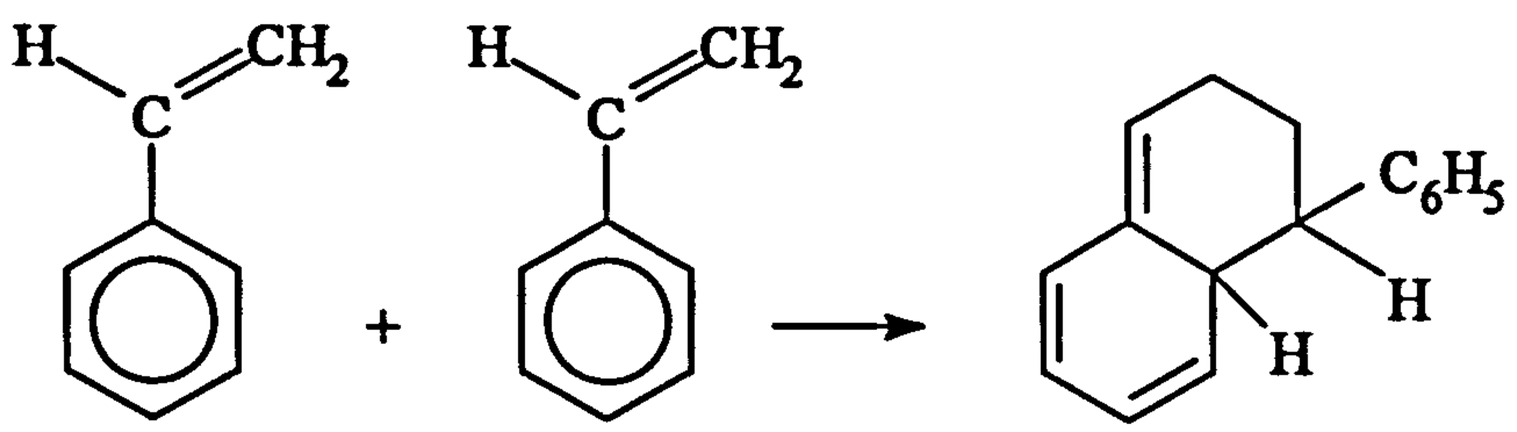

(2.2a)

Diels - Alder dimer

The Diels-Alder dimer has two stereoisomers: axial phenyl and equatorial phenyl. However, only the axial isomer is able to react with another styrene molecule [94] whereby a hydrogen-transfer step results in the production of two monoradicals:

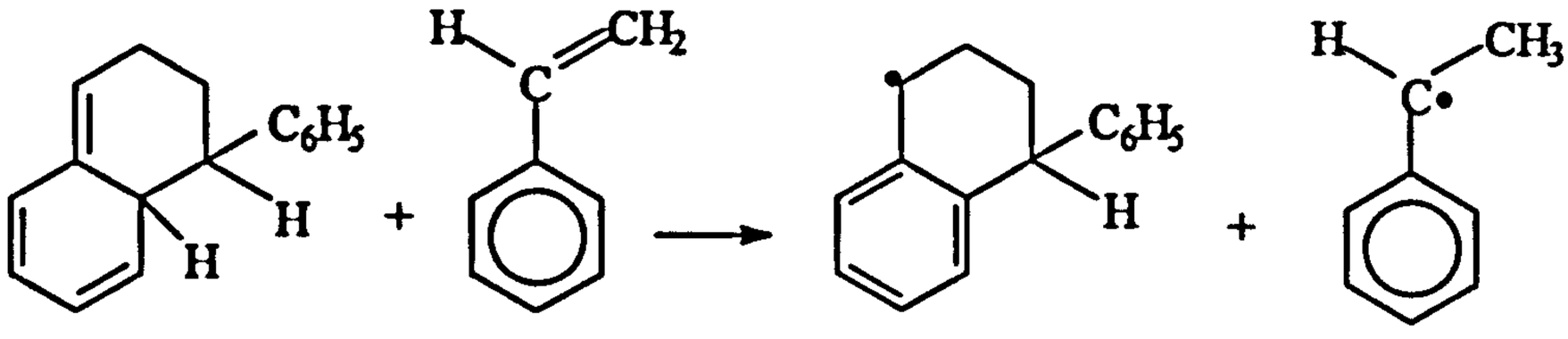

(2.2b)

Each of the above monoradicals subsequently adds a further monomer molecule to form an active centre which then participates in the chain propagation reaction.

2.3.2.1.1.2. Chemical Initiation

Production of free-radicals can also be achieved by the homolytic dissociation of an initiator induced by heat or irradiation.

The suitability of a compound as a heat-induced initiator for a given set of conditions is determined by two factors namely its bond dissociation energy and its half-life at the selected operating temperature. The bond dissociation energy at the point of scission should ideally be in the range 100-170 kJ/mole [86] and only those compounds containing such bonds as O-O, S-S and N-O fulfil this requirement. Of these, the peroxide group of compounds, that is, those compounds having the O-O

bond, are most widely used. The azo compounds are another useful group of compounds frequently employed as chemical initiators. In this special case, although scission of a rather strong C-N bond with bond dissociation energy of about 290 kJ/mole [86] is involved, it is the formation of the extremely stable nitrogen molecule that favours the splitting of the bond to produce free-radicals. The process is shown below for 2,2'- azobisisobutyronitrile (AIBN):

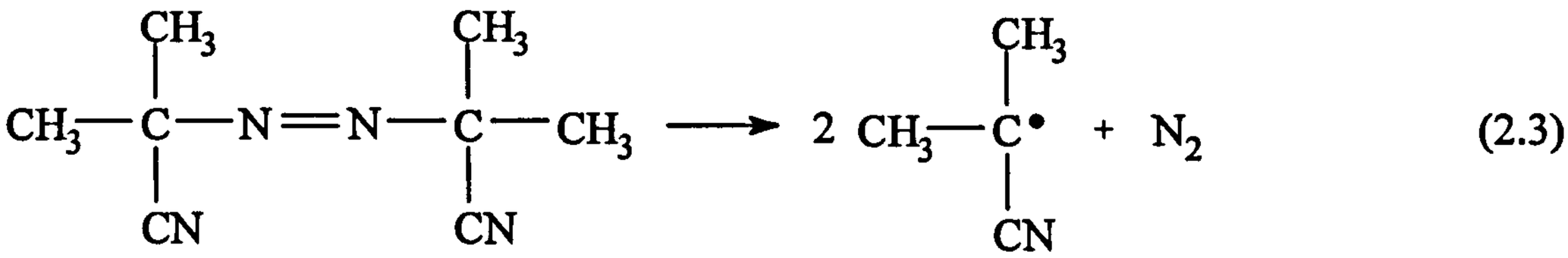

(2.3)

2,2'-azobisisobutyronitrile

The selection of an appropriate initiator for a given polymerisation system is dictated by its decomposition rate at the temperature of polymerisation. A reasonable decomposition rate constant k_d typically lies in the range 10^{-4} to 10^{-6} s^{-1} at the operating temperature [86]. Another parameter often used to select a suitable initiator is its half-life, $t_{1/2}$, which is defined as the time required for half of the initiator originally present to be consumed. The half-life is related to the decomposition rate constant by the following expression:

$$t_{1/2} = \frac{0.693}{k_d} \qquad (2.4)$$

Therefore, the ideal half-life of an initiator should be between 1.9 and 192 hours for appreciable decomposition to occur.

Table 2.1 below lists the half-lives for several common initiators in toluene or benzene at various temperatures [86].

Table 2.1. Half-lives of common initiators in benzene or toluene solutions

Initiator	Half-Life at							
	50°C	60°C	70°C	85°C	100°C	115°C	130°C	145°C
AIBN	74 hr		4.8 hr		7.2 mins			
Benzoyl Peroxide			7.3 hr	1.4 hr	19.8 mins			
Acetyl Peroxide	158 hr		8.1 hr	1.1 hr				
t-Butyl Peroxide					218 hr	34 hr	6.4 hr	1.38 hr
t-Butyl Hydroperoxide					338 hr			

Thus AIBN is preferentially used in systems operating in the temperature range 50°C to 70°C whilst benzoyl peroxide works best between 70°C and 95°C.

Now that a background for a few of the more frequently used thermal initiators has been established, the mechanism for the initiation sequence in the polymerisation of styrene using benzoyl peroxide initiator will be presented. In general terms, the first step is represented by:

$$I \xrightarrow{k_d} 2R^{\bullet} \qquad (2.5a)$$

where I is an initiator molecule
$R^{\bullet}$ is an initiator radical or primary radical species and
k_d is the rate constant for the initiator decomposition

The second part of the initiation step involves the addition of one of the free-radicals produced to a monomer molecule.

$$R^{\bullet} + M \xrightarrow{k_i} RM^{\bullet} \qquad (2.6a)$$

where M is a monomer molecule and
k_i is the rate constant for initiation of polymerisation

For the polymerisation of styrene using benzoyl peroxide as initiator, equations (2.5a) and (2.6a) become:

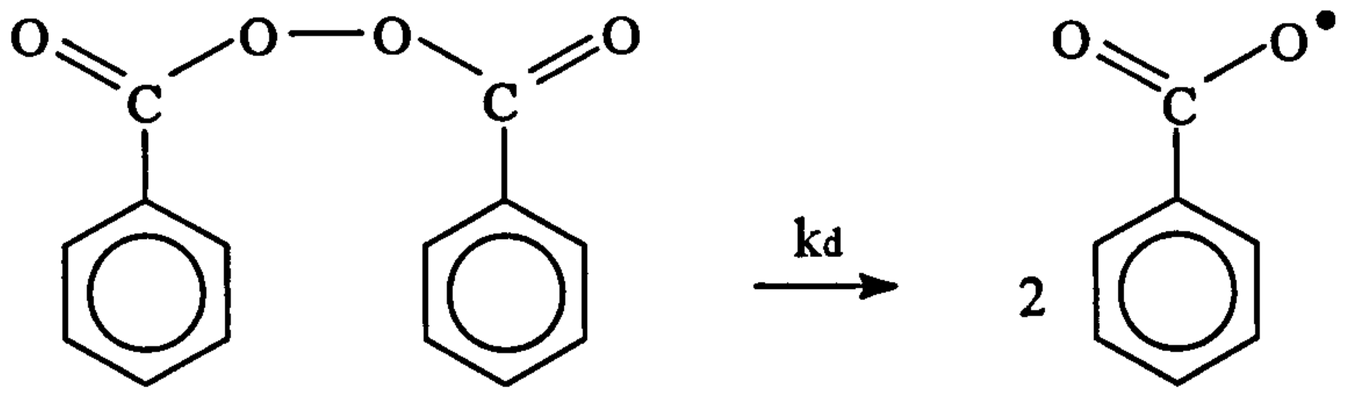

benzoyl peroxide molecule — benzoyl peroxide radicals (2.5b)

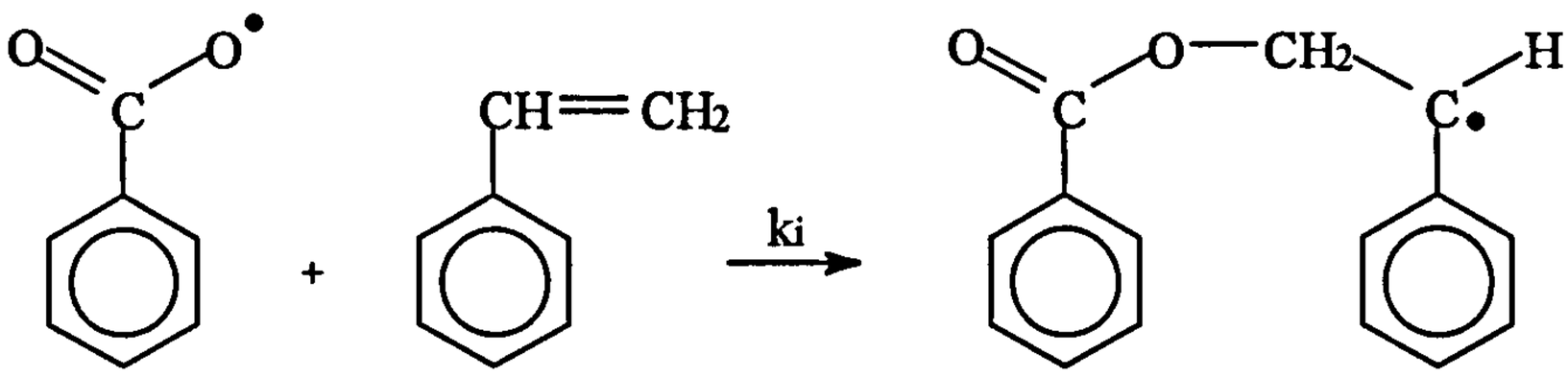

(2.6b)

In equation (2.6b), the mode of addition of the primary benzoyloxy radical to styrene monomer is referred to as tail addition whereby the radical attaches itself to the less substituted carbon on the styrene molecule. Although tail addition is the most favoured process, research findings have shown that, in the case of BPO, initiated species formed by head addition and aromatic substitution are also obtained [130]. In this respect, benzoyloxy radicals are said to have poor regiospecificity in their attack of carbon-carbon double bonds.

2.3.2.1.2. Propagation

The growth of the active chain occurs rapidly by the addition of monomer molecules one at a time to the radical site with the active centre being transferred to the end of the newly formed chain. An appropriate representation of the successive additions is as follows:

$$RM^{\bullet} + M \xrightarrow{k_p} RM_2^{\bullet} \qquad (2.7a)$$

$$RM_2^{\bullet} + M \xrightarrow{k_p} RM_3^{\bullet} \qquad (2.7b)$$

$$RM_3^{\bullet} + M \xrightarrow{k_p} RM_4^{\bullet} \qquad (2.7c)$$

or, in general terms,

$$RM_n^{\bullet} + M \xrightarrow{k_p} RM_{n+1}^{\bullet} \qquad (2.7d)$$

where k_p is the rate of propagation.

The value of n increases very rapidly during propagation reaching several thousand to at least a hundred thousand giving high molecular weight radicals. This is reflected in a large rate constant k_p which for most monomers is of the order of 10^2-10^4 litres/mole-sec [86].

There is quite a wide divergence in k_p values for styrene in the literature applicable to low to intermediate conversion regimes at temperatures in the range 0 to 90°C [131]. Some of the various correlations derived from experimental measurements by different techniques are presented below.

Matheson and co-workers [132] used the rotating sector technique and obtained the following Arrhenius relationship for k_p in the range 0 to 50°C:

$$k_p = 2.16 \times 10^7 \exp\left[\frac{-32592}{RT}\right] \qquad (2.8a)$$

where R is the Universal gas constant in J/mol K
T is the temperature in Kelvin

Mahabadi and O'Driscoll [133] used the technique of spatially intermittent polymerisation (SIP) and their correlation for k_p in the temperature range 15-30°C was of the form:

$$k_p = 10^{7.04} \exp\left[\frac{-29500}{RT}\right] \qquad (2.8b)$$

Berger and Meyerhoff [131] used a least squares fit to k_p data in the range 50-90°C collected using different measuring techniques and obtained the following correlation:

$$k_p = 2.4 \times 10^8 \exp\left[\frac{-37500 \pm 1600}{RT}\right] \qquad (2.8c)$$

More recently the UIPAC Working Party [134] established a new correlation based on measurements of k_p values for styrene using the relatively new technique of pulsed laser polymerisation (PLP) with MWD analysis which has been recommended as the "method of choice" for measurement of k_p. The Arrhenius equation applicable in the temperature range of –12°C to 93°C is:

$$k_p = 10^{7.63} \exp\left[\frac{-32510}{RT}\right] \qquad (2.8d)$$

In simplified radical polymerisation kinetics, the propagation rate constant, k_p, is often assumed to be a function only of temperature while being independent of the viscosity of the reaction mixture as seen in the various expressions above. Even for highly viscous polymer melts where diffusion of reactants in the system is significantly slowed down, the assumption still remains valid particularly if the operating temperature is maintained above the first-order transaction temperature, also referred to as the glass-point temperature. The situations where k_p becomes diffusion controlled are discussed in more detail in section 2.3.7.2 within this chapter.

2.3.2.1.2.1. Modes of Propagation

A propagating radical can be attached to a monosubstituted monomer molecule such as styrene at two possible locations, notably carbon 1 or carbon 2 where carbon 1 has the substituted phenyl group attached to it as shown in the structural arrangement of the styrene molecule below:

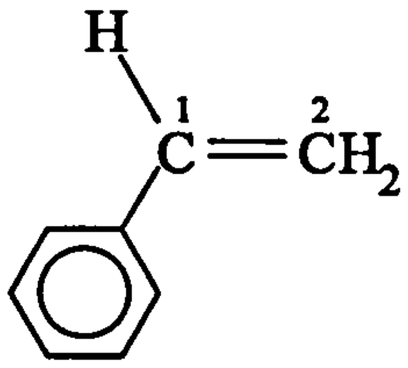

If a radical attaches to carbon 1, the resulting active molecule has the structure shown in equation (2.9a) below:

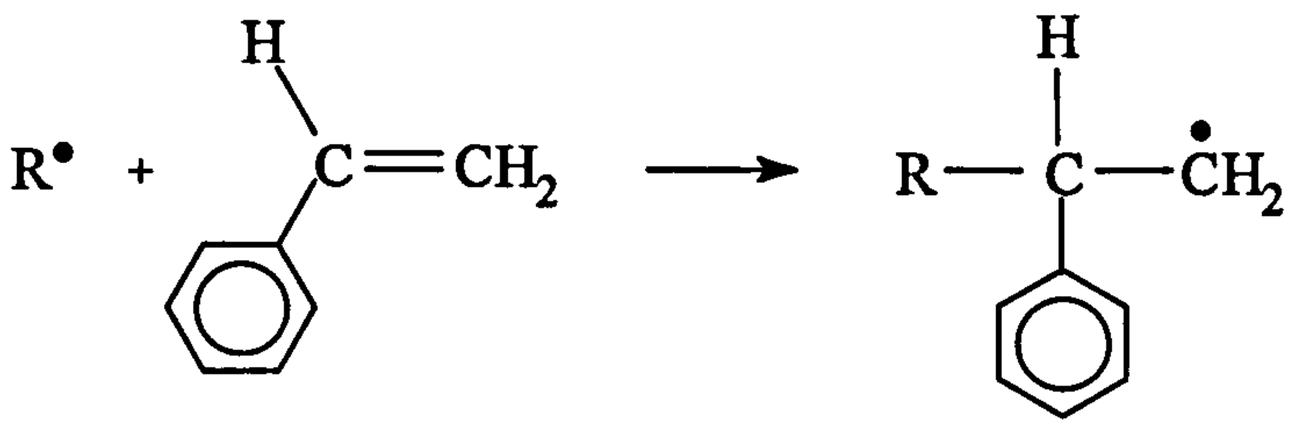

(2.9a)

On the other hand, if attachment occurs at carbon 2, the active species has a slightly different structural arrangement:

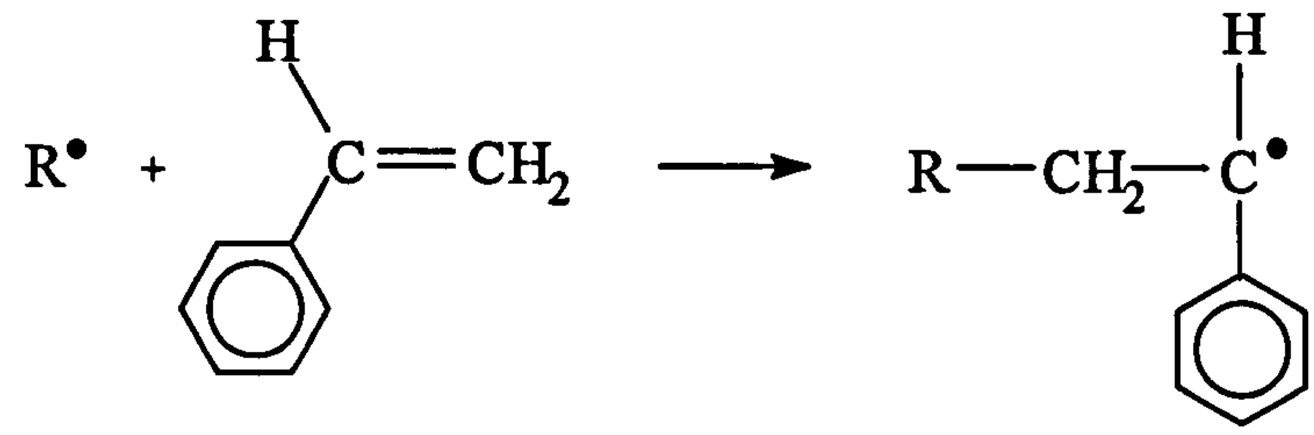

(2.9b)

If each successive addition of monomer molecules to the propagating radical occurs in the same manner either as in equation (2.9a) or (2.9b), monomer units in the final polymer molecule will be arranged such that the substituent which, in the case of styrene is the phenyl group, is placed on alternate carbon atoms.

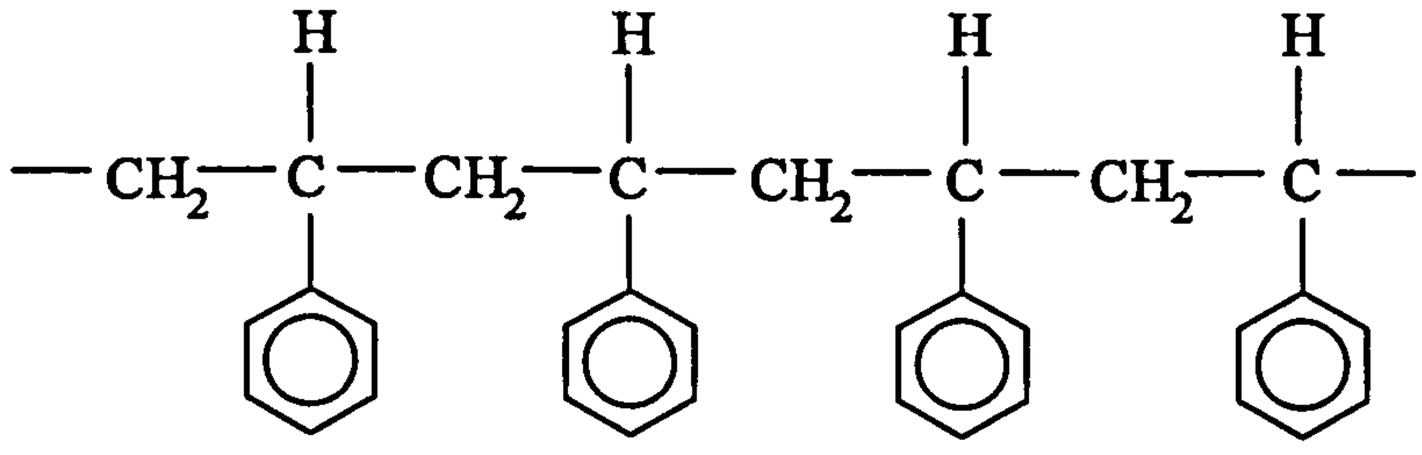

Structure I

This type of arrangement, as shown in Structure I, is referred to as head-to-tail or H-T placement of monomer units.

If on the other hand the propagation of the polymer chain occurs alternately via equations (2.9a) and (2.9b), the resulting arrangement contains both head-to-head (H-H) or tail-to-tail (T-T) placements, as shown below:

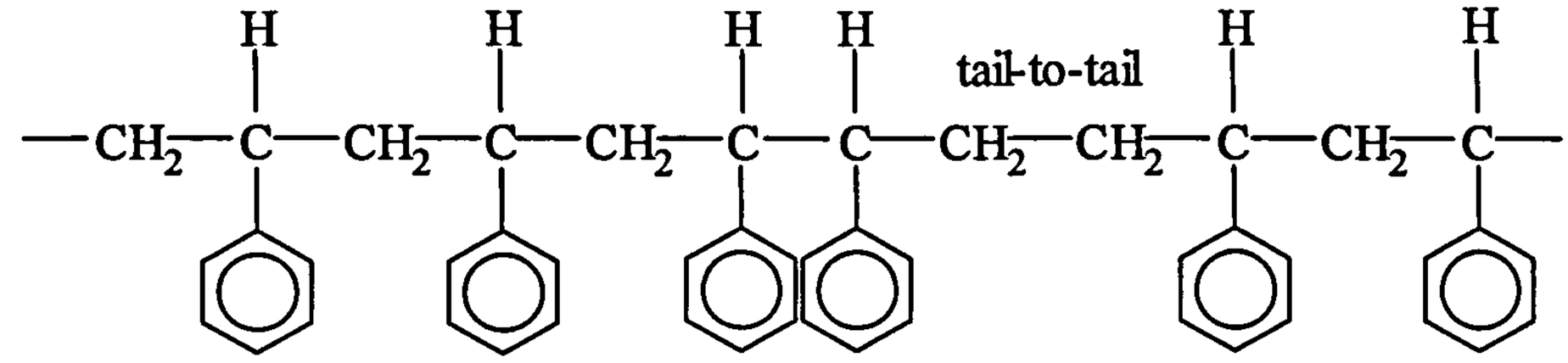

head-to-head

Structure II

The head-to-tail mode of addition is expected to occur almost exclusively in the propagation step since it is favoured on both steric and resonance considerations. The approach and subsequent attachment of a propagating radical at the unsubstituted carbon of a monomer molecule is much less sterically hindered than the approach at the substituted carbon (the carbon having a phenyl group attached to it) since, in the former case, the bulky phenyl groups are not in close proximity. In addition, any structure bearing a radical is an inherently unstable species. However the stability of the propagating radical formed by attachment at carbon 2, as in equation (2.9b), is greatly enhanced by the presence of one or more substituents such as the phenyl ring on the carbon bearing the unpaired electron. The phenyl ring creates resonance effects which are essentially brought about by the delocalisation of the radical over two or more atoms in the structure. Resonance stabilisation for a propagating polystyrene radical is shown below in Structure III.

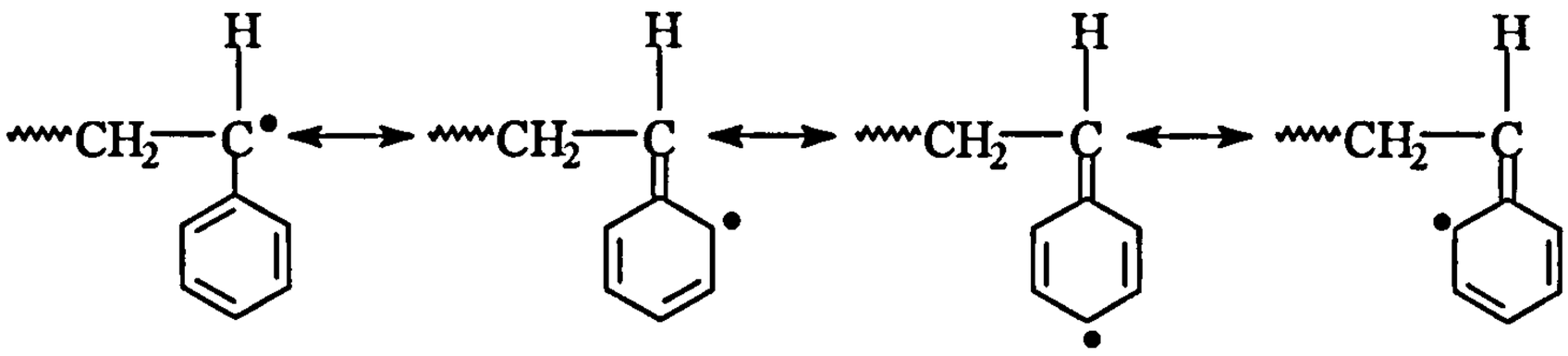

Structure III

On the other hand, the phenyl ring is unable to stabilise the radical formed in equation (2.9a) since it is not attached to the carbon carrying the unpaired electron.

2.3.2.1.3. Termination

At some point in the reaction, the active centre on a polymer chain is destroyed thereby stopping its growth. Termination is then said to occur. Several primary termination reactions have been identified [135] for polymerisation systems in general, but the most likely termination mechanisms referred to consistently in recent publications on styrene polymerisations involve the annihilation of the radical centres

by means of a bimolecular reaction between two radical species. Such mutual termination can occur in two distinct ways: combination (or coupling) and disproportionation.

2.3.2.1.3.1. Combination

Two free radicals each with the active site located on the end of the polymer chain react to form a single polymer molecule. The simultaneous destruction of the two radicals thereby gives rise to a dead polymer molecule with a saturated bond joining the two chains. For styrene polymerisation, this is represented as in equation (2.10a):

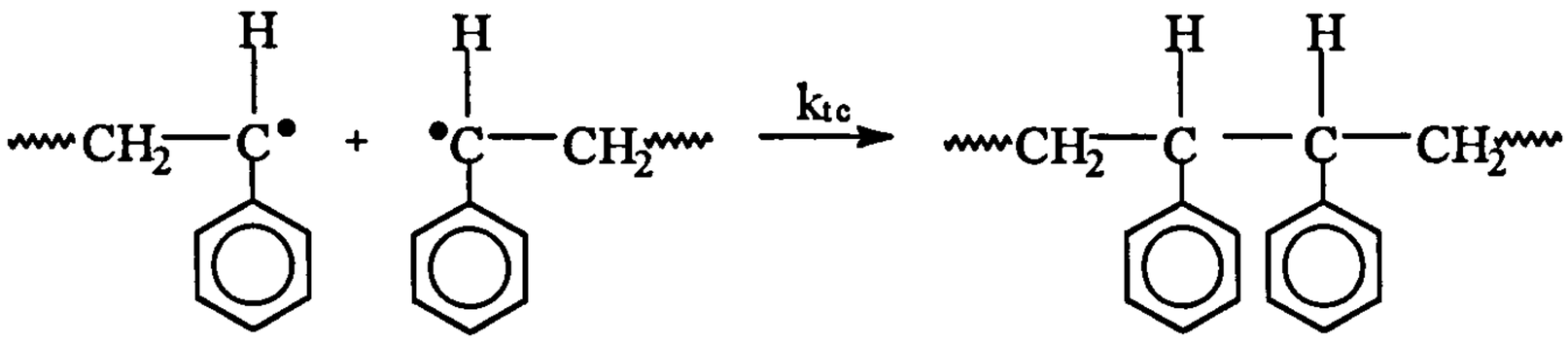

(2.10a)

or, more generally,

$$M_n^{\bullet} + M_m^{\bullet} \xrightarrow{k_{tc}} M_{n+m} \qquad (2.10b)$$

where k_{tc} = rate constant for termination by combination
$M_n^{\bullet}$, $M_m^{\bullet}$ = growing chains consisting of n and m monomer units respectively
M_{n+m} = dead polymer molecule having (n+m) units of monomer

2.3.2.1.3.2. Disproportionation

Disproportionation is also a reaction between two long-chain free radicals but instead of forming one dead molecule out of two growing chains, a collision produces two dead polymer molecules. A hydrogen atom is transferred from one polymeric radical to the other so that a double bond is formed on the end of one polymer molecule (unsaturated molecule) and a single covalent bond on the end of the other (saturated) as illustrated for polystyrene chain in equation (2.11a).

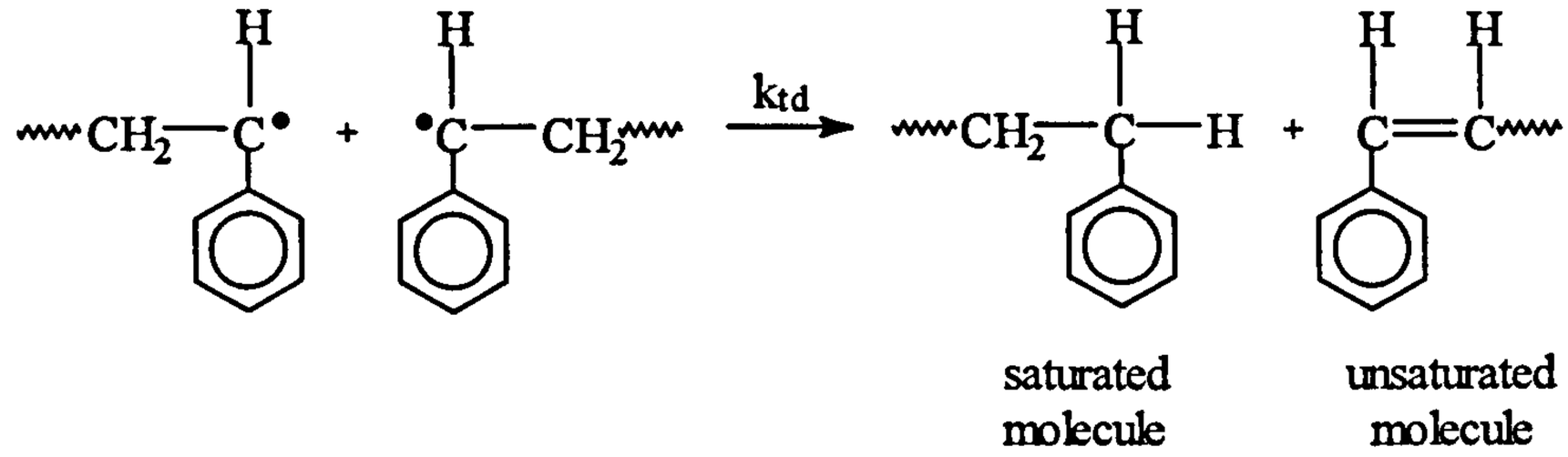

(2.11a)

or, in general terms,

$$M_n^{\bullet} + M_m^{\bullet} \xrightarrow{k_{td}} M_x + M_y \qquad (2.11b)$$

where k_{td} = rate constant for disproportionation reaction
M_n, M_m = growing chains consisting of n and m monomer units respectively
M_x, M_y dead polymer molecules with x and y monomer units respectively

Literature reports that the length of the dead molecules produced by disproportionation need not be the same as those of the original growing molecules due to the random nature of the scission process [135].

Chemical evidence indicates that termination by combination occurs almost exclusively in styrene polymerisation systems operating at temperatures below 80°C [76,136-140]. For temperatures above 80°C, there are contradictory findings about the importance of each mechanism. While some researchers have found evidence to support the fact that disproportionation plays an increasingly important part in terminating polystyrene chains at temperatures above 80°C [141-144], separate kinetic modelling studies have shown that combination as the principal mode of termination for higher temperatures fits molecular weight data better than disproportionation [76].

Other termination reactions notably spontaneous termination and monomer addition to the end of the growing chain, the latter being a temporarily stopped reaction, have been known to take place in some polymerisation processes. As far as polymerisation of styrene is concerned, there is no mention of such termination reactions. They probably do not occur to a significant extent under the process conditions used on a commercial level. Further details about these reactions can be obtained by consulting the literature [135].

If the particular mode of termination is not specified, it is common to formulate the equation for the terminating reaction as:

$$M_n^{\bullet} + M_m^{\bullet} \xrightarrow{k_t} \text{dead polymer} \qquad (2.12)$$

where $k_t = k_{tc} + k_{td}$

In general, typical termination rate constants, k_t, are in the range 10^6-10^8 litres/(mole-sec) [86]. Values for k_t which have been determined for the polymerisation of styrene under a range of conditions have been published collectively in the literature [131]. The data have also been reproduced graphically in the work of Buback and Kuchta [145].

Various correlations for k_t applicable to styrene polymerisation before the onset of diffusion control effects have also been presented. Thus, Matheson et al. [132] correlated k_t for styrene with temperature in the range 0-50°C as:

$$k_t = 1.295 \times 10^9 \exp\left[\frac{-9950}{RT}\right] \qquad (2.13a)$$

where R is the Universal gas constant in J/mol K
T is the temperature in deg. K

Buback and Kuchta [145] obtained an empirical correlation for k_t in the low conversion region of styrene polymerisation in terms of pressure and temperature variables. Their expression applied at atmospheric pressure simplifies to:

$$k_t = 1.064 \times 10^9 \exp\left[\frac{-6260}{RT}\right] \qquad (2.13b)$$

Biesenberger and Sebastian [146] used the correlation below in one of their examples involving the benzoyl peroxide initiated free-radical polymerisation of styrene:

$$k_t = 1.255 \times 10^9 \exp\left[\frac{-7035}{RT}\right] \qquad (2.13c)$$

It is to be noted that k_t in the above correlations refers to the termination rate expression (2.23b) in the section to follow.

It is observed that k_t values are several orders of magnitude greater than the propagation rate constants, k_p. The high values for k_t indicates a strong tendency for the propagating chains to terminate. However, the radical species are present in such low concentrations that the termination process is less likely to occur. Furthermore, the polymerisation rate is inversely proportional to only the one-half power of k_t so that the effect of large k_t values on the overall polymerisation rate is largely diminished.

An important assumption has been made in equations (2.10) to (2.12) in that the rate constants k_{tc}, k_{td} and k_t are independent of the size of the radical as is the propagation rate constant k_p. Kerr [147]concluded from his work in the 1970s that although molecular size does influence radical reactivity to some extent in the initial stages of the polymerisation, the effect of size disappears after the dimer or trimer level is attained. While radical reactivity may be unaffected, it is however argued that in light of the simple collision theory applied to long active chains involved in diffusion-controlled termination reactions (to be discussed later), size dependence of diffusion rates will certainly have an impact on the overall termination rate constant [148,149].

2.3.2.2. Rate Expressions

The detailed mechanism of the chemically initiated radical chain polymerisation of styrene has been outlined in the previous section with the use of equations (2.5), (2.6), (2.7), (2.10), (2.11) and (2.12). These will be used to develop an expression for the overall rate of polymerisation and to determine how the different system parameters involved affect the polymerisation process.

2.3.2.2.1. Initiation

The rate of decomposition of an initiator such as benzoyl peroxide (BPO) following the mechanism laid out in equation (2.5) is given by:

$$R_d = \frac{d[R^\bullet]}{dt} = 2\,k_d[I] \qquad (2.14)$$

where R_d is the rate of decomposition
$[R^{\bullet}]$ is the primary radical concentration in reacting mixture
[I] is the initiator concentration
k_d is the rate constant for initiator decomposition

The factor 2 takes into account the bimolecular nature of the dissociation of the initiator molecule following the general convention adopted in reaction kinetics.

The second stage of the initiation process involves the formation of active polymer chains by radical attack on monomer molecules (equation (2.6)). With the primary radical species being highly reactive, this process is much faster than the initiator decomposition reaction which consequently becomes the rate-controlling step of the initiation sequence. Therefore, the rate of production of active chains or the rate of initiation R_i is expressed as:

$$R_i = \left(\frac{d[M^{\bullet}]}{dt}\right)_{initiation} = 2 f k_d [I] \qquad (2.15)$$

where $[M^{\bullet}]$ is the concentration of newly formed polymer chains
f is the initiator efficiency

The initiator efficiency is defined as the fraction of radicals produced in the primary step of initiator decomposition (equations (2.5a), (2.5b)) which are actually successful in initiating polymerisation. There is wastage of initiator due to two main reactions, one being the induced decomposition of initiator which is also referred to as chain transfer to initiator and the other involving various side reactions of primary radicals. The initiator efficiency is regarded in many literature sources as being related mainly to the latter wastage reaction which is strongly enhanced by the so-called cage effect [86,120]. The initiator efficiency has been shown to exhibit variable dependence on the monomer/solvent system, monomer concentration (hence viscosity) and temperature [130]. In general, the value of f for BPO initiating a styrene/solvent system is expected to decrease with styrene conversion and with increasing viscosity but show a marked increase with temperature rise.

The rate of polymer chain formation or the rate of initiation, denoted by R_i, is equal to the rate at which monomer is consumed during initiation. Hence,

$$R_i = -\left(\frac{d[M]}{dt}\right)_{initiation} = \left(\frac{d[M\bullet]}{dt}\right)_{initiation} = 2 f k_d [I] \qquad (2.16)$$

where [M] is the monomer concentration

2.3.2.2.2. Propagation

Monomer molecules are used up in a series of individual propagation steps according to equations (2.7a) to (2.7d). Since the rate constants, k_p, for all the propagation steps are the same, irrespective of the length of the polymer chain, the rate of monomer consumption during propagation can be formulated as:

$$-\left[\frac{d[M]}{dt}\right]_{propagation} = k_p[M][M\bullet] \qquad (2.17)$$

where [M] is the monomer concentration
[M$^\bullet$] is the total concentration of all chain radicals, that is, all radicals of size $M_1^\bullet$ and larger.

The rate of polymerisation, R_p, is measured by the total rate of monomer consumption during initiation and propagation.

$$R_p = -\left[\frac{d[M]}{dt}\right]_{initiation} + -\left[\frac{d[M]}{dt}\right]_{propagation} \qquad (2.18)$$

However, the rate of removal of monomer during the initiation sequence is far less than the rate of monomer disappearance during propagation where a relatively huge number of monomer molecules are reacting with numerous growing chains at the same instant to produce high polymer. Therefore, to a very close approximation, the term $-\left[\frac{d[M]}{dt}\right]_{initiation}$ can be neglected so that the polymerisation rate is simply expressed as:

$$R_p = -\left[\frac{d[M]}{dt}\right]_{propagation} \qquad (2.19)$$

Combining equations (2.15) and (2.17), we have

$$R_p = k_p\,[M]\,[M^\bullet] \qquad (2.20)$$

2.3.2.2.3. Termination

The general rate expression for termination by combination (equations (2.10a) and (2.10b)) is:

$$R_{tc} = -\left[\frac{d[M^\bullet]}{dt}\right]_{combination} = 2\,k_{tc}[M^\bullet]^2 \qquad (2.21)$$

Similarly, for disproportionation (equations (2.11a) and (2.11b)), the rate is:

$$R_{td} = -\left[\frac{d[M^\bullet]}{dt}\right]_{disproportination} = 2\,k_{td}[M^\bullet]^2 \qquad (2.22)$$

If there is no specification as to whether termination occurs by combination or disproportionation, then the rate expression is as follows:

$$R_t = -\left[\frac{d[M^\bullet]}{dt}\right] = 2\,(k_{tc} + k_{td})\,[M^\bullet]^2 \qquad (2.23a)$$

Putting $k_t = (k_{tc} + k_{td})$, we have

$$R_t = -\left[\frac{d[M^\bullet]}{dt}\right] = 2\,k_t\,[M^\bullet]^2 \qquad (2.23b)$$

The factor 2 in the termination rate expressions has been included to indicate that radicals are being destroyed in pairs.

2.3.3. POLYMERISATION RATE BY STEADY STATE HYPOTHESIS

The correlation for the rate of polymerisation as given by equation (2.20) contains the term $[M^\bullet]$ whose value is difficult to evaluate experimentally since the radical concentration in the mixture is generally extremely low, being of the order of 10^{-8} M [86] . This is because radicals get used up almost instantaneously once they are created due to their extremely reactive nature and hence the possibility of their accumulation is greatly reduced. It is therefore necessary to eliminate the term $[M^\bullet]$ from equation (2.20).

The concentration of radicals in the reaction mixture can be estimated by the steady-state approximation. Such an approximation has been successfully applied in developing the kinetics of many small molecule reaction involving highly reactive intermediates present in very low concentrations. Experimental investigation has shown that the steady-state assumption is applicable to many free-radical systems where all the conditions required to ensure the validity of the assumption are encountered.

Hence, according to the steady-state assumption, the rate of production of free-radicals that induce polymerisation equals their rate of destruction during the termination stage. In other words, the rate of change of the concentration of radicals in the system quickly becomes and remains zero during the course of polymerisation. Typical polymerisations reach steady-state in a very short period which may be at most a minute [86].

In mathematical form,

$$\frac{d[R^\bullet]}{dt} = -\frac{d[M^\bullet]}{dt} \qquad (2.24)$$

rate of production of free radicals during initiation = rate of destruction of free radicals during termination

Substituting for $\frac{d[R^\bullet]}{dt}$ and $-\frac{d[M^\bullet]}{dt}$ from equations (2.14) and (2.23b) respectively, we obtain the following:

$$2\,f\,k_d\,[I] \;=\; 2\,k_t\,[M^\bullet]^2 \qquad (2.25a)$$

It should be noted that the initiator efficiency is included in the rate of radical production to take into account only those primary radicals which participate in the subsequent chain reaction.

After simplifying and rearranging, an expression for $[M^\bullet]$ is generated:

$$[M^\bullet] = \sqrt{\left(\frac{f\,k_d\,[I]}{k_t}\right)} \qquad (2.25b)$$

Substitution for $[M^\bullet]$ in the expression for R_p in equation (2.20) yields:

$$R_p = k_p\,[M]\,\sqrt{\left(\frac{f\,k_d\,[I]}{k_t}\right)} \qquad (2.26)$$

Equation (2.26) is a differential expression which applies to vanishingly small increments in monomer conversion. An integral form of equation (2.26) is desirable for practical manipulations and comparison to experimental data obtained for a finite change in time.

Replacing for R_p by $-\frac{d[M]}{dt}$ and $[I]$ by $[I]_o e^{(-k_d t)}$ for exponential decay of initiator in equation (2.26) gives, after rearrangement:

$$-\frac{d[M]}{[M]} = k_p\sqrt{\left(fk_d[I]_o/k_t\right)}\,e^{(-k_d t/2)}dt \qquad (2.27)$$

In terms of conversion x where $[M]=[M]_o(1-x)$, equation (2.27) becomes:

$$\frac{dx}{dt} = k_p\sqrt{\left(fk_d[I]_o/k_t\right)}\,e^{(-k_d t/2)}(1-x) \qquad (2.28)$$

which, on integration between the limits

$$x = 0 \quad \text{at } t = 0$$

and $\quad x = x \quad \text{at } t = t$

yields

$$x = 1 - \exp\{-2k_p\sqrt{f[I]_o/(k_d k_t)}(1-e^{-k_d t/2})\} \qquad (2.29)$$

The effect of volume contraction has not be considered here. A more general relationship to include this effect has been developed by Nishimura [150]. For low conversion regimes, this effect can be ignored.

In situations where the initiator half-life is long compared to the polymerisation time scale (i.e. initiator decomposition rate is slow ($k_d t \ll 1$) so that the

initiator concentration does not change much over the course of polymerisation), it is common practice to express the differential equation for conversion-time relationship simply as:

$$\frac{dx}{dt} = k_p\sqrt{\left(fk_d[I]_o/k_t\right)}\,(1-x) \qquad (2.30)$$

from which we then get

$$x = 1-\exp\{-k_p(\sqrt{fk_d[I]_o/k_t}\,)t\} \qquad (2.31)$$

As can be seen from the final correlation for R_p from equation (2.26), faster rates of polymerisation can theoretically be achieved by:

1) Increasing the initiator concentration, [I]; a doubling in the concentration causes R_p to increase by a factor of $\sqrt{2}$. In physical terms, this is the result of bimolecular termination reaction between radicals.
2) Increasing the monomer concentration, [M]; doubling [M] doubles the rate of polymerisation.
3) Increasing the temperature; k_d increases to a significant extent with temperature while k_p and k_t, being rate constants for free-radical reactions, are relatively less affected by temperature. Generally, the initiator efficiency, f, shows little variation with temperature. The overall effect is an increase in R_p with temperature.

2.3.3.1. Effect of monomer concentration on polymerisation rate

Although the first-order dependence of the overall polymerisation rate on monomer concentration (equation (2.26)) holds true for most systems, divergence from such behaviour have been known to occur. For instance, Horikx and Hermans [151] have observed a progressively higher order of dependence of R_p on [M] from 1.18-order at [M]=1.8 to 1.36-order at [M]=0.4 for the polymerisation of styrene/toluene system at 80°C initiated by BPO.

These observations may best be explained by a direct effect of a change in monomer concentration on the rate of initiation. Under normal reaction conditions prevailing at the beginning of the polymerisation, the rate of initiation is independent of the monomer concentration, as shown by the expression in equations (2.15) and (2.16). However, as polymerisation proceeds, the rate of initiation becomes dependent on the monomer concentration in various ways. The initiator efficiency, f, for example, has been shown to be related to [M] according to an expression of the form [152]:

$$f = f'\,[M]^a \qquad (2.32)$$

where f' is the limiting value of initiator efficiency

The value of a can vary between zero and 1. If a = 0, f becomes independent of [M]; this occurs at high monomer concentration usually at the beginning of polymerisation. The order of dependence of R_p on [M] is 1 at this stage. As monomer concentration decreases with conversion, the effect of [M] on initiator efficiency becomes more pronounced. At low monomer concentrations or high conversions, 1.5-order dependence of R_p on [M] is seen. Monomer concentrations below 10^{-1}-10^{-2} M

have been predicted to have a large influence on the value of f [153]. The solvent cage effect as described in various standard texts [86,120,152] is responsible for the above-mentioned changes in initiator efficiency during the course of polymerisation. The chances of radical-radical interactions within or out of the solvent cage are increased at low monomer concentrations, thereby giving lower initiator efficiency.

Under certain specific conditions, the rate of polymerisation is observed to be second order with respect to the monomer concentration. This occurs at very high concentrations of primary radicals which react preferentially with the propagating radicals during the termination stage of the polymerisation. Such a reaction can be represented as:

$$RM_n^{\bullet} + R^{\bullet} \xrightarrow{k_{tp}} RM_n\text{—}R \qquad (2.33)$$

where $RM_n^{\bullet}$ is an growing chain
$R^{\bullet}$ is a primary radical formed by initiator decomposition (equations (2.5a) and (2.5b))
RM_n-R is a terminated polymer molecule with n monomer units
k_{tp} is the rate constant

The mode of termination then changes from the normal bimolecular termination as expressed in equations 8 through to 10 to primary termination. Such an effect is further enhanced in the presence of a low monomer concentration, usually <1 mole/litre [154], which fails to absorb the large number of primary radicals being produced. This behaviour has been observed by Moad and Solomon and co-workers [142,155] during their investigation of styrene polymerisation initiated by 0.1M BPO at 60°C. The authors have reported that primary radical termination is responsible for 75% of chain termination at conversions in the range 30% to 70%. Detailed kinetic treatment for primary termination have been presented in several papers [156-158].

By combining rate expressions for equations (2.6a), (2.7d) and (2.33), the polymerisation rate is derived as:

$$R_p = \frac{k_p k_i [M]^2}{k_{tp}} \qquad (2.34)$$

It should also be mentioned that at low monomer concentrations, the second step of the initiation stage (equation 2.6a) becomes the rate determining step giving the rate of initiation, R_i, as:

$$R_i = k_i [R^{\bullet}] [M] \qquad (2.35)$$

2.3.3.2. Effect of initiator concentration on polymerisation rate

Similar arguments can be advanced in an attempt to explain the deviation from square root dependence of the rate of polymer formation on initiator concentration. As seen in equation (2.34), the polymerisation rate becomes independent of the initiator concentration when primary termination is the predominant termination scheme. The Trommsdorff or gel effect is also expected to be responsible for promoting primary

radical termination as diffusion of the small primary radicals is much less hindered than the long polymer chains in the highly viscous medium.

At very high initiator concentrations, for instance, the order of dependence of R_p on [I] that best fits the experimental data is shown to be less than one-half. Nevertheless, it is argued that R_p being less than expected may not truly be a deviation from the correlation. Instead, a decrease in the initiator efficiency, f, may, in fact, be the responsible factor for the effect observed [86].

On the other hand, the dependence of R_p on [I] becomes close to first-order in the Trommsdorff region of some heterogeneous polymerisations since the radical chains are not able to undergo termination [159]. Inhibited polymerisations systems in which premature termination of a growing chain occurs by radical transfer onto an inhibitor can also give rise to first-order dependence on [I]. Odian [86] has given a concise kinetic treatment of such behaviour.

2.3.4. KINETIC CHAIN LENGTH

An important parameter in polymerisation which is commonly employed to obtain information about the individual rate constants k_p and k_t is the average kinetic chain length denoted by ν. The kinetic chain length is defined as the average number of monomer molecules polymerised for each initiated chain. In other words, it is the ratio of the polymerisation rate per unit rate of initiation. In mathematical form, this is expressed as:

$$\nu = \frac{R_p}{R_i} \tag{2.36}$$

Substituting for $R_i = R_t$ from the steady state approximation, $R_p = k_p[M][M^\bullet]$ (equation (2.20)) and $R_t = 2\,k_t\,[M^\bullet]^2$ (equation (2.23b)), the kinetic chain length can be obtained as

$$\nu = \frac{k_p[M]}{2k_t[M^\bullet]} \tag{2.37}$$

Substituting for $[M^\bullet]$ by $\sqrt{\frac{R_i}{2k_t}}$ gives

$$\nu = \left(\frac{k_p^{\,2}}{2k_t}\right)^{1/2} \frac{[M]}{\sqrt{R_i}} \tag{2.38}$$

Alternatively if $[M^\bullet]$ is replaced by $\frac{R_p}{k_p[M]}$ we get instead

$$\nu = \frac{k_p^{\,2}[M]^2}{2k_tR_p} \tag{2.39}$$

In the case of thermal decomposition of an initiator, equation (2.26) can be substituted for R_p in equation (2.39) to give

$$\nu = \frac{k_p[M]}{2\sqrt{(fk_dk_t[I])}} \qquad (2.40)$$

Equations (2.37) to (2.40) indicate that an inverse proportionality dependence exists between the kinetic chain length and both the radical concentration $[M^\bullet]$ and the polymerisation rate R_p. Small-sized or low molecular weight polymer molecules are obtained with an increase in polymerisation rate. For any free-radical polymerisation system, the desired molecular weight to be achieved will dictate the rate of reaction to be imposed.

A knowledge of the kinetic chain length value for a given system allows determination of the ratio $\frac{k_p^2}{2k_t}$ which combined with the measurement of $\frac{k_p}{k_t}$ under non-steady state conditions yields absolute values for the individual rate constants k_p and k_t. The non-steady state conditions are achieved by using widely documented techniques such as the rotating sector and spatially intermittent polymerisation (SIP) [86,160-162]. A more advanced method called pulsed laser photolysis (PLP) has only recently been developed to allow the direct and reliable determination of the value of k_p from the molecular weight distribution curve [163,164].

2.3.5. DEGREE OF POLYMERISATION

The instantaneous number-average degree of polymerisation, $\overline{X}_N$, is defined as the average number of monomer molecules in each polymer molecule. It can also be expressed as:

$$\overline{X}_N = \frac{\text{Rate of monomer consumption}}{\text{Rate of polymer formation}} = \frac{-d[M]/dt}{d[P]/dt} \qquad (2.41)$$

But from equations (2.19) and (2.20), we get

$$-\frac{d[M]}{dt} = k_p[M][M^\bullet] \qquad (2.42)$$

and, assuming there is no chain transfer, $\frac{d[P]}{dt}$ can be expressed in different forms depending on whether termination occurs by combination or disproportionation:

For combination:
$$\frac{d[P]}{dt} = k_{tc}[M^\bullet]^2 \qquad (2.43)$$

For disproportionation: $$\frac{d[P]}{dt} = 2k_{td}[M^{\bullet}]^2 \qquad (2.44)$$

Thus the total rate of polymer formation by both mechanisms is defined as:

$$\frac{d[P]}{dt} = (k_{tc} + 2k_{td})[M^{\bullet}]^2 \qquad (2.45)$$

Hence combining expressions for $-\frac{d[M]}{dt}$ and $\frac{d[P]}{dt}$ from equations (2.42) and (2.45) respectively, $\overline{X}_N$ is obtained as

$$\overline{X}_N = \frac{k_p[M]}{(k_{tc} + 2k_{td})[M^{\bullet}]} \qquad (2.46)$$

When expressed in terms of the kinetic chain length ν using equations (2.37) and (2.46) and applying the relationship $k_t = k_{tc} + k_{td}$, $\overline{X}_N$ becomes

$$\overline{X}_N = 2\nu \left(\frac{k_{tc} + k_{td}}{k_{tc} + 2k_{td}} \right) \qquad (2.47)$$

Two simplified forms of equation (2.47) can be written if termination is assumed to proceed predominantly by combination or disproportionation.

Thus, if combination is the favoured mechanism, $k_{tc} >> k_{td}$ and equation (2.47) yields

$$\overline{X}_N = 2\nu \qquad (2.48a)$$

On the other hand, if disproportionation occurs predominantly, $k_{td} >> k_{tc}$ and we then obtain

$$\overline{X}_N = \nu \qquad (2.48b)$$

If both mechanisms occur to an appreciable extent, then $\overline{X}_N$ lies between ν and 2ν.

The number-average degree of polymerisation is related to the number-average molecular weight, $\overline{M}_n$, of a given polymer by the following expression:

$$\overline{M}_n = M_o \overline{X}_N \qquad (2.49)$$

where M_o is the molecular weight of the monomer.

Thus reliable measurement of $\overline{M}_n$ allows the straightforward evaluation of the value of $\overline{X}_N$.

2.3.5.1. Distribution Functions for Degree of Polymerisation

At all times, a given polymerising system comprises growing radical chains of various sizes or lengths. Owing to the random nature of chain reactions, the degree of polymerisation at any instant is therefore expected to follow a statistical distribution based on the size distribution of radicals participating in the termination reaction. The development of an appropriate distribution function for the degree of polymerisation involving free-radicals has been outlined in great detail in a number of text-books [165] following the early treatment given by North [166].

The number distribution of degree of polymerisation essentially represents the number of polymer molecules having n monomer units in their structure, that is, having a degree of polymerisation of n. Based on the simple termination mechanism of combination and/or disproportionation, this distribution denoted by x_n has been evaluated as [165]:

$$x_n = \frac{1}{\nu}\left(1+\frac{1}{\nu}\right)^{-n} \frac{(n-1)/\nu + 2(k_{td}/k_{tc})}{1+2(k_{td}/k_{tc})} \qquad (2.50)$$

Again the above expression can be simplified by assuming predominance of one mode of termination, giving for combination only:

$$x_n = \frac{n-1}{\nu^2}\left(1+\frac{1}{\nu}\right)^{-n} \qquad (2.51)$$

and for disproportionation reaction only,

$$x_n = \frac{1}{\nu}\left(1+\frac{1}{\nu}\right)^{-n} \qquad (2.52)$$

As specified above, equations (2.50) through to (2.52) represent the number or mole-fraction distribution. The conversion of x_n into weight-fraction distribution (also known as the differential weight distribution), denoted by x_w, is easily done by multiplying x_n by the ratio $\frac{nM_o}{\overline{X}_N M_o}$, where M_o is the monomer molecular weight and $\overline{X}_N$ is replaced by the expression in equation (2.47) to give:

$$x_w = \frac{n}{2\nu^2}\left(1+\frac{1}{\nu}\right)^{-n} \frac{(n-1)/\nu + 2(k_{td}/k_{tc})}{1+(k_{td}/k_{tc})} \qquad (2.53)$$

The molecular weight distribution can be obtained by using the following expression:

$$M_n = nM_o \qquad (2.54)$$

where M_n is the molecular weight of the polymer chain with n monomer units

Hence a plot of x_w against M_n yields the molecular weight distribution (MWD).

It is important to note the difference between M_n and $\overline{M}_n$, the latter being an average value based on the number of molecules in a system while M_n is the weight of a polymer chain with n monomer units.

2.3.6. CHAIN TRANSFER

Chain transfer is an additional step in the chain reaction mechanism whereby growth of a polymer chain is stopped by transfer of the active site to another molecular species which may or may not subsequently reinitiate another chain. The mechanism may be represented by the following equations:

$$M_n^{\bullet} + T \xrightarrow{k_{tr}} M_n + T^{\bullet} \qquad (2.55)$$

$$T^{\bullet} + M \xrightarrow{k_s} TM^{\bullet} \qquad (2.56)$$

where $M_n^{\bullet}$ is a growing polymer chain
T is the chain transfer agent
k_{tr} is the rate constant for chain transfer
M_n is a terminated or inactive polymer molecule
$T^{\bullet}$ is the new active site created from the transfer agent
M is a monomer molecule
k_s is the rate constant for the reinitiation reaction
$TM^{\bullet}$ is the newly initiated polymer chain

While chain transfer agents in the form of solvent (S) are usually involved in this step, it is not uncommon that other species in the system such as monomer (M), initiator (I) or even polymer (P) also participate in chain transfer.

The general rate equation for chain-transfer as expressed by equation (2.55) is given by:

$$R_{tr} = k_{tr} [M^{\bullet}][T] \qquad (2.57a)$$

where R_{tr} is the rate of chain transfer

Similarly, the rate equations for transfer to solvent, monomer, initiator and polymer are:

$$R_{tr,S} = k_{tr,S} [M^{\bullet}][S] \qquad (2.57b)$$

$$R_{tr,M} = k_{tr,M} [M^{\bullet}][M] \qquad (2.57c)$$

$$R_{tr,I} = k_{tr,I} [M^{\bullet}][I] \qquad (2.57d)$$

$$R_{tr,P} = k_{tr,P} [M^{\bullet}][P] \qquad (2.57e)$$

where $k_{tr,S}$, $k_{tr,M}$, $k_{tr,I}$ and $k_{tr,P}$ are the rate constants for transfer to solvent, monomer, initiator and polymer respectively.

Therefore, the total rate of chain transfer, R_{tr}, is calculated as:

$$R_{tr} = R_{tr,S} + R_{tr,M} + R_{tr,I} + R_{tr,P} \qquad (2.57f)$$

2.3.6.1. Effect of chain transfer on molecular weight

Odian [86] has briefly discussed the effects of the relative magnitudes of k_{tr} and k_s compared to k_p on the polymerisation rate, R_p, and the number-average degree of polymerisation, $\overline{X}_N$. Ideally the aim of chain transfer is to achieve a desired and controllable molecular weight without affecting the polymerisation rate. Odian [86] refers to this specific type of chain transfer as "normal chain transfer" which is characterised by unchanged polymerisation rate and kinetic chain length with, however, a decrease in $\overline{X}_N$ and molecular weight. This occurs in situations where the reinitiation rate constant, k_s, is comparable to the propagation rate constant, k_p, so that monomer consumption remains unchanged as the reinitiation reaction (equation (2.56)) generates a new propagating chain to promptly replace the one terminated in the transfer step. Hence, as highlighted by Moad & Solomon [167], it is expected that normal chain transfer is more likely to occur for monomers such as styrene and methyl methacrylate (MMA) having low propagation rate constants k_p.

The process by which chain transfer reduces the number-average degree of polymerisation is more clearly understood by considering the definition for $\overline{X}_N$ given in the previous section as:

$$\overline{X}_N = \frac{\text{Rate of monomer consumption}}{\text{Rate of polymer formation}} = \frac{-d[M]/dt}{d[P]/dt} \qquad (2.41)$$

Chain transfer is, in essence, a termination process and it therefore contributes to the rate of polymer formation $\frac{d[P]}{dt}$ which together with normal bimolecular radical termination becomes:

$$\frac{d[P]}{dt} = (k_{tc} + 2k_{td})[M^\bullet]^2 + R_{tr} \qquad (2.58)$$

Using equations (2.57b) to (2.57f) to replace R_{tr}, we have:

$$\frac{d[P]}{dt} = (k_{tc} + 2k_{td})[M^\bullet]^2 + k_{tr,S}[M^\bullet][S] + k_{tr,M}[M^\bullet][M] + k_{tr,I}[M^\bullet][I] + k_{tr,P}[M^\bullet][P] \qquad (2.59)$$

Substitution for $-\frac{d[M]}{dt}$ and $\frac{d[P]}{dt}$ from equations (2.42) and (2.59) respectively leads, after simplification, to

$$\overline{X}_N = \frac{k_p[M]}{(k_{tc} + 2k_{td})[M^\bullet] + k_{tr,S}[S] + k_{tr,M}[M] + k_{tr,I}[I] + k_{tr,P}[P]} \quad (2.60)$$

On inversion, equation (2.60) becomes

$$\frac{1}{\overline{X}_N} = \frac{(k_{tc} + 2k_{td})[M^\bullet]}{k_p[M]} + C_S\frac{[S]}{[M]} + C_M + C_I\frac{[I]}{[M]} + C_P\frac{[P]}{[M]} \quad (2.61)$$

where C_S, C_M, C_I, C_P are chain transfer constants for transfer to solvent, monomer, initiator and polymer respectively (= $k_{tr,T}/k_p$ where T represents solvent (S), monomer (M), initiator (I) and polymer (P)).

It is often more convenient to replace $[M^\bullet]$ by $\frac{R_p}{k_p[M]}$ in the above equation to yield $\frac{1}{\overline{X}_N}$ in terms of known or measurable variables. Thus

$$\frac{1}{\overline{X}_N} = \frac{(k_{tc} + 2k_{td})R_p}{k_p^2[M]^2} + C_S\frac{[S]}{[M]} + C_M + C_I\frac{[I]}{[M]} + C_P\frac{[P]}{[M]} \quad (2.62)$$

Since transfer to polymer becomes important only at very high conversions, the term $C_p\frac{[P]}{[M]}$ can be neglected for most practical purposes in the low to intermediate conversion region. Thus the final simplified form of equation (2.62) known as the Mayo equation is:

$$\frac{1}{\overline{X}_N} = \frac{(k_{tc} + 2k_{td})R_p}{k_p^2[M]^2} + C_S\frac{[S]}{[M]} + C_M + C_I\frac{[I]}{[M]} \quad (2.63)$$

Equation (2.63) predicts the effect on polymer molecular weight of changes in operating conditions of free-radical polymerisations. Molecular weight decreases when:

1. Solvent concentration, [S], increases and/or a solvent having a higher chain transfer constant C_S is used.
2. Initiator concentration [I] is increased and/or an initiator with a higher chain transfer constant C_I is employed.
3. Rate of polymerisation R_p is increased by either raising the operating temperature or increasing the initiator concentration. In the latter case, the decrease in molecular weight will be accelerated since initiator chain transfer is promoted. The study carried out by Baysal and Tobolsky [168] demonstrates this effect.

Experimental determination of the individual chain transfer constants C_S, C_M and C_I is possible by suitable manipulation of equation 60 and measurement of the appropriate variables as clearly outlined by Odian [86]. A wide range of systems with particular emphasis on styrene polymerisation systems have thus been investigated by

a great number of researchers over the past decades [138,168,169] and the data obtained have been conveniently compiled in several polymer literature sources.

Toluene or ethylbenzene are commonly employed as solvents in the polymerisation of styrene mainly to reduce the solution viscosity for better control of the polymerisation. These solvents have C_S values of $1.25x10^{-5}$ and $6.7x10^{-5}$ respectively at 60°C [170,171], indicating poor chain transfer and negligible effects on the degree of polymerisation.

The value of C_M at 60°C for styrene using BPO as initiator is reported to be $6x10^{-5}$ [138,170] which is considered to be too small to affect the molecular weight in any significant manner.

The initiator chain transfer constant, C_I, attributable to BPO in the polymerisation of styrene at 60°C varies from 0.048 to 0.10 [170] which in itself is quite high. However, the observed molecular weight decrease is not as drastic as would be expected owing to the combined effect of usually low [I]/[M] ratio (of the order of 10^{-3} -10^{-5} [86]) and relatively high C_I values. Chain transfer to BPO initiator in the polymerisation of styrene has been shown to produce high conversion polystyrene having a narrower molecular weight distribution than that obtained with other initiators such as AIBN [130, 216].

2.3.7. HIGH CONVERSION DIFFUSION CONTROLLED POLYMERISATION

For most free radical polymerisation systems, the simple kinetic model outlined in the previous sections has been found to be only applicable to relatively low conversion regions. As pointed out before, such kinetic schemes involve a number of simplifying assumptions in the derivations of rate expressions to enable a straight-forward mathematical manipulation. These assumptions are reiterated below:

1. Long Chain Approximation- The average length of active radical chains is large enough to assume that monomer is consumed solely in the propagation step.
2. Chain Length Independence- The radical reactivity is independent of the radical size, i.e. k_p and k_t are constant for all propagation and termination steps irrespective of the chain length of the reacting radicals.
3. Steady State Assumption- The system operates under steady state conditions whereby the concentration of free radicals at any time is very small and rapidly reaches a constant level soon after the onset of polymerisation.

Intermediate to high conversion experimental data have, in many cases, failed to be accurately predicted from the model developed with those simplifications. This has prompted extensive research into the specific characteristics exhibited by high conversion polymer systems with emphasis on the high viscosity of the reaction medium. The validity of the chain length independence of k_t, in particular, has received a great deal of attention from the polymer chemistry research community. Attempts have also been made at developing a mathematical model to account for such changes in polymerisation kinetics at advanced degrees of conversion [172-175].

One particularly interesting feature observed in many polymerisations is a rapid increase in both polymerisation rate and molecular weight beyond a certain conversion under isothermal conditions. Such an autoaccelerative phenomenon has

been termed the "gel effect" or the "Trommsdorff effect". Obviously the gel effect is a deviation from the classical polymerisation kinetics and polymer scientists have explained this phenomenon in terms of a marked decrease in the termination rate due to increased viscosity at high polymer concentrations [176-178]. In the ensuing section, the main intention is to briefly discuss the changes that occur during the gel-effect situation at both microscopic and macroscopic levels. Detailed model developments to account for the gel effect will not be covered here but these can be obtained from the abundant literature material published on the subject [172-174, 179-185].

It is worthwhile, at this point, to give a qualitative outline of the major features observed in the bulk polymerisation of vinyl monomers in general. According to Soh and Sundberg [181], four distinct phases can be identified in polymerisations where chain transfer is negligible:

1) Phase I- Low conversion regime

   This is dictated by conventional kinetics for steady state polymerisation whereby the polymerisation rate is first order with respect to monomer concentration and half-order with respect to the initiator concentration. The average molecular weights quickly attains a constant value from the start of polymerisation.

2) Phase II- Gel effect

   The onset of the gel effect is characterised by a sharp increase in the polymerisation rate. The conversion at which this occurs is generally independent of the initiator concentration at a given temperature. A broadening of the molecular weight distribution accompanied by large increases in the average molecular weights is observed.

3) During Phase III the molecular weight averages seem to level off although the polymerisation rate is still quite high.

4) In Phase IV, the rate of polymerisation starts to fall off to eventually become zero. A limiting conversion is reached at reaction temperatures below the glass transition temperature of the polymer.

The conversion and molecular weight trends as discussed above are illustrated in Figures 2.17 and 2.18 below.

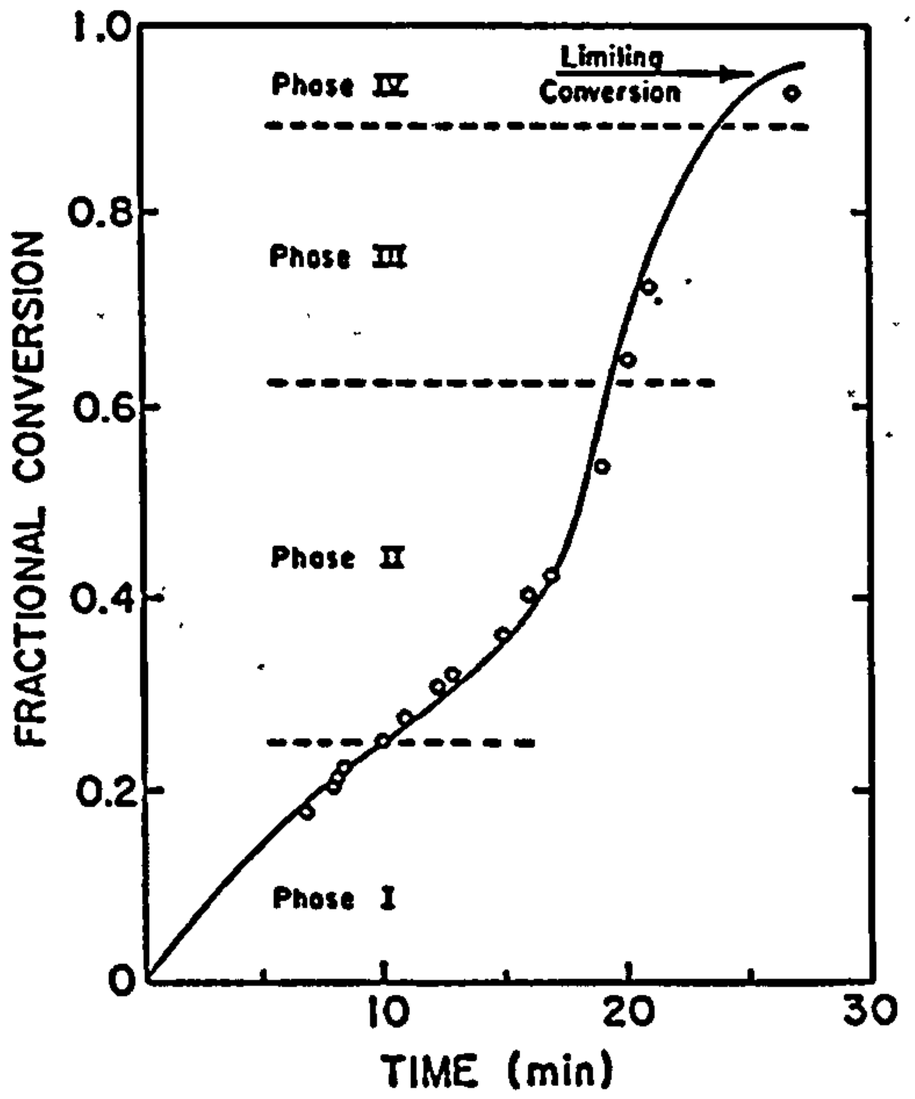

Figure 2.17. Typical high conversion polymerisation profile for methyl methacrylate [181]

The appearance and duration of each phase over the course of a given polymerisation system are broadly determined by the nature and composition of the system itself and the molecular weight of the polymer formed. A severe gel effect can be predicted in bulk polymerisations at conversions between 15-90% [186] while in solution polymerisation systems the onset of the gel effect is delayed until a much higher conversion is attained.

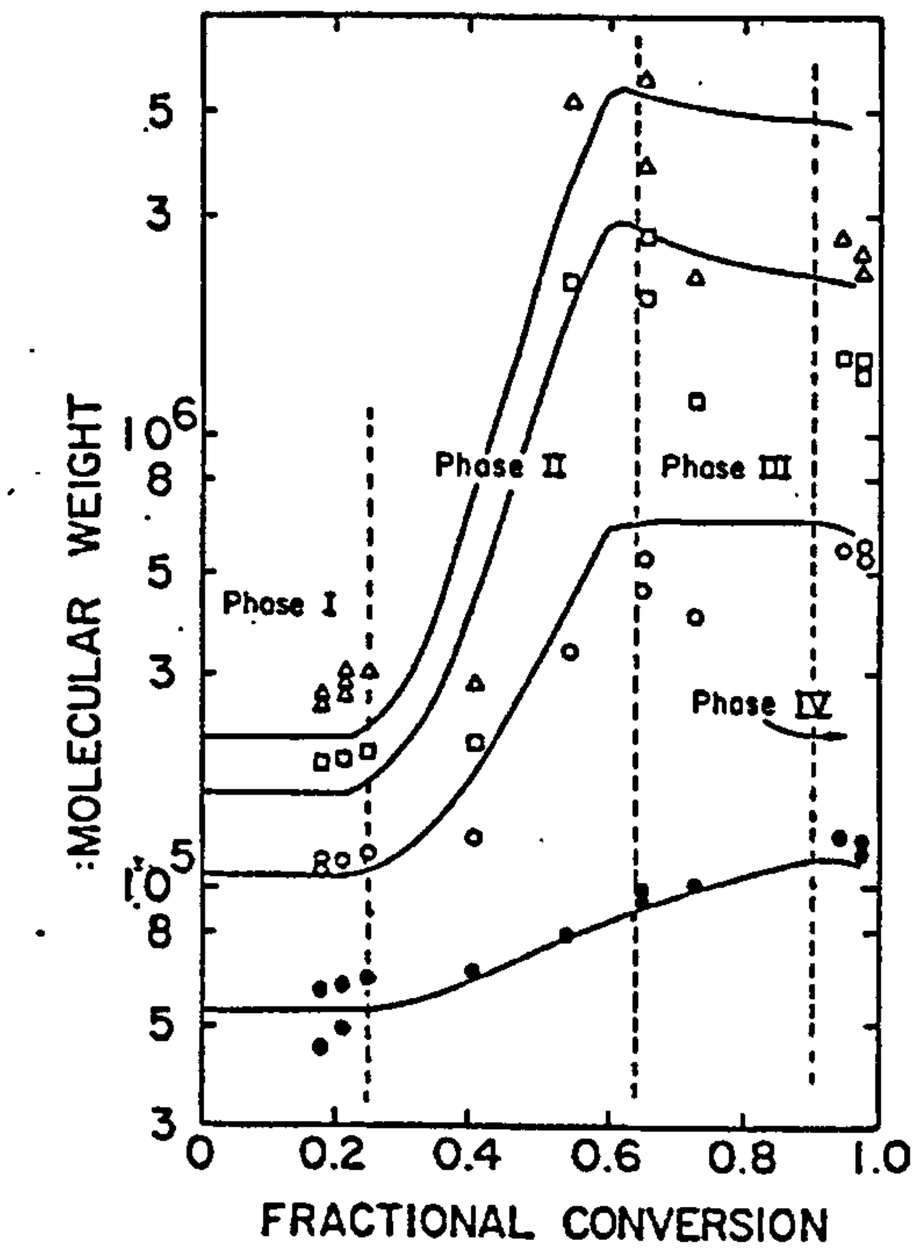

Figure 2.18. Effect of conversion on molecular weight averages during polymerisation of methyl methacrylate (•) $\overline{M}_n$, (○) $\overline{M}_w$, (□) $\overline{M}_z$, (△) $\overline{M}_{z+1}$ [181]

2.3.7.1. Diffusion-Controlled Termination

The occurrence of the gel effect can best be explained by considering the bimolecular termination process as a sequence of three steps, the first two of which proceed by diffusion mechanisms [86,186,187]:

1. Translational diffusion of propagating macroradicals through the bulk of the medium in their approach to each other- rate constant, k_{TD}
2. Segmental diffusion of the entire chain in an entangled region (reptation) followed by segmental motion of the chain ends so that these are positioned in close proximity- rate constant, k_{SD}
3. Chemical reaction to terminate the active sites- rate constant, k_R

Each of these steps is associated with a rate constant as indicated above and together they determine the overall termination rate constant k_t according to the relationship [175]:

$$\frac{1}{k_t} = \frac{1}{k_{TD}} + \frac{1}{k_{SD}} + \frac{1}{k_R} \qquad (2.64)$$

Reaction between two free radicals is typically very fast making k_R very high, of the order of 10^9 litres/mole-sec [86]. Its effect on k_t is therefore negligible in which case equation (2.64) simplifies to:

$$\frac{1}{k_t} = \frac{1}{k_{TD}} + \frac{1}{k_{SD}} \qquad (2.65)$$

The smaller of the two rate constants k_{TD} and k_{SD} becomes the controlling rate for the termination process.

The effect of increasing conversion on each of k_{TD} and k_{SD} is most readily seen from the graphical illustration presented by Dionisio and co-workers [175] which is reproduced below in Figure 2.19.

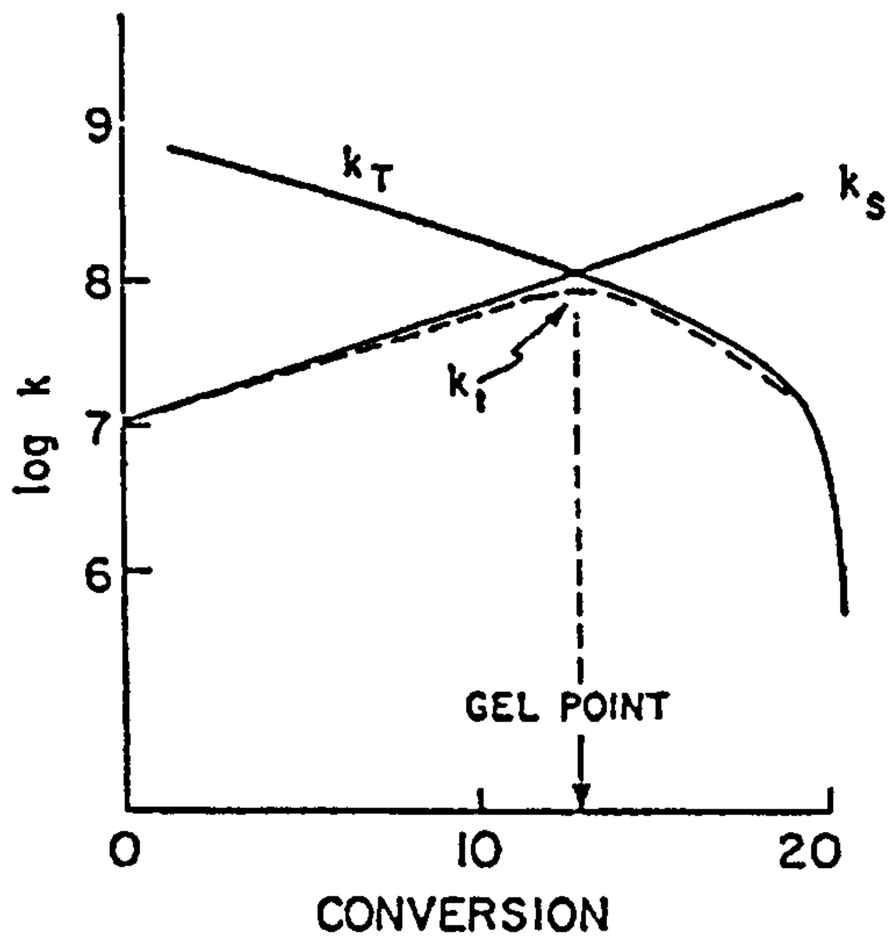

Figure 2.19. Illustration of effect of conversion on k_{TD} , k_{SD} and k_t for polymerisation in a good solvent [175]

At low conversions, segmental diffusion is rate controlling since it occurs within a region of high entanglement in contrast to the relatively rapid translational movement of the long polymer active chains through the bulk of the low viscosity medium. With increasing conversion, more polymer molecules in solution cause a decrease in the goodness of the solvent so that the polymer coil becomes smaller. Under the resulting higher concentration gradient across the smaller coil, the segmental motion of the chain ends is enhanced. A linear increase in k_{SD} with conversion has been previously established in a separate study [188]. As the concentration of polymer rises at high conversion, the viscosity of the solution is increased while the macroradicals get in a highly entangled state and are thus less free to diffuse across the bulk of the solution. Translational diffusion (or k_{TD}) thereby decreases with conversion as shown in Figure 2.19 above. Eventually a conversion is reached in the polymerisation where translational diffusion becomes the rate controlling step instead of the segmental diffusion. Dionisio et al. [175] have denoted this point to be the onset of the gel effect or the "gel point". A sharp decrease in k_{TD} and hence k_t from this point onwards result in the observed rise in polymerisation rate and molecular weight.

It is important to realise that the gel effect is only noticeable in polymerisations where other forms of termination reactions such as primary termination (section 2.3.3.1) and chain transfer (section 2.3.6) are absent. Hence, for high temperature thermal polymerisation of styrene, Husain and Hamielec [124] did not observe the onset of gel effect due to transfer reactions.

2.3.7.2. Diffusion Controlled Propagation

In contrast to the gel effect, the glass effect which arises as a result of diffusion controlled propagation reaction causes a rapid decline in the rate of polymerisation to almost zero and polymerisations stop short of complete conversion. This behaviour has in fact been studied and reported for different systems polymerised under a range of different conditions [185, 189-194]. It has been suggested that the absence of diffusion limitations on the propagation rate constant as observed by some investigators [195] is related to short chain length of the polymer and hence the reduced entanglement.

The propagation step involves the diffusion of a small monomer molecule and as such it is expected to become diffusion controlled only in extremely viscous media at very high conversions. Moreover, the decrease in the propagation rate constant k_p is more noticeable in polymerisations carried out at reaction temperatures well below the glass transition temperature of the polymer and in such cases polymerisations have been shown to stop short of complete conversion [196,197]. Hayden and Melville [189] have indeed observed this effect during the polymerisation of MMA in bulk at 25°C. Under these conditions, the propagation reaction eventually becomes diffusion controlled giving a gradually decaying polymerisation rate after the gel effect until a limiting conversion below 100% is reached. Several mathematical models based on the free volume theory [179,180,193] have been proposed in an attempt to predict the effect of conversion on k_p.

2.3.8. SOME CHARACTERISTIC PROPERTIES OF POLYMERS

As discussed in the previous sections, the elementary reaction steps involved in free-radical polymerisation (initiation, propagation and termination) are all random in nature. As a result, polymers are characterised by a mixture of macromolecules of different sizes or molecular weights and they are said to be polydisperse materials. Therefore, a distribution of molecular weights exists. Together with the different average molecular weights that can be defined, the molecular weight distribution (MWD) gives useful information about the properties of the polymer in question. It is a necessity in most polymerisation processes to adequately control the average molecular weight and the MWD in order to achieve polymer with certain desirable physical properties.

2.3.8.1. Average molecular weights

Several molecular weight averages are used to characterise a polymer product. The definition for each is given below.

1. Number-average molecular weight, $\overline{M}_n$

The number-average molecular weight is defined as the total weight of the whole system divided by the total number of molecules present or, in mathematical form:

$$\overline{M}_n = \frac{\Sigma N_i M_i}{\Sigma N_i} = \frac{\Sigma W_i}{\Sigma N_i} \qquad (2.66)$$

where N_i is the number of molecules i whose weight is M_i
W_i ($=N_iM_i$) is the weight of all molecules with weight M_i

The value of $\overline{M}_n$ is biased towards the low molecular weight polymer fraction. The determination of $\overline{M}_n$ relies on the measurement of a colligative property such as osmotic pressure, boiling point elevation and vapour pressure lowering which effectively gives a count of the number of particles in solution. Experimental and analytical details for these methods are available in general polymer textbooks [198-200].

2. Weight-average molecular weight, $\overline{M}_w$

The weight average molecular weight is defined as:

$$\overline{M}_w = \frac{\Sigma N_i M_i^2}{\Sigma N_i M_i} = \frac{\Sigma W_i M_i}{\Sigma W_i} \qquad (2.67)$$

In contrast to $\overline{M}_n$, the value of $\overline{M}_w$ is influenced by the high molecular weight species in the polymer sample. It is experimentally determined by light scattering and ultracentrifugation techniques [198-200].

3. Higher average molecular weights, $\overline{M}_z$ and $\overline{M}_{z+1}$

Based on the previous definitions, these can similarly be defined as:

$$\overline{M}_z = \frac{\Sigma N_i M_i^3}{\Sigma N_i M_i^2} = \frac{\Sigma W_i M_i^2}{\Sigma W_i M_i} \tag{2.68}$$

$$\overline{M}_{z+1} = \frac{\Sigma N_i M_i^4}{\Sigma N_i M_i^3} = \frac{\Sigma W_i M_i^3}{\Sigma W_i M_i^2} \tag{2.69}$$

4. Viscosity-average molecular weight, $\overline{M}_v$

This is another useful average molecular weight which can be measured by viscosity methods. It is defined according to equation (2.70) below:

$$\overline{M}_v = \left[\frac{\Sigma N_i M_i^{a+1}}{\Sigma N_i M_i} \right]^{1/a} \tag{2.70}$$

where a is a constant.

It is to be noted that if a=1, then $\overline{M}_v = \overline{M}_w$ but on the other hand if a=-1, $\overline{M}_v = \overline{M}_n$. However, in most cases, the value of 'a' varies from 0.5 to 0.9 [201] so that $\overline{M}_n < \overline{M}_v < \overline{M}_w$, with $\overline{M}_v$ being closer to $\overline{M}_w$ than to $\overline{M}_n$.

The solution viscosity method is a relative method for determining molecular weights since it is based on measurement of a property (viscosity) which is dependent on the molecular weight of the polymer. A correlation between viscosity and molecular weight for a given system is required before $\overline{M}_v$ can be evaluated.

2.3.8.2. Molecular weight distribution

In order to assess the suitability of a polymer product for specific applications, only a knowledge of the previously defined molecular weight averages is not sufficient. The exact distribution of molecular weights is an additional requirement which, combined with the molecular weight average data, will give a reliable indication of the physical properties of the polymer such as its mechanical strength. Several distribution functions for molecular weights or degree of polymerisation have been developed to fit the specific mechanisms involved in a given free-radical chain polymerisation. The individual reaction steps (initiation, propagation, chain transfer and chain termination) and their relative rates determine the exact form of the distribution and the many different possibilities have been extensively discussed by Billingham [202]. Of particular relevance to the current work is the analysis presented by Throne [203] for free-radical polymerisation in the batch reactor based on the earlier work of Liu and Amundson [204].

The determination of molecular weight distributions in practice has been greatly simplified with advances in gel permeation chromatography (GPC) techniques which finds extensive use in all polymer characterisation work nowadays. It basically involves separation of the different size molecules using a packed column and amounts of the different fractions collected over time are determined in a detector. A comparison of the collected data with calibration yields the molecular weight distribution and the corresponding average molecular weights.

2.3.8.3. Polydispersity index

The ratio $\overline{M}_w/\overline{M}_n$ is a measure of the breadth of the distribution of molecular weights in a polymer sample. It is often referred to as the polydispersity index. For optimum polymer properties, $\overline{M}_w/\overline{M}_n$ should preferably be in the range 1.5 to 2.0. However, processing limitations in conventional batch or continuous reactors at high conversions often cause a broadening of the distribution giving $\overline{M}_w/\overline{M}_n$ as high as 5 [86].

Chapter 3

Aims of the Present Investigation

3. INTRODUCTION

The primary aim of this chapter is to assess the potential of using a previously built Spinning Disc Reactor for the chemically initiated free-radical polymerisation of styrene on the basis of the characteristics offered by the spinning disc technology which have been discussed at length in the first part of the literature review in Chapter 2. Obviously, a key driving force for shifting research into a completely different reactor technology for polymerisation is the limitations inherent in conventional reactor designs developed to date. An assessment of these limitations and their negative effects on the process will also be presented here coupled with a brief analysis of the way in which the characteristics of the Spinning Disc Reactor may overcome such limitations. Finally an outline of the experimental programme proposed for the current investigation will be given.

3.1. ASSESSMENT OF PREVIOUS WORK

The review of the published literature on spinning disc technology has shown that a vast amount of experimental data has been collected over more than half a century with regard to the hydrodynamics and heat and mass transfer characteristics of the thin film formed on the rotating disc. The general indication obtained from those studies is that highly improved mixing and heat and mass transfer rates to and from the thin film are achieved. These are the key features which places the technology high on the list of intensification strategies.

A range of chemical reactions has also been identified which could potentially benefit from the application of the spinning disc technology. They include gas-liquid reactions which, conventionally, are or become diffusion controlled as a result of the generally slow micromixing ability of other existing reactor designs. This problem is exacerbated for reactions which are kinetically fast and of a highly exothermic nature whereby heat transfer limitations also arise. Poor product quality, reduced yield and product selectivity and inefficient use of reactor volume all result from poor mixing performance of traditional reactors such as the stirred tank reactor.

However, although the potential opportunities of enhancing chemical reactions by the spinning disc technology appear to be attractive, only very few laboratory tests have been performed so far. Of particular interest is the recent preliminary study investigating the polymerisation of unsaturated polyester reported by Jachuck and Ramshaw [73] which also involved the development of a spinning disc reactor (SDR). The results from this work suggested that the diffusion constraints imposed by physical factors such as medium viscosity and which cause the polymerisation to proceed at a slower rate in conventional stirred tank vessels can be effectively eliminated by applying high centrifugal fields so that the reaction is carried out in thin, intensively mixed films.

The positive results obtained are encouraging enough to warrant further extensive investigation in the application of the spinning disc technology to other processes which exhibit similar characteristics and diffusion-control limitations as a result of poor engineering inherent in traditional reaction vessels. Another industrially important reaction identified in the category of diffusion-controlled systems concerns free-radical addition polymerisations of vinyl monomers. The most important monomers polymerised through this route include styrene and ethylene, of which styrene is by far the most studied. Like all polymerisation systems, the rapid rise in viscosity with progress in the polymerisation of styrene renders the bulk process very susceptible to poor mixing levels, reductions in heat transfer ability within the viscous melt and loss of temperature control, the latter being aggravated by the exothermic nature of polymerisations. The polymerisation of styrene therefore appears to be a suitable candidate for application on the spinning disc.

The development of various types of reactor vessels for polystyrene production incorporating varied design features as discussed in Chapter 2 attests to the efforts invested in attempting to suppress the problems related to the highly viscous nature of the reaction mixture. Also, the move towards different polymerisation modes such as solution, suspension and emulsion polymerisation does help to a certain extent in achieving better control but these techniques introduce other specific problems such as the need for separation step to purify the final polymer product.

An interesting feature of continuous polystyrene processes is the sequential increase in operating temperature down the line of reactors from around 100-130°C in the low conversion reactor to above 200°C at high conversions. Evidently the reason for this is to facilitate the flow and agitation of viscous material at high polymer concentration which also means a larger consumption of heating energy although admittedly this is compensated for by the reduced pumping power and agitation power. However the downside of employing higher temperatures is associated with a decrease in kinetic chain length or molecular weight of the polymer. Ideally, if high molecular weights are desirable for a given application, then the lowest economically viable process temperature is preferred.

Furthermore, the need for increased throughput of polymer product as a result of higher consumption of general purpose polystyrene over the years has implied that reactor vessels have grown much larger in size as testified in the literature review of polystyrene reactor technology in Chapter 2. It is well-known that the reduced surface area to volume ratio in such large reactors complicates the issues relating to reactor thermal stability and polymer product quality (MWD). Therefore reactors providing the required throughput without compromising on the surface area to volume ratio are desirable.

3.2. AIMS OF THE PRESENT INVESTIGATION

The present investigation looks into the applicability of the spinning disc reactor to a well known free-radical polymerisation process which has not previously been studied under SDR conditions. In view of the physical nature of the free-radical polymerisation system, the potential for success of SDR application is great. The polymerisation of styrene chemically initiated by benzoyl peroxide has been chosen as

an example of a free-radical polymerisation system mainly because the kinetics and mechanism of this reaction are fairly well-established as a result of the vast amount of past experimental and theoretical work done. Since this study involving free-radical polymerisation is the first of its kind to be explored on the spinning disc, there are various aspects of the reaction to be considered. The aims of the proposed study will therefore include the following:

1. A study of the effect of prepolymer feed conversion/ feed viscosity on conversion and molecular weight properties of the spinning disc product after one pass on the disc rotating at different fixed disc rotational speeds.
2. A study of the effect of disc rotational speed on conversion and molecular weight properties of the spinning disc product after one disc pass for a given prepolymer feed conversion/ feed viscosity.
3. An investigation into the effect of agitation rates on conversion and molecular weight properties for the polymerisation of styrene in a batch reactor which will give an insight into the way mixing affects polymerisation.
4. The ability of the spinning disc to allow intensified operations on its surface suggests that it is a highly energy efficient equipment. As part of this work, it is intended to carry out a case study to estimate the energy usage of an industrially adapted spinning disc reactor for the polymerisation of styrene. This will be compared with the energy consumed in a batch process giving the same polystyrene production capacity.
5. Based on the results of this investigation, a process involving spinning disc surfaces which could be applied to the industrial production of general purpose polystyrene will be proposed.

3.3. OUTLINE OF THE APPROACH

In order make a realistic evaluation of the performance of the existing spinning disc reactor (SDR) for the polymerisation of styrene, it is necessary to compare the relevant data from the SDR with an established type of reactor such as a stirred tank vessel. Batch calibration curves following the progress of styrene polymerisation with time in a temperature controlled laboratory scale glass reactor will be generated for conversion, average molecular weights and polydispersity index. These characteristics of the polymerisation reaction will be measured mostly by gel permeation chromatography (GPC) and in some cases by the method of precipitation.

Spinning disc runs will be performed by feeding a given conversion prepolymer prepared in the batch reactor onto the rotating disc surface set at fixed temperature of 88-90°C and selected rotational speed. The product from the one pass in the SDR will be analysed for conversion, average molecular weights and polydispersity index and compared with the appropriate batch calibration curve. Tests will be carried out for various prepolymer feed conversions/viscosity and disc rotational speeds.

With regard to the agitation study in the batch, the effect of varying the impeller speed from less than 100 rpm to about 1500 rpm on the polymerisation of styrene will be assessed by determining conversion, molecular weights and

polydispersity index of the reaction mixture at regular intervals of time over the duration of the experiment.

Using previously derived expressions for kinetic energy and power dissipation due to friction for thin films flowing on a rotating disc, it is intended to compare the energy usage of a batch process and a combined batch/spinning disc process for the production of 20 tonnes of polystyrene.

Chapter 4

Experimental Apparatus And Procedures

4. INTRODUCTION

Detailed description of the main experimental and analytical equipment employed for the purpose of the current research is given in this chapter together with step-by-step procedures for performing the experimental runs and analysis. The experimental programme has been divided into two parts. The first part relates to the **polymerisation experiments** performed in two pieces of equipment, namely a standard batch vessel and the spinning disc reactor (SDR). The purpose of these experiments was to evaluate the performance of the spinning disc reactor relative to the conventional batch reactor with regard to conversion and molecular weight properties for the polymerisation of styrene. In the second part, details of the **agitation experiments** exploring the effect of various agitation rates on the batch polymerisation of styrene are presented.

Conversion and molecular weight data for both sets of experiments were obtained by sample analysis in a gel permeation chromatography system which will also be described below. The changes in macroscopic properties such as viscosity during polymerisation can often be associated with changes in the polymerisation rate. As part of the experimental programme, a Bohlin Viscometer was used to obtain viscosity data for samples collected over the course of several batch polymerisation runs. Description of the essential parts of the viscometer will be given in this chapter. For safety reasons, all experiments were conducted in either an enclosure fitted with an extractor unit or in a fume cupboard.

4.1. POLYMERISATION EXPERIMENTS

4.1.1. Batch reactor system

The use of the batch vessel was two-fold: (1) to generate a calibration curve following the progress of polymerisation with time which would eventually serve as a benchmark for the performance of the spinning disc reactor and (2) to prepare the desired prepolymer for feeding into the spinning disc reactor. The batch reactor system, shown in Plate 4.1 and schematically in Figure 4.1, consisted of a 250 ml capacity volume 'Pyrex' glass vessel surrounded by a water circulator system. The circulating water was pumped from a constant temperature bath which was provided with a digital controller unit for temperature control. The reactor stood in the centre of a magnetic plate which together with a magnetic stirrer in the reaction mixture was used to provide uniform temperature and adequate mixing levels throughout the polymer melt. The speed of mixing in the batch mixture was manually controlled by a knob on the magnetic plate. Access to the glass vessel was provided by two stopped arms, one of which was inclined at 45^{o} to the horizontal and the other was vertical. A thermocouple was inserted through the inclined arm and was connected to the data logger to record the temperature of the melt. The vertical arm was used for feeding the

Chapter 4. Experimental Apparatus and Procedures

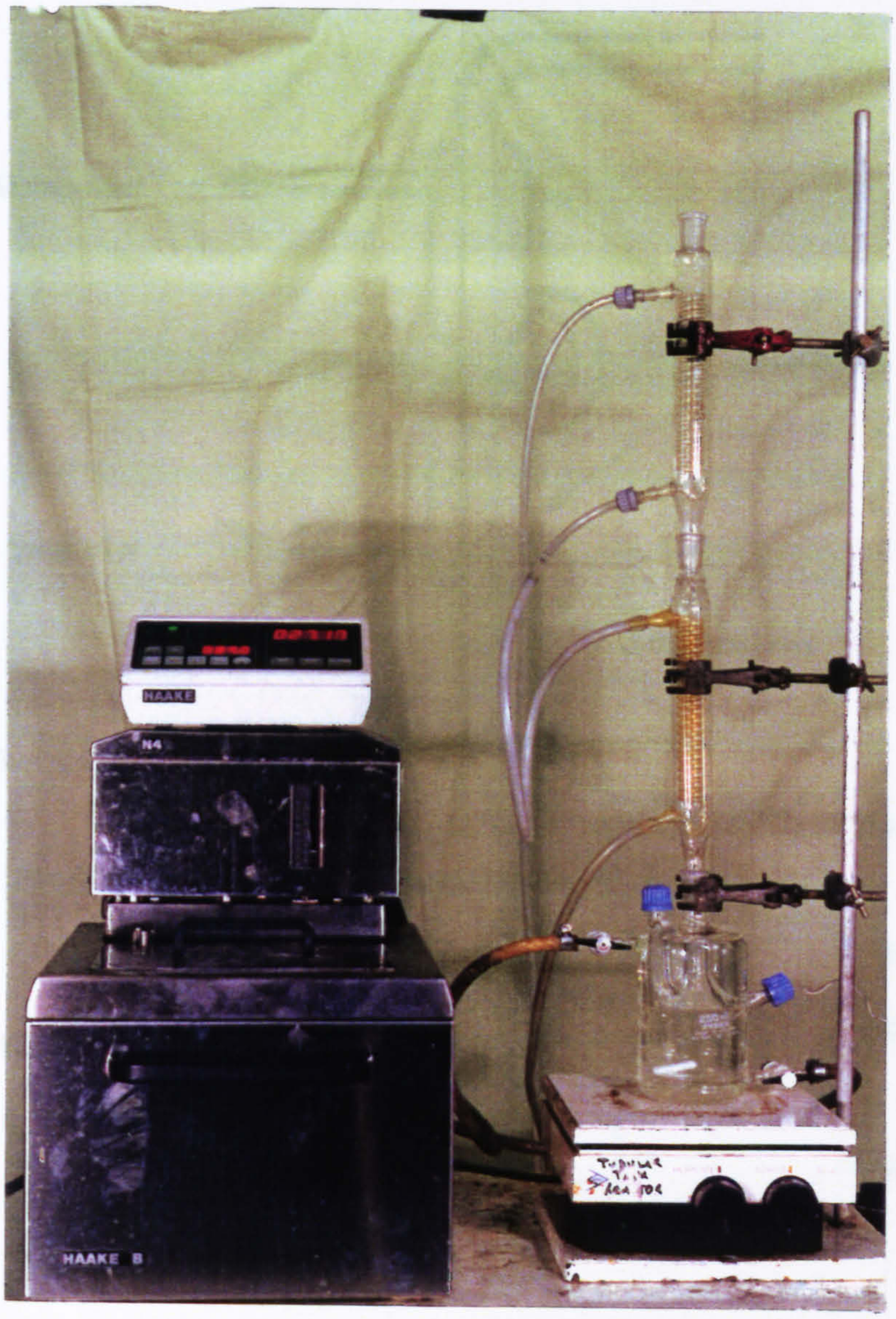

Plate 4.1. Batch reactor set-up

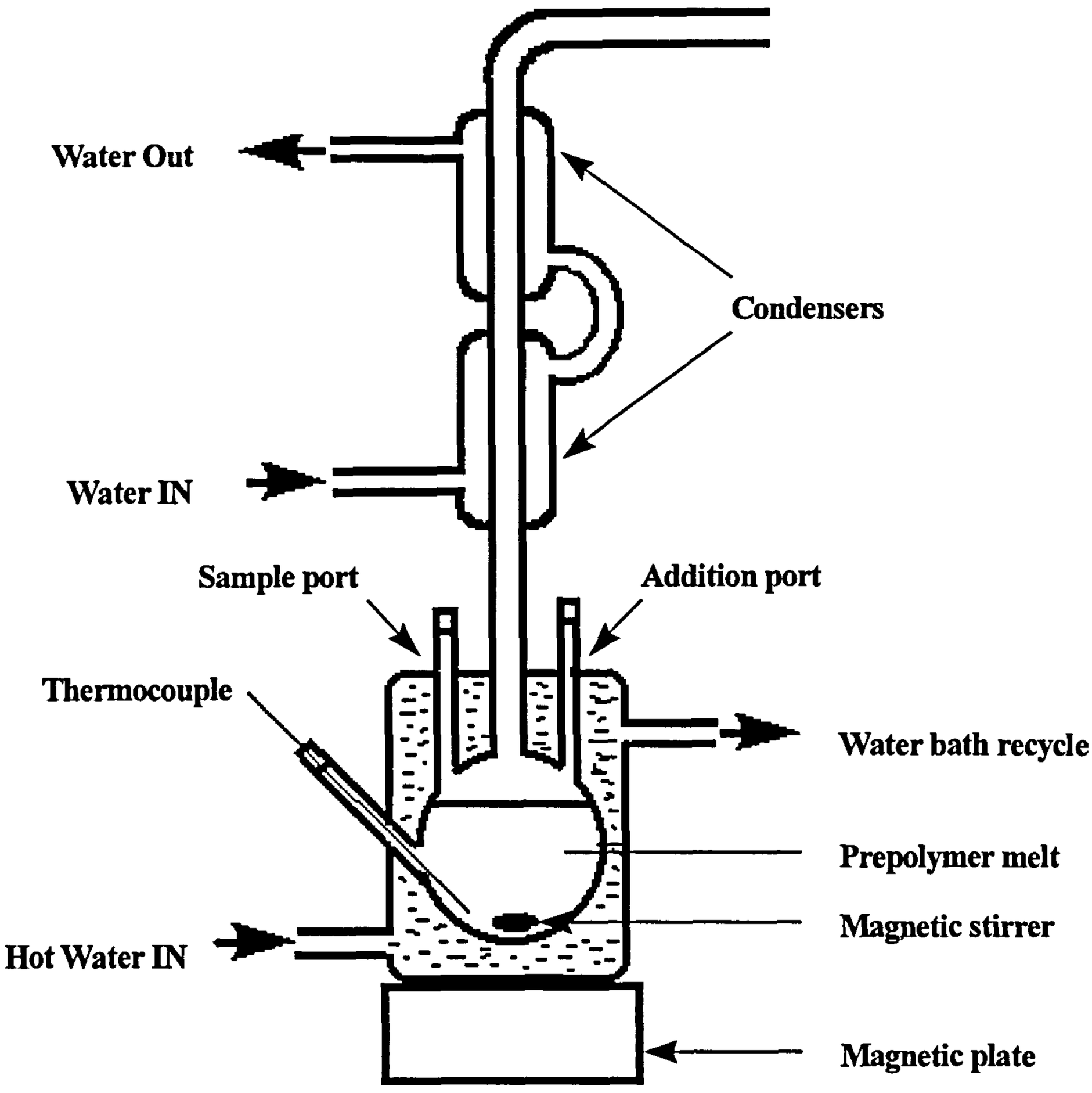

Figure 4.1. Schematic of batch reactor system

monomer, solvent and initiator into the reactor and for taking samples from the reaction mixture as required. The top end of the vessel was fitted with a vertical condenser system to prevent loss of volatile material. In the first stage of the research, the condenser system was comprised of one condenser unit which was replaced by two condensers in series in later experiments to ensure complete condensation.

4.1.2. Spinning Disc Rig

The set-up of the spinning disc rig used in the polymerisation study is shown in Plate 4.2. The rig consisted of three main items as follows:

1) Spinning disc equipment (detailed in section 4.2.2.1)
2) Condenser system
3) Instrumentation (temperature data acquisition unit, temperature controller, speed control regulator and speed measuring device)

4.1.2.1. Spinning disc reactor

The outside and inside views of the spinning disc reactor are displayed in Plates 4.3 and 4.4 respectively and a schematic representation is shown in Figure 4.2. The reactor was made up of the following main components:

1) Spinning disc surface
2) Thermocouples, slip ring assembly and motor arrangement
3) Electric heater
4) Prepolymer feed distributors
5) Product collector
6) Reactor housing
7) Cooling coils

Most of the design features of the spinning disc reactor to be described below were adopted for the purpose of the heat transfer research work [22]. A few modifications with regard to the feed and cooling systems had been made for the polymerisation studies as will become apparent below. Also, the replacement of some damaged thermocouples required that a new slip ring assembly mounted on the bottom surface of the disc arrangement be fitted. The design before and after these modifications were put in place will be described in the section which follows.

4.1.2.1.1. Spinning disc surface

The rotating disc system was made of brass and consisted of a top disc bolted onto a base disc, the contact surfaces of which have been machined to ensure good thermal contact. Brass was selected as the material of construction on the basis of its high thermal conductivity which was an important consideration in the heat transfer work for which the equipment had initially been built. The double disc arrangement was chosen at the design stage to facilitate the replacement of various top discs with different surface configurations. The double disc arrangement was chosen at the design stage to facilitate the replacement of various top discs with different surface configurations.

The base disc measured 360mm in diameter and was 30mm thick. Holes of 1mm diameter had been drilled at chosen locations to allow thermocouples to pass through to the top disc. The top disc also had holes at identical positions which were

Plate 4.2. Spinning Disc Rig

Chapter 4. Experimental Apparatus and Procedures

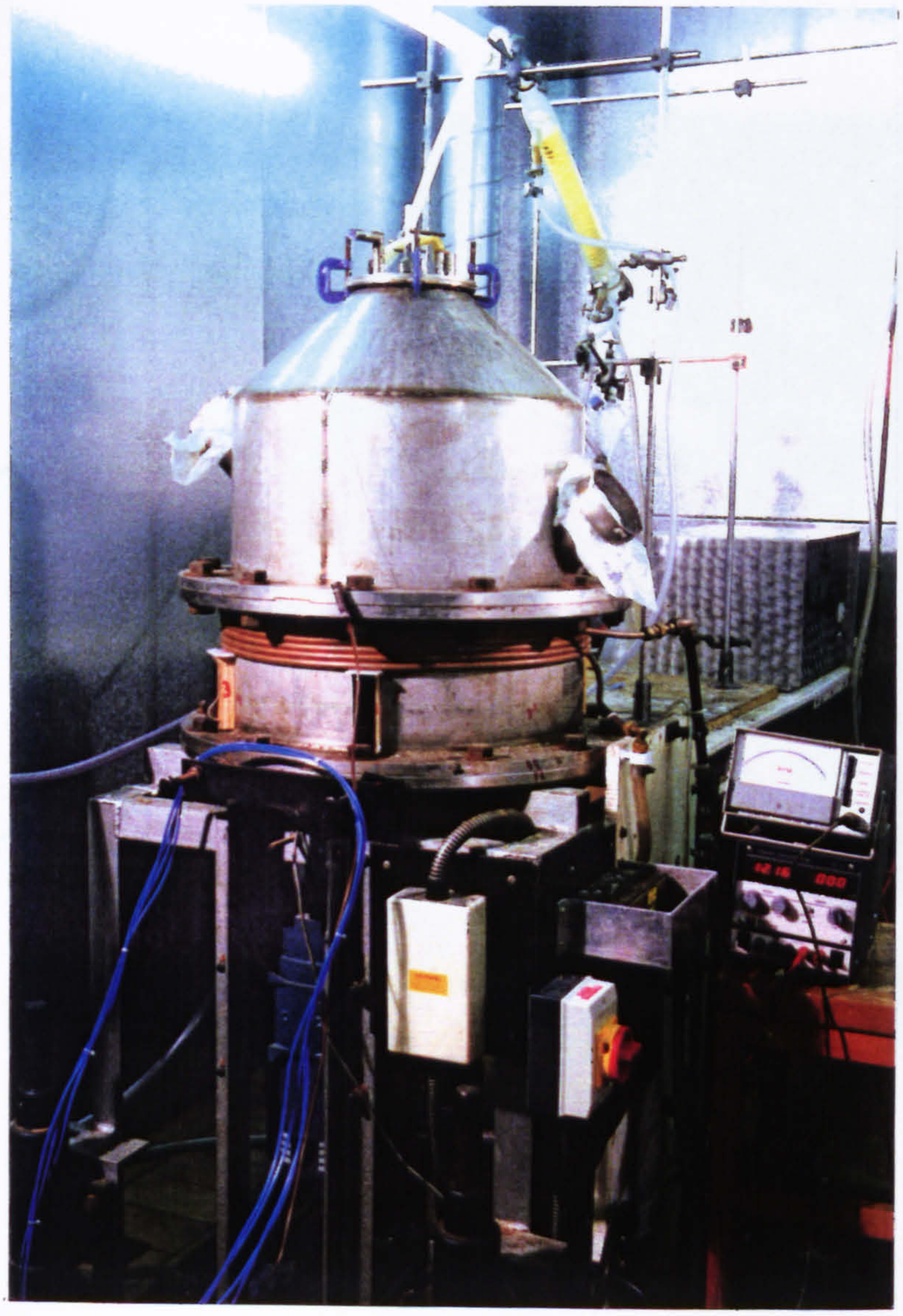

Plate 4.3. Outside view of Spinning Disc Reactor

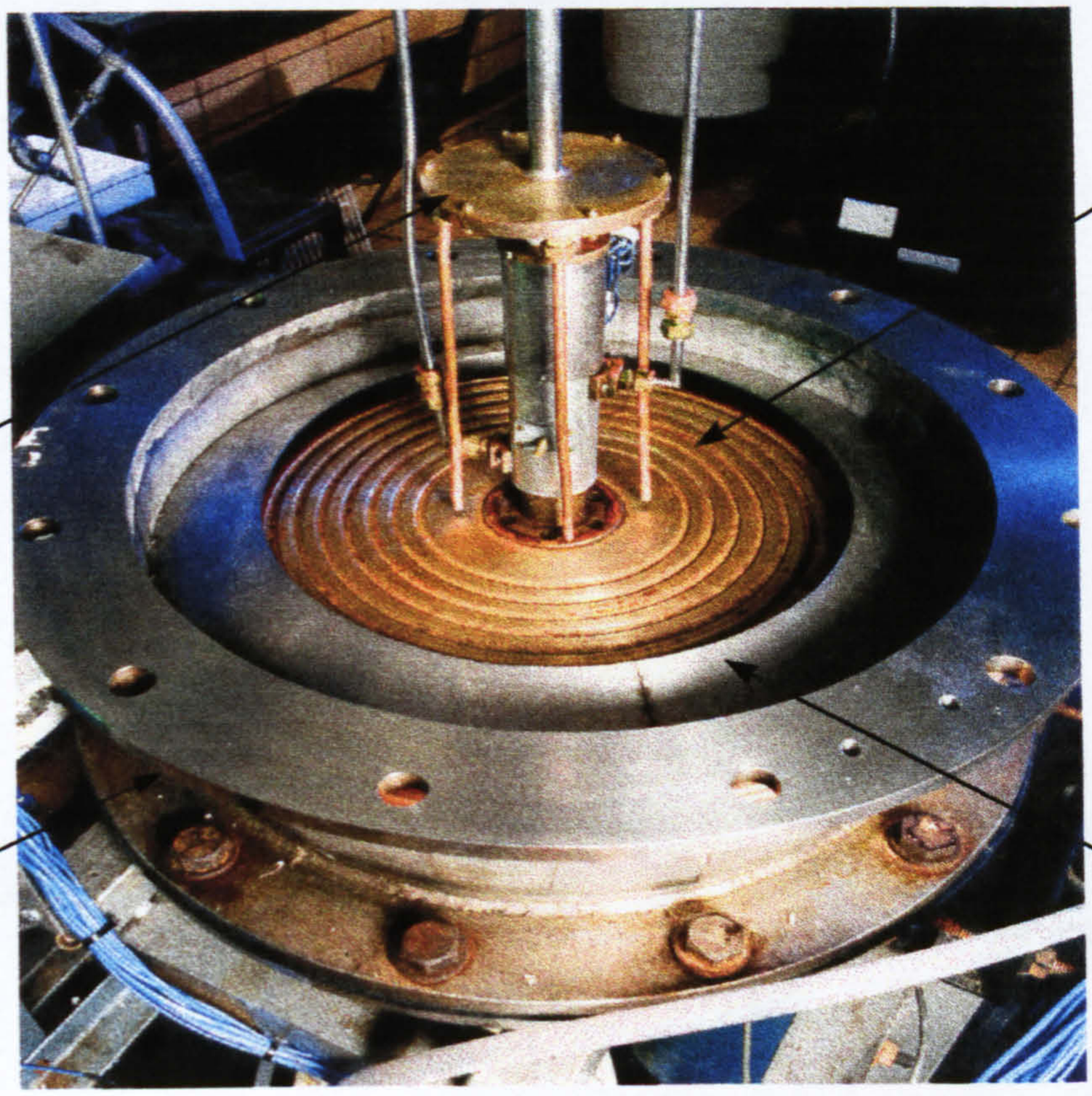

Plate 4.4. Inside view of Spinning Disc Reactor

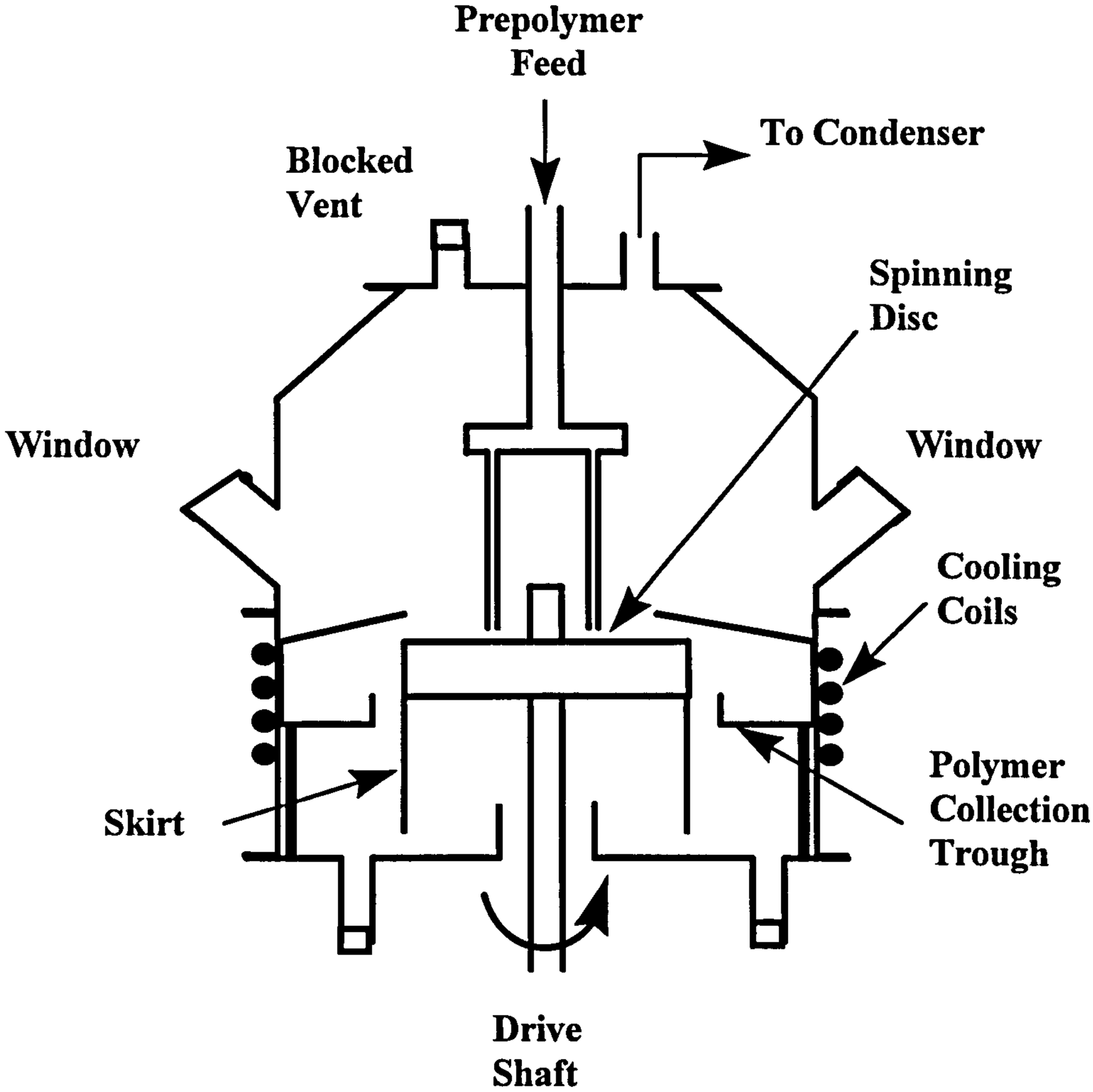

Figure 4.2. Schematic of spinning disc reactor

of 1mm diameter and at distances of 2mm and 11mm below the upper surface for the thermocouples. When bolted together, the two discs rotated about a vertical axis as a single unit. The horizontal displacement of the disc unit, caused by the vibration of the shaft, had been measured by using a dial test indicator and found to be less than 0.05mm which was acceptable.

The top disc was 17mm thick and 360mm in diameter, with a superficial heat transfer area of approximately $0.1m^2$ for the exchange of heat between the liquid film and the disc. Based on the earlier heat transfer results which had established that a normal grooved disc gave the highest heat transfer rates [22], the normal grooved configuration was the obvious choice for the top disc surface. As shown in Plate 4.5, the disc had seven concentric normal grooves machined in its surface at radial distances of 70, 85, 100, 115, 130, 145 and 160 mm. Each groove was 15mm wide which included a 6mm flat section and two inclined sections of 7mm and 2mm. The angle of inclination for the 7mm section was 15° and that for the 2mm section was 45° giving a groove depth of 2mm. The detailed geometry of the grooves can be seen in Figure 4.3. The presence of these grooves in the disc surface helps to enhance the heat and mass transfer performance by inducing the formation of a large number of small waves (Plate 4.6) which create instabilities in the film and at the same time by increasing the exchange area of the disc.

4.1.2.1.2. Thermocouples, slip ring assembly and motor arrangement

In the initial design, six T-type thermocouples were embedded in the top disc at 2mm below the surface at radial distances of 50, 60, 75, 133, 168 and 175mm respectively. By measurement of the surface temperatures at those several positions, a reliable temperature profile was obtained across the disc. For the purpose of the heat transfer work where calculation of the heat flux across the disc arrangement was necessary, another set of five thermocouples were embedded at 11mm below the surface at radial distances of 50, 75, 133, 168 and 175mm respectively. However, the readings from the latter thermocouples were not taken into consideration in the polymerisation study as only the surface temperature of the disc was of practical relevance. Two more thermocouples at radial distances of 50mm and 178mm were left exposed to the liquid film to measure the polymer melt temperature. The connection of the thermocouple wires to the data acquisition computer was made through a slip-ring assembly. The latter which was protected by a shroud and cooled by compressed air during rotation of the disc was supported on a boss of radius 35mm fixed to the centre of the disc.

A new bottom mounted slip ring assembly was subsequently fitted during the course of the experimental programme to replace the previous one which was worn out. Its new position at the bottom of the disc arrangement eliminated the need for cooling by compressed air. All twelve thermocouples initially put in were also replaced by four new T-type ones, two of which were just underneath the disc surface and the other two located right through the disc to measure its temperature. The exact locations of the four thermocouples are given in Appendix E (section E1.2.5).

The disc was rotated by a variable speed electric motor positioned on the central shaft which supported the double disc arrangement.

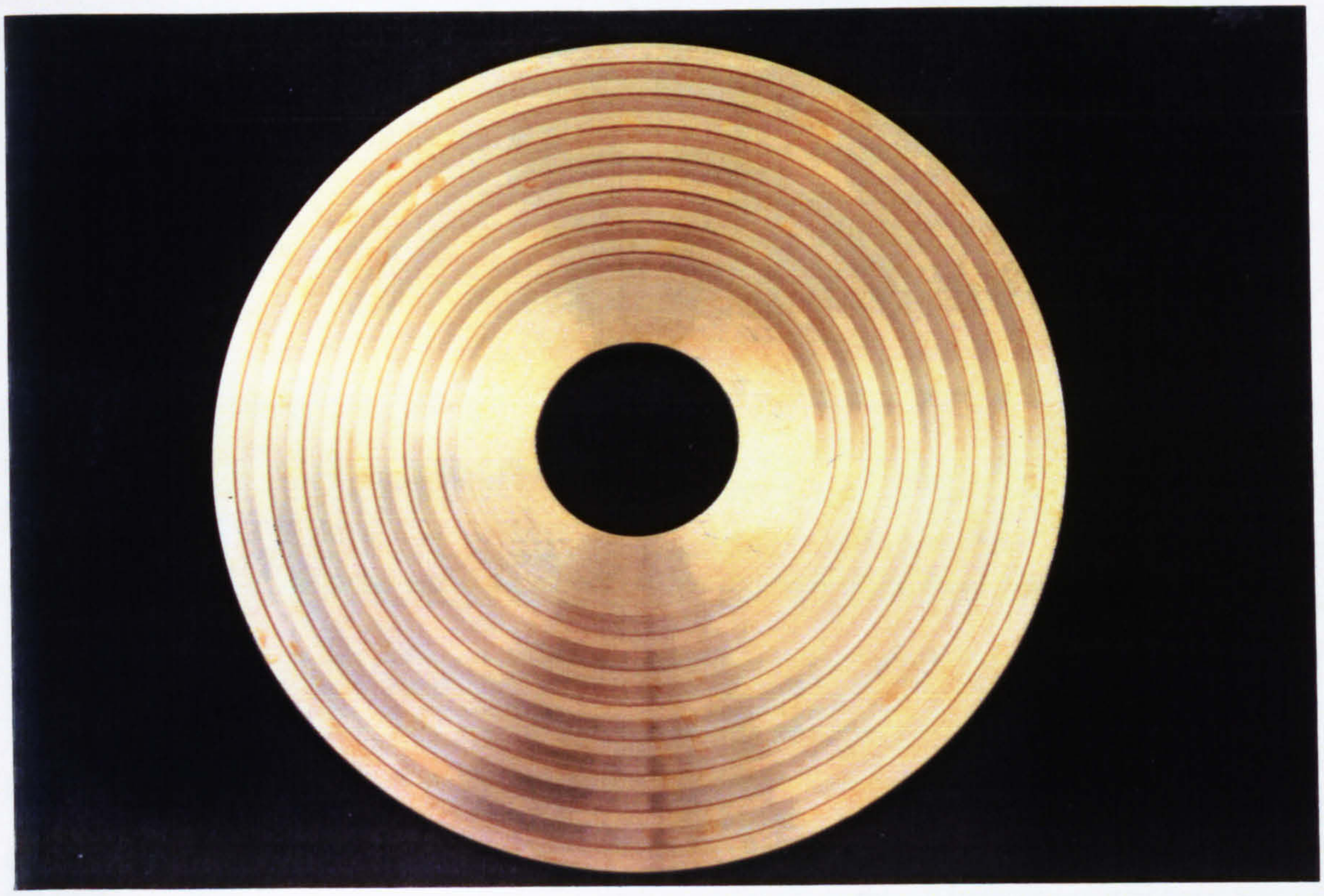

Plate 4.5. Concentric normal grooves in disc surface

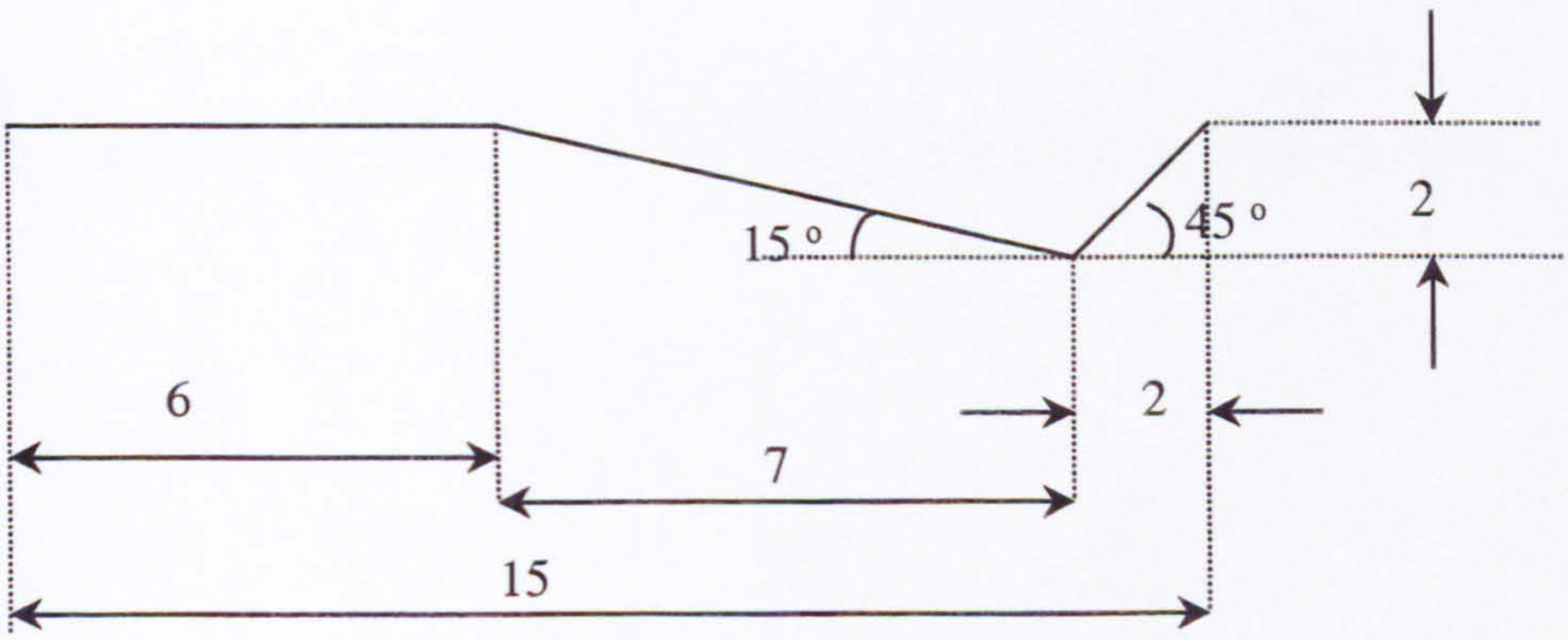

Figure 4.3. Normal groove geometry

Chapter 4. Experimental Apparatus and Procedures

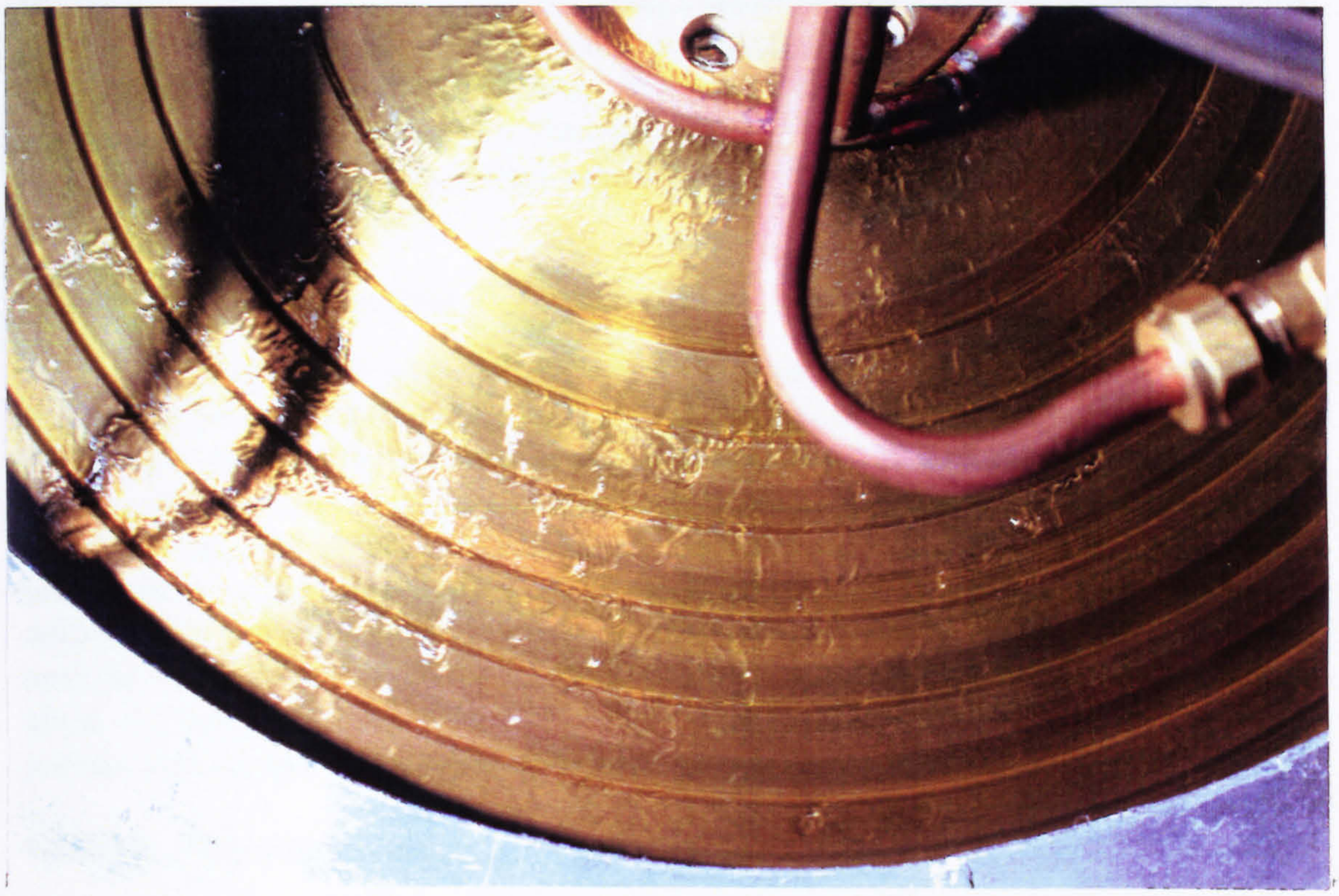

Plate 4.6. Surface waves on thin liquid film flowing on rotating disc

4.1.2.1.3. Electric heater

Radiant heat was supplied to the disc by concentric heating rings having a power rating of 3.9 kW and placed 40mm underneath the base disc. A skirt extending from the edge of the base disc and completely surrounding the heating unit shielded the latter from any liquid flowing off the disc and bouncing off from the collector wall.

4.1.2.1.4. Prepolymer feed distributors

The prepolymer was fed into the spinning disc reactor through a central port in the lid of the reactor where it flowed down a small pipe to a circular distributor. Four evenly spaced thin copper tubes extended downwards from the distributor as shown in Plate 4.7. When in place in the reactor, the ends of the copper tubes were about ½ cm above the disc surface at a radial distance of about 50mm from the centre of the disc as shown in Plate The prepolymer was delivered onto the disc surface after passing through the distributor tubes.

4.1.2.1.5. Product collector

An annular ring made of stainless steel positioned against the external wall of the reactor housing was used to collect the spinning disc product after it was thrown off the disc surface. The collector is displayed in Plate 4.8. The inner, cylindrical ring of the collector was 39 cm in diameter and about 3 cm high while the outer 49 cm diameter ring, also cylindrical, was about 7 cm in height. A cone of about 8 cm wide was welded to the outer ring at an angle of about 30^{o} to the horizontal acting as deflectors to prevent product bouncing off the wall of the collector to be thrown back onto the disc surface. When the collector was in place, the inner ring was located at about 1-2 cm below the edge of the disc to ensure that the most of the polymer product was thrown into the collector after leaving the disc.

4.1.2.1.6. Reactor housing

The spinning disc surface and its associated parts described above were housed in a stainless steel enclosure which consisted of a removable top section and a bottom section, the latter being fixed to the framework support. The top section consisted of a bottom cylindrical portion and a top conical shaped portion. Two viewing windows covered by transparent plastic material were provided on opposite sides of the cylindrical part to enable direct visual observation of the flow on the spinning disc. During operation of the reactor, the flanges of the top and bottom sections were bolted together with PTFE joint sealant between the two surfaces to ensure a complete seal from the surrounding environment. A central lid with provision for a port leading to the distributor tubes and other ports for gaseous outlet and thermocouples was located on the conical end of the top section. Ports in the lid not in use during operation of the reactor were blanked off by rubber bungs.

4.1.2.1.7. Cooling coils

Several copper cooling coils wound around the outside of the base of the reactor housing were used as a water jacket for cooling the collection trough in an attempt to cool the polymer product collected from the disc, thereby preventing further

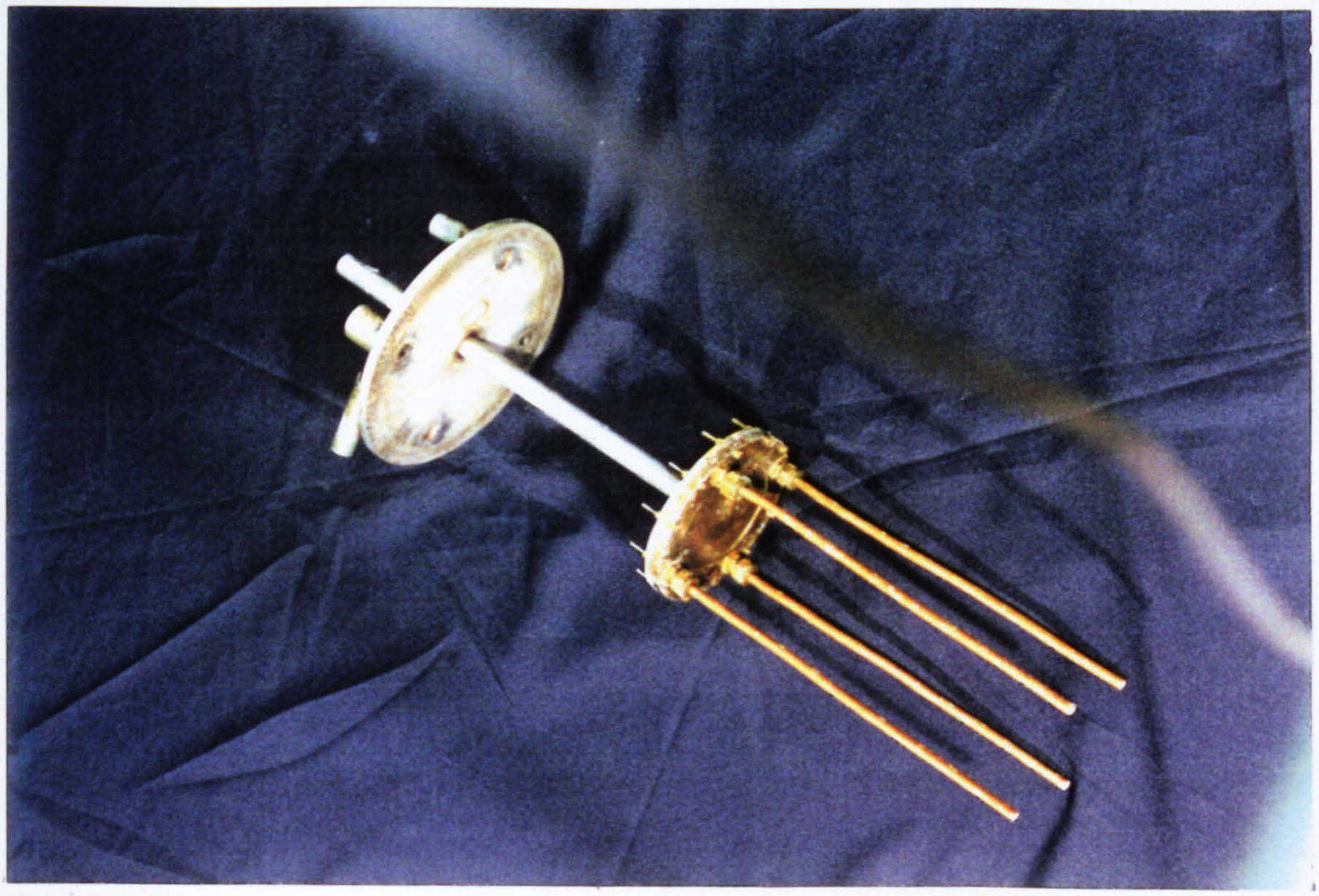

Plate 4.7. Prepolymer feed distributor tubes

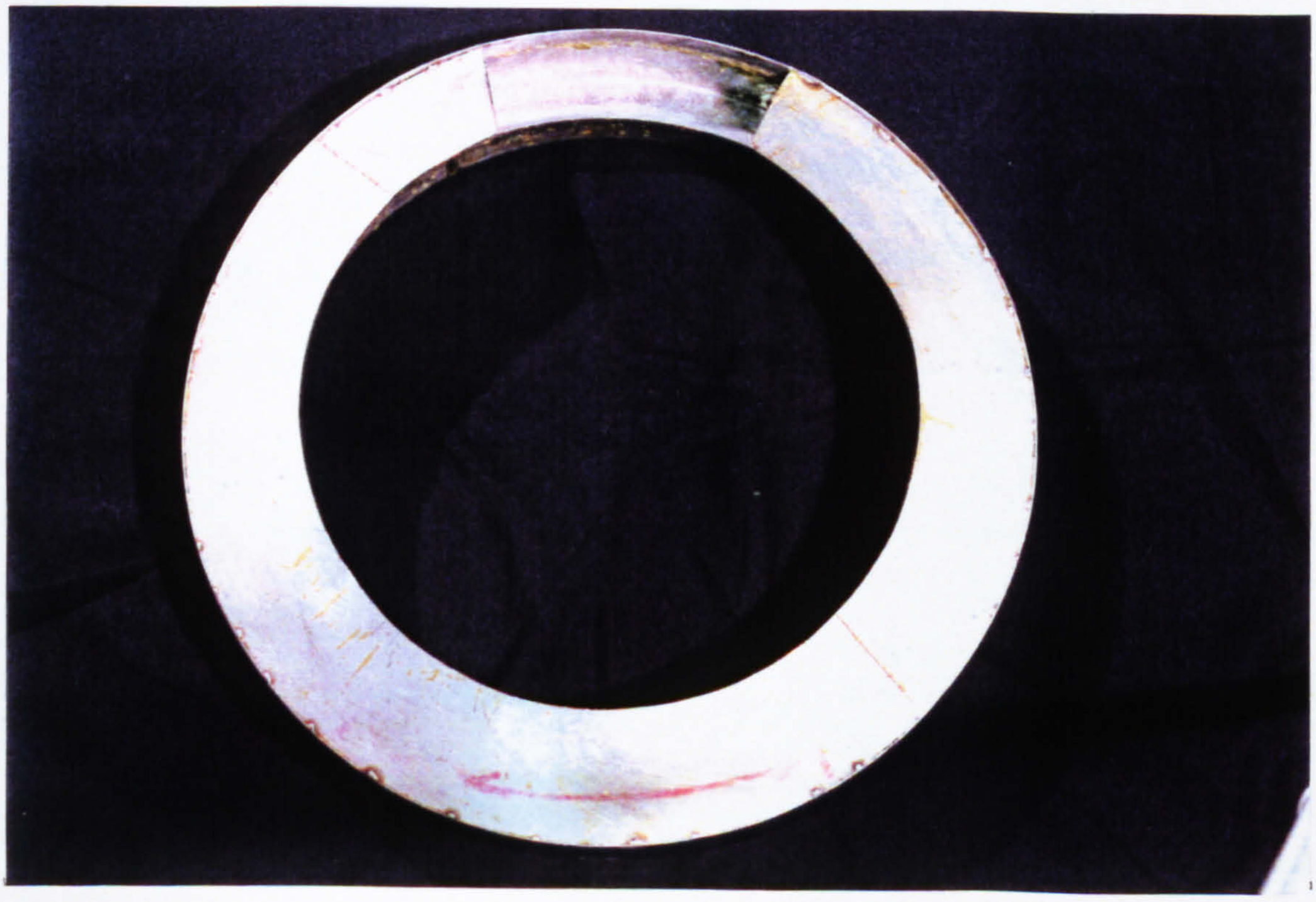

Plate 4.8. Annular ring product collector

polymerisation. This was to ensure that the sample collected was a true representation of the product leaving the disc surface.

4.1.2.2. Condenser system

The gas outlet pipe in the lid of the reactor was connected to an inclined condenser unit to condense any volatile material evaporating from the disc surface. A flask was placed at the end of the condenser to collect the condensate formed. Mains water flowed through the condenser as coolant.

4.1.2.3. Instrumentation

The disc temperature was regulated by a temperature control unit from which the desired temperature and heating rate was set. A trip system was designed to prevent the temperature of the vapour above the disc surface to rise beyond the flash point temperature of the chemicals used. This was achieved by measuring the vapour space temperature by a probe which automatically shut down the heater via the control box as soon as the temperature rose beyond the set temperature of the probe. Data from thermocouples in the disc surface were processed in a data acquisition unit.

A speed control regulator system was used to vary the disc speed in the range 0-1500 rpm. The rotational speed of the disc was measured initially by a stroboscopic lamp which was later replaced by an analogue tachometer with a sensitivity within ± 10 rpm.

4.1.3. Procedures

4.1.3.1. Batch calibration runs

Batch runs were performed to produce calibration curves of conversion, molecular weights and polydispersity index against time. These curves were then used to bench mark the performance of the spinning disc polymeriser as far as such characteristics were concerned. Since variations in different sets of batch data inevitably occurred, a batch calibration curve was produced for each set of experiments in the spinning disc reactor operating under different conditions in order to ensure that valid comparisons between the batch and spinning disc data were made at all times.

Styrene monomer and toluene solvent were preheated and stirred for about 15 minutes in the glass vessel until the desired starting temperature of 88^{o}C was reached. The toluene/styrene initial molar concentration ratio was increased from 0.05 to 0.22 during the course of the experimental work to extend the batch reaction time without the difficulty of handling very viscous polymer melts and to achieve improved temperature control in the batch mixture. The temperature of the water bath surrounding the vessel was set at 88^{o}C on the control panel. The magnetic stirrer was switched on to provide uniform temperature throughout the mixture. Water was allowed to flow at a reasonable rate through the condenser connected to the top end of the reactor. The stop clock was started on addition of benzoyl peroxide initiator through the vertical stopped arm of the batch vessel.

Temperature measurements were taken at intervals of 10 minutes. Samples were removed from the batch at 10 minute intervals by means of a teat-pipette and crash cooled in cold water to prevent any further polymerisation before analysis.

4.1.3.2. Spinning Disc Runs

The general procedure of performing a disc run involved two stages, the first being the preparation of the desired prepolymer feed for the SDR in the batch vessel (prepolymer stage) followed by transfer of the prepolymer onto the spinning disc (spinning disc stage).

4.1.3.2.1. Prepolymer stage

The prepolymerisation was carried out in the batch reactor to a selected level of conversion which was known from the calibration curve obtained as outlined in the previous section. The operating procedure for the prepolymer stage was the same as that used for the batch runs and samples were taken at intervals of 10 minutes until the time selected for termination of the stage was reached. As soon as the preparation of the prepolymer was completed, it was poured down onto the spinning disc surface via the feed distributor tubes.

4.1.3.2.2. Spinning disc stage

The spinning disc was started at a low rotational speed and the electric heater was switched on. Cooling water to the condenser and skirt jacket were turned on. The flow of air to the slip-ring assembly was also turned on. However, after the new slip-ring was fitted at the bottom of the disc arrangement (see section 4.1.2.1.2), the latter step was no longer applicable. Shortly before the final operating temperature of 88°C was reached, the disc was brought up to the required rotational speed and the prepolymer was poured down the feed port. The disc was allowed to rotate for about 2-3 minutes to ensure that almost all of the feed introduced had sufficient time to flow down the distributor tubes and come into contact with the disc surface. After passing over the disc surface, the polymer melt was thrown off the disc surface into the collecting trough. Samples were taken immediately after the disc stopped rotating and they were crash-cooled in cold water before analysis was carried out by either GPC or precipitation method.

4.2. AGITATION EXPERIMENTS

4.2.1. Apparatus

The set-up of the test facility employed in the agitation study is shown in Plate 4.9. The essential parts of the equipment were a glass polymerisation vessel, an impeller driven by an electric motor and a temperature controlled water bath. The polymerisation reactor consisted of two parts, namely a 6 cm inner diameter Pyrex glass cylinder about 10 cm high and a hemispherical top cover. In operation, the flanges of the two sections were tightly held together by a metal coil. The vessel cover had provisions for a bent side arm used to connect two condensers in series, a central opening for the agitator shaft and finally two capped openings on each side of the central port, one for pouring the reaction mixture and the other for insertion of a

thermocouple (K-type). In one of the preliminary experiments, a brass turbine impeller was used as the mixing device during the polymerisation. However, after it was found that some complex reaction between one or more of the reagents and the brass material was inhibiting the progress of reaction, the brass impeller was subsequently replaced by a 5 cm diameter stainless steel propeller fixed to a 13.5 cm long stainless steel shaft (Plate 4.10) The end of the agitator shaft was fixed onto a rotor seal (Premex Reactor AG 10 Ncm) which, when fitted into the central opening, ensured that an air-tight environment was obtained. When in place, the propeller was located at a distance of 3 cm from the bottom of the vessel. The other end of the rotor seal was locked onto the variable speed electric motor mounted in a vertical position above the seal. The cylindrical portion of the reactor was surrounded by an outer glass jacket fed with water pumped from the digitally controlled temperature bath (supplied by Haake). A tap opening located at the bottom of the vessel allowed samples to be removed from the reactor during the course of the experiment.

A portable stroboscope was used to measure the rotational speed of the agitator.

4.2.2. Procedures

The motor/agitator speed in revolutions per minute (rpm) was first calibrated by rotating the impeller in a styrene/toluene mixture heated to an average temperature of 88°C and measuring the speed of rotation by the stroboscope. The calibration details and results are presented in Appendix F.

The experimental procedures adopted for the agitation runs were similar to those for the batch runs as detailed in section 4.2.3.1. The toluene/styrene molar concentration ratio was maintained constant at 0.22 in all the experiments. However an increase from 240 ml to 270 ml in total initial reagent volume was necessary in later experiments (as a result of a slight change in the dimensions of the vessel used in these experiments) to ensure that the impeller was positioned about half-way in the polymerisation mixture for good mixing throughout the contents. The height of the liquid in the reactor was then about 8 cm. The motor was switched on to rotate the impeller at low speed during the preheating period of the styrene and the toluene mixture, thus providing a uniform temperature distribution. Just before the addition of benzoyl peroxide initiator to the vessel, the motor was geared up to the required speed. Temperature measurements were taken at regular intervals of 5 minutes from the start of the polymerisation by means of a hand-held temperature recorder. The speed was also constantly monitored at intervals of 5 to 10 minutes throughout the course of each experiment by means of the stroboscope and was readjusted if necessary to the set value. Samples were taken every 20 minutes from the mixture from the tap at the bottom of the reactor. In order to check that samples collected from the tap were representative of the bulk polymer mixture, one further sample was taken at the end of the polymerisation run from inside the vessel after it was opened.

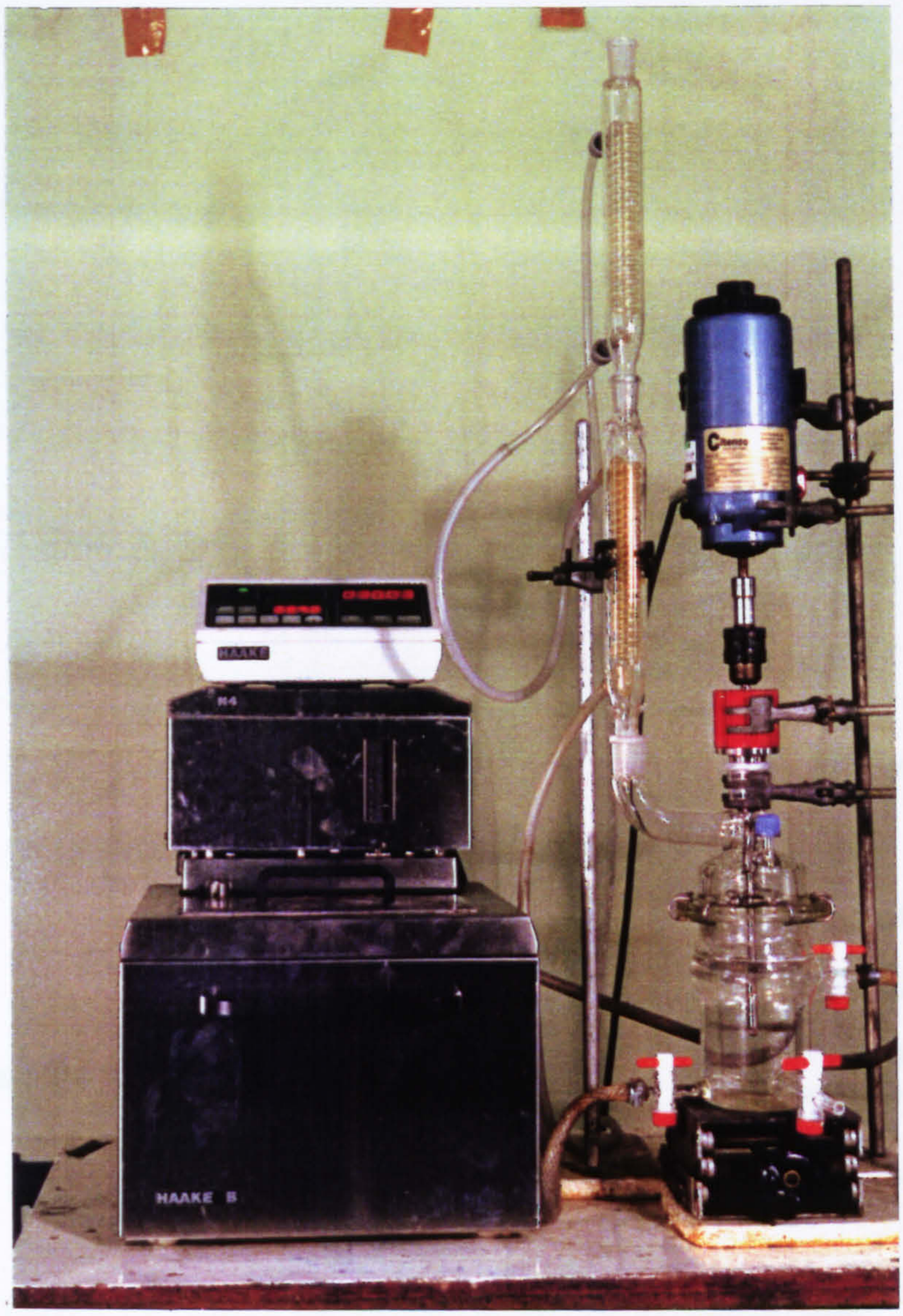

Plate 4.9. Test facility for agitation study

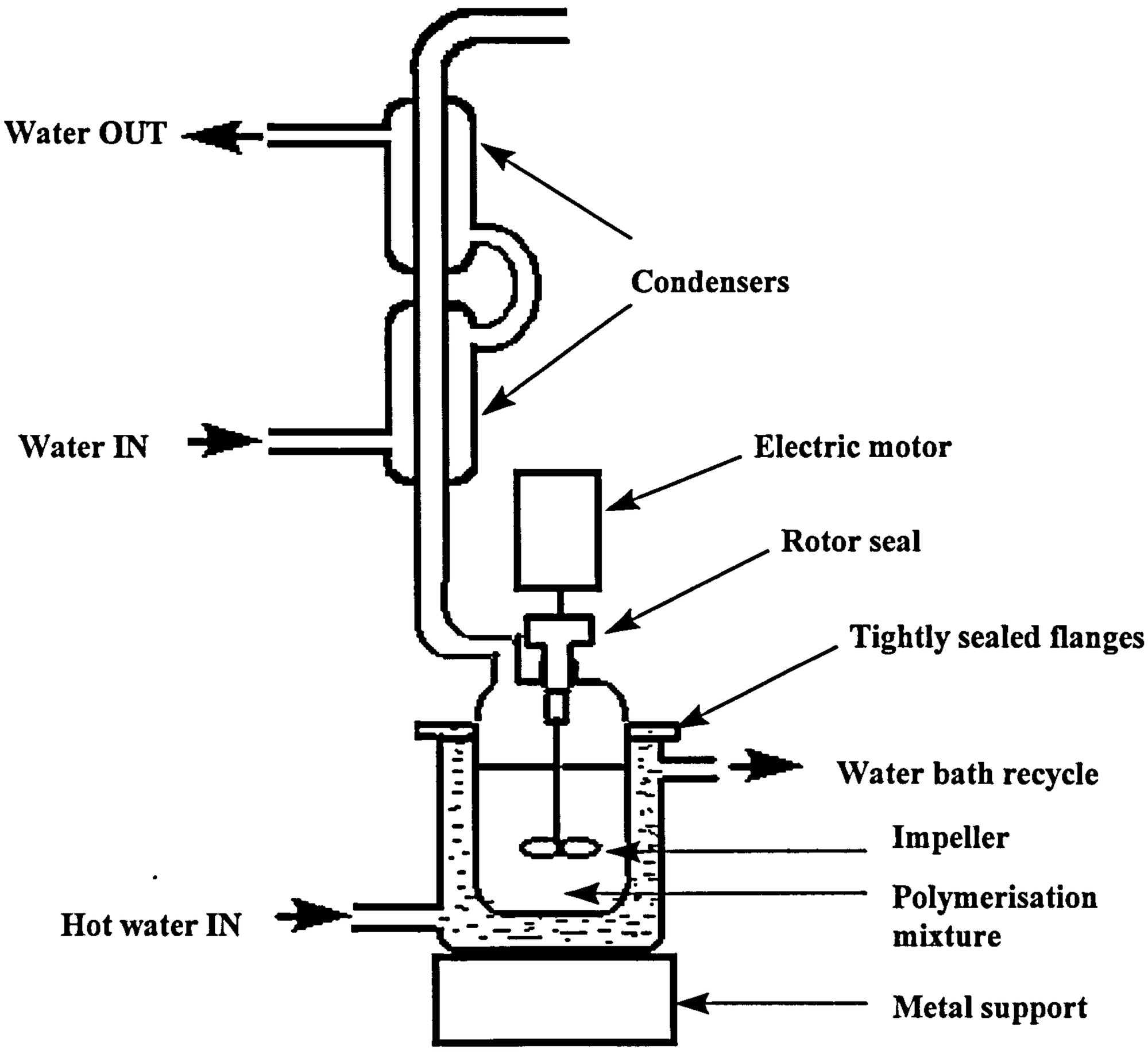

Figure 4.4. Schematic of test facility for agitation study

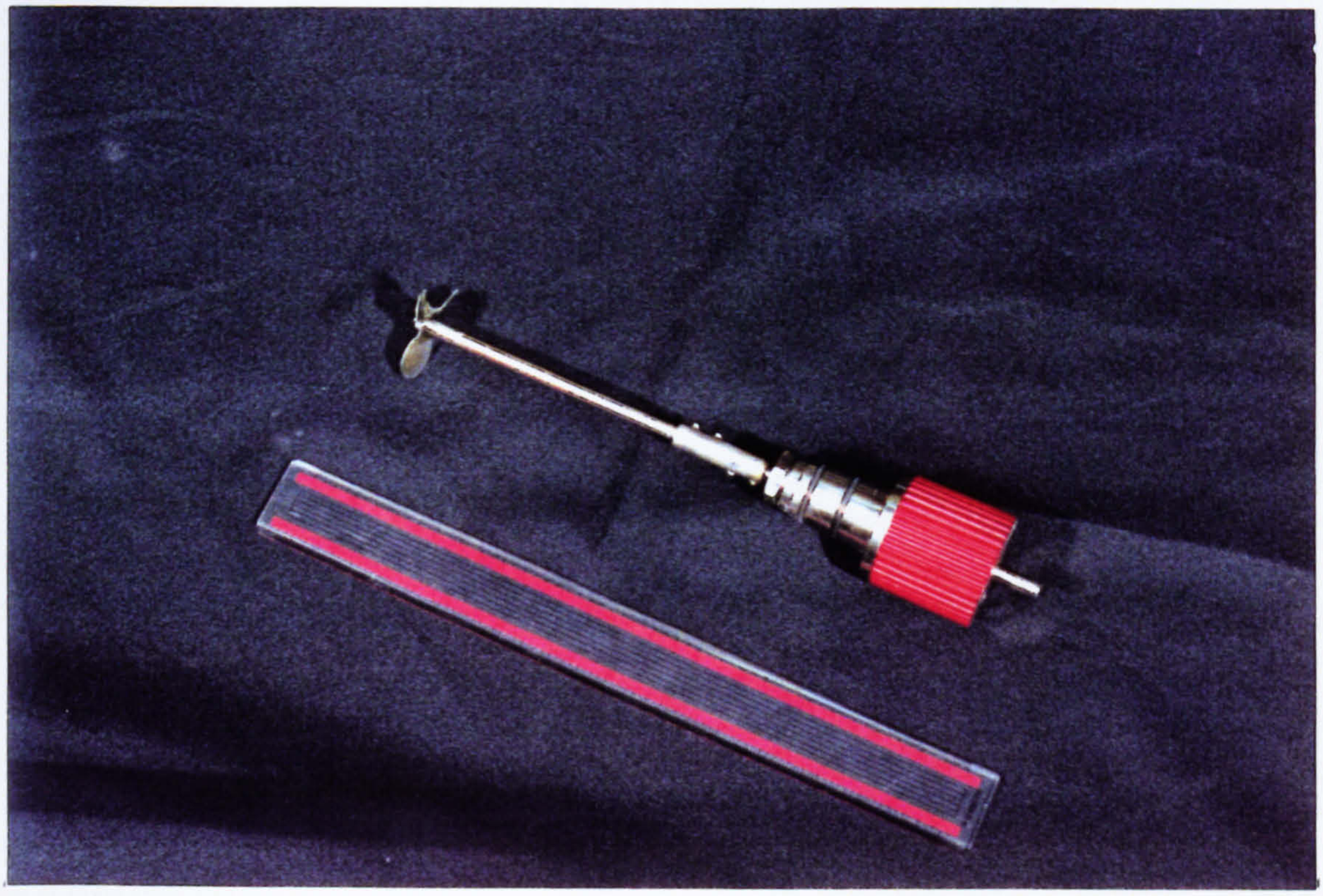

Plate 4.10. Propeller agitator with rotor seal

4.3. ANALYTICAL METHODS

4.3.1. Precipitation

In the preliminary stages of the experimental runs, precipitation of the polymer by methanol was the main analytical tool used to obtain conversion. Excess methanol was added to a known weight of sample contained in a sample bottle. The mixture was shaken vigorously and left overnight for the polymer to separate out as a white precipitate. After the remaining solution was carefully poured out, the precipitate was washed with more methanol and dried at 65-70°C on a hot plate to constant weight. The weight of the dry precipitate corresponded to the mass of polymer in the given sample. Details of conversion calculations using this method are given in Appendix D. The shortcoming of this analysis was that it did not provide any information about the molecular weight properties of the polymer. It was henceforth decided to perform all subsequent analysis for conversion and molecular weight properties in a gel permeation chromatography (GPC) equipment supplied by Polymer Laboratories.

4.3.2. Gel Permeation Chromatography (GPC)

4.3.2.1. Apparatus

The GPC set-up, as displayed in Plate 4.11, consisted of the following main items of equipment:

1) THF Solvent reservoir with inlet filter
2) Degasser (Model ERC-3215)
3) Pump (Model LC1120)
4) Column oven (SSI Model 505)
5) Analytical columns (2 x PLgel 5μm Mixed-C columns with 5μm PLgel guard)
6) Refractive index (RI) detector (Model ERC-7515A)
7) Data Converter Unit (DCU) (supplied by Polymer Laboratories)
8) Computer with PL Caliber® GPC/SEC and LC-GC softwares designed by Polymer Laboratories

Where relevant, more details about the description and operating conditions of individual components listed above can be found in Appendix D.

4.3.2.2. Sample preparation and analysis

Prior to injection into the analytical columns, the samples were prepared by dissolving a known mass (ca. 50 mg) in 10 ml of THF solvent measured by a pipette. The concentration of the prepared solutions should be in the range 0.4%- 0.6% g of sample/ml of solvent in order not to overload the columns. Damage to the column from large impurity particles was avoided by passing the solution through a 0.45μm filter before injection of 100 μl into the column by means of a syringe. Conversion and molecular weight data from calibration samples made up from PS Easical standards were processed by the LC-GC and GPC/SEC softwares respectively to generate data for experimental samples. Details of calibrations results can be found in Appendix D.

4.3.3. Viscometry

4.3.3.1. Apparatus

The Bohlin Visco 88 BV viscometer supplied by Bohlin Instruments Ltd. is shown in Plate 4.12 together with a temperature controlled water bath and an external computer. The viscometer featured a built-in Pt-100 temperature sensor which when fully immersed in a given sample recorded the temperature of the sample. However, this is only possible with coaxial cylinders (or cup and bob) as measuring systems. In the current set-up, water from the bath was pumped to a small reservoir beneath the base plate which was thus heated up to the temperature of the water.

In the current viscometry analysis, three different cone and plate geometries namely CP5/30, CP2.5/15, CP2.5/30 (where CP5/30 refers to a cone angle of 5° and a cone diameter of 30 mm etc.) were used to measure shear stress, shear rate and viscosity of polymer samples collected from a number of batch polymerisation runs.

4.3.3.2. Sample analysis

The gap between the truncated cone and the plate was first set using the appropriate shims provided, that is 70 μm for 2.5° cone and 150 μm for the 5° cone. The temperature of the water bath was set at 30-35°C initially but was later increased to about 50°C for the most viscous samples. A small amount of the test sample was placed on the plate and the cone was lowered to the preset position determined by the gap setting procedure described above. The excess sample after compression was removed, leaving only a slight bulge around the edge of the cone. Measurements were immediately started via the software "Viscometry" (supplied by Bohlin Instruments Ltd) installed on the external computer system. The data was collected and processed by the software together with an associated file converter used to save the data in ANSI format in order to enable direct transfer into Microsoft Excel for producing the required rheological plots.

Plate 4.11. GPC analytical set-up

Plate 4.12. Set-up of viscometry apparatus

Chapter 5

Experimental Results

5. INTRODUCTION

This chapter reports the results of the experimental runs performed for the polymerisation study involving the spinning disc reactor and for the agitation study. Following the lay-out of the previous chapter, it is felt appropriate, for reasons of clarity, to divide the presentation of the results of the two investigations in two separate sections within this chapter.

5.1. POLYMERISATION STUDY IN SDR

The principal aim of the styrene polymerisation experiments was to assess, in a quantitative manner, the feasibility of applying the spinning disc technology to a free-radical polymerisation process. The performance of the spinning disc reactor (SDR), in terms of increases in conversion and changes in molecular weight properties in one disc pass, was measured against the capabilities of a standard laboratory stirred tank reactor.

A detailed description of the apparatus in which the polymerisation runs were performed can be found in Chapter 4. Four different sets of experiments were conducted in the SDR during the course of the current experimental programme. Each of these experiments explored the effects of different system parameters of the SDR on the polymerisation process, as detailed in section 5.1.2 within this chapter.

The reagents used in the majority of the runs were styrene monomer, toluene as solvent and benzoyl peroxide initiator with initial concentrations varied over the course of the experimental programme in order to cope with large increases in viscosity during the progress of polymerisation. Hence, the reaction medium evolved from a purely bulk system in experiment A which was conducted during a previous research [205] to a moderately solvated one by the end of the current investigation. The concentrations of each species as well as the actual volumes used in each experiment are given in Appendix E where the detailed operating conditions and raw experimental data are also presented.

5.1.1. Batch Calibration Runs

A meaningful evaluation of polymerisation data (conversion, molecular weights and MWD) from the spinning disc rested on comparisons with polymerisation conducted under a given set of conditions in a stirred tank vessel which was described in Chapter 4. In this respect, calibration runs following the progress of polymerisation to high conversion in the batch were performed for each set of experiments B, C, D & E, data for which will be presented in the ensuing sections. For comparison purposes, the batch calibration data for experiment A gathered from a separate research study conducted prior to the present investigation will also be reproduced herein.

5.1.1.1. Temperature Profile

A profile following the reaction temperature in the batch reactor was established over an average polymerisation time of about 130 minutes for each experimental set of runs C, D and E, as shown in Figure 5.1.

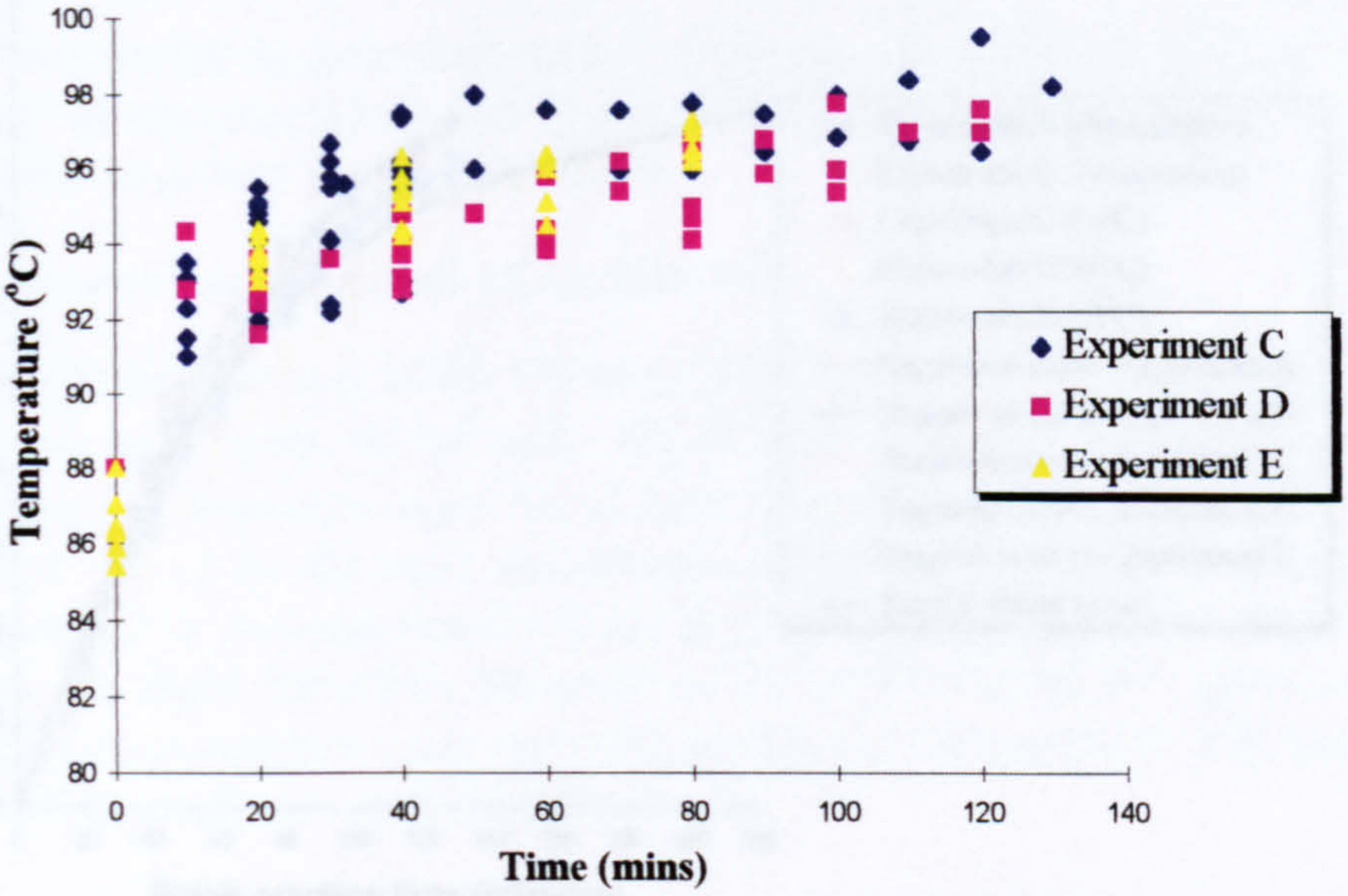

Figure 5.1. Batch polymerisation temperature profile

The temperature was seen to rise gradually from the starting temperature of 88°C and level out at around 96°C after 30 minutes from the onset of polymerisation. This initial increase in temperature indicates that the heat generated during polymerisation exceeds the heat removal capacity of the surrounding water bath in the initial stages of reaction when the rate of polymerisation is at its highest due to large monomer concentrations. This rise in temperature is important and should be taken into account when changes in conversion and molecular weight properties are being considered.

5.1.1.2. Conversion

The calibration data for conversion corresponding to each experimental set are plotted below in Figure 5.2.

The label for each calibration curve indicates the method used to analyse the experimental samples.

It is observed that the polymerisation trends in the batch for all five experiments are fairly similar, except for experiment D where the conversion at any given time is lower than in any of the other experiments. This was initially attributed to the fact that two vertical condensers in series were used, instead of one as in experiments A, B and C, which helped to minimise styrene and toluene losses by evaporation from the batch. However, with the same set-up as in experiment D, the batch results for experiments E were seen to be higher than expected and in fact were in reasonable agreement with the previous calibration curves A, B and C. This led to the conclusion that reproducibility in the batch polymerisation was not easily achieved and hence it was necessary to collect samples from the batch even during the

prepolymer feed preparation for a disc run. In this way, the conversion history in the batch prepolymer stage allowed any adjustment to be made in the feed and product conversions so that reliable comparisons between spinning disc data and the appropriate calibration curve could be made.

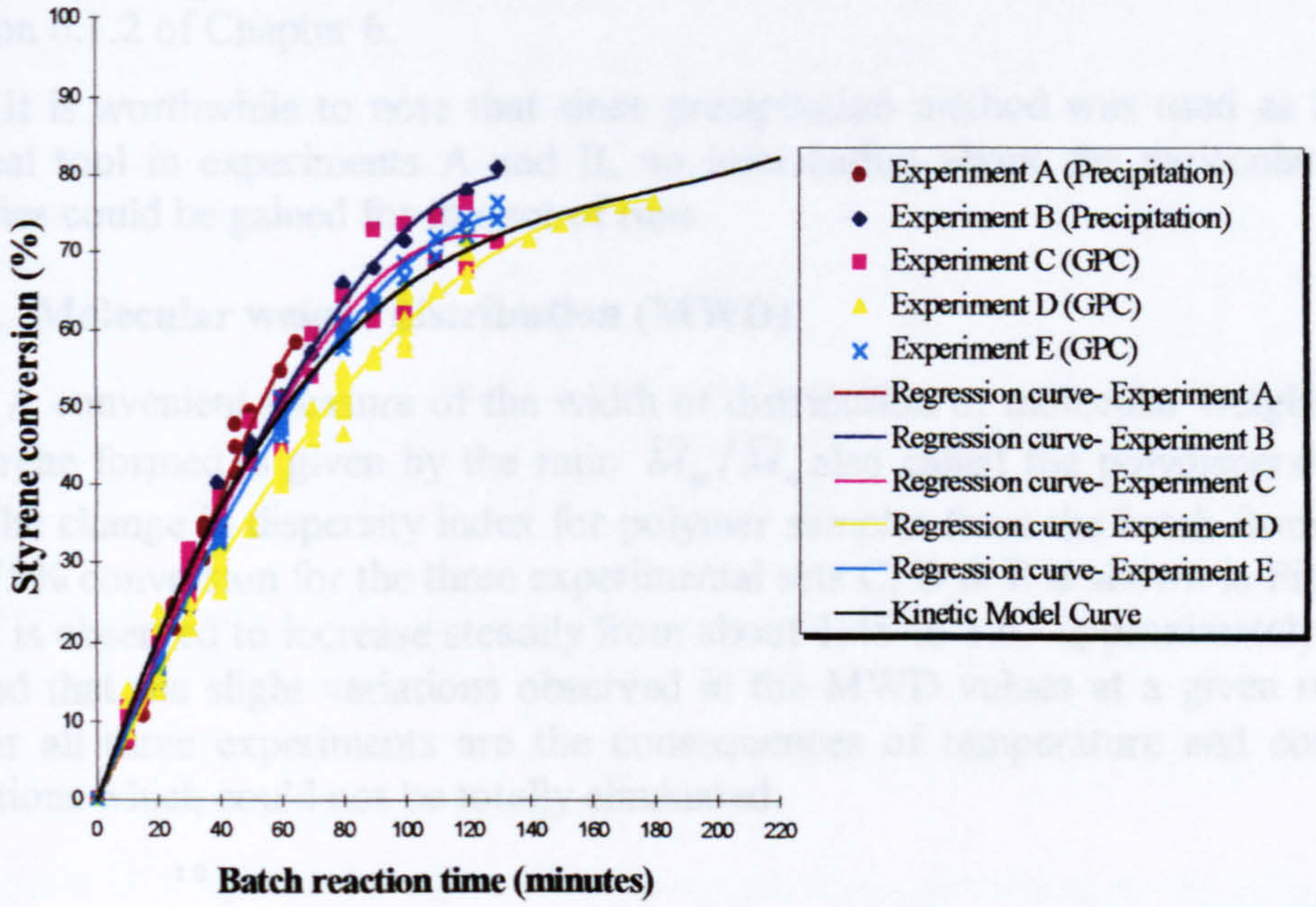

Figure 5.2. Experimental and predicted conversions for styrene polymerisation in the batch reactor

5.1.1.3. Molecular weights, M_n and M_w

The changes in number-average and weight-average molecular weights, M_n and M_w respectively with progress in polymerisation in the batch experimental runs for the present study are illustrated in Figure 5.3 below.

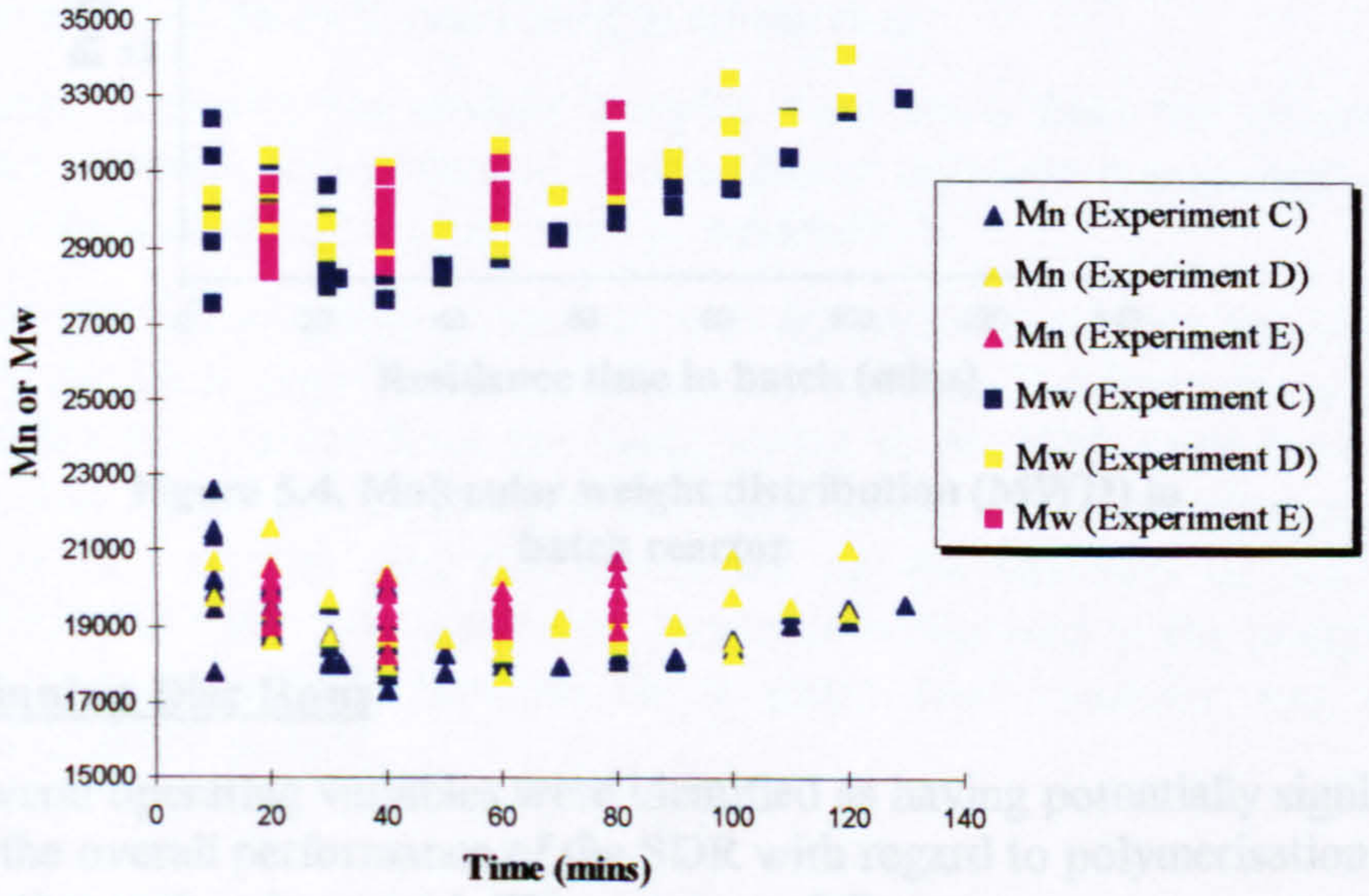

Figure 5.3. Molecular weight profiles in experimental batch polymerisations

The average value of M_w decreases from about 30000 at 10 minutes to a value of around 28500 at 40 minutes approximately and thereafter rises steadily to 32500 at the end of the batch reaction. Similarly, M_n falls from an initial average value of about 20000 to 18000 after 60 minutes of polymerisation and then experiences a gradual rise to reach an average value of 20000 at 130 minutes. These observations are discussed in section 6.1.2 of Chapter 6.

It is worthwhile to note that since precipitation method was used as the only analytical tool in experiments A and B, no information about the molecular weight properties could be gained for this set of runs.

5.1.1.4. Molecular weight distribution (MWD)

A convenient measure of the width of distribution of molecular weights of the polystyrene formed is given by the ratio $\overline{M}_w/\overline{M}_n$ also called the polydispersity index (DI). The change in dispersity index for polymer samples from the batch from zero to about 75% conversion for the three experimental sets C, D & E is shown in Figure 5.4. The DI is observed to increase steadily from about 1.45 to 1.65 approximately. It is to be noted that the slight variations observed in the MWD values at a given residence time for all three experiments are the consequences of temperature and conversion fluctuations which could not be totally eliminated.

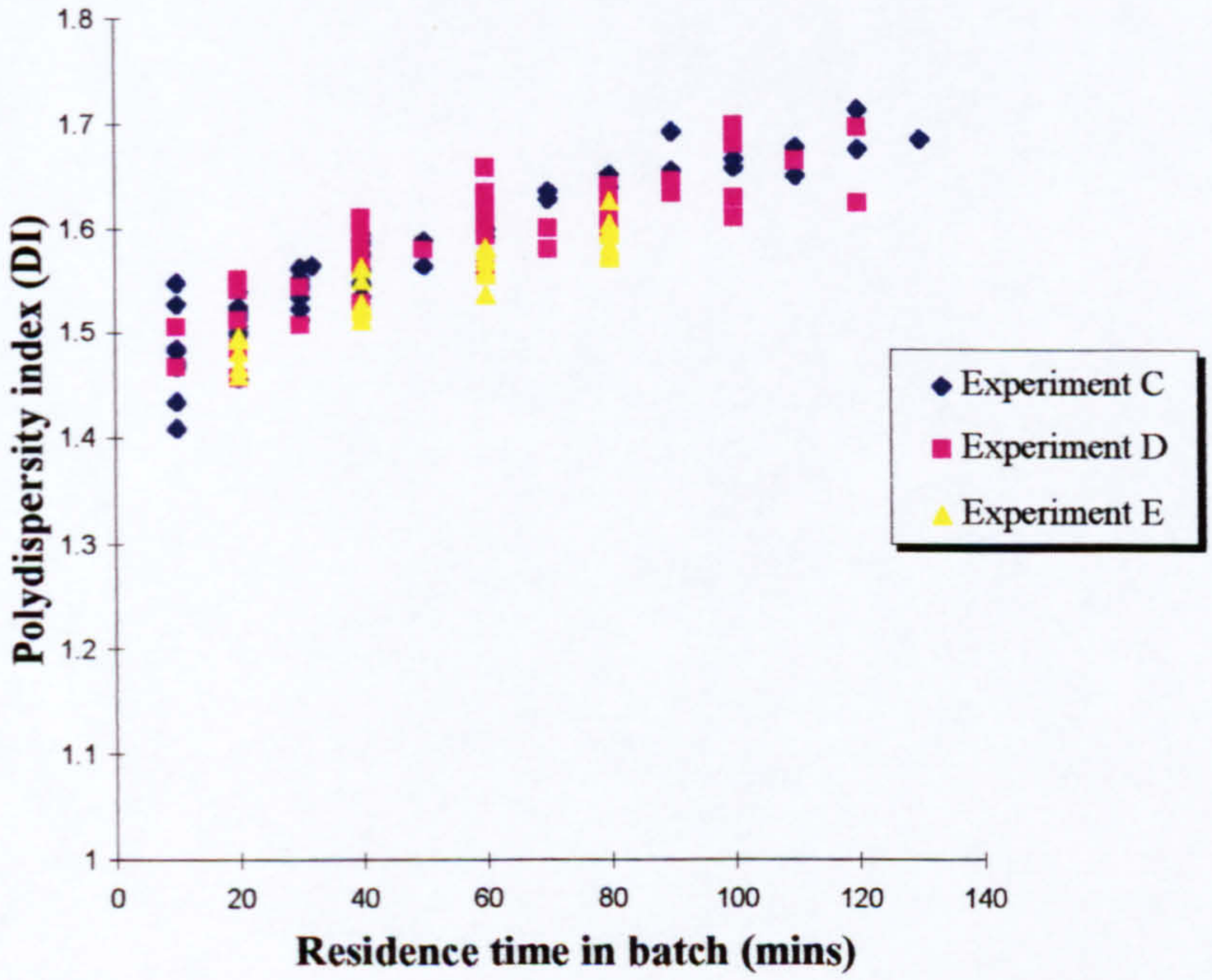

Figure 5.4. Molecular weight distribution (MWD) in batch reactor

5.1.2. Spinning Disc Runs

Several operating variables were identified as having potentially significant effects on the overall performance of the SDR with regard to polymerisation processes or any reaction system in general. These were as follows:

1. Disc rotational speed
2. Disc temperature

3. Disc diameter
4. Feed viscosity/conversion
5. Feed flowrate

It was intended to concentrate the research effort on studying the effect of at least two of these variable parameters. As a continuation of a previously reported preliminary study of styrene polymerisation in the SDR [205], four different sets of experimental runs were carried out as part of the present research programme. The experiments explored the effects of prepolymer feed viscosity (or conversion since viscosity is dependent on the concentration of polymer which in turn is determined by the monomer conversion) and disc rotational speed on the level of conversion and molecular weight properties of the product from the SDR. Only one of these parameters was varied at a time in each experiment to enable a straightforward appraisal of the extent to which the selected parameter affects the polymerisation on the disc. Details pertaining to the operating conditions for each experimental set are as follows:

Experiment B: Study of the effect of prepolymer feed conversion in the range ca. 37-66% for fixed disc rotational speed of 350-400 rpm.

Experiment C: Study of the effect of disc speed in the range 300-1000 rpm for fixed prepolymer conversion of ca. 37%.

Experiment D: Study of the effect of prepolymer feed conversion in the range ca. 29-67% for fixed disc rotational speed of 850 rpm.

Experiment E: Study of the effect of rotational speeds in the range 400-1500 rpm for fixed prepolymer feed conversion of ca. 58%.

As mentioned earlier, experiment A which looked into the effect of prepolymer feed conversion in the range ca. 12- 37% for fixed disc rotational speed of 350-400 rpm was conducted prior to the present investigation, the results for which have already been reported [205].

A grooved disc surface of fixed diameter of 360 mm and an average disc temperature between 88-90°C were used in all the runs.

A minimum of three product samples were taken from the spinning disc in each run and the SDR data presented in this chapter represent a numerical average of the results, details of which can be found in Appendix E.

Each individual spinning disc run was divided into a batch prepolymer stage followed by the final stage on the rotating disc surface. The procedures adopted in transferring the prepolymer from the batch vessel to the SDR were kept simple by pouring the feed under gravity into the distributor tubes. Unfortunately this meant that the feed flowrate on the disc was dependent on the viscosity of the feed. The interdependency of these two parameters has to be recognised in the interpretation of the results. Also, the feed flowrate for a given feed viscosity was subject to fluctuations in different runs.

5.1.2.1. Experiment A

Results of the tests with conditions as outlined for experiment A above have been displayed in Table 5.1.

The net average increase in conversion due to polymerisation on the rotating disc as shown in the above table has been attained after the possible losses of styrene due to evaporation from the reaction mixture have been taken into consideration. Details regarding the calculation of styrene loss by evaporation from the spinning disc surface and its effects on the product conversions have been presented in Appendices C and E respectively. As a result of these adjustments, the increments in conversion on the disc shown here are rather lower than those presented in an earlier report [205]. Modifications in the results for experiments A reported before are therefore necessary. The adjusted results will be presented in this section.

Table 5.1. Changes in conversion and time savings in Spinning Disc Reactor (Experiment A)

Prepolymer residence time in batch (mins)	Feed conversion (%)	Average increase in conversion due to polymerisation in SDR (%)	Equivalent batch time (Time saving in SDR) (mins)
15	13.3	4.0	4
20	18.2	5.7	6
25	23.3	3.1	4
30	27.6	6.2	7
35	33.0	7.2	9
40	36.9	9.8	11

Disc temperature: 88°C
Disc speed: 350-400 rpm

The equivalent batch time which is necessary to achieve the same given increase in conversion obtained in only a few seconds on the rotating disc is also given in the table above.

The increases in conversion at the various feed conversions have been plotted in Figure 5.5 below. There is only a small increase in conversion not exceeding 10% at the highest feed conversion from one pass on the disc rotating at 350-400 rpm.

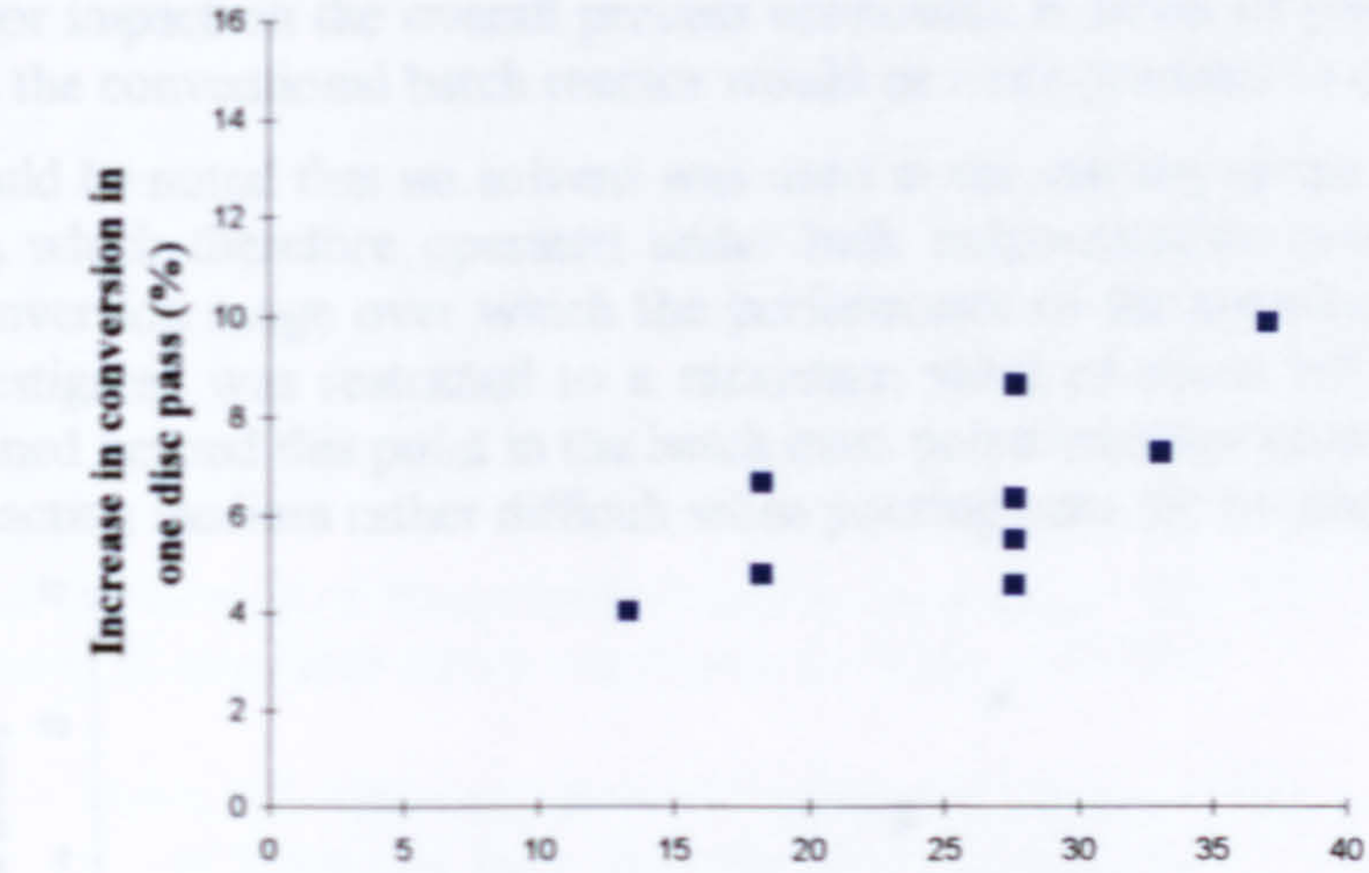

Figure 5.5. Effect of prepolymer feed conversion on increase in disc product conversion (Experiment A)

The equivalent batch times or, more conveniently, the time savings in the SDR corresponding to the range of feed conversions studied in experiment A are calculated from the batch polymerisation profile as illustrated in Figure 5.6 below.

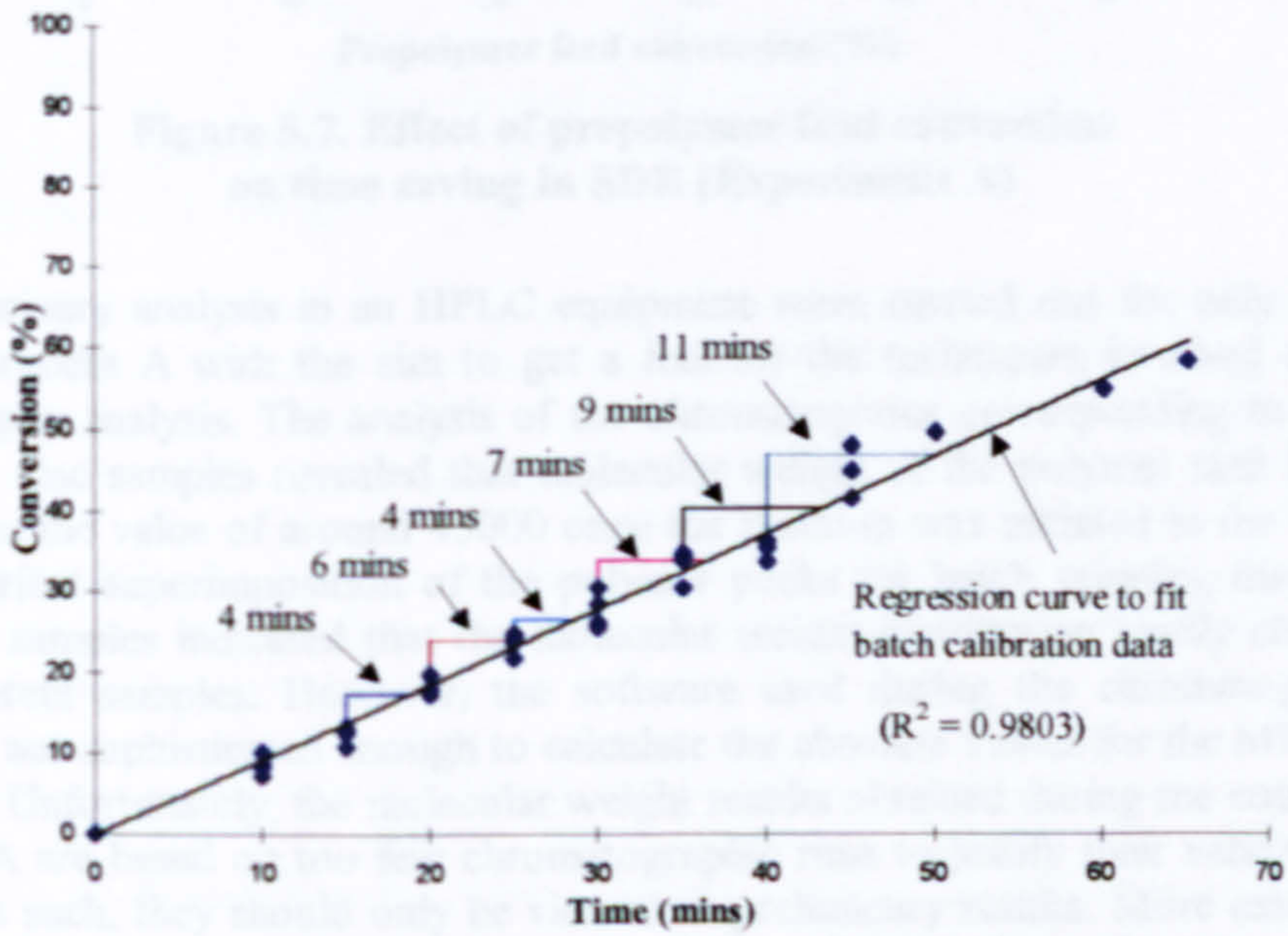

Figure 5.6. Time saving in SDR (Experiment A)

The time savings derived from Figure 5.6 are plotted in Figure 5.7 below to show the effect of prepolymer feed conversion.

As seen in Figure 5.7, there is a small but gradual increase in the time saved from 4 minutes to 11 minutes as the feed conversion rises to 37%, indicating a moderate improvement in the performance of the spinning disc reactor with increasing prepolymer conversion. However, the increases in conversions on the disc for runs in experiment A, especially for feed conversions below 25%, are deemed to be too small

to have a major impact on the overall process economics in terms of processing time. In these cases the conventional batch reactor would be more practical to operate.

It should be noted that no solvent was used in the starting recipe of all runs in experiment A which therefore operated under bulk polymerisation conditions. As a result, the conversion range over which the performance of the spinning disc reactor has been investigated was restricted to a maximum value of about 60% as the high viscosity attained beyond this point in the batch mass polymerisation process makes the flow of the reacting medium rather difficult when pouring onto the rotating surface.

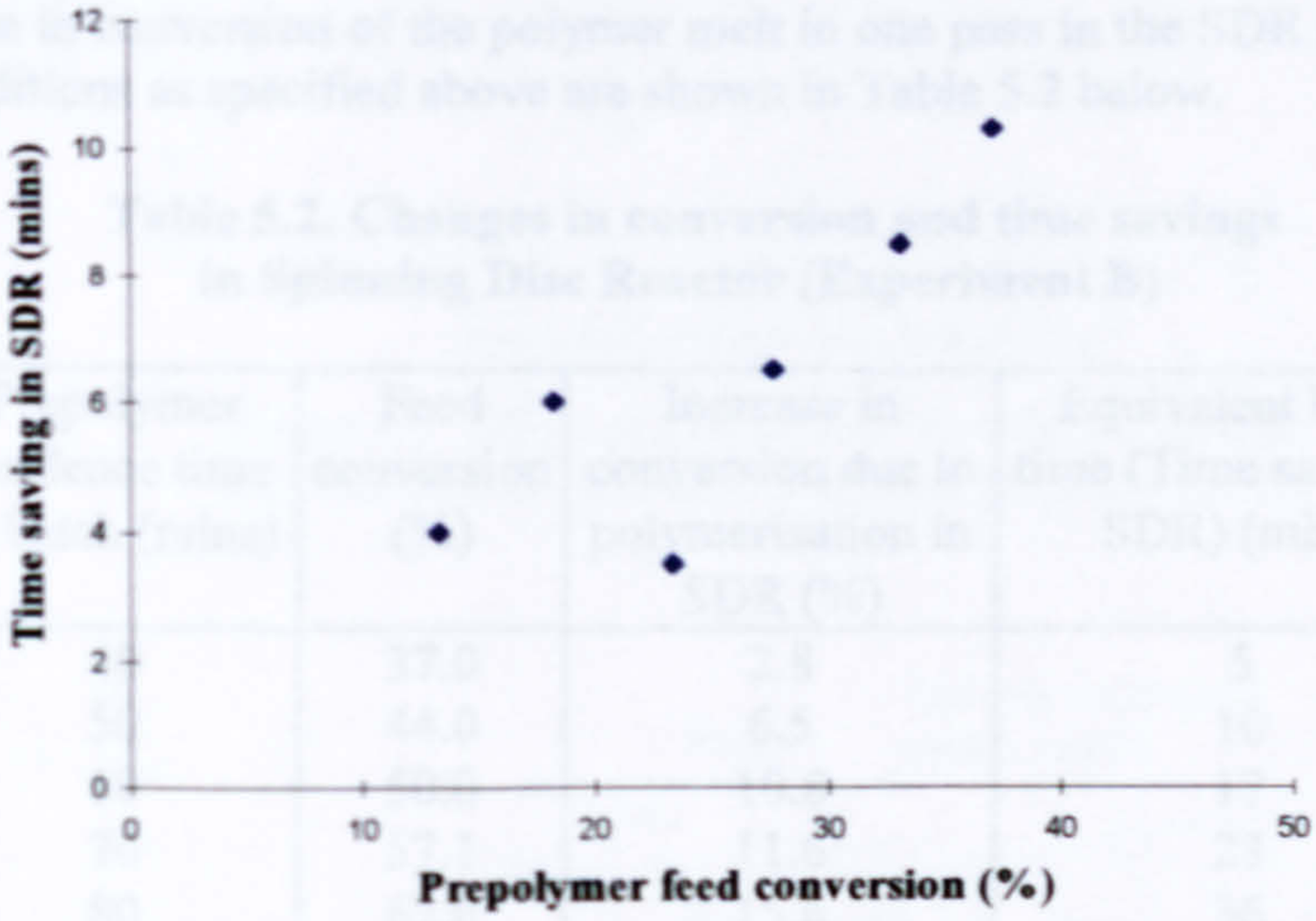

Figure 5.7. Effect of prepolymer feed conversion on time saving in SDR (Experiment A)

Preliminary analysis in an HPLC equipment were carried out for only a few runs in experiment A with the aim to get a feel for the techniques involved during chromatography analysis. The analysis of the chromatograms corresponding to batch and spinning disc samples revealed that molecular weight of the polymer melt hardly deviated from the value of around 45000 once the reaction was initiated in the batch. Also, the perfect superimposition of the polymer peaks for batch samples, disc feed and product samples indicated that the molecular weight distribution hardly changed for the different samples. However, the software used during the chromatography analysis was not sophisticated enough to calculate the absolute values for the MWD of the samples. Unfortunately, the molecular weight results obtained during the course of experiment A are based on too few chromatographic runs to justify their validity and accuracy. As such, they should only be viewed as preliminary results. More extensive chromatography analysis as performed in experiments C, D & E would give a more conclusive set of results regarding the molecular weight properties, as the results presented in the ensuing sections demonstrate.

5.1.2.2. Experiment B

This set of runs followed on from the previous experiment with higher feed conversion levels being more easily handled by using a small amount of toluene solvent (10 ml) in the batch recipe which helped to reduce the viscosity of the reaction mixture with the assumption that the polymerisation kinetics of styrene are not significantly affected by the presence of the solvent. This assumption was validated by the close agreement of the batch calibration curves for the two experiments (see Figure 5.2 above).

The increase in conversion of the polymer melt in one pass in the SDR for experiment B with conditions as specified above are shown in Table 5.2 below.

Table 5.2. Changes in conversion and time savings in Spinning Disc Reactor (Experiment B)

Prepolymer residence time in batch (mins)	Feed conversion (%)	Increase in conversion due to polymerisation in SDR (%)	Equivalent batch time (Time saving in SDR) (mins)
40	37.0	2.8	5
50	44.0	6.5	10
60	50.0	10.8	17
70	57.1	11.6	23
80	62.0	15.6	36

Disc temperature: 88°C
Disc speed: 350-400 rpm

As has been specified in the previous section, these increments are due to polymerisation on the disc after the theoretical loss of monomer by evaporation from the disc surface has been taken into account as explained in Appendix C. Graphical illustrations of these results are given in Figures 5.8 to 5.10 below.

As seen in Figure 5.8, the relationship between the change in disc product conversion with prepolymer feed conversion closely follows an exponential trend described by the following expression:

Increase in conversion = 0.3212 exp (0.0646*prepolymer feed conversion)

The above expression was been obtained from a "transformed regression model" used by Microsoft Excel which also yields an R-squared value of 0.8901 showing that the fit of the regression model to the data points is quite satisfactory.

Figure 5.9 below shows the time savings achieved in one disc pass for experimental set B. The results indicate that the spinning disc reactor gives bigger savings in reaction time as the feeding times increase from 40 to 80 minutes. The time saved is seen to rise substantially from 14 to 54 minutes as the % PS concentration in the prepolymer feed changes from 37% (at 40 minutes batch residence time) to 62% (at 80 minutes batch residence time) respectively.

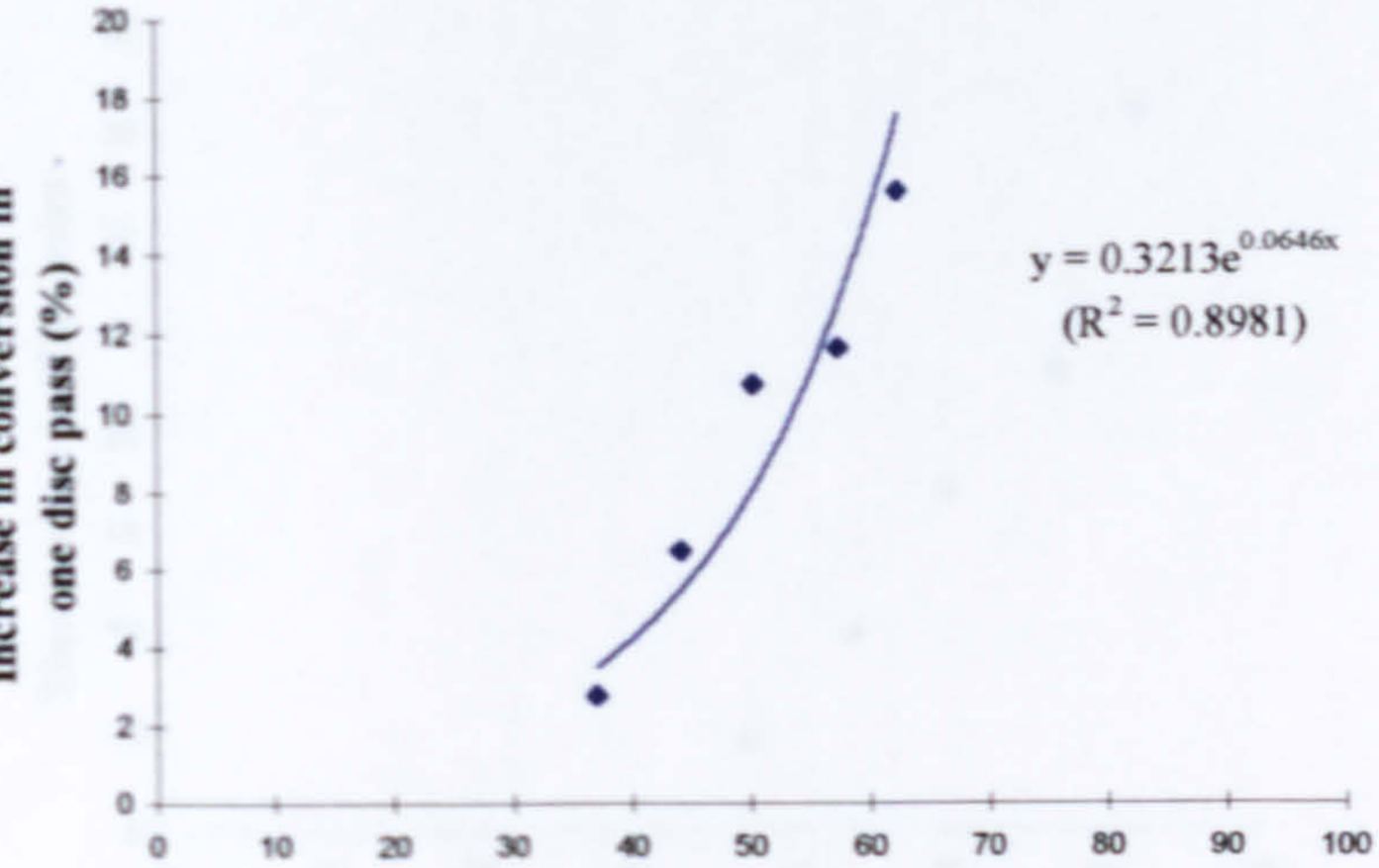

Figure 5.8. Effect of prepolymer feed conversion on increase in disc product conversion (Experiment B)

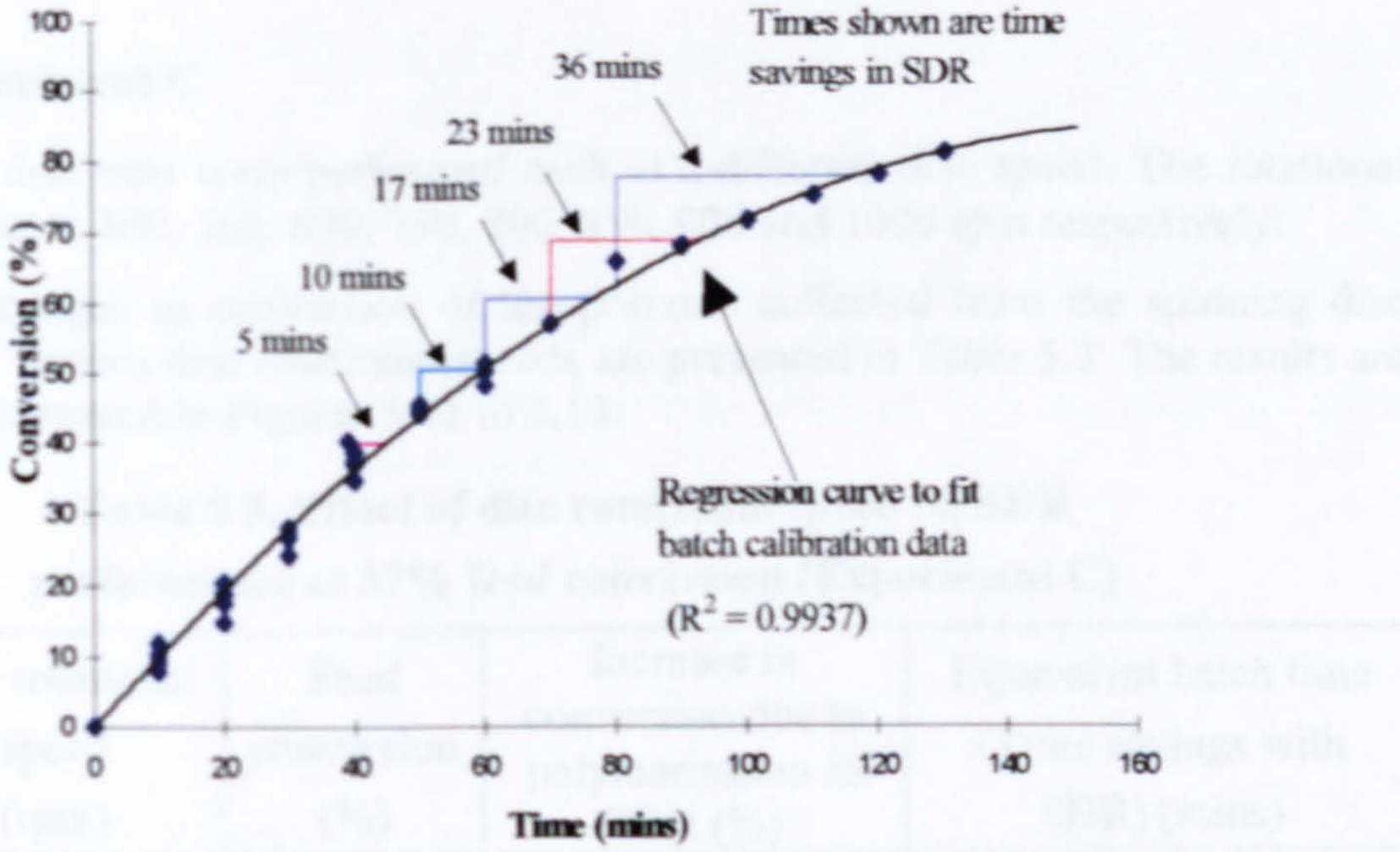

Figure 5.9. Time saving in SDR (Experiment B)

The trend in the effect of prepolymer feed conversions on the time saved in the SDR operating under the set of conditions specified in section 5.1.2 for experiment B is explicitly shown in Figure 5.10 below. It is obvious that the time saved experiences an exponential increase with a rise in feed conversion and hence viscosity. It should be noted, however, that the calculation of time saving in the SDR is very much dependent on the batch polymerisation profile as seen in Figure 5.9. It is therefore not wise to attempt to directly correlate time saving with prepolymer feed conversion as has been done for the change in disc conversion (Figure 5.8).

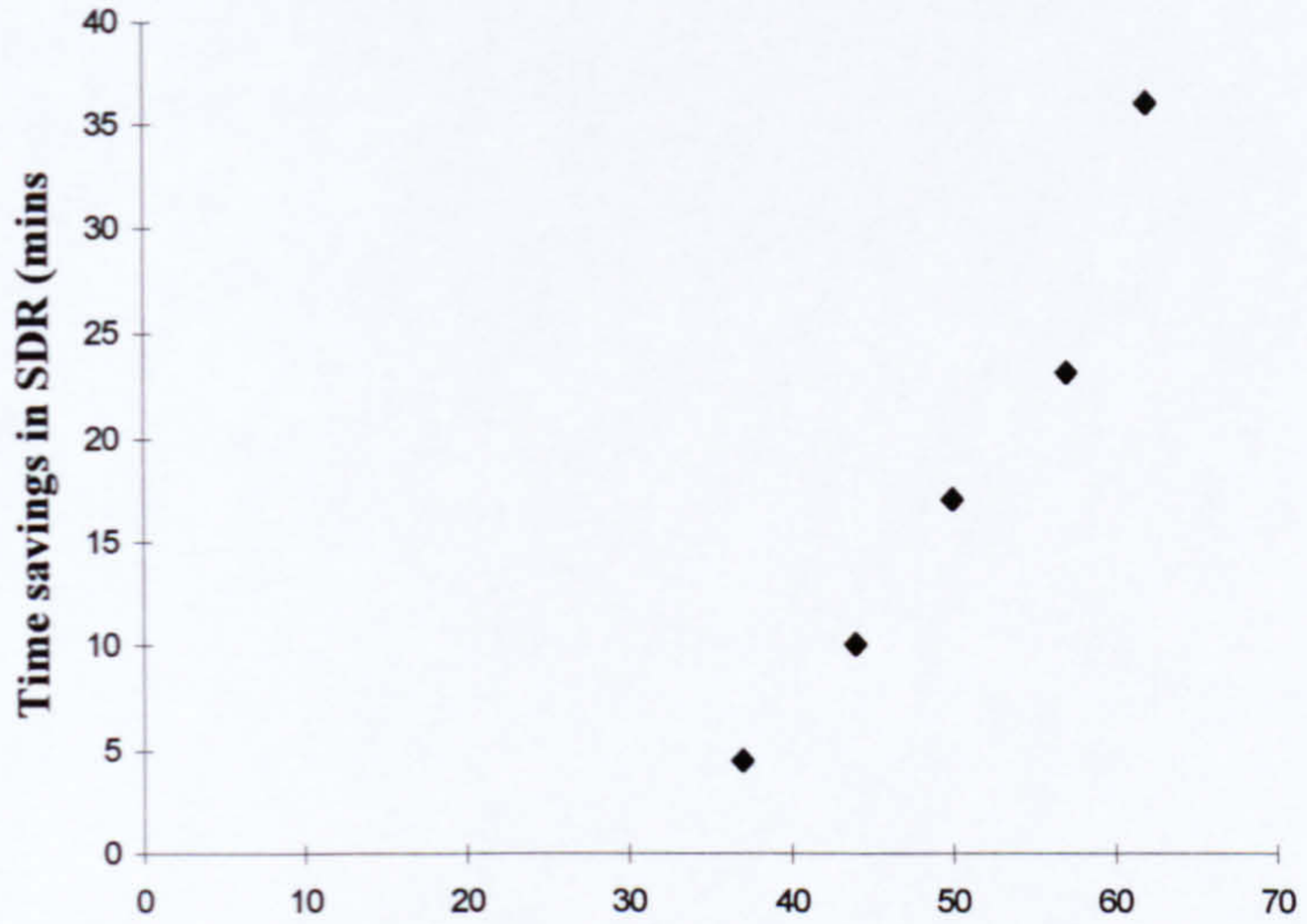

Figure 5.10. Effect of prepolymer feed conversion on time saving in SDR (Experiment B)

5.1.2.3. Experiment C

Eight disc runs were performed each at a different disc speed. The rotational speeds were set at 300, 500, 600, 750, 800, 850, 900 and 1000 rpm respectively.

The changes in conversion of the polymer collected from the spinning disc surface at the various disc rotational speeds are presented in Table 5.3. The results are also clearly illustrated in Figures 5.11 to 5.13.

Table 5.3. Effect of disc rotational speed on SDR performance at 37% feed conversion (Experiment C)

Disc rotational speed (rpm)	Feed conversion (%)	Increase in conversion due to polymerisation in SDR (%)	Equivalent batch time (Time savings with SDR) (mins)
300	36.4	3.9	6
400	36.4	4.6	7
500	36.4	2.8	5
600	36.4	8.2	13
750	36.4	6.8	10
800	36.4	9.7	15
850	36.4	17.2	27
900	36.4	13.3	21
1000	36.4	8.4	13

Disc temperature : 88°C
Time of feeding onto the disc: 40 minutes

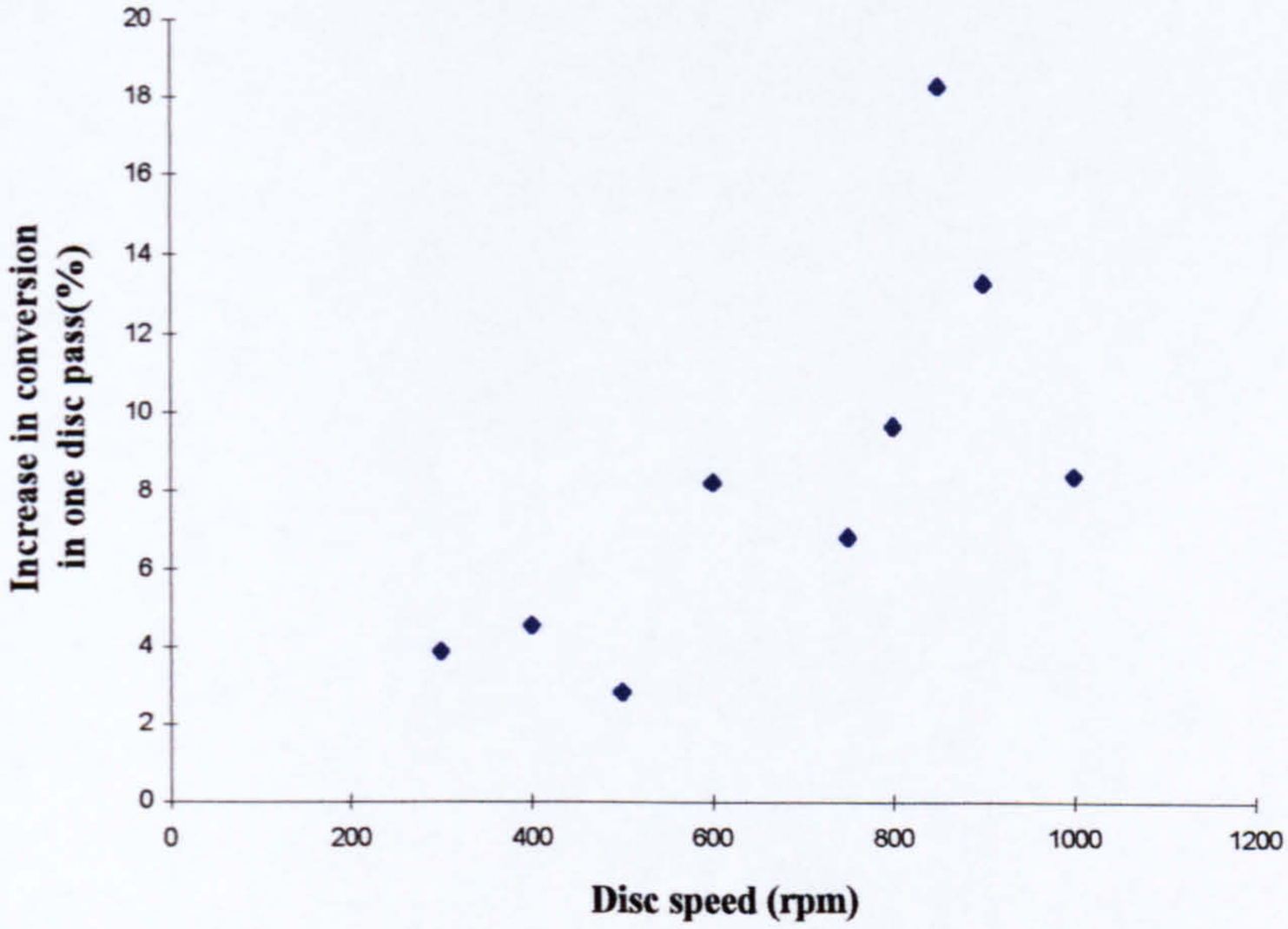

Figure 5.11. Effect of disc speed on increase in conversion in SDR for prepolymer conversion of 37% (Experiment C)

Figure 5.11 above indicates that the increase in conversion slowly increases from around 3% to 7-8% as the speed of rotation creeps up from 300 to 750 rpm. From this point onwards, there is a steep rise in the change in conversion to 17% with only a change of 100 rpm from 750 to 850 rpm. Beyond 850 rpm, however, the increase in conversion declines rapidly to about 8% at 1000 rpm. An optimal speed of 850 rpm is therefore observed in this set of runs.

Figure 5.12 below shows the time savings obtained by comparing the SDR performance with batch data for experiment C.

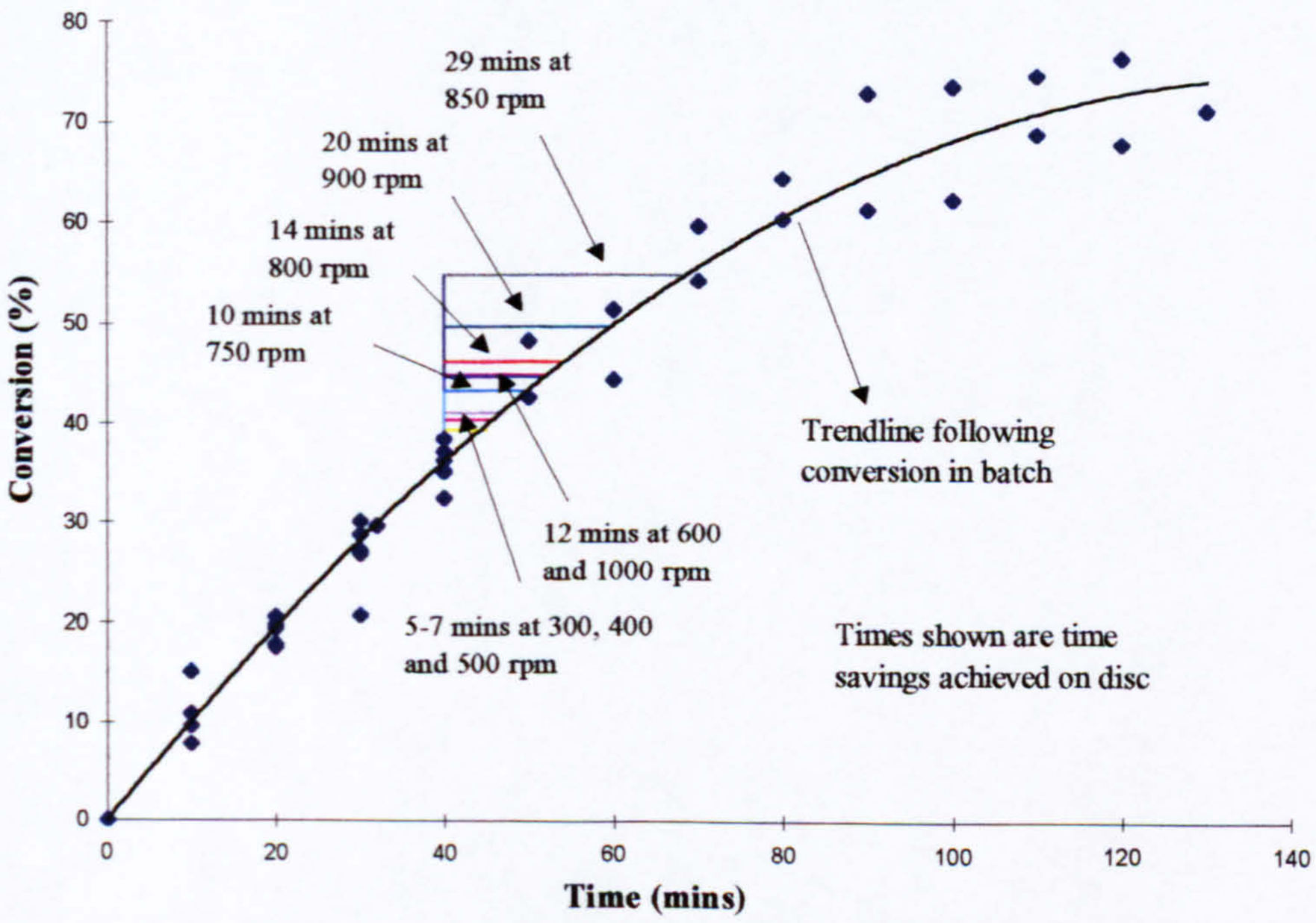

Figure 5.12. Time savings in SDR at different disc speeds for prepolymer feed conversion of 37% (Experiment C)

The effect of disc rotational speed on SDR time savings is more clearly presented in Figure 5.13 below. It is seen that the time saving achieved on the disc remains almost unchanged up to 750 rpm. Beyond this rotational speed, however, there is a notable increase in the time saving which attains a maximum value of 29 minutes at 850 rpm. Further increases in the speed of rotation result in a significant decline in the time saving to 15 minutes at 1000 rpm. A similar trend has also been observed for the change in disc conversion as seen earlier in Figure 5.11.

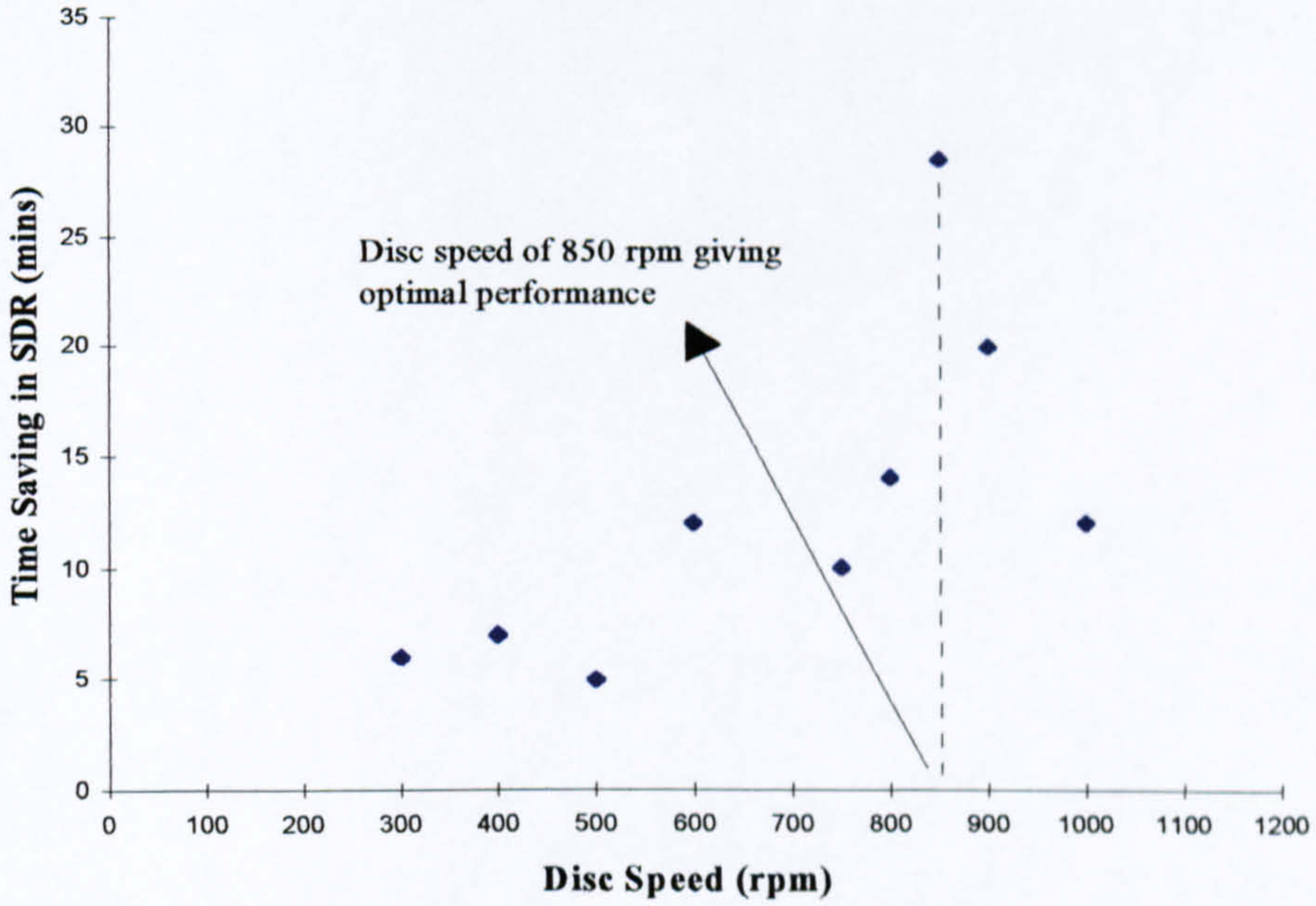

Figure 5.13. Effect of disc rotational speed on reaction time savings for 37% prepolymer feed conversion (Experiment C)

The molecular weight averages, M_n and M_w, for product samples at a given speed of rotation are presented and compared with batch molecular weights in Figures 5.14 to 5.17.

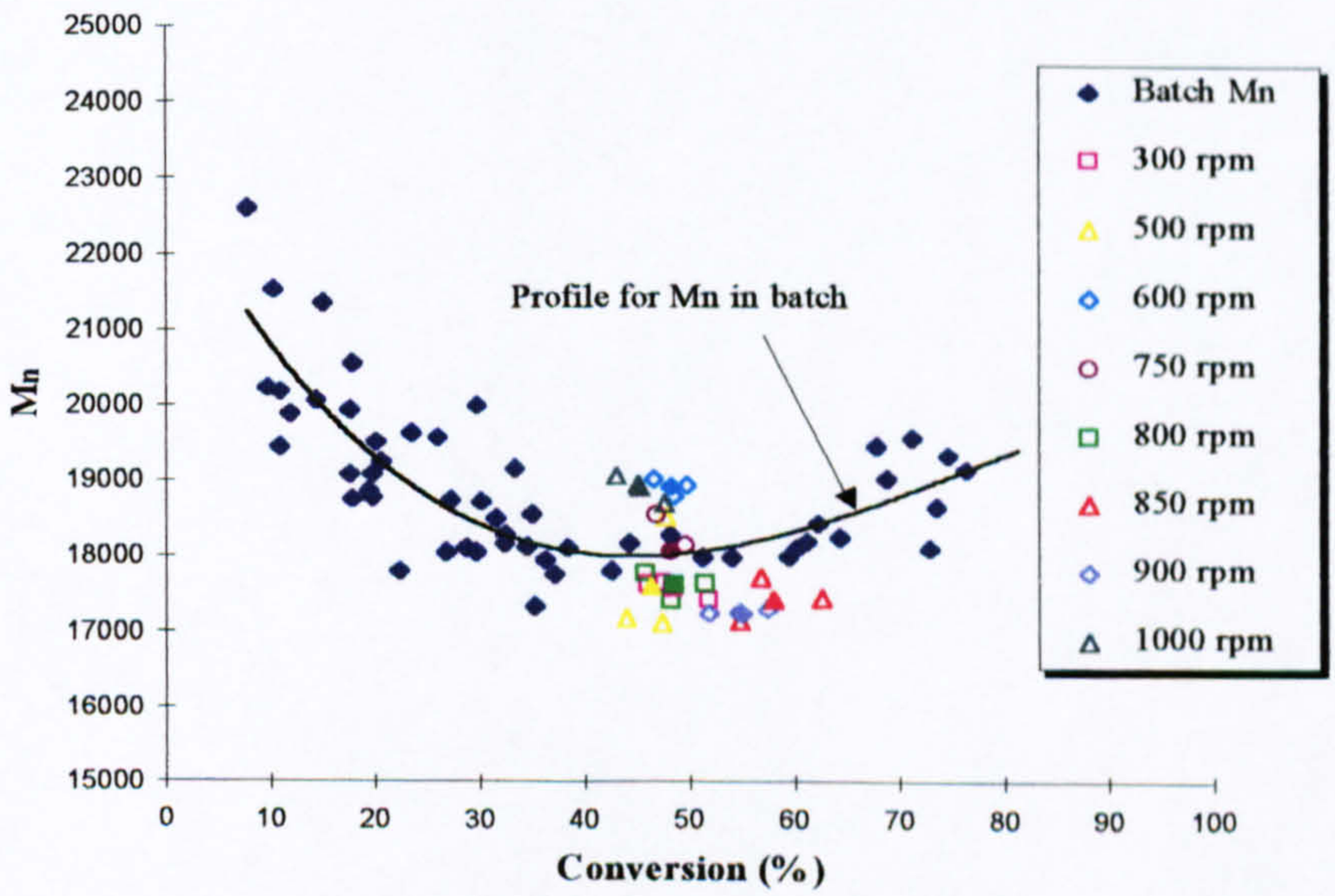

Figure 5.14. Mn for batch and SDR polymerisations (Experiment C)
(SDR filled labels-average, SDR unfilled labels- measured data)

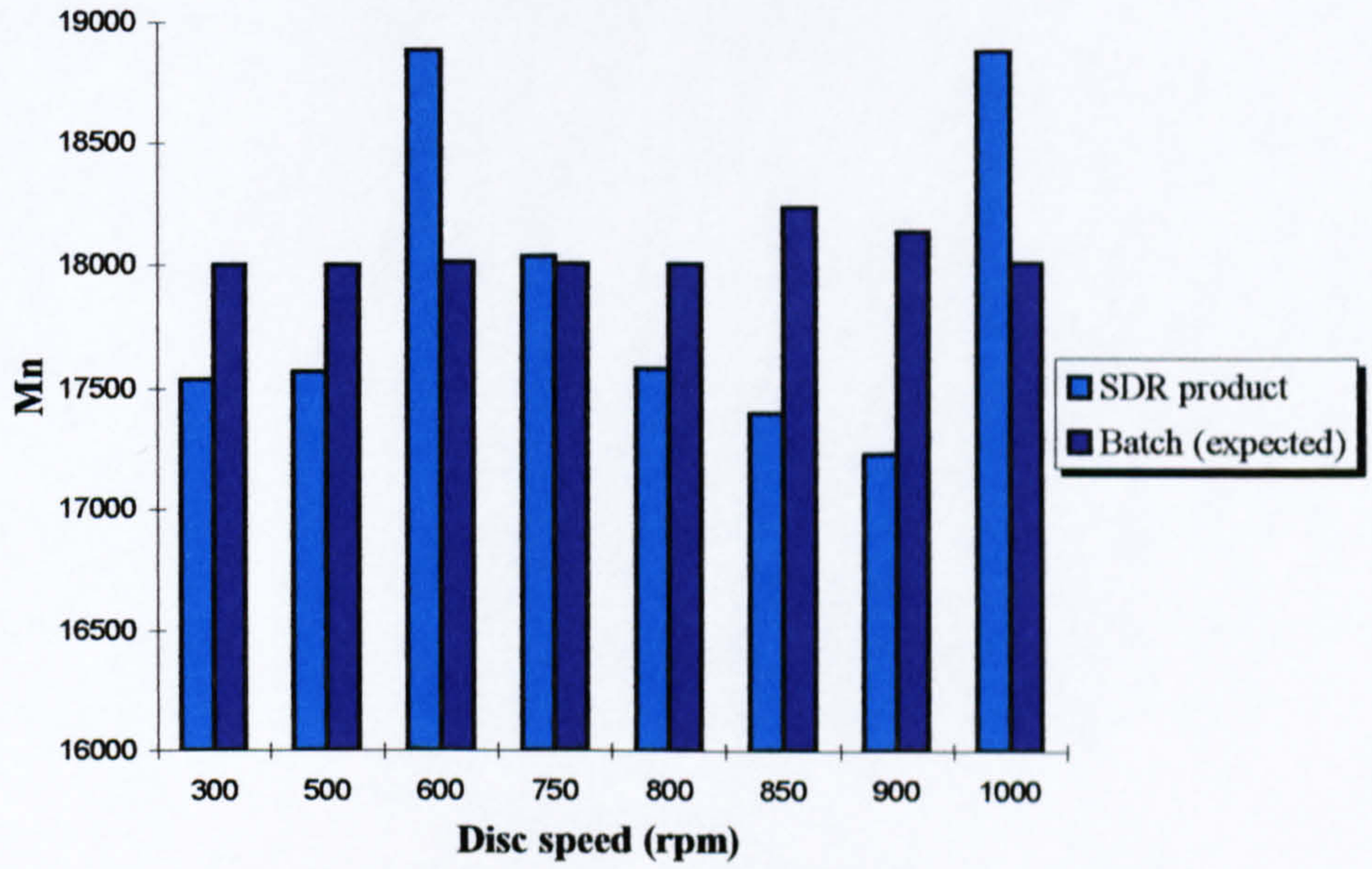

Figure 5.15. Comparison of average SDR product Mn and expected batch Mn at same conversion (Experiment C)

It is to be noted that for all speeds, comparison is made between the SDR product and polymer obtained from the batch at the same conversion. The batch profiles for M_n and M_w are established with the use of batch data points corresponding to samples collected from batch runs and prepolymer preparation in the batch. The large scatter between the batch data points as plotted in Figures 5.14 and 5.16 is the result of temperature variations in the batch which have a significant effect on the molecular weight properties.

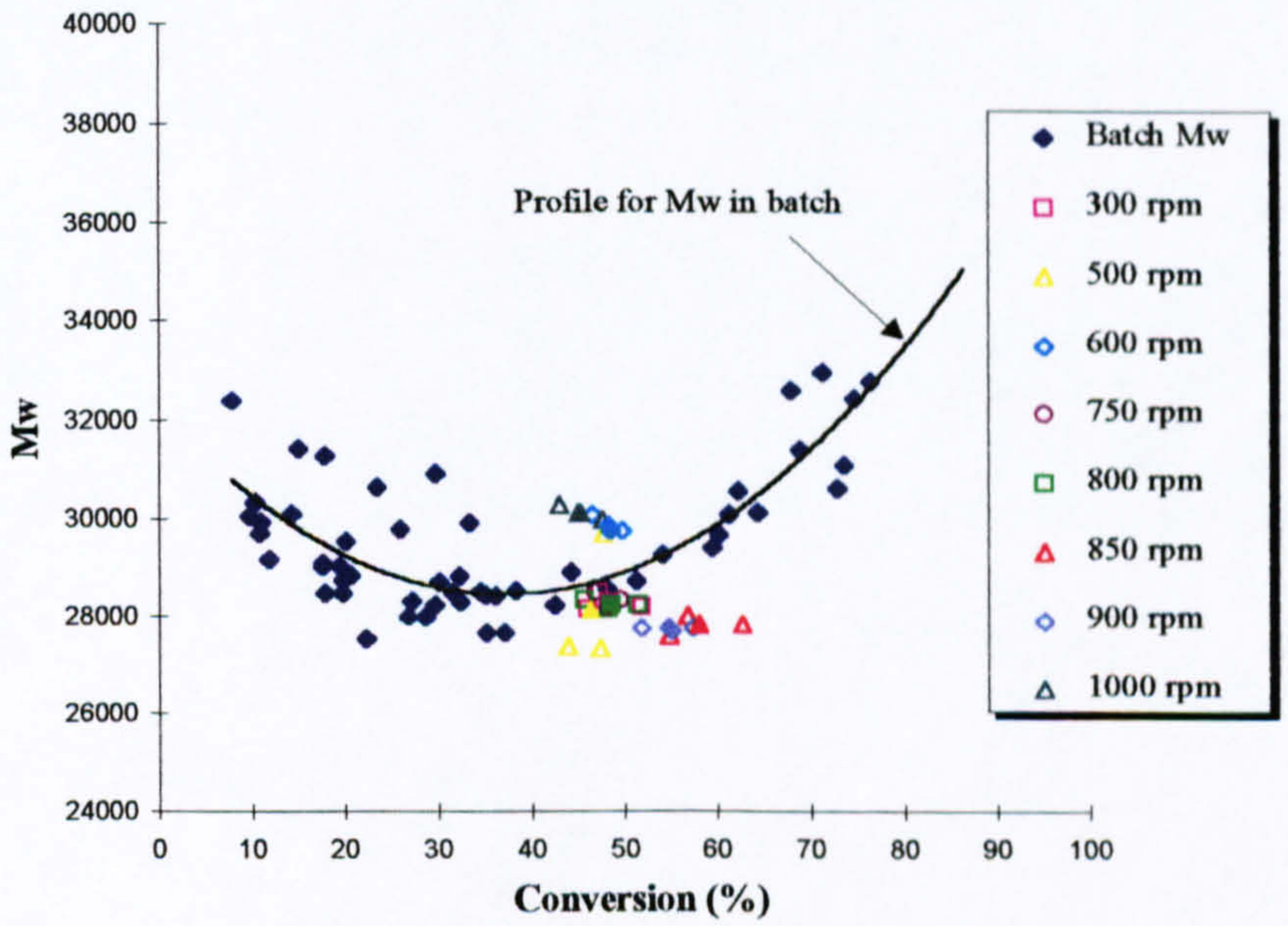

Figure 5.16. Mw for batch and SDR polymerisations (Experiment C)
(SDR filled labels- average, SDR unfilled labels- measured data)

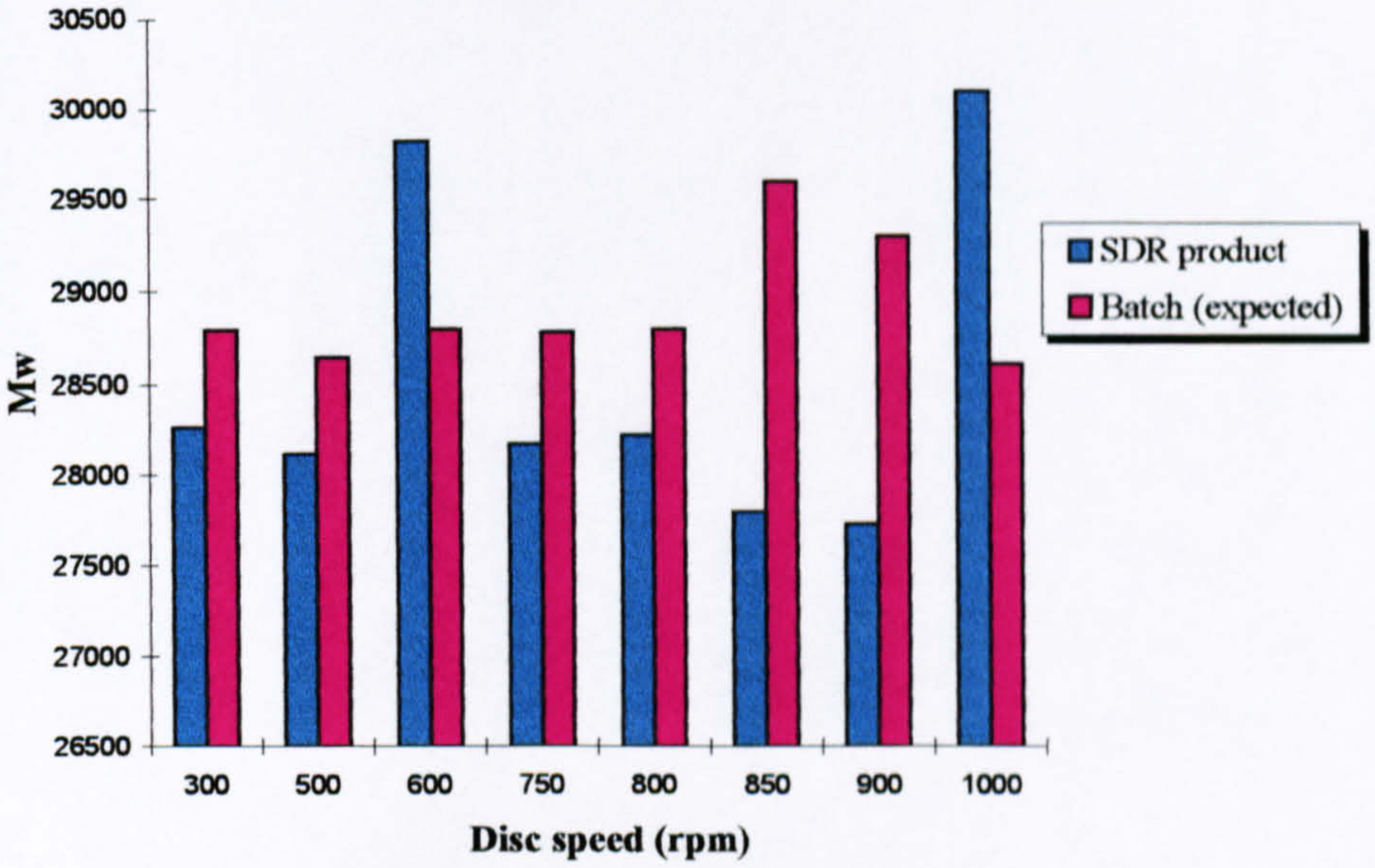

Figure 5.17. Comparison of average SDR product Mw and expected batch Mw at same conversion (Experiment C)

For the range of speeds considered, the product from the disc has a lower average M_n and M_w with the decreases representing no more than around 7.7% for M_n and 6.3% for M_w. It is also observed from Figures 5.15 and 5.17 that SDR products from the disc rotating at 600 and 1000 rpm had M_n and M_w that were higher than the values expected from the batch. This was due to variations in temperature during the prepolymer stage preparation in the batch as was discussed in section 5.1.1.1. As seen in Appendix E, the batch temperature for these runs at 40 minutes of reaction time (i.e. the feed time) were 93°C and 92.7°C respectively compared to the expected value of around 96°C. Therefore at such low temperatures, the molecular weights M_n and M_w of the feed are higher. It follows that the corresponding SDR product M_n and M_w are also higher, hence explaining the anomaly in the results obtained.

The effect of rotation on the spread of the molecular weight distribution (MWD) which is measured by the polydispersity index (DI) is presented in Figures 5.18 and 5.19 below. The data points in Figure 5.18 correspond to batch and spinning disc product samples from the disc rotating at the speed shown. Both the measured and average data for samples from the SDR are included in the plot but only the average data are taken into consideration for a realistic comparison with batch data in Figure 5.19.

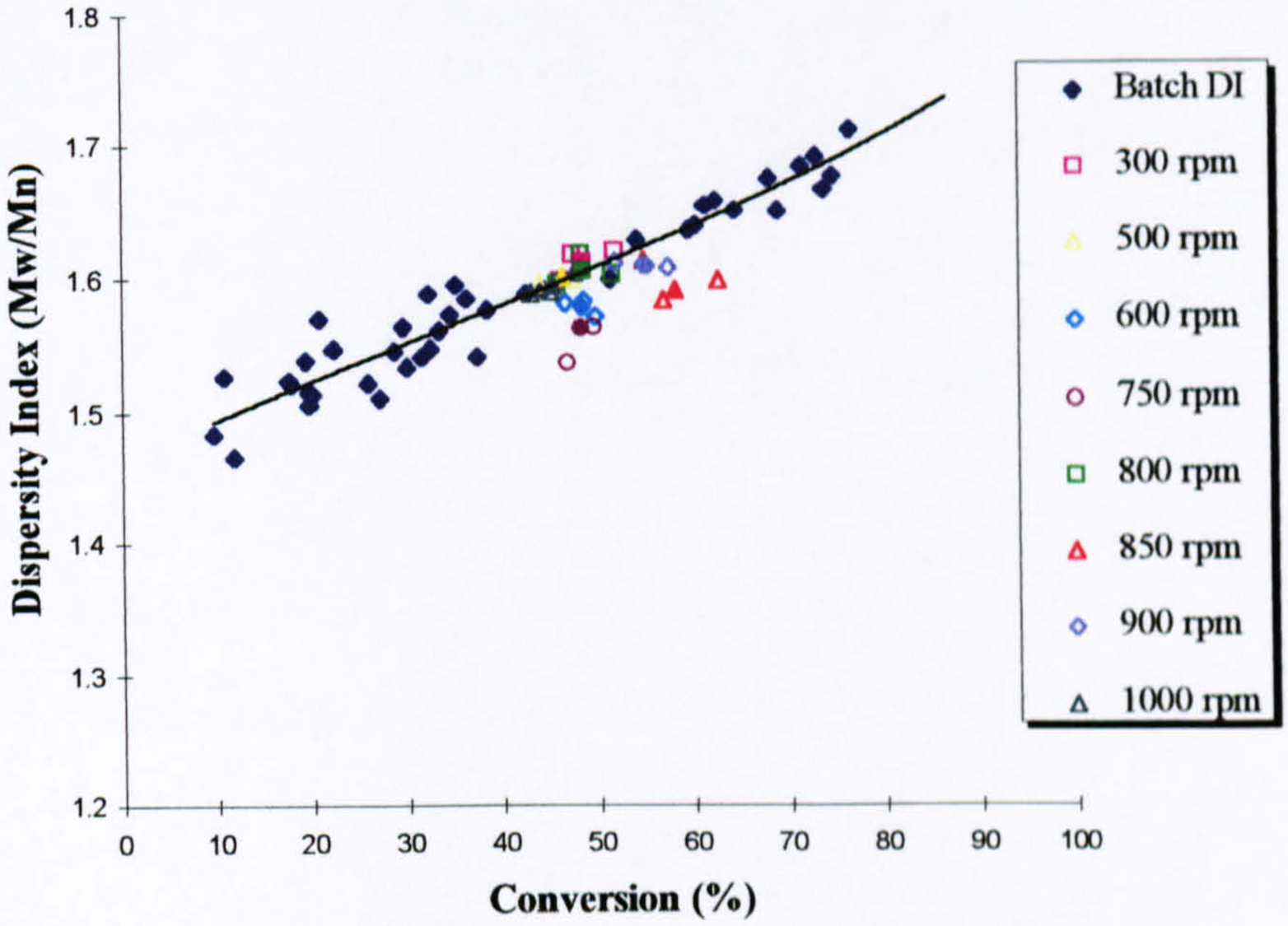

Figure 5.18. Polydispersity index (DI) for batch and SDR polymerisations (Experiment C)
(SDR filled labels- average, SDR unfilled labels- measured data)

It is seen from Figure 5.18 that the majority of the SDR product data points fall below the profile established for the batch DI. In other words, most of the runs (apart from those at 300, 500 and 800 rpm) gave SDR products with a dispersity index lower than the DI expected for a polymer at the same conversion produced in the batch.

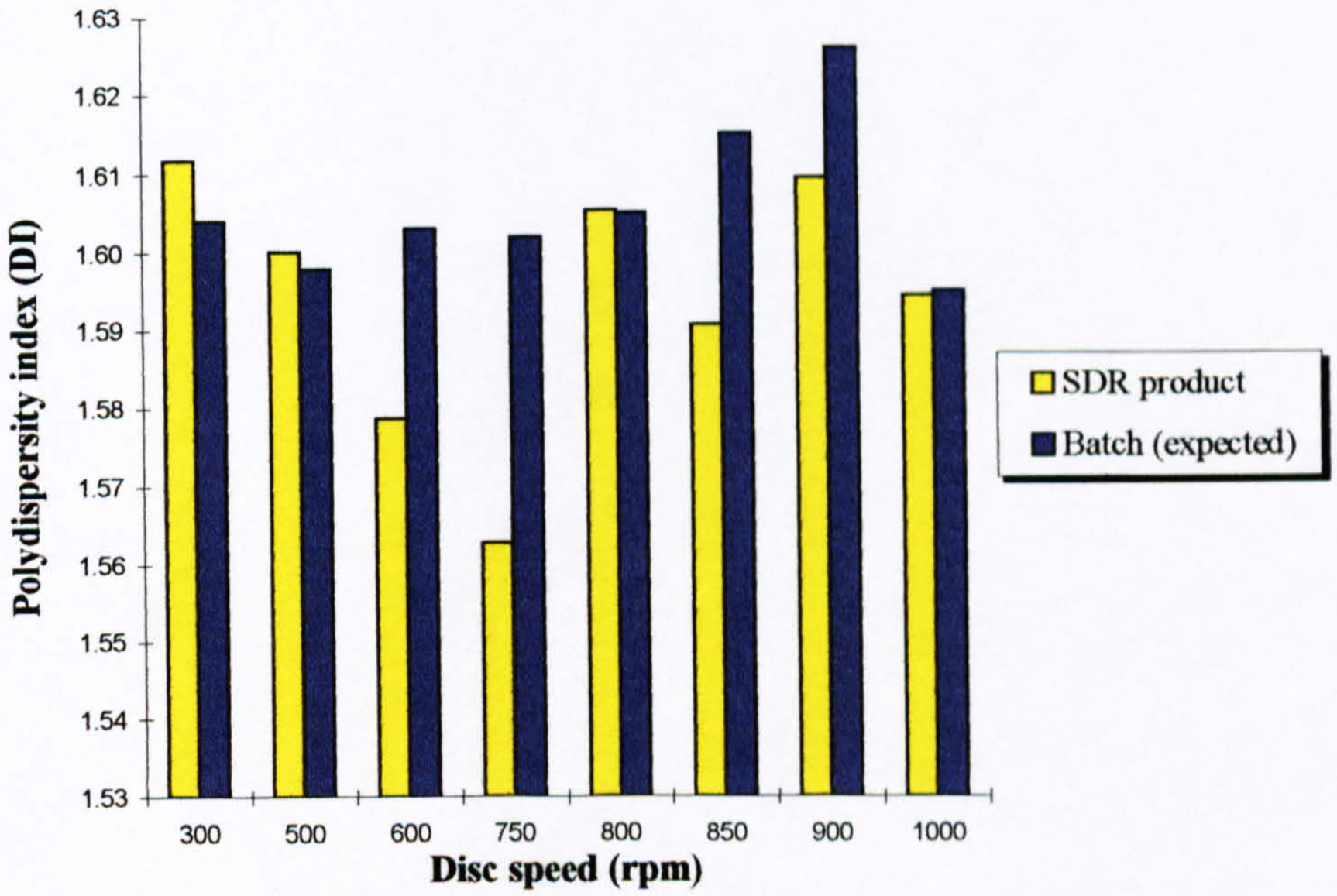

Figure 5.19. Comparison of average SDR product DI and batch DI at same conversion (Experiment C)

The results can be quantitatively analysed by comparing the average DI value of the product from the disc (having an average product conversion) with the batch DI as in Figure 5.19. The percentage decrease in DI observed in one pass of the disc

varies from around 1-2.5% for speeds in the range 600-850 rpm, with the best result of 2.5% decrease seemingly obtained at speed 750 rpm.

It is to be noted that the determination of the spread of the molecular weight distribution is very sensitive to the integration limits used in the analysis of the chromatograms. Since experiment C was the first set of runs for which the PL Caliber® GPC was used to calculate molecular weight properties, familiarity and experience with manipulation of the software and integration limits were minimal. For this reason, the results relating to the polydispersity index for experiment C should be treated with caution.

5.1.2.4. Experiment D

The conversion results of runs from experiment D are given in Figures 5.20 to 5.23 below.

From Figure 5.20, it can be seen that a rise in the conversion of the feed into the SDR from 29% to 61% is accompanied by a steady increase in conversion from about 6% to 16% in one pass on the disc rotating at 850 rpm. However, with a still higher feed conversion of 67%, a drop in the change in SDR conversion to 11.5% is observed.

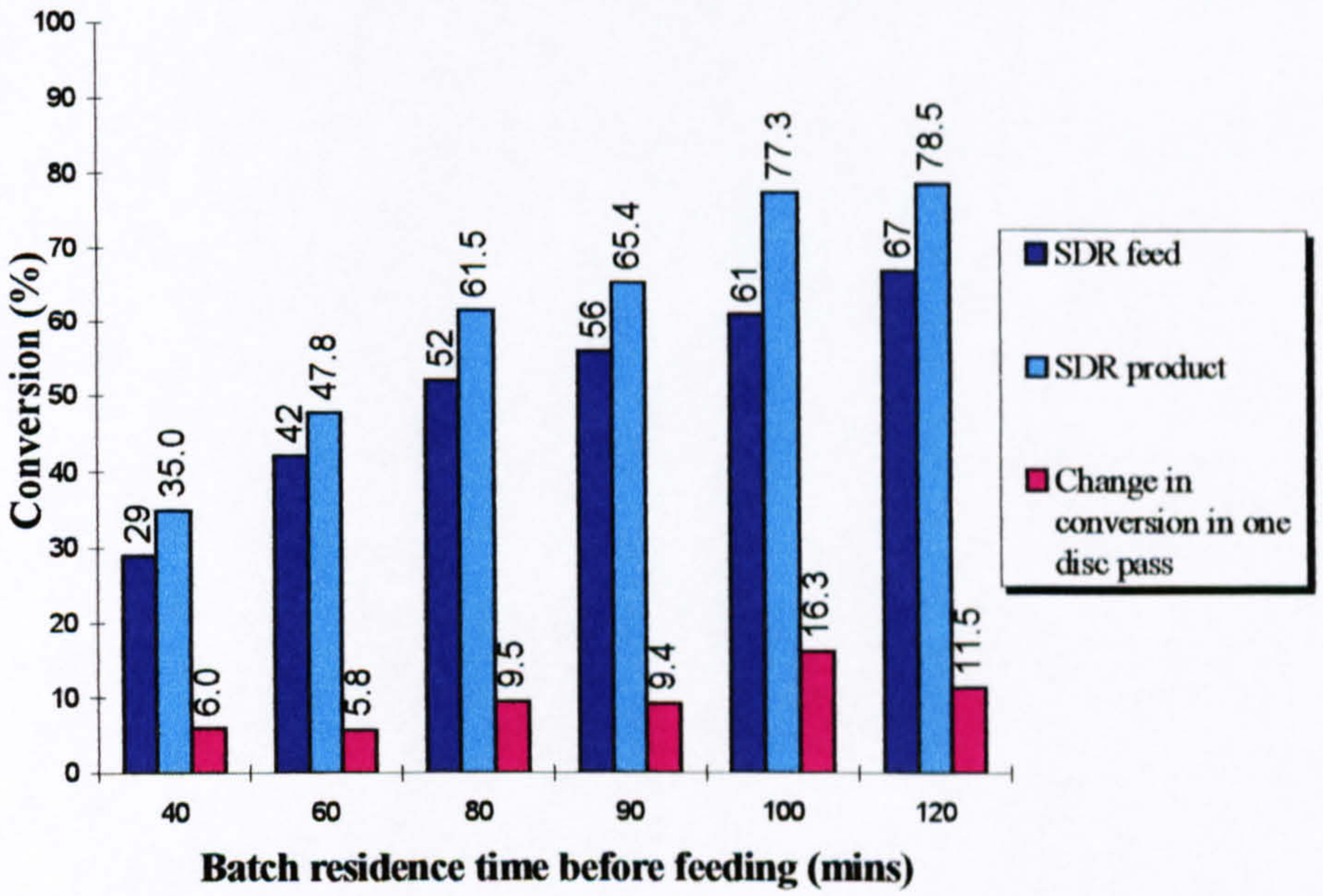

Figure 5.20. Effect of prepolymer feed residence time in batch on SDR product conversion for fixed disc speed of 850 rpm (Experiment D)

The presence of an optimal feed conversion whereby the SDR performs at its best for a disc rotational speed of 850 rpm is more clearly illustrated in Figure 5.21.

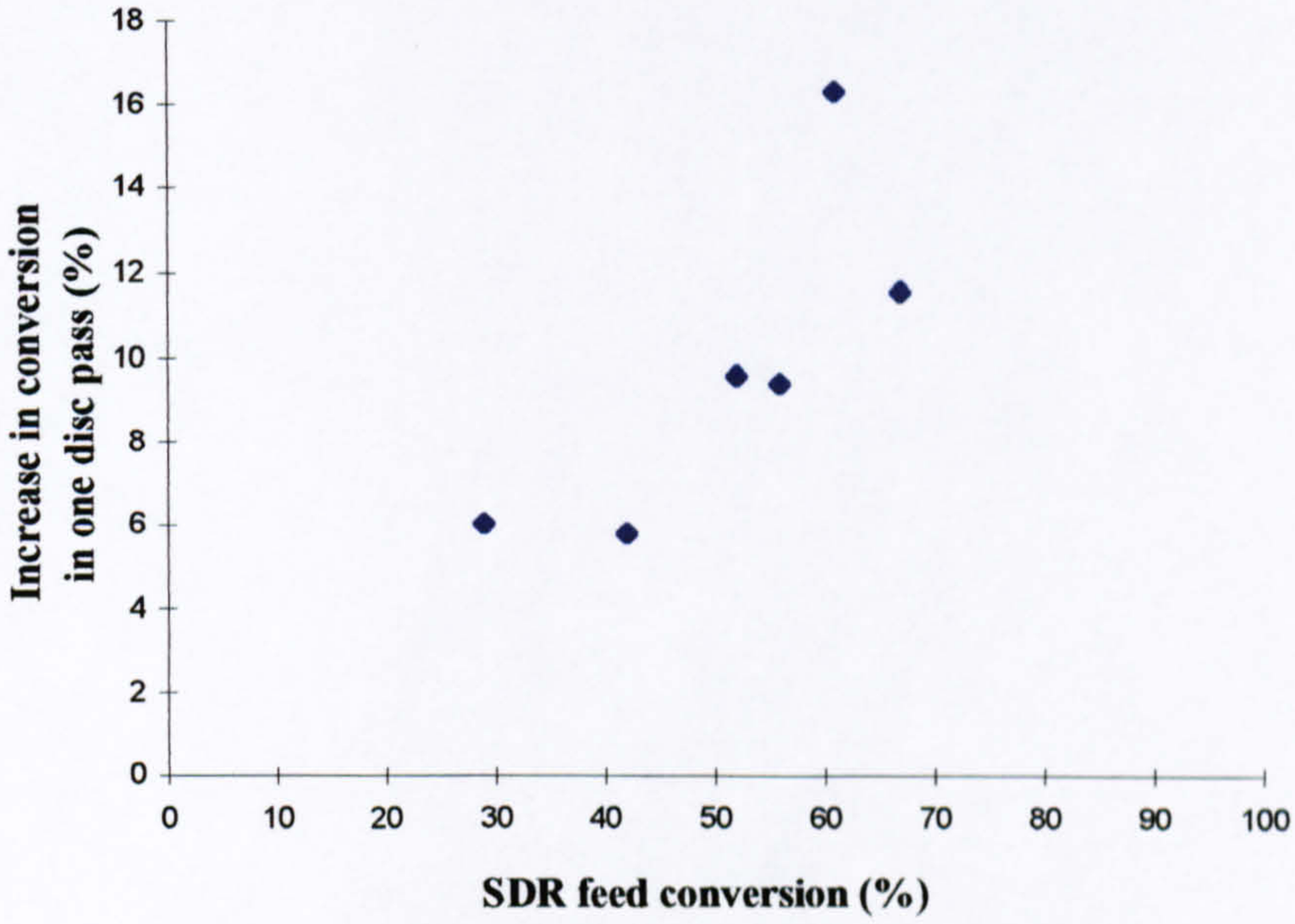

Figure 5.21. Increase in SDR conversion at fixed disc speed of 850 rpm (Experiment D)

As shown below, Figures 5.22 and 5.23 display the same results but this time in terms of the time savings achieved in the SDR which measures the effectiveness of the SDR as a polymer reactor in comparison to the stirred tank.

The time savings essentially represent the equivalent batch time needed to reach the same product conversion in the STR as that obtained in less than 2 minutes in the SDR (including the transfer time from batch to SDR). As seen above, there is a remarkable increase in the time saving from 10 minutes to over 100 minutes as the SDR feed conversion is raised from 29% to 67%.

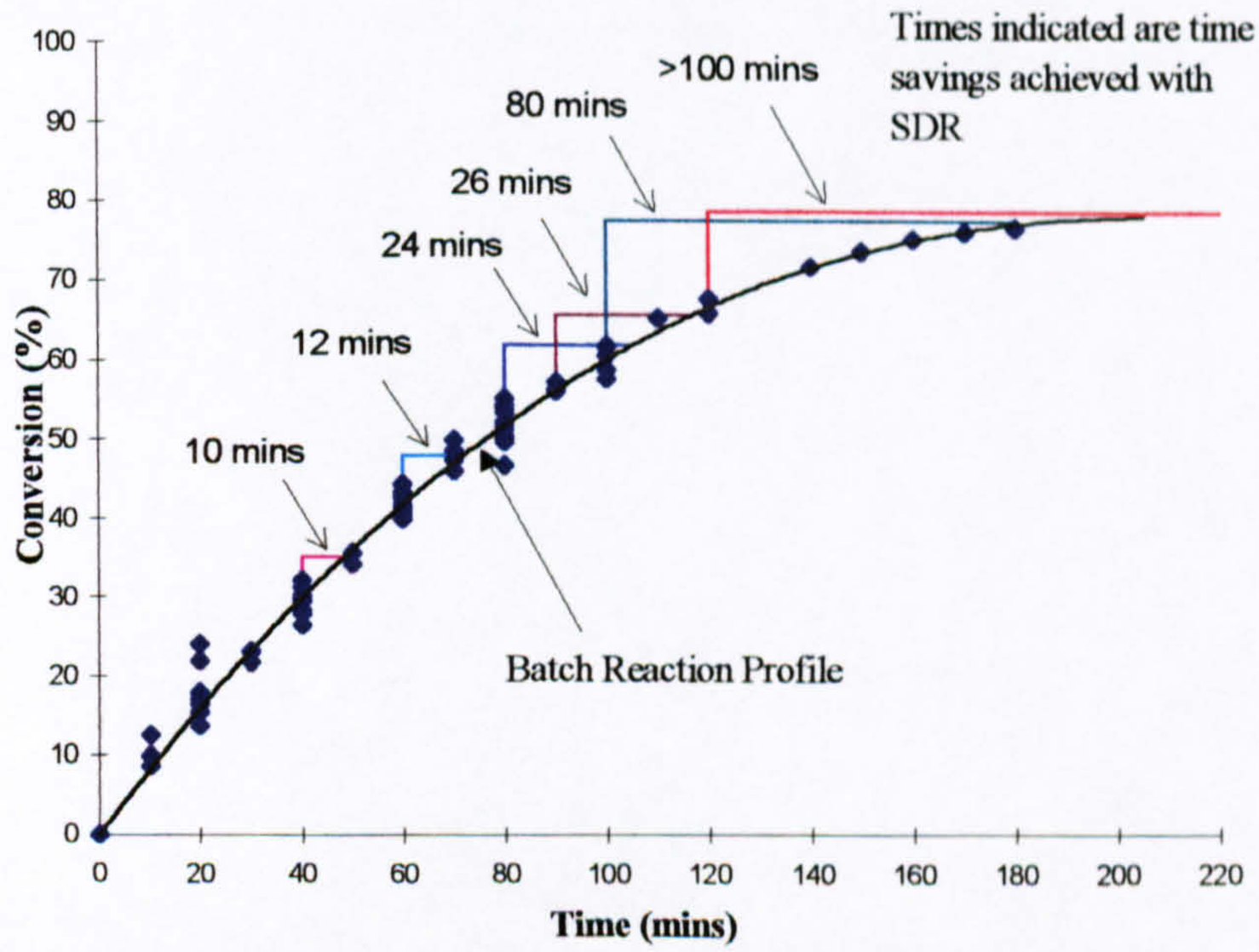

Figure 5.22. Time savings in SDR at fixed disc speed of 850 rpm (Experiment D)

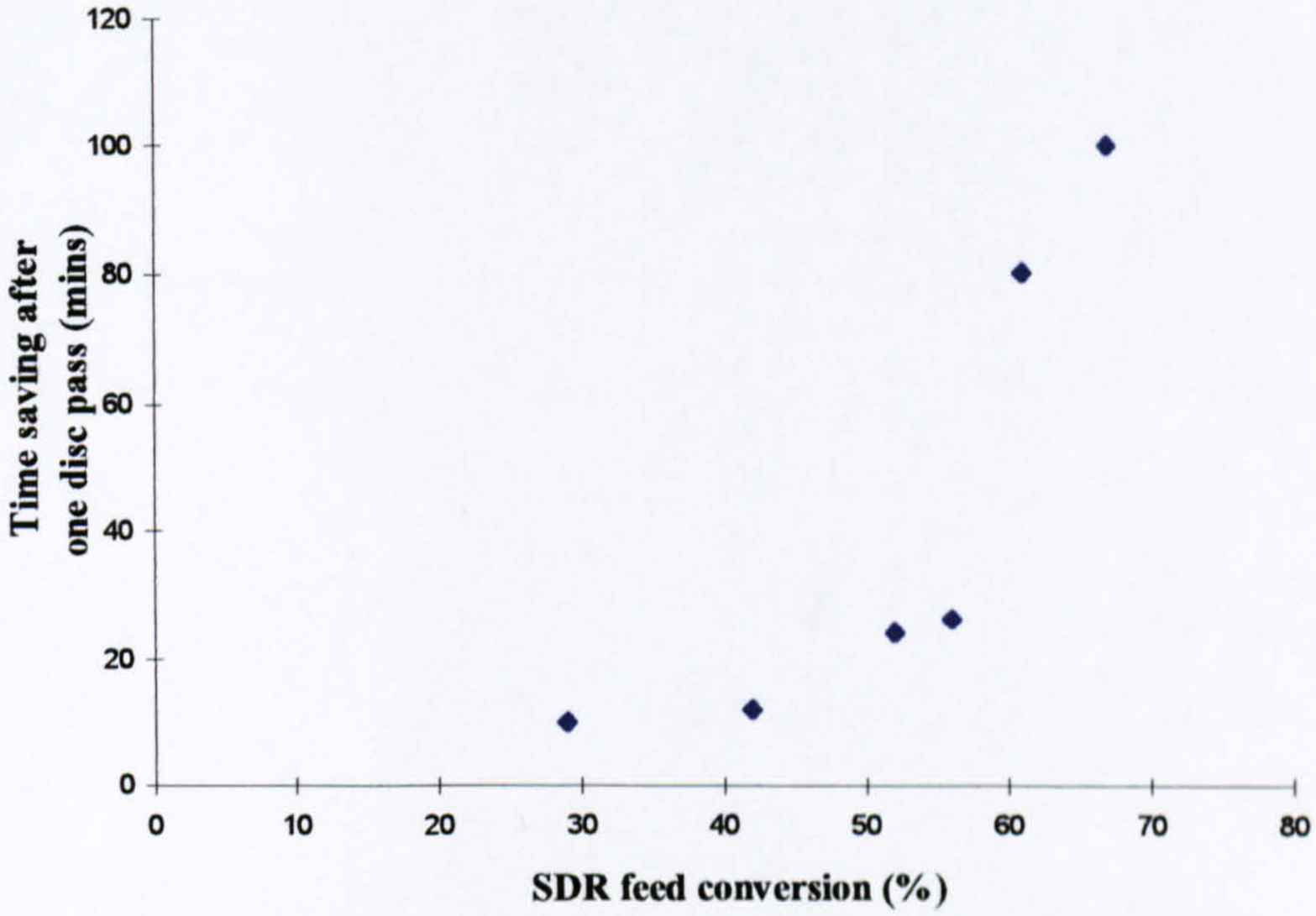

Figure 5.23. Effect of prepolymer feed conversion on time saving at fixed disc speed of 850 rpm (Experiment D)

The changes observed in molecular weights M_n and M_w for runs in experiment D are presented in Figure 5.24 through to Figure 5.28 below. The results indicate that, generally, the product from the rotating disc surface has considerably lower average M_n and M_w values in comparison with those expected in the stirred tank reactor at the same conversion. This is clearly seen in Figure 5.24 and Figure 5.26 from the SDR product molecular weight averages falling below the profile for the batch data.

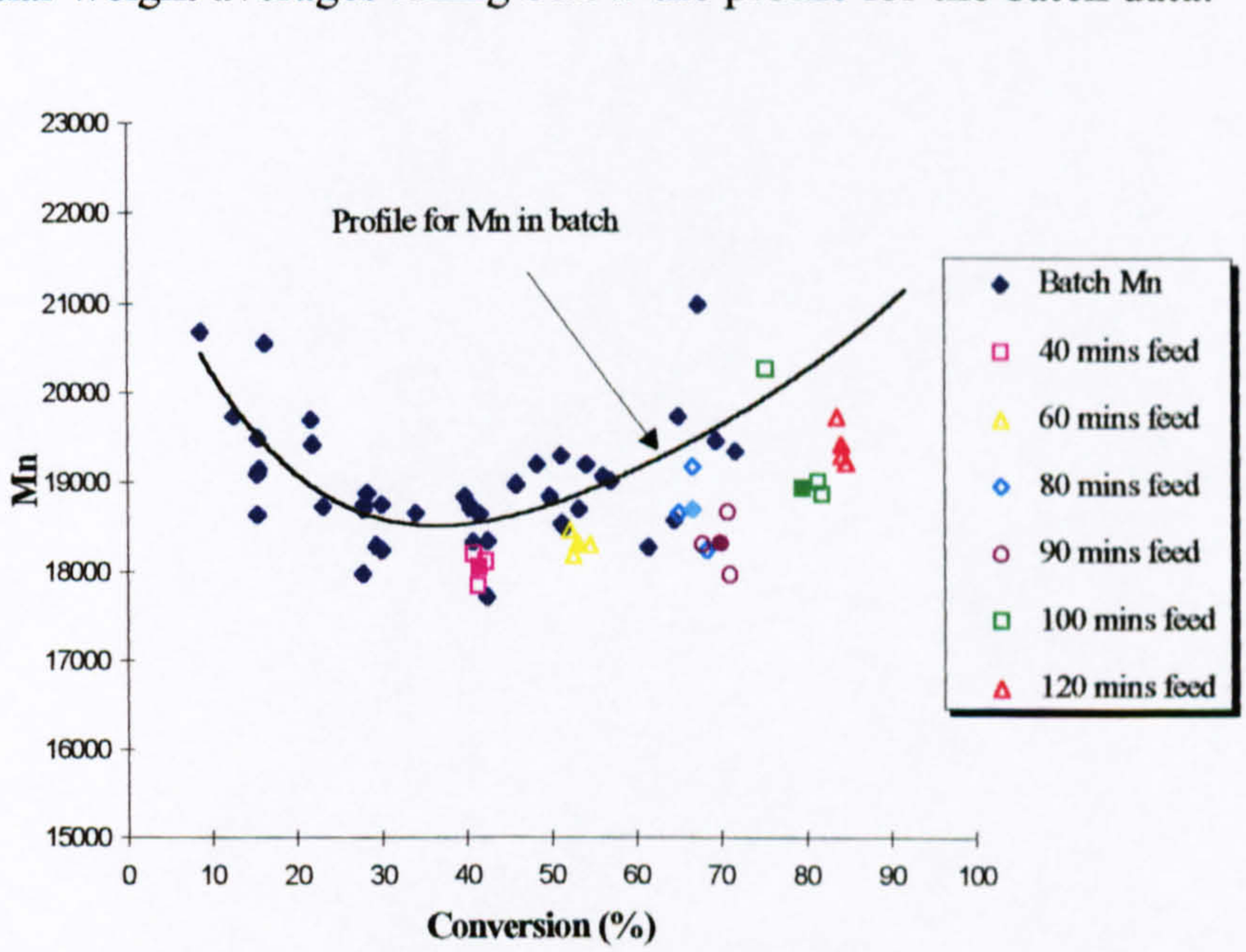

Figure 5.24. Mn for batch and SDR polymerisations (Experiment D)
(SDR filled labels- average, SDR unfilled labels- measured data)

From Figures 5.24 and 5.25, the % decrease in M_n is calculated to be in the range 2.8% to 6.6% as the feed conversion is increased from 29% (at 40 minutes feed time) to 67% (at 120 minutes feed time). The difference becomes more significant at

higher conversions because of the rapid build-up of viscosity in the batch which encourages more monomer molecules to add to the active growing chain hence giving high molecular weights. This effect has been discussed in some detail in Chapter 2.

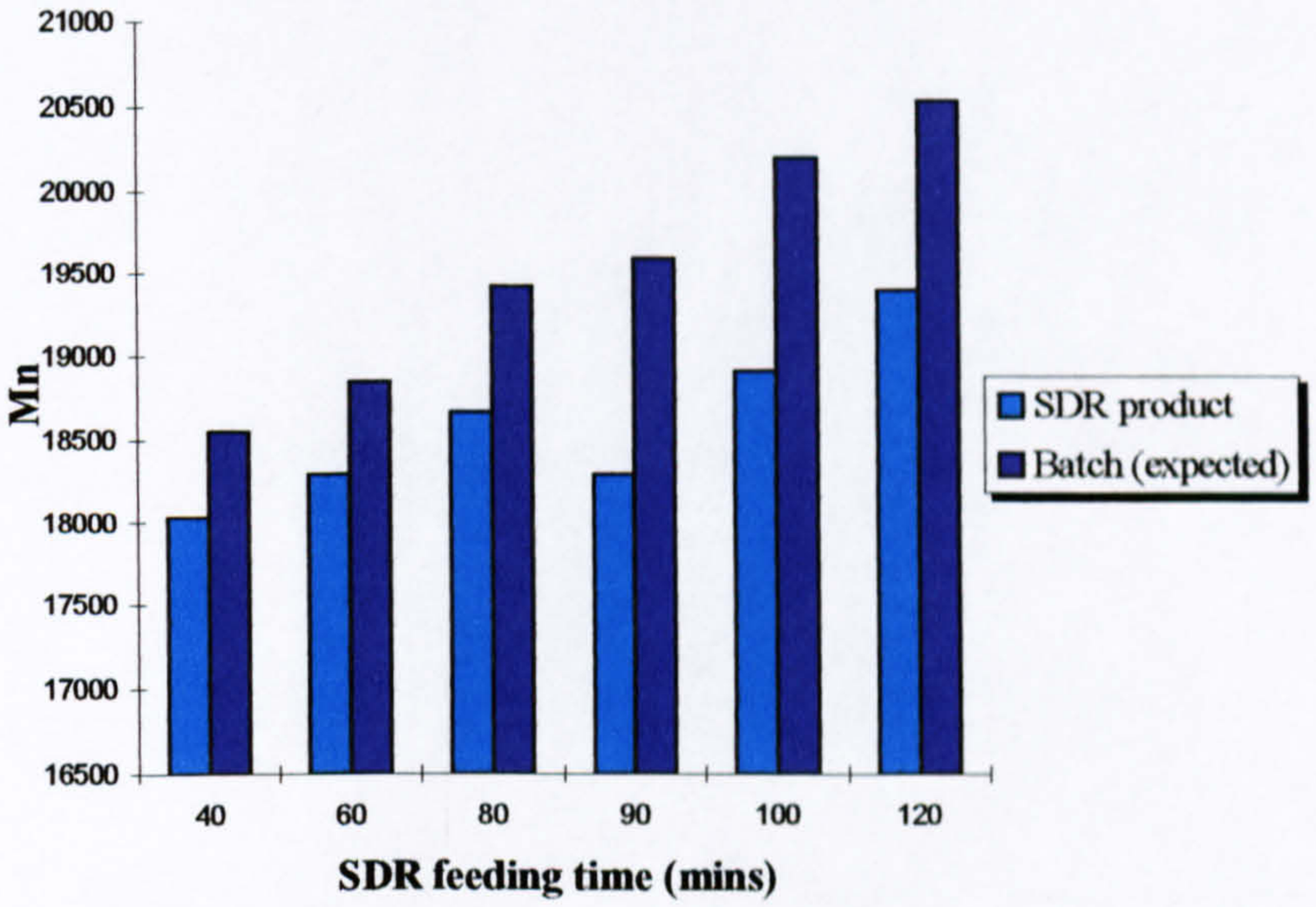

Figure 5.25. Comparison of average SDR product Mn and expected batch Mn at same conversion (Experiment D)

Figures 5.26 and 5.27 display similar results for M_w. Here the % decline in M_w ranges from 3.4% to 5.8%.

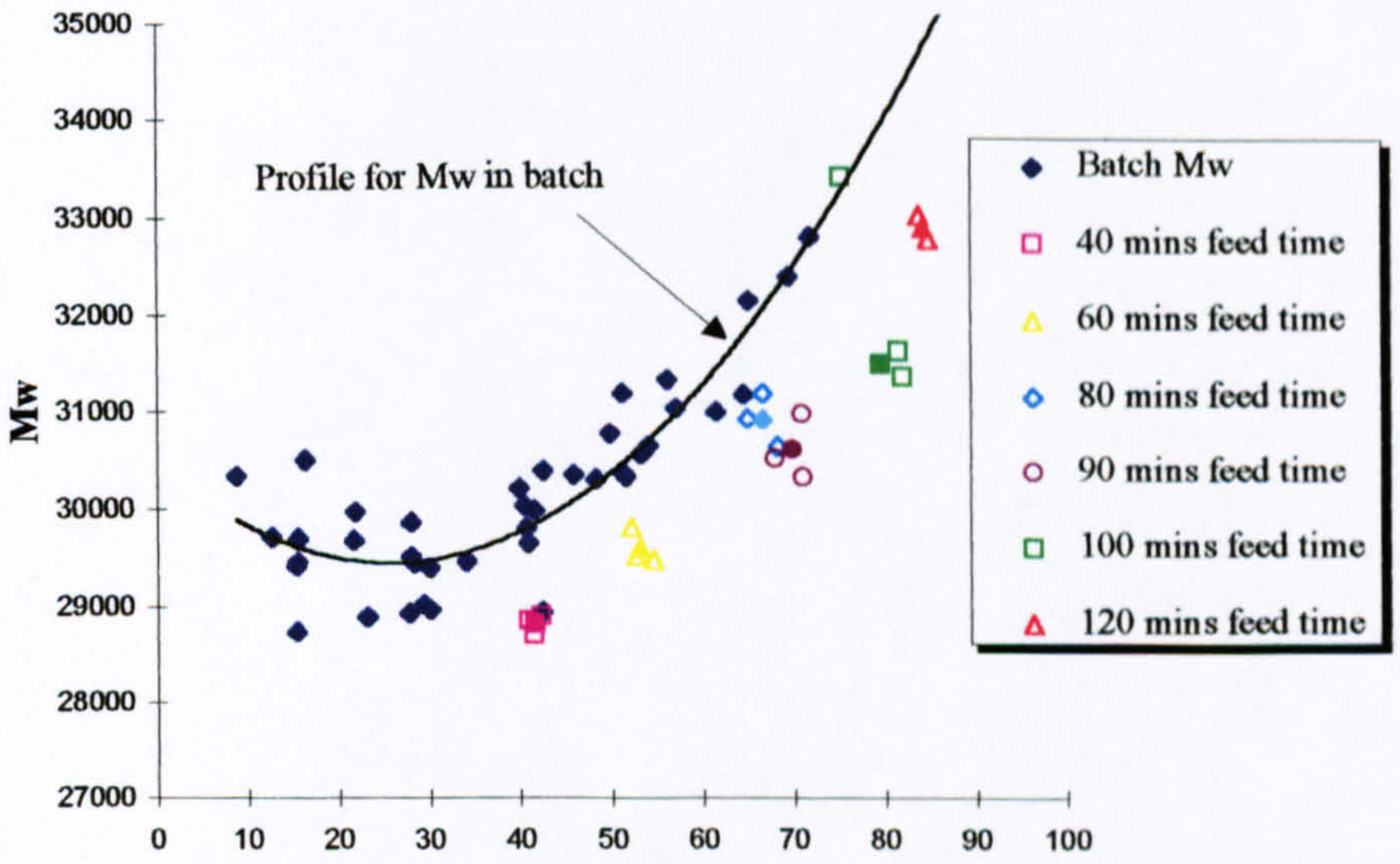

Figure 5.26. Mw for batch and SDR polymerisations (Experiment D)
(SDR filled labels- average, SDR unfilled labels- measured data)

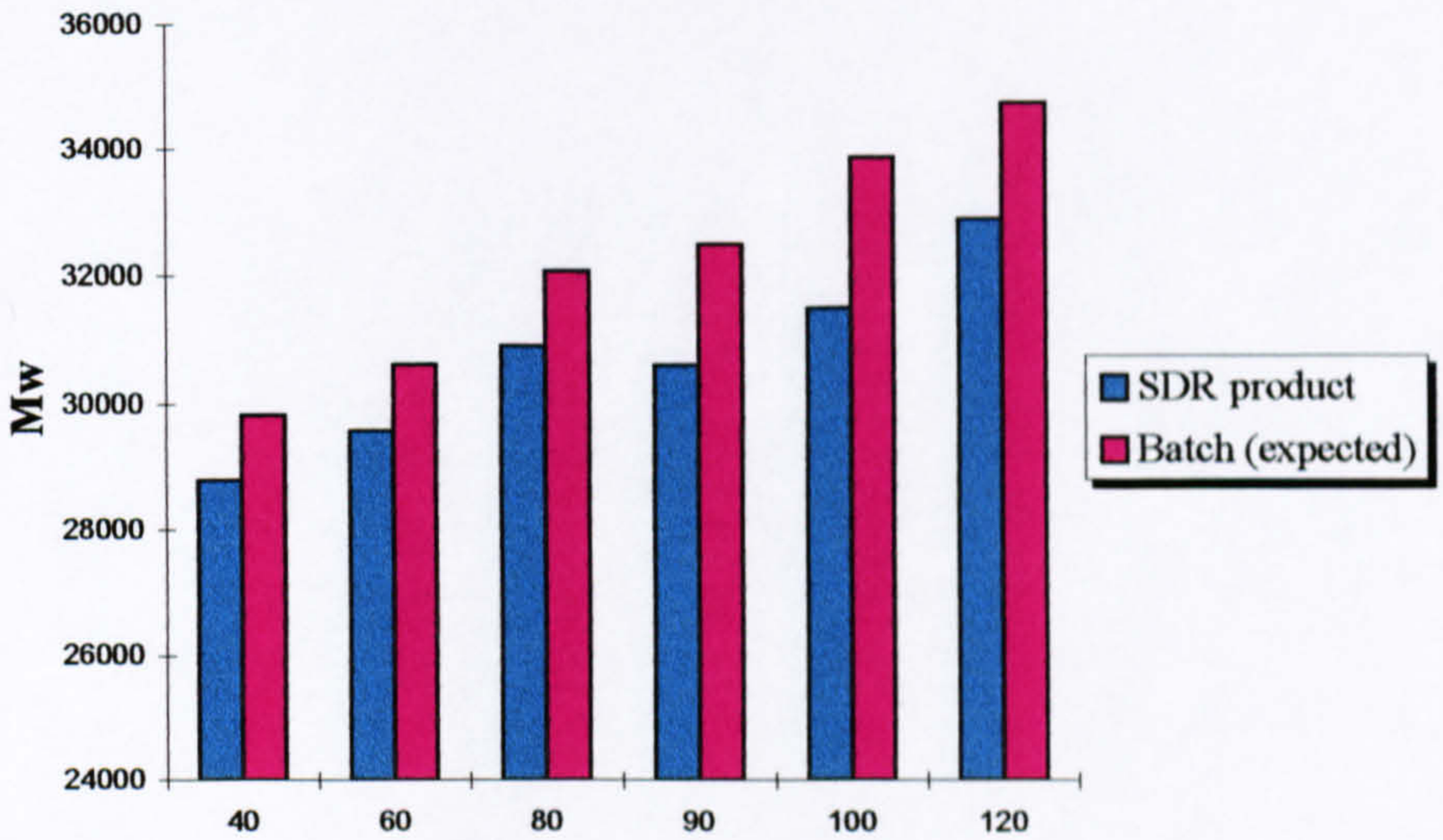

Figure 5.27. Comparison of average SDR product Mw and expected batch Mw at same conversion (Experiment D)

Analysis of the results for the polydispersity index (DI) of the SDR polymer product (Figures 5.28 and 5.29 below) reveals a similar pattern as that for M_n and M_w.

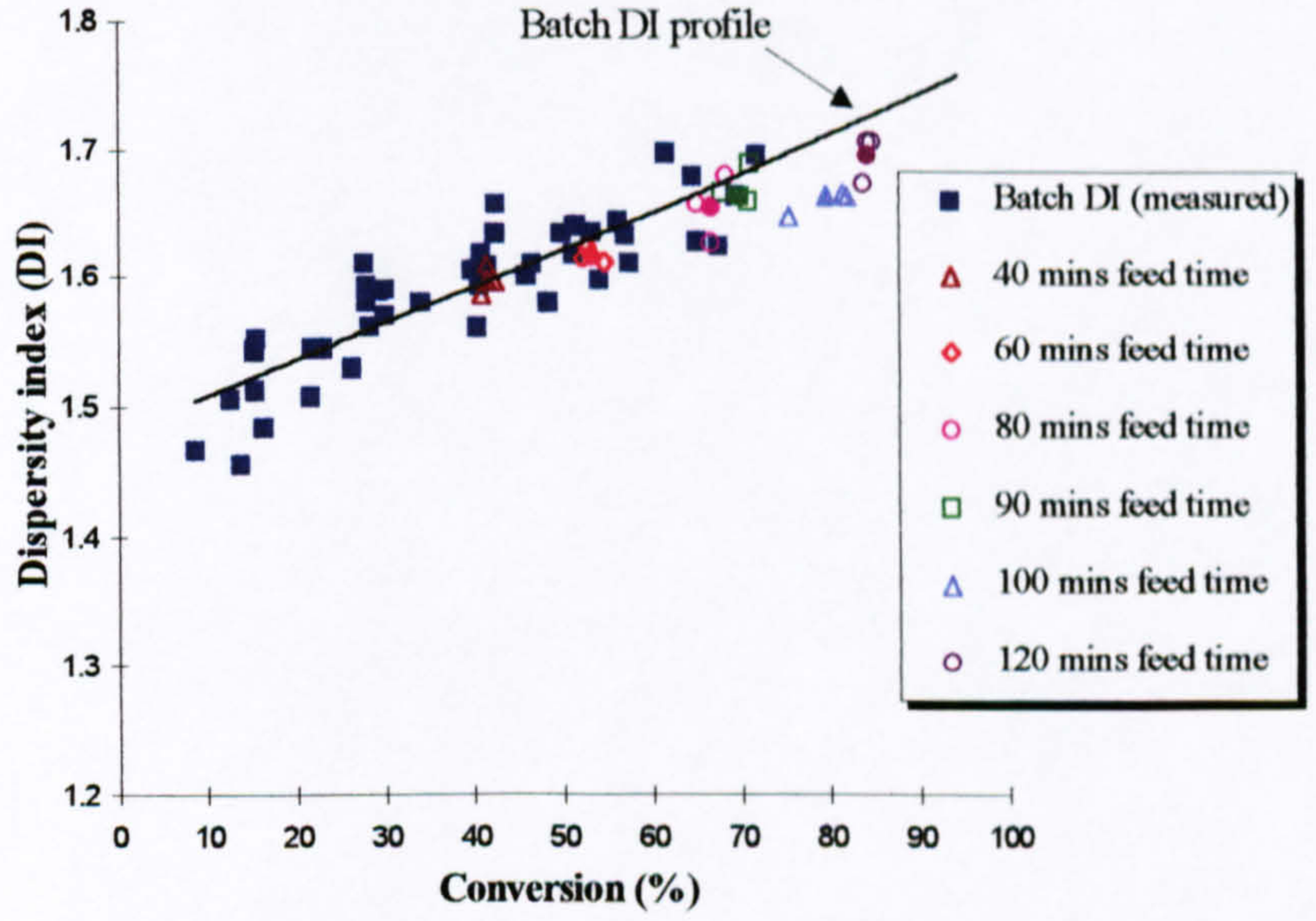

Figure 5.28. Dispersity index (DI) for batch and SDR polymerisations (Experiment D)
(SDR filled labels- average, SDR unfilled labels- measured data)

Hence, for the range of feeding times considered in experiment D, the SDR yields a polymer having a lower DI than that expected to be produced from the conventional batch system for the same polymer product conversion.

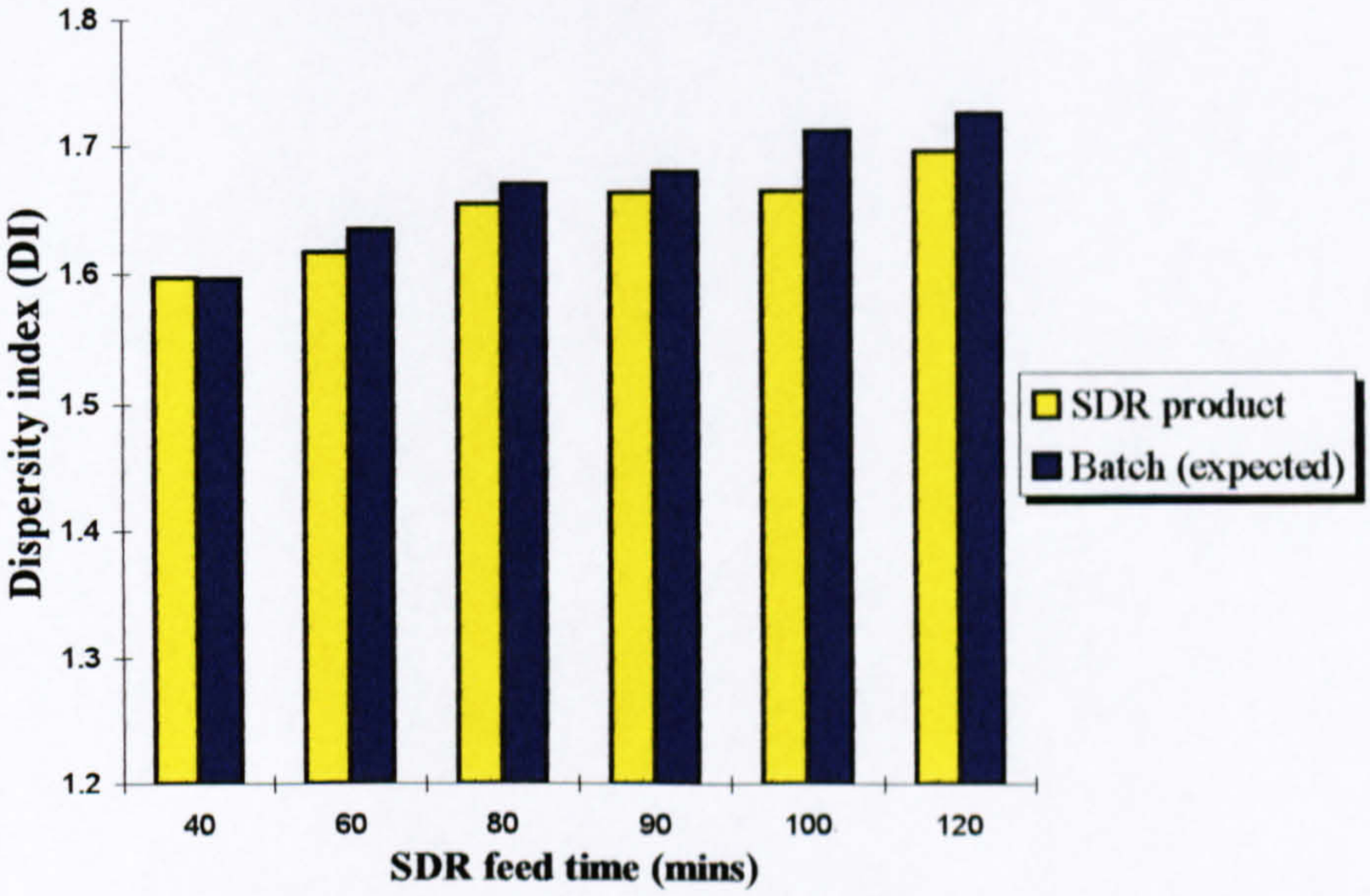

Figure 5.29. Comparison of average SDR product DI and expected batch DI at same conversion (Experiment D)

5.1.2.5. Experiment E

The conversion results for runs in experiment E in which rotational speeds ranging from 400 to 1500 rpm were tested at fixed prepolymer feed conversion of 58% (80 minutes batch reaction time) are given in Figures 5.30 to 5.33. The measured raw data can be found in Appendix E.

The increases in conversion of the polymer collected from the spinning disc surface at the different speeds are presented in Figures 5.30 and 5.31 below. For a realistic evaluation of the effect of disc speed on the polymerisation of styrene, the measured conversion of the SDR feed in each run has been standardised to the constant value of 58% predicted from the batch calibration curve. All corresponding SDR product conversions have been adjusted accordingly, as seen in the summary table for each experimental set given in Appendix E. This procedure was also adopted for experiment C. Also, all SDR product conversions presented in the graphs below have been appropriately modified to account for styrene losses due to evaporation.

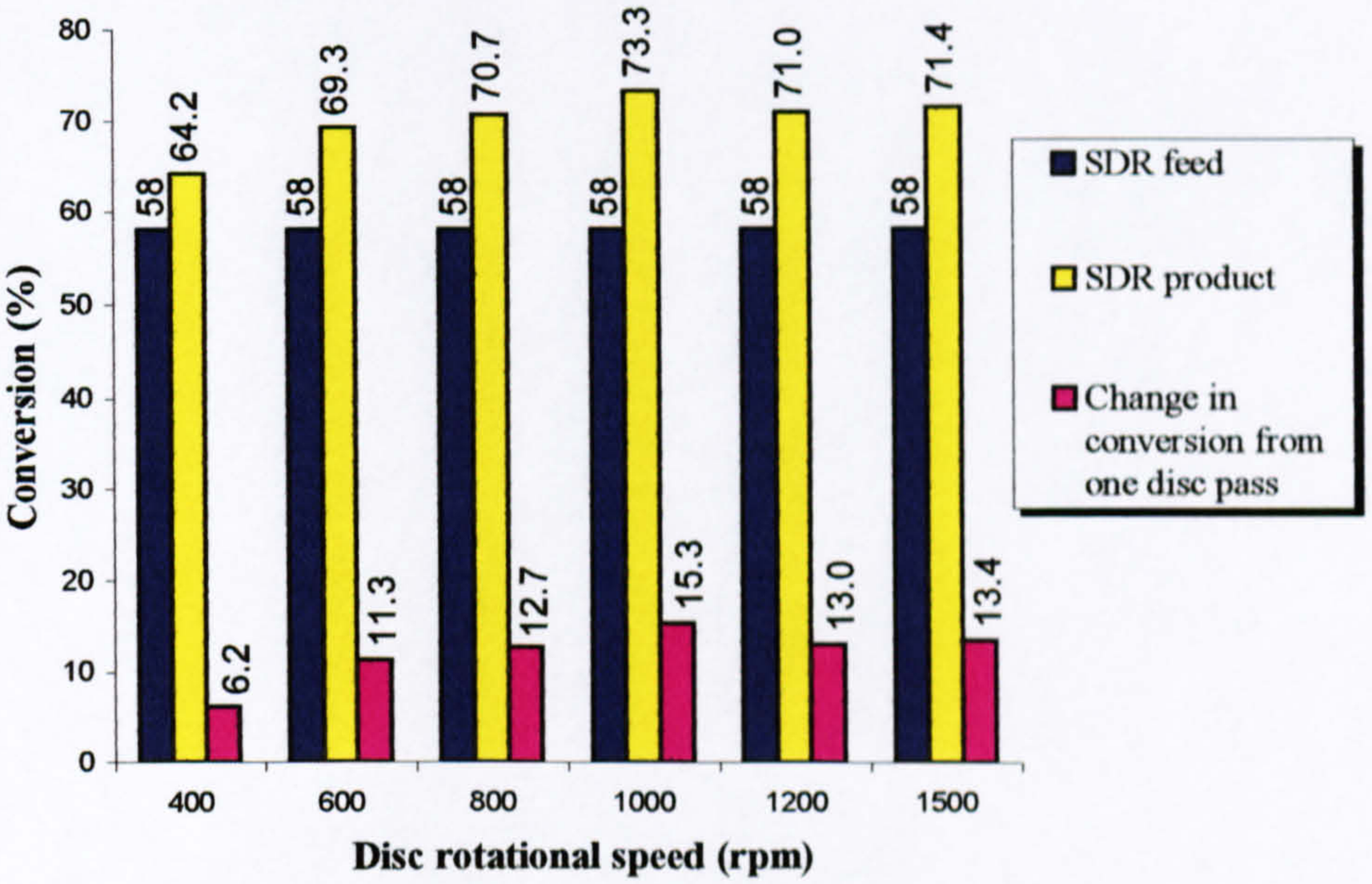

Figure 5.30. Effect of disc speed on SDR product conversion for fixed SDR feed conversion of 58% (Experiment E)

A gradual increase in conversion with higher disc speed is observed with a peak value of 15.3% recorded at a disc speed in the region of 1000 rpm. Further increases in the disc speed beyond 1000 rpm result in a decline in the change in conversion in the SDR. This trend is clearly visible in Figure 5.31 and is remarkably similar to the one obtained in experiment C (section 5.1.2.3).

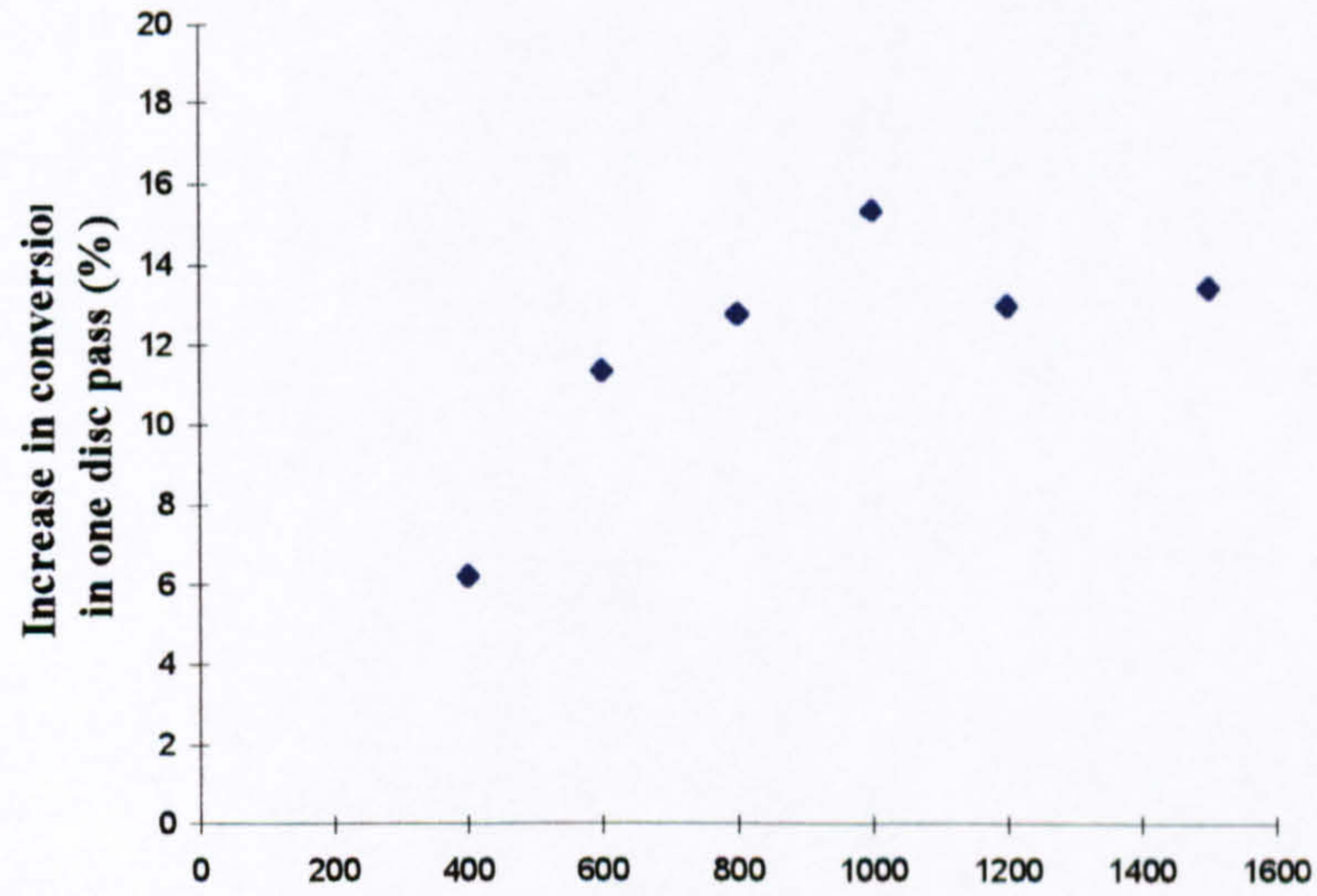

Figure 5.31. Increase in SDR conversions at fixed prepolymer feed of 58% (Experiment E)

The time saving results for experiment E are illustrated in Figures 5.32 and 5.33.

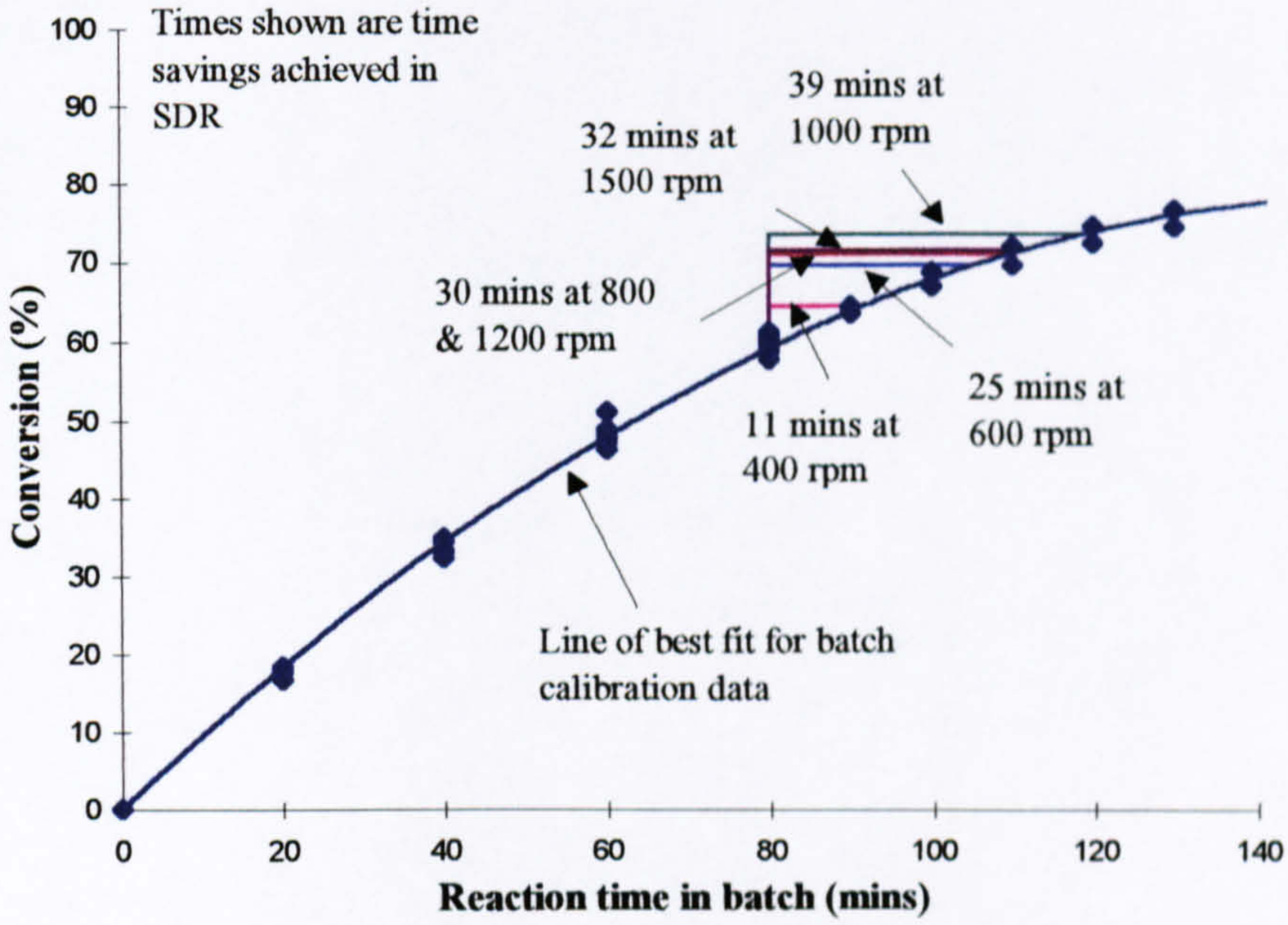

Figure 5.32. Time savings in SDR at fixed prepolymer feed conversion of 58% (Experiment E)

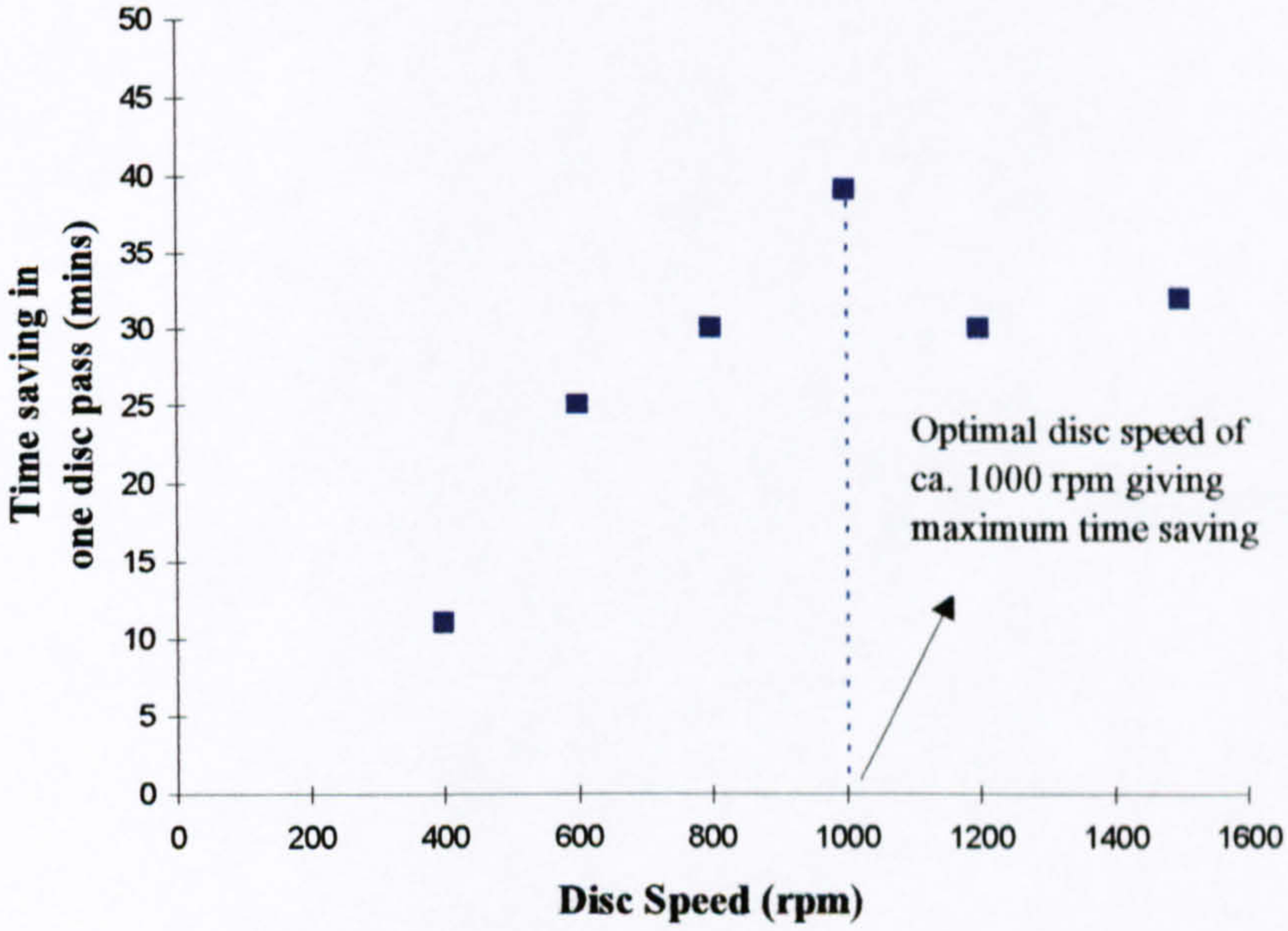

Figure 5.33. Effect of disc rotational speed on time saving for 58% SDR feed (Experiment E)

The time saved rises steadily from 11 minutes to 30 minutes as the rotational speed is doubled from 400 rpm to 800 rpm. It peaks at about 40 minutes at an optimal speed of around 1000 rpm. Beyond this point, the saving in time by the SDR falls to around 30 minutes. It is worthwhile noting that the trend identified here is similar to the one in experiment C (Figure 5.13).

Changes in average molecular weights M_n and M_w for SDR products from the disc rotating at the various speeds investigated are shown in Figures 5.34 to 5.37.

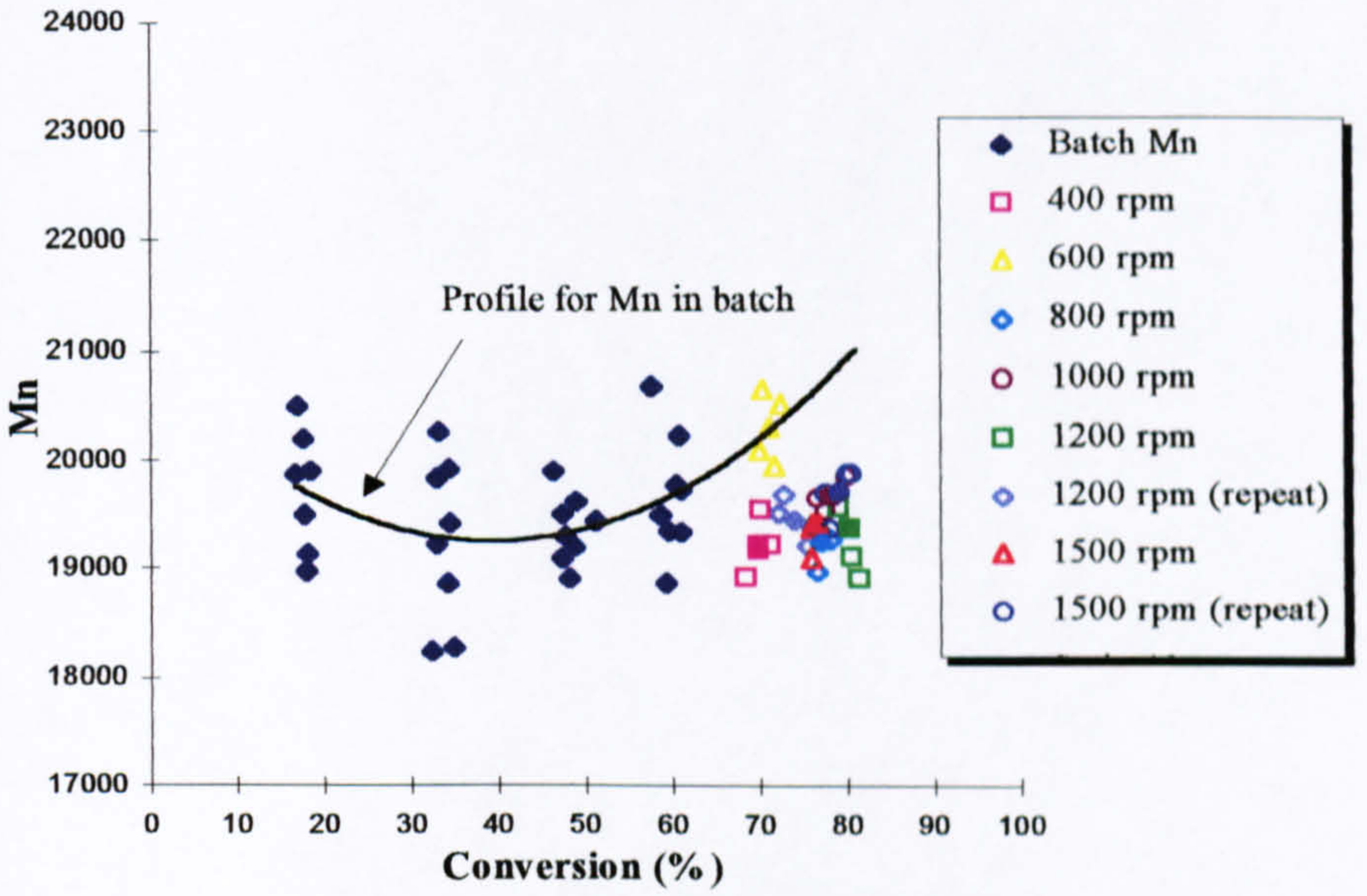

Figure 5.34. Mn for batch and SDR polymerisations (Experiment E)
(SDR filled labels- average, SDR unfilled labels- measured data)

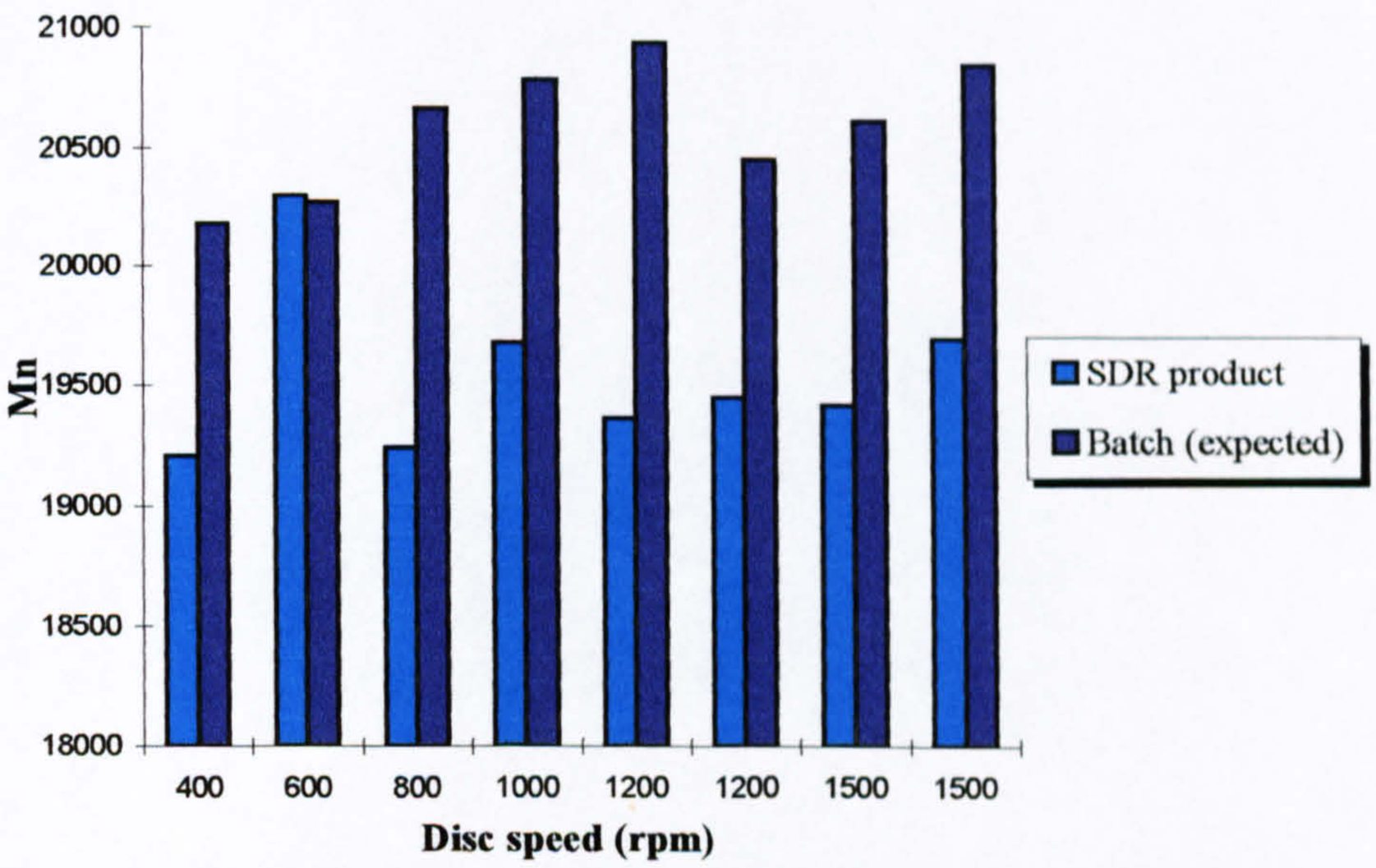

Figure 5.35. Comparison of average SDR product Mn and expected batch Mn at same conversion (Experiment E)

Comparison between SDR polymer and batch polymer at the same conversion as the SDR product average conversion shows that both M_n and M_w for the SDR polymer are lower than the value expected in the batch for all the speeds tested except at 600 rpm. The maximum % decrease of 9.3% in M_n occurs at 400 rpm while the maximum % decrease of 8.4% in M_w occurs at 1200 rpm.

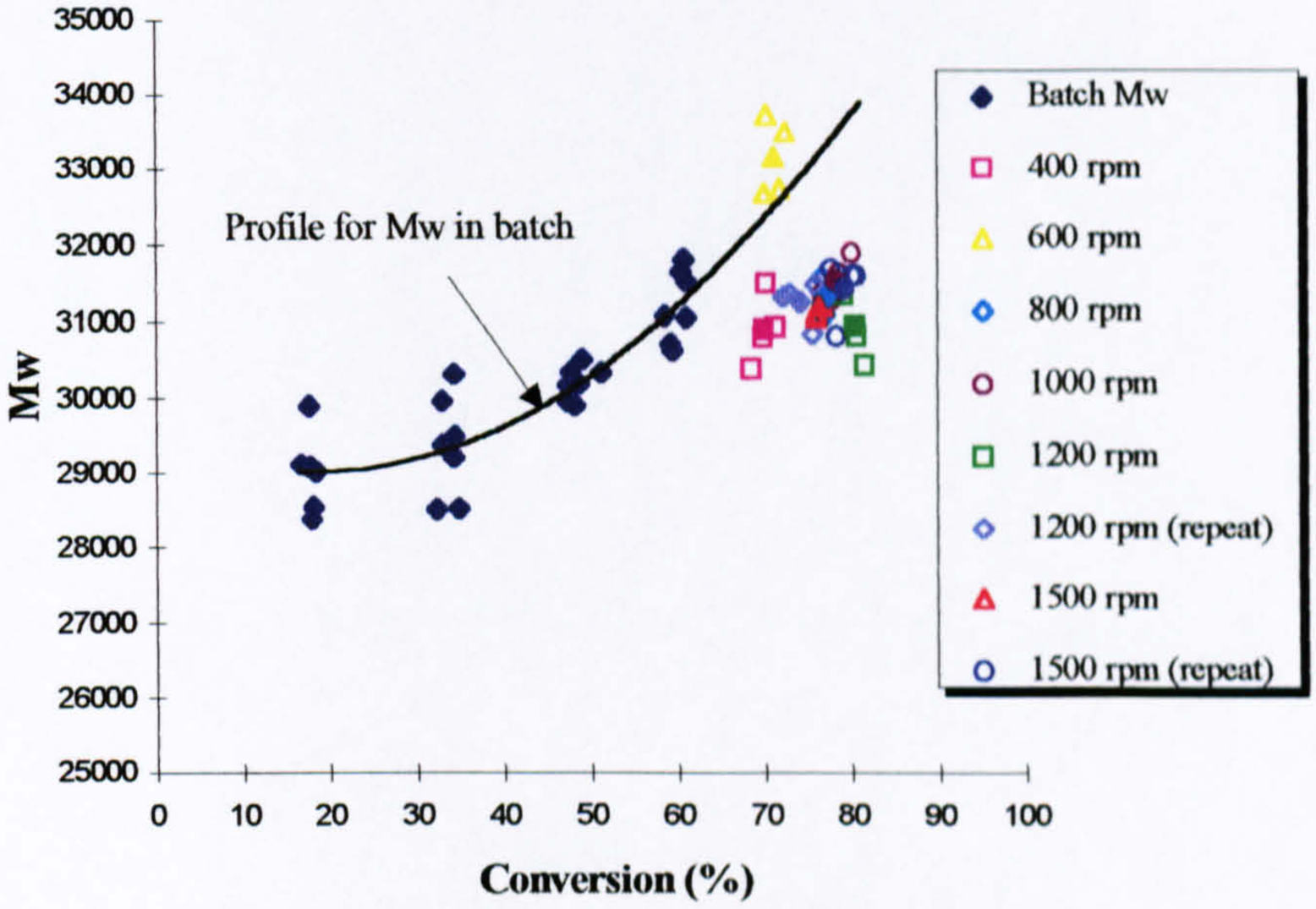

Figure 5.36. Mw for batch and SDR polymerisations (Experiment E)
(SDR filled labels- average, SDR unfilled labels- measured data)

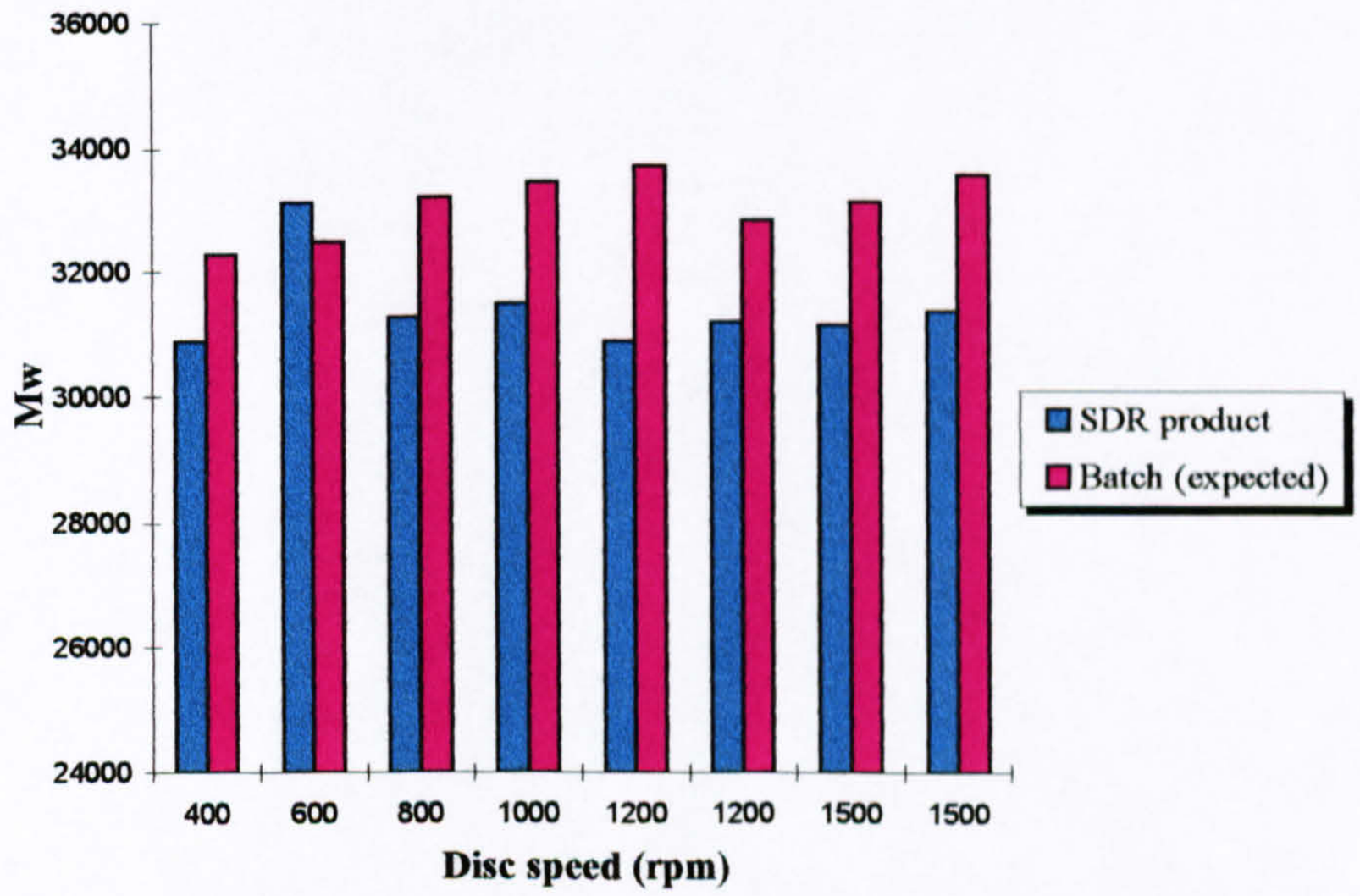

Figure 5.37. Comparison of average SDR product Mw and expected batch Mw at same conversion (Experiment E)

Although there does not seem to be any apparent trend in the change of M_n and M_w with variation in speed, these results suggest that the control of molecular weight in the SDR can be more readily achieved with enhancement in the rate of polymerisation on the disc.

Similarly, the effect of rotation on the spread of the molecular weight distribution (MWD) which is measured by the polydispersity index (DI) is presented in Figures 5.38 and 5.39 below.

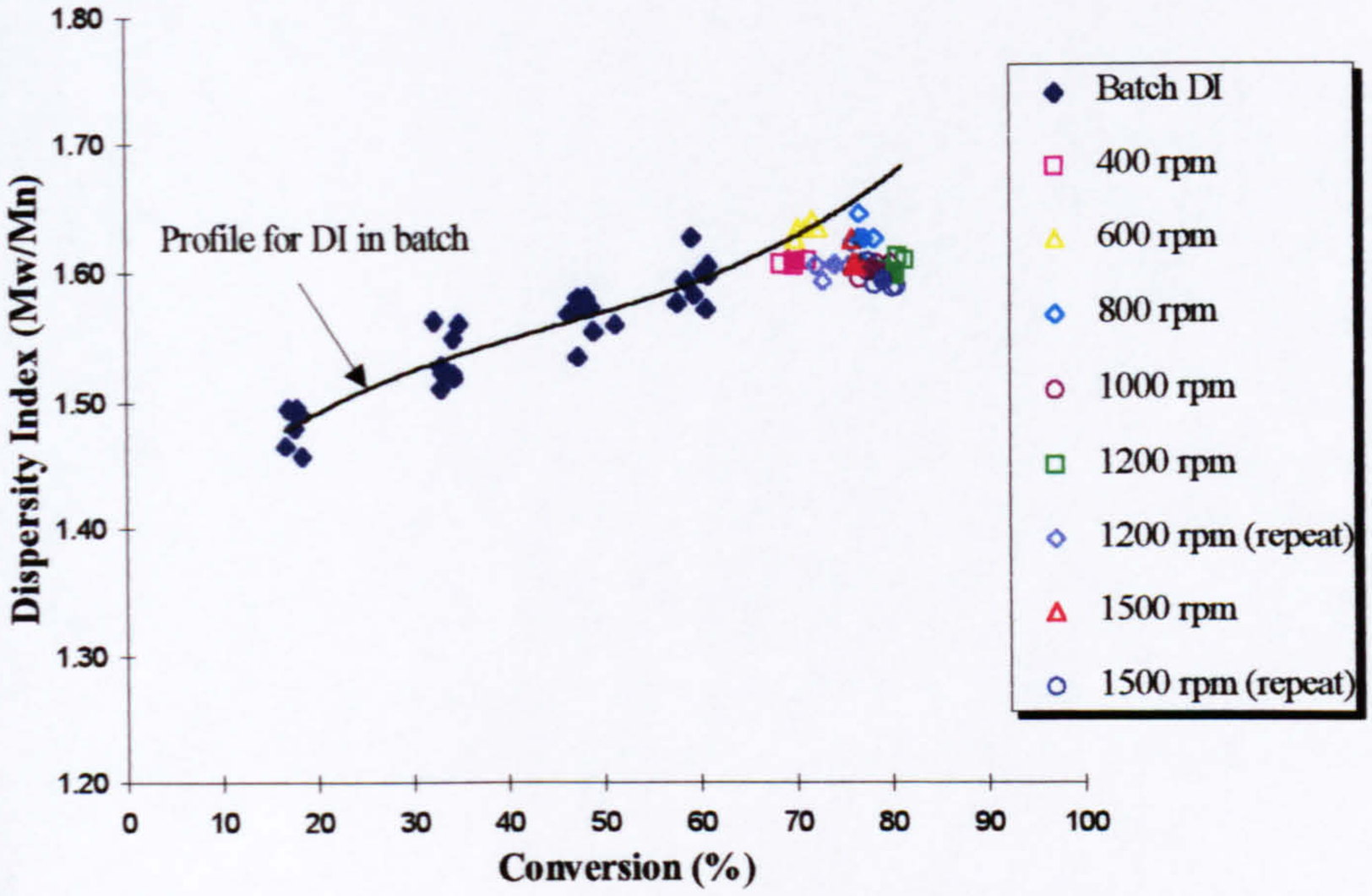

Figure 5.38. Polydispersity index (DI) for batch and SDR polymerisations (Experiment E)
(SDR filled labels- average, SDR unfilled labels- measured data)

It is seen in Figure 5.38 that the SDR measured data points as well as the average calculated values are all found below the batch DI profile except for the data at 600 rpm. This is indeed emphasised in Figure 5.39 below whereby the SDR products DI values averaged over all samples collected for each test speed are compared with the expected DI predicted from the batch profile for a batch polymer at the same conversion. The % decreases in SDR product DI with respect to the batch DI are evaluated to be in the range 1.8% to 4.9% for the speeds tested.

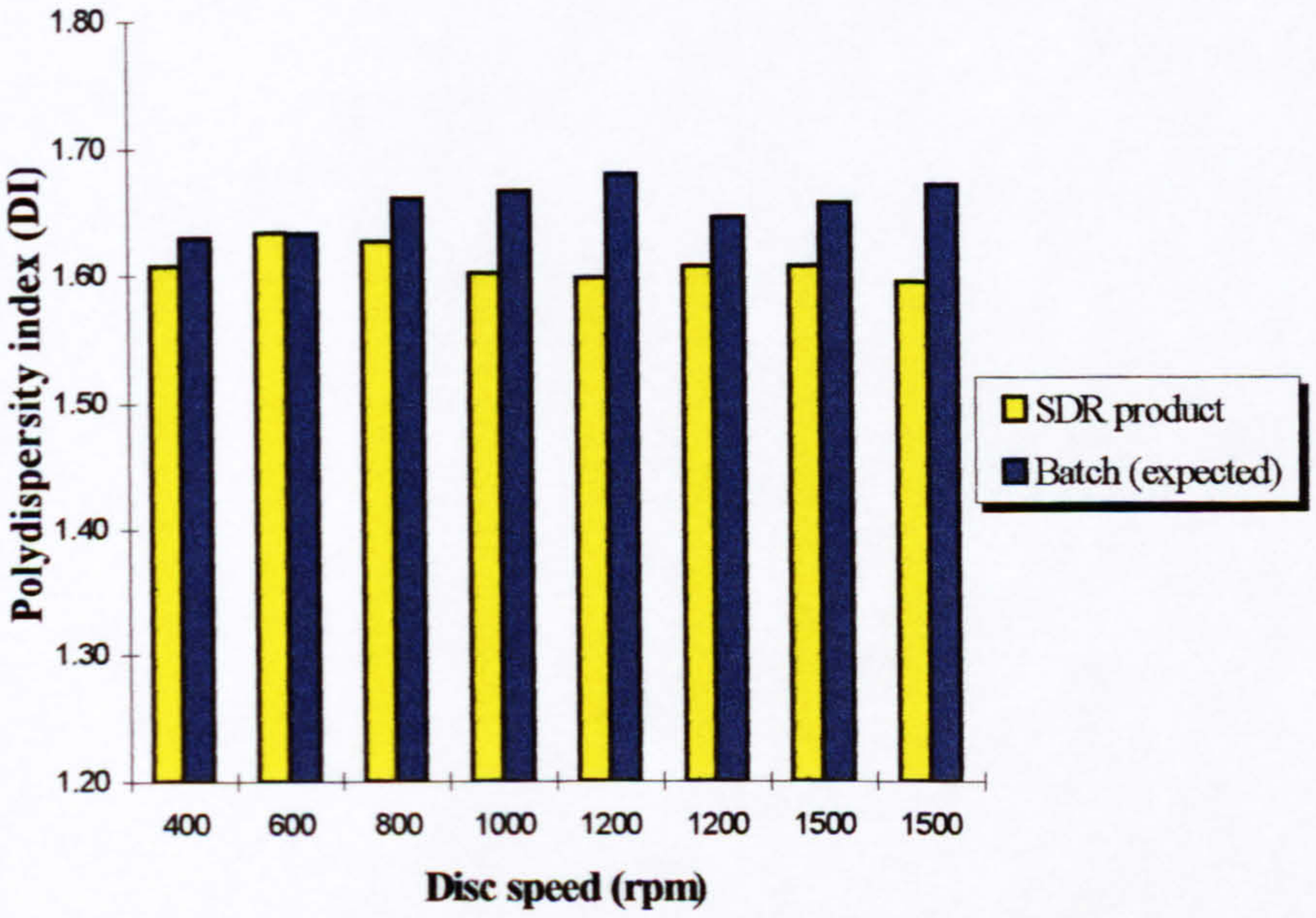

Figure 5.39. Comparison of average SDR product dispersity index (DI) and expected batch DI at same conversion (Experiment E)

5.2. BATCH AGITATION STUDY

The batch agitation experiments were performed in an attempt to quantify the effect of different agitation rates on the conversion and molecular weight properties of the styrene polymerisation system. The results of the agitation experiments would thus enable us to assess the type of flow and the mixing levels sustained on the rotating disc by direct comparison with the SDR results presented in the previous section.

Details of the experimental set-up and procedures have been given in Chapter 4. Four different agitation speeds in the range 50 rpm to 1500 rpm were tested, with a repeat run at 500 rpm to check the reproducibility and accuracy of the data. The conversion and molecular weight data of samples from each run can be found in Appendix F together with operating conditions for each run. The effect of agitator speed on conversion, M_w, M_n and polydispersity index (DI) will be examined in turn in the ensuing section.

5.2.1. Conversion

The conversion profile is very much dependent on the reaction temperature in the batch reactor. In order to separate the effects of any temperature variation in the reaction mixture from those of agitation, it was necessary to establish a temperature profile for each of the runs performed. This is shown in Figure 5.40 below.

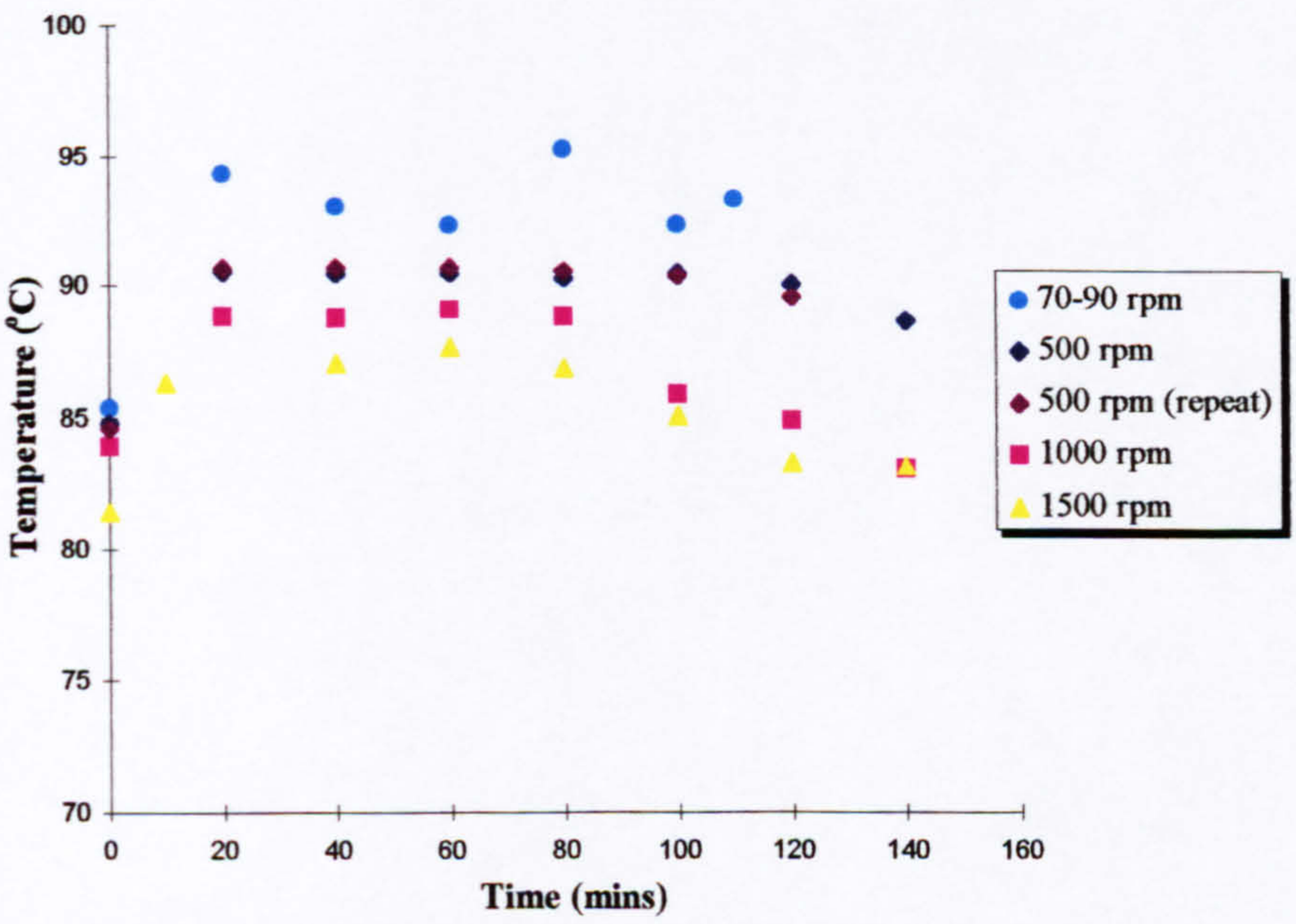

Figure 5.40. Temperature variation in batch reaction mixture with time

The temperature profile for each speed of agitation shows an initial rise in temperature which is followed by a steady decrease at large reaction times. The temperature at any given time of reaction increases as the speed of agitation in the mixture is reduced. Extreme vortices were observed in the reaction mixture especially at the highest agitation rates. This was due to the absence of baffles around the walls of the glass vessel. In the presence of these vortices, the thermocouple had the tendency to drift towards the upper surface of the mixture. Although the position of

the thermocouple was constantly monitored and adjusted, it is possible that some temperature readings were not those of the bulk mixture. Assuming that the changes in temperature predicted by the profiles in Figure 5.40 are accurate enough, they could affect changes in conversion and molecular weight properties and should therefore be accounted for.

The progress of styrene polymerisation in terms of monomer conversion was monitored for various agitator speeds and the results are given in Figure 5.41 below.

The conversion-time profile is seen to be dependent on the speed of agitation in the reactor with the lowest speed of 70-90 rpm giving the highest conversion at any given time. Divergence between the curves at 500, 1000 and 1500 rpm is noticeable approximately beyond the 15% conversion level and tends to become larger with increases in conversion. The data for the two runs at 500 rpm are close enough to deduce that good reproducibility can be expected in the results.

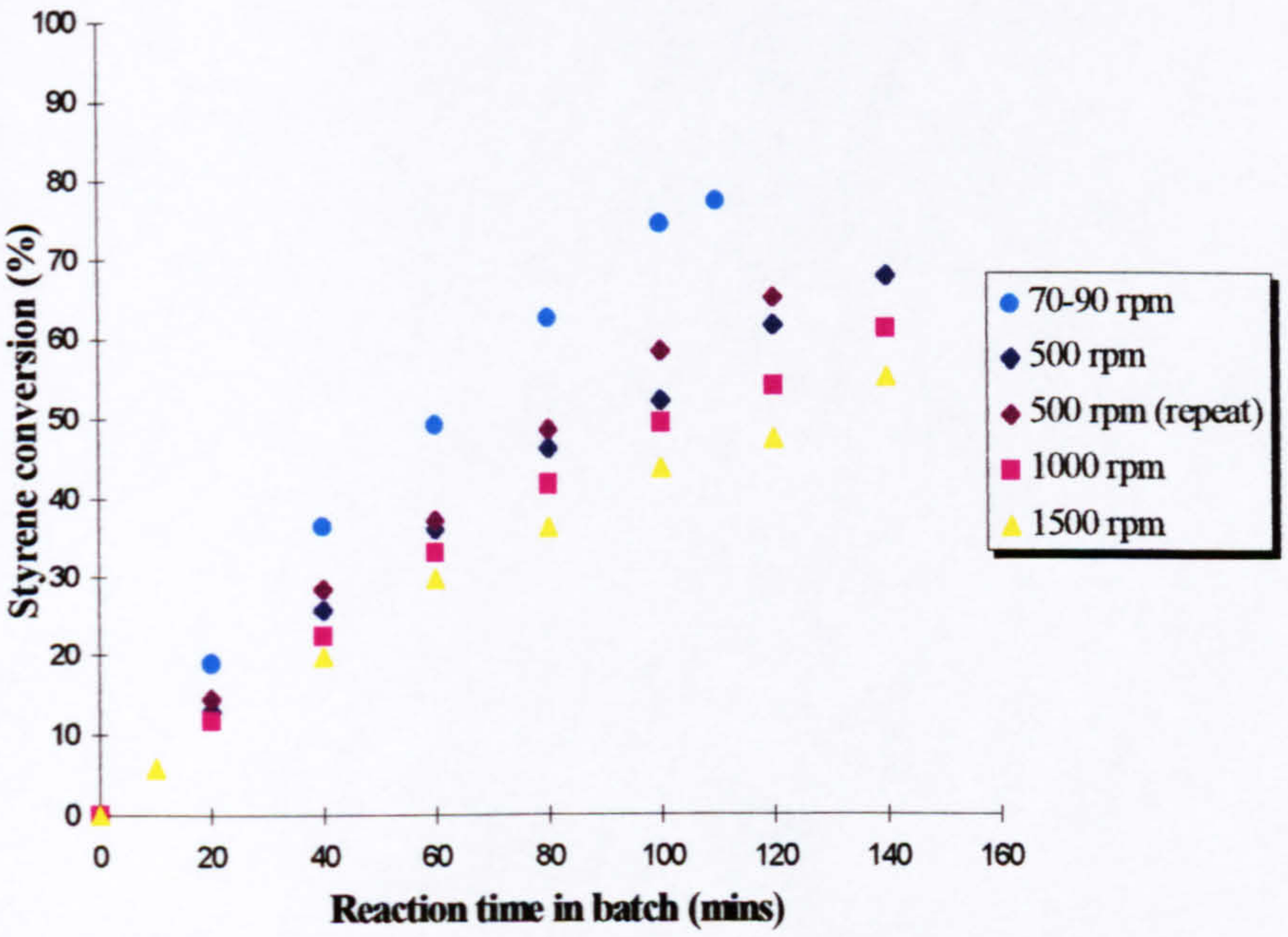

Figure 5.41. Effect of agitator speed on conversion in the batch polymerisation of styrene

The measured experimental conversions obviously include effects due to temperature variations in the reaction mixture which have been presented in Figure 5.40 above. In an attempt to eliminate these from the experimental conversion data, kinetic modelling curves with temperature as the main variable are plotted in Figure 5.42 for each agitator speed.

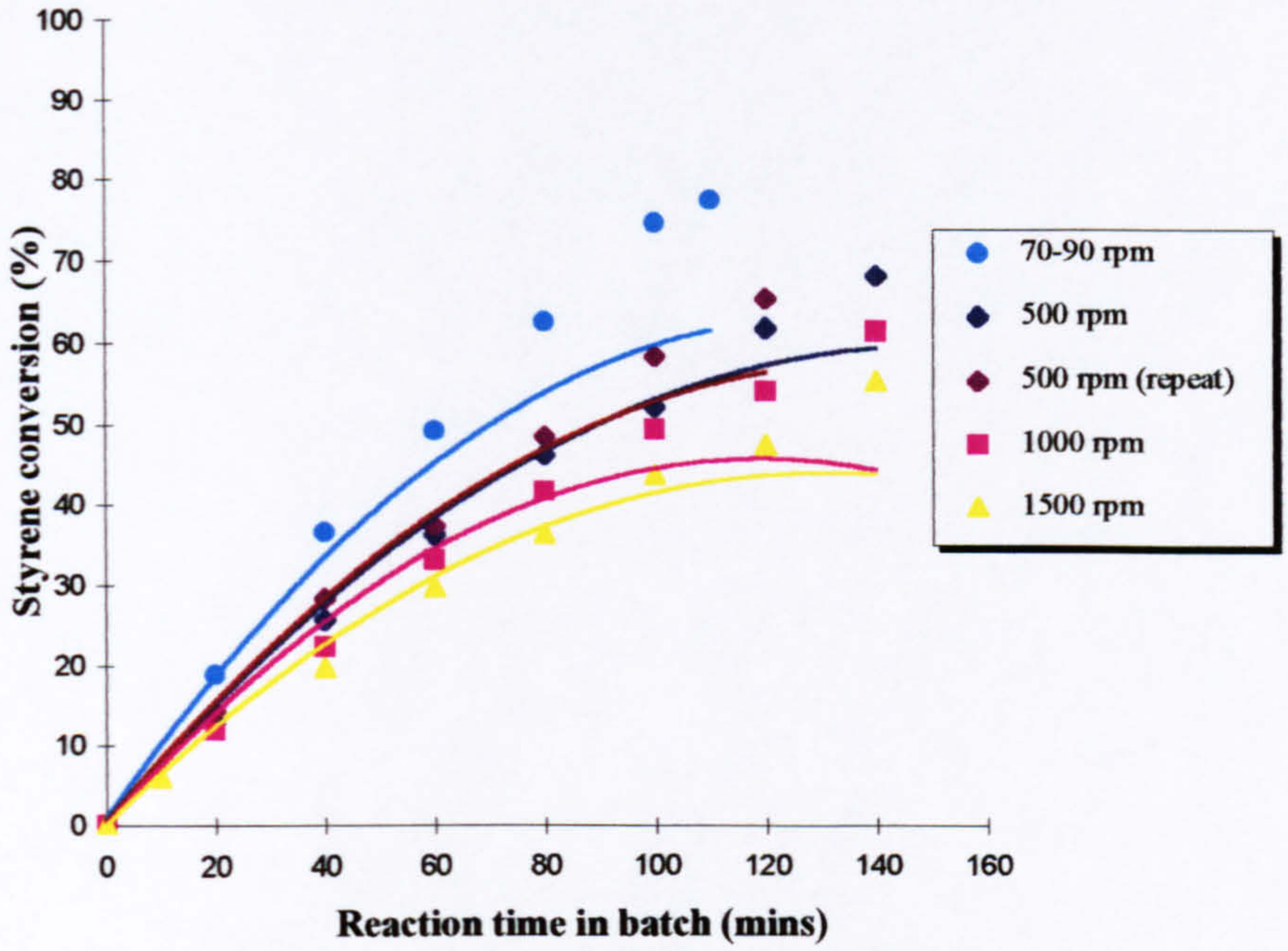

Figure 5.42. Comparison of measured data at various agitator speeds with corresponding model curves calculated with temperature as the main variable

The temperature data used are those measured in the experiments. The rate constants used in the computations of the model data are given in Appendix F together with the model data calculated for each run.

For the range of agitator speeds considered, it is seen from Figure 5.42 that the model curves all tend to be lower than the experimental data in the intermediate to high conversion range (30-50%) indicating that the changes in temperature in the reaction mixture then have minimal effect on the level of conversion actually achieved during the experimental runs. It appears that the deviation from the model curve becomes more pronounced with a fall in the agitation rate. Hence, to a good approximation, differences in experimental conversions observed at high conversions can be attributed to some other mixing effects due to the agitation rate of the impeller.

5.2.2. Molecular weights, M_n and M_w

The changes in M_n and M_w with reaction time for each agitator speed are shown in Figures 5.43 and 5.44 respectively.

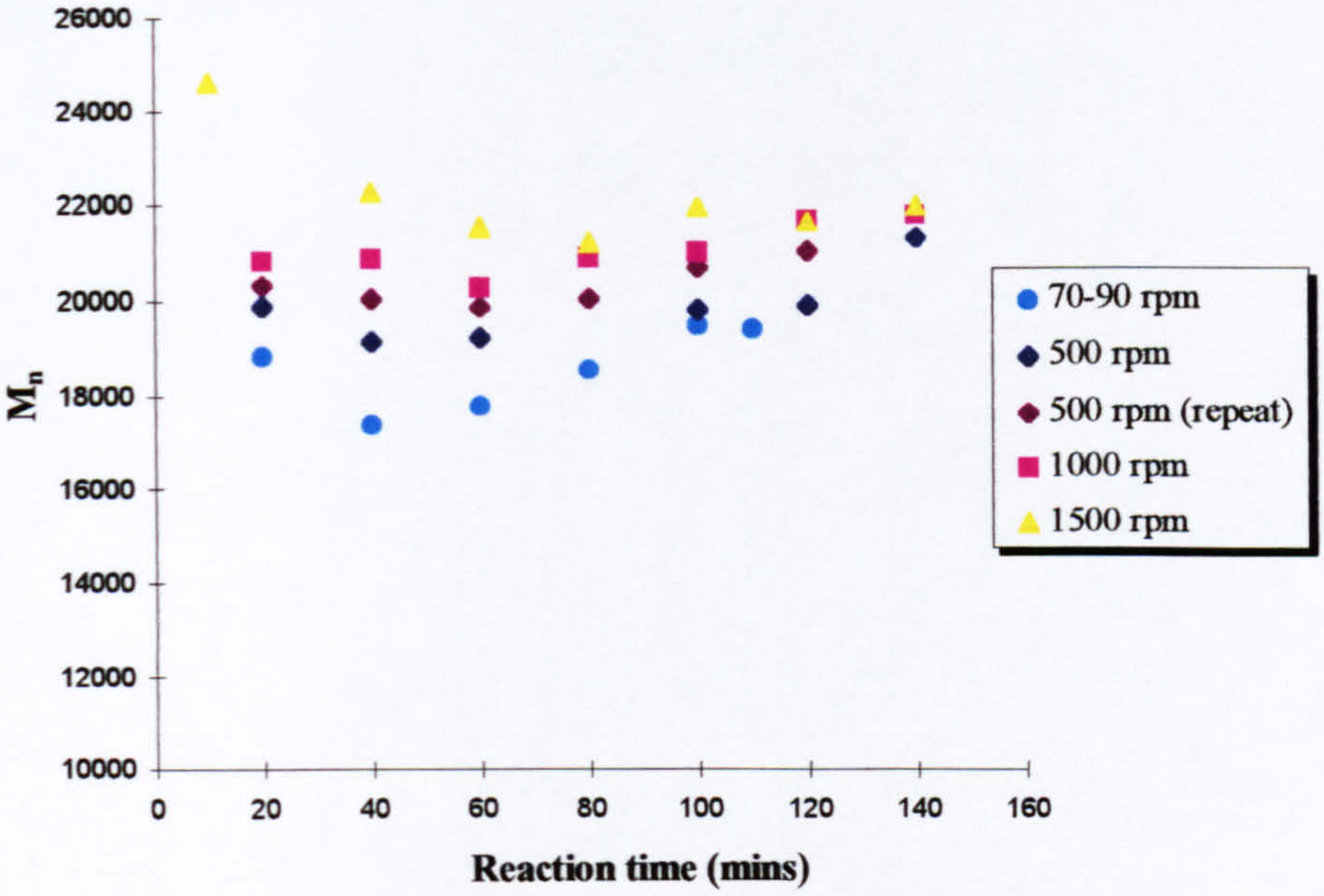

Figure 5.43. Effect of agitator speed on Mn

At a given speed, the values of M_n and M_w are seen to drop initially and then start to rise beyond a certain conversion during the polymerisation. These changes are similar to those observed in Figure 5.3 earlier in this chapter. As will be discussed in more detail in Chapter 6 (section 6.1.2), this is related to the competing effects of temperature and viscosity.

The interesting feature here is the effect of agitator speed on the molecular weights. In the experiment where the lowest speed of 70-90 rpm was tested, the molecular weights are observed to be lower than those at the higher agitation rates. This observation is unmistakably related to the reaction temperature profile as plotted in Figure 5.40 which is always higher for the low agitation rates. The higher the temperature, the lower are the molecular weights M_n and M_w and this is exactly the effect seen at the different agitation speeds.

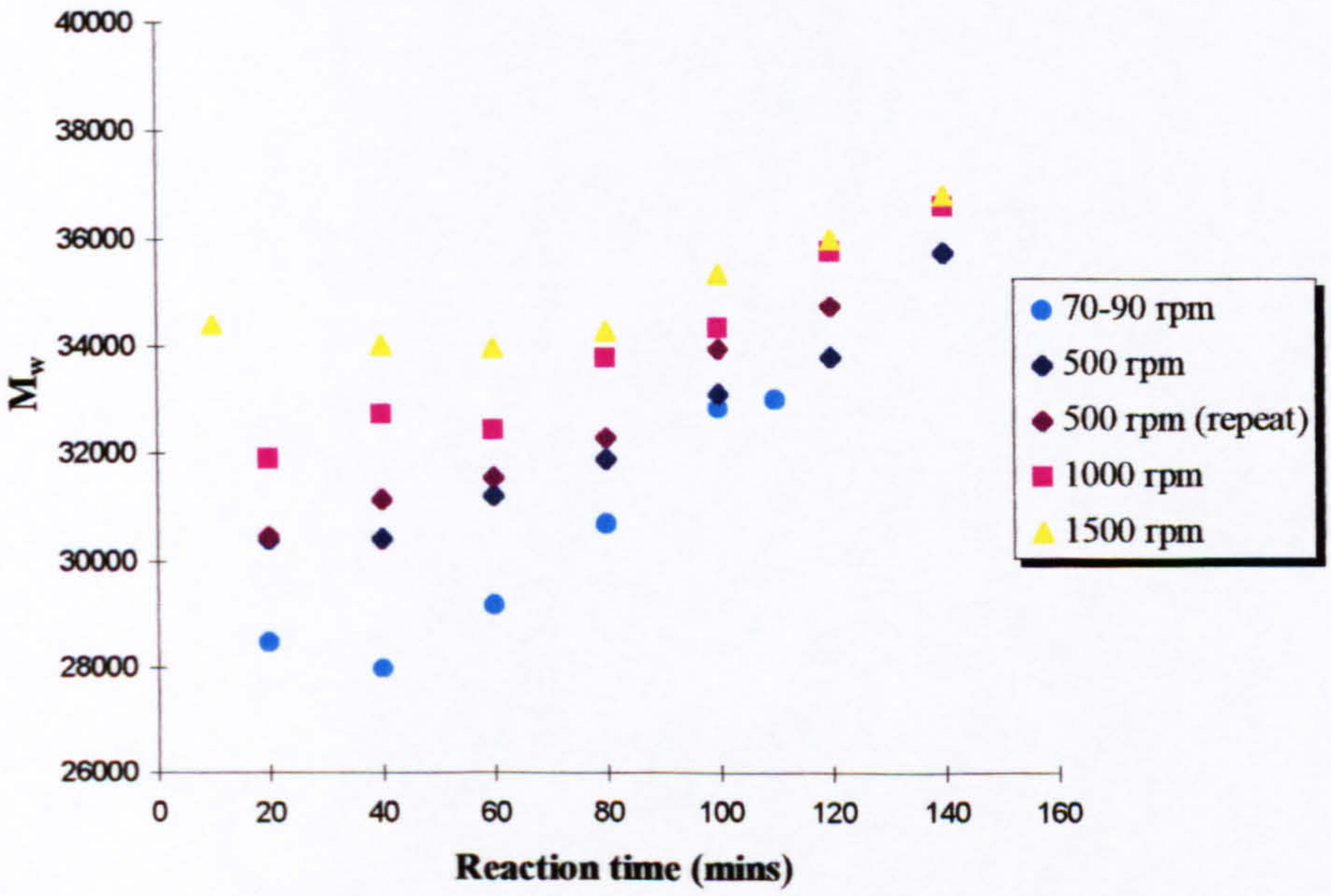

Figure 5.44. Effect of agitator speed on Mw

5.2.3. Molecular Weight Distribution (MWD)

A quantitative measure of the MWD is calculated from the ratio $\overline{M}_w/\overline{M}_n$ called the polydispersity index (DI). The changes in DI over the course of the polymerisation for the range of agitator speeds tested are shown in Figure 5.45 below.

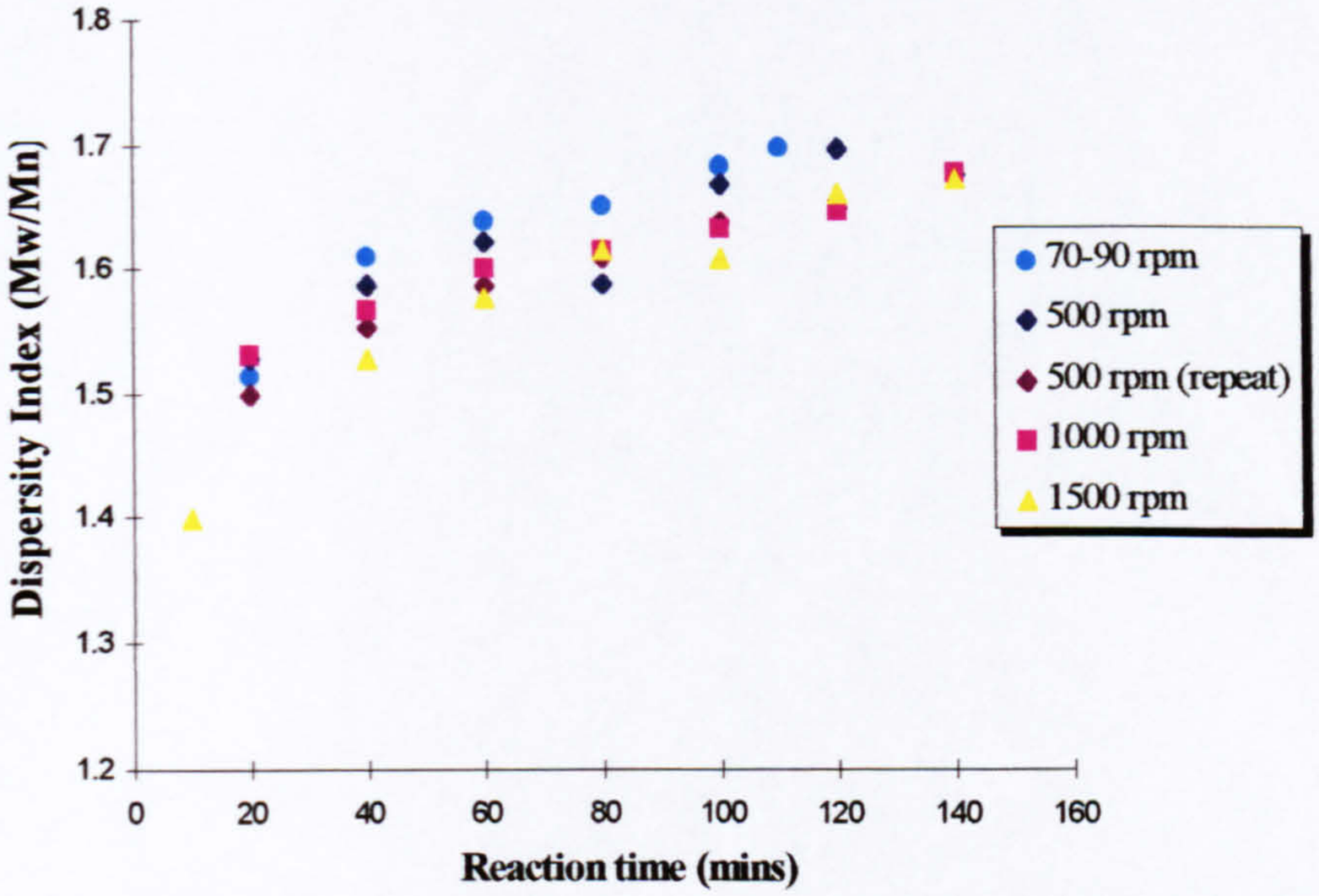

Figure 5.45. Effect of agitator speed on polydispersity index (DI)

The general trend observed is a small but steady increase in DI with reaction time for all the agitation rates investigated. This increase is associated with the increases in viscosity expected with a rise in polymer concentration as will be extensively discussed in section 6.1.3 in Chapter 6.

Once again, the rate of agitation is seen to have a major influence on the polydispersity index. The DI at low agitator speed is generally higher than that at an increased speed. This observation is clearly the result of a change in levels of mixing at the different agitation rates which will be discussed in Chapter 6 later.

Chapter 6

Discussion

6. INTRODUCTION

The results of the polymerisation study in the SDR and the batch agitation study presented in Chapter 5 will be discussed in the following sections. The effect of the disc rotational speed and the feed viscosity on the overall performance of the SDR will be discussed in terms of the mean film thickness and residence time and the types of flow patterns prevailing on the rotating disc. An attempt will be made to provide a theoretical explanation of the polymerisation rate enhancement observed in the SDR by considering the effect of the rotating disc hydrodynamics on the kinetic parameters involved in the chemically initiated polymerisation of styrene. Micromixing effects on the batch reactor performance applied to the polymerisation of styrene are then discussed based on the results obtained in the agitation study. This will be followed by a theoretical assessment of the energy saving potential of the spinning disc reactor employed in the second stage of a semi-batch process in comparison to a purely batch process for the production of polystyrene. Finally, an industrial scale continuous process for the polymerisation of styrene is proposed where a first stage reaction in a tubular reactor having static mixing inserts is envisaged followed by polymerisation to high conversion in the spinning disc reactor.

6.1. BATCH RESULTS

6.1.1. Conversion

A kinetic model to predict the progress of styrene polymerisation with time in the batch reactor was used to assess the validity and reliability of the experimental batch conversion data. The theoretical conversions were calculated according to equation (2.29) derived in Chapter 2 which is:

$$x = 1 - \exp\{-2k_p\sqrt{f[I]_o / (k_d k_t)}(1 - e^{-k_d t/2})\} \qquad (2.29)$$

For simplicity, the initiator efficiency for benzoyl peroxide used in the theoretical prediction was assumed to be constant at 0.8 although this is not strictly true in practice, as has already been discussed in Chapter 2. Furthermore, the simple Arrhenius expressions for the individual kinetic rate constants (see section E1.1.5 in Appendix E) do not take into account the effects of increasing polymer concentration and reduced chain mobility on the rate constants, particularly on the termination rate constant k_t. The model used here therefore represents an idealised situation from which significant deviations are expected to occur in practice especially in the high conversion regimes of very viscous reaction medium due to the diffusion control effects. In fact, this behaviour is clearly demonstrated in Figure 5.2 in Chapter 5 where the experimental conversions agree reasonably well with the model curve in the low to intermediate conversion range but become higher than those predicted by the model in the high conversion range of the polymerisation where diffusion controlled reactions come into play.

It must be pointed out that in the range of operating temperature in the batch, the rate of thermal polymerisation of styrene is about 1%/hour [94,206] which can effectively be neglected over the relatively short time span of the polymerisation in this investigation.

It should be noted that the degree of agitation provided by the magnetic stirrer in the glass reactor was not measured. Hence it has not been possible to relate the batch calibration data to a given agitation speed. On the misguided basis that high rates of agitation result in better mixing and high conversions in a batch system, it might be argued that the non-optimised and inadequate agitation rates in the batch reactor gave lower conversions than theoretically achievable and hence comparisons with the SDR results were flawed and unreliable. However, as the results of the agitation experiments have shown (section 5.2), polymerisation reaction mechanisms are unique in that auto-acceleration effects which are accompanied by a dramatic rise in monomer conversion become more pronounced in poorly mixed batch systems. Improving mixing in the batch delays the onset of the auto-acceleration stage and hence conversion is lower in perfectly mixed systems operated batchwise. This observation is in marked contrast to the effect of perfect micromixing in continuous flow systems which has been experimentally studied for the homogeneous polymerisation of styrene by Harada et *al.* [233]. Assuming that the mixing provided by the magnetic stirrer in the batch calibration experiments was far from adequate to achieve good mixing levels, then the conversion profile is higher than it should have been under better mixing conditions. Therefore any performance comparison between the SDR and the batch under the conditions of the present investigation represents a very conservative estimate which can only improve under different conditions of operation. In any case, the sensitivity of monomer conversion to micromixing effects is known to be much less than that exhibited by the molecular weight distribution of the polymer [207,208], as discussed in the ensuing sections. Hence, an assessment of the degree of micromixing in the batch should preferably be based on the MWD of the polymer instead of the extent of conversion achieved.

6.1.2. Average molecular weights, Mn and Mw

Based purely on the free-radical mechanism encountered in the current study of styrene polymerisation, the molecular weight of the polymer melt is expected to remain at a constant level which is determined primarily by the initial concentration of the reagents and temperature. In other words, the free-radical mechanism ideally causes polymer chains of a certain fixed length to be formed in a fraction of a second from the start of reaction and as reaction proceeds, the chain length does not grow, but rather more chains of the same initial length are being formed. This theoretical behaviour as illustrated in Figure 2.16 in Chapter 2 is in sharp contrast with that seen in step polymerisation where high molecular weight polymer is produced only at near completion of the reaction.

The variations in molecular weights M_w and M_n observed with the progress of polymerisation in the experimental batch runs are somewhat in contradiction to the constant theoretical molecular weights expected for the free-radical mechanism. The presence of a minimum point in both experimental curves for M_n and M_w as shown in Figure 5.3 seems to be indicative of the competing effects of increasing temperature against increasing concentration and viscosity which affect the

length of the growing polymer chain differently. At the beginning of the reaction, the rise in temperature causes more free radicals and more growing chains to occur, thus increasing the probability of termination. With more chains undergoing termination, the average molecular weights M_w and M_n of the polymer drop with temperature. At the same time, the increase in polymer concentration translates into an increase in viscosity whereby the diffusion of polymer chains towards one another in the reaction medium becomes hindered. The tendency is then for longer chains and hence higher molecular weight products to be formed. This sequence of events aptly describes the changes in molecular weights seen in the batch polymerisations where up to between 40 and 60 minutes, the viscosity build-up is hardly significant from visual observation and hence temperature is the controlling factor, giving a net decrease in M_w and M_n. Beyond this point, temperature is seen to be almost constant at 96°C (Figure 5.1) while the viscosity of the polymer mixture increases in a gradual manner with conversion. Hence, there is a net increase in M_w and M_n values.

A similar trend in molecular weight to the one described above was obtained in the bulk polymerisation of styrene initiated with dimethyl 2,2'-azobis(isobutarate) (MAIB) at 70°C studied by Yamada et al. [195]. The authors attributed the initial decline in their average M_n values to a fall in styrene concentration. Perfectly isothermal conditions were presumably achieved over the duration of their polymerisation. In view of these results, part of the decrease in molecular weights in the present investigation could also be due to changes in the monomer concentration, the effects of which have been masked by temperature increases.

6.1.3. Molecular weight distribution (MWD)

The MWD is an important parameter in polymerisation processes as it directly influences the physical and mechanical properties of the polymer and hence its quality. As already mentioned in Chapter 2, a measure of the MWD is given by the polydispersity ratio ($= \overline{M}_w / \overline{M}_n$).

The gradual increase in the polymer dispersity index from an average of 1.45 to about 1.65 (on average) over a conversion range of 0% to 75% in the current experimental batch polymerisation runs agrees reasonably well with the computations performed by Tadmor and Biesenberger [209] for a batch reactor based on a similar kinetic scheme.

The observed increase in DI is most definitely related to the changes occurring mainly on microscopic levels as reaction progresses. In general, the increase in polymer concentration is accompanied by a rise in viscosity which may be of several orders of magnitude as is certainly the case in the current study. Such a tremendous increase in viscosity in the batch reactor has important implications on the mixing process, reaction kinetics and transport properties (e.g. molecular diffusion and heat transfer) of the reaction system. The effects of viscosity on many aspects of any polymerisation process have been studied in great detail by Reichert and Moritz [210]. Of particular relevance to the MWD are the severe limitations in micromixing that arise with an increase in viscosity [211]. The resulting segregation, partial or complete, of the growing chains in the polymerisation mixture invariably leads to the formation of a wider range of polymer chain lengths than would have been expected in a mixture with good levels of micromixing. Hence a broadening of the molecular weight distribution takes place with increasing polymer concentration or medium

viscosity. This situation is equally applicable to batch and continuous flow systems as discussed in the literature [211,212]. The importance of good mixing in polymerisation processes, especially on a molecular scale (i.e. micromixing) and at high monomer conversions, is therefore widely recognised for control of the molecular weight distribution of polymer molecules in homopolymerisation systems such as styrene polymerisation. The scenario described here for the changes in molecular weight properties is typical of batch systems in which the rate of initiation as well as the monomer concentration declines with conversion and the termination is predominantly bimolecular [202,203].

However, the increase in dispersity index encountered in the laboratory-scale batch reactor used in the current investigation is deemed to be too small to cause any major changes in the properties of the polymer. It is expected that with a scaled-up version of the batch reactor it would be difficult to control the molecular weight distribution to such a narrow range as the one achieved here unless very complex reactor design features are incorporated. The reduced surface area to volume ratio in a large reactor results in poor heat removal and non-uniform temperatures. This problem is obviously exacerbated with high viscosity materials. The installation of additional cooling surfaces inside the reactor can help in taking the heat away but they can also create new problems altogether by interfering with mixing equipment [85]. Therefore large batch reactors designed for industrial use are prone to have wider molecular weight distributions than encountered in the small batch reactor employed in the current investigation.

6.2. SPINNING DISC RESULTS

Very rough estimates of the rate of polymerisation in one pass on the rotating disc can be obtained by considering the increase in conversion of the SDR product per minute after allowing for the polymerisation in the batch during transfer. A transfer time of 2 minutes has been assumed for all experimental runs and the extent of conversion in that time has been calculated from the rate of polymerisation at the selected time in the batch deduced from the gradient of the batch calibration curves corresponding to each experiment. The time of reaction on the disc will be of the order of seconds but a very conservative value of 1 minute has been used to take into account the time spent in the collector (about 4-5 minutes) during which some polymerisation could have occurred.

6.2.1. Effect of SDR feed conversion/viscosity

The results of the effect of feed conversion/viscosity on SDR performance were presented in sections 5.1.2.1, 5.1.2.2 and 5.1.2.4 of Chapter 5 for experiments A, B and D respectively.

6.2.1.1. Conversion

The results of experiment A will be compared with those of experiment B since both were carried out under the same disc operating conditions of 88-90°C temperature and 350-400 rpm rotational speed. The range of feed conversion studied in experiment A (13% to 37%) was extended to 62% in experiment B by the use of a small amount of toluene solvent. The purpose of the solvent was to reduce the

viscosity of the polymer solution at high conversions so that the feeds could be introduced in the SDR distributor tubes without much difficulty. From the close agreement between the conversion profiles of A and B, it is seen that the solvent did not greatly affect the polymerisation kinetics in the batch reactor. However, the viscosity of the polymer solution in B at the same conversion was significantly reduced as demonstrated by the increase in conversion in one pass of the SDR. For the same feed conversion at 40 minutes, the increase in conversion in experiment B was 2.8% compared to 9.8% in experiment A. The difference is clearly due to the effect of higher feed viscosity in A.

It would seem that the viscosity level at 37% conversion in experiment A is more or less equalised at 50% conversion in experiment B from the similar increase in conversion of about 10% in the SDR for these two feed conversions. The corresponding time saving is nevertheless higher in experiment B than in A because of the increasingly flat profile in the batch calibration curve in high conversions regimes.

The time saving plots for both low and high conversion feeds (experiments A & B respectively) emphasise the tremendous improvement in the performance of the spinning disc reactor in the region of high degree of prepolymerisation. Thus, an increase in conversion of 15.6% over a very short exposure time (of the order of seconds) in the SDR for the highest feed conversion of 62% in experiment B represents a significant change which is only achievable in the batch process after an additional 36 minutes of polymerisation time. The physical significance of the time saving analysis can be translated into a higher rate of reaction on the disc surface than in the batch reactor. The rates of polymerisation in the SDR estimated from the data collected for experiments A and B are compared with batch polymerisation rates in Tables 6.1 and 6.2 below.

Table 6.1. Rates of polymerisation in SDR and batch (Experiment A)

Prepolymer residence time in batch (mins)	Prepolymer feed conversion in batch (%)	R_p in batch (%/min)	Estimated average R_p in SDR (%/min)	$\frac{R_p(SDR)}{R_p(batch)}$
15	13.3	0.9282	2.26	2.32
20	18.2	0.9312	3.87	4.25
25	23.3	0.9342	1.27	1.36
30	27.6	0.9372	4.37	4.66
35	33.0	0.9402	5.37	5.71
40	36.9	0.9432	7.95	8.43

The viscous nature of the highly concentrated polymer solution impedes good mixing of the reacting species at a molecular level in the batch. At these low monomer concentrations, auto-acceleration effects are effectively suppressed and hence the polymerisation rate in the batch decays steadily as seen in Tables 6.1 and 6.2. On the other hand, it would seem that micromixing is enhanced in the thin film flowing over

the rotating disc promoting a more rapid rate of polymerisation. The estimated rates of polymerisation for the SDR should be treated with caution at this stage because they have been deduced by a very crude methodology involving assumed values and hence are not to be taken as being very precise. However, they do give an indication of the trend in rate increases expected in the SDR.

Table 6.2. Rates of polymerisation in SDR and batch (Experiment B)

Prepolymer residence time in batch (mins)	Prepolymer feed conversion in batch (%)	Rp in batch (%/min)	Estimated average R_p in SDR (%/min)	$\frac{R_p(SDR)}{R_p(batch)}$
40	37.0	0.7838	1.19	1.52
50	44.0	0.7218	5.06	7.01
60	50.0	0.6598	9.43	14.29
70	57.1	0.5978	10.44	17.46
80	62.0	0.5358	14.55	27.16

In experiment D, the effect of feed conversion/viscosity was investigated at a higher disc rotational speed of 850 rpm. This speed was chosen as it was identified as the optimal speed in the previous experimental set C. A higher concentration of solvent was used for runs in experiment D as compared to experiment B which reduced the viscosity of the polymer solution even further. A steady increase in conversion and rate of polymerisation and hence time saving in one pass in the SDR are again observed for feed conversions up to 61% while a somewhat peculiar result is obtained for the highest feed conversion of 67%. The calculated rates of polymerisation in the batch and SDR are compared in Table 6.3 below. Again the rate calculations are based on the same method outlined in section 6.2 above.

Table 6.3. Rates of polymerisation in batch and SDR (Experiment D)

Prepolymer residence time in batch (mins)	Prepolymer feed conversion in batch (%)	R_p in batch (%/min)	Estimated average Rp in SDR (%/min)	$\frac{R_p(SDR)}{R_p(batch)}$
40	29	0.6461	4.73	7.33
60	42	0.5541	4.67	8.43
80	52	0.4621	8.63	18.67
90	56	0.4161	8.53	20.50
100	61	0.3701	15.55	42.03
120	67	0.2781	10.93	39.31

The higher rotational speed employed in D seems to improve the performance of the SDR when similar feed conversions rather than feed times are compared to runs in B. However caution should be exercised when comparing the data since, at a given feed conversion, the viscosity of the batch polymerising medium is lower in experimental set D. This can be inferred from the batch polymerisations rates shown in Tables 6.2 and 6.3 whereby it is clearly seen that rates in the batch are lower in experiment D than in experiment B due to the increased dilution effect of the higher solvent concentration in set D. If the viscosity levels of the feeds can be assumed to be equalised at the same polymer concentrations, then it can be said that the higher rotational speed of 850 rpm employed in set D results in a superior performance of the SDR in terms of largely increased rates and extent of product conversions.

The influential part played by viscosity in the performance of the SDR with regard to conversion is made very obvious from the data presented so far. From previous studies on the rotating disc [17] it is known that a direct proportionality relationship exists between the residence time on the disc and liquid viscosity. Hence as SDR feed viscosity (Newtonian viscosity) increases by more than ten-fold from about 0.2 Pas to about 2 Pas, it is expected that the corresponding rise in exposure time on the spinning disc allows polymerisation to proceed to higher conversions even though the residence times still remain of the order of seconds. The opposing effect presented by an increase in the film thickness with higher viscosity feed would undoubtedly have an adverse effect on the performance of the SDR but the thickness would still be small enough for enhanced reaction. The individual contribution of the film thickness and residence time parameters to the performance of the SDR will be discussed in greater depth at a later stage in this chapter.

6.2.1.2. Molecular weight properties

The molecular weight properties (M_n, M_w and DI) of the SDR product show a definite improvement in comparison to the polymer produced from the batch at the same degree of polymerisation. The difference seems to be more appreciable with an increase in the feed viscosity.

The enhanced mixing state of the film flowing over the rotating disc is undoubtedly a highly contributory factor in the improvement seen. The importance of good molecular mixing in high viscosity polymerising media for the control of molecular weight properties cannot be over-emphasised. Progress in polymerisation in a conventional stirred tank reactor is usually accompanied by a steady increase in molecular weights, M_n and M_w and in the polydispersity index ratio DI. In the extreme case, the well known 'gel effect' or 'Trommsdorff effect' taking place under certain conditions of polymerisation is characterised by a tremendous rise in molecular weights together with a severe broadening of MWD of the polymer. It has long been recognised that the gel-effect is related to diffusion-controlled termination mechanisms which become pronounced in poorly mixed, highly viscous systems, as has been discussed at length in Chapter 2.

While increases in conversion in the stirred tank reactor are usually achieved at the expense of a rise in molecular weights and a broadening of the MWD, the SDR appears to be capable of producing high conversion polymers having tightly controlled molecular weight characteristics. The mixing limitations at high viscosity which are characteristic of conventional stirred tanks are believed to be overcome in the SDR by

a much reduced diffusion path length together with an intense mixing mechanism within the thin film.

6.2.2. Effect of disc rotational speed

Experiments C and E explored the effect of the speed of rotation of the disc on the conversion and molecular weight properties of the SDR product. The two experiments served to compare the effect of speed at two different feed conversions (37% and 58% for experiments C and E respectively) or viscosities. In this case, the feed conversion can be taken as a reliable measure of its viscosity since the solvent concentration in the starting recipe used throughout the two experiments was kept constant, as seen in Appendix E.

6.2.2.1. Conversion

The conversion results from both set of experiments indicate that, for a given set of fixed operating variables such as disc temperature and feed viscosity, an optimal speed exists at which the polymerisation on the spinning disc proceeds at its fastest rate, giving the highest conversion and the maximum saving in reaction time. Tables 6.4 and 6.5 below show a comparison between the estimated rates of polymerisation in the SDR and the batch for experiments C and E respectively.

Table 6.4. Rates of polymerisation in batch and SDR (Experiment C)

Disc rotational speed (rpm)	Prepolymer feed conversion in batch (%)	R_p in batch (%/min)	Estimated average R_p in SDR (%/min)	$\frac{R_p(SDR)}{R_p(batch)}$
300	36.4	0.7573	2.37	3.12
400	36.4	0.7573	3.04	4.01
500	36.4	0.7573	1.32	1.75
600	36.4	0.7573	6.70	8.85
750	36.4	0.7573	5.28	6.97
800	36.4	0.7573	8.13	10.74
850	36.4	0.7573	16.77	22.15
900	36.4	0.7573	11.73	15.49
1000	36.4	0.7573	6.85	9.05

Table 6.5. Rates of polymerisation in batch and SDR (Experiment E)

Disc rotational speed (rpm)	Prepolymer feed conversion in batch (%)	R_p in batch (%/min)	Estimated average Rp in SDR (%/min)	$\frac{R_p(SDR)}{R_p(batch)}$
400	58	0.4885	5.22	10.69
600	58	0.4885	10.36	21.21
800	58	0.4885	11.77	24.10
1000	58	0.4885	14.32	29.32
1200	58	0.4885	11.98	24.52
1500	58	0.4885	12.43	25.45

As expected, the value of the optimal or critical speed varies with the feed conversion and hence the feed viscosity which in turn affects the film thickness and the residence time on the disc surface. Hence, the optimal speed has shifted from 850 rpm for a feed conversion of 37% to 1000 rpm for a feed conversion of 58%. The increase in film thickness due to higher feed viscosity can only be counteracted by increasing the speed of rotation and hence the centrifugal acceleration. The same reasoning is applicable to the residence time on the spinning disc. The film thickness and the residence time of the polymer flowing on the disc are believed to be two of the most important parameters which strongly dictate the extent of conversion of the final disc product as will be discussed below.

It is interesting to note that the changes in conversion with speed of rotation are quite abrupt and steep for feed conversion of 37% (experiment C) especially in the region of the critical speed. In contrast, the changes in conversion are more subtle and gradual in experiment E. The difference is most likely related to the viscosity of the feed and the corresponding flow patterns generated on the reaction surface.

Once again, the effect of viscosity as a controlling system parameter is clearly seen by comparing the increases in conversion at the same rotational speed for the two feed conversions studied in experiments C and E. For instance, at each of the speeds of 400, 600 and 800 rpm, the increase in conversion is always higher by about 3% for the higher feed conversion of 58% in experiment E. These observations are in agreement with the previous discussion in section 6.2.1 where the effect of feed conversion or viscosity was examined.

It should be pointed out that with an increase in the prepolymer viscosity fed onto the disc, the polymer flowrate on the disc surface was also reduced since feeding was performed under gravity. Therefore, the impact on the residence time and film thickness will be greater as a result of a change in not one but two variables at the same time.

6.2.2.2. Molecular weight properties

A general decrease in M_n, M_w and DI for SDR polymer product is again noted in both experiments when these properties are measured against the batch values at the same conversion, except for a few abnormal results pointed out in the results section. One of the potential merits attributed to the SDR with regard to polymerisation reactions is the formation of narrow molecular weight distribution polymers. The decline in DI values in the SDR observed in each of the experiments, regardless of the disc rotational speed, provides enough evidence to support this claim.

A primary difficulty encountered during the treatment of the molecular weight results concerns the direct correlation between the changes in the molecular weight properties in the SDR with the parameters investigated in the experiments herein (i.e. rotational speed and prepolymer feed conversion/viscosity) as many other factors also come into play. Thus, the changes on the disc, as calculated here, is not only dependent on the speed or the feed conversion, if at all, but also on the expected batch values for that particular product conversion and, more importantly, on the SDR feed M_n, M_w or DI which can be strongly influenced by the conditions in the batch during the prepolymer stage preparation. Therefore the profile for the batch for each of the properties needs to be determined accurately by taking a larger sample of data points spanning the whole conversion range from 0 to near 100%.

The decreases in molecular weights and tightening of the MWD would seem to suggest that the increase in polymerisation rates on the rotating surface is taking place by mechanisms different from those observed in the gel effect phenomenon which, in contrast, gives high polymerisation rates at the expense of an increase in molecular weights and a severe broadening of their distribution.

6.2.3. Film thickness, residence time and flow regimes in SDR

The results of the present polymerisation study in the SDR seem to indicate that the extent of conversion of the final product from the disc is strongly dictated by the two most important SDR parameters: the liquid film thickness and the mean residence time on the disc. The film thickness determines the molecular diffusion path length which is an important consideration when micromixing effects comes into play especially in viscous reaction media. The mean residence time controls the time of exposure to conditions imposed in the SDR and can thus have a great impact on the productivity and properties of the end-product.

Based on the centrifugal model, the average thickness δ and the mean residence time t_{res} of a Newtonian liquid film flowing over a smooth disc have been derived as:

$$\delta = \left(\frac{3}{2\pi}\frac{\nu Q}{\omega^2 r^2}\right)^{1/3} \qquad (6.1)$$

and

$$t_{res} = \left(\frac{81\,\pi^2\,\nu}{16\,\omega^2\,Q^2}\right)^{1/3}\left(r_o^{4/3} - r_i^{4/3}\right) \qquad (6.2)$$

where ν is the kinematic viscosity (= η/ρ)
Q is the volumetric flowrate
ω is the angular velocity (= $2\pi N/60$)
N is the rotational speed
r is the radial distance
subscripts o and i refer to outlet and inlet respectively

The present investigation concerns polymerisation reactions on the spinning disc. In general, polymers dissolved in their monomers exhibit pronounced non-Newtonian characteristics, especially at high concentrations. Polystyrene-styrene mixtures fall into the non-Newtonian fluids category and they obey the so-called "power-law relationship" over a relatively wide range of shear rates [109]. The power-law model can be expressed as:

$$\eta_{app} = K \dot{\gamma}^{\,n-1} \tag{6.3}$$

where η_{app} is the apparent viscosity
K is the consistency index
$\dot{\gamma}$ is the shear rate
and n is the power law index

Using the expression for the power-law model, modified equations can be derived to predict the flow characteristics of non-Newtonian fluids such as the polystyrene-styrene mixtures on the rotating disc. Thus the film thickness δ and the radial velocity distribution v_r are obtained as:

$$\delta = \left(\frac{1+2n}{2\pi n}\right)^{\frac{n}{1+2n}} \left(\frac{Q}{r}\left[\frac{K}{\rho\omega^2 r}\right]^{1/n}\right)^{\frac{n}{1+2n}} \tag{6.4}$$

$$v_r = \frac{n}{n+1}\left(\frac{\rho}{K}\omega^2 r\right)^{1/n}\left(\delta^{\frac{n+1}{n}} - (\delta - z)^{\frac{n+1}{n}}\right) \tag{6.5}$$

The derivations based on the Newtonian and non-Newtonian flow models can be found in Appendix A.

When n approaches the value of 1, K=η and hence the system behaves as a Newtonian fluid. This is the case for pure styrene monomer and this approximation can also be used for dilute solutions of polystyrene dissolved in styrene. However, as styrene conversion rises, the value of n decreases steadily to a minimum of 0.32 for pure polystyrene melt [109].

Shear thinning effects are only apparent for a certain range of shear rates. At very low shear rates, the viscosity/shear rate profile is relatively flat. The more or less constant viscosity is referred to as the zero-shear or low shear limiting Newtonian viscosity. Similarly, at high enough shear rates, Newtonian flow characteristics are obtained and the constant viscosity in this regime is called the Newtonian viscosity. Assuming that the centrifugal force acting on a film flowing on a rotating disc produces very high shear rates within the film, the Newtonian flow approximation can

be applied to the polystyrene/styrene/toluene solutions, even at high polymer concentrations. Hence, equations (6.1) and (6.2) can be used in calculating film thickness and residence times.

A few inaccuracies are expected to arise on applying the above expressions for mean film thickness and mean residence time to the present investigation. First of all, the equations have been derived in an earlier research [17,18] for a smooth disc and are not completely accurate for the present study which involves in-built surface roughness (i.e. grooves) in the rotating disc. Also, they are based on the assumption of the negligible Coriolis forces or negligible slip in the angular direction so that the liquid film flows in an outward radial direction from the centre of the disc. While the validity of the latter assumption may be justified for thin films of high viscosity liquids [213], it has been shown experimentally that considerable angular slip occurs in low viscosity liquid films making the path on the rotating disc spiral rather than radial [44, 214].

According to the condition

$$\nu >> \omega \delta^2 \qquad (6.6)$$

put forward by Emslie et al. [213] for negligible Coriolis effect, the minimum kinematic viscosity of a feed solution onto the disc can be calculated for the present study. Thus, taking the worst possible conditions likely to be encountered in the investigation (film thickness of about 200 microns halfway across the disc and a maximum disc speed of about 1200 rpm), the minimum kinematic viscosity required is obtained as 5.03×10^{-6} m^2/s which is equivalent to 0.0048 Pas dynamic viscosity for a solution of average density of 950 kg/m^3. Hence from the viscosity data presented in the Appendix G, it would appear that the validity of the centrifugal model is maintained for solutions of PS concentrations greater than 50% at 90°C. Therefore the applicability of the above expressions for film thickness and residence time based on the centrifugal model would involve some limitations for dilute solutions of polystyrene (< 50%).

Despite the inaccuracies involved in applying these expressions to the current investigation for the reasons mentioned above, they are nevertheless considered useful in providing a valuable insight into how the different independent variables affect each parameter. It is expected that, in the case of the grooved surface configuration, similar dependencies on the different variables will be seen with the inclusion of an appropriate correction factor to account for the surface roughness.

On inspection of equations (6.1) and (6.2), it is found that the film thickness and the mean residence time are controlled by the angular velocity ω (hence rotational speed) and kinematic viscosity (hence dynamic viscosity) among other variables. Increases in the speed of rotation translate into shorter residence times and thinner films while increases in the liquid viscosity result in longer residence times and thicker films. The two system parameters would seem to be more sensitive to changes in the rotational speed variable because of the $2/3$-power inverse proportionality dependence of each parameter on this variable as compared to the $1/3$-dependence on the viscosity variable. On this basis, if comparable changes in rotational speed and liquid viscosity take place simultaneously, the dominant influence of rotational speed

on both film thickness and mean residence time is expected to override any opposing effect caused by changes in the liquid viscosity.

The theoretical changes in mean residence time and average film thickness on the disc surface for a range of operating conditions, as calculated by the above expressions, are graphically illustrated in Figures 6.1 to 6.4 below.

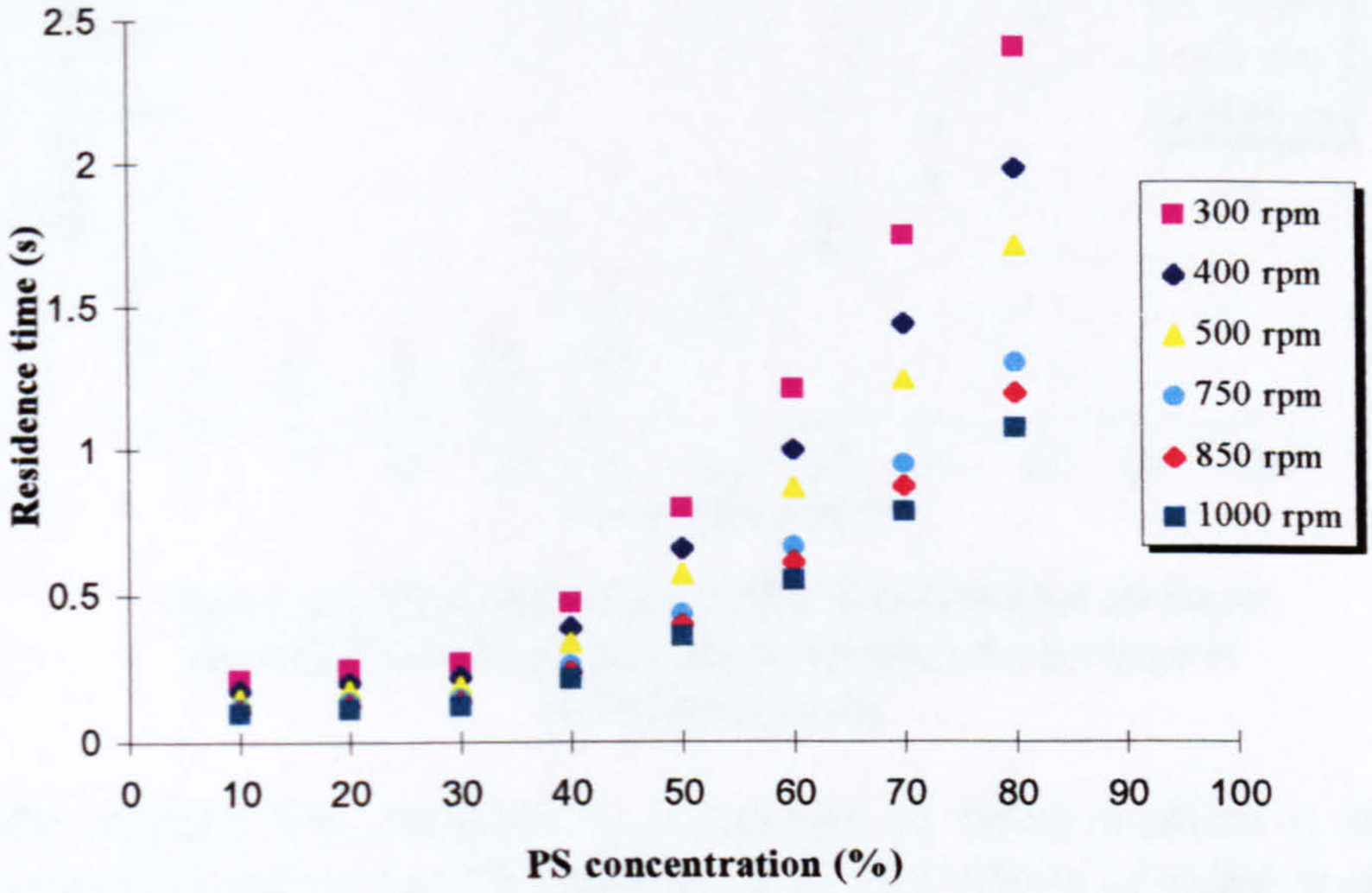

Figure 6.1. Predicted effect of PS concentration (and hence viscosity) on time of residence on spinning disc surface at different rotational speeds

As seen in Figures 6.1 and 6.2, the divergence between the film thickness and residence time curves at different rotational speeds becomes more pronounced beyond 40% PS concentration as a result of a 5 to 10-fold increase in viscosity for each 10% rise in conversion predicted from the viscosity data in Appendix G.

It is to be noted that polymerisation reactions in the SDR represent a special case in that the average film thickness and mean residence time on the disc are expected to change continuously across the disc surface due to increases in viscosity with the progress of polymerisation. For instance, if a feed of 40% PS concentration is introduced onto the rotating disc at 850 rpm and an SDR product of 60% PS concentration is obtained, the mean residence time would lie somewhere between 0.23 seconds and 0.61 seconds which are the values corresponding to the two concentrations respectively. Similarly the film thickness which is a decreasing function of radial distance at constant viscosity would tend to remain constant or rise depending on the magnitude of viscosity increase. The development of appropriate mathematical models for the two parameters would thus involve viscosity as a function of radial position on the disc instead of a constant viscosity as implied in the derivations herein. Unfortunately the complexity of such models is beyond the scope of this present study.

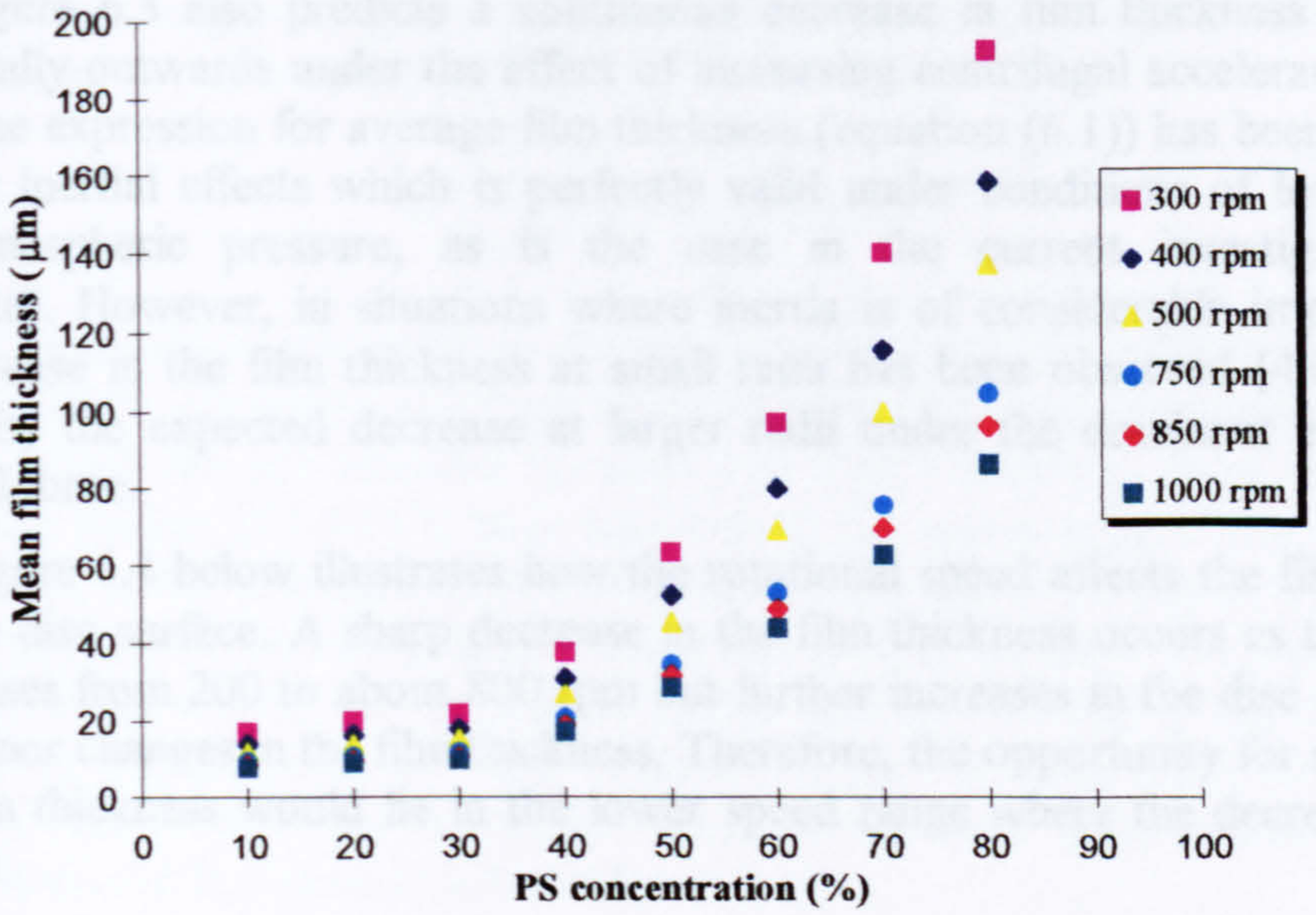

Figure 6.2. Predicted effect of PS concentration on mean film thickness at edge of disc (r=0.18m) for a range of rotational speeds

The average film thickness is a function of radial position r, disc angular velocity ω and viscosity ν (or PS concentration). The effects of radial position on the film thickness at fixed disc rotational speed and fixed PS concentration (or viscosity) are clearly illustrated below in Figures 6.3 and 6.4 respectively.

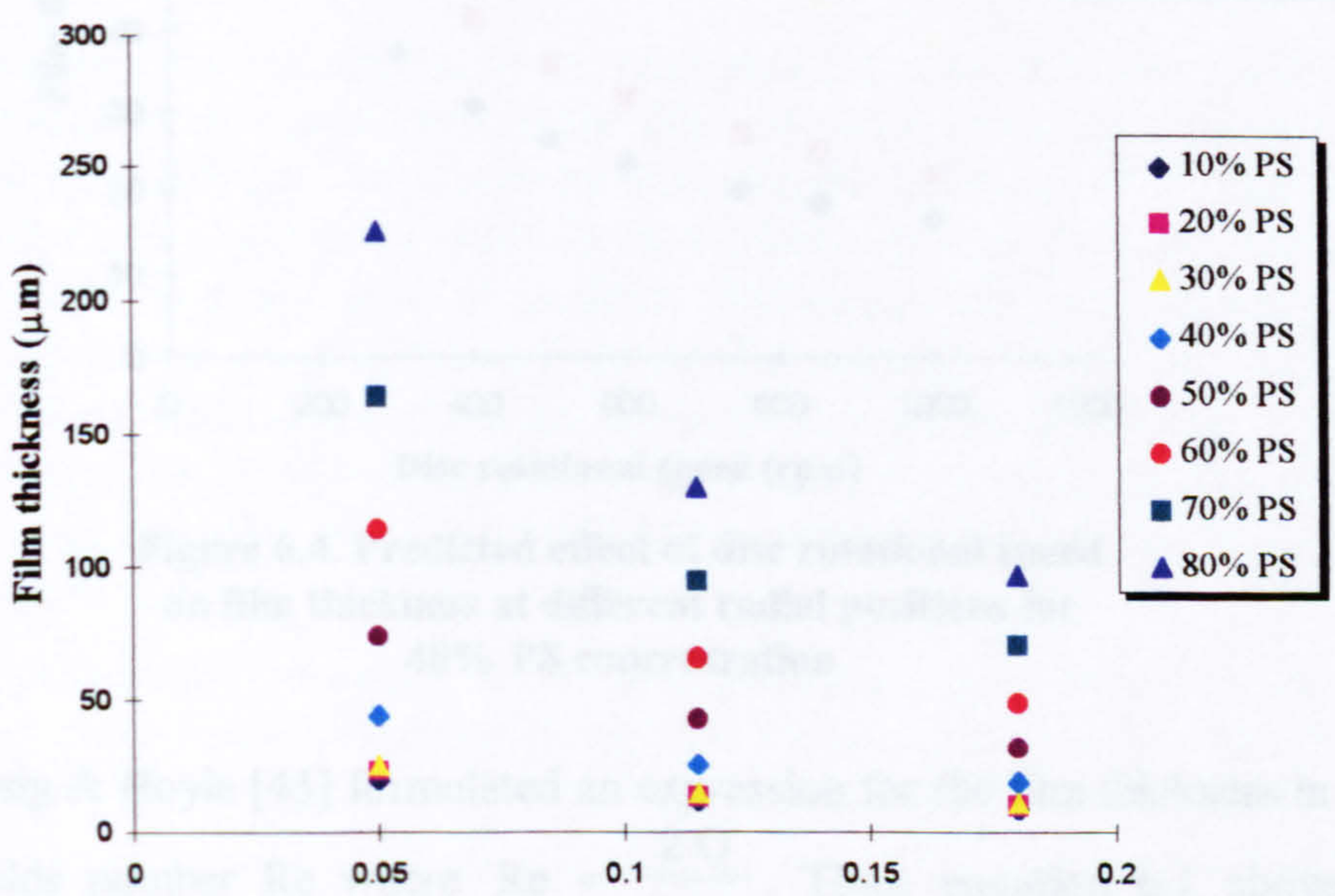

Figure 6.3. Predicted effect of radial position on film thickness for various PS concentrations at fixed rotational speed of 850 rpm

As seen in Figure 6.3, the decrease in film thickness across the disc is more noticeable for high polymer concentrations which again emphasises the importance of viscosity in determining the film thickness.

Figure 6.3 also predicts a continuous decrease in film thickness as the film flows radially outwards under the effect of increasing centrifugal acceleration. This is because the expression for average film thickness (equation (6.1)) has been derived by neglecting inertial effects which is perfectly valid under conditions of low flowrates under atmospheric pressure, as is the case in the current investigation (Q<1 litre/minute). However, in situations where inertia is of considerable importance, an initial increase in the film thickness at small radii has been observed [45,58,59,215] followed by the expected decrease at larger radii under the dominant effect of the centrifugal force.

Figure 6.4 below illustrates how the rotational speed affects the film thickness across the disc surface. A sharp decrease in the film thickness occurs as the speed of rotation rises from 200 to about 800 rpm but further increases in the disc speed result in only minor changes in the film thickness. Therefore, the opportunity for optimisation of the film thickness would lie in the lower speed range where the decrease is most significant.

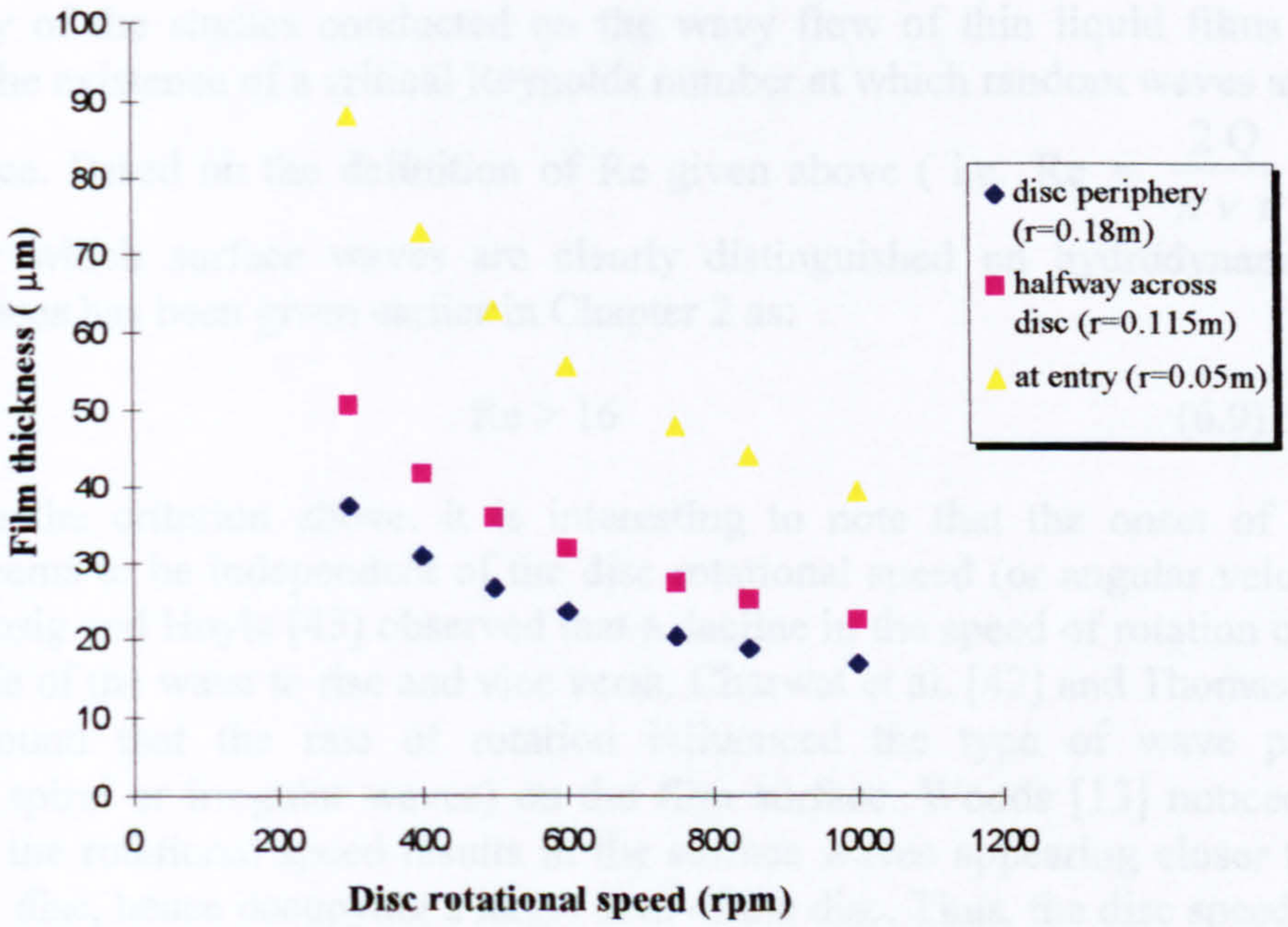

Figure 6.4. Predicted effect of disc rotational speed on film thickness at different radial positions for 40% PS concentration

Epsig & Hoyle [43] formulated an expression for the film thickness in terms of the Reynolds number Re where $\mathrm{Re} = \dfrac{2\,Q}{\pi\,\nu\,r}$. Thus, equation 6.1 above can be rewritten as:

$$\delta \left(\frac{r\,\omega^{2}}{\nu^{2}} \right)^{1/3} = 0.909\,\mathrm{Re}^{1/3} \qquad (6.7)$$

The above expression is analogous to the derivation obtained based on Nusselt's theory [26] for fully developed laminar flow down inclined surfaces with the

acceleration due to gravity g has been replaced by the centrifugal acceleration $r\omega^2$. Nusselt's equation can be expressed as:

$$\delta \left(\frac{g}{\nu^2} \right)^{1/3} = 0.909 \, \mathrm{Re}^{1/3} \qquad (6.8)$$

All expressions presented so far are based on smooth laminar or streamline flow of thin films. However, this type of flow is only achieved under certain specific conditions which are not satisfied in most real flow situations. Thus, several early experimental studies [27-32,43] have established the presence of a large number of random waves on the free surface of a thin liquid film. Various types of wave patterns have been observed in recent years by many different researchers [13,19,22,42] for a wide range of flowrates, disc rotational speeds and disc diameters as described in Chapter 2. In the presence of such random waves, the maximum film thickness occurring at the crest of the waves has been shown to be greater than the mean thickness predicted by equation 6.7 or 6.8.

Many of the studies conducted on the wavy flow of thin liquid films have established the existence of a critical Reynolds number at which random waves appear on the surface. Based on the definition of Re given above (i.e. $\mathrm{Re} = \frac{2\,Q}{\pi\,\nu\,r}$), the criterion for which surface waves are clearly distinguished on hydrodynamically smooth surfaces has been given earlier in Chapter 2 as:

$$\mathrm{Re} > 16 \qquad (6.9)$$

From the criterion above, it is interesting to note that the onset of wave formation seems to be independent of the disc rotational speed (or angular velocity). However, Epsig and Hoyle [43] observed that a decline in the speed of rotation causes the amplitude of the wave to rise and vice versa. Charwat et al. [42] and Thomas et al. [45] also found that the rate of rotation influenced the type of wave pattern (concentric, spiral or irregular waves) on the film surface. Woods [13] noticed that increases in the rotational speed results in the surface waves appearing closer to the centre of the disc, hence occupying a larger area of the disc. Thus, the disc speed is an important parameter after all as it affects the waves generated on the free surface of the film in some way.

Re values for the range of PS concentrations encountered in the present investigation have been calculated using the given definition for Re at various positions across the rotating disc. The results are plotted in Figure 6.5 below.

The condition of Re>16 for the presence of surface waves is satisfied for all concentrations $\leq$ 50% at all radii. Hence it is expected that wavy laminar flow conditions prevail at these polymer concentrations whereas completely smooth films are predicted at higher concentrations. While polymerisation proceeds along the disc surface, the flow regime is expected to change from turbulent to wavy laminar to smooth laminar depending on the extent of the increase in polymer concentration and hence the solution viscosity.

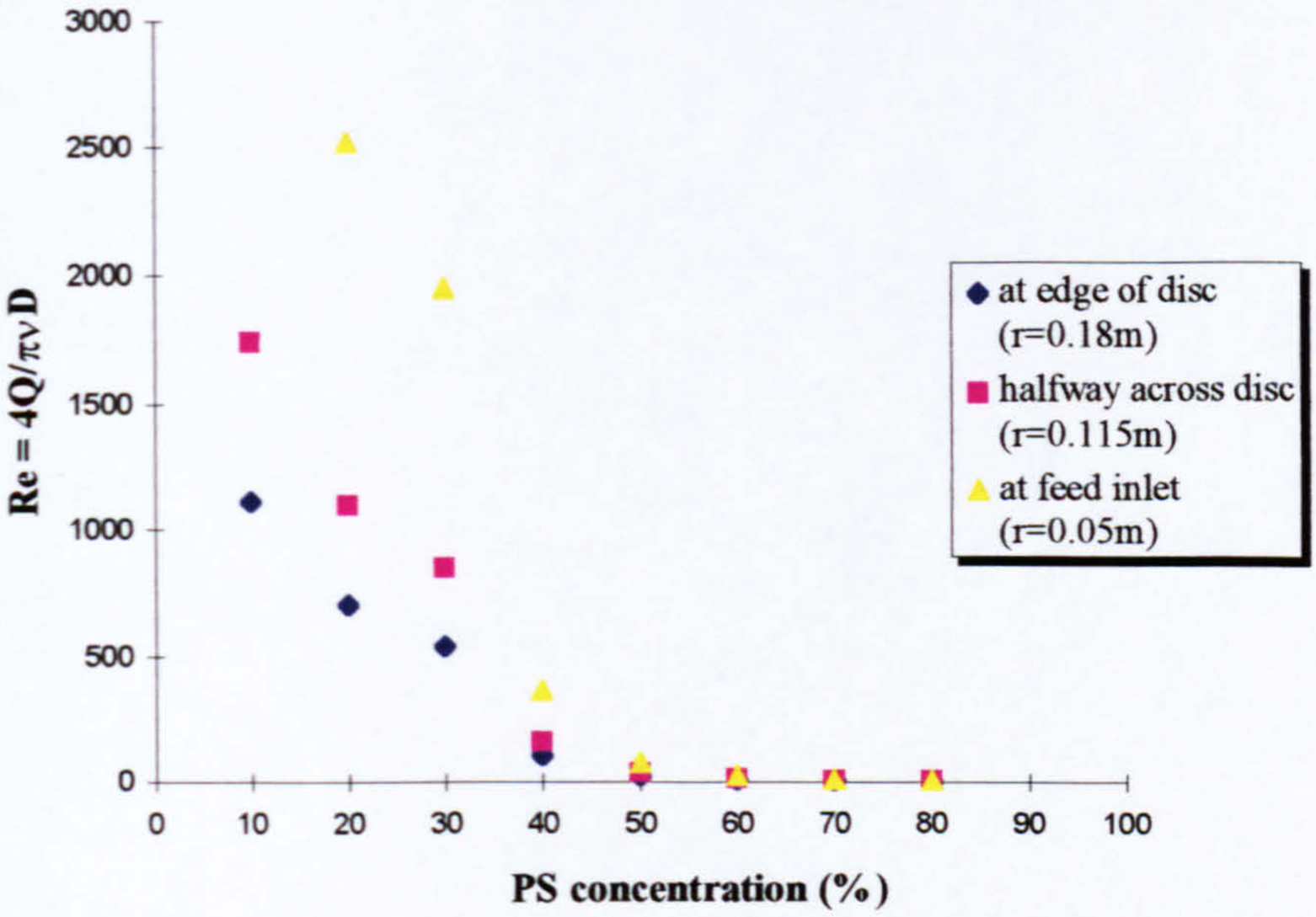

Figure 6.5. Effect of PS concentration (and hence viscosity) on Re at various radial positions across the rotating disc for fixed prepolymer flowrate of 10 cc/s

It is worth mentioning that the effect of grooves in the disc surface has not been taken into consideration in the above predictions. Based on the results of a recent flow visualisation study involving grooved discs [22] which are discussed in Chapter 2, it may be that surface waves are induced at a much lower Re than that predicted by expression (6.9) in which case the wavy laminar flow condition would extend to polymer concentrations higher than 50%.

The enhanced mixing effect of surface waves have long been recognised and investigated in early studies of films flowing on inclined surfaces under gravity [35-38]. Of particular interest to the present investigation are the significant increases in heat and mass transfer rates which have been reported for thin liquid films on the rotating disc [19,20,22]. The most recent study on mixing characteristics involving dye-tracer measurements on a grooved surface [23] is indeed indicative of vigorous mixing action, the extent of which is influenced by disc rotational speed, volumetric flowrate and radial position. The intensely mixed regime provided by the numerous instabilities on the film surface may well have an active part to play in the enhancement of the polymerisation rate seen in the SDR during the course of the current research.

6.2.4. Polymerisation rate enhancement in SDR: a theoretical explanation

The rate of styrene polymerisation has been shown to rise dramatically in one pass on the rotating disc especially under conditions of viscous feeds or high prepolymer feed conversions and optimised disc rotational speed. Two possible theories will be put forward in this section in an attempt to explain the superior performance demonstrated by the SDR.

The first theory centres around steady state kinetics for which the rate of polymerisation, R_p, has previously been derived as (see section 2.3.3 Chapter 2):

$$R_p = k_p [M] \sqrt{\left(\frac{f k_d [I]}{k_t} \right)} \qquad (2.26)$$

From the above expression, it is seen that there may be four possible causes of an enhancement in R_p: an increase in the propagation rate constant k_p, a decrease in the termination rate constant k_t, an increase in initiator decomposition rate constant k_d and finally an increase in the initiator efficiency f.

A decrease in the rate of termination k_t is highly unlikely to be responsible for the increase in R_p on the rotating disc for two main reasons. Firstly, the accompanying increases in molecular weights which is characteristic of reduced termination, as demonstrated by the gel-effect phenomenon, are conspicuously absent. As a matter of fact, M_n and M_w values for the SDR products are almost unchanged in comparison to the SDR feeds. In addition, the decline in termination rates is the result of diffusion limitations which arise in systems where micromixing is severely restricted, for example in a viscous reaction medium. However, the polymerising film on the rotating disc has the potentials of an intensely mixed environment with its extremely short diffusion path length and large number of surface instabilities or ripples. Hence it is expected that the termination process will proceed at more or less the same rate on the disc even under conditions of increasing viscosity.

With regard to the initiator decomposition rate constant k_d, studies into initiation kinetics are rather scarce. But in a recent investigation, Moad and co-workers [216] have found that it remained almost unchanged in the solution polymerisation of styrene initiated by AIBN with toluene as solvent. It is considered reasonable, on the basis of the findings of the latter authors, to assume that changes in k_d with conversion are effectively negligible under conditions of steady state polymerisation.

As detailed in Chapter 2, the effects of increased viscosity on propagation rate constants are more important in bulk polymerisation systems performed at temperatures well below the glass transition temperature, T_g, of the polymer. In the current study involving formation of quite low molecular weight polystyrene, T_g is taken to be about 95°C [217]. In view of the reaction temperature in the batch being between 88°C and 96°C and of a moderately solvated process instead of a purely bulk system, there is a very remote possibility of the propagation rate becoming diffusion controlled in the batch polymerisation. Hence, in the absence of any limitations on the propagation step, it is unlikely that the hydrodynamics of the polymerising film on the rotating disc will affect the rate of propagation k_p.

The remaining factor which could have a significant effect on R_p is the initiator efficiency f. A number of recent studies [193, 194, 218] have focused on the effect of conversion on the initiator efficiency which, for a simplified kinetic treatment, is often assumed to be constant over the whole duration of a chemically initiated polymerisation. The idea of initiator efficiency was briefly examined in section 2.3.3.1 in Chapter 2 with regard to the change of the order of dependence of R_p on monomer concentration. The detailed mechanism controlling the efficiency of initiation will be discussed below with reference to mechanistic equations presented in Chapter 2.

The initiator efficiency f is defined as:

$$f = \frac{\text{Rate of initiation of polymerisation chains}}{2 \times \text{Rate of decomposition of initiator into primary radicals}}$$

The factor 2 accounts for the fact that primary radicals are generated in pairs from an initiator molecule.

The initiator efficiency is unity when all the primary radicals produced during decomposition of the initiator (equations (2.5a) and (2.5b)) participate in chain initiation (equations (2.6a) and (2.6b)). However, this is rarely the case in practical situations due to a number of wastage reactions taking place as a result of what is commonly known as the cage effect. In such cases, the decomposition of initiator and chain initiation steps are not as straightforward as depicted by equations (2.5) and (2.6). Instead a number of competing side reactions are involved between radicals confined in cages formed by solvent molecules as illustrated in the sequence of reaction steps below for benzoyl peroxide initiator [86]:

$$\phi COO - OOC\phi \leftrightarrow [2\ \phi COO^{\bullet}] \qquad (6.10)$$

$$[2\ \phi COO^{\bullet}] \rightarrow [\phi COO\phi + CO_2] \qquad (6.11)$$

$$[2\phi COO^{\bullet}] + M \rightarrow \phi CO_2^{\bullet} + \phi COOM^{\bullet} \qquad (6.12)$$

$$[2\phi COO^{\bullet}] \rightarrow 2\phi COO^{\bullet} \qquad (6.13)$$

$$\phi COO^{\bullet} + M \rightarrow \phi COOM^{\bullet} \qquad (6.14)$$

$$\phi COO^{\bullet} \rightarrow \phi^{\bullet} + CO_2 \qquad (6.15)$$

$$\phi^{\bullet} + M \rightarrow \phi M^{\bullet} \qquad (6.16)$$

$$\phi^{\bullet} + \phi COO^{\bullet} \rightarrow \phi COO\phi \qquad (6.17)$$

$$2\phi^{\bullet} \rightarrow \phi\text{-}\phi \qquad (6.18)$$

The square brackets around the species denote a shell or cage formed by surrounding solvent molecules. Of the above steps, equations (6.12), (6.14) and (6.16) result in chain initiation while steps (6.11), (6.17) and (6.18) reduce the efficiency of initiation due to consumption of radicals in reactions resulting in inert species. Equation (6.13) represents the diffusion of the trapped radicals out of the solvent cage whereby truly free radicals in solution are formed. If the diffusive process (6.13) is slow as in highly viscous media, for instance, decomposition inside the solvent cage (as in step 6.11) is more likely to occur. It is obvious that the latter reaction within the solvent cage competes with initiation reaction (6.12) also within the solvent cage. However, the radical-radical interactions inside the solvent cage are favoured on the grounds of high radical concentrations (≈10M) and their higher rate constants (10^7 litres/(mole.sec)) than the monomer addition having a rate constant generally between 10-10^5 litres/mole.sec [86]. Once the radicals are released from the solvent cage, they

react preferentially with monomer as in equations (6.14) and (6.16) due to the large monomer concentration in the bulk of the polymerisation medium and the usually high reactivity towards monomers. Reactions (6.17) and (6.18) are therefore suppressed to a large degree in the early stages of most polymerisations.

It is clear from the above description that radical decomposition within the solvent cage represents the main cause of reduced initiator efficiency and the decomposition is in turn determined by the rate of diffusion of the radicals out of the cage. A slow diffusion process leads to increased lifetimes of primary radicals in close proximity inside the solvent cage thereby promoting decomposition. In the case of BPO, reaction step (6.11) involves β scission at the phenyl ring and the carbon atom linkage, the rate of which is much slower than the diffusion process at low conversions of monomer [219]. Hence, the efficiency of thermal decomposition of BPO is expected to be higher than most initiators including AIBN and LPO during the early stages of polymerisation.

The importance of the cage effect has been shown to increase with a rise in the viscosity of the polymerising medium [220,221]. The interactions between primary initiator radicals and monomer molecules suffer as a consequence of poor mixing efficiency. The effect of viscosity has been demonstrated in numerous experimental studies by a fall in the initiator efficiency f with progress in polymerisation for various systems [193,222-225]. Faldi et al. [194] have modelled the decrease of initiator efficiency with conversion on the basis of reduced mobility of radical fragments and hence diffusion with a rise in polymer concentration. Their model fits the initiator efficiency estimates from various sources [191,192,226] reasonably well. It is to be noted that a few investigations, however, still found no obvious dependence of f on viscosity [227].

In addition, reactions such as those described by steps (6.17) and (6.18) above which also result in a decrease in f are more prone to occur at monomer concentrations below 10^{-1} and 10^{-2} M [153]. In fact, the effect of monomer concentration on f during the AIBN initiated polymerisation of styrene was experimentally studied by Bevington [228] and more recently by Solomon and Moad [225]. The latter authors reported a decrease in AIBN efficiency from 0.75 at conversions up to 30% to 0.20 at 90-95% conversion. A similar decrease in efficiency was noted by Stickler and Dumont [224] for BPO initiator in the polymerisation of MMA whereby the formation of phenyl benzoate was evidence for the loss of primary benzoyloxy radicals. From equation (2.26) above, such a drop in the initiator efficiency is predicted to have a detrimental effect on the speed of polymerisation R_p but in many experimentally determined rate values, the fall in R_p may be masked and indeed overcome by the parallel decrease in k_t which has an opposite effect on R_p.

The experimental results gathered by Robertson [222] are considered instrumental in predicting the onset of diffusion control in the present study of styrene polymerisation. The author's data on f, in particular, will be used as reference marks to estimate the starting initiator efficiency and the decrease of f with styrene conversion under the operating conditions of the current experimental analysis. Taking the data from Experiment 12 in Robertson's work as the reference [222], the initial efficiency for the present study would most likely be around 0.8 if allowances are made for the increase in temperature from 60°C in Robertson's work to 90°C (present study), for the reduced initial styrene concentration of about 82% (present

study) and finally for the lower initial BPO concentration of 0.052 M or 12.6 g/litre (present study). The onset of diffusion control of f in conventional agitated reactors applicable to the current polymerisation system would be somewhere between 30% and 40% styrene conversion which is higher than the 20% conversion for experiment 12 of Robertson's work. The shift of the diffusion control process to a later stage in the polymerisation would be expected in the present research in view of the increase in viscosity being delayed by the presence of the solvent (toluene), the higher temperature (90°C) and the lower average chain length (about 100), all of which would contribute to lower the viscosity of the polymerising medium. Hence a comparable viscosity level to Experiment 12 would only be reached at a higher polymer concentration or higher conversion. If the decrease in f with conversion follows the trend established in Robertson's study, then a steady fall in initiator efficiency from 0.8 to about 0.5 in the region of 80% conversion, as shown in Figure 6.6, can be estimated for the purpose of the current investigation.

This method of estimating the initiator efficiency is admittedly a very crude one but, in the absence of any other data for systems similar to the one investigated in this research, the estimates herein represent a good starting point in assessing the performance of the SDR.

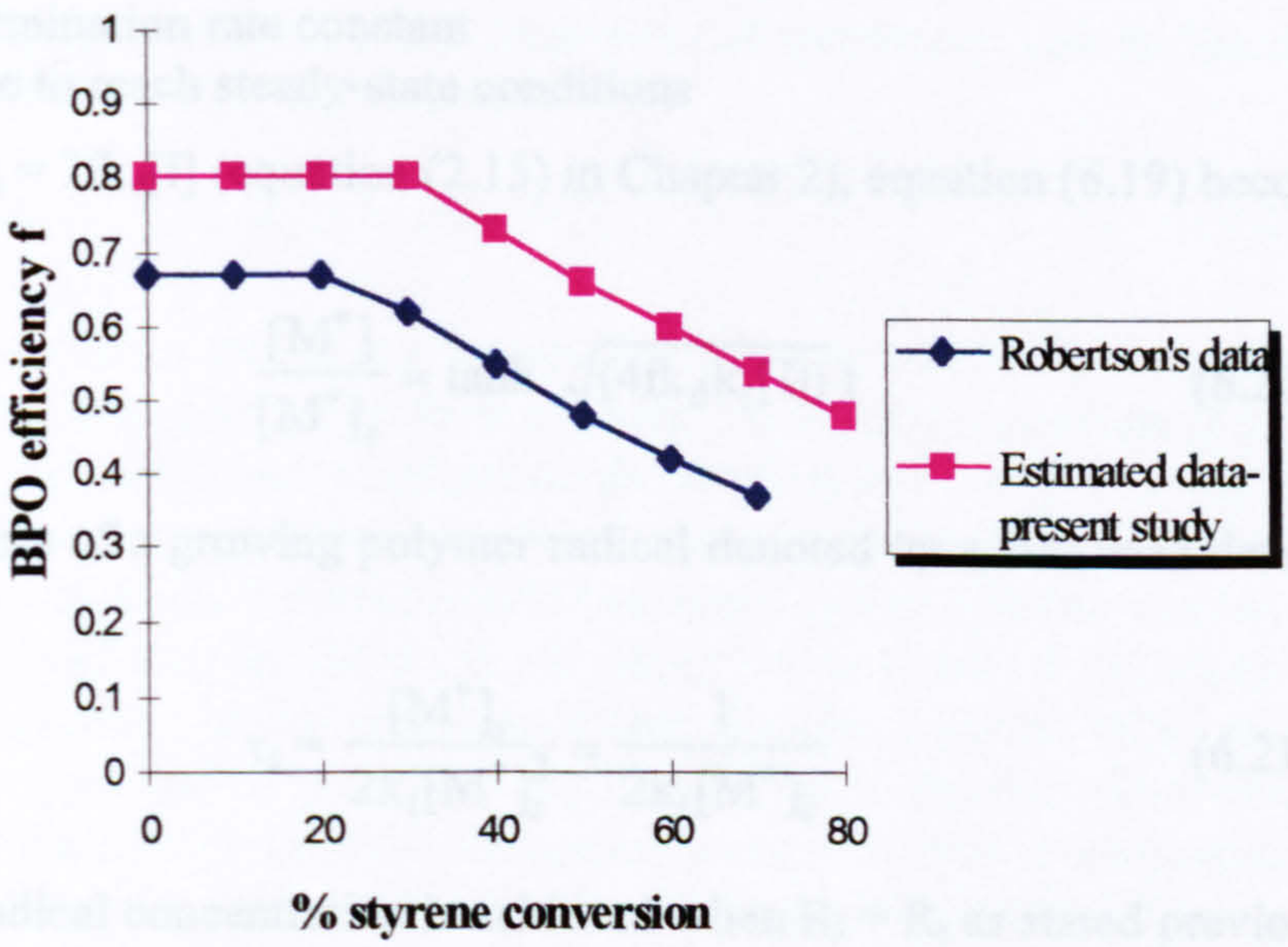

Figure 6.6. Variation of BPO efficiency with conversion in conventional polymer reactors

Under the influence of the improved mixing characteristics of the rotating disc environment, it is quite probable that the BPO efficiency can be increased and maintained to values of 0.8 or higher still even in the case of viscous systems. Let us consider for example a feed at 60% conversion into the SDR for which the efficiency f in the batch can be predicted to be close to 0.6 based on the data given in Figure 6.6. If it is assumed that the SDR can increase the efficiency to the value of 0.8 at which cage effects are negligible and also that k_p and k_t remain constant at their respective non-diffusion limited values k_{po} and k_{to}, then the ratio of the rate of polymerisation in SDR to that in the batch i.e. $R_p(SDR)/R_p(batch)$ which is proportional to $\sqrt{f_{SDR}}/\sqrt{f_{batch}}$ would have a value of 1.15. Only a 15% improvement in the rate of

polymerisation in the SDR would be expected from the rise in efficiency of the initiator. However, as shown in Tables 6.1 to 6.5 previously, the rates of polymerisation in the SDR appear to be much higher than can be accounted for solely by an improvement in f due to enhanced micromixing in the thin polymerising film. It is plausible therefore to expect that polymerisation in the SDR is proceeding in a rather unique manner due to the influence of the high centrifugal acceleration caused by rotation of the disc surface.

The second theory which, combined with the high initiator efficiency, could provide a meaningful explanation for the enhanced performance of the SDR is based on non-steady state kinetics. The time for the radical concentration to reach steady state after a sudden change in conditions e.g. an increase in the rate of initiation can be obtained from the expression below [86,161,171]:

$$\frac{[M^\bullet]}{[M^\bullet]_s} = \tanh \sqrt{(2R_i k_t)}\, t \qquad (6.19)$$

where $[M^\bullet]$ is the transient polymer radical concentration
$[M^\bullet]_s$ is the steady-state polymer radical concentration
R_i is the rate of chain initiation
k_t is the termination rate constant
t is the time to reach steady-state conditions

Substituting for $R_i = 2fk_d[I]$ (equation (2.15) in Chapter 2), equation (6.19) becomes:

$$\frac{[M^\bullet]}{[M^\bullet]_s} = \tanh \sqrt{(4fk_d k_t[I])}\, t \qquad (6.20)$$

The average lifetime of a growing polymer radical denoted by τ_s has been defined by Odian [86] as:

$$\tau_s = \frac{[M^\bullet]_s}{2k_t[M^\bullet]_s^2} = \frac{1}{2k_t[M^\bullet]_s} \qquad (6.21)$$

The steady state radical concentration is achieved when $R_i = R_t$ as stated previously in Chapter 2. Hence $[M^\bullet]_s$ is conveniently expressed in terms of rate parameters as:

$$[M^\bullet]_s = \sqrt{\frac{f k_d[I]}{k_t}} \qquad (6.22)$$

Replacing $[M^\bullet]_s$ in equation (6.21) with the expression in (6.22), we get

$$\tau_s = \sqrt{\frac{1}{(4fk_d k_t[I])}} \qquad (6.23)$$

In terms of τ_s , equation (6.20) is simply written as:

$$\frac{[M^\bullet]}{[M^\bullet]_s} = \tanh \frac{t}{\tau_s} \qquad (6.24)$$

Using typical rate constants for the BPO initiated polymerisation of styrene at 88-90°C e.g. $k_d = 10^{-5}$ s^{-1}, $k_t = 10^7$ litre/mole.sec [86,229] and assuming [I]=0.051 mol/litre and f = 0.8, the radical lifetime of polystyrene radicals is then about 0.3 seconds and the time to reach a new steady state after an abrupt change in the radical concentration is found from equation (6.24) to be less than 1 second.

Conventional polymer reactors operate at residence times of the order of hours and the use of the stationary state approximation is highly justified in such reactors. However, it has been shown theoretically in section 6.2.3 above that residence times on the rotating disc surface are of the order of seconds. Therefore it would appear that the polymerisation of styrene in the SDR could well have taken place under non-steady state conditions so that the much simplified stationary state kinetics are no longer applicable. Therefore steady state kinetics with typical rate constants fail to predict the rate of polymerisation in the SDR.

The rate of polymerisation under conditions of non-steady state is described by equation (2.20) as given earlier in Chapter 2:

$$R_p = k_p [M] [M^\bullet] \qquad (2.20)$$

It is obvious from the above expression that the rate of polymerisation is dependent on the radical population in the system. If a radical concentration higher than normal can be achieved and sustained on the rotating disc surface during the non-stationary state, then many monomer molecules would be consumed by addition to the large number of newly formed radical chains and hence polymerisation would proceed at a much more rapid rate in the SDR. In order for the radical concentration to increase upon introduction of the prepolymer onto the disc surface, either the rate of initiation should rise dramatically or there should be a fall in the rate of termination of active chains. But from the relatively unchanged molecular weight properties of the SDR polymer product, it is unlikely that termination is inhibited on the disc especially under the conditions of improved micromixing characteristics in the liquid film. It is our belief therefore that the rate of chain initiation or more precisely the decomposition rate of the initiator could well be a responsible factor at the root of the polymerisation rate enhancement observed in the SDR. Previous research carried out into the decomposition rates of initiators during the course of polymerisation have been limited but they have generally been assumed to be constant in most systems. In fact Moad and co-workers [216] recently reported unchanged decomposition rate for AIBN in the polymerisation of styrene. This finding was however based on measurements at steady state condition of polymerisation. Unfortunately, not much information is available for unsteady state kinetics for decomposition of initiators since the possibility of carrying out polymerisations in non-stationary state did not arise before. The SDR is believed to possess all the required characteristics to improve the rates of the chain reactions involved in free-radical polymerisations even in very viscous media in a short period of time.

The theories put forward above appear to be plausible suggestions which could explain the rate enhancements and improved polymer product quality observed in the study of the polymerisation of styrene in the SDR. However, thorough experimental investigations into the kinetics of polymerisations in the thin liquid film need to be undertaken before any definite conclusions can be reached.

6.3. AGITATION RESULTS

6.3.1. Effect of agitation rate on conversion

From the results of the agitation study of the batch polymerisation of styrene which have been presented in section 5.2 of Chapter 5, it can be deduced that the rate of polymerisation drops with increasing agitator speed.

This effect may be explained by considering the expression derived in Chapter 2 for the rate of polymerisation which is:

$$R_p = k_p [M] \sqrt{\left(\frac{f k_i [I]}{k_t}\right)} \qquad (2.26)$$

As the speed of agitation increases, the recirculation rate of the reactive species in the polymerising mixture rises. Segregated regions are progressively destroyed and the micromixing process which involves mixing on a molecular scale improves considerably. The individual rate constants for the consecutive reaction steps of initiation, propagation and termination are all expected to increase as the active species come in close proximity to one another more frequently and hence have a greater chance of colliding and combining during reaction. However, the greatest impact is on the termination reaction which involves diffusion and joining of the ends of two relatively long polymer chains. The diffusion step makes the termination process more susceptible to improvements in mixing than the propagation or the initiation processes. The termination rate constant k_t therefore becomes significantly higher at large agitation rates, hence reducing R_p and the extent of conversion achieved after a given polymerisation time. In contrast, at low impeller speeds where poor mixing levels and negligible recirculation rates are encountered, the termination reaction is effectively suppressed to a large degree so that a considerable rise in the rate of polymerisation is seen. The gel-effect can then set in and in extreme cases, the polymerisation can spiral out of control.

Vortex formation was also observed to become more significant with increases in the agitation rate which in turn resulted in lower polymer concentration and lower solution viscosity. It may well be that the swirling action contributed in some way in improving the mixing of species in the system and hence has some disguised benefits on the reactor performance.

Thus the apparent effect of enhanced micromixing at higher agitation rates in the current polymerisation of styrene is to reduce the conversion at a given time. In fact, many studies into the effects of micromixing [229-231] have shown that perfect mixing in systems having reaction orders greater than 1 leads to lower conversions. From equation (2.26) above, the overall reaction order is 1.5 which explains the lower conversion results at high rates of impeller rotation. Also, as seen earlier on in Chapter

2 (sections 2.3.3.1 and 2.3.3.2), the overall reaction order has been known to rise with the progress in polymerisation.

Micromixing effects become important in systems where fast reaction kinetics and high viscosity media are involved. Polymerisations can be fast under suitable operating conditions but in many practical instances, they are commonly characterised by high viscosities. Harada and co-workers [232] have indeed shown that polymerisations carried out under low viscosity regimes can be assumed to operate under conditions of perfect micromixing at all times. This work was followed up by experimentation in a more viscous medium where the sensitivity of styrene conversion on micromixing becomes more significant as a direct consequence of the auto-acceleration effects [233]. More recently, the effect of micromixing or backmixing in a copolymerisation system was also mathematically analysed in the presence of the gel-effect [234]. It was again noted that as a result of the gel-effect, the conversion was more dependent on the extent of backmixing. It is reasonable to expect that any diffusion limitation imposed by the high viscosity of the reaction medium would make a given polymerisation system more responsive to changes in micromixing levels.

6.3.2. Effect of agitation rate on Mn and Mw

The molecular weights M_n and M_w are both lowered as the speed of agitation drops from 1500 rpm to 70-90 rpm as seen in Figures 5.43 and 5.44 in Chapter 5. Under conditions of poor mixing and reduced chain termination, the average molecular weight of the polymer is predicted to rise substantially as the active polymer chains grow much longer by adding a large number of monomer molecules. The analysis performed by Chen and Steenrod [212] as applied to batch systems operating under various degrees of mixing indeed shows that complete segregation results in lower M_n, higher M_w and consequently increased polydispersity of the polymer. The current results for M_n and polydispersity index seem to agree well with the theoretical analysis of Chen and Steenrod whereas the M_w results are quite the opposite.

This anomaly in the current results is probably best explained by taking account of the non-uniform temperatures in the polymerising mixture at the various speeds as shown in Figure 5.40 in the previous chapter. Inadequate mixing is invariably linked to poor heat transfer from the reaction mixture and hence non-uniform temperature distribution within a poorly to moderately mixed system in comparison to a completely micromixed system. Following on from the earlier discussion in section 6.1.2, a rise in temperature is accompanied by low molecular weights. It would therefore appear that, in the present investigation, temperature has a more dominant influence on the molecular weights.

6.3.3. Effect of agitation rate on MWD

The instantaneous molecular weight distribution is seen to become broader as the level of micromixing in the agitated system is reduced. This is indeed indicated in Figure 5.45 in the preceding chapter by the increased polydispersity index as the speed of agitation is lowered.

The effect of reduced mixing capabilities on heat transfer performance and hence temperature distribution in the reaction mixture contributes largely to broadening the MWD of the polymer product. The importance of the degree of

micromixing with regard to molecular weight distribution has long been recognised and one of the earliest studies in this subject is attributed to Biesenberger and Tadmor [209]. The latter investigators compared molecular weight distributions of free-radical chain polymerisation in 3 types of reactors: the batch reactor, the homogeneous CSTR (HCSTR) having perfect micromixing and the segregated CSTR (SCSTR) which exhibits complete microscopic segregation in its contents. Their results indicated that at a given conversion the narrowest MWD was achieved for the HCSTR and the broadest for the SCSTR. This result is only applicable when the mean life time of active chains is much shorter than the mean residence time [235]. Furthermore, Biesenberger and Tadmor [209] found that the variation of the polydispersity index with conversion was more pronounced in the SCSTR with large increases observed from conversions as low as 20-30%.

The way in which micromixing affects general reactor performance for polymerisation processes depends strongly on whether the process operates in continuous flow or in batch mode. In a continuous system, feeds are continuously added to the reactor and product is continuously removed from the other end. Mixing is of paramount importance as the feed streams need to be rapidly and efficiently incorporated into the polymerising mixture which can be quite viscous. The problems posed by local segregation of initiator feed stream, for example, under conditions of improper mixing include poor initiator efficiency and local temperature rise leading to "hot-spots" and possible reactor runaway [211]. With regard to conversion, an increase in the degree of micromixing is expected to lower the conversion achieved as a result of greater uniformity of dispersion of reactants in the feed. However, the results for the polymerisation of styrene obtained by Harada et *al.* in a CSTR [233] indicate a surprisingly different effect whereby perfect micromixing leads to much higher conversion than the condition of no micromixing. Their finding was related to the autoacceleration phenomenon which is unique to polymerisation systems. The situation in this particular case can be imagined as the increased micromixing enabling the monomer molecules in the feed to reach and add to the growing active chains thus aiding in the autoacceleration process. However, it would seem that the enhanced micromixing is still not adequate to completely overcome the diffusion limitations of the termination process. Under these circumstances, it would appear that the degree of micromixing is such that it is selectively dispersing small monomer molecules in the entangled polymer network but not promoting bimolecular termination of the longer polymer chains.

The tests in the agitation study were carried out with a marine propeller in an unbaffled batch reactor. Such an axial flow agitator was a purely arbitrary choice and it could well be that its performance was not adequate for the whole range of viscosities encountered. However, the purpose of the agitation study was to get a feel for the effect of stirring rates on the polymerisation of styrene in general terms and the agitator has fulfilled this purpose.

Hence, on the basis of the results obtained in the present agitation study, it can be said that the selection of an appropriate agitator speed rests on an acceptable compromise between the conversion and the molecular weight distribution of the final polymer product. The compromise in the case of the laboratory-scale batch reactor used in the investigation appears quite insignificant at low agitation rates (much higher conversion at the expense of only a minor increase in polydispersity index). However, several other factors such as heat removal, temperature control, power

requirements, reactor stability etc. would have to be considered in an industrial scale reactor operating at much higher conversions and viscosities with much lower diffusivities. Stirring rates would then have to kept at a reasonably high level to prevent loss of control, poor product quality and potential reactor runaway situations.

6.4. CASE STUDY: ENERGY SAVING POTENTIAL OF SPINNING DISC REACTOR

One of the most attractive features of the spinning disc reactor is its potential to increase reaction rates thereby reducing the energy consumption without compromising production and product quality. An attempt to theoretically quantify its energy usage would substantiate the claim that the spinning disc is a highly energy efficient device.

The objective of this case study is to compare the energy consumed by using the batch reactor and a combination of the batch vessel and a number of spinning disc surfaces to reach the same conversion level. The energy consumption will be based on total batch reactor volume of 35 m^3 (measured at 20°C) with 84% v/v styrene, 16% v/v toluene and 0.05 mole/litre of benzoyl peroxide initiator initially, to produce 20 tonnes of polystyrene at a conversion of 75%. It is assumed that agitation in the batch is provided by a close-clearance type of impeller [110] to cope with the high viscosities during the course of the reaction. In practice, polymerising melt is transferred from a low conversion type of reactor to a high conversion reactor during the process, with both type of reactors equipped with agitators of different designs and adequate heat transfer surfaces to ensure good mixing and high heat transfer rates over the wide range of viscosity build up.

6.4.1. Batch Reactor Energy Usage

Using only the batch reactor, the required conversion level of 75% is achieved after 2 hours from the onset of polymerisation, assuming the small glass vessel can be scaled up to give the same reaction profile in the industrial scale reactor.

Energy in the batch is mainly consumed in the following ways:

6.4.1.1. Preheating energy to reaction mixture

Assuming that styrene monomer and toluene solvent are heated to the required operating temperature of 88°C by transfer of heat from heating oil circulating through the hollow agitator shaft, the heat required is calculated as:

$$\Delta H_1 = m_s C_{ps} \Delta T + m_t C_{pt} \Delta T$$
$$= (m_s C_{ps} + m_t C_{pt}) \Delta T \qquad (6.25)$$

where m_s, m_t : mass of styrene and toluene respectively
C_{ps}, C_{pt} : specific heat capacity of styrene and toluene respectively
ΔT : temperature rise = 88-20 = 68 K

Also since $M_s = \rho_s V_s$ and $M_t = \rho_t V_t$, equation (6.25) becomes:

$$\Delta H_1 = (\rho_s V_s C_{ps} + \rho_t V_t C_{pt}) * \Delta T \qquad (6.26)$$

Taking ρ_s :density of styrene = 906 kg/m^3 at 20°C
V_s: volume of styrene used = 29.4 m^3
ρ_t : density of toluene = 867 kg/m^3 at 20°C
V_t : volume of toluene used = 5.6 m^3
C_{ps} = 1.598 kJ/kg K
C_{pt} = 1.738 kJ/kg K

$$\Delta H_l = (906*29.4*1.598 + 867*5.6*1.738)*68$$
$$= 3.47 \times 10^6 \text{ kJ}$$
$$= 3.47 \times 10^9 \text{ J}$$

Assuming a heat transfer efficiency of 50%, the energy delivered by the heating oil is then obtained as:

$$\Delta H_{coils} = \underline{6.94 \times 10^9 \text{ J}}$$

6.4.1.2. Pumping energy of heating oil

It is assumed that Dow Corning heating fluid (200 cS at 25°C) is used as the oil in the heating. Based on an average fluid velocity of 2 m/s in a 40 mm diameter pipe and 20 m equivalent length of coil, the estimated pressure drop is calculated as 105 kN/m^2. The pumping power requirement is given by:

$$\text{Power} = V * \Delta P_{drop} \qquad (6.27)$$

where V is the volumetric flowrate (m^3/s)
ΔP_{drop} is the pressure drop (N/m^2)

The volumetric flowrate is calculated as:

$$V = uA \qquad (6.28)$$

where u is the water velocity (m/s) (= 2 m/s)
A is the area of cross-section of pipe ($=\pi d^2/4$)

Thus the volumetric flow is 0.0025m3/s giving a power requirement of 263W.

If the period of operation of the pump is 2 hours, the energy input of the pump having an efficiency of say 60% is $\underline{3.16 \times 10^6 \text{ J}}$.

6.4.1.3. Pumping energy of cooling water in jacket

Assume the water of mass flowrate of 1kg/s flows in a carbon steel pipe of optimum diameter, d(optimum), given (for water) by [236]:

$$d_{optimum} = 293 * \dot{m}^{0.53} \rho^{0.37} \qquad (6.29)$$

where $\dot{m}$ is the mass flowrate (kg/s)
ρ is the density of water ($\approx$ 1000 kg/m^3 at 20°C)

The optimum diameter is calculated as 22.7mm giving a fluid velocity of 2.5 m/s. The pressure drop in an equivalent pipe length of 20 m is estimated to be 56

kN/m^2. From equation (6.27) above, the pumping power requirement is calculated as 56W giving a total energy input of 6.75×10^5 J over a period of 2 hours of operation based on a pump efficiency of 60%.

6.4.1.4. Agitation power

The stirring action of the magnetic stirrer used in the batch mixture acts as a source of power consumption. However, it is difficult to calculate the energy used up by this magnetic stirrer and for this reason, we will consider instead the power requirement of a conventional agitator design employed commercially for this type of polymerisation process. We assume that the polymerisation reaction proceeds in bulk as the proportion of toluene used, 16 % v/v, is relatively low. Close-clearance impellers, such as an anchor impeller or a helical impeller, are the most suitable agitators to handle the highly viscous mixtures formed at high conversion levels of the bulk process. The typical power requirement of a close-clearance type of impeller in a bulk polymerisation process is between 1.0 and 6.0 kW/m^3 [110].

For the purpose of this study, we will assume that the average agitator power requirement is 5 kW/m^3.

For a total volume of reaction mixture of 35 m^3, the power consumed, P_2, is given by:

$$P_2 = 5*35 = 175 \text{ kW}$$

Hence average energy input, ΔH_2, over 2 hours of polymerisation time is:

$$\Delta H_2 = 175*120*60 = \underline{1.26 \times 10^9 \text{ J}}$$

The total energy requirement to reach 75% conversion in the batch process

$$= (6.94 \times 10^9 + 3.16 \times 10^6 + 6.75 \times 10^5 + 1.26 \times 10^9) \text{ J}$$
$$= \underline{\underline{8210 \text{ MJ}}}$$

6.4.2. Batch / Spinning Disc Reactor Combined Energy Usage

The prepolymerisation is carried out in the batch vessel over the first 40 minutes giving a conversion of 29%. The melt is then fed onto the spinning discs rotating at 850 rpm. We assume that the cascade arrangement of 4 rotating discs in series each of 360mm diameter can be replaced by a single disc of diameter 1.44m to give the required performance. Three such discs will be used in a parallel arrangement with a prepolymer feed rate of 200 cc/s to each disc in order to handle the volume of material leaving the prepolymer reactor. The required processing time in the spinning disc stage for 35.9 m^3 of 29% converted prepolymer is estimated to be about 16.6 hours. This time can be reduced if a feed flowrate much higher than 200 cc/s can be employed providing the increase in film thickness and reduction in residence time would not have any significant effect on the rate of polymerisation on the disc. For the feed flow of 200 cc/s chosen in this case study, the film thickness at the periphery of the disc (r=0.72m), halfway across the disc (r=0.36m) and at r=0.18m are calculated from equation (6.1) as 158 microns, 250 microns and 397 microns respectively. The corresponding residence time is obtained by the use of equation (6.2) as 1.87 seconds.

6.4.2.1. Batch energy usage

The sources of batch energy usage for the period of prepolymer preparation until 29% conversion is achieved are similar to those in section 6.4.1 above, the difference being a reduction in reaction time from 2 hours to 40 minutes. Hence the individual sources of energy consumption during the prepolymer preparation in the batch is as follows:

Heat input to batch reaction mixture
to increase temperature from 15°C to 88°C = 6.94×10^9 J

Pumping energy to heating fluid in coil immersed in reaction mixture = 1.05×10^6 J

Pumping energy for water in cooling jacket = 2.25×10^5 J

Agitation energy consumption in batch = 8.41×10^7 J (assuming an average power requirement of 1 kW/m^3 of reactor volume for agitation of low viscosity reaction mixture at 29% conversion [110])

Hence energy requirement for prepolymerisation in batch = $(6.94 \times 10^9 + 1.05 \times 10^6 + 2.25 \times 10^5 + 8.41 \times 10^7)$ J
= 7030 MJ

6.4.2.2. Spinning disc energy usage

In the spinning disc equipment power is consumed in heating and rotating the discs and pumping heat transfer fluid through the internal parts of the disc system.

6.4.2.2.1. Energy requirement of heating fluid

Heat and pumping energy need to be imparted to the heating fluid.

It will be assumed that heating of the disc surface is achieved by circulation of a heating fluid (e.g. water) underneath the disc surface through the shaft system. For each of the 3 disc systems, the heating fluid will be heated in a 50 litre capacity constant temperature bath by electric coils with an efficiency assumed to be 50%. The pump operates at 60% efficiency and delivers water from the bath at the rate of 10 litres/minute (assumed).

On the basis of the above operating conditions, the heat and pumping energy can be calculated.

Heat input to raise the temperature of 50 litres of water
in the bath from 15°C to 88°C for 1 disc system = $m_{water} * Cp_{water} * (T_{out} - T_{in})$/efficiency
= 50*4.18*(88-15)/0.5 kJ
= 3.05×10^7 J

Assuming that disc reaches the required temperature of 88°C in 30 minutes and that the maximum temperature drop in the heating water circulating through the system during the heat up period is 2 K, then additional heat energy is needed to bring the water back to 88°C.

Additional power requirement to
maintain constant temperature in bath = $\dot{m}_{water} * Cp_{water} * (T_{out} - T_{in})$
= (10/60)* 4.18 * 2 kW

$$= 1.4 \text{ kW}$$

Additional heat to be supplied by coils = $1.4*1000*30*60/0.5 = 5.02 \times 10^6$ J

Total heat supplied for 3 disc systems = $3*(3.05 \times 10^7 + 5.02 \times 10^6) = \underline{1.07 \times 10^8 \text{ J}}$

Pumping power requirement is given by equation (6.27). Assuming a pressure drop of 101.3 kN/m^2 through the rotating system, then the power required to overcome friction in 1 disc is 16.8 W. Then the power developed by a 60% efficient pump is 28.1W.

Based on a processing time of 16.7 hours on 3 parallel discs, the total energy consumed in pumping heating fluid = $\underline{5.06 \times 10^6 \text{ J}}$.

6.4.2.2.2. Rotational energy requirement

The rotational energy is provided by an electric motor operating at an assumed efficiency of 70%.

Rotational energy of dry disc

Assuming a torque of 0.5 Nm is required to keep the disc rotating at constant speed against the retarding frictional forces of the bearings, rotary union and surrounding medium (air), then the rotational power consumed on a dry disc at 850 rpm is given by:

$$\begin{aligned} P_{dry} &= \text{Torque x Angular velocity} \\ &= \text{Torque x } 2\pi N/60 \\ &= 0.5* 2*\pi*850/60 \text{ W} \\ &= 44.5 \text{ W} \end{aligned} \qquad (6.30)$$

With a motor efficiency of 70% and operating time of 16.7 hours, the total rotational energy delivered to the 3 disc systems is $\underline{1.14 \times 10^7 \text{ J}}$.

Kinetic energy of liquid film

In addition to the rotational energy of the dry disc, the motor also supplies the kinetic energy for the flow of the thin liquid film on the rotating disc.

The change in kinetic energy of the film per unit time has been formulated by Khan [20] as:

$$P_{K.E} = \frac{1}{2} Q_f \{\rho_o (r^2\omega^2 + u^2_m)_o - \rho_i (r^2\omega^2 + u_m^2)_I\} \qquad (6.31)$$

where Q_f: volumetric flowrate taken to be 200 cc s^{-1}
ρ: film density (kg/m^3)
r : radial distance from centre of disc (m)
ω: angular velocity ($=2\pi N/60$) ($rads^{-1}$)
N: rotational speed (rpm)
u_m: mean velocity of film on disc (m/s)
subscripts o, i: outer and inner respectively

An expression for the mean velocity u_m of a thin film under the effect of a centrifugal force is derived in Appendix A as:

$$u_m = \left(\frac{\rho Q_f^2 \omega^2}{12 \pi^2 \mu r} \right)^{1/3} \qquad (6.32)$$

where μ: dynamic viscosity (Ns/m^2)

Taking r_i = 0.03m and r_o = 0.72 m, ρ_o= 978 kg/m^3 and ρ_l= 892 kg/m^3, μ_o =10 Pas, μ_i=0.001 Pas, N= 850 rpm, the energy supplied by the motor due to the increase in kinetic energy for 3 discs over a total processing time of 16.7 hours is estimated to be $\underline{8.69x10^7\ J}$.

Frictional energy dissipation

Another source of energy consumption in the disc system is the energy required to compensate for the power dissipated by the polymer melt due to friction with the disc surface. The frictional power dissipation is derived by Khan [20] as:

$$P_{friction} = \tfrac{1}{2} Q_f \omega^2 (\rho_o r_o^2 - \rho_i r_i^2) \qquad (6.33)$$

From (6.33), the power requirement for 1 disc is calculated as 401 W.

Over the total period of operation of the 3 discs, the energy to be delivered by 70% efficient motors is estimated as $\underline{1.03x10^8\ J}$.

The overall energy requirement in the 3-disc system = ($1.07x10^8$ + $5.06x10^6$+ $1.14x10^7$ + $8.69x10^7$+ $1.03x10^8$) J
= $\underline{3.13x10^8\ J}$

Batch / spinning disc reactor combined energy usage = 7030 MJ + 313 MJ
= $\underline{7343\ MJ}$

6.4.3. Energy Saving

Energy saved by using spinning disc surfaces = 8210 - 7343 = $\underline{867\ MJ}$

A realistic estimation of the % saving in energy achieved from the use of the rotating disc system can be obtained by comparing the energy consumed in the batch process to raise the conversion from 29% to 75% and that consumed by the SDR for the same conversion change. The energy usage in the batch for the stated change in conversion amounts to about 1180 MJ (=8210 MJ- 7030 MJ) while the SDR uses up about 313 MJ to reach the same conversion. Hence the % saving in energy is calculated to be about $\underline{70\%}$ (=1180-313 /1180) which highlights the tremendous energy saving potential of the SDR as a polymer reactor.

6.5. PROPOSED INDUSTRIAL POLYMERISATION PROCESS

In a real process situation, the use of the spinning disc reactor as a polymer reactor would appear to be more advantageous in a staged continuous process scheme. In the initial stage of the reaction, the prepolymer may be prepared in an enhanced tubular reactor where conversions up to about 30% may be achieved. The tubular reactor is essentially regarded as the continuous version of the batch reactor. The usefulness of tubular reactors fitted with static mixers in polymerisation processes has recently been demonstrated in the large-scale commercial production of polystyrene [105]. This stage of operation is relatively easier as the viscosities are low. The pre-polymer exiting the tubular reactor may then be introduced on to the spinning disc reactor where, on the basis of the results of the present investigation, rapid polymerisation rates would enable high conversions to be reached in a short period of time. The flowsheet representing the proposed process is illustrated in Figure 6.7 below.

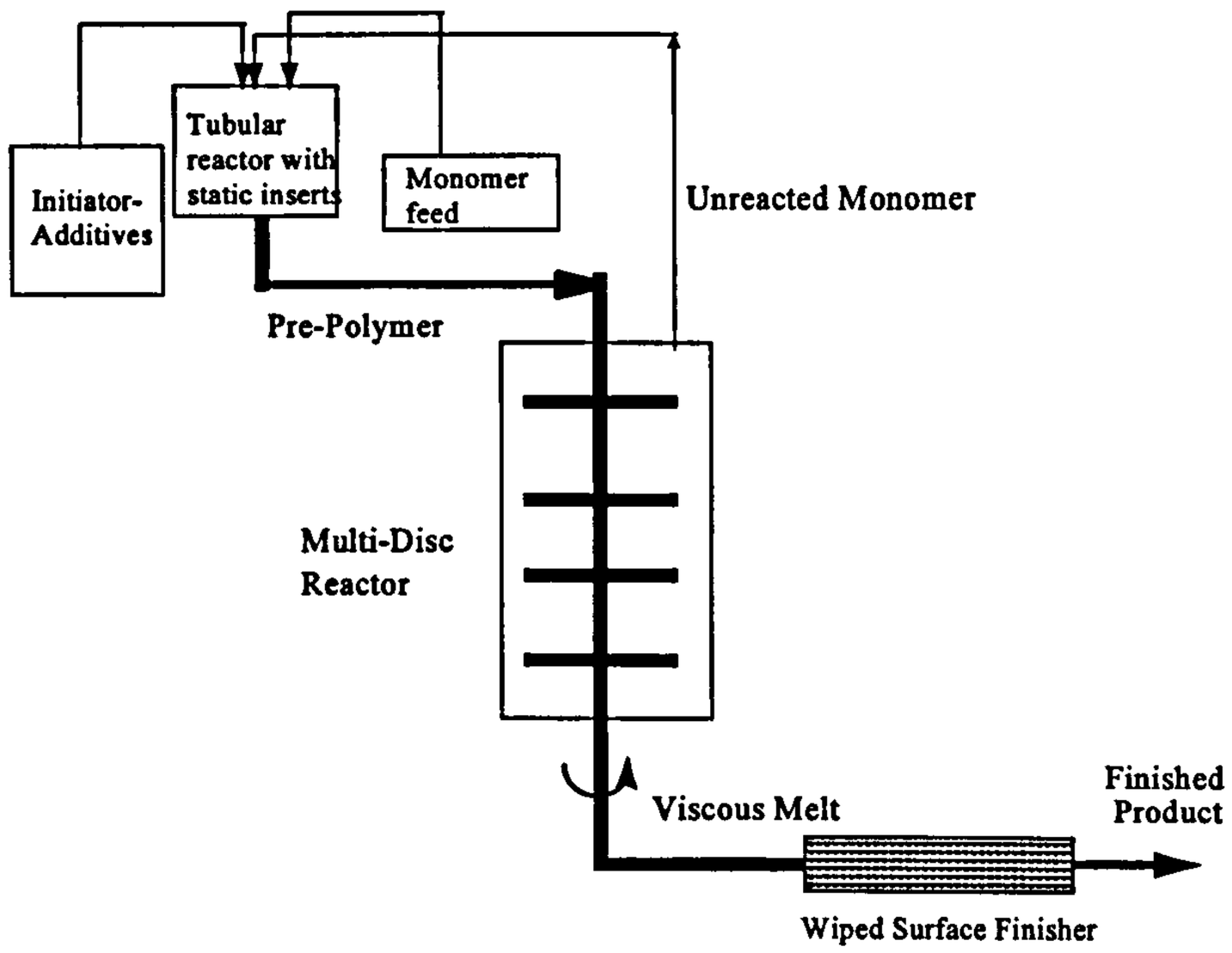

Figure 6.7. Simplified flowsheet of proposed polymerisation process

Based on the test results in the present investigation, it is predicted that a cascade of 4 successive disc passes (360 mm diameter discs) fed with a 29% converted prepolymer mix from the first stage would be able to achieve the desired performance with a large saving in time as illustrated in Figure 6.8 below.

The spinning disc reactor depicted in the process flowsheet in Figure 6.7 above is seen to consist of several rotating surfaces arranged in series in a vertical cascade. A number of design problems would be anticipated for such an arrangement, one of which being the transfer of product from the periphery of one disc to the centre of the next surface. It is envisaged that the performance of a cascade of discs could be adequately matched by having a single disc which would be approximately n times as large as each of the n discs in the cascade. Hence a conservative estimate would suggest that a single disc of about 1.4m diameter rotating at 850 rpm would be capable of achieving the desired conversion. Also depending on the feed flow rate which can be handled on the disc, it might be necessary to have several large discs

operating in parallel in order to reduce the processing time as has been highlighted in section 6.4.2 above.

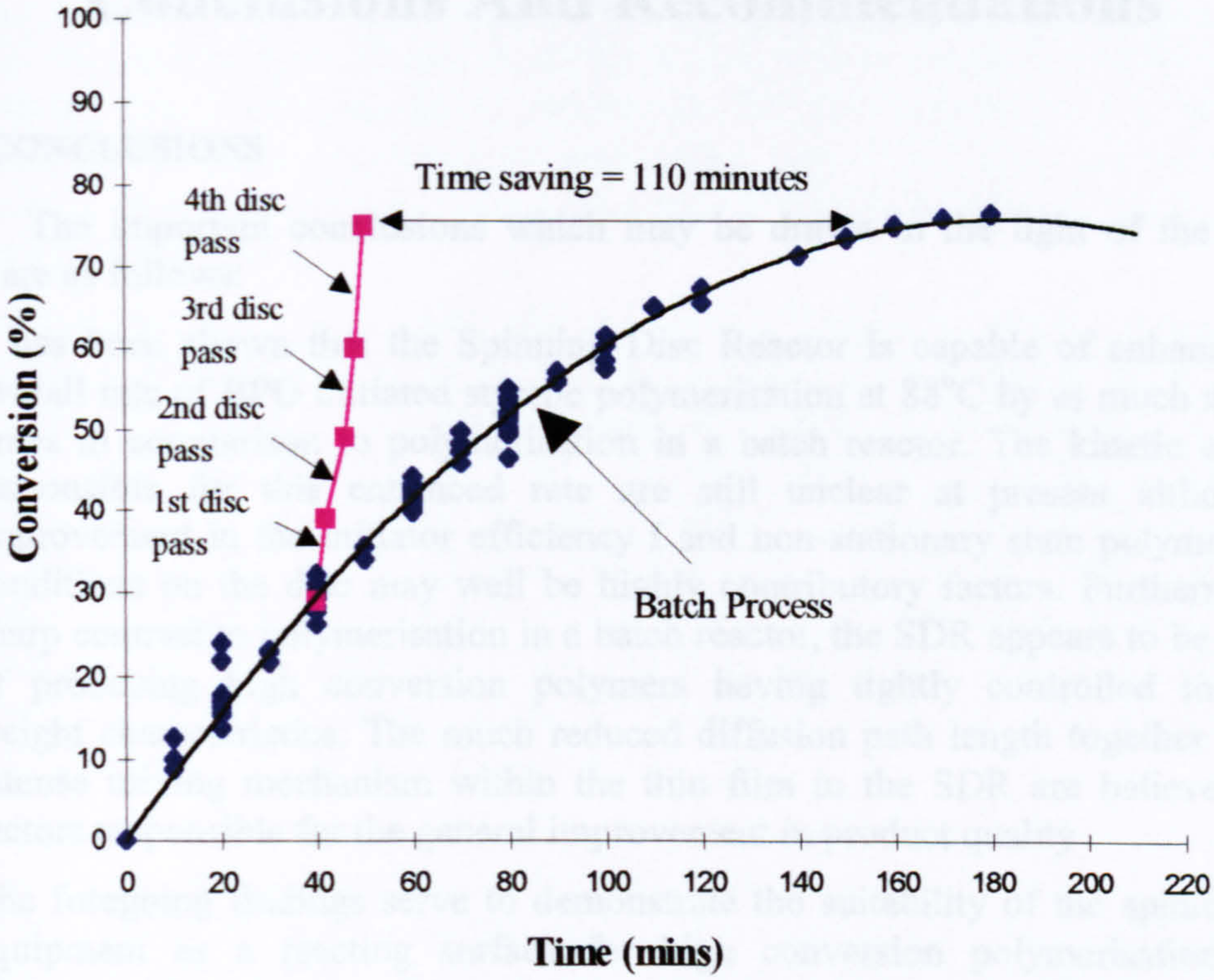

Figure 6.8. Predicted performance of proposed process using a cascade of discs rotating at 850 rpm

The use of spinning disc surfaces at a commercial level may be associated with several other important benefits. It is envisaged that the shorter residence times and exceptionally good heat transfer characteristics that can be achieved on the rotating disc will allow the use of higher temperatures which cannot be used in the existing reactors due to their heat removal limitations leading to possible runaway reactions and fear of thermal degradation of the polymer. Use of higher temperature will significantly reduce the viscosity even for very high molecular weight melts thereby improving mixing and hence enhancing heat and mass transfer rates. Furthermore, as the process described above will be operated under continuous mode and the reaction times will be significantly reduced, the amount of inventory in the reactor at any given time will be small and therefore the intrinsic safety of the process will be improved. The extremely high surface area to volume ratio offered by the rotating disc surface which is estimated to be of the order of 10000 m^2/m^3 for an average film thickness of 100 μm also compares most favourably with the conventional industrial scale stirred tank reactor which has a ratio as low as 1.3 for typical reactor dimensions of 4m diameter and 4m liquid level [237].

Chapter 7

Conclusions And Recommendations

7.1. CONCLUSIONS

The important conclusions which may be drawn in the light of the present study are as follows:

1. It has been shown that the Spinning Disc Reactor is capable of enhancing the overall rate of BPO initiated styrene polymerisation at 88°C by as much as 30-40 times in comparison to polymerisation in a batch reactor. The kinetic elements responsible for this enhanced rate are still unclear at present although an improvement in the initiator efficiency f and non-stationary state polymerisation conditions on the disc may well be highly contributory factors. Furthermore, in sharp contrast to polymerisation in a batch reactor, the SDR appears to be capable of producing high conversion polymers having tightly controlled molecular weight characteristics. The much reduced diffusion path length together with an intense mixing mechanism within the thin film in the SDR are believed to be factors responsible for the general improvement in product quality .

   The foregoing findings serve to demonstrate the suitability of the spinning disc equipment as a reacting surface for high conversion polymerisation where viscosity often poses serious problems in the mixing and diffusion of active species and monomer molecules in conventional batch processes.

2. Changes in prepolymer feed conversion or viscosity were found to have a profound effect on the general performance of the SDR. A steady increase in conversion and rate of polymerisation and hence time saving in one pass in the SDR were observed with a rise in the prepolymer feed conversion or viscosity. Increases in conversion as high as 16.3% in one pass on the disc rotating at 850 rpm were achieved with a time saving as large as 80-100 minutes. With regard to molecular weight properties, the SDR product is seen to have improved characteristics in terms of narrower molecular weight distribution when compared to polymer prepared in the batch at the same conversion.

3. The disc rotational speed was identified as another largely influential system variable in the polymerisation reaction conducted in the SDR. The presence of an optimal speed of rotation which gave the highest rate of polymerisation in the SDR and hence the largest time saving was established for a given set of fixed operating conditions such as disc temperature and prepolymer feed viscosity (or conversion). The value of the optimal speed rose from 850 rpm to 1000 rpm as the prepolymer feed conversion was increased from 37% to 58% at constant disc temperature of 88-90°C. Again, for all speeds tested, there is a general decrease in M_n, M_w and polydispersity index of SDR product in comparison with the batch polymer at the same conversion although no discernible trend with changes in rotational speed can be identified.

4. The individual contributions of the film thickness and residence time parameters as well as the film surface instabilities to the performance of the SDR have all

been extensively discussed in relation to the polymerisation of styrene on the disc. These hydrodynamic factors were shown to be functions of disc rotational speed, prepolymer feed viscosity and radial position. Previously derived correlations for smooth discs were used to predict changes in film thickness and residence times and the onset of wave formation for the polymerisation of styrene on the grooved rotating disc. Such predictions, although not completely accurate for the present study, nevertheless provided a valuable insight into the effect of system variables such as disc speed and disc feed viscosity on the hydrodynamic aspects of thin film polymerisation.

5. An agitation study in the batch was carried out to verify the effect of agitation rate on the conversion and molecular weight properties of the styrene polymerisation system. With increasing agitator speed, the rate of polymerisation was seen to drop, molecular weights M_n and M_w were increased and the instantaneous molecular weight distribution became narrower. Temperature effects were found to responsible for the anomalous result for M_w. The results were explained in terms of improved micromixing efficiency at high agitation rates. High degrees of micromixing in a continuous system such as the SDR would have an opposite effect on the rate of polymerisation and molecular weight properties compared to that observed in the batch agitation study.

6. A case study was performed in an attempt to provide a theoretical estimation of the energy saving potential of Spinning Disc Reactors. It was shown that the production of 20 tonnes of polystyrene at 75% in a semi-batch process involving 3 large discs of 1.4 m diameter rotating at 850 rpm and a feed flow of 200 cc/s on each disc could be achieved with more than 70% saving in energy in comparison to polymerisation in an industrial scale batch reactor.

7. A two-stage continuous industrial process for free-radical polymerisations has been proposed consisting of an enhanced tubular reactor in the first stage followed by a parallel arrangement of several rotating disc surfaces. Based on the test results in the present investigation, a conservative prediction suggests that up to 4 large discs of 1.4m diameter each rotating at 850 rpm, fed with a 29% converted prepolymer mix from the first stage, would be able to achieve the desired performance. Other potential benefits besides enhanced polymerisation rates and better polymer product quality to be gained from the proposed process may include an improvement in its intrinsic safety as a result of reduced inventory in the system at any given time and minimal risk of polymer degradation and thermal runaways at high operating temperatures due to short residence times and enhanced heat removal rates.

7.2. RECOMMENDATIONS FOR FUTURE WORK

The present investigation has undoubtedly shed much light into the performance of the SDR with regard to polymerisation processes. However, a number of avenues still remain to be explored before a complete and thorough understanding of the principles behind the spinning disc technology as applied to polymerisation systems in general can be acquired. It is hoped that the following suggestions are given most consideration and attention in the future exploration of Spinning Disc Reactors for polymerisation.

1. The present research involved the use of a normal grooved rotating disc for which no hydrodynamic measurements have as yet been performed. It is imperative to carry out tests to measure film thickness and radial velocity at various radial positions as well as residence times for various types and geometry of grooves such as the normal and re-entry groove. Empirical correlations and models similar to the centrifugal model for smooth discs need to be developed to establish the dependencies of film thickness, velocity distribution and residence time on the different operating variables such as disc speed and liquid flowrate and viscosity.

2. All of the earlier hydrodynamic measurements and derivations focused on the flow of liquid with constant viscosity. On the other hand, polymerisations involve constantly increasing conversion and viscosity with progress in reaction across the rotating disc. It is therefore considered necessary to obtain a viscosity/conversion profile across the disc surface for a particular polymerisation system by direct measurement across the disc of either conversion or viscosity combined with the use of appropriate correlations linking conversion and viscosity. This would make determination of other parameters which rely heavily on viscosity such as film thickness and residence time more precise.

3. It is important that the influence of other variables such as disc temperature, disc diameter and prepolymer flowrate on the polymerisation of styrene and other monomers are studied in great detail. It is also proposed that more tests be performed with different starting recipes to confirm the effect of feed viscosity and disc speed on the polymerisation of styrene observed in the present research. The development of an empirical relationship which will predict the effect of all the spinning disc variables on the product conversion and molecular weight properties of polymerisation systems in general will be most useful.

4. It is recommended that a detailed kinetic study into polymerisation carried out on the rotating disc be undertaken to determine the elements responsible for the rate enhancements observed in the present investigation. The measurement of individual rate coefficients for the decomposition of initiator and elementary chain steps (i.e. initiation, propagation and termination) under the effect of high acceleration environments should be performed. Furthermore, the measurement of initiator efficiency f together with the determination of radical concentration across the disc should be carried out to confirm the causes of polymerisation rate increases as put forward in this study.

5. Many problems associated with polymer reactors are related to mixing and it is believed that the success of the spinning disc concept for the styrene polymerisation system is due to its improved mixing characteristics especially on a molecular scale (i.e. micromixing). An experimental investigation into the level of micromixing and its effects on polymerisation reactions on the disc surface should constitute a relevant part in the future exploration work into the spinning disc technology.

6. It may be worthwhile to investigate the possibility of extending the use of Spinning Disc Reactors to co-polymerisation systems whose product properties are particularly sensitive to micromixing. The SDR may also be a suitable alternative reactor for bulk polymerisations of monomers such as methyl methacrylate which

suffer from severe gel-effect in conventional reactors. The enhanced mixing mechanism on the rotating disc may help in promoting termination reactions.

7. Finally, the development of a pilot plant scale multi-disc reactor such as the one shown in Figure 6.7 operating in continuous mode would allow relevant industrial processes to be realistically evaluated in the Spinning Disc Reactor.

NOMENCLATURE

		Units
A	Area of cross-section	m^2
a	Constant	-
a_{Cor}	Coriolis acceleration	ms^{-2}
b	Constant	-
C_I	Chain transfer constant to initiator	-
C_M	Chain transfer constant to monomer	-
C_P	Chain transfer constant to polymer	-
C_S	Chain transfer constant to solvent	-
c_p	Specific heat capacity	J/kg/K
D	Diameter at point of measurement on disc	m
DI	Polydispersity index	-
d	Pipe diameter	m
f	Initiator efficiency	-
f'	Limiting value of initiator efficiency	-
g	acceleration due to gravity	ms^{-2}
g	Gravitational acceleration vector ($= i g_x + j g_y + k g_z$)	-
ΔH	Change in enthalpy	J
h	Film heat transfer coefficient on disc surface	kW/m^2K
I	Initiator molecule	-
i, j, k	Unit vectors in positive x, y and z -directions respectively	-
K	consistency index	-
k_d	Initiator decomposition rate constant	s^{-1}
k_i	Initiation rate constant	$l.mol^{-1}s^{-1}$
k_p	Propagation rate constant	$l.mol^{-1}s^{-1}$
k_R	Rate constant for chemical reaction in termination process	$l.mol^{-1}s^{-1}$
k_s	Rate constant for reinitiation reaction	$l.mol^{-1}s^{-1}$
k_{SD}	Rate constant for segmental diffusion in termination process	$l.mol^{-1}s^{-1}$
k_t	Overall termination rate constant	$l.mol^{-1}s^{-1}$
k_{tc}	Rate constant for termination by combination	$l.mol^{-1}s^{-1}$
k_{td}	Rate constant for termination by disproportionation	$l.mol^{-1}s^{-1}$
k_{TD}	Rate constant for translational diffusion in termination process	$l.mol^{-1}s^{-1}$
k_{tp}	Rate constant for primary termination	$l.mol^{-1}s^{-1}$
k_{tr}	Rate constant for chain transfer	$l.mol^{-1}s^{-1}$
$k_{tr,I}$	Rate constant for chain transfer to initiator	$l.mol^{-1}s^{-1}$
$k_{tr,M}$	Rate constant for chain transfer to monomer	$l.mol^{-1}s^{-1}$
$k_{tr,S}$	Rate constant for chain transfer to solvent	$l.mol^{-1}s^{-1}$
M	Monomer	-
M_i	Molecule i whose weight is M	
M_{n+m}	Inactive polymer molecule with (n+m) monomer units	-
$\overline{M}_n$	Number-average molecular weight	kg/kmol
$\overline{M}_w$	Weight-average molecular weight	kg/kmol

Nomenclature

$\overline{M}_v$	Viscosity-average molecular weight	kg/kmol
$\overline{M}_z$, $\overline{M}_{z+1}$	Higher weight average molecular weights	kg/kmol
M_n	Molecular weight of a polymer chain consisting of n monomer units	kg/kmol
M_o	Molecular weight of monomer	kg/kmol
$M_n^\bullet$, $M_m^\bullet$	Active polymer chain with n,m monomer units respectively	-
MWD	Molecular weight distribution	-
m	mass	kg
$\dot{m}$	mass flowrate	kg/s
N	Number of molecules	-
N	Rotational speed	rpm
n	Degree of polymerisation	-
n	Number of moles	moles
n	Power law index	-
P	Polymer	-
ΔP	Pressure drop	N/m^2
P	Power	W
p	Pressure or partial pressure	N/m^2 or Pa
Q, Q_v	Volumetric flowrate	m^3/s
R	Universal gas constant	J/(mol K)
$R^\bullet$	Primary radical	-
R_d	Rate of initiator decomposition	mol. $l^{-1}s^{-1}$
R_i	Rate of initiation	mol. $l^{-1}s^{-1}$
R_p	Rate of polymerisation	mol. $l^{-1}s^{-1}$
R_t	Rate of termination	mol. $l^{-1}s^{-1}$
R_{tc}	Rate of termination by combination	mol. $l^{-1}s^{-1}$
R_{td}	Rate of termination by disproportionation	mol. $l^{-1}s^{-1}$
R_{tr}	Rate of chain transfer	mol. $l^{-1}s^{-1}$
$R_{tr,I}$	Rate of chain transfer to initiator	mol. $l^{-1}s^{-1}$
$R_{tr,M}$	Rate of chain transfer to monomer	mol. $l^{-1}s^{-1}$
$R_{tr,P}$	Rate of chain transfer to polymer	mol. $l^{-1}s^{-1}$
$R_{tr,S}$	Rate of chain transfer to solvent	mol. $l^{-1}s^{-1}$
r	Radial distance	m
S	Solvent	-
T	Chain transfer agent	-
T	Liquid film temperature	°C or K
ΔT	Temperature rise	K
t	Reaction time, time to reach steady state	s
t_{res}	Mean residence time	s
$t_{1/2}$	Half-life	s
V	Volume	m^3
u,v	Velocity	m/s
$\bar{v}$	Average film velocity	m/s
v	Velocity vector ($= \mathbf{i}\, v_x + \mathbf{j} v_y + \mathbf{k} v_z$)	-
W_i	Total weight of all molecules with weight M_i	kg
$\overline{X}_N$	Instantaneous number-average degree of polymerisation	-

x_n	Number/mole-fraction distribution of degree of polymerisation	-
x_w	Weight-fraction distribution of degree of polymerisation	-
z	Vertical upward distance	m

Greek

ν	Kinetic chain length	-
η,μ	Dynamic viscosity	Pas
ρ	Density	kg/m^3
ν	Kinematic viscosity	m^2/s
θ	Angle of inclination of plane surface to the horizontal	-
ω	Angular velocity	s^{-1}
$\dot{\gamma}$	Shear rate	s^{-1}
δ	Average film thickness	m
σ	Surface tension	N/m
τ	Shear stress	N/m^2
∇	Del operator $\left(= \mathbf{i}\frac{\partial}{\partial x} + \mathbf{j}\frac{\partial}{\partial y} + \mathbf{k}\frac{\partial}{\partial z}\right)$	m^{-1}

Dimensionless group

Re	Reynolds number $\left(=\frac{4\rho Q_v}{\pi\mu D}\right)$	-

Symbols

[X]	Concentration of component X	mol/litre

Subscripts

app	apparent
D	disc surface
f	feed
i	inlet
m	mean
o	outlet
r, θ, z	radial, angular and vertical directions respectively in cylindrical co-ordinates
x, y, z	x, y and z-directions respectively in rectangular Cartesian co-ordinates

REFERENCES

1. Etchells, J., Runaway. *The Chemical Engineer*, No.618, 17-21 (1996)
2. "Small is beautiful: Are miniaturised factories the way forward?", in *IChemE Future Life Report- Engineering Solutions for the Next Generation,* pp. 14-16, IChemE Publication, 1997.
3. Butcher, C., More poke, less pounds. *The Chemical Engineer*, No.532, 18 (1992)
4. Caruana, C.M., ChEs seek big gains from process miniaturisation. *Chem. Eng. Prog.*, **92**, 12-19 (April 1996)
5. Fell, N., Bespoke Reactions. *The Chemical Engineer*, No.643, 17-18 (1997)
6. Green, A., Process intensification: the key to survival in global markets? *Chemistry & Industry*, No.5, 168-172 (1998)
7. Semel, J., Process intensification- Today's challenge for the chemical industry, in *2nd International Conference on Process Intensification in Practice- Applications and Opportunities*, 21-23 October 1997, Antwerp, Belgium, BHR Conference Series No.28 (1997)
8. Ramshaw, C., A game for n-players. *The Chemical Engineer*, No.415, 30-33 (1985)
9. Gardner, G., Small is beautiful. *The Chemical Engineer*, No.571, 15 (1994)
10. Charlesworth, R.J., Steam reforming and combustion of methane on a micro-thin catalyst for use in a catalytic plate reactor, *Ph.D. Thesis,* University of Newcastle Upon Tyne (1996)
11. Burns, J.R., Liquid distribution in a rotating packed bed, *Ph.D. Thesis,* University of Newcastle Upon Tyne (1996)
12. Hassan-Beck, H.M., Process intensification: Mass transfer and pressure drop for counter-current rotating packed beds, *Ph.D. Thesis,* University of Newcastle Upon Tyne (1997)
13. Woods, W., The hydrodynamics of thin liquid films flowing over a rotating disc, *Ph.D. Thesis,* University of Newcastle Upon Tyne (1995)
14. Jachuck, R.J. and Ramshaw, C., Process intensification: Polymer film compact heat exchanger (PFCHE). *Trans. Inst. Chem. Engnrs*, **72**, Part A, 255-262 (1994)
15. Reay, D.A., Heat transfer enhancement- A review of techniques and their possible impact on energy efficiency in the UK. *Heat Recovery Systems & CHP*, **11**(1), 1-40 (1991)
16. Ramshaw, C., The opportunities for exploiting centrifugal fields. *Heat Recovery Systems & CHP*, **13**(6), 493-513 (1992)
17. Bell, C., The hydrodynamics and heat transfer characteristics of liquid films on a rotating disc, *Ph.D. Thesis,* University of Newcastle Upon Tyne (1975)
18. Jazayeri, A., The hydrodynamics of Newtonian and non-Newtonian liquid films flowing across a rotating disc, *Ph.D. Thesis,* University of Newcastle Upon Tyne (1980)

19. Lim, S.T., Hydrodynamics and mass transfer processes associated with the absorption of oxygen in liquid films flowing across a rotating disc, *Ph.D. Thesis,* University of Newcastle Upon Tyne (1980)

20. Khan, J.R., Heat transfer on a rotating disc with and without phase change, *Ph.D. Thesis,* University of Newcastle Upon Tyne (1986)

21. Moore, R.S., Mass transfer to thin liquid films on rotating surfaces with and without chemical reaction, *Ph.D. Thesis,* University of Newcastle Upon Tyne (1986)

22. Jachuck, R.J. and Ramshaw, C., Process Intensification: Heat transfer characteristics of tailored rotating surfaces. *Heat Recovery Systems & CHP*, **14**(5), 475-491 (1994)

23. Turnbull, J., Mixing characteristics on a rotating disc, *MEng. Report*, University of Newcastle Upon Tyne (1997)

24. Waldram, S., Batch runaway rethink. *The Chemical Engineer*, No.657, 15-16 (1998)

25. Fell, N., Innovation offers a new spin on drug production. *The Chemical Engineer*, No.656, 23-25 (1998)

26. Nusselt, *Ver. Deut. Ingr Z.*, **60**, 549, 569 (1916)

27. Kirkbride, C.G., Heat transfer by condensing vapour on vertical tubes. *Ind. Eng. Chem.*, **26**(4), 425-428 (1934)

28. Friedman, S.J. and Miller, C.O., Liquid films in the viscous flow region. *Ind. Eng. Chem.*, **33**(7), 885-891 (1941)

29. Grimley, S.S., Liquid flow conditions in packed towers. *Trans. Instn. Chem. Engrs*, **23**, 228-235 (1945)

30. Kapitza, P.L., Wave motion of a thin liquid layer of a viscous liquid. *J. Exp. Theo. Phys., USSR*, **18**, 3-28 (1948)

31. Benjamin, T.B., Wave formation in laminar flow down an inclined plane. *J. Fluid Mech.*, **2**, 554-574 (1957)

32. Binnie, A.M., Experiments on the onset of wave formation on a film of water flowing down a vertical plane. *J. Fluid Mech.*, **2**, 551-553 (1957)

33. Wilkes, J.O. and Nedderman, R.M., The Measurement of Velocities in Thin Films of Liquid. *Chem. Eng. Sci.*, **17**, 177-187 (1962)

34. Andreev, A.F., Stability of the laminar flow of thin liquid layers. *J. Exp. Theo. Phys., USSR*, **18**(2), 519-521 (1964)

35. Hikita, H., *Chem. Eng. (Tokyo)*, **23**, 23 (1959)

36. Jackson, M.L., Liquid films in viscous flow. *AIChE J.*, **1**, 231 (1955)

37. Stirba, C. and Hurt, D.M., Turbulence in falling liquid films. *AIChE J.*, **1**, 178 (1955)

38. Brauer, H., *Chem.- Ing.-Tech.*, **30**, 75 (1958)

39. Emmert, R.E. and Pigford, R.L., A study of gas absorption in falling liquid films. *Chem. Eng. Progr.*, **50**(2), 87-93 (1964)

40. Davies, J.T. and Warner, K.V., The effect of large scale roughness in promoting gas absorption. *Chem. Eng. Sci.*, **24**, 231-240 (1969)

41. Fulford, G.D., The flow of liquids in thin films, in *Advances in Chemical Engineering* Vol.5, Academic Press, New York, pp.151-236, 1964.

42. Charwat, A.F. et *al.*, The flow and stability of thin liquid films on a rotating disk. *J. Fluid Mech.*, **53**(2), 227-255 (1972)

43. Epsig, H. and Hoyle, R., Waves in a thin liquid layer on a rotating disc. *J. Fluid Mech.*, **22**(4), 671-677 (1965)

44. Wood, R.M. and Watts, B.E., The flow, heat and mass transfer characteristics of liquid films on rotating discs. *Trans. Instn. Chem. Engrs*, **51**, 315-322 (1973)

45. Thomas, S. et *al.*, Experimental analysis and flow visualisation of a thin liquid film on a stationary and rotating disc. *ASME J. Fluids Eng.*, **113**(1), 73-80 (1991)

46. Brauer, H., Stromung und warmeubergang bes rieselfilmen. *Ver. Deat. Ingr. - Forschungsheft*, 457-462 (1956)

47. Hickman, K.C.D., Centrifugal boiler compression still. *Ind. Eng. Chem.*, **49**(5), 786-789 (1957)

48. Cross, W.T. and Ramshaw, C., European Pat. 119776 (1983)

49. Ramshaw, C., European Pat. 207630 (1985)

50. Ramshaw, C. and Winnington, T., European Pat. 327230 (1986)

51. Mallinson, R. and Ramshaw, C., European Pat. 2568B (1979)

52. Mallinson, R. and Ramshaw, C., US Pat. 4263255 (1981)

53. Bromley, L.A. *et al.*, Condensation on and evaporation from radially grooved rotating discs. *ASME J. Heat Transfer*, **88**, 80-86 (1966)

54. Yanniotis, S. and Kolokotsa, D., Experimental study of water vapour condensation on a rotating disc. *Int. Commun. Heat and Mass Transfer*, **23**(5), 721-729 (1996)

55. Yanniotis, S. and Kolokotsa, D., Boiling on the surface of a rotating disc. *Journal of Food Engineering*, **30**(3/4), 313-325 (1996)

56. Yanniotis, S. and Kolokotsa, D., Boiling in a centrifugal field: the case of films formed between two closely spaced horizontal spinning discs, in *1st International Conference on Process Intensification for the Chemical Industry- Practical Applications of New Technology*, 6-8 December 1995, Antwerp, Belgium, BHR Group Conference Series No.18 (1995)

57. Rahman, M.M. *et al.*, Prediction of heat transfer to a thin liquid film in plane and radially spreading flows. *ASME J. Heat Transfer*, **112**, 822-824 (1990)

58. Rahman, M.M. and Faghri, A., Analysis of heating and evaporation from a liquid film adjacent to a horizontal rotating disc. *Int. J. Heat Mass Transfer*, **35**(10), 2655-2664 (1992)

59. Rahman, M.M. and Faghri, A., Numerical simulation of fluid flow and heat transfer in a thin liquid film over a rotating disk. *Int. J. Heat Mass Transfer*, **35**(6), 1441-1453 (1992)

60. Butozov, A.I. and Rifert, V.G., Heat transfer in evaporation of liquid from a film on a rotating disc. *Heat Transfer- Soviet Res.*, **5**, 57-61(1973)

61. Sparrow, E.M. and Gregg, J.L., A theory of rotating condensation. *ASME J. Heat Transfer*, **81**, 113-120 (1959)

62. Brauner, N. and Maron, D.M., Modelling of wavy flow in inclined thin films. *Chem. Eng. Sci.*, **35**(5), 775-788 (1983)

63. Venkataraman, R.S., Mass transfer to an expanding surface, *Ph.D. Thesis,* Leeds University (1966)

64. Javdani, K., Mass Transfer in Wavy Liquid Films. *Chem. Eng. Sci.*, **29**, 61-69 (1974)

65. Ravetkar, D.D. and Kale, D.D., Gas absorption into non-Newtonian fluids in rotating disc contactors. *Chem. Eng. Sci.*, **36**, 399-403 (1981)

66. Suga, K. and Boongorsrang, A., A new model of mass transfer in a rotating disc contactor. *Chem. Eng. Sci.*, **39**(4), 767-773 (1984)

67. Long, R. and Pattni, T., Mass transfer in a laminar rippling film in a conical centrifugal film reactor. Part I: Film thickness profile and velocity profile, in *Industrial Mixing Fundamentals with Applications* Vol.91, *AIChE Symposium Series No. 305*, pp.61-69, 1995.

68. Long, R. and Pattni, T., Mass transfer in a laminar rippling film in a conical centrifugal film reactor. Part II: Stability analysis for the film flow, in *Industrial Mixing Fundamentals with Applications* Vol.91, *AIChE Symposium Series No. 305*, pp.70-79, 1995.

69. Long, R. and Pattni, T., Mass transfer in a laminar rippling film in a conical centrifugal film reactor. Part III: enhanced mass transfer in ripple Flow, in *Industrial Mixing Fundamentals with Applications* Vol.91, *AIChE Symposium Series No. 305*, pp.80-87, 1995.

70. Cheong, S.I. and Choi, K.Y., A study of the polymer layer-forming phenomena in a rotating disc polycondensation reactor. *J. Appl. Polym. Sci.*, **55**(13), 1819-1826 (1995)

71. Cheong, S.I. and Choi, K.Y., Melt polycondensation of poly(ethylene terephthalate) in a rotating disc reactor. *J. Appl. Polym. Sci.*, **58**(9), 1473-1483 (1995)

72. Cheong, S.I. and Choi, K.Y., Modelling of a continuous rotating disc polycondensation reactor for the synthesis of thermoplastic polyesters. *J. Appl. Polym. Sci.*, **61**(5), 763-773 (1996)

73. Jachuck, R.J. and Ramshaw, C., Process intensification: Spinning disc polymeriser, in *The 1995 IChemE Research Event- First European Conference for Young Researchers in Chemical Engineering*, 5-6 January 1995, Edinburgh (1995)

74. Richter, P. *et al.*, Immobilised enzyme reactors. Diffusion/convection, kinetics and a comparison of packed column and rotating bioreactors for use in continuous flow systems. *Anal. Chem.*, 68(10), 1701-1705 (1996)

75. Menikheim, V., Polymerisation procedures, Industrial, in *Concise Encyclopaedia of Polymer Science and Engineering* (J. Kroshwitz, Ed.), John Wiley & Sons, Inc., New York, pp.840-843, 1990.

76. Meister, B.J. and Malanga, M.T., Styrene Polymers - Polymerisation, in *Concise Encyclopaedia of Polymer Science and Engineering* (J.I. Kroschwitz, Ed.), John Wiley & Sons, Inc., New York, pp.1113-1117, 1990.

77. Mallikarjun, R. and Nauman, E.B., Optimal Processes for Crystal Polystyrene. *Polym.-Plast. Technol. Eng.*, 28(2), 137-149 (1989)

78. Ku, P.L., Polystyrene and styrene copolymers. I. Their manufacture and application. *Adv. Polym. Technol.*, 8(2), 177-196 (1988)

79. Ku, P.L., Polystyrene and styrene copolymers. II. Their manufacture and application. *Adv. Polym. Technol.*, 8(3), 201-223 (1988)

80. Simon, R.H.M. and Chappelear, D.C., Technology of styrenic polymerisation reactors and processes, Ch.4 in *Polymerisation Reactors and Processes* (J.N. Henderson and T.C. Bouton, Eds.), *ACS Symposium Series No. 104*, pp.71-110, 1979.

81. Bishop, R.B., *Practical Polymerisation for Polystyrene*, Ch.3, pp. 107-156, Cahers, Boston, 1971.

82. Amos, J.L., The development of impact polystyrene - A review. *Polym. Eng. Sci.*, 14(1), 1-11 (1974)

83. Albright, L.F., *Processes for Major Addition-Type Plastics and Their Monomers*, Ch.8, pp. 312-376, Mc Graw-Hill, New York, 1974.

84. Platzer, N., Design of continuous and batch polymerisation processes. *Ind. Eng. Chem.*, 62(1), 6-20 (1970)

85. Beckmann, G., Design of large polymerisation reactors. *Chem. Tech.*, 304-310 (May 1973)

86. Odian, G.G., *Principles of Polymerisation*, Ch.3, pp. 198-334, 3rd ed., John Wiley & Sons, New York, 1991.

87. Pasztor, A.J., Styrene Polymers - Thermal Properties, in *Concise Encyclopaedia of Polymer Science and Engineering* (J.I. Kroschwitz, Ed.), John Wiley & Sons, Inc., New York, pp.1123-1125, 1990.

88. Albright, L.F., Polymerisation, in *Encyclopedia of Chemical Processing and Design* (J.J. Mc Ketta, Ed.), Vol.39, Marcel Dekker Inc., New York, pp.281-313, 1992.

89. Albright, L.F. and Bild, C.G., Designing reaction vessels for polymerisation. *Chem. Eng.*, 121-128 (September 1975)

90. Schildknecht, C.E., Other Bulk Polymerisations, Ch.4 in *Polymerisation Processes* (C.E. Schildknecht and I. Skeist, Eds.), *High Polymers Vol.29*, Wiley-Interscience, New York, pp.88-105, 1977.

91. Dunlop, R.D. and Reese, F.E., Continuous polymerisation in Germany. *Ind. Eng. Chem.*, 40(4), 654-660 (1948)

92. Boundy, R.H. and Boyer, R.F., *Styrene: Its polymers, copolymers and derivatives*, Reinhold, New York, 1952.

93. Mc Donald, D.L. *et al.*, Process of mass polymerisation in vertical unmixed strata, U.S. Pat. 2,727,884 (to Dow Chemical Company) (Dec. 20, 1955)

94. Platt, A.E. and Wallace, T.C., Styrene Plastics, in *Encyclopaedia of Chemical Technology* (Kirk-Othmer, Ed.), 3rd ed., Vol.21, John Wiley & Sons, New York, pp.825-827, 1983.

95. Allen, I.J. *et al.*, Continuous bulk polymerisation of styrene, U.S. Pat. 2,496,653 (to Union Carbide Corporation) (Feb. 7, 1950)

96. Kii, T. and Suka, M., Process and apparatus for treating viscous material, Canadian Pat. 864047 (to Mitsui Toatsu Chemicals Inc.) (Feb. 16, 1971)

97. Weber, A.P., Continuous flow reactor for high viscosity materials, U.S. Pat. 4,007,016 (to The Bethlehem Corporation) (Feb. 8, 1977)

98. Walas, S.M., *Reaction Kinetics for Chemical Engineers*, pp. 88, McGraw-Hill, New York, 1959.

99. Wallis, J.P.A. *et al.*, Continuous production of polystyrene in a tubular reactor. *AIChE J.*, **21**(4), 686-698 (1975)

100. Agarwal, S.S. and Kleinstreuer, C., Analysis of styrene polymerisation in a continuous flow tubular reactor. *Chem. Eng. Sci.*, **41**(12), 3101-3110 (1986)

101. Lynn, S. and Huff, J.E., Polymerisation in a tubular reactor. *AIChE J.*, **17**, 475-481 (1971)

102. Lynn, S., Comments on polymerisation of styrene in a tubular reactor. *AIChE J.*, **23**(3), 387-389 (1977)

103. Cunningham, M.F. *et al.*, Bulk polymerisation in tubular reactors I. Experimental observations on fouling. *Can. J. Chem. Eng.*, **69**, 630-638 (1991)

104. Chen, C.C., A continuous bulk polymerisation process for crystal polystyrene. *Polym.-Plast. Technol. Eng.*, **33**(1), 55-81 (1994)

105. Stone, J., Polystyrene process showcases static mixing. *Chem. Eng.*, **98**(2), 213-215 (September 1991)

106. Tauscher, W.A., A styrene polymerisation process based on static mixing technology, paper presented at CHISA Congress in Prague on August 29, 1990.

107. Yoon, W.J. and Choi, K.Y., Polymerisation of styrene in a continuous filled tubular reactor. *Polym. Eng. Sci.*, **36**(1), 65-77 (1996)

108. Streiff, F.A. and Rogers, J.A., Don't Overlook Static-Mixer Reactors. *Chem. Eng.*, **101**(6), 76-82 (June 1994)

109. Henderson, L.S., Polymerisation. Stability analysis in turbine-agitated reactors, in *Encyclopaedia of Chemical Processing and Design* (J.J. Mc Ketta, Ed.), Vol.39, Marcel Dekker, New York, pp.334-352, 1992.

110. Oldshue, J.Y., *Fluid Mixing Technology*, Ch.15, pp. 295-337, 1983.

111. Uhl, V.W. and Voznick, H.P., The anchor agitator. *Chem. Eng. Prog.*, **56**(3), 72-77 (1960)

112. Coyle, C.K. et *al.*, Heat transfer to jackets with close clearance impellers in viscous material. *Can. J. Chem. Eng.*, **48**, 275-278 (1970)

113. Metzner, A.B. and Otto, R.E., Agitation of non-Newtonian fluids. *AIChE J.*, **3**, 3-10 (1957)

114. Metzner, A.B. and Taylor, J.S., Flow patterns in agitated vessels. *AIChE J.*, **6**, 109-114 (1960)

115. Calderbank, P.H., The prediction of power consumption in the agitation of non-Newtonian fluids. *Trans. Inst. Chem. Engnrs*, **37**, 26-33 (1959)

116. Throne, J.L., *Plastics Process Engineering*, Ch. 3, pp. 137, Marcel Dekker, New York, 1979.

117. Henderson, L.S.I. and Cornejo, R.A., Temperature control of continuous, bulk styrene polymerisation reactors and the influence of viscosity: an analytical study. *Ind. Eng. Chem. Res.*, **28**(11), 1644-1653 (1989)

118. Flory, P.J., *Principles of Polymer Chemistry*, Ch.4, Cornell University Press, Ithaca, New York, 1973.

119. Odian, G.G., *Principles of Polymerisation*, Ch.1, pp. 8, 3rd ed., John Wiley & Sons, New York, 1991.

120. North, A.M., *Kinetics of Free-Radical Polymerisation*, Ch.4, pp. 36-50, Pergamon Press, London, 1966.

121. Bamford, C.H., Redox initiators, Ch.9 in *Comprehensive Polymer Science* (G. Allen, J.C. Bevington, and G.C. Eastmond, Eds.), 1st ed., Vol.3, Pergamon Press, Oxford, pp.123-140, 1989.

122. Moad, G. et *al.*, Other initiating systems, Ch.10 in *Comprehensive Polymer Science* (G. Allen, J.C. Bevington, and G.C. Eastmond, Eds.), 1st ed., Vol.3, Pergamon Press, Oxford, pp.141-146, 1989.

123. Hui, A.W. and Hamielec, A.E., Thermal Polymerisation of Styrene at High Conversions and Temperatures. An Experimental Study. *J. Appl. Polym. Sci.*, **16**, 749-769 (1972)

124. Husain, A. and Hamielec, A.E., Thermal polymerisation of styrene. *J. Appl. Polym. Sci.*, **22**, 1207-1223 (1978)

125. Mayo, F.R., Chain transfer in the polymerisation of styrene VIII. Chain transfer with bromobenzene and mechanism of thermal initiation. *J. Am. Chem. Soc.*, **75**, 6133-6141 (1953)

126. Flory, P.J., The mechanism of vinyl polymerisations. *J. Am. Chem. Soc*, **59**, 241-253 (1937)

127. Pryor, W.A. and Lasswell, L.D., Diels-Alder and 1,4-diradical intermediates in the spontaneous polymerisation of vinyl monomers, Ch.2 in *Advances in Free-Radical Chemistry* (G.H.Williams, Ed.), Vol.5, Elek Science, London, 1975.

128. Priddy, D.B., Recent advances in styrene polymerisation. *Adv. Polym. Sci.*, **111**, 68-114 (1994)

129. Buzanowski, W.C. et *al.*, *Polymer*, **33**, 3055 (1992)

130. Moad, G. and Solomon, D.H., *The Chemistry of Free-Radical Polymerisation*, Ch.3, pp. 43-144, Elsevier Science, Oxford, 1995.

131. Berger, K.C. and Meyerhoff, G., Propagation and termination constants in free-radical polymerisation, in *Polymer Handbook* (J. Brandrup and E.H. Immergut, Eds.), 3rd ed., Wiley-Interscience, New York, pp.II/67-II/79, 1989.

132. Matheson, M.S. et *al.*, Rate constants in free radical polymerisation. III. Styrene. *J. Am. Chem. Soc.*, **73**, 1700-1706 (1951)

133. Mahabadi, H.K. and O'Driscoll, K.F., *J. Macromol. Sci. Chem.*, **A11**, 967 (1977)

134. Buback, M. et *al.*, Critically evaluated rate coefficients for free-radical polymerisation. I. Propagation rate coefficient for styrene. *Macromol. Chem. Phys.*, **196**, 3267-3280 (1995)

135. Throne, J.L., *Plastics Process Engineering*, Ch.2, pp.66-67, Marcel Dekker, New York, 1979.

136. Bevington, J.C. et *al.*, The termination reaction in radical polymerisations. II. Polymerisations of styrene at 60°C and of methyl methacrylate at 0 and 60°C and the copolymerisation of these monomers at 60°C. *J. Polym. Sci.*, **14**, 463-476 (1954)

137. Burnett, G.M. and North, A.M., Free-radical polymerisation using a bifunctional initiator. III. The termination reaction. *Makromol. Chem.*, **73**, 77-84 (1964)

138. Mayo, F.R. *et al.*, Chain Transfer in the Polymerisation of Styrene. *J. Am. Chem. Soc.*, **73**, 1691-1699 (1951)

139. Johnson, D.H. and Tobolsky, A.V., Monoradical and diradical polymerisation of styrene. *J. Am. Chem. Soc.*, **74**, 938-943 (1952)

140. Bamford, C.H. and Jenkins, A.D., Termination reactions in vinyl polymerisation: preparation of block co-polymers. *Nature (London)*, **176**, 78 (1955)

141. Moad, G. and Solomon, D.H., Chemistry of bimolecular termination, Ch.11 in *Comprehensive Polymer Science* (G. Allen, J.C. Bevington, and G.C. Eastmond, Eds.), 1st ed., Vol.3, Pergamon Press, Oxford, pp.147-160, 1989.

142. Moad, G. et *al.*, *Macromolecules*, **15**, 1188 (1982)

143. Berger, K.C., *Makromol. Chem.*, **176**, 3575 (1975)

144. Olaj, O.F. et *al.*, *J. Polym. Sci. Polym. Lett. Ed.*, **15**, 229 (1977)

145. Buback, M. and Kuchta, F.-D., Termination kinetics of free-radical polymerisation of styrene over extended temperature and pressure range. *Macromol. Chem. Phys.*, **198**, 1455-1480 (1997)

146. Biesenberger, J.A. and Sebastian, D.H., *Principles of Polymerisation Engineering*, Ch.1, pp. 79, John Wiley & Sons, New York, 1983.

147. Kerr, J.A., Rate processes in the gas phase, Ch.1 in *Free Radicals* (J.K. Kochi, Ed.), Vol.I, Wiley-Interscience, New York, pp.1-36, 1973.

148. Allock, H.R. and Lampe, F.W., *Contemporary Polymer Chemistry*, Ch.12, pp. 284, 2nd ed., Prentice-Hall, New Jersey, 1990.

149. North, A.M., *Kinetics of Free-Radical Polymerisation*, Ch.1 & 6, pp. 17-18, 74, Pergamon Press, London, 1966.

150. Nishimura, N., *J. Macromol.. Chem.*, **1**, 257 (1966)

151. Horikx, M.W. and Hermans, J.J., Application of the steady-state method to benzoyl peroxide initiated polymerisation of styrene. *J. Polym. Sci.*, **11**, 325-352 (1953)

152. Bamford, C.H. *et al.*, *The Kinetics of Vinyl Polymerisation by Free-Radical Mechanism*, Ch.6, pp. 203-226, Butterworths, London, 1958.

153. Koenig, T. and Fisher, H., Cage effects, Ch.4 in *Free Radicals* (J.K.Kochi, Ed.), Vol.I, Wiley-Interscience, New York, pp.157-189, 1973.

154. North, A.M., *Kinetics of Free-Radical Polymerisation*, Ch.6, pp. 79, Pergamon Press, London, 1966.

155. Moad, G. et *al.*, *Macromolecules*, **17**, 1094 (1984)

156. Ito, K., Evaluation of polymerisation rate by chain length dependence on polymer-polymer termination and primary termination in radical polymerisation. *J. Polym. Sci. Polym. Chem. Ed.*, **18**(2), 701-707 (1980)

157. Mahabadi, H.K. and O'Driscoll, K.F., *Makromol. Chem.*, **178**, 2629 (1977)

158. Deb, P.C. and Ray, S., *Eur. Polym. J.*, **14**, 607 (1978)

159. Ueda, M. et *al.*, *Macromolecules*, **17**, 2800 (1984)

160. Moad, G. and Solomon, D.H., *The Chemistry of Free-Radical Polymerisation*, Ch.4, pp. 145-205, Elsevier Science, Oxford, 1995.

161. North, A.M., *Kinetics of Free-Radical Polymerisation*, Ch.3, pp. 22-35, Pergamon Press, London, 1966.

162. Stickler, M., Experimental techniques in free radical polymerisation kinetics. *Makromol. Chem. Macromol. Symp.*, **10/11**, 17-69 (1987)

163. Buback, M. et *al.*, Consistent values of rate parameters in free-radical polymerisation systems. *J. Polym. Sci., Part C: Polym. Lett.*, **26**, 293-297 (1988)

164. Buback, M. et *al.*, Consistent values of rate parameters in free-radical polymerisation system. II. Outstanding dilemmas and recommendations. *J. Polym. Sci., Part A: Polym. Chem.*, **30**(5), 851-863 (1992)

165. Allock, H.R. and Lampe, F.W., *Contemporary Polymer Chemistry*, Ch.12, pp. 294-298, 2nd ed., Prentice-Hall, New Jersey, 1990.

166. North, A.M., *Kinetics of Free-Radical Polymerisation*, Ch.2, pp. 14-16, Pergamon Press, London, 1966.

167. Moad, G. and Solomon, D.H., *The Chemistry of Free-Radical Polymerisation*, Ch.5, pp. 234-259, Elsevier Science, Oxford, 1995.

168. Baysal, B. and Tobolsky, A.V., Rates of initiation in vinyl polymerisation. *J. Polym. Sci.*, **8**, 529 (1952)

169. Gregg, R.A. and Mayo, F.R., Chain transfer in the polymerisation of styrene. II. The reaction of styrene with carbon tetrachloride. *J. Am. Chem. Soc.*, **70**, 2373-2378 (1948)

170. Ueda, A. and Nagai, S., Transfer constants to monomers, polymers, catalysts and initiators, solvent and additives and sulfur compounds in free radical polymerisation, in *Polymer Handbook* (J. Brandrup, E.H. Immergut, and A.E. Grulke, Eds.), Wiley-Interscience, New York, pp.II/97-II-162, 1999.

171. Eastmond, G.C., The kinetics of free-radical polymerisation of vinyl monomers in homogeneous solution, Ch.1 in *Comprehensive Chemical Kinetics* (C.H. Bamford and C.F.H. Tipper, Eds.), Vol.14A, Elsevier, Oxford, pp.1-103, 1976.

172. Cardenas, J.N. and O'Driscoll, K.F., High conversion polymerisation. I. Theory and application to methyl methacrylate. *J. Polym. Sci. Polym. Chem. Ed.*, **14**, 883-897 (1976)

173. Cardenas, J.N. and O'Driscoll, K.F., High conversion polymerisation. II. Influence of chain transfer on the gel effect. *J. Polym. Sci. Polym. Chem. Ed.*, **15**, 1883-1888 (1977)

174. Cardenas, J.N. and O'Driscoll, K.F., High conversion polymerisation. III. Kinetic behaviour of ethyl methacrylate. *J. Polym. Sci. Polym. Chem. Ed.*, **15**, 2097-2108 (1977)

175. Dionisio, J. et *al.*, High conversion polymerisation. IV. A definition of the onset of the gel effect. *J. Polym. Sci. Polym. Chem. Ed.*, **17**, 1891-1900 (1979)

176. Turner, D.T., Autoacceleration of free-radical polymerisation 1. The critical concentration. *Macromolecules*, **10**(2), 221-226 (1977)

177. Balke, S.T. and Hamielec, A.E., Bulk polymerisation of methyl methacrylate. *J. Appl. Polym. Sci.*, **17**, 905-949 (1973)

178. Lee, H.B. and Turner, D.T., Autoacceleration of free-radical polymerisation 2. Methyl methacrylate. *Macromolecules*, **10**(2), 226-230 (1977)

179. Marten, F.L. and Hamielec, A.E., High conversion diffusion controlled polymerisation, in *Polymerisation Reactors and Processes* (J.N. Henderson and T.C. Bouton, Eds.), *ACS Symposium Series No.104*, pp.43-70, 1979.

180. Marten, F.L. and Hamielec, A.E., High conversion diffusion-controlled polymerisation of styrene. I. *J. Appl. Polym. Sci.*, **27**, 489-505 (1982)

181. Soh, S.K. and Sundberg, D.C., Diffusion-controlled vinyl polymerisation. I. The gel effect. *J. Polym. Sci. Polym. Chem. Ed.*, **20**, 1299-1313 (1982)

182. Soh, S.K. and Sundberg, D.C., Diffusion-controlled vinyl polymerisation. II. Limitations on the gel effect. *J. Polym. Sci. Polym. Chem. Ed.*, **20**, 1315-1329 (1982)

183. Soh, S.K. and Sundberg, D.C., Diffusion-controlled vinyl polymerisation. III. Free volume parameters and diffusion controlled propagation. *J. Polym. Sci. Polym. Chem. Ed.*, **20**, 1331-1344 (1982)

184. Soh, S.K. and Sundberg, D.C., Diffusion-controlled vinyl polymerisation. IV. Comparison of theory and experiment. *J. Polym. Sci. Polym. Chem. Ed.*, **20**, 1345-1371 (1982)

185. Stickler, M., Free-radical polymerisation kinetics of methyl methacrylate at very high conversions. *Makromo. Chem.*, **184**, 2563-2579 (1983)

186. Moad, G. and Solomon, D.H., *The Chemistry of Free-Radical Polymerisation*, Ch.5, pp. 207-233, Elsevier Science, Oxford, 1995.

187. Mahabadi, H.K., A review of the kinetics of the low conversion free radical termination process. *Makromol. Chem. Macromol. Symp.*, **10/11**, 127-150 (1987)

188. Mahabadi, H.K. and O'Driscoll, K.F., *Macromolecules*, **10**, 55 (1977)

189. Hayden, P. and Melville, H., The kinetics of the polymerisation of methyl methacrylate. I. The bulk reaction. *J. Polym. Sci.*, **43**, 201-214 (1960)

190. Ballard, M.J. et *al.*, *Macromolecules*, **19**, 1303 (1986)

191. Shen, J. et *al.*, *Makromol. Chem. Rapid Commun.*, **8**, 615 (1987)

192. Sack, R. et *al.*, Free-radical polymerisation of methyl methacrylate up to the glassy state. Rates of propagation and termination. *Macromolecules*, **21**(12), 3345-3352 (1988)

193. Achilias, D.S. and Kiparissides, C., Development of a general mathematical framework for modelling diffusion controlled free-radical polymerisation reactions. *Macromolecules*, **25**, 3739-3750 (1992)

194. Faldi, A. et *al.*, Monomer diffusion and the kinetics of methyl methacrylate radical polymerisation at intermediate to high conversion. *Macromolecules*, **27**, 4184-4192 (1994)

195. Yamada, B. et *al.*, Dependence of propagation and termination rate constants on conversion for radical polymerisation of styrene in bulk as studied by ESR spectroscopy. *Macromolecules*, **24**, 5234-5236 (1991)

196. Horie, K. et *al.*, Calorimetric investigation of polymerisation reactions. I. Diffusion-controlled polymerisation of methyl methacrylate and styrene. *J. Polym. Sci., Part A-1*, **6**, 2663 (1968)

197. Mita, I. and Horie, K., Diffusion-controlled reactions in polymer systems. *J. Macromol. Sci.-Rev. Macromol. Chem. Phys.*, **C27**(1), 91-169 (1987)

198. Allock, H.R. and Lampe, F.W., *Contemporary Polymer Chemistry*, Ch.14, pp. 335-378, 2nd ed., Prentice-Hall, New Jersey, 1990.

199. Rodriguez, F., *Principles of Polymer Systems*, 3rd ed., McGraw-Hill, New York, 1989.

200. Pollock, D.J. and Kratz, R.F., Polymer molecular weights, Ch.2 in *Methods of Experimental Physics* (R.A. Fava, Ed.), Vol. 16 Part A, Academic Press, New York, pp. 13-72, 1980

201. Odian, G.G., *Principles of Polymerisation*, Ch.1, pp. 22, 3rd ed., John Wiley & Sons, New York, 1991.

202. Billingham, N.C., Molecular weight distributions, Ch.4 in *Comprehensive Polymer Science* (G. Allen, J.C. Bevington, and G.C. Eastmond, Eds.), Vol.3, Pergamon Press, Oxford, pp.43-57, 1989.

203. Throne, J.L., *Plastics Process Engineering*, Ch.3, pp. 100-110, Marcel Dekker, New York, 1979.

204. Liu, S.-I. and Amundson, N.R., *Rubber Chem. Tech.*, **34**, 995-1133 (1961)

205. Boodhoo, K., Spinning disc polymeriser for the production of polystyrene, *MEng. Report*, University of Newcastle Upon Tyne (1995)

206. O'Driscoll, K.F. and White, P.J., Kinetics of polymerisation of styrene initiated by substituted peroxides. II. Decomposition rate constants and efficiencies. *J. Polym. Sci.: Part A*, **3**, 283-299 (1965)

207. Lhila, R.C. and Forsyth, T.H., Mixing in viscous polymer reactors. *Polym.-Plast. Technol. Eng.*, **15**(2), 155-168 (1980)

208. Nauman, E.B. and Buffham, B.A., *Mixing in Continuous Flow Systems*, Ch.5, pp. 163-177, John Wiley & Sons, New York, 1983.

209. Tadmor, Z. and Biesenberger, J.A., Influence of segregation on molecular weight distribution in continuous linear polymerisations. *Ind. Eng. Chem. Fundamentals*, **5**(3), 336-343 (1966)

210. Reichert, K.-H. and Moritz, H.-U., Polymer Reaction Engineering, Ch.24 in *Comprehensive Polymer Science* (G. Allen, J.C. Bevington, and G.C. Eastmond, Eds.), 1st ed., Vol.3, Pergamon Press, Oxford, pp.327-363, 1989.

211. Choplin, L. and Villermaux, J., Viscous mixing in polymer reactors. *Industrial Mixing Technology*, **90**(299), 123-129 (1994)

212. Chen, H.T. and Steenrod, J., *Polym. Eng. Sci.*, **15**(5), 357-359 (1975)

213. Emslie, A.G. et *al.*, Flow of a viscous liquid on a rotating disk. *J. Appl. Phys.*, **29**(5), 858-862 (1958)

214. Dixon, B.E. et *al.*, Liquid films formed by means of rotating disks. *Brit. J. Appl. Phys.*, **3**, 115-119 (1952)

215. Thomas, S. et *al.*, One-dimensional analysis of the hydrodynamic and thermal characteristics of thin film flows including the hydraulic jump and rotation. *ASME J. Heat Transfer*, **112**, 728-735 (1990)

216. Moad, G. et *al.*, *Macromolecules*, **17**, 1094 (1984)

217. Bueche, F., *Physical properties of polymers*, Ch.5, pp. 114, Interscience, New York, 1962.

218. Russell, G.T. et *al.*, Initiator efficiencies in high-conversion bulk polymerisations. *Macromolecules*, **21**(7), 2141-2148 (1988)

219. Moad, G. and Solomon, D.H., Azo and peroxy initiators, Ch.8 in *Comprehensive Polymer Science* (G. Allen, J.C. Bevington, and G.C. Eastmond, Eds.), 1st ed., Vol.3, Pergamon Press, Oxford, pp.98-121, 1989.

220. Niki, E. and Kamiya, Y., Cage reactions of tert-butoxy radicals. *J. Am. Chem. Soc.*, 96(7), 2129-2133 (1974)

221. Noyes, R.M., Effects of Diffusion Rates on Chemical Kinetics, in *Progress in Reaction Kinetics* (G. Porter, Ed.), Vol.1, Pergamon Press, Oxford, 1961.

222. Robertson, E.R., Diffusion control in the polymerisations of methyl methacrylate and styrene. *Trans. Faraday Soc.*, **52**, 426-437 (1956)

223. De Schrijver, F. and Smets, G., Polymerisation kinetics in highly viscous media. *J. Polym. Sci.: Part A-1*, **4**, 2201-2210 (1966)

224. Stickler, M. and Dumont, E., *Makromol. Chem.*, **187**, 2663 (1986)

225. Solomon, D.H. and Moad, G., Initiation. The reaction of primary radicals. *Makromol. Chem. Macromol. Symp.*, **10/11**, 109-125 (1987)

226. Adams, M.E. et *al.*, *Makromol. Chem. Macromol. Symp.*, **35/36**, 1 (1990)

227. Brooks, B.W., Viscosity effects in the free-radical polymerisation of methyl methacrylate. *Proc. Roy. Soc. London. A*, **357**, 183-192 (1977)

228. Bevington, J.C., The sensitized polymerisation of styrene. The rate and efficiency of initiation. *Trans. Faraday Soc.*, **51**, 1392 (1955)

229. Biesenberger, J.A. and Sebastian, D.H., *Principles of Polymerisation Engineering*, Ch.3, pp. 298-326, John Wiley & Sons, New York, 1983.

230. Nauman, E.B., Mixing in polymer reactors. *Journal of Macromolecular Science - Reviews in Macromolecular Chemistry*, **C10**(1), 75-112 (1974)

231. Hatate, Y. et *al.*, A study of copolymerisation in a continuous stirred tank reactor. *J. Chem. Eng. Japan*, **4**(4), 348-354 (1971)

232. Harada, M. et *al.*, *J. Chem. Eng. Japan*, **29**, 301 (1965)

233. Harada, M. et *al.*, The effect of micromixing on the homogeneous polymerisation of styrene in a continuous flow reactor. *J. Chem. Eng. Japan*, **1**(2), 148-152 (1968)

234. Atiqullah, M. et *al.*, Influence of the gel-effect and mixing on the dynamics and rate parameters of bulk copolymerisation in a tubular reactor- theoretical analysis. *Chem. Eng. J.*, **48**, 71-81 (1992)

235. Denbigh, K., Continuous reactions. Part II. The kinetics of steady state polymerisation. *Trans. Faraday Soc.*, **43**, 648-660 (1947)

236. Sinnott, R.K., *Chemical Engineering, Vol. 6*, Ch.5, pp. 189, 2nd ed., Pergamon Press, Oxford, 1993.

237. Middleton, J.C., Applicability of high-intensity gas-liquid reactors to typical chemical processes, in *2nd International Conference on Process Intensification in Practice; Applications and Opportunities*, Antwerp, Belgium (1997)

Appendix A

Hydrodynamics of thin film flow

A1.1. NAVIER-STOKES EQUATION

A1.1.1. Flow down an inclined plane

The derivation of the modified Navier-Stokes equations for momentum transfer as applied to incompressible fluids of constant dynamic viscosity has been given in a number of standard textbooks [A1,A2]. The vector form of the equation using rectangular coordinates (x,y,z) can be expressed as:

$$\rho \frac{D\mathbf{v}}{Dt} = \mu \nabla^2 \mathbf{v} - \nabla p + \rho \mathbf{g} \qquad \text{(A1.1)}$$

where

$$\frac{D}{Dt} = \frac{\partial}{\partial t} + \mathbf{v}_x \frac{\partial}{\partial x} + \mathbf{v}_y \frac{\partial}{\partial y} + \mathbf{v}_z \frac{\partial}{\partial z}$$

$$\nabla = \mathbf{i} \frac{\partial}{\partial x} + \mathbf{j} \frac{\partial}{\partial y} + \mathbf{k} \frac{\partial}{\partial z}$$

$$\mathbf{v} = \mathbf{i} v_x + \mathbf{j} v_y + \mathbf{k} v_z$$

$$\mathbf{g} = \mathbf{i} g_x + \mathbf{j} g_y + \mathbf{k} g_z$$

$$\nabla^2 = \frac{\partial^2}{\partial x^2} + \frac{\partial^2}{\partial y^2} + \frac{\partial^2}{\partial z^2}$$

p: pressure
μ: dynamic viscosity
ρ: density

For flow down an inclined plane, the system is considered to be two-dimensional with x and z being the relevant coordinates in the direction of flow and normal to it respectively. Flow in the y-direction is negligible. The system representing flow down an inclined plane can be represented by Figure A1 below. Equation (A1.1) then reduces to:

$$\frac{\partial^2 v_x}{\partial z^2} = -\frac{\rho g}{\mu} \sin\theta \qquad \text{(A1.2)}$$

$$\frac{\partial p}{\partial z} = \rho g \cos\theta \qquad \text{(A1.3)}$$

$$\frac{\partial P}{\partial y} = 0 \qquad \text{(A1.4)}$$

The equations can be solved by integration with the appropriate boundary conditions.

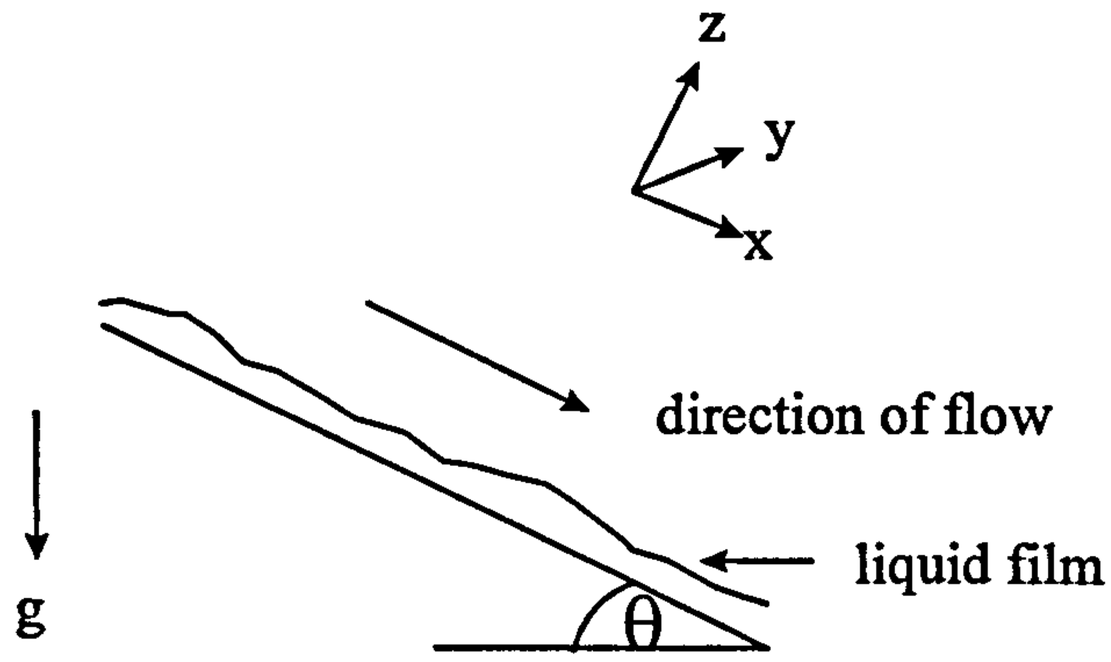

Figure A1. Flow down an inclined plane

A1.1.2. Flow on a rotating disc

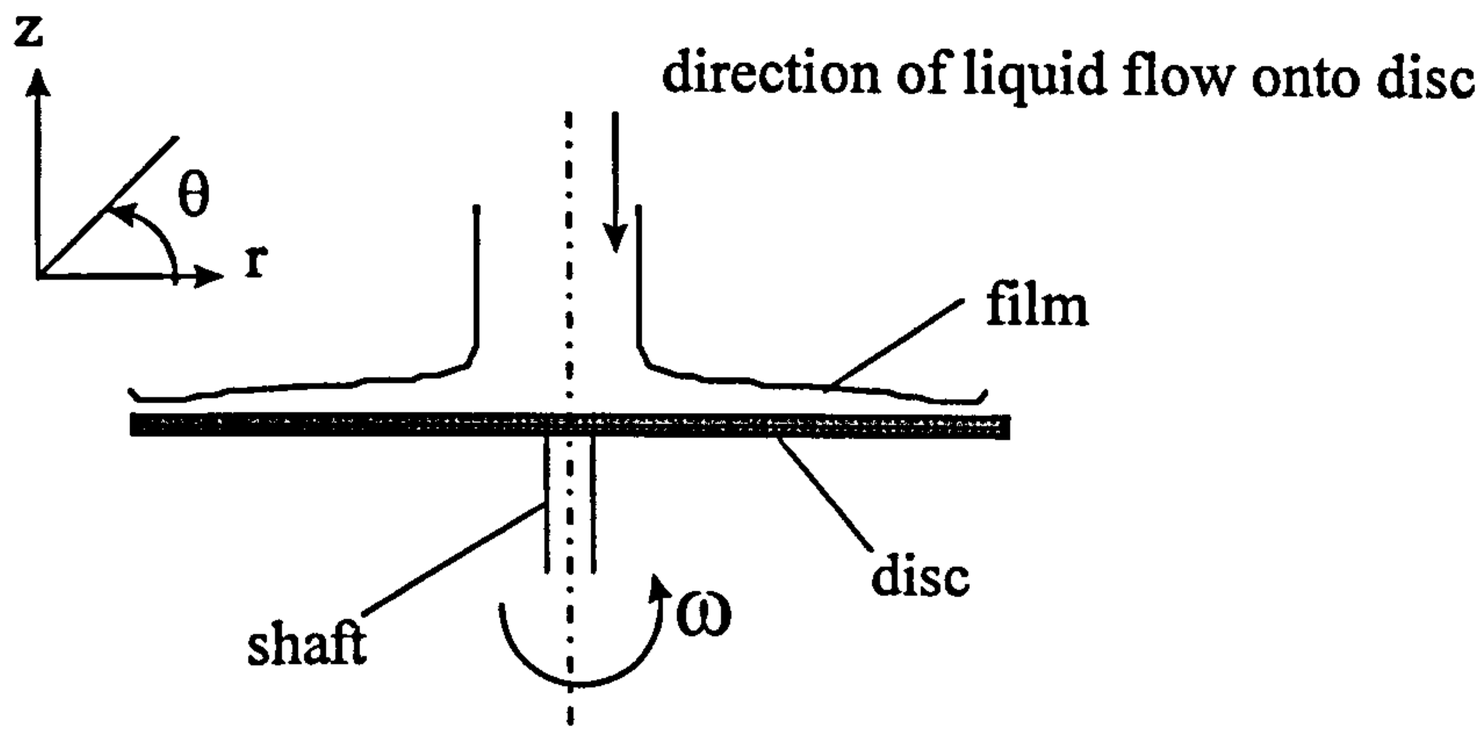

Figure A2. Thin film flow on a rotating disc

Flow on a horizontal smooth disc rotating about a vertical axis (Figure A2) can be more appropriately represented by considering vertical cylindrical coordinates (r, θ, z). The modified Navier-Stokes equation is then given by the following expressions:

In the radial direction, r

$$\rho \frac{Dv_r}{Dt} - \rho \frac{v_\theta^2}{r} = \mu\left(\nabla^2 v_r - \frac{v_r}{r^2} - \frac{2}{r^2}\frac{\partial v_\theta}{\partial \theta}\right) - \frac{\partial p}{\partial r} + \rho g_r \qquad \text{(A1.5)}$$

In the angular direction, θ:

$$\rho \frac{Dv_\theta}{Dt} - \rho \frac{v_\theta v_r}{r} = \mu\left(\nabla^2 v_\theta - \frac{v_\theta}{r^2} + \frac{2}{r^2}\frac{\partial v_r}{\partial \theta}\right) - \frac{1}{r}\frac{\partial p}{\partial \theta} + \rho g_\theta \qquad \text{(A1.6)}$$

In the vertical z- direction:

$$\rho \frac{Dv_z}{Dt} = \mu \nabla^2 v_z - \frac{\partial p}{\partial z} - \rho g_z \qquad \text{(A1.7)}$$

where

$$\frac{D}{Dt} = \frac{\partial}{\partial t} + v_r \frac{\partial}{\partial r} + v_\theta \frac{\partial}{\partial \theta} + v_z \frac{\partial}{\partial z}$$

$$\nabla^2 = \frac{\partial^2}{\partial r^2} + \frac{1}{r}\frac{\partial}{\partial r} + \frac{1}{r^2}\frac{\partial^2}{\partial \theta^2} + \frac{\partial^2}{\partial z^2}$$

The equation governing the conservation of mass also termed the continuity equation must also be satisfied for the flow system and it is given by:

$$\frac{\partial \rho}{\partial t} + \nabla . (\rho \mathbf{v}) = 0 \qquad \text{(A1.8)}$$

Equation (A1.8) can be expressed for the horizontal rotating disc system as [A1]:

$$\frac{\partial \rho}{\partial t} + \frac{1}{r}\frac{\partial}{\partial r}(\rho r v_r) + \frac{1}{r}\frac{\partial}{\partial \theta}(\rho v_\theta) + \frac{\partial}{\partial z}(\rho v_z) = 0 \qquad \text{(A1.9)}$$

Considering an incompressible fluid where the density ρ is constant, equation (A1.9) can be further simplified to give:

$$\frac{1}{r}\frac{\partial}{\partial r}(r v_r) + \frac{1}{r}\frac{\partial v_\theta}{\partial \theta} + \frac{\partial v_z}{\partial z} = 0 \qquad \text{(A1.10)}$$

or, on expansion,

$$\frac{\partial v_r}{\partial r} + \frac{v_r}{r} + \frac{1}{r}\frac{\partial v_\theta}{\partial \theta} + \frac{\partial v_z}{\partial z} = 0 \qquad \text{(A1.11)}$$

Therefore, fluid flow in a rotating system is fully defined by equations (A1.5), (A1.6), (A1.7) and (A1.11).

The general Navier-Stokes equations (A1.5), (A1.6), (A1.7) have been simplified by a number of workers to obtain an adequate model describing the flow on the rotating disc [A3-A5]. The following assumptions have been considered in their analysis:

1. The flow of liquid in any direction on the disc is steady so that

$$\frac{\partial v_r}{\partial t} = 0 \;, \frac{\partial v_\theta}{\partial t} = 0 \;, \frac{\partial v_z}{\partial t} = 0$$

2. The influence of gravity, surface tension and interfacial shear with the surrounding medium are not important which means that the terms involving the g components disappear.
3. The pressure is everywhere constant.
4. Since the flow is symmetric about the axis of rotation, there is no variation of velocity in the angular direction [A4] $\left(\frac{\partial v_r}{\partial \theta} = 0\,,\ \frac{\partial v_\theta}{\partial \theta} = 0\,,\ \frac{\partial v_z}{\partial \theta} = 0\right)$.
5. Since the film thickness δ is much smaller than the corresponding radius r, it can be assumed that $v_z << v_r$ or v_θ and $\frac{\partial}{\partial z} >> \frac{\partial}{\partial r}$ [A4, A6].

The simplified set of Navier-Stokes equations obtained on implementation of the above assumptions can be expressed as:

$$-\frac{v_\theta^2}{r} = \nu \frac{\partial^2 v_r}{\partial z^2} \qquad \text{(A1.12)}$$

$$v_r \frac{\partial v_\theta}{\partial r} + \frac{v_\theta v_r}{r} = \nu \frac{\partial^2 v_\theta}{\partial z^2} \qquad \text{(A1.13)}$$

where ν is the kinematic viscosity

The development of the different models based on these equations will be discussed below.

A2.1. CENTRIFUGAL MODEL

Emslie and co-workers [A3] have described the hydrodynamics of thin film flow on a smooth disc by means of a simple balance between the centrifugal force and the opposing viscous forces in the radial direction:

$$-\frac{v_\theta^2}{r} = \nu \frac{\partial^2 v_r}{\partial z^2} \qquad \text{(A1.14)}$$

The following considerations are inherent in the development of the centrifugal model represented by equation (A1.14):

1. The radial velocity component, v_r, is negligibly small compared to the angular velocity v_θ.
2. The angular rate of rotation of the liquid is equal to the rate of rotation of the disc at all radii so that $v_\theta = r\omega$.

Substituting for $v_\theta = r\omega$, where ω is the angular velocity, equation (A1.14) becomes:

$$-\omega^2 r = \nu \frac{\partial^2 v_r}{\partial z^2} \qquad \text{(A1.15)}$$

A2.1.1. Velocity profile

The radial velocity profile across the thin film on the rotating disc can be obtained by integration of equation (A1.15) subject to the boundary conditions:

at $z = 0$ $\quad v_r = 0$ (condition of 'no slip' at the disc surface)

at $z = \delta \dfrac{\partial v_r}{\partial z} = 0$ (condition of zero shear at the free surface of the film)

Thus,

$$v_r = \frac{\omega^2 r}{\nu}(\delta z - \frac{z^2}{2}) \qquad \text{(A1.16)}$$

where δ is the thickness of the film

Equation (A1.16) predicts that the radial velocity follows a parabolic path across the film thickness with maximum velocity at the free surface at a given radius.

A2.1.2. Film thickness

Using the result for the velocity distribution in the film, the average radial film velocity can be computed as:

$$\bar{v}_r = \frac{1}{\delta}\int_0^{\delta} v_r dz = \frac{\omega^2 r \delta^2}{3\nu} \qquad \text{(A1.17)}$$

The average film velocity can also be expressed in terms of the volumetric flowrate Q per unit area of cross-section available for flow:

$$\bar{v}_r = \frac{Q}{2\pi r \delta} \qquad \text{(A1.18)}$$

An expression for the film thickness as a function of the system parameters is then formulated by equating equations (A1.17) and (A1.18):

$$\frac{Q}{2\pi r \delta} = \frac{\omega^2 r \delta^2}{3\nu}$$

which, on rearrangement, yields:

$$\delta = \left(\frac{3}{2\pi}\frac{\nu Q}{\omega^2 r^2}\right)^{1/3} \qquad \text{(A1.19)}$$

Putting $\mathrm{Re} = \dfrac{2\,Q}{\pi\,\nu\,r}$, the film thickness can also be written in the form [A7]:

$$\delta \left(\frac{r\,\omega^2}{\nu^2}\right)^{1/3} = 0.909\,\mathrm{Re}^{1/3} \qquad \text{(A1.20)}$$

The above expression is analogous to the derivation obtained based on Nusselt's theory [A8] for fully developed laminar flow down inclined surfaces with the acceleration due to gravity g having been replaced by the centrifugal acceleration $r\omega^2$. Nusselt's equation can be expressed as [A7]:

$$\delta \left(\frac{g}{\nu^2}\right)^{1/3} = 0.909\,\mathrm{Re}^{1/3} \qquad \text{(A1.21)}$$

A2.1.3. Mean residence time

The mean residence time of the film between two radial positions on the disc can be calculated from equation (A1.17). Thus:

$$\bar{v}_r = \frac{dr}{dt} = \frac{\omega^2 r \delta^2}{3\,\nu}$$

Substituting for δ from equation (A1.19), we have, after simplification:

$$\frac{dr}{dt} = \left(\frac{\omega^2\,Q^2}{12\,\pi^2\,\nu}\right)^{1/3} r^{-1/3} \qquad \text{(A1.22)}$$

This equation is integrated within the limits given below:

$$t = 0,\ r = r_i$$
$$t = t_{res},\ r = r_o$$

where r_i is the radial distance of the inlet from the centre of the disc
r_o is the radius at exit

The resulting expression for the residence time t_{res} is then obtained as:

$$t_{res} = \left(\frac{81\,\pi^2\,\nu}{16\,\omega^2\,Q^2}\right)^{1/3} \left(r_o^{4/3} - r_i^{4/3}\right) \qquad \text{(A1.23)}$$

The centrifugal model is the simplest formulation of the Navier-Stokes equation. Its validity is strongly dependent on many assumptions which do not hold true for some

systems. In such cases, alternative models such as the Coriolis model and other more general models [A6] have to be applied.

A3.1. CORIOLIS MODEL

The centrifugal model is based on negligible radial velocity, v_r, which allows what is referred to as the "Coriolis acceleration" to be disregarded since:

$$a_{Cor} = 2v_r\omega \qquad \text{(A1.24)}$$

where a_{Cor} is the Coriolis acceleration

The Coriolis model has been formulated to give a more rigorous description of film flow where the radial velocity component is taken into account. From equation (A1.24), it then follows that a force acts on the film in an azimuthal direction opposite to the direction of disc rotation. As a result, the fluid velocity in the angular direction is lower than that for the disc. Taking the Coriolis effect into consideration, Bell [A9] and other subsequent researchers [A6,A10,A11] have used equations (A1.13) and (A1.14) in their analysis:

$$-\frac{v_\theta^2}{r} = \nu\frac{\partial^2 v_r}{\partial z^2} \qquad \text{(A1.13)}$$

$$\frac{v_\theta v_r}{r} + v_r\frac{\partial v_\theta}{\partial r} = \nu\frac{\partial^2 v_\theta}{\partial z^2} \qquad \text{(A1.14)}$$

Replacing v_θ by $r\omega$ on the left-hand side allows the above equations to be transformed into:

$$-\omega^2 r = \nu\frac{\partial^2 v_r}{\partial z^2} \qquad \text{(A1.25)}$$

$$2v_r\omega = \nu\frac{\partial^2 v_\theta}{\partial z^2} \qquad \text{(A1.26)}$$

which have been solved by Bell [A9] and Lim [A6] to obtain a velocity profile for v_θ in terms of the radial position r and the upward vertical distance z.

Emslie et al [A3] have stipulated that the Coriolis effect can be ignored if the condition below is satisfied:

$$2v_r\omega << \omega^2 r \qquad \text{(A1.27)}$$

or, after rearranging:

$$v_r << \omega r/2 \qquad \text{(A1.28)}$$

The maximum value of the radial velocity occurs at the free surface of the film. Putting $z = \delta$ in equation (A1.16), we have:

$$v_{r(max)} = \frac{r\omega^2\delta^2}{\nu} \qquad \text{(A1.29)}$$

Hence, substituting for $v_{r(max)}$ in inequality (A1.28), the condition is of the form:

$$\nu >> \omega\delta^2 \qquad \text{(A1.30)}$$

Therefore, the applicability of the much simplified centrifugal model (where the Coriolis effect is taken to be negligible) is limited to relatively thin films of high viscosity fluids at a given angular velocity.

A4.1. GENERAL MODELS

Several other models have also been proposed [A12-A15] to include inertial and gravitational effects on the film flowing on a rotating disc. Interested readers should consult the above mentioned references for an in-depth discussion of these models.

For the purpose of this current investigation, it will suffice to mention that that inertia, gravity and indeed Coriolis acceleration were found to have any significant effect on the thin film flow behaviour only at relatively small distances from the discharge point of the fluid on the disc [A12, A16]. Therefore, the simple centrifugal model is adequate to describe the flow on a fairly large disc.

A5.1. NON-NEWTONIAN FLOW MODELS

Jazayeri [A10] reported the development of a centrifugal model by Zinnatulin [A17] for non-Newtonian power law fluids. The author used a power law equation as an approximation to the rheological properties of non-Newtonian fluids:

$$\tau = K\left(\frac{\partial v_r}{\partial z}\right)\left(\frac{\partial v_r}{\partial z}\right)^{n-1} \qquad \text{(A1.31)}$$

where τ is the shear stress

$\frac{\partial v_r}{\partial z}$ is known as the velocity gradient, often referred to as the shear rate γ

K, n are the characteristic parameters of the fluid

The equation of motion of the thin film is again described by equation (A1.15) for the case of the centrifugal model which may be transformed to take into account the non-Newtonian nature of the fluid:

$$\frac{\partial \tau}{\partial z} = -\omega^2 r \qquad \text{(A1.32)}$$

Substituting for τ from (A1.31) in (A1.32) gives:

$$\frac{K}{\rho}\frac{\partial}{\partial z}\left(\left(\frac{\partial v_r}{\partial z}\right)^{n-1}\left(\frac{\partial v_r}{\partial z}\right)\right) = -\omega^2 r \qquad \text{(A1.33)}$$

A5.1.1. Velocity profile

Integration of the above equation subject to the boundary conditions:

$$\text{at } z = 0 \qquad v_r = 0$$

$$\text{at } z = \delta \qquad \frac{\partial v_r}{\partial z} = 0$$

yields an expression for the radial velocity distribution:

$$v_r = \frac{n}{n+1}\left(\frac{\rho}{K}\omega^2 r\right)^{1/n}\left(\delta^{\frac{n+1}{n}} - (\delta - z)^{\frac{n+1}{n}}\right) \qquad \text{(A1.34)}$$

A5.1.2. Film thickness

The average radial velocity is obtained by substituting equation (A1.34) into (A1.17) and carrying out the integration between limits of $z = 0$ and $z = \delta$:

$$\bar{v}_r = \frac{n}{2n+1}\left(\frac{\rho\omega^2 r}{K}\right)^{1/n}\delta^{\frac{n+1}{n}} \qquad \text{(A1.35)}$$

Also, as before,

$$\bar{v}_r = \frac{Q}{2\pi r\delta} \qquad \text{(A1.18)}$$

Equating (A1.35) and (A1.18), we get the film thickness δ as:

$$\delta = \left(\frac{1+2n}{2\pi n}\right)^{\frac{n}{1+2n}}\left(\frac{Q}{r}\left[\frac{K}{\rho\omega^2 r}\right]^{1/n}\right)^{\frac{n}{1+2n}} \qquad \text{(A1.36)}$$

It should be noted that for n=1 and K=μ, equations (A1.33) to (A1.36) become equal to those derived using the centrifugal model for the Newtonian fluids.

Model equations describing non-Newtonian flow using the Coriolis model originally developed by Zinnatulin [A17] were also presented in Jazyeri's work [A10].

However since the centrifugal model for non-Newtonian flow is deemed suitable to predict the flow characteristics for the purpose of this present investigation, details of the Coriolis model for non-Newtonian flow will not be considered.

References

A1. Holland, F.A., *Fluid Flow for Chemical Engineers*, Ch.12, pp.203-221, Edward Arnold, London, 1973.

A2. Bird, R.B., Stewart, W.E., Lightfoot, E.N., *Transport Phenomena*, John Wiley & Sons, New York, 1960.

A3. Emslie, A.G. et *al.*, Flow of a viscous liquid on a rotating disk. *J. Appl. Phys.*, **29**(5), 858-862 (1958)

A4. Rahman, M.M. and Faghri, A., Analysis of heating and evaporation from a liquid film adjacent to a horizontal rotating disc. *Int. J. Heat Mass Transfer*, **35**(10), 2655-2664 (1992)

A5. Acrivos, A. et *al.*, On the flow of a non-Newtonian liquid on a rotating disk. *J. Appl. Phys.*, **31**(6), 963-968 (1960)

A6. Lim, S.T., Hydrodynamics and mass transfer processes associated with the absorption of oxygen in liquid films flowing across a rotating disc, *Ph.D. Thesis,* University of Newcastle Upon Tyne (1980)

A7. Epsig, H. and Hoyle, R., Waves in a thin liquid layer on a rotating disc. *J. Fluid Mech.*, **22**(4), 671-677 (1965).

A8. Nusselt, *Ver. Deut. Ingr Z.*, **60**, 549, 569 (1916)

A9. Bell, C., The hydrodynamics and heat transfer characteristics of liquid films on a rotating disc, *Ph.D. Thesis,* University of Newcastle Upon Tyne (1975)

A10. Jazayeri, A., The hydrodynamics of Newtonian and non-Newtonian liquid films flowing across a rotating disc, *Ph.D. Thesis,* University of Newcastle Upon Tyne (1980)

A11. Woods, W., The hydrodynamics of thin liquid films flowing over a rotating disc, *Ph.D. Thesis,* University of Newcastle Upon Tyne (1995)

A12. Venkataraman, R.S., Mass transfer to an expanding surface, *Ph.D. Thesis,* Leeds University (1966)

A13. Marshall, W.R. (Jr.) and Seltzer, E., Principles of spray drying. *Chem. Eng. Prog.*, **46**, 501, 575 (1950)

A14. Marshall, W.R. (Jr.) and Adler, C.R., Performance of spinning disc atomisers. Part I and II. *Chem. Eng. Prog.*, **47**(10), 515, 601-608 (1951)

A15. Rauscher, J.W. *et al.*, An aymptotic solution for the laminar flow of a thin liquid film on a rotating disc. *ASME J. Appl. Mechanics*, **40**, 43-47 (1975)

A16. Dixon, B.E. et *al.*, Liquid films formed by means of rotating disks. *Brit. J. Appl. Phys.*, **3**, 115-119 (1952)

A17. Zinnatullin, N.K. *et al.*, The two-dimensional flow of a non-Newtonian fluid over the open surface of a rapidly rotating flat disc. *J. Eng. Physics*, **15**, 701-704 (1968)

Appendix B

Heat transfer calculations on disc surface

The heat balance on a thin liquid film flowing outwards from the centre across a rotating disc can be obtained by considering the heat exchange from the heated disc to a small annular element of fluid of width dr at a radial distance r from the centre of the rotating disc as illustrated in the schematic diagram below in Figure B1.

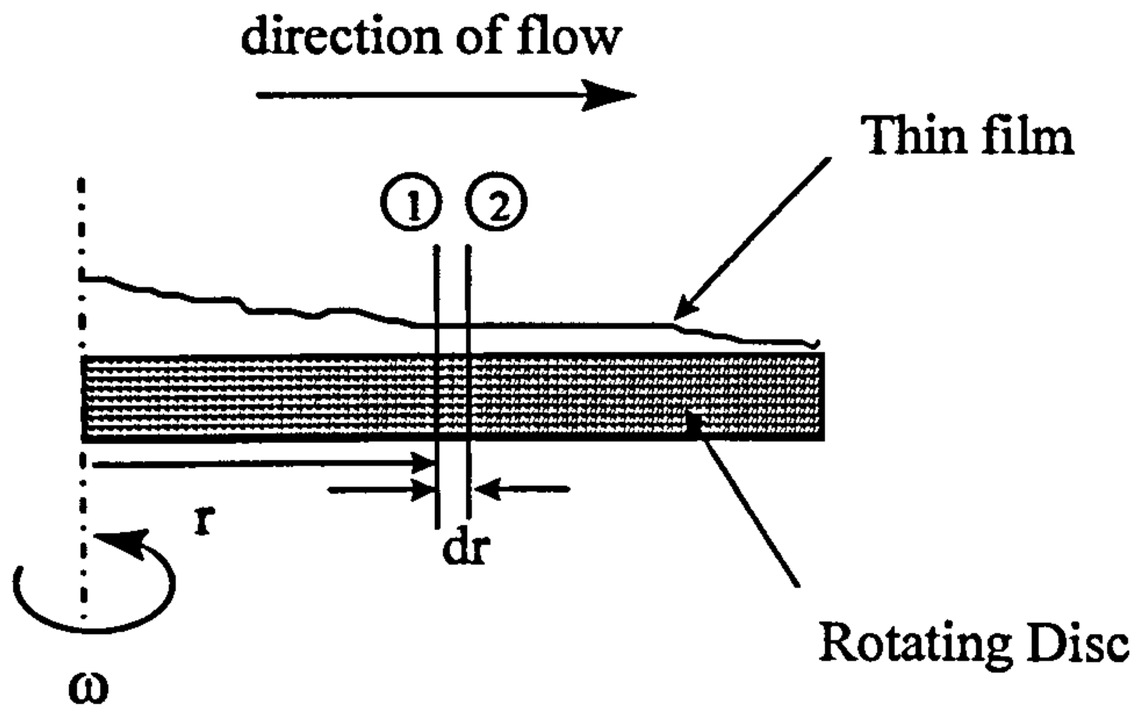

Figure B1. Heat balance on small element of fluid

A simple heat balance on the fluid element between sections 1 and 2 is given by:

$$\text{Rate of heat change} = \text{Heat out} - \text{Heat in}$$

$$Qc_p dT = [\pi(r+dr)^2 h(T_D - T)] - \pi r^2 h(T_D - T)] \qquad \text{(B1.1)}$$

or, in simplified form,

$$Qc_p dT = 2\pi r dr\, h\,(T_D - T) \qquad \text{(B1.2)}$$

where Q = liquid mass flowrate
c_p = specific heat capacity of fluid
T = liquid film temperature
T_D= disc temperature (assumed constant)
r = radial distance from centre of disc
h = disc surface film heat coefficient

The derivation of the above equation is subject to the following simplifying assumptions:

1. Heat transfer occurs mainly by convection from the disc surface to the liquid film in a direction perpendicular to the plane surface of the disc.
2. The thickness of the film is considered to be so small and mixing within the film is so intense that temperature variations across the height of the film are assumed to be negligible. Only temperature differences in the radial direction are significant.

The boundary conditions applicable in this case are as follows:

at $r = r_i$, $T = T_i$

and at $r = r_o$, $T = T_o$

where r_i = inner radial feed point
r_o = outlet disc radius
T_i = inlet film temperature
T_o = outlet film temperature

Integration of equation (B1.2) within the above set of integral limits yields:

$$\frac{\pi h}{Qc_p}(r_o^2 - r_i^2) = \ln\left(\frac{T_D - T_i}{T_D - T_o}\right) \qquad \text{(B1.3)}$$

After rearrangement, equation (B1.3) can be expressed as:

$$T_o = T_D - \frac{(T_D - T_i)}{\exp\left\{\frac{\pi h}{Qc_p}(r_o^2 - r_i^2)\right\}} \qquad \text{(B1.4)}$$

Previous heat transfer work on the spinning disc has shown that an average film heat transfer coefficient as high as 10 kW/m^2K can be achieved along the rotating surface [B1].

For the case of styrene polymerisation with an average flow of 10 cc/s for a 30% converted prepolymer feed, the following properties and conditions are applicable for the system considered in this research:

$\rho = 892\ kg/m^3$ (see Appendix G for density calculation)
$Q = 10 \times 10^{-6} \times 892 = 0.00892\ kg/s$
$r_i = 0.05\ m$
$r_o = 0.36\ m$
$T_i = 60°C$ (assumed)
$T_D = 90°C$

Substitution of the above values in equation (B1.4) gives the final film temperature exiting the edge of the disc as 90°C.

This implies that the film quickly reaches the temperature of the disc over which it is flowing as a result of the enhanced heat transfer from the disc surface to the liquid film. It is interesting to see the gradual increase in film temperature across the disc radius. The results of the Excel computations are shown in Table B1 below.

Table B1. Change in film temperature across rotating disc

Disc temperature temperature T_D (°C)	Inlet feed temperature T_i (°C)	Radius of inlet r_i (m)	Radius of outlet r_o(m)	Outlet film T_o (°C)
90	60	0.025	0.03	71.536
90	60	0.025	0.04	84.632
90	60	0.025	0.06	89.843
90	60	0.025	0.08	89.999
90	60	0.025	0.10	90.000
90	60	0.025	0.15	90.000
90	60	0.025	0.18	90.000

References

B1. Jachuck, R.J. and Ramshaw, C., Process Intensification: Heat transfer characteristics of tailored rotating surfaces. *Heat Recovery Systems & CHP*, **14**(5), 475-491 (1994)

Appendix C

Calculations for evaporation from spinning disc surface

C1. INTRODUCTION

The previous use of the spinning disc surface as an efficient evaporator raised some important concerns in the present investigation. The measurement of conversion of the disc product was based on the relative amounts of styrene and polystyrene in the collected sample and hence was directly affected by any monomer loss which might have taken place. It was therefore necessary to check whether any significant loss of styrene and toluene by evaporation from the rotating disc was taking place. Experiments were carried out to monitor the amount of styrene relative to o-xylene in the product collected from the disc and in the vapour space above the disc surface in order to assess the extent of styrene loss by evaporation. Based on the results of these experiments, a theoretical quantification which gave a conservative estimate of the loss of both styrene and toluene was performed. This was adjusted for in the extensive experimental data gathered for the polymerisation of styrene in the Spinning Disc Reactor.

C1.1. EXPERIMENTAL EVALUATION

An assessment of the loss of styrene by evaporation from the disc was only possible if the styrene loss was measured against the loss of a compound acting as a 'marker'. The conditions to be satisfied for an effective marker were:

1. Similar volatility as styrene
2. Non-reactive with toluene, styrene or polystyrene
3. Easily separable from styrene and toluene in a suitable gas chromatography column

O-xylene was chosen based on its boiling point of 144.4°C which is very close to the boiling point of styrene (145.1°C), its chemical inertness and its complete separation from styrene using a 0.25μ DB-WAX coated fused silica capillary column.

C1.1.1. Methodology

The underlying principle in assessing whether evaporation of styrene from the disc occurred to any significant extent was based on a comparison of the mass ratio of styrene to o-xylene in product collected from the rotating disc with the ratio in the feed to the disc. The results of this comparison led to further analysis of the mass ratio of the two components in the vapour space above the disc.

Starting from a given recipe in the batch and assuming that styrene is consumed solely in polymerisation in the batch and that no o-xylene is lost from the batch, then the ratio of styrene to o-xylene should decrease in a continuous manner

from the start of the reaction in the batch up to the time of feeding onto the disc. If evaporation of styrene rather than polymerisation is taking place from the disc, then it is expected that the mass ratio of styrene to o-xylene in the disc product should be the same as that in the feed since both components, having similar volatility, would evaporate in similar proportion as they exist in solution (Raoult's Law). If on the other hand styrene remains in solution and some of it polymerises while the extent of o-xylene evaporation is unchanged, then their mass ratio in the SDR product would be increased.

In order to confirm the results from the SDR product samples, it is also important to directly evaluate the mass ratio of styrene to o-xylene in the vapour phase. A ratio similar to the mass ratio in the feed would indicate that evaporation is taking place according to Raoult's Law while a very small ratio would suggest that negligible amounts of styrene is lost through evaporation. Furthermore, from the experimentally determined concentration of each of the individual components in the vapour space of the SDR, the partial pressure of each component in the mixture can be deduced and this may yield important information about the vapour saturation in the SDR.

C1.1.2. Experimental Set-up

The experiments were carried in the same set-up as described in section 4.1 in Chapter 4. A slight modification was put in place for collection of the vapour from the enclosure volume of the spinning disc reactor. The components added to the overall set-up arrangement are shown schematically in Figure C1 below.

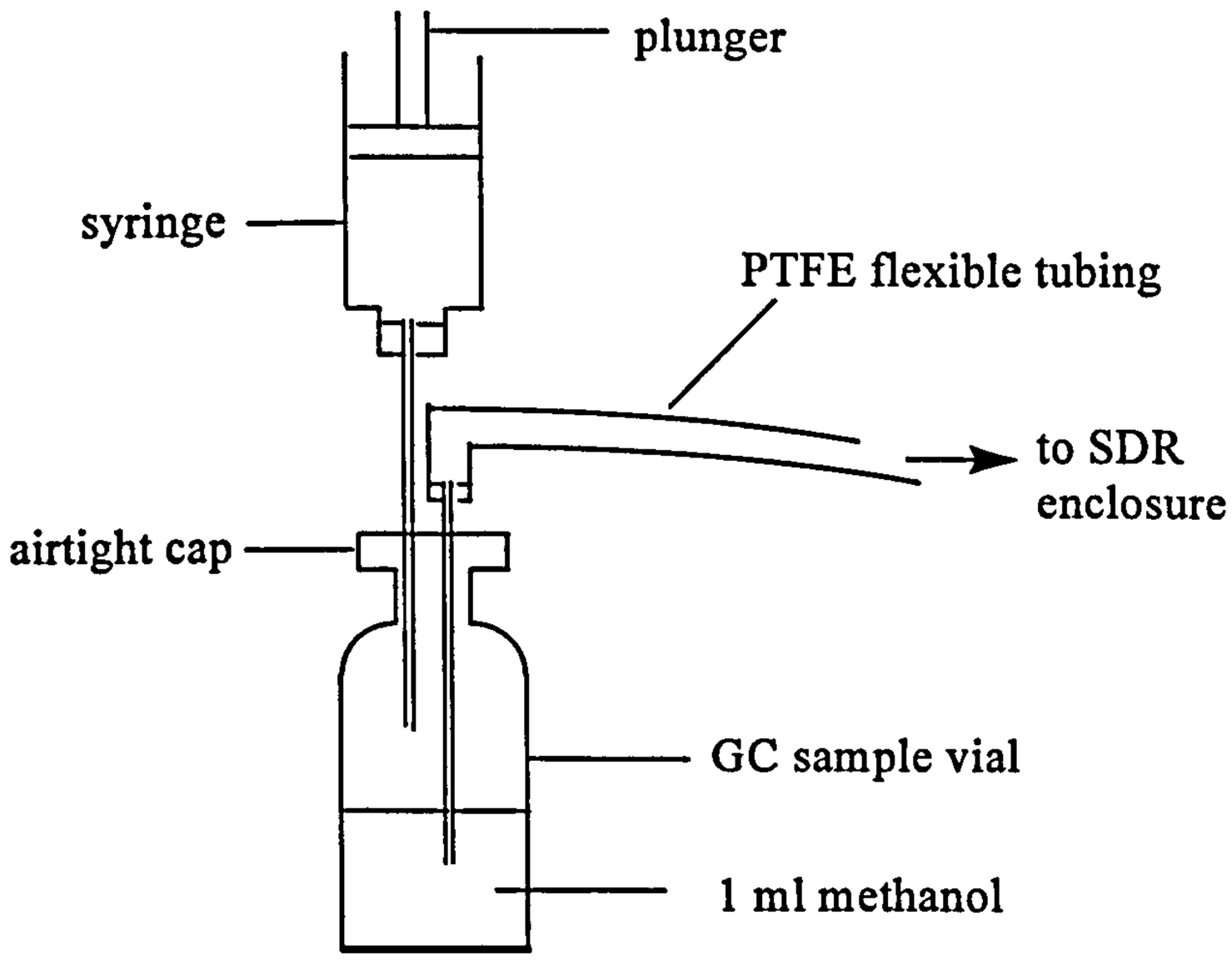

Figure C1. Set-up for SDR vapour collection

The set-up consisted of a vial containing 1 ml of methanol in which a hollow syringe needle at the end of a length of flexible PTFE tubing was dipped. The other end of the tubing was placed inside the SDR housing. The needle from a 100 ml

syringe was also located inside the vial in the air space above the level of methanol as shown in Figure C1 above.

C1.1.3. Experimental Procedure

Four disc runs were performed, two of which (Runs 1 and 2) were aimed at collecting SDR product samples while the other two (Runs 3 and 4) were conducted to collect vapour samples from above the rotating disc. The procedures for the prepolymer feed preparation and disc runs were essentially the same as that used in the normal disc runs as described in section 4.1.3.2, Chapter 4 except for a change in starting recipe. The recipe used in the runs was as follows: 200 ml styrene, 20 ml toluene and 20 ml o-xylene and 3.0g benzoyl peroxide (BPO) initiator. In order to check that the presence of o-xylene did not have any major effect on the progress of polymerisation, samples were collected at regular intervals of time during the course of the batch reaction for Runs 1 and 2. Two to three disc product samples were also collected for Runs 1 and 2.

A simple procedure for collecting vapour samples in Runs 3 and 4 was employed. Soon after the feed was poured down the distributor tubes of the SDR, the plunger of the syringe shown in Figure C1 was pulled upwards until the 100 ml mark was reached. As the air was sucked out of the vial, vapour from the SDR enclosure was thus bubbled through and dissolved in the methanol.

C1.1.4. Sample Preparation and Analysis

Part of the samples from Runs 1 and 2 were prepared for GPC analysis in the same way as described in section 4.3.2.2 in Chapter 4. The rest of the samples from these two runs were prepared for gas chromatography (GC) analysis for which the procedure will be outlined in this section. Vapour samples from Runs 3 and 4 as collected by the procedure given in the previous section did not require further preparation before GC analysis.

Before injection into the GC capillary column, the feed and product samples from Runs 1 and 2 were mixed with methanol to precipitate out all polymer present. After it was ensured that the remaining solutions were completely free of polystyrene, they were ready for injection into the GC. The size of sample injection was varied from 1 μl to 4 μl in order to obtained reasonably sized component peaks.

The column specifications and operating conditions used in the GC for an efficient separation of the individual components (methanol, styrene, o-xylene and toluene) were as follows:

Column: Fused Silica Capillary column, 30m x 0.25mm
Coating: DB-WAX, 0.25μ film
Temperature programme: 50°C (1 min), 75°C (4°C/min ramp) to 100°C (10°C/min)
Carrier gas and flowrate: Helium, 40.6 cm/s (= 1.14 ml/min)
Detector: FID, 250°C
Injection: Split (1:25), 225°C

C1.1.5. Calibration of GC column

Calibration of the GC capillary column for each of the components in the mixture was performed prior to the injection of samples collected from the polymerisation runs. Solutions of various known concentrations in g/ml of methanol, styrene, toluene and o-xylene were prepared and run through the GC and the area of the peaks obtained were matched with the given concentrations. A linear fit to the calibration data of each of the four components was appropriate. The coefficients of the linear fit for each component are shown in Table C1 below.

Table C1. Calibration data for styrene, toluene, o-xylene and methanol

Component	Retention time (minutes)	Coefficients for A+Bx A	B	Data fit to correlation
Methanol	2.232	0.00	9.186E-08	0.90765
Toluene	3.690	0.00	8.859E-08	0.94471
Styrene	6.547	0.00	4.174E-08	0.96063
O-xylene	8.336	0.00	4.121E-08	0.96471

C1.1.6. Experimental Results

GPC results

The conversion data from GPC for samples from the batch in Runs 1 and 2 are compared in Figure C2 with batch calibration data in which only styrene, toluene and BPO were used.

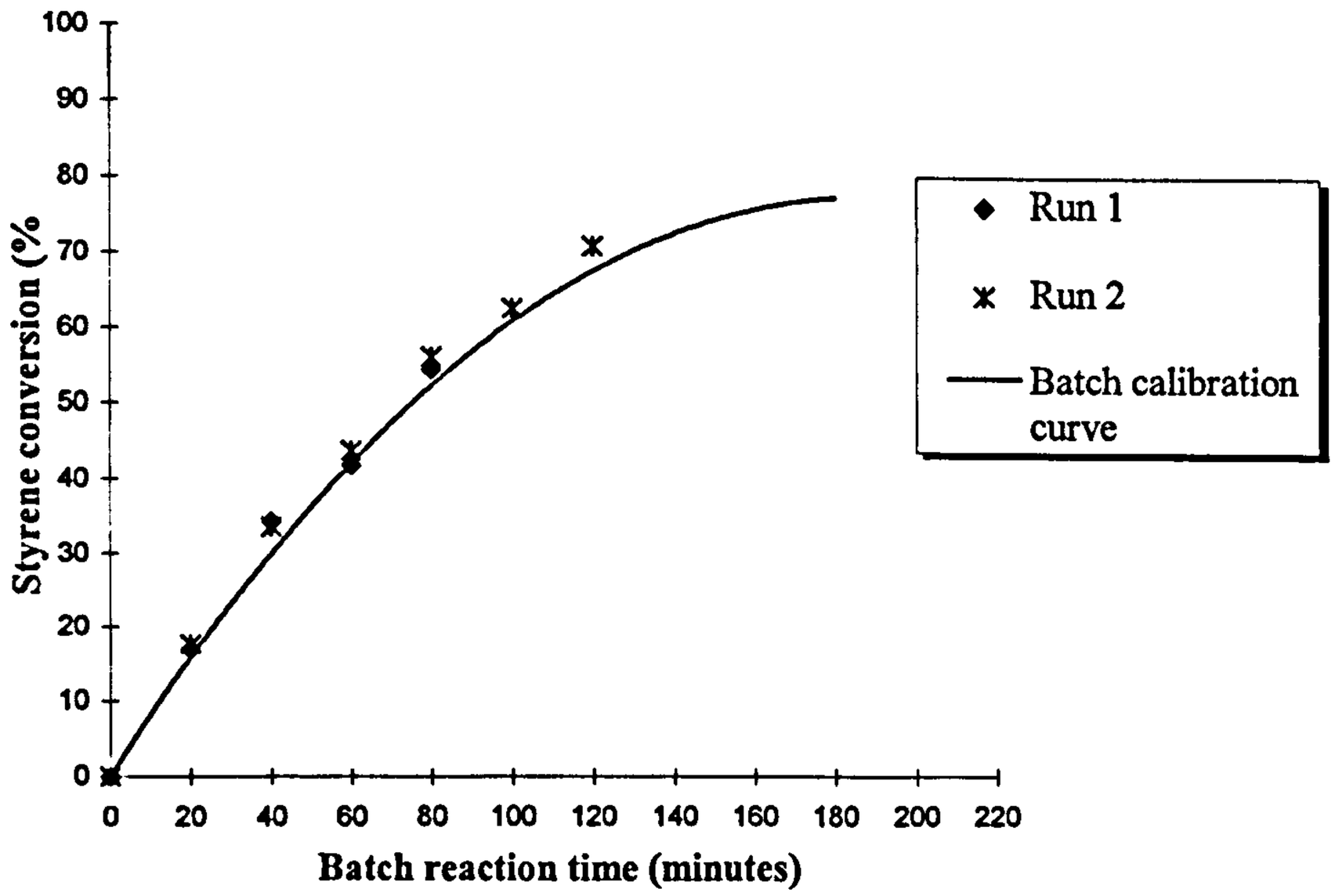

Figure C2. Effect of o-xylene marker on extent of polymerisation in batch reactor

The general indication from the above conversion results is that the presence of o-xylene has not affected the polymerisation kinetics. Thus, as seen in Figure C2

above, the progression in polymerisation in Runs 1 and 2 is in close agreement with the calibration curve for batch runs employing styrene, toluene and BPO as the starting reagents.

GC results

Typical peaks and retention times obtained from a GC run are shown in Figure C3. The mass ratio of styrene to o-xylene for all the samples analysed was calculated from the concentration data generated by peaks in the GC chromatograms. Hence,

$$\text{Mass ratio S:X} = \frac{\text{Styrene concentration (g / ml)}}{\text{O - xylene concentration (g / ml)}} \qquad \text{(C1.1)}$$

The data obtained for each of the four runs are presented below with the operating conditions corresponding to each.

Run 1

Recipe: 200 ml styrene, 20 ml toluene, 20 ml o-xylene, 3 g BPO
Prepolymer feed time: 80 minutes
Disc rotational speed: 850 rpm
Disc temperature: 89°C
Enclosure temperature before feeding: 43.3°C
Maximum enclosure temperature after feeding: 47.3°C

Batch reaction time (mins)	Sample	Styrene conc from GC (g/ml)	O-xylene conc. from GC (g/ml)	S:X ratio
40	M40	0.0526	0.0076	6.92
60	M60	0.1180	0.0205	5.76
80	M80	0.0444	0.0088	5.045
Disc product samples	MS1(1)	0.0075	0.0014	5.36
	MS1(2)	0.0059	0.0011	5.36
	MS2(1)	0.0288	0.0054	5.33
	MS2(2)	0.0367	0.0071	5.17

Note
MS1(2) and MS2(2) denote repeat GC runs of samples MS1 and MS2 respectively using fresh product samples.

Run 2

Recipe: 200 ml styrene, 20 ml toluene, 20 ml o-xylene, 3 g BPO
Prepolymer feed time: 120 minutes
Disc rotational speed: 850 rpm
Disc temperature: 89-90°C
Enclosure temperature before feeding: 41.3°C
Maximum enclosure temperature after feeding: 46.4°C

Batch reaction time (mins)	Sample	Styrene conc. from GC (g/ml)	O-xylene conc. from GC (g/ml)	S:X ratio
60	N60	0.0538	0.0092	5.84
80	N80	0.0589	0.0114	5.17
100	N100	0.0266	0.0063	4.22
120	N120	0.0179	0.0053	3.38
Disc product samples	NS1	0.0024	0.0005	4.8
	NS2(1)	0.0017	0.0004	4.25
	NS2(2)	0.0034	0.0008	4.25
	NS3	0.0050	0.0011	4.55

Run 3

Recipe: 200 ml styrene, 40 ml toluene, 3 g BPO
Prepolymer feed time: 90 minutes
Disc rotational speed: 850 rpm
Disc temperature: 88-90°C
Enclosure temperature before feeding: 36.2°C (top)
41.6°C (near disc surface)
Maximum enclosure temperature after feeding: 41.4°C (top part)
45.8°C (near disc surface)

Two vapour samples were collected from the disc enclosure volume and analysed in GC. But no styrene peak was detected in the GC chromatogram although a small toluene peak was obtained.

Run 4

Recipe: 200 ml styrene, 20 ml toluene, 20 ml o-xylene, 3 g BPO
Prepolymer feed time: 80 minutes
Disc rotational speed: 850 rpm
Disc temperature: 89-90°C
Enclosure temperature before feeding: 42.1°C
Maximum enclosure temperature after feeding: 46.6°C

Sample	Styrene conc. from GC (g/ml)	o-xylene conc. from GC (g/ml)	Toluene conc. from GC ratio (g/ml)	S:X
SDR Vapour Mix 1	0.0017	0.0004	0.0049	4.25
SDR Vapour Mix 2	0.0022	0.0006	0.0053	3.67

C1.1.7. Discussion

The results of Runs 1 and 2 clearly show a gradual decrease in the mass ratio of styrene to o-xylene in the batch samples up to the point of feeding. This is in accord with styrene being used up in polymerisation while the mass of o-xylene in the batch remains essentially unchanged. On the other hand, the mass ratio of the SDR products

```
***** MODEL 1020 RUNLOG for run: RUN___04 ******

End Time altered manually on Channel A.


File : RUN___04.D01              DISC PROD MS1(2)                    KAMELIA
Run  : 01                                                      Type : Sample
Path : C:\CHROM\KAMELIA\MARKER
Collection : 11:37:30 May 15 1997   Method : KAMCAP   [ 16:50:43 May 14 1997 ]
Integration: 11:37:30 May 15 1997   Method : KAMCAP   [ 16:50:43 May 14 1997 ]
Report     : 11:47:07 May 15 1997   Method : KAMCAP   [ 11:47:03 May 15 1997 ]

Sample Amt : 2.00000e+0    Dilution: 1.00000e+0

                        EXTERNAL STANDARD ( AREA )

   RT        Area  BC    ExpRT      RF                    g/ml    Name

  2.267    7715774 V     2.232  9.18642e-8                0.3544    METHANOL
  3.693     351760 V     3.689  3.85967e-8                0.0068    TOLUENE
  6.546     392673 V     6.546  4.17449e-8                0.0082    O-XYLENE
  8.400    2036237 V     8.336  4.12104e-8                0.0420    STYRENE
```

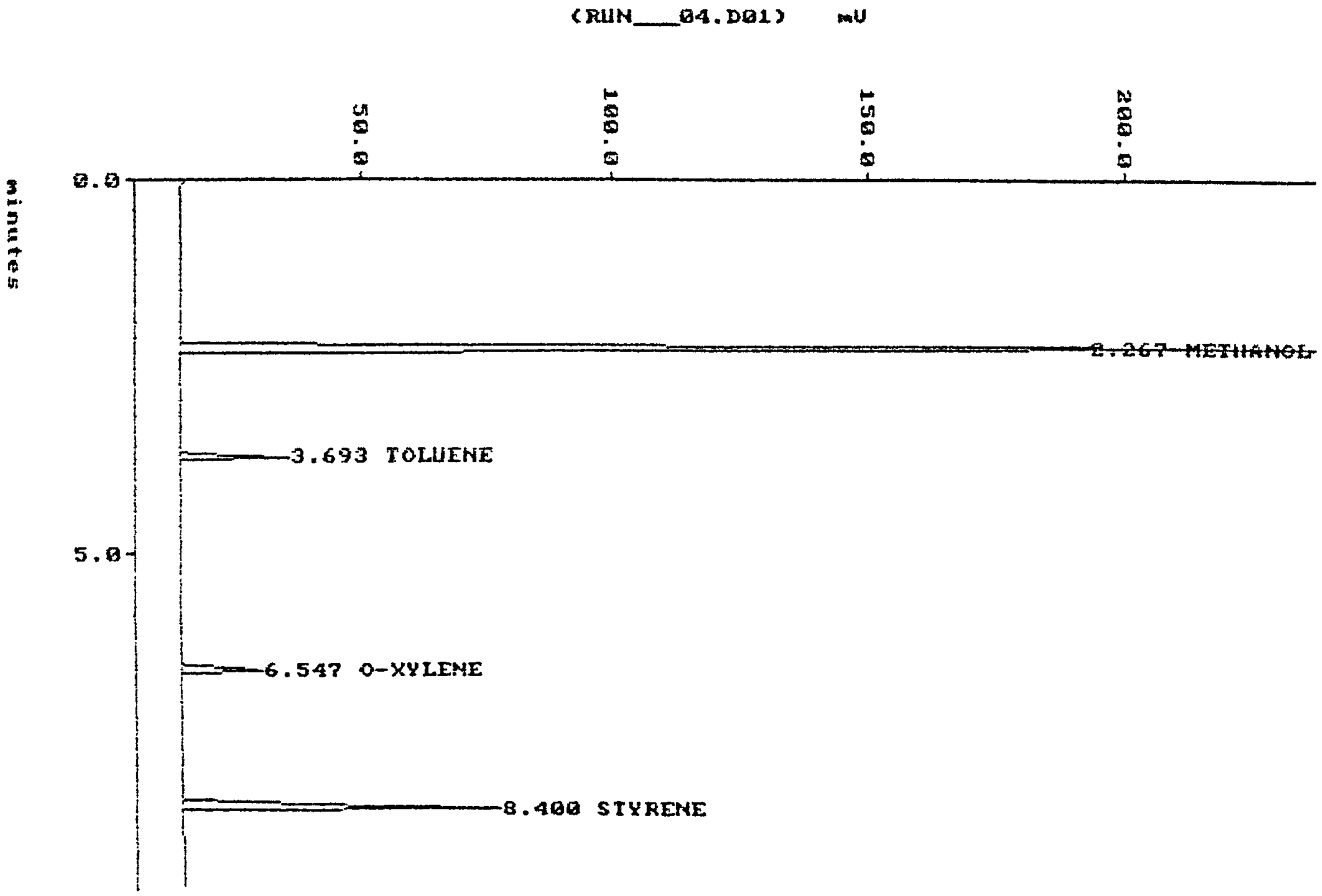

Figure C3. Peaks and results from a typical GC run

is increased in comparison to the ratio in the corresponding feed which is indicative of more o-xylene than styrene being lost by evaporation from the disc surface.

The data from Runs 3 and 4 show that styrene in the vapour is less giving a reduced mass ratio S:X than would be predicted on the basis of Raoult's law applied to the solution flowing on the disc. If Raoult's Law did hold, then S:X ratio in the vapour would be the same as the ratio in the feed which may be approximated by sample M80 in Run 1 (i.e. S:X ratio of 5.045) where the same operating conditions prevail.

The concentration data from Run 4 can be manipulated to deduce the partial pressure of the individual components in the vapour mixture. The calculations involved are outlined below.

Average concentration of:

styrene = (0.0017+0.0022)/2 = 0.00195 g/ml
o-xylene = (0.0004+0.0006)/2 = 0.0005 g/ml
toluene = (0.0049+0.0053)/2 = 0.0051 g/ml

Based on 100 ml of air sucked out by syringe and accounting for the volume of vapour (about 10 ml) remaining in length of PTFE tubing from enclosure volume to sample vial, the volume of vapour mixture bubbled through 1 ml methanol = 90 ml

Hence mass of each component in 90 ml of vapour mixture is:

styrene = 0.00195 g
o-xylene = 0.0005 g
toluene = 0.0051 g

The dimensions of the SDR enclosure are as given below, from which the total volume can be calculated as 60 litres.

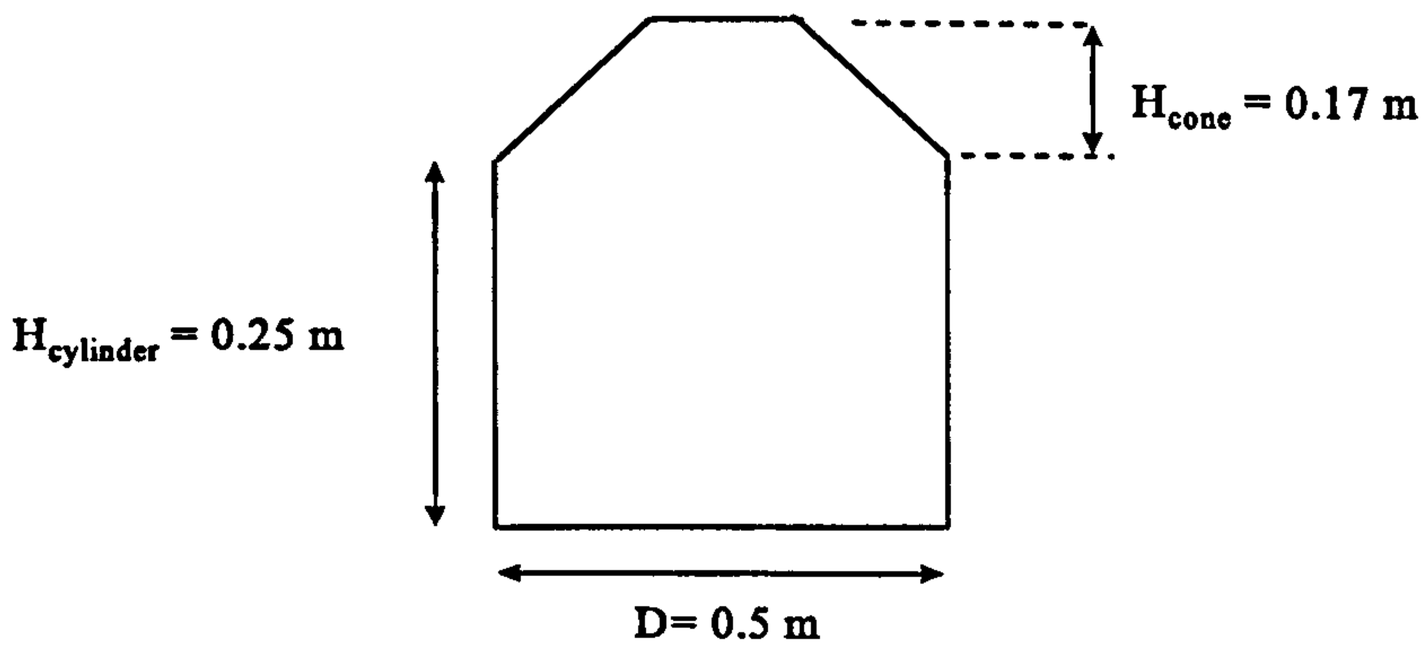

Thus the total mass of each component in the enclosed volume of the SDR is:

styrene = $0.00195/90 * 60*10^3 = 1.3$ g
o-xylene = $0.0005/90 *60*10^3 = 0.33$ g
toluene = $0.0051/90 *60*10^3 = 3.40$ g

With known molecular weights of 104, 106 and 92 g/mol for styrene, o-xylene and toluene respectively, the molar composition is evaluated to be:

styrene = 0.00125 moles
o-xylene = 0.00314 moles
toluene = 0.03696 moles

Appendix C

Repeated temperature measurements of the air/vapour mixture in the enclosure volume indicate that the temperature hardly ever rises above 50°C but it is more likely to vary in the range between 42°C and 48°C. The temperature of 50°C will thus be assumed in the ensuing calculations.

Component partial pressure, p, is given by the equation:

$$pV = nRT \qquad \text{(C1.2)}$$

where V: volume occupied by vapour = 60 litres

n: number of moles of component present in vapour

R: Universal gas constant = 8.314 J/mol K

T: enclosure temperature = 50+273 = 323 K

The partial pressures for each component is thus calculated from the experimental data as:

$p_{(styrene)} = 553$ Pa

$p_{(o\text{-}xylene)} = 139$ Pa

$p_{(toluene)} = 1634$ Pa

If the partial pressures of the individual components were to be calculated on the basis of the formation of an ideal solution of the three components namely styrene, toluene and o-xylene, then Raoult's Law would be applicable, whereby

$$p_i = x_i \, Pvp_i \qquad \text{(C1.3)}$$

where p: partial pressure

x: mole fraction of component i in solution

Pvp: vapour pressure of component i at the given temperature

The component mole fractions in 180 cc of a 54% converted (80 minutes batch time) prepolymer feed solution are calculated as:

$x_{(styrene)} = 0.72$

$x_{(o\text{-}xylene)} = 0.13$

$x_{(toluene)} = 0.15$

Also the vapour pressure of each component is given by the Antoine equation [C1]:

$$\ln (Pvp_{(styrene)} (mmHg)) = 16.0193 - \frac{3328.57}{(T(K) - 63.72)} \qquad \text{(C1.4)}$$

$$\ln (Pvp_{(o\text{-}xylene)} (mmHg)) = 16.1156 - \frac{3395.7}{(T(K) - 59.46)} \qquad \text{(C1.5)}$$

$$\ln (Pvp(toluene) (mmHg)) = 16.0137 - \frac{3096.52}{(T(K) - 53.67)} \qquad \text{(C1.6)}$$

The vapour pressures are calculated at the enclosure temperature of 50°C instead of the solution temperature of 88-90°C. The evidence of lower enclosure temperature indicates that total equilibrium between the liquid and vapour phases is not achieved in the short time of exposure on the disc. Hence it would not be justified

to perform the calculations at 88°C. Temperature of 50°C is a better estimate although not completely accurate.

The partial pressures are thus evaluated to be:

$$p_{(styrene)} = 0.72 * 3200 = 2304 \text{ Pa}$$

$$p_{(o\text{-}xylene)} = 0.13 * 3360 = 436.8 \text{ Pa}$$

$$p_{(toluene)} = 0.15 * 12160 = 1824 \text{ Pa}$$

If the calculated partial pressures are compared to those determined from the experimental data above, it is seen that theoretically, the mass ratio of styrene to o-xylene in the vapour can be approximated by the ratio of their partial pressures which is 5.27. However, the experimentally evaluated ratio is 3.97. This discrepancy in the two ratios may be explained by the non-ideality of the feed solution. A strong interaction between styrene and polystyrene molecules would cause the actual partial pressure of styrene to be less than that predicted by Raoult's Law. Hence, Raoult's Law would overestimate the predicted loss of styrene in the saturated vapour which is what seems to be indicated by the GC analysis of the vapour mixture and the rather unexpected increase in the S/X ratio of the product samples. Also, the actual volume of styrene in solution would be much less than that assumed in the calculations with a significant proportion of the monomer being converted to polymer on the disc. All experimental evidence seem to indicate that loss of styrene by evaporation occurs to a very small extent which is not enough to account for the measured consumption of styrene in the disc runs. Therefore, polymerisation which also removes styrene from solution is obviously taking place to a large degree on the disc surface.

C1.2. THEORETICAL CALCULATIONS

The experimental and predicted data presented in the previous section provide the basis for the theoretical quantification of the loss of styrene and toluene by evaporation from the disc surface in experiments conducted during the course of this investigation. Hence conservative estimates of the losses involved may be predicted by Raoult's Law applied at the enclosure temperature of 50°C. An example of the calculations involved for each individual disc run will be presented below.

It is assumed in this specimen calculation that a feed solution which is 29% converted in the batch is to be introduced onto the rotating disc. For simplification purposes, the extent of evaporation is taken to be independent of the disc rotational speed which may not apply in practice. The total volume of prepolymer solution is assumed to be 200 ml and the starting recipe is made up of styrene, toluene and BPO in the following quantity: 200 ml styrene, 40 ml toluene and 3 g BPO.

Assuming complete conservation of mass in the batch system, then the volumetric amount of individual component in the feed solution is:

$$\text{Toluene} = (40/240 * 200) = 33.3 \text{ ml}$$

$$\text{Styrene + Polystyrene} = (200\text{-}33.3) = 166.7 \text{ ml}$$

Taking the density of toluene to be 867 kg/m^3 and that of a 29% solution mixture of styrene and polystyrene to be 892 kg/m^3 (see Appendix G for density correlation of styrene/PS mixtures), then the mass of the components are:

Toluene = 33.3 *0.867 = 28.9 g

Styrene + PS = 148.7 g

Styrene = (100-29)/100 * 148.7 = 105.6 g

PS = (148.7-105.6) = 43.1 g

The molar quantities of styrene and toluene in solution can be deduced as:

Styrene = 105.6/104 = 1.02 moles

Toluene = 28.9/92 = 0.314 moles

In terms of mole fractions,

Styrene = 1.02/(1.02+0.314) = 0.765

Toluene = 0.314/(1.02+0.314) = 0.235

The vapour pressures of toluene and styrene at 50°C have already been calculated earlier in section 1.1.7 as 12160 Pa and 3200 Pa respectively.

Hence the partial pressures are obtained from Raoult's Law (equation C1.3) as:

$p_{(styrene)}$ = 0.765*3200 = 2448 Pa

$p_{(toluene)}$ = 0.235*12160 = 2858 Pa

The molar quantities corresponding to the above partial pressures are obtained by rearranging equation (C1.2) as:

n = pV/RT

Hence,

Moles of styrene lost in vapour = $2448*60*10^{-3}/(8.314*323)$= 0.055

Moles of toluene lost in vapour = 2858*60*10-3/(8.314*323) = 0.064

In terms of mass,

Mass of styrene lost = 0.055*104 = 5.72 g

Mass of toluene lost = 0.064*92 = 5.89 g

Mass of styrene remaining in solution = 105.6-5.72 = 99.9 g

% PS in remaining solution after loss of styrene

= 43.1/(43.1+99.9)*100 = 30.1%

Hence, after styrene evaporation, it would appear that the conversion in the disc product has changed from 29% to 30.1%.

The above calculations were undertaken for a range of prepolymer feed conversions and different starting recipes used in the five experimental sets (A-E) of disc runs in the present study. Operating conditions of each experiment can be found in Appendix E. The predicted losses for runs in experiments A to E as calculated by the above method are given below in Tables C2 to C6 respectively.

References

C1. Sinnott, R.K., *Chemical Engineering, Vol. 6*, pp. 857-877, 2nd ed., Pergamon Press, Oxford, 1993.

Experiment A

Starting recipe: 200 ml styrene and 3 g BPO

Basis: 180 ml of prepolymer feed on disc

180 ml of styrene (S)/polystyrene (PS) mixture in feed solution

$Pvp_{(styrene)}$ at 50°C = 3200 Pa

Table C2. Predicted losses by evaporation from disc for experiment A

Feed conversion (%)	Density of solution (kg/m^3)	S+PS on disc	S on disc (g)	PS on disc (g)	S in solution (mole fraction) (g)	p_s (Pa)	S in vapour (g)	S left in solution (g)	PS in remaining solution (%)
13.3	864	155.4	134.8	20.7	1.00	3200	7.46	127.3	14.0
18.2	873	157.2	128.6	28.6	1.00	3200	7.46	121.1	19.1
23.3	883	159.0	121.9	37.0	1.00	3200	7.46	114.5	24.4
27.6	890	160.2	116.0	44.2	1.00	3200	7.46	108.5	28.9
33.0	898	161.7	108.4	53.4	1.00	3200	7.46	100.9	34.6
36.9	905	163.0	102.8	60.2	1.00	3200	7.46	95.4	38.7

Notes

1) Feed conversions given here are average values from batch calibration curve. Measured feed conversions from each disc run as given in Appendix E are adjusted to the average value before the final increase in conversion on the disc is evaluated as seen in Appendix E.

2) The **% PS remaining in solution is the apparent conversion** of the disc product after loss of styrene by evaporation. If polymerisation also takes place on the disc, then the measured experimental conversion should be greater than the apparent conversion due to loss, the difference representing the increase in conversion due to polymerisation on the disc.

Experiment B

Starting recipe: 200 ml styrene, 10 ml toluene and 3.0 g BPO

Basis: 180 ml of prepolymer feed on disc

8.6 ml of toluene (T) in feed (or 7.4 g toluene)

171.4 ml of styrene (S)/polystyrene (PS) mixture in feed solution

$Pvp_{(styrene)}$ at 50°C = 3200 Pa

$Pvp_{(toluene)}$ at 50°C = 12160 Pa

Table C3. Predicted losses by evaporation from disc for experiment B

Run no.	Feed conv. (%)	Density of solution (kg/m^3)	S+PS on disc (g)	S on disc (g)	PS on disc (g)	S in solution (mole fraction)	T in sol (mole fraction)	p_s (Pa)	p_T (Pa)	S in vapour (g)	T in vapour (g)	S left in sol. (g)	PS in remaining sol. (%)	Toluene left in sol. (%w/w)
B1	37.0	905	155.2	97.8	57.4	0.921	0.079	2947	962	6.9	2.0	90.9	38.7	3.51
B4	44.0	920	157.7	88.3	69.4	0.913	0.087	2922	1056	6.8	2.2	81.5	46.0	3.33
B2	50.0	931	159.6	79.8	79.7	0.905	0.095	2895	1158	6.8	2.4	73.1	52.2	3.17
B5	57.1	942	161.5	69.3	92.2	0.892	0.108	2854	1314	6.7	2.7	62.7	59.5	2.94
B3	62.0	954	163.5	62.1	101.4	0.881	0.119	2819	1449	6.6	3.0	55.5	64.6	2.73

Notes

(1) to (2) As above

3) Runs no. correspond to those used in Appendix E. The operating conditions for each run can be found in Appendix E.

4) The % w/w of toluene left in solution after evaporation from the disc surface is calculated from the following expression:

$$\% \text{ toluene remaining in solution} = \frac{(\text{Initial mass of toluene in feed} - \text{Mass of toluene lost})}{\text{Mass of remaining toluene} + \text{Mass of S left in solution} + \text{Mass of PS on disc}} \times 100$$

Experiment C

Starting recipe: 200 ml styrene, 40 ml toluene and 3.0 g BPO

Basis: 200 ml of prepolymer feed on disc

33.3 ml of toluene (T) in feed (or 28.9 g toluene)

166.7 ml of styrene (S)/polystyrene (PS) mixture in feed solution

$Pvp_{(styrene)}$ at 50°C = 3200 Pa

$Pvp_{(toluene)}$ at 50°C = 12160 Pa

Table C4. Predicted losses by evaporation from disc for experiment C

Run no.	Feed conv. (%)	Density of solution (kg/m^3)	S+PS on disc (g)	S on disc (g)	PS on disc (g)	S in solution (mole fraction)	T in sol. (mole fraction)	p_s (Pa)	p_T (Pa)	S in vapour (g)	T in vapour (g)	S left in sol. (g)	PS in remaining sol. (%)	Toluene left in sol. (%w/w)
C1-C10	37.0	905	150.9	95.1	55.8	0.744	0.256	2382	3110	5.5	6.4	89.5	38.4	13.4

Notes: As above

Experiment D

Starting recipe: 200 ml styrene, 40 ml toluene and 3.0 g BPO

Basis: 200 ml of prepolymer feed on disc

33.3 ml of toluene (T) in feed (or 28.9 g toluene)

166.7 ml of styrene (S)/polystyrene (PS) mixture in feed solution

$Pvp_{(styrene)}$ at 50°C = 3200 Pa

$Pvp_{(toluene)}$ at 50°C = 12160 Pa

Table C5. Predicted losses by evaporation from disc for experiment D

Run no.	Feed conv. (%)	Density of solution (kg/m^3)	S+PS on disc (g)	S on disc (g)	PS on disc (g)	S in solution (mole fraction)	T in sol. (mole fraction)	p_s (Pa)	p_T (Pa)	S in vapour (g)	T in vapour (g)	S left in sol. (g)	PS in remaining sol. (%)	Toluene left in sol (%w/w)
D9	29	892	148.6	105.5	43.1	0.764	0.236	2443	2875	5.7	5.9	99.8	30.2	13.86
D7	42	914	152.4	88.4	64.0	0.730	0.270	2336	3282	5.4	6.8	82.9	43.6	13.09
D4	52	933	155.5	74.6	80.9	0.696	0.304	2226	3702	5.2	7.6	69.4	53.8	12.39
D8	56	940	156.7	68.9	87.7	0.678	0.322	2171	3910	5.1	8.1	63.9	57.9	12.09
D6	61	950	158.3	61.7	96.6	0.654	0.346	2093	4208	4.9	8.7	56.8	62.9	11.65
D5	67	959	159.9	52.8	107.1	0.618	0.382	1976	4650	4.6	9.6	48.2	69.0	11.06

Notes: As above

Experiment E

Starting recipe: 180 ml styrene, 36 ml toluene and 2.7 g BPO

Basis: 180 ml of prepolymer feed on disc

30 ml of toluene (T) in feed (or 26.0 g toluene)

150 ml of styrene (S)/polystyrene (PS) mixture in feed solution

$Pvp_{(styrene)}$ at 50°C = 3200 Pa

$Pvp_{(toluene)}$ at 50°C = 12160 Pa

Table C6. Predicted losses by evaporation from disc for experiment E

Run no.	Feed conv. (%)	Density of solution (kg/m^3)	S+PS on disc (g)	S on disc (g)	PS on disc (g)	S in solution (mole fraction)	T in sol. (mole fraction)	p_s (Pa)	p_T (Pa)	S in vapour (g)	T in vapour (g)	S left in sol. (g)	PS in remaining sol. (%)	Toluene left in sol. (%w/w)
E1-E8	58	944	141.6	59.5	82.1	0.669	0.331	2141	4023	5.0	8.3	54.5	60.1	11.48

Notes: As above

Appendix D

Analytical Methods: Operation, Calibration and Calculation details

D1.1. PRECIPITATION

The precipitation method was used for conversion analysis in the early stages of the present investigation for runs in experimental sets A and B. The procedure adopted in this analysis was described in section 4.3.1 of Chapter 4. A sample calculation of conversion by this method is given below. All conversion calculations for experiment B which have been presented in Appendix E follow the same procedures as set out below.

D1.1.1. Sample calculation

The following calculation is for sample A10 from Run B1.

Mass of vial = 12.978 g
Mass of vial with collected sample of styrene and polystyrene = 22.288 g
Mass of vial and polystyrene after precipitation with methanol = 13.827 g

Hence,

Mass of styrene and polystyrene, A = 22.288 - 13.827 = 8.461g
Mass of polystyrene only, B = 13.827 - 12.978 = 0.849 g
Mass of styrene, C = 8.461 - 0.849 = 7.612 g
Conversion = (A - C)*100/A = (8.461 - 7.612)*100/ 8.461 = 9.11 %

D2.1. GEL PERMEATION CHROMATOGRAPHY (GPC)

D2.1.1. Operating conditions

Solvent flowrate: 1ml/min
Column temperature: 30°C
Single injection volume: 100 µl
RI detector response: fast

D2.1.2. Column and detector response calibrations

D2.1.2.1. Column calibration for molecular weight

The column was calibrated twice (at the beginning and in the middle of the research programme) for molecular weight of polystyrene by using Easical Standards PS-2 and PS-1 respectively supplied by Polymer Laboratories. The standards were in the form of spatulas coated with a mixture of narrow molecular weight distribution polystyrene calibrants. Two types of spatulas each coated with polystyrene having a range of different molecular weights were available. The relevant characterisation data

for Easical PS-1 and PS-2 were as follows:

Easical PS-1

Plain spatula

Peak No.	M_w/M_n	Assigned M_p
1	1.10	7500000
2	1.05	841700
3	1.02	148000
4	1.03	28500
5	1.04	2930

Hole punched spatula

Peak No.	M_w/M_n	Assigned M_p
6	1.06	2560000
7	1.04	320000
8	1.02	59500
9	1.02	10850
10	1.13	580

Easical PS-2

Plain spatula

Peak No.	M_w/M_n	Assigned M_p
1	1.04	380000
2	1.04	96000
3	1.03	22000
4	1.05	5050
5	1.07	1320

Hole punched spatula

Peak No.	M_w/M_n	Assigned M_p
6	1.03	2560000
7	1.03	320000
8	1.03	59500
9	1.05	10850
10	1.17	580

One of each type of spatula was immersed in 2 ml of THF solvent for about 30 minutes with occasional agitation to allow the polymer to dissolve in the solvent. Solutions of 0.25% g/ml concentration were thus obtained. After filtering the prepared solutions, 100µl of each was separately injected into the column and retention times for each polystyrene peak were recorded and stored in a calibration file on the computer. The molecular weight calibration data thus generated for the two sets of calibration are presented in graphical form in Figures D1 and D2. Coefficients of a 1st order polynomial curve fit between log M and the retention time T are also shown. The fit ratio of the calibration points on the calibration line varies between 0.995 and 1.013 which is very satisfactory.

D2.1.2.2. Detector response calibration for concentration

The detector response was calibrated for three components namely polystyrene, styrene and toluene in an attempt to obtain absolute amounts of each in a given unknown sample. A three level calibration was used by making up solutions of three concentrations (0.5% w/v, 0.3% w/v and 0.1% w/v) of each component. Desired concentrations of polystyrene and styrene were mixed together while toluene was prepared and run through the column separately. The polystyrene standard PS 28500 was used as the polymer calibrant in each calibration sample as its molecular weight characteristics were the closest match to the polymer produced during polymerisation in the present study.

The calibration plots of peak area against concentration for polystyrene, styrene and toluene are given in Figures D3 to D5 respectively. Data for response factors and closeness of fit of the calibration line are also included.

GPC Calibration Editor

Calib. Graph for - GPCCALIB.30

13:55 Fri Nov 20 1998

Curve Fitting Using : 1st Order Polynomial

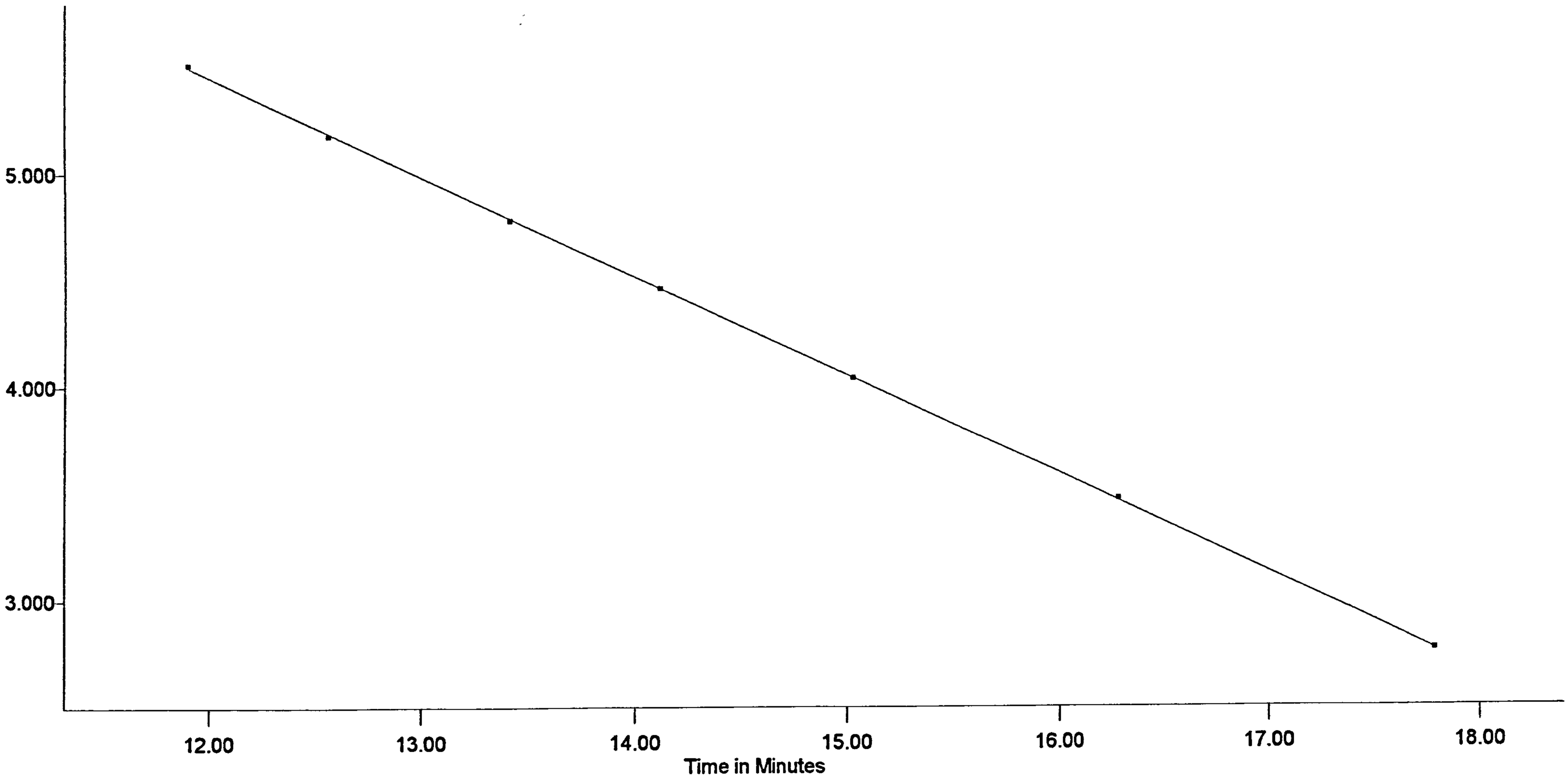

Polynomial Coefficients: LogM = A + BT
A=1.099860e+001, B=-4.628282e-001

Figure D1. Molecular weight calibration plot using Easical standards PS-1

GPC Calibration Editor

Calib. Graph for - GPCCALIB.10

13:47 Fri Nov 20 1998

Curve Fitting Using : 1st Order Polynomial

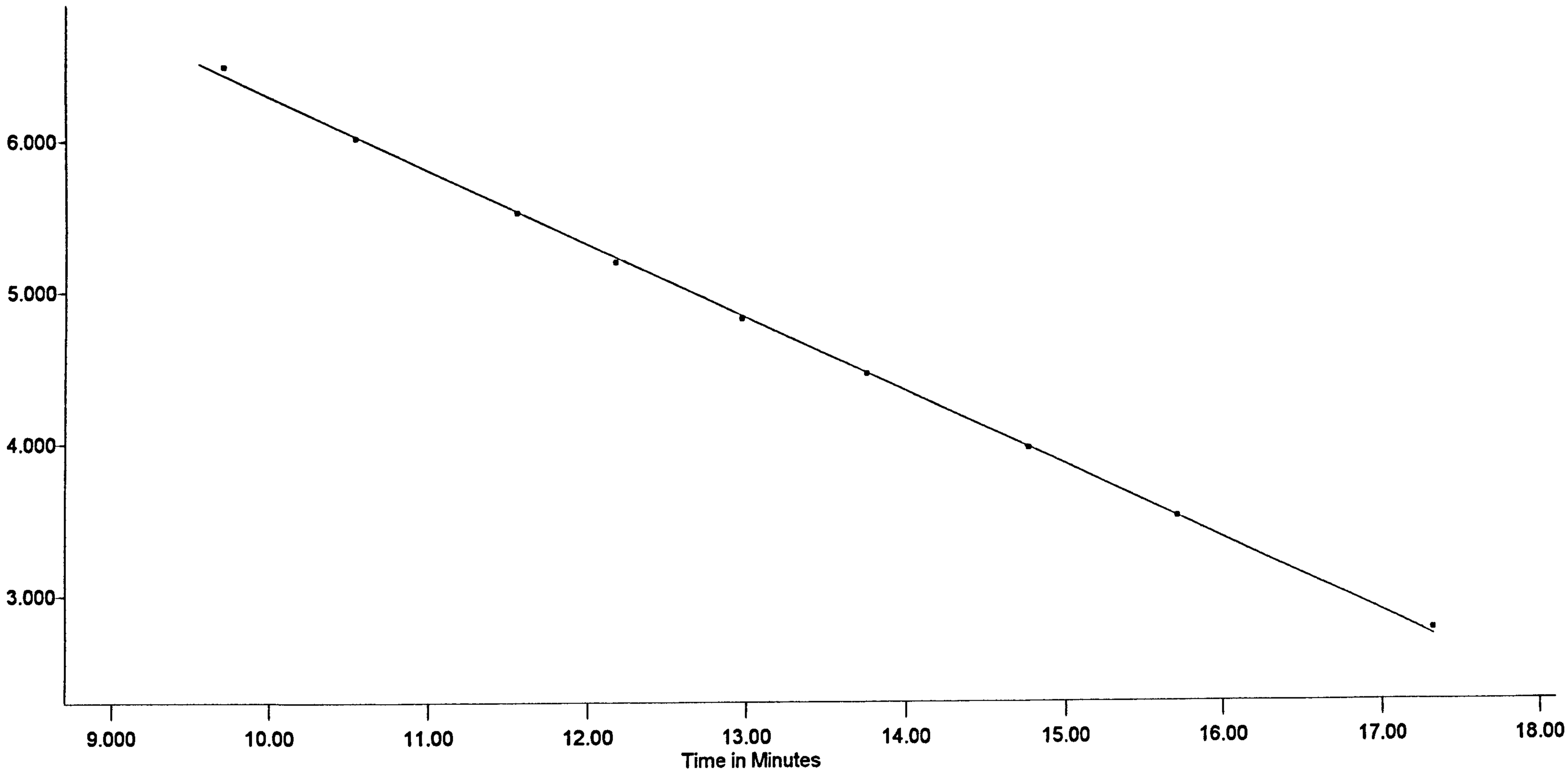

Polynomial Coefficients: LogM = A + BT
A=1.114918e+001, B=-4.859316e-001

Figure D2. Molecular weight calibration plot using Easical standards PS-2

Appendix D

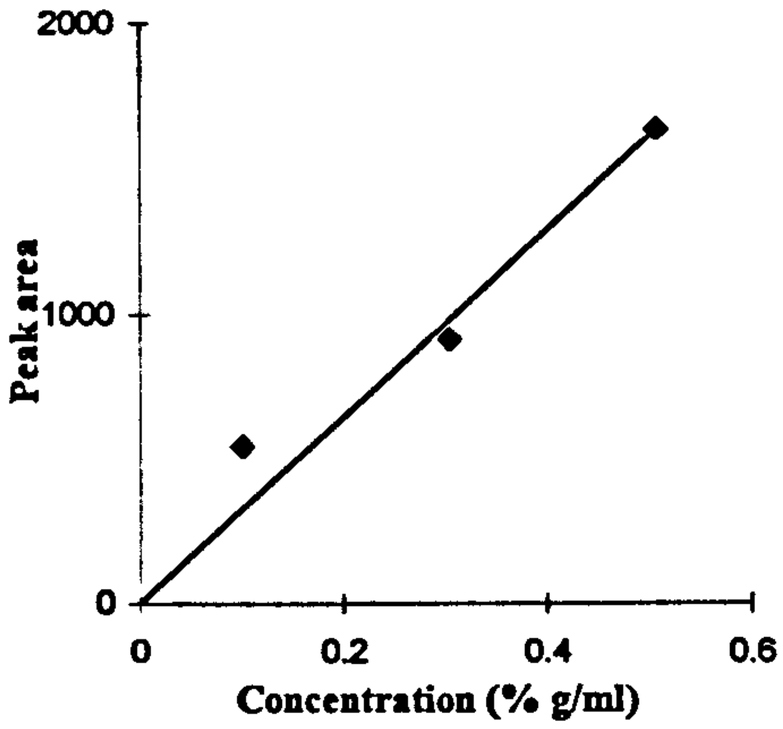

Peak : PS
RT(mins) : 13.883
Area = 0.000 * C^2 + 3225.559 * C + 0.000
Residual Std Dev : 124.246
Residual Mean : 36.613
Coefficient of Determination : 0.96844

	Use	Area	Samples	Max	Min	Conc	Residual
1	Y	1633.192	1	-	-	0.50700	-2.166
2	Y	915.598	1	-	-	0.30500	-68.198
3	Y	542.599	1	-	-	0.10100	216.818

Figure D3. Detector response calibration for polystyrene

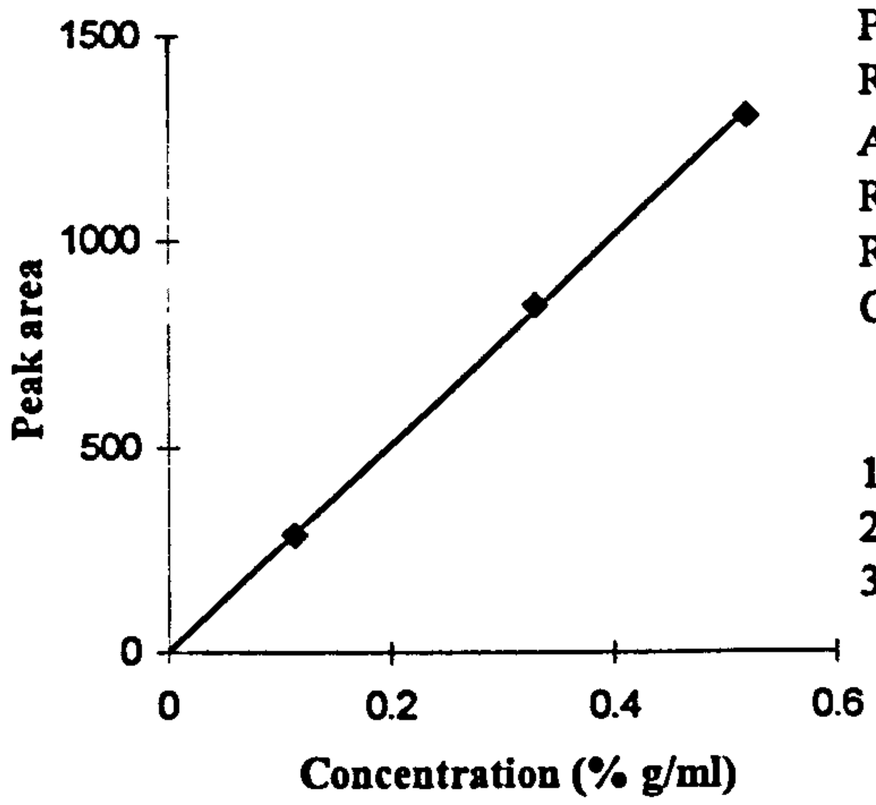

Peak : styrene
RT(mins) : 20.061
Area = 0.000 * C^2 + 2527.060 * C + 0.000
Residual Std Dev : 9.669
Residual Mean : 1.506
Coefficient of Determination : 0.99972

	Use	Area	Samples	Max	Min	Conc	Residual
1	Y	286.612	1	-	-	0.11300	1.504
2	Y	848.165	1	-	-	0.33000	14.235
3	Y	1304.809	1	-	-	0.52000	-9.262

Figure D4. Detector response calibration for styrene

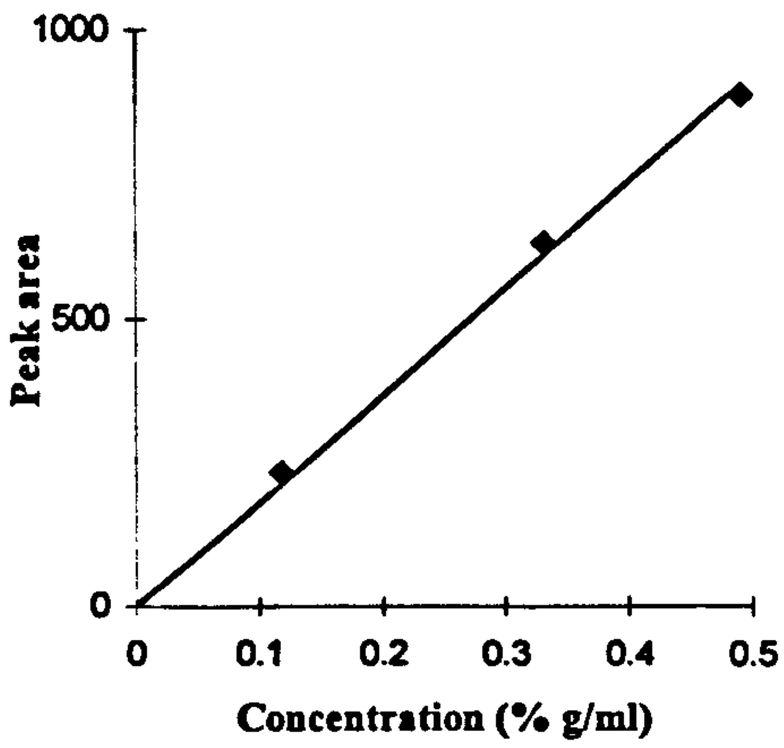

Peak : toluene
RT(mins) : 20.306
Area = 0.000 * C^2 + 1838.299 * C + 0.000
Residual Std Dev : 18.600
Residual Mean : 5.689
Coefficient of Determination : 0.99761

	Use	Area	Samples	Max	Min	Conc	Residual
1	Y	884.490	1	-	-	0.49100	-18.115
2	Y	629.341	1	-	-	0.33200	19.025
3	Y	238.766	1	-	-	0.11800	21.847

Figure D5. Detector response calibration for toluene

D2.1.3. Molecular weight analysis

Molecular weight analysis of unknown samples collected from batch polymerisation mixture and from the rotating disc were performed against the polystyrene calibrants with characteristics as given in Figure D1 and D2. The unknown samples were prepared prior to injection as described in section 4.3.2.2 of Chapter 4. Peaks obtained in a typical chromatogram generated by the GPC/SEC software for an unknown sample are shown in Figure D6 together with the corresponding data for molecular weight properties.

D2.1.4. Analysis methods for component concentration

Two methods were used for determining component concentration and hence styrene conversion from chromatograms generated by the GPC: normalisation method and external standard method.

D2.1.4.1. Normalisation method

This is the simplest analysis method which calculates relative amounts of components based on the ratio of individual component peak areas to the sum of the area of all peaks in the chromatogram. Hence, for component i,

$$(\%\ \text{Area})_i = \frac{\text{Area}_i}{\sum_{i=0}^{i=n} \text{Area}_i} \times 100 \qquad \text{(D1.1)}$$

where n is the number of peaks in the sample chromatogram

Using the normalisation method, styrene conversion to polystyrene is obtained by the following expression:

$$\%\ \text{conversion} = \frac{\text{Area}_{PS}}{\text{Area}_{PS} + \text{Area}_{styrene}} \times 100 \qquad \text{(D1.2)}$$

The problem with this method of analysis is that the area for the styrene peak cannot be determined accurately since the styrene peak coincides with the toluene peak in the chromatogram. Hence the peak area in fact consists of areas attributable to both styrene and toluene. The overestimation of the styrene peak area will cause the % conversion to be lower than the true conversion. However, calculation by the normalisation method is a good enough estimate of the % conversion since toluene is present only in a very small quantity in the sample.

A typical calculation by the normalisation method using the LC-GC software is shown in Figure D7 together with the peaks generated during the chromatography run.

Conversion data calculated by the normalisation method are presented in Appendix E for samples from experiments C to E.

DEPARTMENT OF CHEMICAL AND PROCESS ENGINEERING
UNIVERSITY OF NEWCASTLE UPON TYNE

15:46 Tue Jun 09 1998

Unknown SDR33.006
QS1: 1500 rpm, 80 mins feed time
Operator : K.Boodhoo
Detector : RI Temperature : 30oC
Column Set : 2 PLgel 5um MIXED-C column, dimen. 300*7.5 mm PLgel 5um guard
Standards : polystyrene
Flow Rate : 1.000
Flow Rate Marker :
found at 20.78

Method : 30
Last Calibrated Sun Jun 07 12:34:06 1998
Calib. Start 11.97 End 17.90 Mins
Peak Start 12.58 End 16.60

Results

Mp :	29114	Mz :	44678
Mn :	19879	Mz+1 :	57937
Mw :	31557	Mv :	29747

Polydispersity 1.587
Peak Area 164338

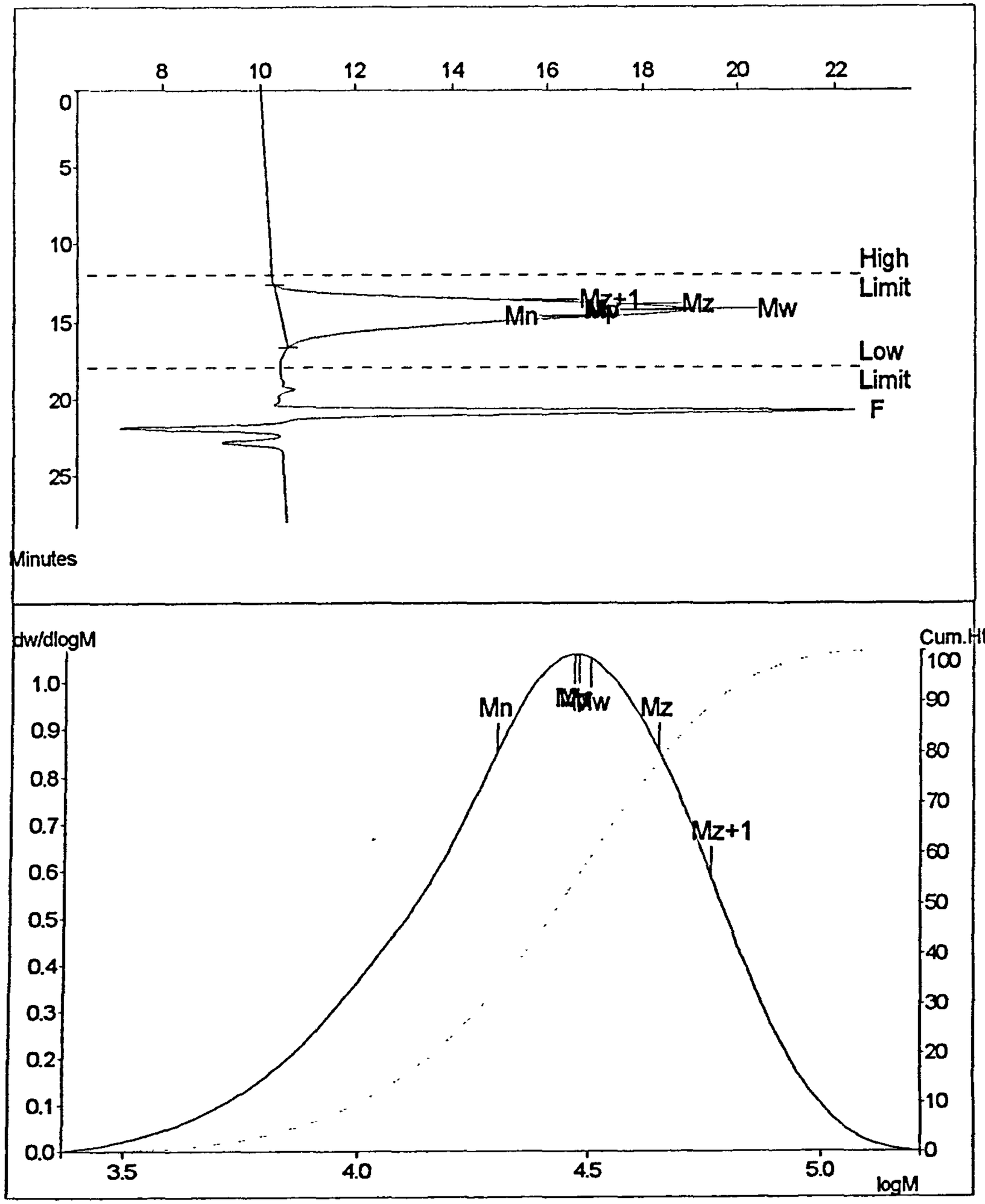

Figure D6. Typical GPC chromatogram and dW/dlogM plot used in the evaluation of molecular weight properties of polystyrene in an unknown sample

Run Type : Unknown

File Description	Date	Name
Sample Strip:	20:41 Sat Nov 21 1998	C:\LC-GC\SYSTEM\QS4.STR
Method:	00:15 Wed May 13 1998	C:\LC-GC\METHODS\KAM1
Raw Data:	13:46 Mon Jun 08 1998	C:\GPC\RAWDATA\GPC\SDR33.004
Results:	20:44 Sat Nov 21 1998	C:\LC-GC\RESULTS\RSDR33.004

Mode : Manual

Sample Name : Q80

Scale : 1.0000000

Sample Amount : 1.0000000

Comment:

Analysis method: Normalisation
Last peak in chromatogram is due to both
styrene and toluene

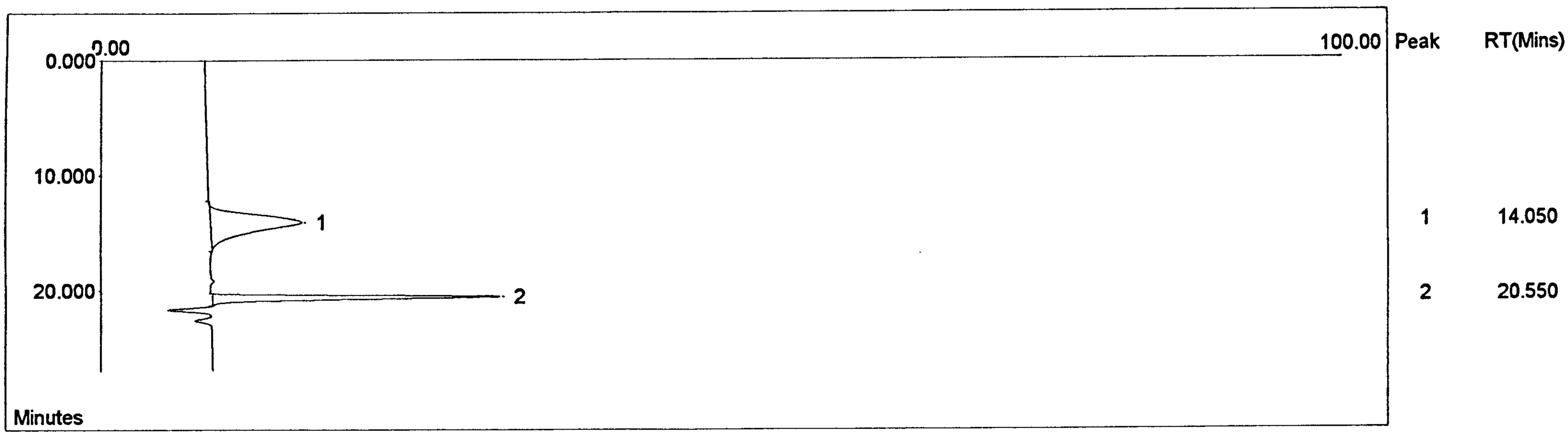

Peak	Name	Type	RT(Mins)	Area	Height	Base	Conc(% Area)
1		BB	14.050	683.638	7.318	8.925	57.259
2		BBMM	20.550	510.300	23.087	9.098	42.741

Figure D7. Typical chromatogram used in determining component concentration by normalisation method

D2.1.4.2. External standard method

The external standard method calculates absolute concentrations of each component using response factors obtained from prior calibration data which have been presented in Figures D3 to D5 for each component.

When unknown samples are run with this method, peaks are matched by retention times with those in the calibration file. From the calibration response factors which relate the component peak area A_i to the concentration C_i, as:

$$A_i = RF2_i * C_i^2 + RF1_i * C_i + RF0_i \qquad \text{(D1.3)}$$

where RF2, RF1 and RF0 are the response factors obtained from calibration

The order of the polynomial in equation (D1.3) is determined by the best fit to the calibration data for each component. As shown in Figures D3 to D5, a polynomial of order 1 is chosen to fit the data for polystyrene, styrene and toluene.

The results of a typical calculation based on the external standard method is shown below the chromatogram in Figure D8.

The peak named "styrene" in the chromatogram is, in fact, a peak corresponding to both styrene and toluene which elute at more or less the same time from the GPC column ($RT_{styrene}$ (mins) = 20.061, $RT_{toluene}$ (mins)= 20.306). The LC-GC software calculates the concentration corresponding to this peak as though it was styrene only (i.e. using the response factor for styrene).

While it is not possible to adjust the peak area for the presence for toluene in the normalisation method, the determination of response factors for toluene in the external standard method provides a means for adjustment and hence more accurate conversion data for the polymerisation study can be expected. The sequence of calculations involved in adjusting the concentration data generated by the LC-GC software using the external standard method of analysis to take into account the presence of toluene is outlined below for sample .

The calculations will be performed for batch sample Q80 from Run E4 (see Appendix E for details of this run).

Mass of sample Q80 dissolved in 10 ml THF solvent = 0.057 g
Concentration of solution injected in GPC = 0.57% g/ml

From the starting recipe of 180 ml styrene, 36 ml toluene and 2.7 g BPO used for Run E4, the % w/w of toluene in the sample is calculated to be 15.77% assuming that no loss of toluene occurs during polymerisation in the batch.

Hence,

Concentration of toluene in injected sample =15.77/100 *0.57
= 0.0899 % g/ml

From the calibration data for toluene given in Figure D5, the toluene peak area is related to its concentration as follows:

$$Area_{(toluene)} = 1838.299 * C_{(toluene)} \qquad \text{(D1.4)}$$

Therefore, the peak area corresponding to toluene in the injected sample Q80 is obtained as:

$$\text{Area}_{(\text{toluene})} = 1838.299 * 0.09 = 165.26 \text{ units}$$

Combined peak area for styrene and toluene
(from LC-GC software) = 511.599 units

Area due to styrene peak only = 511.599 - 165.26
= 346.339 units

The response factor for styrene obtained from calibration in Figure D4 is:

$$\text{Area}_{(\text{styrene})} = 2527.06 * C_{(\text{styrene})} \qquad \text{(D1.5)}$$

Concentration of styrene in injected sample = 346.339/2527.06
= 0.137 % g/ml

Polystyrene concentration calculated by LC-GC software
= 0.212 % g/ml

% conversion = 100* 0.212/(0.212+0.137) = 60.74 %

It is to be noted that the % w/w of toluene in samples from the batch is higher than that in samples collected off the rotating disc due to some toluene being lost by evaporation from the surface of the rotating disc. The loss of toluene for runs in experiments B-E has been estimated in Appendix C. From this, the % w/w of toluene remaining in solution in disc product samples have also been calculated. These % w/w data have been used to calculate the concentration of toluene in the injected samples collected from the surface of the rotating disc.

Conversions evaluated by the above calculations are presented in Appendix E under the name "conversion by external standard method".

Run Type : Unknown

File Description	Date	Name
Sample Strip:	20:41 Sat Nov 21 1998	C:\LC-GC\SYSTEM\QS4.STR
Method:	16:22 Wed Mar 26 1997	C:\LC-GC\METHODS\RF
Calib File:	22:23 Mon Jun 17 1996	C:\LC-GC\METHODS\RF
Raw Data:	13:46 Mon Jun 08 1998	C:\GPC\RAWDATA\GPC\SDR33.004
Results:	20:51 Sat Nov 21 1998	C:\LC-GC\RESULTS\RSDR33.004

Mode : Manual

Response Factors : Replace

Sample Name : Q80

Scale : 1.0000000

Sample Amount : 1.0000000

Comment:

Analysis method:EXTERNAL STD
Peak 2 is due to both styrene and toluene;
calculated area and conc to be adjusted for
presence of toluene.

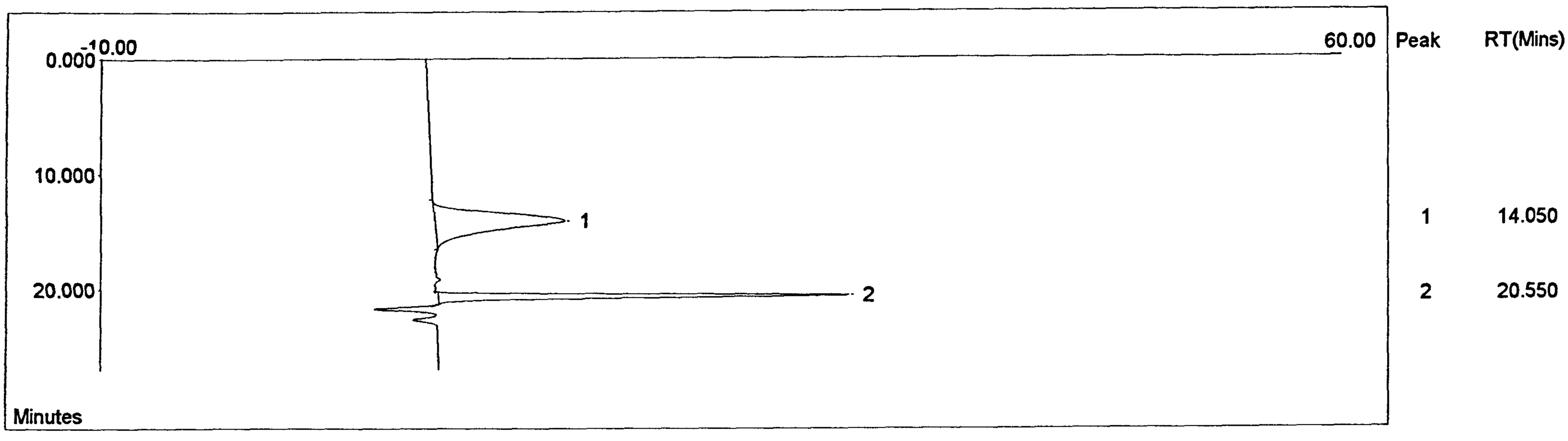

Peak	Name	Type	RT(Mins)	Area	Height	Base	Conc (%g/ml)
1	PS	BB	14.050	683.638	7.318	8.925	0.212
2	styrene	BBMM	20.550	509.232	23.077	9.109	0.202

Figure D8. Typical chromatogram used in determining component concentration by external standard method

Appendix E

Polymerisation Experiments: Batch and SDR Data

E1.1. BATCH POLYMERISATION DATA

Data used to establish batch calibration profiles were collected during individual batch runs solely performed to monitor the polymerisation in the batch and also during prepolymer preparation in the batch during the course of spinning disc runs. The data to be presented in this appendix reflects this procedure in that batch runs extend over a period of more than 2 hours while prepolymer preparation time for disc runs varies according to the selected feeding time on the disc.

E1.1.1. Experiment B

The recipe used in all runs in this set was 200 ml styrene, 10 ml toluene and 3.0 g BPO which corresponded to concentrations of 8.32 mole/litre styrene, 0.448 mole/litre toluene and 0.059 mole/litre BPO. All volumetric quantities were measured at room temperature.

Conversion was calculated by measuring the difference in weight before and after precipitation of the polymer with methanol. Sample calculation details for this method can be found in Appendix D. Information about molecular weight properties could not be obtained for experiment B because of precipitation being used as the main analytical method.

Run B1

Time (mins)	Sample	Vial V mass(g)	V+PS+S (g)	V+PS (g)	Conversion (%)	Comments
5	A5	17.748	32.137	18.845	7.624	
10	A10	12.978	22.288	13.827	9.119	
15	A15	12.833	21.042	13.849	12.377	
20	A20	12.925	19.564	13.912	14.867	
25	A25	12.789	20.271	14.309	20.315	
30	A30	13.143	20.534	14.934	24.232	
35	A35	13.039	18.312	14.714	31.766	
40	A40	12.841	18.618	15.166	40.246	

Run B2

Time (mins)	Sample	Vial V mass(g)	V+PS+S (g)	V+PS (g)	Conversion (%)	Comments
10	B10	18.067	25.732	18.984	11.963	
20	B20	12.893	18.84	14.117	20.582	
30	B30	12.881	17.773	14.255	28.087	
40	B40	13.219	20.061	15.862	38.629	
50	B50	12.479	17.899	14.947	45.535	
60	B60	12.828	14.546	13.655	48.137	

Run B3

Time (mins)	Sample	Vial V mass(g)	V+PS+S (g)	V+PS (g)	Conversion (%)	Comments
10	C10	17.528	28.066	18.377	8.057	
20	C20	12.982	18.885	14.108	19.075	
30	C30	13.100	19.926	14.764	24.377	
40	C40	12.337	16.239	13.687	34.598	
50	C50	12.938	18.347	15.327	44.167	
60	C60	12.929	19.691	16.41	51.479	
70	C70	12.316	17.832	15.471	57.197	
80	C80	12.911	17.845	16.163	65.910	

E1.1.2. Experiment C

Unless otherwise stated, the recipe used in all runs for Experiment C was 200 ml styrene, 40 ml toluene and 3.0 g benzoyl peroxide. All volumetric quantities were measured at room temperature. The given quantities correspond to concentrations of 7.28, 1.567 and 0.0517 moles/litre of styrene, toluene and benzoyl peroxide respectively, as stipulated earlier in Chapter 5.

All analysis was performed by gel permeation chromatography (GPC). In most cases, conversions were calculated by both the normalisation method and the external standard method (see details of both methods in Appendix D). Where the two values were fairly close, an average was taken as the real time batch conversion and used in the calibration plot for conversion as shown in Chapter 5.

Run C1

Time (mins)	Sample	Batch Temp. (°C)	M_n	M_w	M_w/M_n	Conversion (Norm. Mtd) (%)	Comments
0		88.0				0	
10	K10	93.5	20183	29911	1.482	10.874	
20	K20	95.5	19245	28819	1.497	20.542	
30	K30	96.7	18033	27985	1.552	26.757	
40	K40	97.5	17732	27634	1.558	37.141	

Run C2

Time (mins)	Sample	Batch Temp. (°C)	M_n	M_w	M_w/M_n	Conversion (Norm. Mtd) (%)	Comments
0		88.0				0	
10	L10	93.0	17789	27529	1.548	22.268	Too high
20	L20	95.0	19925	29001	1.456	17.589	
30	L30	95.5	18724	28293	1.511	27.17	
40	L40	96.0	18265	28267	1.548	32.43	
50	L50	96.0	17773	28226	1.588	42.498	
60	L60	96.0	18148	28883	1.592	44.306	
70	L70	96.0	17952	29226	1.628	54.103	
80	L80	96.0	18077	29630	1.639	60.183	
90	L90	96.5	18165	30054	1.655	61.206	
100	L100	96.9	18408	30517	1.658	62.241	
110	L110	96.8	19005	31361	1.650	68.813	Too high
120	L120	96.5	19443	32564	1.675	67.853	
130	L130	98.2	19543	32918	1.684	71.266	

Run C3

Time (mins)	Sample	M_n	M_w	M_w/M_n	Conversion (Norm. Mtd) (%)	Comments
10	M10	19709	29963	1.520	15.12	Too high
20	M20	18742	28472	1.519	17.85	
30	M30	18341	28413	1.549	20.686	Too low
40	M40	18529	28423	1.534	35.032	

Run C4

Time (mins)	Sample	Batch Temp. (°C)	M_n	M_w	M_w/M_n	Conversion (Norm. Mtd) (%)	Conversion (Ext. Std Mtd) (%)	Comments
10	N10(R)	91.0	21345	31391	1.471	14.995	13.960	
20	N20(R)	91.8	20063	30074	1.499	14.323	12.755	Low temp ∴ low conv
30	N30(R)	92.2	19617	30632	1.562	23.435	21.698	As above
40	N40(R)	92.7	19993	30894	1.545	29.699	28.445	As above

Run C5

Time (mins)	Sample	Batch Temp. (°C)	M_n	M_w	M_w/M_n	Conversion (Norm. Mtd) (%)	Conversion (Ext. Std Mtd)	Comments
0		88.0				0	0	
10	O10	93.5	22590	32373	1.433	7.766	9.826	
20	O20	95.1	20546	31257	1.521	17.8	19.574	
30	O30	96.2	18698	28679	1.534	30.084	28.509	
40	O40	97.4	18076	28493	1.576	38.365	36.751	
50	O50	98.0	18252	28534	1.563	48.2	49.838	

60	O60	97.6	17955	28715	1.599	51.278	51.195	
70	O70	97.6	17964	29375	1.635	59.483	61.545	
80	O80	97.8	18230	30096	1.651	64.342	66.798	
90	O90	97.5	18075	30575	1.692	72.848	79.625	Conv. by Ext. Std Mtd too high, maybe due to toluene loss
100	O100	98.0	18630	31046	1.666	73.536	77.404	As above
110	O110	98.4	19319	32393	1.677	74.594	81.180	As above
120	O120	99.5	19120	32734	1.712	76.356	81.573	As above

Run C6

Time (mins)	Sample	Batch Temp. (°C)	M_n	M_w	M_w/M_n	Conversion (Norm. Mtd) (%)	Conversion (Ext. Std Mtd) (%)	Comments
10	P10	93.1	20237	30030	1.484	9.673	8.746	
20	P20	94.6	18854	29023	1.539	19.413	17.831	
32	P30	95.6	18033	28206	1.564	29.627	28.968	
40	P40	95.8	17923	28402	1.585	36.228	35.059	

Run C7

Time (mins)	Sample	Batch Temp. (°C)	M_n	M_w	M_w/M_n	Conversion (Norm. Mtd) (%)	Conversion (Ext. Std Mtd) (%)	Comments
0		88.0				0	0	
10	Q10	93.1	17704	27799	1.570	20.774	18.946	Too high ∴ unreliable
20	Q20	94.8	18767	28448	1.516	19.712	18.636	
30	Q30	95.8	18087	27964	1.546	28.695	27.553	
40	Q40	96.2	17325	27631	1.595	35.201	34.235	

Run C8

Time (mins)	Sample	Batch Temp. (°C)	M_n	M_w	M_w/M_n	Conversion (Norm. Mtd) (%)	Conversion (Ext. Std Mtd) (%)	Comments
0		87.1				0	0	
10	R10(R)	92.3	21526	30317	1.408	10.29	9.430	
20	R20(R)	93.4	19074	29073	1.524	17.55	16.317	
30	R30(R)	94.1	18476	28484	1.542	31.51	28.715	Overpressure in GPC ∴ not reliable
40	R40(R)	95.5	18139	28814	1.589	32.30	31.656	

Run C9

Time (mins)	Sample	Batch Temp. (°C)	M_n	M_w	M_w/M_n	Conversion (Norm. Mtd) (%)	Conversion (Ext. Std Mtd) (%)	Comments
10	S10(R)	93.0	19444	29690	1.527	10.83	10.051	
20	S20(R)	94.1	19070	28722	1.506	19.76	18.787	
30	S30(R)	95.5	18454	28450	1.542	37.45	40.012	Too high ∴ unreliable
40	S40(R)	97.4	18106	28489	1.573	34.53	34.647	

Run C10

Time (mins)	Sample	Batch Temp. (°C)	M_n	M_w	M_w/M_n	Conversion (Norm. Mtd) (%)	Conversion (Ext. Std Mtd) (%)	Comments
0		88.0				0	0	
10	U10	91.5	19882	29148	1.466	11.83	10.761	
20	U20	92.0	19500	29519	1.514	20.09	18.353	
30	U30	92.4	19552	29769	1.523	25.93	23.803	Low temp ∴ low conversion
40	U40	93.0	19149	29888	1.561	33.33	32.440	As above

E1.1.3. Experiment D

Unless otherwise stated, the following recipe was used in all runs for Experiment D: 200 ml styrene, 40 ml toluene and 3 g benzoyl peroxide. All volumetric quantities were measured at room temperature. The given quantities correspond to concentrations of 7.28, 1.567 and 0.0517 moles/litre of styrene, toluene and benzoyl peroxide respectively, as stipulated earlier in Chapter 5. The speed of the magnetic agitator in the batch was set at between mark 4 and mark 5 on the magnetic plate.

All sample analysis were performed by GPC. As seen below, conversion calculated by both the normalisation method and the external standard method (see details of both methods in Appendix D) are given to enable a direct comparison. Since the two values agree quite reasonably, an average was taken as the batch conversion and used in the calibration plot in Chapter 5.

Run D1

Time (mins)	Sample	Batch Temp. (°C)	M_n	M_w	M_w/M_n	Conversion (Norm. Mtd) (%)	Conversion (Ext. Std Mtd) (%)	Comments
0		88.0				0	0	
20	D20	90.7	21566	31387	1.455	15.431	13.73	
40	D40	91.5	20336	31070	1.528	28.32	26.31	
60	D60	91.1	20290	31639	1.559	39.872	40.32	
80	D80	89.0	20234	32578	1.610	49.5	46.56	
100	D100	88.9	20758	33429	1.610	58.479	57.50	

Run D2

Time (mins)	Sample	Batch Temp. (°C)	Mn	Mw	Mw/Mn	Conversion (Norm. Mtd) (%)	Conversion (Ext. Std Mtd) (%)	Comments
0		87.8				0	0	
20	E20	93.6	19415	29964	1.543	23.924	21.863	
60	E60	94.3	18698	30018	1.605	41.726	40.486	
70	E70	95.4	19177	30293	1.580	49.8	48.333	
80	E80	94.7	18521	30352	1.639	52.119	51.328	

Run D3

Time (mins)	Sample	Batch Temp. (°C)	Mn	Mw	Mw/Mn	Conversion (Norm. Mtd) (%)	Conversion (Ext. Std Mtd) (%)	Comments
0		88.0				0	0	
10	F10	94.3	20688	30334	1.466	9.962	8.688	
20	F20	92.6	19142	29687	1.551	17.094	15.509	
30	F30	93.6	19693	29670	1.507	22.981	21.659	
40	F40	93.9	18222	28963	1.589	32.128	30.056	
50	F50	94.8	18649	29448	1.579	35.489	34.054	
60	F60	94.3	18630	29970	1.609	43.267	41.541	
70	F70	96.2	18959	30339	1.600	47.278	45.887	
80	F80	96.8	18684	30546	1.635	53.967	53.256	
90	F90	96.8	19047	31327	1.645	55.895	56.153	
100	F100	95.4	18565	31172	1.679	64.188	64.502	
110	F110	97.0	19461	32386	1.664	64.978	69.402	
120	F120	97.6	20980	34080	1.624	65.59	67.404	

Run D4

Time (mins)	Sample	Batch Temp. (°C)	Mn	Mw	Mw/Mn	Conversion (Norm. Mtd) (%)	Conversion (Ext. Std Mtd) (%)	Comments
0		88.0				0	0	
20	G20	91.6	20564	30502	1.483	17.826	16.337	
40	G40	92.8	18746	29849	1.592	29.568	27.950	
60	G60	93.8	18333	30380	1.657	44.237	42.530	
80	G80	94.1	19282	31185	1.617	51.532	51.209	

Run D5

Time (mins)	Sample	Batch Temp. (°C)	Mn	Mw	Mw/Mn	Conversion (Norm. Mtd) (%)	Conversion (Ext. Std Mtd) (%)	Comments
0		88.0				0	0	
20	H20	92.4	19488	29454	1.511	17.11	15.455	
40	H40	93.0	18276	29015	1.588	31.166	29.328	
60	H60	94.3	18824	30195	1.604	41.352	39.816	
80	H80	95.0	19175	30634	1.598	55.0	54.124	
100	H100	97.8	19738	32138	1.628	60.32	65.038	
120	H120	97.0	19338	32785	1.695	69.766	71.735	

Run D6

Time (mins)	Sample	Batch Temp. (°C)	Mn	Mw	Mw/Mn	Conversion (Norm. Mtd) (%)	Conversion (Ext. Std Mtd) (%)	Comments
0		88.0				0	0	
20	I20	92.6	19086	29411	1.541	16.959	15.348	
40	I40	93.1	18864	29434	1.560	30.201	28.336	
60	I60	94.4	18313	29629	1.618	42.467	40.814	
80	I80	96.3	18819	30759	1.634	50.373	49.815	
100	I100	96.0	18263	30993	1.697	61.442	61.497	

Run D7

Time (mins)	Sample	Batch Temp. (°C)	Mn	Mw	Mw/Mn	Conversion (Norm. Mtd) (%)	Conversion (Ext. Std Mtd) (%)	Comments
0		88.0				0	0	
20	J20	92.7	16007	28327	1.770	25.749	22.923	
40	J40	93.7	18688	29509	1.579	29.908	27.901	
60	J60	94.1	18703	29786	1.593	42.781	40.634	

Run D8

Time (mins)	Sample	Batch Temp. (°C)	Mn	Mw	Mw/Mn	Conversion (Norm. Mtd) (%)	Conversion (Ext. Std Mtd) (%)	Comments
0		88.0				0	0	
20	K20	93.6	18545	29584	1.595	28.856	26.880	
40	K40	94.8	18743	29389	1.568	31.905	30.009	
60	K60	95.8	17714	28932	1.633	43.798	42.422	
80	K80	94.8	18482	30314	1.640	51.919	51.561	
90	K90	95.9	18997	31023	1.633	55.827	57.041	

Run D9

Time (mins)	Sample	Batch Temp. (°C)	Mn	Mw	Mw/Mn	Conversion (Norm. Mtd) (%)	Conversion (Ext. Std Mtd) (%)	Comments
0		88.0				0	0	
10	L10	92.8	19739	29703	1.505	14.064	12.590	
20	L20	93	18626	28729	1.542	16.952	15.367	
30	L30	93.6	18717	28885	1.543	25.041	23.094	
40	L40	93.8	17969	28923	1.610	29.612	27.762	

E1.1.4. Experiment E

The recipe consisting of 200 ml styrene, 40 ml toluene and 3.0 g BPO, as used in the previous experiments C and D was retained for Run 30. As before, the speed of

agitation for the magnetic stirrer in the batch polymerisation mixture was set at mark 4 on the magnetic plate.

All sample analysis were performed by GPC. As seen below, conversion calculated by both the normalisation method and the external standard method (see details of both methods in Appendix D) are given to enable a direct comparison. Since the two values agree quite reasonably, an average was taken as the batch conversion and used in the calibration plot in Chapter 5.

Run E1

Time (mins)	Sample	Batch Temp. (°C)	Mn	Mw	Mw/Mn	Conversion (Norm. Mtd) (%)	Conversion (Ext. Std Mtd) (%)	Comments
0		85.4				0	0	
20	J20	93.3	20005	28944	1.447	18.636	17.993	
40	J40	94.2	18536	28727	1.550	32.4	32.381	
60	J60	95.1	18534	29659	1.600	46.464	47.368	
80	J80	96.3	19591	31165	1.591	55.823	58.620	

The recipe for all subsequent runs in the current experimental set was altered to 180 ml styrene, 36 ml toluene and 2.70 g BPO initiator to reduce the total volume of reagents in the glass vessel to 220 ml and hence prevent the reactor from overflowing from the thermocouple insertion port in the side arm. The initial concentration of each reagent was unaffected by this change in volume. All other parameters were kept constant.

Run E2

Time (mins)	Sample	Batch Temp. (°C)	Mn	Mw	Mw/Mn	Conversion (Norm. Mtd) (%)	Conversion (Ext. Std Mtd) (%)	Comments
0		86.3				0	0	
20	K20	93.6	19901	29009	1.458	19.353	18.472	
40	K40	94.4	19831	29951	1.510	33.488	33.013	
60	K60	94.5	19086	30153	1.580	46.413	47.370	
80	K80	96.2	18865	30677	1.626	56.841	59.230	

Run E3

Time (mins)	Sample	Batch Temp. (°C)	Mn	Mw	Mw/Mn	Conversion (Norm. Mtd) (%)	Conversion (Ext. Std Mtd) (%)	Comments
0		87.0				0	0	
20	L20	94.2	15769	26931	1.708	23.946	22.773	Chromat. not reliable ∴reject
40	L40	96.3	18271	28516	1.561	35.315	34.964	
60	L60	96.4	19433	30314	1.560	50.045	51.262	
80	L80	97.2	19335	31028	1.605	57.542	61.002	

Run E4

Time (mins)	Sample	Batch Temp. (°C)	Mn	Mw	Mw/Mn	Conversion (Norm. Mtd) (%)	Conversion (Ext. Std Mtd) (%)	Comments
0		87.0				0	0	
20	M20	94.2	19128	28534	1.492	18.944	18.176	
40	M40	95.5	18851	29203	1.549	34.712	34.323	
60	M60	96.2	18901	29885	1.581	46.514	48.208	
80	M80	97.0	19730	31506	1.597	58.016	60.998	

Run E5

Time (mins)	Sample	Batch Temp. (°C)	Mn	Mw	Mw/Mn	Conversion (Norm. Mtd) (%)	Conversion (Ext. Std Mtd) (%)	Comments
0		88				0	0	
20	N20	94.4	19908	30395	1.527	17.977	16.998	Mn & Mw
40	N40	95.8	19232	30477	1.585	33.805	33.212	unusually
60	N60	96.2	19553	31080	1.590	45.71	46.403	high for all
80	N80	96.5	20199	32421	1.605	55.612	57.648	samples

Run E6

Time (mins)	Sample	Batch Temp. (°C)	Mn	Mw	Mw/Mn	Conversion (Norm. Mtd) (%)	Conversion (Ext. Std Mtd) (%)	Comments
0		86.3				0	0	
20	O20	93.0	19864	29111	1.466	17.728	16.766	
40	O40	95.4	19215	29364	1.528	33.538	33.055	
60	O60	96.2	19292	30335	1.572	46.963	47.680	
80	O80	97.3	19339	30599	1.582	56.27	59.539	

Run E7

Time (mins)	Sample	Batch Temp. (°C)	Mn	Mw	Mw/Mn	Conversion (Norm. Mtd) (%)	Conversion (Ext. Std Mtd) (%)	Comments
0		86.4				0	0	
20	P20	93.7	19492	29068	1.491	18.809	17.801	
40	P40	95.4	19414	29487	1.519	35.007	34.436	
60	P60	96.0	19617	30493	1.554	48.076	48.994	
80	P80	96.3	19777	31626	1.599	57.992	60.399	

Run E8

Time (mins)	Sample	Batch Temp. (°C)	Mn	Mw	Mw/Mn	Conversion (Norm. Mtd) (%)	Conversion (Ext. Std Mtd) (%)	Comments
0		85.9				0	0	
20	Q20	93.8	20199	29894	1.480	18.650	17.692	
40	Q40	95.1	19911	30303	1.522	34.732	34.359	
60	Q60	96.4	19190	30175	1.572	47.801	48.738	
80	Q80	96.6	20228	31784	1.571	57.197	60.728	

E1.1.5. Kinetic Model

The modelling equation used to generate the kinetic model curve for comparison with the experimental batch data is:

$$x = 1 - \exp\{-2k_p\sqrt{f[I]_o/(k_d k_t)}(1 - e^{-k_d t/2})\} \qquad (2.29)$$

This equation has been derived in Chapter 2. All parameters used in the equation have also been defined in the same chapter.

The expressions for the various kinetics rate constants applicable to styrene polymerisation using benzoyl peroxide initiator which have been taken from the literature and used in the above equation are as follows:

	Ref.
$f k_d = 6.378 \times 10^{13} \exp\left(-29700/RT\right)$	[E1]
$f = 0.8$	[E2]
$k_p = 10^{7.630} \exp\left(-7740/RT\right)$	[E3,E4]
$k_t = 1.255 \times 10^{9} \exp\left(-1675/RT\right)$	[E1]

where R is the Universal gas constant = 1.986 cal/mol K
T is the reaction temperature in Kelvin

(See reference section at the end of this appendix for references given in square brackets)

With $[I]_o$ = 0.051mole/litre and f =0.8, the conversion data obtained over a time period of 220 minutes after taking into account the effects of increasing temperature (see Figure 5.1 in Chapter 5) in the reaction mixture are given below.

Time (min)	T (K)	k_d (s^{-1})	k_p (litre. mol^{-1} s^{-1})	k_t (litre. mol^{-1} s^{-1})	Conversion (%)
0	361	8.14E-05	843.0	1.21E+08	0
10	363	1.02E-04	894.8	1.23E+08	8.077
20	365	1.28E-04	949.2	1.24E+08	17.655
30	367	1.60E-04	1006.3	1.26E+08	28.255
40	369	2.00E-04	1066.1	1.28E+08	39.167
50	369	2.00E-04	1066.1	1.28E+08	45.325
60	369	2.00E-04	1066.1	1.28E+08	50.553

70	369	2.00E-04	1066.1	1.28E+08	55.019
80	369	2.00E-04	1066.1	1.28E+08	58.856
90	369	2.00E-04	1066.1	1.28E+08	62.170
100	369	2.00E-04	1066.1	1.28E+08	65.046
110	369	2.00E-04	1066.1	1.28E+08	67.555
120	369	2.00E-04	1066.1	1.28E+08	69.753
130	369	2.00E-04	1066.1	1.28E+08	71.687
140	369	2.00E-04	1066.1	1.28E+08	73.395
150	369	2.00E-04	1066.1	1.28E+08	74.909
160	369	2.00E-04	1066.1	1.28E+08	76.256
170	369	2.00E-04	1066.1	1.28E+08	77.459
180	369	2.00E-04	1066.1	1.28E+08	78.536
190	369	2.00E-04	1066.1	1.28E+08	79.503
200	369	2.00E-04	1066.1	1.28E+08	80.374
210	369	2.00E-04	1066.1	1.28E+08	81.160
220	369	2.00E-04	1066.1	1.28E+08	81.872

E1.2. SPINNING DISC POLYMERISATION DATA

For each spinning disc run, at least 3 product samples were collected from the collecting trough immediately after the disc stopped rotating. This was done after it was discovered early in the research programme during experiment A that some polymerisation still occurred while the product was left to stand for a couple of hours in the collector.

In the following sections, only data for feed and disc product samples will be presented for each disc run performed in each experimental set. Data about the progress of polymerisation during the prepolymer feed preparation stage in the batch reactor can be found in section E1.1 under the same run number where appropriate.

E1.2.1. Experiment A

The raw data for feed and SDR product samples collected from experiment A have been presented in a previous report as mentioned in Chapter 5. However, some adjustments to the reported disc product conversions were required as a result of styrene losses by evaporation as determined theoretically in Appendix C. The modified results will be given in this section.

Table E1. Increase in conversion in SDR for Experiment A

Feed time (mins)	Measured conv.[1] Feed (%)	Disc Product (%) (A)	Average feed conv. (from BCC) (%) (B)	(A)-(B) (%)	Adjusted Disc Product conv. (%)[2] (C)	(%)[3] (D)	Apparent disc prod. conversion due to loss[4] (%)	Increase in conv. due to polym.[5] (%)
15	11.93	21.61	13.30	-1.37	16.61	17.97	14.0	4.00
20	23.23	35.79	18.20	5.03	30.79	25.77	19.1	6.66
20	21.28	31.96	18.20	3.08	26.96	23.88	19.1	4.77
25	26.40	33.67	23.30	3.10	30.67	27.56	24.4	3.11
30	29.72	39.52	27.59	2.13	36.52	34.39	28.9	5.45
30	32.77	41.63	27.59	5.18	38.63	33.45	28.9	4.52
30	32.06	44.98	27.59	4.47	41.98	37.51	28.9	8.57

30	31.59	42.23	27.59	4.00	39.23	35.22	28.9	6.29
35	41.62	53.41	33.00	8.62	50.41	41.80	34.6	7.20
40	42.46	57.01	36.91	5.55	54.01	48.46	38.9	9.78

Notes

1) Data for the measured feed and averaged disc product conversions were obtained from a previous report on a preliminary study of styrene polymerisation in the SDR [E5].

2) The measured conversions for disc products are assumed to include loss of 3%-5% of monomer by evaporation which occurred during the feeding process onto the disc when the solution was left exposed to the atmosphere. The adjusted disc product conversions in column (C) represent the conversion of the product from the disc after accounting for this loss.

3) The fluctuations in measured feed conversions at a given batch reaction time are accounted for in the measured disc product conversion. Hence the value of the disc product conversion as given in column (D) in Table E1 is increased or decreased by the % difference in conversion between the measured (A) and average feed conversions (B) determined from the batch calibration curve (BCC).

4) The apparent disc product conversion has been estimated on the basis of styrene loss from the feed solution. The calculations procedures have been outlined in detail in Appendix C.

5) The increase in conversion due to polymerisation on the disc is obtained by the difference in the apparent conversion due to loss and the adjusted measured product conversion in column (D). It is used to calculate the time saving on the disc from the batch calibration curve as seen in Chapter 5.

E1.2.2. Experiment B

Run B1
Disc speed: 350-400 rpm
Disc temperature: 90°C
Variable Parameter: Feed conversion
Prepolymer feeding time (after start of reaction in batch): 40 minutes

	Sample	Vial V mass(g)	V+PS+S (g)	V+PS (g)	Conversion (%)	Comments
Feed	AF1	12.841	18.618	15.166	40.246	
Disc	AP1	12.839	13.607	13.198	46.686	
Product	AP2	12.916	15.422	14.126	48.278	
Samples	AP3	12.564	14.847	13.625	46.492	
	AP4	12.928	15.846	14.371	49.438	
Disc product average conversion					47.724	

Run B2

Disc speed: 350-400 rpm
Disc temperature: 89°C
Variable Parameter: Feed conversion
Prepolymer feeding time (after start of reaction in batch): **60 minutes**

	Sample	Vial V mass(g)	V+PS+S (g)	V+PS (g)	Conversion (%)	Comments
Feed	CF1	12.828	14.546	13.655	48.137	
Disc	CP1	12.292	13.753	13.163	59.606	
Product	CP2	12.892	14.304	13.823	65.963	
Samples	CP3	12.924	13.94	13.551	61.708	
	CP4	12.649	13.816	13.409	65.141	
Disc product average conversion					63.105	

Run B3

Disc speed: 350-400 rpm
Disc temperature: 89°C
Variable Parameter: Feed conversion
Prepolymer feeding time (after start of reaction in batch): **80 minutes**

	Sample	Vial V mass(g)	V+PS+S (g)	V+PS (g)	Conversion (%)	Comments
Feed	EF1	12.911	17.845	16.163	65.910	
Disc	EP1	10.113	12.082	11.765	83.891	
Product	EP2	10.011	11.458	11.267	86.808	
Samples	EP3	10.484	12.964	12.651	87.379	
	EP4	10.515	13.035	12.695	86.496	
Disc product average conversion					86.144	

Run B4

Disc speed: 350-400 rpm
Disc temperature: 89°C
Variable Parameter: Feed conversion
Prepolymer feeding time (after start of reaction in batch): **50 minutes**

	Sample	Vial V mass(g)	V+PS+S (g)	V+PS (g)	Conversion (%)	Comments
Feed	BF1	13.941	20.158	16.729	44.848	
Disc	BP1	13.843	21.782	18.183	54.672	
Product	BP2	12.406	21.616	17.754	58.063	
	BP3	11.953	19.201	16.077	56.903	
	BP4	13.291	21.598	17.920	55.724	
Disc product average conversion					56.341	

Run B5
Disc speed: 350-400 rpm
Disc temperature: 90°C
Variable Parameter: Feed conversion
Prepolymer feeding time (after start of reaction in batch): 70 minutes

	Sample	Vial V mass(g)	V+PS+S (g)	V+PS (g)	Conversion (%)	Comments
Feed	D70	12.638	18.038	15.712	56.932	
Disc Product	DP1	12.753	16.926	15.671	69.917	
	DP2	13.047	19.417	17.836	75.184	
	DP3	12.732	17.923	16.472	72.046	
	DP4	12.751	17.385	16.223	74.931	
Disc product average conversion					73.020	

Table E2. Increase in conversion in SDR for Experiment B

Run no.	Feed time (mins)	Measured conv. Feed (%) (A)	Measured conv. Disc Product (%)	Average feed conv. (from BCC) (%) (B)	(A)-(B) (%)	Adjusted Disc Product conv. (%)[1] (C)	Adjusted Disc Product conv. (%)[2] (D)	Apparent disc prod. conversion due to loss[3] (%)	Increase in conv. due to polym.[4] (%)
B1	40	40.25	47.72	37.00	3.25	44.72	41.47	38.7	8.57
B4	50	44.85	56.34	44.00	0.85	53.34	52.49	46.0	6.29
B2	60	48.15	63.10	49.98	-1.83	61.10	62.94	52.2	7.20
B5	70	56.93	73.02	57.07	-0.14	71.02	71.16	59.5	9.78
B3	80	65.92	86.14	62.00	3.92	84.14	80.22	64.6	2.76

Notes

1) The measured conversions for disc products are assumed to include loss of 2%-3% of monomer by evaporation which occurred during the feeding process onto the disc when the solution was left exposed to the atmosphere. The adjusted disc product conversions in column (C) represent the conversion of the product from the disc after accounting for this loss.

2) The fluctuations in measured feed conversions at a given batch reaction time are accounted for in the measured disc product conversion. Hence the value of the disc product conversion as given in column (D) in Table E2 is increased or decreased by the % difference in conversion between the measured (A) and average feed conversions (B).

3) The apparent disc product conversion has been estimated on the basis of styrene loss from the feed solution. The calculations procedures have been outlined in detail in Appendix C.

4) The increase in conversion due to polymerisation on the disc is obtained by the difference in the apparent conversion due to loss and the adjusted measured product conversion in column (D). It is used to calculate the time saving on the disc from the batch calibration curve as seen in Chapter 5.

E1.2.3. Experiment C

Run C1

Prepolymer feed time (after start of reaction in batch): 40 minutes
Disc temperature: 88°C
Variable Parameter: Disc speed
Disc speed: 500 rpm

Sample		M_n	M_w	M_w/M_n (DI)	Conversion (Norm. Mtd)	Comments
Feed	KF1	17732	27634	1.558	37.141	
Disc Product	KP1	17147	27363	1.596	43.915	
	KP2	18476	29669	1.606	47.750	
	KP3	17088	27320	1.599	47.383	
Disc Product Averages		17118	27342	1.600	46.349	

Run C3

Prepolymer feed time (after start of reaction in batch): 40 minutes
Disc temperature: 88°C
Variable Parameter: Disc speed
Disc speed: 750 rpm

Sample		M_n	M_w	M_w/M_n (DI)	Conversion (Norm. Mtd)	Comments
Feed	MF1	18529	28423	1.534	35.032	
Disc Product	MP1	18522	28479	1.538	46.835	
	MP2	18113	28324	1.564	49.558	
	MP3	17470	27724	1.587	34.427	Too low.∴reject
Disc Product Averages		18318	28402	1.551	48.197	

Run C4

Prepolymer feed time (after start of reaction in batch): 40 minutes
Disc temperature: 88°C
Variable Parameter: Disc speed
Disc speed: 1000 rpm

Sample		M_n	M_w	M_w/M_n (DI)	Conversion (Norm. Mtd)	Conversion (Ext. Std Mtd)	Comments
Feed	NF1(R)	19993	30894	1.545	29.699	28.445	
Disc Product	NP1(R)	18993	30182	1.589	43.04	40.961	
	NP2(R)	18127	29706	1.639	47.633	46.644	
	NP3(R)	18820	29992	1.594	45.069	43.310	
Disc Product Averages		18647	29960	1.607	45.247	43.638	

Run C6

Prepolymer feed time (after start of reaction in batch): 40 minutes
Disc temperature: 93°C
Variable Parameter: Disc speed
Disc speed: 300 rpm

	Sample	M_n	M_w	M_w/M_n (DI)	Conversion (Norm. Mtd)	Conversion (Ext. Std Mtd)	Comments
Feed	PF1	17923	28402	1.585	36.228	35.059	
Disc Product	PP1	17347	27984	1.613	46.079	45.811	
	PP2	17794	28266	1.589	51.785	50.633	
	PP3	17283	28325	1.639	47.294	46.735	
Disc Product Averages		17475	28192	1.614	46.687	46.273	

Run C7

Prepolymer feed time (after start of reaction in batch): 40 minutes
Disc temperature: 89°C
Variable Parameter: Disc speed
Disc speed: 900 rpm

	Sample	M_n	M_w	M_w/M_n (DI)	Conversion (Norm. Mtd)	Conversion (Ext. Std Mtd)	Comments
Feed	QF1	17325	27631	1.595	35.201	34.235	
Disc Product	QP1	16559	27438	1.657	57.422	58.438	
	QP2	16775	27522	1.641	51.804	51.461	
	QP3	16853	27434	1.628	55.071	54.731	
Disc Product Averages		16729	27465	1.642	54.766	54.877	

Run C8

Prepolymer feed time (after start of reaction in batch): 41 minutes
Disc temperature: 88.8°C
Variable Parameter: Disc speed
Disc speed: 800 rpm

	Sample	M_n	M_w	M_w/M_n (DI)	Conversion (Norm. Mtd)	Conversion (Ext. Std Mtd)	Comments
Feed	RF1(R)	18139	28814	1.589	32.30	31.656	
Disc Product	RP1(R)	17584	28233	1.606	58.79	62.606	Not reliable due to overpressure of HPLC pump ∴ rejected
	RP2(R)	17747	28318	1.596	45.74	44.858	
	RP3(R)	17605	28214	1.603	51.51	51.975	
	RP4(R)	17389	28128	1.618	48.26	47.563	
Disc Product Averages		17580	28220	1.605	48.501	48.132	

Run C9

Prepolymer feed time (after start of reaction in batch): 41.5 minutes
Disc temperature: 89°C
Variable Parameter: Disc speed
Disc speed: 850 rpm

	Sample	M_n	M_w	M_w/M_n (DI)	Conversion (Norm. Mtd)	Conversion (Ext. Std Mtd)	Comments
Feed	SF1(R)	18106	28489	1.573	34.53	34.647	
Disc Product	SP1(R)	17677	27994	1.584	56.77	60.387	
	SP2(R)	17108	27588	1.613	54.80	55.728	
	SP3(R)	17411	27820	1.598	62.63	64.801	Conv. too high ∴ reject
Disc Product Averages		17544	27907	1.591	55.788	58.058	

Run C10

Prepolymer feed time (after start of reaction in batch): 41.5 minutes
Disc temperature: 89.4°C
Variable Parameter: Disc speed
Disc speed: 600 rpm

	Sample	M_n	M_w	M_w/M_n (DI)	Conversion (Norm. Mtd)	Conversion (Ext. Std Mtd)	Comments
Feed	UF1	19149	29888	1.561	33.33	32.440	
Disc Product	UP1	18994	30045	1.582	46.56	44.902	
	UP2	18911	29713	1.571	49.76	49.957	
	UP3	18768	29713	1.583	48.55	47.784	
Disc Product Averages		18891	29824	1.579	48.289	47.548	

Table E3. Increase in conversion in SDR for Experiment C

Run no.	Disc speed (rpm)	Measured conv. Feed (%) (A)	Disc Product (%)	Average feed conv. (from BCC) (%) (B)	(A)-(B) (%)	Adjusted Disc Product conv. (%)[1] (C)	(%)[2] (D)	Apparent disc prod. conversion due to loss[3] (%)	Increase in conv. due to polym.[4] (%)
C6	300	36.23	46.48	36.39	-0.17	42.48	42.65	38.4	4.23
C2	400	36.8	47.72	36.39	0.41	43.72	43.32	38.4	4.90
C1	500	37.14	46.35	36.39	0.75	42.35	41.60	38.4	3.19
C10	600	33.33	47.92	36.39	-3.06	43.92	46.98	38.4	8.57
C3	750	35.03	48.20	36.39	-1.36	44.20	45.56	38.4	7.14
C8	800	32.30	48.32	36.39	-4.10	44.32	48.41	38.4	10.00
C9	850	34.53	59.19	36.39	-1.87	55.19	57.05	38.4	18.64
C7	900	35.20	54.82	36.39	-1.19	50.82	52.01	38.4	13.60
C4	1000	29.70	44.44	36.39	-6.69	40.44	47.13	38.4	8.72

Notes

1) The measured conversions for disc products are assumed to include loss of 4% of monomer by evaporation which occurred during the feeding process onto the disc

when the solution was left exposed to the atmosphere. The adjusted disc product conversions in column (C) represent the conversion of the product from the disc after accounting for this loss.

2) The fluctuations in measured feed conversions at a given batch reaction time are accounted for in the measured disc product conversion. Hence the value of the disc product conversion as given in column (D) in Table E3 is increased or decreased by the % difference in conversion between the measured (A) and average feed conversions (B).

3) The apparent disc product conversion has been estimated on the basis of styrene loss from the feed solution. The calculations procedures have been outlined in detail in Appendix C.

4) The increase in conversion due to polymerisation on the disc is obtained by the difference in the apparent conversion due to loss and the adjusted measured product conversion in column (D). It is used to calculate the time saving on the disc from the batch calibration curve as seen in Chapter 5.

E1.2.4. Experiment D

Run D4
Disc speed: 850 rpm
Disc temperature: 88°C
Variable Parameter: Feed conversion
Prepolymer feeding time (after start of reaction in batch): **80 minutes**

	Sample	M_n	M_w	M_w/M_n (DI)	Conversion (Norm. Mtd)	Conversion (Ext. Std Mtd)	Comments
Feed	GF1	19282	31185	1.617	51.532	51.209	
Disc Product	GP1	19163	31184	1.627	66.636	65.346	
	GP2	18643	30915	1.658	65.016	65.218	
	GP3	18227	30622	1.680	68.327	68.804	
Disc Product Averages		18678	30907	1.655	65.826	65.282	

Run D5
Disc speed: 850 rpm
Disc temperature: 88°C
Variable Parameter: Feed conversion
Prepolymer feeding time (after start of reaction in batch): **120 minutes**

	Sample	M_n	M_w	M_w/M_n (DI)	Conversion (Norm. Mtd)	Conversion (Ext. Std Mtd)	Comments
Feed	HF1	19338	32785	1.695	69.766	71.735	
Disc Product	HP1	19723	33017	1.674	83.715	86.891	
	HP2	19207	32765	1.706	84.736	87.398	
	HP3	19284	32889	1.706	84.219	87.350	
Disc Product Averages		19246	32827	1.706	84.223	87.213	

Run D6
Disc speed: 850 rpm
Disc temperature: 88°C
Variable Parameter: Feed conversion
Prepolymer feeding time (after start of reaction in batch): 100 minutes

	Sample	M_n	M_w	M_w/M_n (DI)	Conversion (Norm. Mtd)	Conversion (Ext. Std Mtd)	Comments
Feed	IF1	18263	30993	1.697	61.442	61.497	
Disc Product	IP1	20259	33392	1.648	75.314	76.488	
	IP2	18850	31352	1.663	81.923	84.197	
	IP3	18987	31620	1.665	81.463	84.508	
Disc Product Averages		18919	31486	1.664	79.567	81.731	

Run D7
Disc speed: 850 rpm
Disc temperature: 88°C
Variable Parameter: Feed conversion
Prepolymer feeding time (after start of reaction in batch): 60 minutes

	Sample	M_n	M_w	M_w/M_n (DI)	Conversion (Norm. Mtd)	Conversion (Ext. Std Mtd)	Comments
Feed	JF1	18703	29786	1.593	42.781	40.634	
Disc Product	JP1	18165	29500	1.624	52.643	51.810	
	JP2	18286	29461	1.611	54.632	53.303	
	JP3	18444	29788	1.615	52.188	50.804	
Disc Product Averages		18365	29625	1.613	53.154	51.972	

Run D8
Disc speed: 850 rpm
Disc temperature: 88°C
Variable Parameter: Feed conversion
Prepolymer feeding time (after start of reaction in batch): 90 minutes

	Sample	M_n	M_w	M_w/M_n (DI)	Conversion (Norm. Mtd)	Conversion (Ext. Std Mtd)	Comments
Feed	KF1	18997	31023	1.633	55.827	57.041	
Disc Product	KP1	18300	30509	1.667	67.863	68.642	
	KP2	17955	30321	1.689	71.047	71.259	
	KP3	18658	30976	1.660	70.866	71.285	
Disc Product Averages		18307	30649	1.674	70.957	71.272	

Run D9
Disc speed: 850 rpm
Disc temperature: 90°C
Variable Parameter: Feed conversion
Prepolymer feeding time (after start of reaction in batch): 40 minutes

	Sample	M_n	M_w	M_w/M_n (DI)	Conversion (Norm. Mtd)	Conversion (Ext. Std Mtd)	Comments
Feed	LF1	17969	28923	1.610	29.612	27.762	
Disc Product	LP1	17830	28688	1.609	41.391	39.130	
	LP2	18185	28838	1.586	40.853	37.723	
	LP3	18099	28883	1.596	42.3	39.976	
Disc Product Averages		18142	28861	1.591	41.515	38.943	

Table E4. Increase in conversion in SDR for Experiment D

Run no.	Feed time (mins)	Measured conv. Feed (%) (A)	Disc Product (%)	Average feed conv. (from BCC) (%) (B)	(A)-(B) (%)	Adjusted Disc Product conv. (%)[1] (C)	(%)[2] (D)	Apparent disc prod. conversion due to loss[3] (%)	Increase in conv. due to polym.[4] (%)
D9	40	27.76	38.94	29.0	-1.24	34.94	36.18	30.2	6.03
D7	60	40.63	51.97	42.0	-1.37	47.97	49.34	43.6	5.78
D4	80	51.21	65.55	52.0	-0.79	62.55	63.35	53.8	9.55
D8	90	57.04	71.27	56.0	1.04	68.27	67.23	57.9	9.36
D6	100	61.50	81.73	61.0	0.50	79.73	79.23	62.9	16.29
D5	120	71.74	87.21	67.0	4.74	85.21	80.48	69.0	11.49

Notes

1) The measured conversions for disc products are assumed to include loss of 2%-4% of monomer by evaporation which occurred during the feeding process onto the disc when the solution was left exposed to the atmosphere. The adjusted disc product conversions in column (C) represent the conversion of the product from the disc after accounting for this loss.

2) The fluctuations in measured feed conversions at a given batch reaction time are accounted for in the measured disc product conversion. Hence the value of the disc product conversion as given in column (D) in Table E4 is increased or decreased by the % difference in conversion between the measured (A) and average feed conversions (B).

3) The apparent disc product conversion has been estimated on the basis of styrene loss from the feed solution. The calculations procedures have been outlined in detail in Appendix C.

4) The increase in conversion due to polymerisation on the disc is obtained by the difference in the apparent conversion due to loss and the adjusted measured product conversion in column (D). It is used to calculate the time saving on the disc from the batch calibration curve as seen in Chapter 5.

E1.2.5. Experiment E

Experiment E was performed after the new disc thermocouples and slip ring assembly as described in section 4.2.2.1.2 in Chapter 4 were fitted. The location of the four thermocouples in the disc were as follows:

T1: 11 mm below disc surface at radial distance of 168mm
T2: 2mm below the disc surface at radial distance of 168mm
T3: 2mm below the disc surface at radial distance of 75mm
T4: 11mm below the disc surface at radial distance of 75mm

Temperature readings from all four thermocouples were recorded during the course of each run and an average value was then calculated.

Run E1

Prepolymer feed time (after start of reaction in batch): 80 minutes
Disc temperature: T_1= 88.5°C
T_2= 90.3°C
T_3= 89.3°C
T_4= 89.2°C
T(ave)= 89.325°C
Variable Parameter: Disc speed
Disc speed: 400 rpm

	Sample	M_n	M_w	M_w/M_n (DI)	Conversion (Norm. Mtd)	Conversion (Ext. Std Mtd)	Comments
Feed	JF1	19591	31165	1.591	55.823	58.620	
Disc Product	JP1	18910	30355	1.605	66.205	68.486	
	JP2	19167	30752	1.604	66.411	69.876	
	JP3	19540	31465	1.610	67.514	70.151	
	JP4	19212	30894	1.608	67.437	71.258	
Disc Product Averages		19221	30905	1.608	66.892	69.943	

Run E2

Prepolymer feed time (after start of reaction in batch): 80 minutes
Disc temperature: T_1=85°C
T_2= 91.2°C
T_3= 87.7°C
T_4= 88.1°C
T(ave)= 88°C
Variable Parameter: Disc speed
Disc speed: 800 rpm

	Sample	M_n	M_w	M_w/M_n (DI)	Conversion (Norm. Mtd)	Conversion (Ext. Std Mtd)	Comments
Feed	KF1	19519	31359	1.607	57.855	60.933	
Disc Product	KP1	19331	31053	1.606	73.151	76.955	
	KP2	19400	31532	1.625	71.967	76.572	
	KP3	18967	31199	1.645	73.177	76.641	

KP4	19265	31316	1.626	73.43	78.238
Disc Product Averages	19241	31275	1.619	72.931	77.101

Run E3

Prepolymer feed time (after start of reaction in batch): 80 minutes

Disc temperature: T_1=83.6°C
T_2=90.6°C
T_3=84.5°C
T_4=82.5°C
T(ave)= 85.3°C

Variable Parameter: Disc speed

Disc speed: 1200 rpm

	Sample Comments	M_n	M_w	M_w/M_n (DI)	Conversion (Norm. Mtd)	Conversion (Ext. Std Mtd)	
Feed	LF1(F)	19860	31168	1.569	62.625	64.085	
Disc Product	LP1	19880	31133	1.566	70.753	74.701	Viscosity and conv. too low ∴ reject
	LP2	19102	30773	1.611	76.288	80.633	
	LP3	19563	31303	1.600	74.063	79.061	
	LP4	18899	30393	1.608	76.683	81.478	
Disc Product Averages		19188	30823	1.606	75.678	80.391	

General remarks and observations

(1) Disc temperatures T1, T3 & T4 declined very rapidly from 88-89°C as the disc was brought up to the required speed before the feed was introduced into the disc. However, it is believed that the erroneous readings were caused by the high speed of disc rotation which affected the connection of the thermocouples through the slip ring assembly. The disc temperature was therefore considered to be within the required range of 88-90°C in spite of the low readings.

(2) The feed sample in this run LF1(F) was taken from the end of the funnel (hence the (F) for funnel) which delivered the melt to the distributor tube system of the SDR. This was done to verify whether any major change in conversion occurred in the hot feed while it was left exposed to the atmosphere during the feeding process. It was indeed found that about 2-4% apparent increase in conversion took place as a result of styrene evaporation from the exposed feed. Hence in all subsequent runs, the funnel was covered by a lid while feeding took place to eliminate any styrene loss by evaporation. The similarity in conversion between samples from the batch immediately prior to feeding and from the end of the funnel during feeding indicated that almost no loss occurred.

Run E4

Prepolymer feed time (after start of reaction in batch): 80 minutes

Disc temperature: T_1=83.6°C
T_2=87.4°C
T_3=84.2°C
T_4=82.5°C
T(ave.)= 84.425°C

Variable Parameter: Disc speed

Disc speed: **1000 rpm**

	Sample Comments	M_n	M_w	M_w/M_n (DI)	Conversion (Norm. Mtd)	Conversion (Ext. Std Mtd)
Feed	MF1(F)	19698	31502	1.599	57.01	60.790
Disc Product	MP1	19647	31324	1.594	72.832	76.630
	MP2	19673	31582	1.605	74.159	78.565
	MP3	19848	31867	1.606	72.548	80.007
	MP4	19532	31248	1.600	72.685	77.627
Disc Product Averages		19675	31505	1.601	73.056	78.207

General remarks and observations

Again, as in Run E3, thermocouples T1, T3 & T4 read low temperatures as disc was spinning at high speed for more than 15 minutes. The attributed cause was as in (2) above.

Run E5

Prepolymer feed time (after start of reaction in batch): 80 minutes

Disc temperature: T_1=88.5°C
T_2=88.5°C
T_3=89.3°C
T_4=87.9°C
T(ave)= 88.55°C

Variable Parameter: Disc speed

Disc speed: **600 rpm**

	Sample Comments	M_n	M_w	M_w/M_n (DI)	Conversion (Norm. Mtd)	Conversion (Ext. Std Mtd)
Feed	NF1(F)	20332	32987	1.622	53.935	56.785
Disc Product	NP1	20090	32655	1.625	67.655	69.955
	NP2	20648	33718	1.633	67.04	70.289
	NP3	19949	32715	1.640	69.134	71.806
	NP4	20512	33488	1.633	69.203	72.392
Disc Product Averages		20300	33144	1.633	68.258	71.111

Run E6

Prepolymer feed time (after start of reaction in batch): 80 minutes

Disc temperature: T_1=88.0°C
T_2=89.4°C
T_3=90.2°C
T_4=89.2°C
T(ave)= 89.2°C

Variable Parameter: Disc speed

Disc speed: **1500 rpm**

	Sample Comments	M_n	M_w	M_w/M_n (DI)	Conversion (Norm. Mtd)	Conversion (Ext. Std Mtd)	
Feed	OF1(F)	19816	31673	1.598	58.935	61.595	
Disc Product	OP1	19777	31389	1.587	77.605	84.798	Too high ∴ reject
	OP2	19415	31156	1.605	73.112	76.768	
	OP3	19092	31018	1.625	71.681	75.927	
	OP4	19367	31076	1.605	72.584	76.002	
Disc Product Averages		19291	31083	1.611	72.459	76.232	

Run E7 (Repeat of Run E3)

Prepolymer feed time (after start of reaction in batch): 80 minutes

Disc temperature: T_1=89.9°C
T_2=90.8°C
T_3=91.0°C
T_4=89.0°C
T(ave)= 90.175°C

Variable Parameter: Disc speed

Disc speed: **1200 rpm**

	Sample Comments	M_n	M_w	M_w/M_n (DI)	Conversion (Norm. Mtd)	Conversion (Ext. Std Mtd)
Feed	PF1(F)	19353	30744	1.589	57.246	60.333
Disc Product	PP1	19504	31293	1.604	69.519	72.147
	PP2	19679	31329	1.592	69.158	72.854
	PP3	19209	30803	1.604	72.171	75.502
	PP4	19392	31451	1.622	71.547	75.867
Disc Product Averages		19446	31219	1.605	70.599	74.092

Run E8 (Repeat of Run E6)

Prepolymer feed time (after start of reaction in batch): 80 minutes

Disc temperature: T_1=89.1°C
T_2=92.1°C
T_3=89.3°C
T_4=91.2°C

T(ave)= 90.425°C

Variable Parameter: Disc speed

Disc speed: **1500 rpm**

	Sample Comments	M_n	M_w	M_w/M_n (DI)	Conversion (Norm. Mtd)	Conversion (Ext. Std Mtd)
Feed	QF1(F)	19755	31933	1.616	59.720	62.866
Disc Product	QP1	19879	31557	1.587	74.969	80.104
	QP2	19875	31561	1.588	76.081	80.601
	QP3	19359	30772	1.590	74.314	78.248
	QP4	19691	31649	1.607	73.978	77.646
Disc Product Averages		19701	31385	1.593	74.835	79.150

Table E5. Increase in conversion in SDR for Experiment E

Run no.	Disc speed (rpm)	Measured conv. Feed (%) (A)	Measured conv. Disc Product (%)	Average feed conv. (from BCC) (%) (B)	(A)-(B) (%)	Adjusted Disc Product conv. (%)[1] (C)	Adjusted Disc Product conv. (%)[2] (D)	Apparent disc prod. conversion due to loss[3] (%)	Increase in conv. due to polym.[4] (%)
E1	400	58.62	69.94	58.0	0.62	66.94	66.32	60.1	6.20
E5	600	57.65	71.11	58.0	-0.35	71.11	71.46	60.1	11.34
E2	800	59.23	77.1	58.0	1.23	74.1	72.87	60.1	12.75
E4	1000	60.79	78.21	58.0	2.79	78.21	75.42	60.1	15.30
E3	1200	61.0	80.39	58.0	3.0	77.39	74.39	60.1	14.27
E7	1200	60.33	74.09	58.0	2.33	74.09	71.76	60.1	11.64
E6	1500	61.59	76.23	58.0	3.59	76.23	72.64	60.1	12.52
E8	1500	60.73	79.15	58.0	2.73	77.15	74.42	60.1	14.30

Notes

1) The measured conversions for disc products in Runs E1 to E3 are assumed to include loss of 2%-3% of monomer by evaporation which occurred during the feeding process onto the disc when the solution was left exposed to the atmosphere. The adjusted disc product conversions in column (C) represent the conversion of the product from the disc after accounting for this loss.

2) The fluctuations in measured feed conversions at a given batch reaction time are accounted for in the measured disc product conversion. Hence the value of the disc product conversion as given in column (D) in Table E5 is increased or decreased by the % difference in conversion between the measured (A) and average feed conversions (B).

3) The apparent disc product conversion has been estimated on the basis of styrene loss from the feed solution. The calculations procedures have been outlined in detail in Appendix C.

4) The increase in conversion due to polymerisation on the disc is obtained by the difference in the apparent conversion due to loss and the adjusted measured product conversion in column (D). It is used to calculate the time saving on the disc from the batch calibration curve as seen in Chapter 5.

References

E1. Biesenberger, J.A. and Sebastian, D.H., *Principles of Polymerisation Engineering*, Ch.1, pp. 79, John Wiley & Sons, New York, 1983

E2. Moad, G. and Solomon, D.H., *The Chemistry of Free-Radical Polymerisation*, Ch.3, pp. 43-144, Elsevier Science, Oxford, 1995

E3. Buback, M. et *al.*, Critically evaluated rate coefficients for free-radical polymerisation. I. Propagation rate coefficient for styrene. *Macromol. Chem. Phys.*, **196**, 3267-3280 (1995)

E4. Berger, K.C. and Meyerhoff, G., Propagation and termination constants in free-radical polymerisation, in *Polymer Handbook* (J. Brandrup and E.H. Immergut, Eds.), 3rd ed., Wiley-Interscience, New York, pp.II/67-II/79, 1989.

E5. Boodhoo, K., Spinning disc polymeriser for the production of polystyrene, *MEng. Report*, University of Newcastle Upon Tyne (1995)

Appendix F

Batch Agitation Experimental Data

F1. INTRODUCTION

This appendix contains details of the relevant measured data relating to samples collected from agitation experiments performed in a batch reactor. Kinetic modelling data to predict conversion levels at continuously changing temperatures and the calibration data for the portable stroboscope will also be included in this appendix. The apparatus and experimental procedures used in the agitation runs have been described in Chapter 4. Analysis and discussion of the data have been presented in Chapters 5 (section 5.2) and 6 (section 6.3) respectively.

Four different speeds of 70-90 rpm, 500 rpm, 1000 rpm and 1500 rpm were investigated with a duplicate run carried out at 500 rpm to check the accuracy of the measurements. The following recipe was used in all runs: 225 ml styrene, 45 ml toluene and 3.375 g benzoyl peroxide. All volumetric quantities were measured at room temperature. The given quantities correspond to concentrations of 7.28, 1.567 and 0.0517 moles/litre of styrene, toluene and benzoyl peroxide respectively which are the same concentrations used in the polymerisation study in the SDR (see Appendix E).

All sample analysis were performed by GPC which gave conversion, average molecular weights and polydispersity index for individual samples. As seen below, conversion calculated by both the normalisation method and the external standard method (see details of both methods in Appendix D) are given to enable a direct comparison. Since the two values agree quite reasonably, an average was taken as the experimental conversion.

F1.1. EXPERIMENTAL DATA

Run 1

Agitator speed: **500 rpm**

Time (mins)	Sample	Batch Temp. (°C)	M_n	M_w	M_w/M_n	Conversion (Norm. Mtd) (%)	Conversion (Ext. Std Mtd) (%)	Comments
0		84.8				0	0	
20	EM20	90.5	19875	30376	1.528	14.408	12.871	
40	EM40	90.4	19149	30384	1.587	27.959	25.668	
60	EM60	90.4	19228	31190	1.622	37.900	36.152	
80	EM80	90.2	20046	31841	1.588	47.586	46.254	
100	EM100	90.4	19791	33054	1.670	52.302	52.094	
120	EM120	90.0	19871	33738	1.698	61.242	61.605	Very viscous
140	EM140	88.6	21269	35679	1.678	66.340	67.957	As above

Run 2

Agitator speed: 1000 rpm

Time (mins)	Sample	Batch Temp. (°C)	M_n	M_w	M_w/M_n	Conversion (Norm. Mtd) (%)	Conversion (Ext. Std Mtd) (%)	Comments
0		83.9				0	0	
20	FM20	88.8	20814	31867	1.531	13.147	11.758	
40	FM40	88.7	20871	32699	1.567	24.037	22.270	
60	FM60	89.0	20246	32410	1.601	35.138	32.997	
80	FM80	88.7	20890	33731	1.615	43.156	41.646	
100	FM100	85.8	20989	34289	1.634	50.015	49.284	
120	FM120	84.8	21656	35692	1.648	54.028	53.941	Very viscous, no vortex
140	FM140	83.0	21764	36542	1.679	60.285	61.175	As above
143	FM143(bulk)		22443	37251	1.660	58.215	58.830	As above

General remark

Significant vortex formation in the agitated mixture until reaction time of 120 minutes.

Note

In this and all subsequent runs, a sample was taken at the end of the run from inside the reactor in order to ensure that the sample delivered from the tap at the bottom of the glass reactor was representative of the bulk of the mixture.

Run 3

Agitator speed: 1500 rpm

Time (mins)	Sample	Batch Temp. (°C)	M_n	M_w	M_w/M_n	Conversion (Norm. Mtd) (%)	Conversion (Ext. Std Mtd) (%)	Comments
0		81.4				0	0	
10	GM10	86.3	24603	34383	1.398	6.598	5.793	
40	GM40	87.0	22246	33982	1.528	21.497	19.635	
60	GM60	87.6	21518	33928	1.577	31.647	29.610	
80	GM80	86.8	21185	34236	1.616	37.912	36.230	
100	GM100	85.0	21921	35265	1.609	45.090	43.629	
120	GM120	83.2	21622	35928	1.662	48.120	47.295	
140	GM140	83.1	21953	36737	1.673	55.639	55.093	
141.5	GM141.5(bulk)		22911	37699	1.645	53.696	53.667	

General remark

Extreme vortices observed at this speed throughout the run.

Run 4

Agitator speed: **70-90 rpm**

Time (mins)	Sample	Batch Temp. (°C)	M_n	M_w	M_w/M_n	Conversion (Norm. Mtd) (%)	Conversion (Ext. Std Mtd) (%)	Comments
0		85.4				0	0	
20	HM20	94.3	18811	28474	1.514	19.604	18.808	
40	HM40	93.0	17375	27970	1.610	36.902	36.516	
60	HM60	92.3	17782	29154	1.640	47.634	49.245	
80	HM80	95.2	18547	30634	1.652	59.541	62.503	very viscous
100	HM100	92.3	19455	32776	1.685	68.268	74.565	As above
110	HM110	93.3	19390	32944	1.699	71.654	77.453	As above
112	HM112(Bulk)		19918	33802	1.697	69.295	75.808	As above

General remark

The stroboscope could not record such a low speed which had to be calculated instead by timing 30 revolutions at regular intervals of time.

Run 5 (Repeat of Run 1)

Agitator speed: **500 rpm**

Time (mins)	Sample	Batch Temp. (°C)	M_n	M_w	M_w/M_n	Conversion (Norm. Mtd) (%)	Conversion (Ext. Std Mtd) (%)	Comments
0		84.6				0	0	
20	IM20	90.6	20310	30448	1.499	15.226	14.363	
40	IM40	90.6	20033	31117	1.553	29.076	28.349	
60	IM60	90.6	19864	31523	1.587	37.200	37.238	
80	IM80	90.5	20030	32244	1.610	47.633	48.545	
100	IM100	90.3	20682	33896	1.639	54.469	58.298	very viscous
120	IM120	89.5	21001	34681	1.651	61.960	65.231	As above
122	IM122(Bulk)		20960	35061	1.673	59.403	62.668	As above

F1.2. KINETIC MODELLING

The approach to deriving the model curves is similar to the one given in section E1.1.5 in Appendix E. The same modelling equation has been used:

$$x = 1 - \exp\{-2k_p\sqrt{f[I]_o/(k_d k_t)}(1 - e^{-k_d t/2})\} \qquad (2.29)$$

All parameters used in the above equation have been defined in Chapter 2.

The expressions for the various kinetics rate constants applicable to styrene polymerisation using benzoyl peroxide initiator which have been used in the above equation are as follows:

	Ref.
$f k_d = 6.378 \times 10^{13} \exp\left(-29700/RT\right)$	[F1]
$f = 0.8$	[F2]

$$k_p = 10^{7.630} \exp\left(-7740/RT\right) \qquad [F3,F4]$$

$$k_t = 1.255 \times 10^{9} \exp\left(-1675/RT\right) \qquad [F1]$$

where R is the Universal gas constant = 1.986 cal/mol K
T is the reaction temperature in Kelvin

With $[I]_o$ = 0.051mole/litre and an assumed value for f of 0.8, the conversion data obtained according to the changes in temperature for each agitation speed are given below.

Run1
Agitator speed: **500 rpm**

Time (min)	T (K)	k_d (s^{-1})	k_p (litre. mol^{-1} s^{-1})	k_t (litre. mol^{-1} s^{-1})	Conversion (%)
0	357.8	5.62E-05	765.1	1.19E+08	0
20	363.5	1.08E-04	908.2	1.23E+08	15.854
40	363.4	1.07E-04	905.5	1.23E+08	28.241
60	363.4	1.07E-04	905.5	1.23E+08	38.274
80	363.2	1.05E-04	900.1	1.23E+08	45.943
100	363.4	1.07E-04	905.5	1.23E+08	53.054
120	363.0	1.02E-04	894.8	1.23E+08	57.618
140	361.6	8.72E-05	858.3	1.22E+08	59.008

Run 2
Agitator speed: **1000 rpm**

Time (min)	T (K)	k_d (s^{-1})	k_p (litre. mol^{-1} s^{-1})	k_t (litre. mol^{-1} s^{-1})	Conversion (%)
0	356.9	5.06E-05	744.4	1.18E+08	0
20	361.8	8.92E-05	863.4	1.22E+08	13.985
40	361.7	8.82E-05	860.8	1.22E+08	25.262
60	362.0	9.13E-05	868.6	1.22E+08	35.291
80	361.7	8.82E-05	860.8	1.22E+08	42.485
100	358.8	6.31E-05	788.8	1.20E+08	42.131
120	357.8	5.62E-05	765.1	1.19E+08	45.058
140	356.0	4.55E-05	724.0	1.17E+08	45.211

Run 3
Agitator speed: **1500 rpm**

Time (min)	T (K)	k_d (s^{-1})	k_p (litre. mol^{-1} s^{-1})	k_t (litre. mol^{-1} s^{-1})	Conversion (%)
0	354.4	3.76E-05	689.0	1.16E+08	0
10	359.3	6.69E-05	800.9	1.20E+08	6.014
40	360.0	7.26E-05	818.0	1.21E+08	22.484
60	360.6	7.77E-05	832.9	1.21E+08	32.402
80	359.8	7.09E-05	813.1	1.20E+08	38.175

100	358.0	5.75E-05	769.8	1.19E+08	40.254
120	356.2	4.66E-05	728.5	1.18E+08	41.181
140	356.1	4.60E-05	726.3	1.18E+08	45.460

Run 4
Agitator speed: **70-90 rpm**

Time (min)	T (K)	k_d (s^{-1})	k_p (litre. mol^{-1} s^{-1})	k_t (litre. mol^{-1} s^{-1})	Conversion (%)
0	358.4	6.03E-05	779.3	1.19E+08	0
20	367.3	1.66E-04	1015.1	1.26E+08	20.695
40	366.0	1.43E-04	977.4	1.25E+08	33.138
60	365.3	1.33E-04	957.6	1.25E+08	42.425
80	368.2	1.83E-04	1041.9	1.27E+08	57.184
100	365.3	1.33E-04	957.6	1.25E+08	57.403
110	366.3	1.48E-04	986.0	1.26E+08	62.341

Run 5 (Repeat of Run 1)
Agitator speed: **500 rpm**

Time (min)	T (K)	k_d (s^{-1})	k_p (litre. mol^{-1} s^{-1})	k_t (litre. mol^{-1} s^{-1})	Conversion (%)
0	357.6	5.49E-05	760.5	1.19E+08	0
20	363.6	1.09E-04	910.9	1.23E+08	15.970
40	363.6	1.09E-04	910.9	1.23E+08	28.604
60	363.6	1.09E-04	910.9	1.23E+08	38.707
80	363.5	1.08E-04	908.2	1.23E+08	46.636
100	363.3	1.06E-04	902.8	1.23E+08	52.820
120	362.5	9.66E-05	881.6	1.23E+08	56.453

F1.3. CALIBRATION OF MOTOR SPEED

The motor driving the agitator shaft had 10 different speed settings on the controls. With the agitator immersed in a solution made up of 200 ml styrene and 40 ml toluene (measured at room temperature) and heated to 88-90°C, a calibration of the motor speed settings was performed. Actual speed measurements to an accuracy of ± 1 rpm were recorded by a portable stroboscope. The calibration data are presented in Figure F1 below.

Unfortunately speed settings beyond 7 could not be calibrated due to the formation of extreme vortices in the mixture which made operation at such high speeds impractical. It is to be noted that although the above calibration data was useful in setting the initial speed of the motor at the start of each experiment, the speed nevertheless had to be monitored intermittently during the course of the polymerisation by the strobe. This was mainly done because of the build-up of viscosity with increasing conversion which inevitably slowed down the impeller.

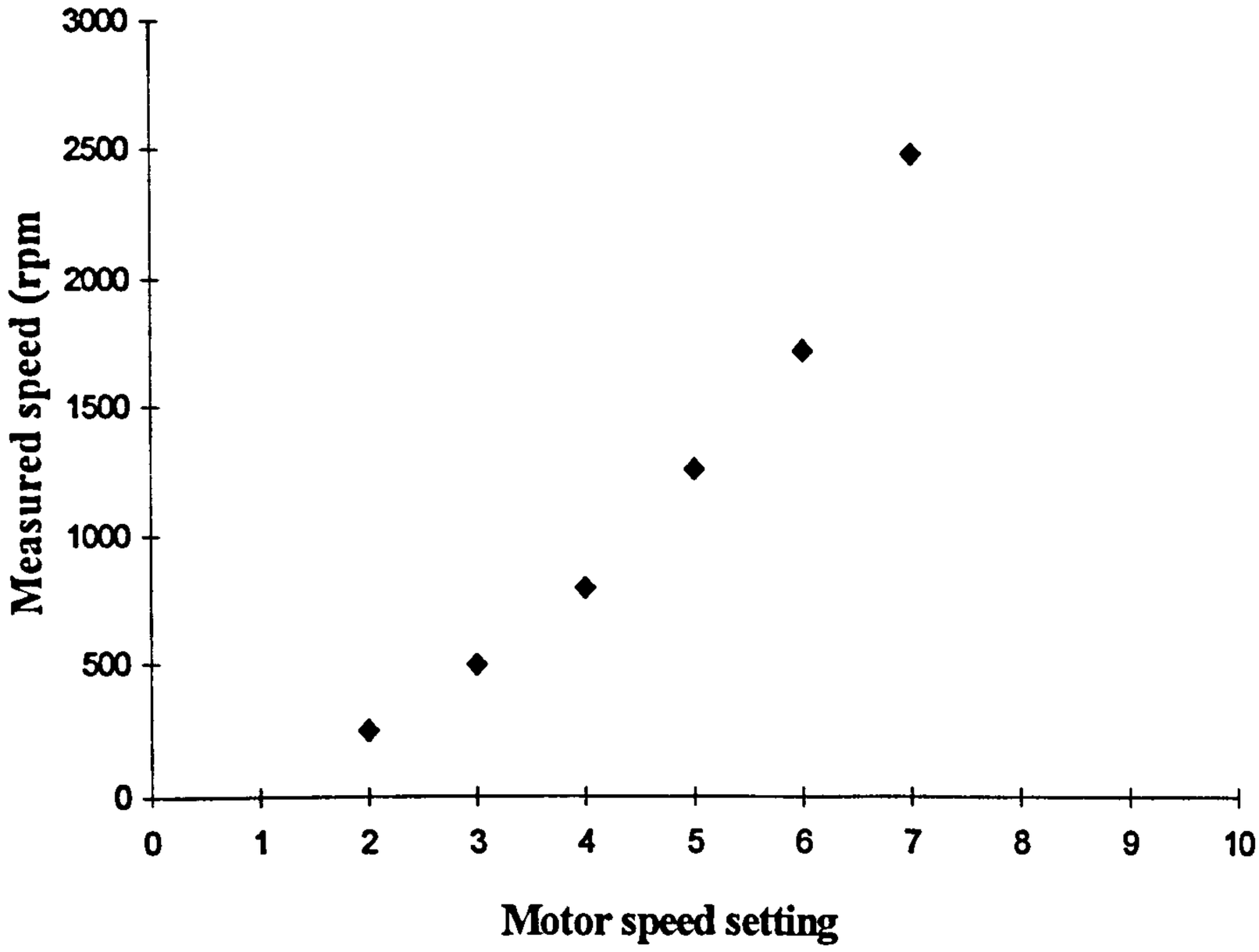

Figure F1. Calibration of motor speed

References

F1. Biesenberger, J.A. and Sebastian, D.H., *Principles of Polymerisation Engineering*, Ch.1, pp. 79, John Wiley & Sons, New York, 1983

F2. Moad, G. and Solomon, D.H., *The Chemistry of Free-Radical Polymerisation*, Ch.3, pp. 43-144, Elsevier Science, Oxford, 1995

F3. Buback, M. et *al.*, Critically evaluated rate coefficients for free-radical polymerisation. I. Propagation rate coefficient for styrene. *Macromol. Chem. Phys.*, **196**, 3267-3280 (1995)

F4. Berger, K.C. and Meyerhoff, G., Propagation and termination constants in free-radical polymerisation, in *Polymer Handbook* (J. Brandrup and E.H. Immergut, Eds.), 3rd ed., Wiley-Interscience, New York, pp.II/67-II/79, 1989.

Appendix G

Viscometry And Density Data

G1. INTRODUCTION

Two separate batch runs, Run V1 and Run V2, were performed to collect samples used to determine the viscosity of different concentrations of polystyrene dissolved in a styrene/toluene solution. The rheological behaviour of each sample was analysed in a viscometer apparatus which has been described in Chapter 4. The measured data relating to the viscometry analysis will be presented in this appendix.

Also, the density of polymer solutions over a wide range of polymer concentration will be estimated by a density correlation. The density data presented in this appendix was used in all calculations in this research.

G1.1. VISCOSITY MEASUREMENTS

The starting recipe for each of the runs V1 and V2 is as follows: 200 ml styrene, 40 ml toluene and 3.0 g BPO. All volumetric quantities were measured at room temperature. The given quantities correspond to concentrations of 7.28, 1.567 and 0.0517 moles/litre of styrene, toluene and benzoyl peroxide respectively. They are exactly the same concentrations used in Experiments C, D and E for polymerisation in the spinning disc reactor.

Sample conversion and molecular weight properties as determined by gel permeation chromatography (GPC) are given below.

Run V1

Time (mins)	Sample	Batch Temp. (°C)	M_n	M_w	M_w/M_n	Conversion (Norm. Mtd) (%)	Conversion (Ext. Std Mtd) (%)	Comments
0		86.4				0	0	
20	VA20	93.6	17673	26390	1.493	19.273	18.550	
40	VA40	94.2	18230	28076	1.540	35.711	35.790	
60	VA60	94.8	17357	28998	1.671	49.668	51.252	
80	VA80	94.6	18307	30210	1.650	57.474	61.263	
100	VA100	95.5	18349	30920	1.685	66.448	71.444	
120	VA120	96.1	18978	32452	1.710	71.973	79.090	
140	VA140	101.1	20118	34294	1.705	79.441	88.428	High temp. due to loss of agitation

Run V2

Time (mins)	Sample	Batch Temp. (°C)	M_n	M_w	M_w/M_n	Conversion (Norm. Mtd) (%)	Conversion (Ext. Std Mtd) (%)	Comments
0		87.8				0	0	
20	VB20	93.1	18863	28405	1.506	18.743	18.161	

40	VB40	94.1	18276	29514	1.615	34.322	34.267
60	VB60	94.7	17875	29306	1.639	45.757	47.538
80	VB80	94.7	19092	30950	1.621	56.477	59.367
100	VB100	94.5	19420	32039	1.650	63.285	68.660
120	VB120	97	19475	33117	1.700	70.604	77.159
140	VB140	97	20721	35503	1.713	76.572	85.151

G1.1.1. Rheological behaviour

G1.1.1.1. Concentration dependence of viscosity

Rheological plots of the apparent viscosity η_a at various shear rates for a range of concentrations can be seen in Figures G1 and G2. All measurements presented here were obtained at a temperature of 35°C.

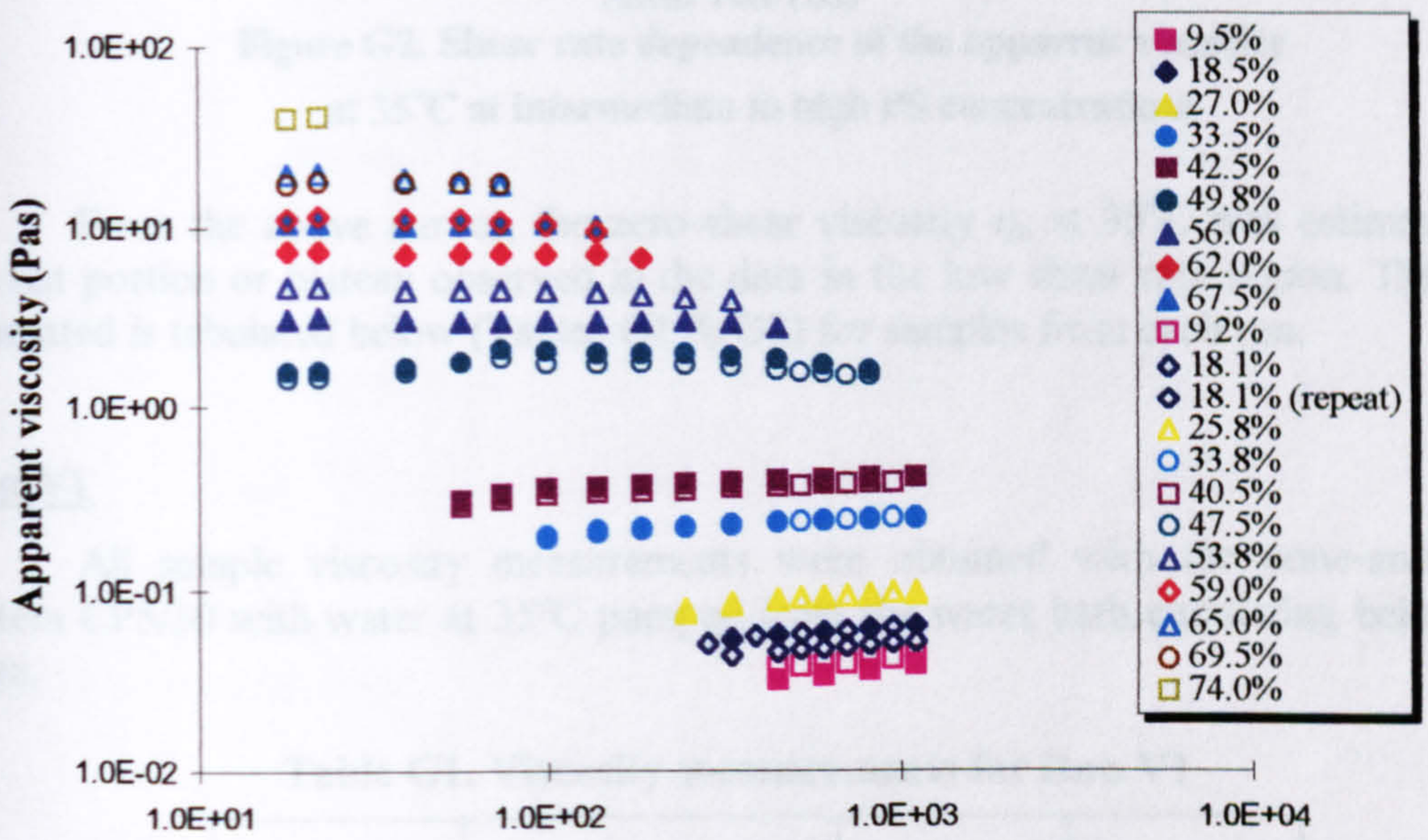

Figure G1. Shear rate dependence of the apparent viscosity at 35°C at low to intermediate PS concentrations
(Filled labels-Run V1, unfilled labels-Run V2)

The marked difference in viscosity for each separate run V1 & V2 at similar concentrations as seen in Figure G1 is most likely due to the higher molecular weight for samples from run V2, especially beyond 60 minutes of reaction time in the batch or 47.5% conversion. The molecular weight differences are related to the variations in temperature in the batch reactor which become more pronounced at high polymer concentrations as a result of non-uniform mixing. The rheological data presented here compares reasonably well with the measurements of Ide and White for various concentrations of higher molecular weight PS in styrene solutions [G1].

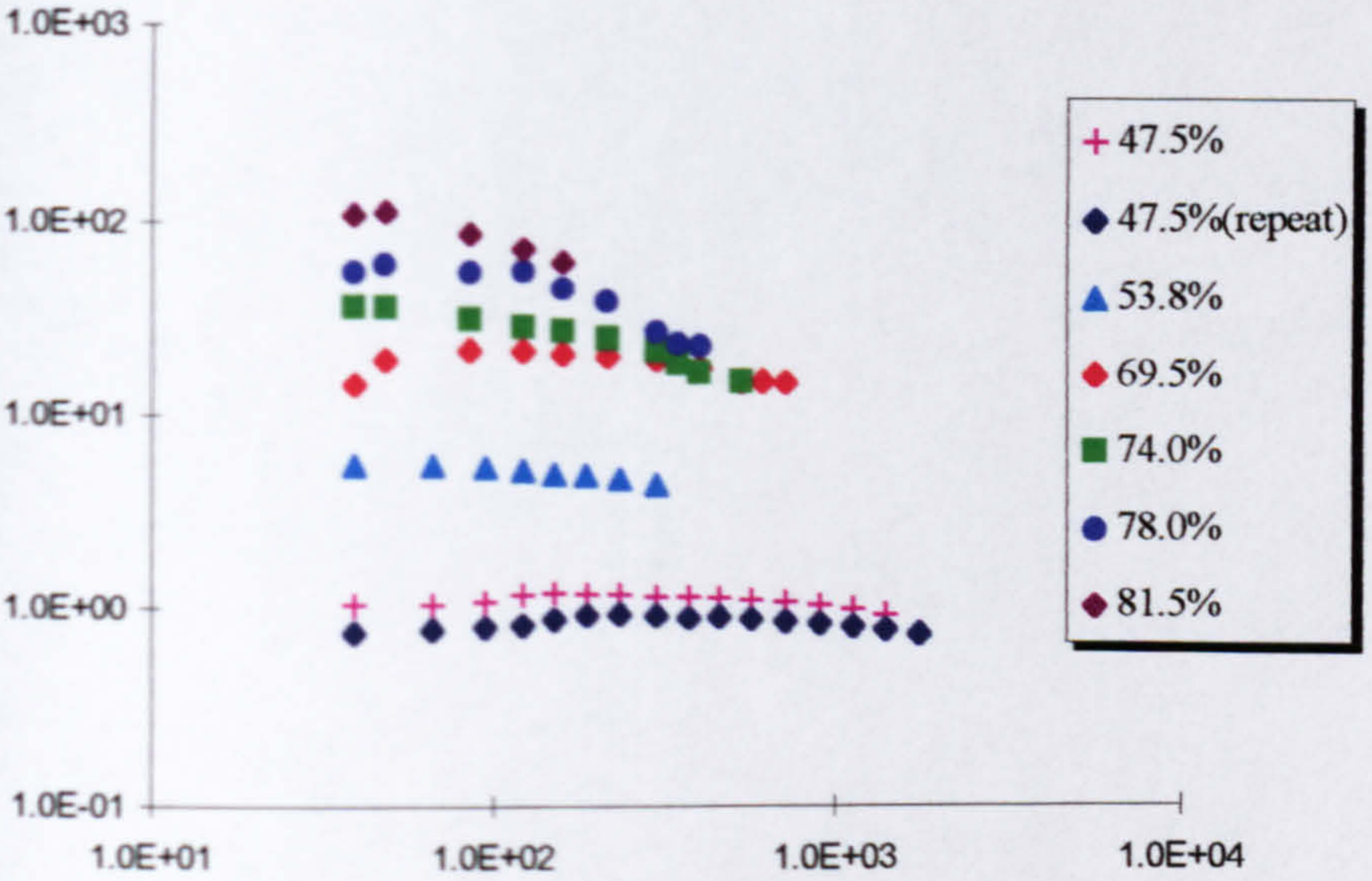

Figure G2. Shear rate dependence of the apparent viscosity at 35°C at intermediate to high PS concentrations

From the above curves, the zero-shear viscosity η_o at 35°C was estimated by the flat portion or plateau observed in the data in the low shear rate region. The data generated is tabulated below (Tables G1 & G2) for samples from each run.

Run V1

All sample viscosity measurements were obtained with the cone-and-plate system CP5/30 with water at 35°C pumped from the water bath circulating below the plate.

Table G1. Viscosity measurements for Run V1

Sample	PS concentration (%)	M_w	η_o (35°C) (Pas)
VA10	9.5	25380	0.03
VA20	18.5	26390	0.05
VA30	27.0	27250	0.07
VA40	34.5	28076	0.19
VA50	42.5	28600	0.30
VA60	49.8	28998	1.55
VA70	56.0	29600	3.1
VA80	62.0	30070	7.4
VA90	67.5	30500	10.6

Run V2

Table G2. Viscosity measurements for Run V2

Sample	PS concentration (%)	M_w	η_o (35°C) (Pas)
VB10	9.2	28100	0.036
VB20	17.9	28500	0.05
VB30	25.8	28800	0.077
VB40	33.8	29515	0.19
VB50	40.5	29500	0.28
VB60	47.5	29306	1.44
VB70	53.8	30200	4.7
VB80	59.0	30950	11.1
VB90	65.0	31200	19.7
VB100	69.5	32039	17.3
VB110	74.0	32500	35.9
VB120	78.0	33117	39.7
VB130	81.5	34300	109

It is assumed that the correlation between η_o , concentration C and molecular weight M_w is of the form:

$$\eta_o = KC^{\beta} M_w{}^{\alpha} \qquad \text{(G1.1)}$$

Also, a value of $\alpha = 1$ is justified for the system under study since the average molecular weights , $\overline{M}_w$,over the whole concentration range satisfies the condition [G2]:

$$\overline{M}_w < \left(\overline{M}_w\right)_{cr}$$

where $\left(\overline{M}_w\right)_{cr}$ is the critical molecular weight for entanglement which is defined, for polystyrene as [G2]:

$$\left(\overline{M}_w\right)_{cr} = \frac{40000}{C} \qquad \text{(G1.2)}$$

where C is the polymer concentration measured in terms of the weight fraction.

Hence, a log-log plot of η_o / M_w against C can be drawn for the data collected. The plot is presented in Figure G3 below.

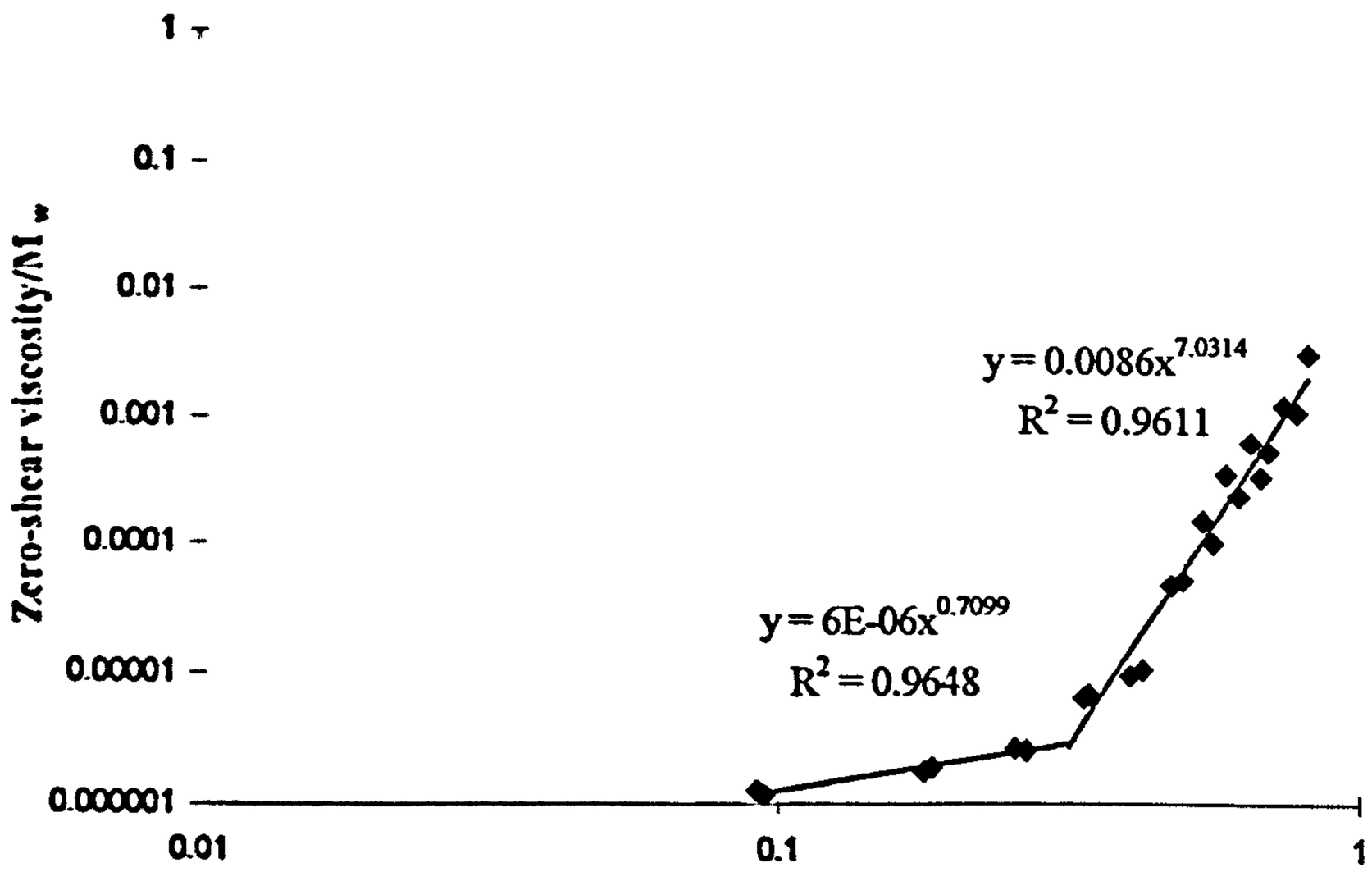

Figure G3. Dependence of zero-shear viscosity at 35°C (normalised for molecular weight) on PS concentration

Two distinct ranges of concentrations can be identified for the PS/styrene/toluene system for which remarkably different rheological behaviours are observed. Thus, in the low concentration region (ca. 0.09-0.30 wt fraction of PS), a rather weak dependence of the zero-shear viscosity on concentration is predicted as given below:

$$\eta_o = 6x10^{-6} C^{0.71} M_w \qquad \text{(G1.3)}$$

In contrast, for concentrations in the range ca. 0.3-0.8, the dependence is as high as 7.03. Hence the relationship in this case is:

$$\eta_o = 8.6x10^{-3} C^{7.03} M_w \qquad \text{(G1.4)}$$

These results compare relatively well with the analysis presented by Biesenberger and Sebastian [G2] where a greater than 4.7-dependence of the zero-shear viscosity of PS in solution was predicted for the high concentration regime while a dependency lower than 1 is expected at low polymer concentrations. The 4.7-dependence for PS/toluene solution at 40°C for η_o >0.3 Pas was first obtained by Onogi et al. [G3]. On the other hand, the correlation derived by Mendelson [G4] predicts a 10.7-dependence on concentration for highly concentrated PS solutions in ethylbenzene at 200°C.

G1.1.1.2. Temperature dependence of viscosity

The concentration dependence in the previous section has been established at a constant temperature of 35°C which was the temperature at which all viscosity measurements were made. However, the present investigation is concerned with polymer processing in the higher temperature range of 88-96°C and it is therefore necessary to derive a relationship for the temperature dependence of viscosity to

enable viscosity data at 35°C to be used to evaluate the viscosity at the desired higher temperature.

Two temperature dependence relationships exists for zero-shear viscosity of polymer melts [G2]: the William-Landel-Ferry (WLF) relation and the Arrhenius relation, both of which are given below:

WLF:
$$\ln\frac{\eta_o(T)}{\eta_o(T_g)}=\frac{C_1(T-T_g)}{C_2+(T-T_g)} \qquad \text{(G1.5)}$$

Arrhenius:
$$\ln\frac{\eta_o(T)}{\eta_o(T_R)}=\frac{E_a}{R}\left(\frac{1}{T}-\frac{1}{T_R}\right) \qquad \text{(G1.6)}$$

where $\eta_o(T)$ is the zero-shear viscosity at temperature T (K)

$\eta_o(T_g)$ is the zero-shear viscosity at the glass transition temperature T_g

$\eta_o(T_R)$ is the zero-shear viscosity at the arbitrarily chosen reference temperature T_R

C_1, C_2: constants in the WLF equation equal to -40 and 52 respectively [G5] for pure polymer melts

E_a: activation energy for viscous flow

R: Universal gas constant

The WLF equation above can be more simply written in terms of a reference temperature T_s which is taken to be 50°C above T_g [G5] whereby the expression becomes:

$$\ln\frac{\eta_o(T)}{\eta_o(T_s)}=\frac{-20.4(T-T_s)}{102+(T-T_s)} \qquad \text{(G1.7)}$$

The constants in the above equation will vary with polymer concentration in solution and can be evaluated experimentally from a plot of shift factors as was done in the work of Onogi and co-workers [G6].

The use of either the WLF equation (G1.7) or the Arrhenius type function (G1.6) is dependent on the proximity of the temperature of the system under consideration to its glass transition temperature. Thus, WLF has been found to be applicable to systems whose temperature lies within the range $T_g < T < T_g+120$ while the Arrhenius expression is most appropriate for temperatures well above T_g. Evaluation of T_g is therefore important in determining the most suitable temperature dependence relation. Bueche [G7] has developed an expression for calculating the glass transition temperature of a polymer diluent system based on the free volume concepts. The equation is :

$$T_g=[\alpha_p V_p T_{gp}+\alpha_d(1-V_p)T_{gd}]/(\alpha_p V_p+\alpha_d(1-V_p)) \qquad \text{(G1.8)}$$

where T_g is the glass transition temperature of the solution

T_{gp} is the glass transition temperature of the pure polymer

T_{gd} is the glass transition temperature of the pure solvent or diluent

V_p is the polymer volume fraction

α_p is the difference between the volumetric coefficients of expansion of liquid and glassy state of the polymer
α_d is the difference between the volumetric coefficients of expansion of liquid and glassy state of the diluent

For the polystyrene/styrene/toluene system under study, the following approximations were used in equation (G1.8) to evaluate T_g at different polymer concentrations:

T_{gp} = 95°C for average polystyrene molecular weight of 30000 [G7]

T_{gd} =-20.4°C (estimated for styrene from the general rule of asymmetric molecules where $T_{gd} = 2/3\ T_m$, [G4] with T_m (melting point of styrene) being -30.7°C [G8]

V_p can be calculated from:

$$V_p = \frac{W_p/\rho_p}{(W_p/\rho_p)+(1-W_p/\rho_m)} \qquad \text{(G1.9)}$$

where W_p: polymer weight fraction in solution

ρ_p: density of polystyrene = 1067 kg/m3 (from density correlation in reference [G9])

ρ_m: density of styrene at 35°C = 893 kg/m3 [G9]

$\alpha_p = 4.8 \times 10^{-4}$ per °C [G7]

$\alpha_d = 10^{-3}$ per °C [G7]

The values of T_g calculated for samples from viscometry Runs V1 and V2 are reproduced in Tables G3 and G4 respectively.

Table G3. T_g values for samples from Run V1

Sample	PS conc. (%)	PS conc (wt fraction)	Vp	Tg (K)	Tg (°C)	Tg+120 (°C)
VA10	9.5	0.095	0.081	257.3	-15.7	104.3
VA20	18.5	0.185	0.160	262.3	-10.7	109.3
VA30	27	0.27	0.236	267.6	-5.4	114.6
VA40	34.5	0.345	0.306	272.9	-0.1	119.9
VA50	42.5	0.425	0.382	279.2	6.2	126.2
VA60	49.8	0.498	0.454	285.7	12.7	132.7
VA70	56	0.56	0.516	291.8	18.8	138.8
VA80	62	0.62	0.577	298.5	25.5	145.5
VA90	67.5	0.675	0.635	305.3	32.3	152.3

Table G4. T_g values for samples from Run V2

Sample	PS conc. (%)	PS conc (wt fraction)	V_p	Tg (K)	Tg (°C)	Tg+120 (°C)
VB10	9.2	0.092	0.078	257.1	-15.9	104.1
VB20	17.9	0.179	0.154	262.0	-11.0	109.0
VB30	25.8	0.258	0.225	266.8	-6.2	113.8
VB40	33.8	0.338	0.299	272.4	-0.6	119.4
VB50	40.5	0.405	0.363	277.5	4.5	124.5
VB60	47.5	0.475	0.431	283.5	10.5	130.5
VB70	53.8	0.538	0.494	289.6	16.6	136.6
VB80	59	0.59	0.546	295.1	22.1	142.1
VB90	65	0.65	0.608	302.1	29.1	149.1
VB100	69.5	0.695	0.656	308.0	35.0	155.0
VB110	74	0.74	0.704	314.4	41.4	161.4
VB120	78	0.78	0.748	320.6	47.6	167.6
VB130	81.5	0.815	0.787	326.6	53.6	173.6
VB140	84.5	0.845	0.820	332.0	59.0	179.0

The reaction temperature of styrene polymerisation in the present investigation lies between 88-96°C. Therefore, as seen in Tables G3 and G4 above, the reaction temperature T fulfils the requirement that $T_g < T < T_g+120$ so that the WLF equation (G1.7) is applicable. In addition setting T_s=35°C roughly satisfies the condition $T_s = T_g+50$°C for polymer concentration in the range 0.1 and 0.8 weight fraction.

The viscosity data calculated at an average reaction temperature of 90°C using the WLF relation given in equation (G1.7) are presented in Tables G5 and G6 below for samples from Run V1 and V2 respectively.

Table G5. Viscosity at 90°C for Run V1

Sample	T_s (°C)	$\eta_o(T_s)$ (Pas)	T (°C)	η_o (T) (Pas)
VA10	35	0.03	90	2.36E-05
VA20	35	0.05	90	3.94E-05
VA30	35	0.07	90	5.51E-05
VA40	35	0.19	90	1.50E-04
VA50	35	0.3	90	2.36E-04
VA60	35	1.55	90	1.22E-03
VA70	35	3.1	90	2.44E-03
VA80	35	7.4	90	5.83E-03
VA90	35	10.6	90	8.35E-03

Table G6. Viscosity at 90°C for Run V2

Sample	T_s (°C)	$\eta_o(T_s)$ (Pas)	T (°C)	η_o (T) (Pas)
VB10	35	0.036	90	2.84E-05
VB20	35	0.05	90	3.94E-05
VB30	35	0.077	90	6.06E-05
VB40	35	0.19	90	1.50E-04
VB50	35	0.28	90	2.21E-04
VB60	35	1.44	90	1.13E-03
VB70	35	4.7	90	3.70E-03
VB80	35	11.1	90	8.74E-03
VB90	35	19.7	90	1.55E-02
VB100	35	17.3	90	1.36E-02
VB110	35	35.9	90	2.83E-02
VB120	35	37.9	90	2.99E-02
VB130	35	109	90	8.59E-02

G1.2. DENSITY CORRELATION

The density of PS/styrene solutions of varying conversion (or polymer concentration) can be calculated by addition of the specific volume of each of the components in the mixture. It is to be noted here that although toluene was also present in the solution mixture in the current investigation, its contribution in the evaluating the density of the mixture is effectively lumped in with the styrene contribution since both have nearly the same density.

The method is illustrated by the specimen calculation below.

Assume a PS/styrene mixture of 30% conversion. The density of pure styrene and polystyrene at 88°C are estimated from the following correlations [G9]:

$$\rho_{(styrene)} = 924 - 0.918\,(T-273.1) \qquad \text{(G1.10)}$$

$$\rho_{(PS)} = 1084.8 - 0.605\,(T-273.1) \qquad \text{(G1.11)}$$

Hence,

Density of styrene at 88°C = 843 kg/m^3

Density of PS at 88°C = 1032 kg/m^3

For density calculation of the 30% converted solution at 88°C, the calculation is based on a mass of 1000 kg of mixture.

Volume of styrene =[(100-30)/100]*1000/843

= 0.830 m^3

Volume of PS = (30/100)*1000/1032

= 0.291 m^3

Total volume of mixture = 0.830 + 0.291 = 1.121 m^3

Density of mixture = 1000/1.121 = <u>892 kg/m^3</u>

Appendix G

The density of a range of mixtures having conversions from 0 to 100% can thus be calculated. The data obtained are plotted in Figure G4 below.

The correlation obtained from a linear fit to the calculated data is:

$$\rho_{(solution)} = 1.8617\,x + 837.11 \quad (R^2 = 0.9963) \qquad \text{(G1.12)}$$

where x is the conversion (%)

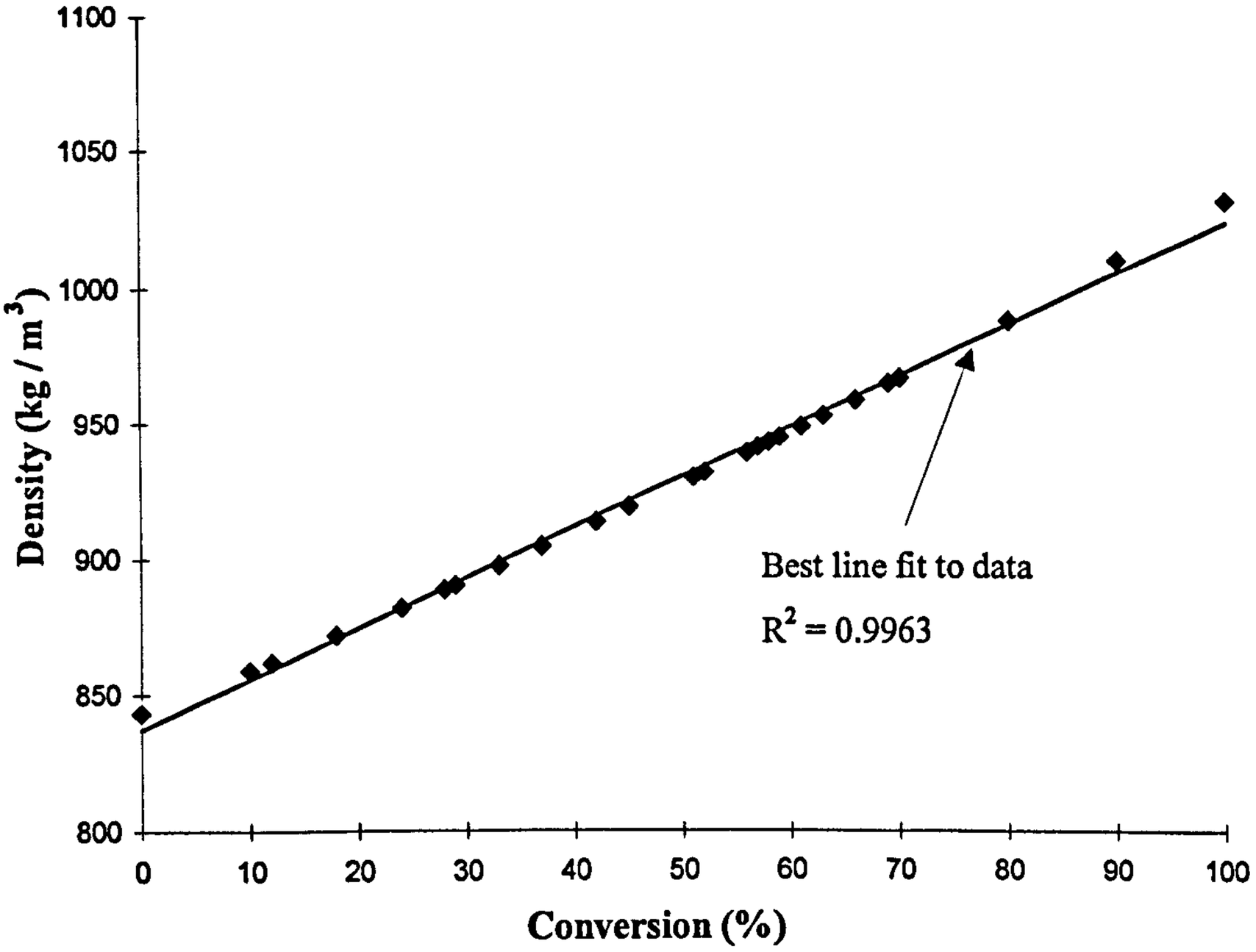

Figure G4. Variation of PS/styrene solution density at 88°C with conversion

References

G1. Ide, Y. and White, J.L., Rheological phenomena in polymerisation reactors: Rheological properties and flow patterns around agitators in polystyrene-styrene solutions. *J. Appl. Polym. Sci.*, **18**, 2997-3018 (1974)

G2. Biesenberger, J.A. and Sebastian, D.H., Flow Phenomena, Ch.5 in *Principles of Polymerisation Engineering*, John Wiley & Sons, New York, pp.514 -572, 1983.

G3. Onogi, S. *et al.*, Effects of molecular weight and concentration on flow properties of concentrated polymer solutions. *J. Polym. Sci.*, **15**, 381-406 (1966)

G4. Mendelson, R.A., Concentrated solution viscosity behaviour at elevated temperatures - Polystyrene in ethylbenzene. *Jou. Rheology*, **24**(6), 765-781 (1980)

G5. Bueche, F., Physical Properties of Polymers, Ch. 4, pp. 104-108, Interscience, New York, 1962

G6. Onogi, S. *et al.*, Non-Newtonian flow of concentrated solutions of high polymers. *J. Appl. Polym. Sci.*, 7, 847-859 (1963)

G7. Bueche, F., Physical properties of polymers, Ch. 5, pp. 112-117, Interscience, New York, 1962

G8. Sinnott, R.K., *Chemical Engineering, Vol. 6*, pp. 857-877, 2nd ed., Pergamon Press, Oxford, 1993.

G9. Husain, A. and Hamielec, A.E., Thermal polymerisation of styrene. *J. Appl. Polym. Sci.*, 22, 1207-1223 (1978)

Appendix H

Publications

The results relevant to the research presented in this thesis have been/will be published in the following conference /journal papers:

1. Boodhoo, K.V.K and Jachuck, R.J.J., Process Intensification: Spinning Disc Reactor for Styrene Polymerisation. *Accepted for publication in Heat Recovery Systems & CHP* (1999)
2. Boodhoo, K.V.K., Jachuck, R.J.J., Ramshaw, C., Process Intensification: Spinning Disc Reactor for Styrene Polymerisation, *Paper presented at the IChemE International Conference on Process Innovation and Intensification*, 21-22 October 1998, Manchester, UK
3. Boodhoo K.V.K., Jachuck, R.J.J., Ramshaw, C., Process Intensification: Spinning Disc Reactor for the Intensification of Styrene Polymerisation, in *2nd International Conference on Process Intensification in Practice- Applications and Opportunities* (J. Semel, Ed.), 21-23 October 1997, Antwerp, Belgium, BHR Conference Series No.28, pp.125-133 (1997)
4. Jachuck, R.J.J., Ramshaw, C., Boodhoo, K.V.K., Dalgleish, J.C., Process Intensification: The Opportunities Presented by Spinning Disc Reactor Technology. *IChemE Symposium Series No. 141*, pp. 417- 424 (1997)
5. Boodhoo, K.V.K., Jachuck, R.J.J, Ramshaw, C., Process Intensification: Spinning Disc Polymeriser for the Manufacture of Polystyrene, in *1st International Conference on Process Intensification* (C. Ramshaw, Ed.), 6-8 December 1995, Antwerp, Belgium, BHR Group Conference Series No.18, pp.175-180 (1995)